Changyou Gao *Editor*

Polymeric Biomaterials for Tissue Regeneration

From Surface/Interface Design to 3D Constructs

Springer

Polymeric Biomaterials for Tissue Regeneration

Changyou Gao
Editor

Polymeric Biomaterials for Tissue Regeneration

From Surface/Interface Design to 3D Constructs

Springer

Editor
Changyou Gao
Department of Polymer Science
and Engineering
Zhejiang University
Hangzhou, Zhejiang, China

ISBN 978-981-10-2292-0 ISBN 978-981-10-2293-7 (eBook)
DOI 10.1007/978-981-10-2293-7

Library of Congress Control Number: 2016954948

© Springer Science+Business Media Singapore 2016
This work is subject to copyright. All rights are reserved by the Publisher, whether the whole or part of the material is concerned, specifically the rights of translation, reprinting, reuse of illustrations, recitation, broadcasting, reproduction on microfilms or in any other physical way, and transmission or information storage and retrieval, electronic adaptation, computer software, or by similar or dissimilar methodology now known or hereafter developed.
The use of general descriptive names, registered names, trademarks, service marks, etc. in this publication does not imply, even in the absence of a specific statement, that such names are exempt from the relevant protective laws and regulations and therefore free for general use.
The publisher, the authors and the editors are safe to assume that the advice and information in this book are believed to be true and accurate at the date of publication. Neither the publisher nor the authors or the editors give a warranty, express or implied, with respect to the material contained herein or for any errors or omissions that may have been made.

Printed on acid-free paper

This Springer imprint is published by Springer Nature
The registered company is Springer Nature Singapore Pte Ltd.
The registered company address is: 152 Beach Road, #22-06/08 Gateway East, Singapore 189721, Singapore

Contents

Chapter 1
An Introduction to Scaffolds, Biomaterial Surfaces, and Stem Cells

Jun Deng and Changyou Gao

1.1 Introduction

The loss of tissues and organs is one of the most serious threats to human health, leading to suffering or death of millions of people each year [1]. Up to present, repair and regeneration of damaged tissues and failed organs is still a hard nut to crack in clinic [2]. Organ transplantation by using autografts and allografts is considered as the most effective technique and remains the dominating therapy for damaged tissues, which has improved the living conditions of millions of patients [2]. However, the application of organ transplantation is compromised because of their drawbacks such as immune response, donor shortage, and donor site morbidity [3].

The idea of "tissues engineering" was firstly put forward in the 1980s, which combines the principles of biology, medicine, materials, and engineering to fabricate in vitro substitutes for subsequent in vivo implantation [4]. During the past three decades, great achievements have been made by using the tissue engineering method. For example, Dermagraft®, a full-thickness skin substitute composed of poly(lactic acid) (PLA), poly(glycolic acid) (PGA), and fibroblasts, has been commercialized to treat diabetic ulcers and has achieved great success [5]. However, some critical issues in tissue engineering still remain. For example, the formation of new tissues needs complicated cell isolation, expansion, and long-term maturation in vitro [6]. The sources of autologous cells are limited. In particular, remodeling of tissues in vitro is difficult to mimic the integrated structures and comprehensive functions of the real in vivo extracellular matrix (ECM) [6]. To overcome these drawbacks, the idea of in situ tissue regeneration is developed by implanting tissue-specific biomaterials alone or combining with cells and biomolecules to the sites of injury [7]. The in situ tissue regeneration can take the advantage of the in vivo

J. Deng • C. Gao (✉)
MOE Key Laboratory of Macromolecular Synthesis and Functionalization, Department of Polymer Science and Engineering, Zhejiang University, Hangzhou 310027, China
e-mail: cygao@mail.hz.zj.cn; cygao@zju.edu.cn

© Springer Science+Business Media Singapore 2016

C. Gao (ed.), *Polymeric Biomaterials for Tissue Regeneration*,
DOI 10.1007/978-981-10-2293-7_1

microenvironment aiming to guide the fate of cells to regenerate new tissues in situ without complicated in vitro manipulation [7]. Therefore, since its emergence, the in situ tissue regeneration has gained great attention and is a promising therapeutic alternative for tissue loss [2, 8].

Biomaterials play a crucial role in the success of in situ tissue regeneration because they can support cell growth and ECM formation. Thus, various formats of biomaterials such as porous scaffolds [9], hydrogels [10], membranes [11], tubes [12], and micro- and nanospheres [13] are available and can be fabricated specifically according to the requirements of different damaged tissues. Multiple technologies including freeze-drying [14], gas foaming [15], electrospinning [16], layer-by-layer (LbL) assembly [17], and three-dimension (3D) printing [18] are used to process biomaterials with organized structures and well-defined functions. Various types of biomaterials such as natural biomaterials [19, 20], synthetic polymers [19, 21], bioceramics [22], and ECM-based biomaterials [23] are employed for the in situ tissue regeneration.

Most studies regarding matrices as regulators of cell behaviors have attributed the effects of the matrix to their "bulk" mechanical and chemical properties [24, 25]. In fact, upon implant into the living body, it is the biomaterial surface/interface that directly contacts with the biological systems [26]. Cells interact with the matrix through the cell-matrix interface, and thereby the "interfacial" properties such as energy [27], wettability [28], and surface topography [29] play a pivotal role in regulating cell adhesion, proliferation, differentiation, and functions. In addition, the biological microenvironment is comprised of the aqueous milieu enriched with soluble proteins and sugars [30]. Upon contact with physiological fluids (e.g., blood), various types of proteins such as albumin, immunoglobulin (IgG), fibrinogen (Fg), fibronectin (Fn), and vitronectin (Vn) adsorb onto the implant surface from body fluids within seconds to minutes [26]. Thus, the cell-surface interaction is ultimately an interaction between cells and surface-bound proteins. The type, amount, conformation/orientation, and bioactivity of the adsorbed proteins subsequently influence the overall kinetics and thermodynamics of the binding events between cells and implant surface [31]. On one hand, certain adsorbed adhesive proteins mediate the attachment and activation of platelets, macrophages, and other inflammatory cells, triggering clotting and immune responses in the host [32]. On the other hand, the adsorbed ECM proteins assist in specific cell adhesion and spreading through integrin binding and regulate other subsequent signaling events (proliferation, differentiation, motility, gene expression, and survival) [33]. Therefore, the interfacial interactions are crucial in determining the success of implant devices.

Stem cells are the focus of many applications for in situ tissue regeneration and tissue engineering due to their extensive abilities to self-renew and to generate differentiated progeny [34]. There are main three broad categories of stem cells, including resident stem cells, embryonic stem cells, and pluripotent stem cells [35]. Tissues that can now be engineered using stem cells comprise a diverse range from

epithelial surfaces (skin, cornea, and mucosal membranes) to skeletal tissues [36]. In addition, one of the strategies in the in situ tissue regeneration is to treat patients by transplanting stem cells or their differentiated derivatives [35]. Although the chemical compositions and physical properties of ECM vary considerably [37], they are the key niche for stem cells in almost all tissues. It has been demonstrated that the ECM not only anchors stem cells but also directs their fate [38]. The adhesion molecules (e.g., proteins and growth factors) on the ECM can regulate the interactions between stem cells and ECM [39]. The interaction of ECM with stem cells depends not only on its surface protein composition but also on its physical and chemical properties. There is strong evidence that ECM surface topography, bulk stiffness, surface energy, and chemical composition can profoundly influence on stem cell behaviors [37, 40].

All these finding are increasingly directing the design of appropriate scaffolds for tissue repair and regeneration [40]. Considerable progress has been made in the design of bioactive and bioresorbable scaffolds that support tissue regeneration. ECM protein motifs, growth factors, and/or genes can be incorporated into the scaffolds by physical incorporation or chemical immobilization, which are used to regulate cell activity and functions by providing signals to stimulate or inhibit cellular adhesion, recruitment, migration, growth, differentiation, and gene expression [40, 41]. Thus, many carriers such as micelles [42], vesicles [43], microgels/nanogels [44], and microcapsules [45] are developed for delivery and controlled release of soluble factors and/or genes.

1.2 Scaffolds

The scaffolds are defined as 3D porous solid biomaterials designed to perform some or all the biological functions and play a unique role in tissue engineering and regenerative medicine. The major function of the scaffolds is to provide a temporary support to body structures, allowing the stress transfer overtime to injured sites and facilitating tissue regeneration on the scaffolds. Meanwhile, the scaffolds should have some other functions, such as (*1*) sufficient transport of gases, nutrients, and regulatory factors to cell survival, (*2*) biodegradable at a controllable rate matching the tissue regeneration, and (*3*) without or with very low inflammation and toxicity. Therefore, design and fabrication of scaffolds is one of the major tasks of biomaterial research in tissue engineering and regenerative medicine. So far different types of scaffolds, including sponges (porous scaffolds), microsphere scaffolds, hydrogel scaffolds, and micro-/nanostructured scaffolds, have been extensively developed (Fig. 1.1).

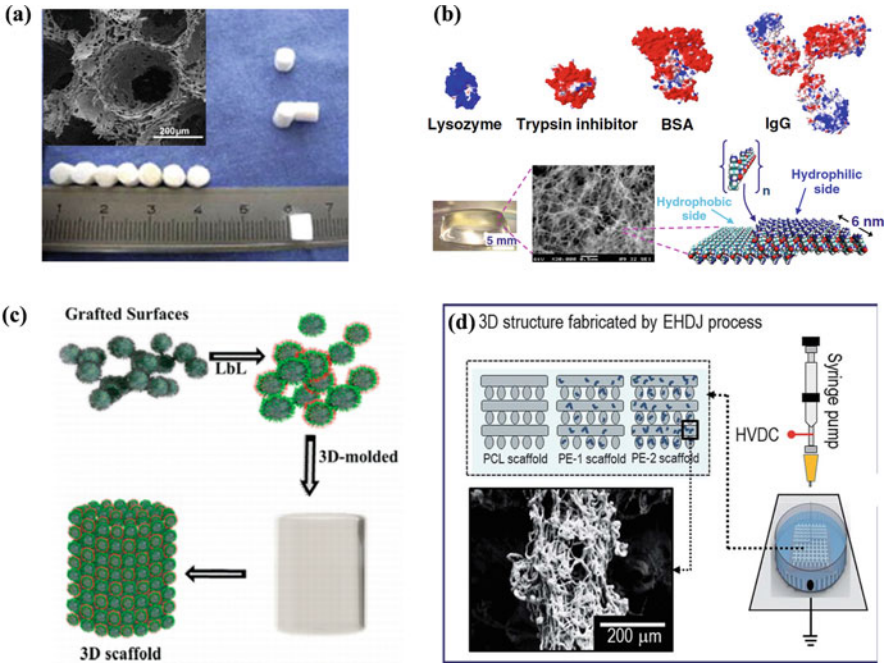

Fig. 1.1 Different types of scaffolds. (**a**) Images of PLGA porous scaffolds ([46, 47], copyright 2010 Elsevier). (**b**) Graphical representation of protein hydrogels ([48], copyright 2009 PNAS). (**c**) Schematic of microsphere scaffolds (Adapted with permission from [49], copyright 2016 American Chemical Society). (**d**) Micro-/nanostructured scaffolds ([50], copyright 2016 Royal Society of Chemistry. Reprinted with permission)

1.2.1 Porous Scaffolds

The 3D polymeric porous scaffolds with higher porosity and interconnected pore network are highly useful for tissue engineering and regeneration. The porous network of the scaffold simulates the ECM, allowing effective cell infiltration and interaction with the outside environment and providing a good substrate for gas and nutrient exchange. Ideal pore size and porosity can be varied for different types of tissues and cells [51, 52]. The porosity and pore size of the scaffolds govern their mechanical properties and play a pivotal role in cell proliferation, migration, and differentiation [52]. Ma et al. fabricated 3D poly(ethylene terephthalate) (PET) nonwoven fibrous scaffolds with variable pore size and porosity using thermal compression [53]. The high porosity (HP) matrices have a porosity of 0.896 and average pore size of 39 μm, while the low porosity (LP) ones have a porosity of 0.849 and average pore size of 30 μm. Cells cultured in the LP matrix could spread across adjacent fibers more easily, leading to faster cell proliferation, while the smaller pore size of LP matrices limits the formation of large cell aggregates and reduces

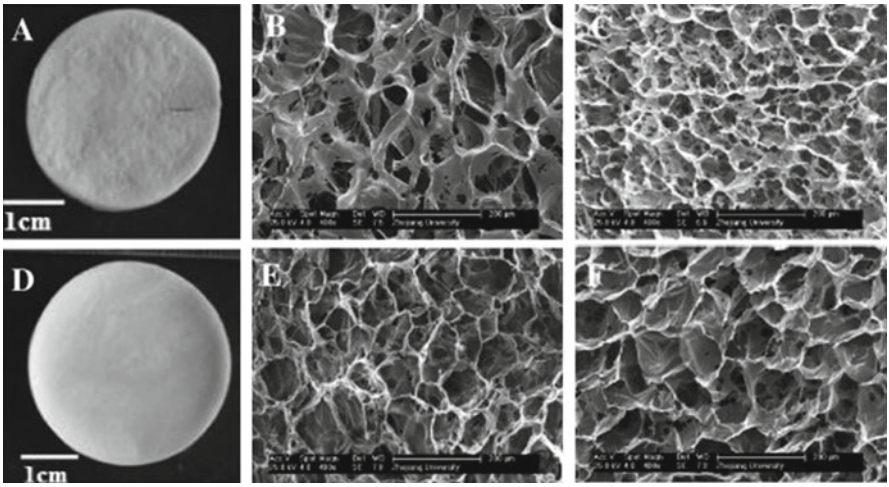

Fig. 1.2 Macroscopic shape of S1 (**a**) and S2 (**d**) and the corresponding microstructure from the surface (**b**, **e**) and cross-sectional view (**c**, **f**) (Reprinted from [55] with permission. Copyright 2012 Elsevier)

cell differentiation. Conversely, cells cultured in HP matrices show a higher degree of cell aggregation and differentiation. The porosity and pore size significantly influence the mechanical properties as well. Although higher porosity and pore size in scaffolds can enhance the nutrient and gas exchange, the mechanical properties of the scaffolds will be compromised due to the large amount of void volume [54]. In general, scaffolds should have strong enough mechanical strength that matches the native tissues in vivo to maintain integrity until new tissue regeneration and sufficient space for cell proliferation and nutrient exchange. Therefore, there is a limit to the amount of porosity and pore size that could be incorporated into a scaffold without compromising its mechanical properties.

The porous scaffold can be fabricated with specific pore size, porosity, and structure using various methods, such as salt leaching [56], phase separation [57], freeze-drying [58], electrospinning [59], selective laser sintering [60], and 3D printing [61]. A variety of natural molecules (e.g., collagen, fibrinogen, and chitosan) and synthetic biodegradable polymers (e.g., poly(L-lactic acid) (PLLA), poly(glutamic acid), poly(lactide-co-glycolide) (PLGA), poly(ε-caprolactone) (PCL), poly(D, L-lactic acid) (PDLLA), and poly(ethylene oxide) (PEO)) are widely used as the scaffolding materials [62]. For example, Liu et al. developed a facile glutaraldehyde (GA) cross-linking method to prepare collagen/chitosan porous scaffolds (S2) by one step of cross-linking and freeze-drying. Compared to the S1 scaffolds prepared by the traditional method consisting of multisteps including freeze-drying, cross-linking, and refreeze-drying [55], the S2 can overcome the shortcomings such as rough surface and inner structure collapse, resulting in a smooth surface and more controllable pore size (Fig. 1.2) [55].

1.2.2 Hydrogel Scaffolds

Since the use of hydrophilic networks of cross-linked poly(2-hydroxyethyl methacrylate) (PHEMA) as soft contact lens material in 1960 [63], the hydrogels have gained increasing interest in biomedical applications [64]. Hydrogels are defined as physically or chemically cross-linked polymer networks that can absorb and maintain large amount of water [65], which is from 10 % to 20 % (an arbitrary lower limit) up to thousands times of their dry weight [66]. The networks are formed by molecular entanglements, covalent bonding, and/or secondary forces including ionic, H-bonding, and hydrophobic forces. The networks can also be formed by biospecific recognitions such as the interactions between Concanavalin A and polysaccharide [67] and between avidin and biotin [68], respectively.

Hydrogels are classified into different categories depending on various parameters including the preparation method, the overall charge, and the mechanical and structural characteristics. The homopolymer and copolymer hydrogels can be distinguished based on the preparation method. The hydrogels can also be classified as neutral, anionic, and cationic depending on the charges of the building blocks, respectively. Moreover, classification of hydrogels can be made according to their physical structures: amorphous, semicrystalline, hydrogen-bonded, supramolecular, and hydrocolloidal, respectively.

Because of their soft and rubbery consistence, they closely resemble the structures and properties of many types of living tissues. Meanwhile, the high water content of the hydrogels contributes largely to their excellent biocompatibility [64]. Therefore, hydrogels are especially suitable for the applications in the revolutionary field of tissue engineering as scaffolds to guide the growth of new tissues, such as cartilage healing, bone regeneration, and wound care. They can act as carriers for drug delivery too [66]. By loading cell growth factors, they can more strongly support the proliferation [67], migration [69], and differentiation of cells [70] during tissue regeneration. Hydrogels in tissue engineering application should meet a number of design criteria including physical parameters (e.g., degradation rate and mechanics) and biological parameters. Therefore, the properties of hydrogels should be well defined and characterized with good reproducibility.

The hydrogels fabricated from naturally derived polymers have potential advantages of biocompatibility, cell-controlled degradability, and intrinsic cellular interactions. However, they may exhibit a narrow and limited range of mechanical properties. Although the synthetic polymers can be prepared with precisely controlled structures, mechanical properties, and functions, the biocompatibility is limited. Thus, various types of hydrogels are prepared by combinations of these two classes of materials. So far a wide and diverse range of polymers have been used to fabricate hydrogels, which contain natural polymers (e.g., collagen, chitosan, hyaluronan, and gelatin), synthetic polymers (e.g., PEG-PLGA-PEG, PEG-PCL-PEG, and PEG-bis-(PLA-acrylate)), and their hybrids (e.g., poly(N-(2-hydroxypropyl) methacrylamide)-g-peptide (P(HPMA-g-peptide)) and P(PLGA-co-serine)). Recently, Mosiewicz et al. developed a hydrogel that could be used for in situ cell

manipulation through enzymatic hydrogel photopatterning [71]. Briefly, a peptide substrate of activated transglutaminase factor XIII (FXIIIa), a key ECM cross-linking enzyme, is rendered photosensitive by masking its active site with a photolabile cage group. Then, covalent incorporation of the caged FXIIIa substrate into PEG hydrogels and subsequent laser-scanning lithography affords highly localized biomolecule tethering (Fig. 1.3) [71].

1.2.3 Micro-/Nanostructured Scaffolds

Nature structural materials are built at ambient temperature from a fairly limited selection of components and are usually comprised of hard and soft phases arranged in complex hierarchical architectures with the dimensions varying from nanoscale to macroscopic physiological scale. The nano-/microstructure of some natural materials such as bone, teeth, and antler has been well characterized [72]. For example, bone is composed of cells embedded in the bone ECM, which is an ordered network assembled from two major nanophases: collagen fibrils made of type I collagen molecules (~300 nm long, ~1.5 nm in diameter) and hydroxyapatite ($Ca_{10}(PO_4)_6(OH)_2$) nanocrystals (plate-shaped, 50 × 25 nm in size, 1.5–4 nm thick) distributing along the collagen fibrils [72]. These structures inspire the investigators to fabricate new micro-/nanostructured scaffolds mimicking the nature materials in tissue regeneration application, such as fibrous scaffolds, microsphere scaffolds, and hybrid (polymer-bioceramic composite) scaffolds. For instance, the development of nanofibers has enhanced the scope for fabricating scaffolds that can potentially mimic the architecture of natural human tissues at the nanometer scale. Microsphere scaffolds have spatial extension and temporal duration control, providing the stiffness gradient for interfacial tissue engineering [73]. The micro-/nanostructured scaffolds possess a larger surface area, which provides much more adsorption sites for bioactive molecules. Thus, the micro-/nanostructured design is also proved to be a strategic method in improving the bioactivity and biological responses of the scaffolds.

Up to present, various technologies have been developed to fabricate the micro-/nanostructured scaffolds, such as biomimetic mineralization [75, 76], layer-by-layer deposition [77], solution casting [78], self-assembly [79], thin-film or tape deposition [80], freeze casting [81], and additive manufacturing (e.g., 3D inkjet printing, robocasting, stereolithography, or two-photon polymerization) [82, 83]. For example, freeze casting has been widely used to fabricate hybrid scaffolds (e.g., poly(methyl methacrylate) (PMMA)/ceramic and PMMA/SiC hybrid materials) with fine lamellar or brick-and-mortar architectures [72, 73, 84]. Lin et al. fabricated the HAp bioceramics with distinct nanostructured topographies using a hydrothermal treatment method [74]. The HAp bioceramics with nanosheet, nanorod, and micro-/nano-hybrid-structured surfaces in macroscopical size are obtained by controlling the compositions of the reaction media (Fig. 1.4) [74]. Compared with the traditional sample with flat and dense surface, the fabricated HAp bioceramics with

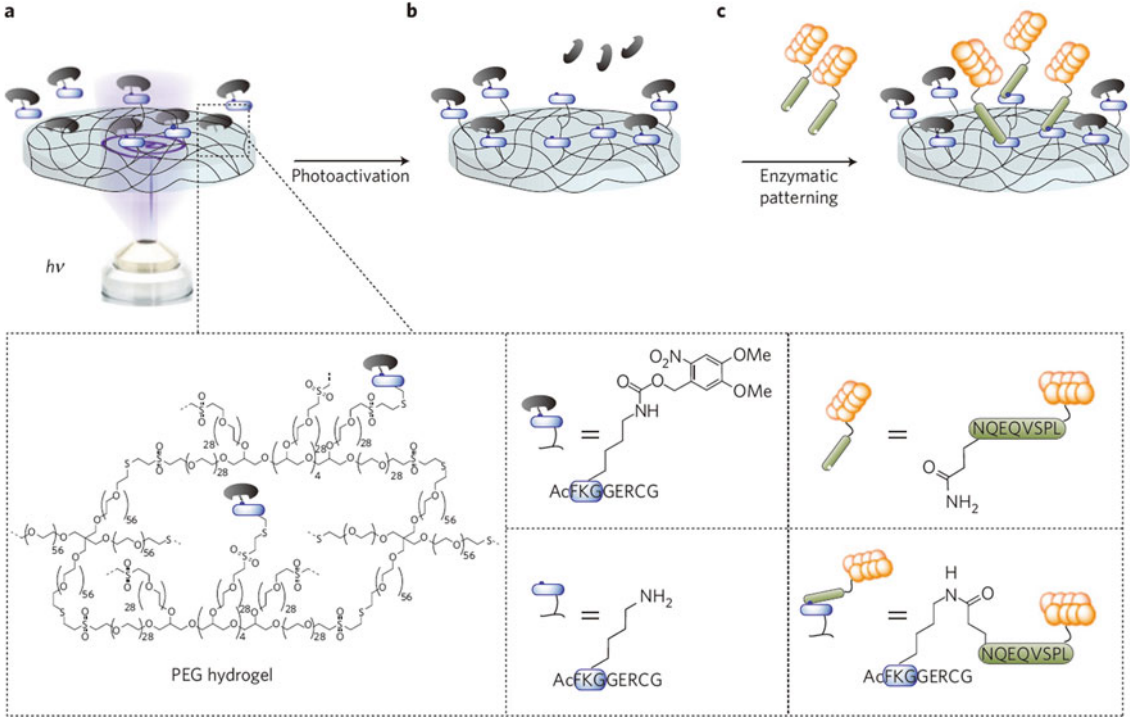

Fig. 1.3 Concept of light-controlled enzymatic biomolecule patterning of hydrogels. (**a**) A photolabile, caged, and therefore inactive enzymatic peptide substrate is covalently incorporated into PEG hydrogels and can be activated by light. (**b**) Localized cleavage of the cage by controlled light exposure from a confocal laser allows reactivation of the enzyme substrate. (**c**) Enzyme-catalyzed (here the transglutaminase factor XIII) reaction of the uncaged substrate with a counter-reactive substrate on a biomolecule of interest allows covalent biomolecule tethering in a highly localized, user-defined pattern (Reprinted from [71] with permission. Copyright 2013 Nature)

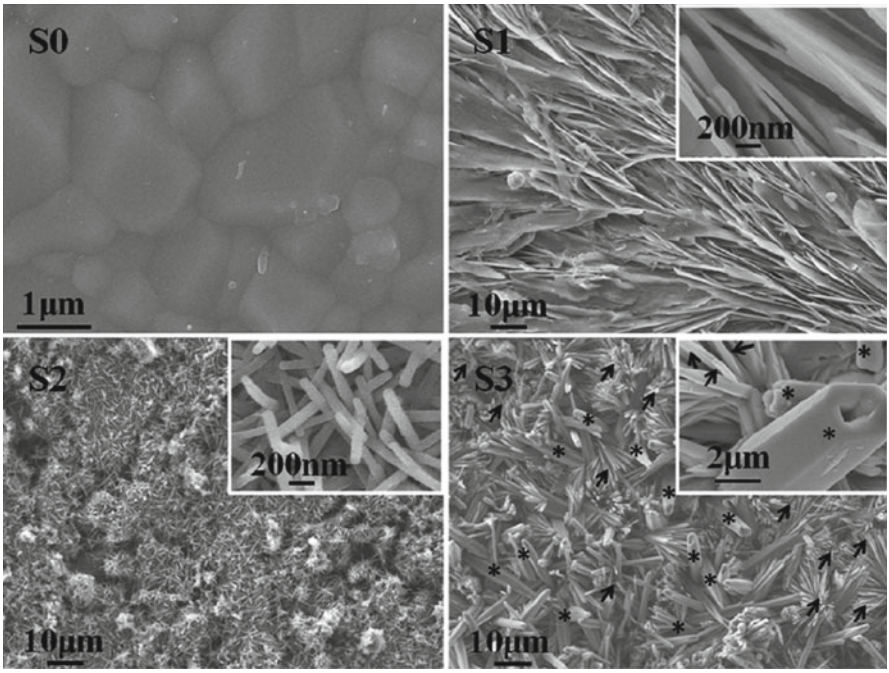

Fig. 1.4 FESEM images of the control sample *S0* and the fabricated HAp bioceramics with different topographic surfaces: nanosheet (*S1*), nanorod (*S2*), and micro-/nano-hybrid (*S3*) (Reprinted with permission from [74]. Copyright 2013 American Chemical Society)

hierarchical 3D micro-/nanotextured surfaces possess higher specific surface area, which selectively enhances adsorption of specific proteins including Fn and Vn in plasma and thereby stimulates osteoblast adhesion, growth, and osteogenic differentiation [74].

1.3 Biomaterial Surface/Interface and Bio-interactions

Upon contact with the biological systems, it is the biomaterial surface that interacts directly with biomacromolecules and living cells, and thereby the cell behaviors are significantly influenced by the surface properties (Fig. 1.5). Hence, the properties of biomaterial surface play a vital role in determining the biological identity and biocompatibility. So far much attention has been paid to understanding the bio-interactions of biomaterial surface and the living systems.

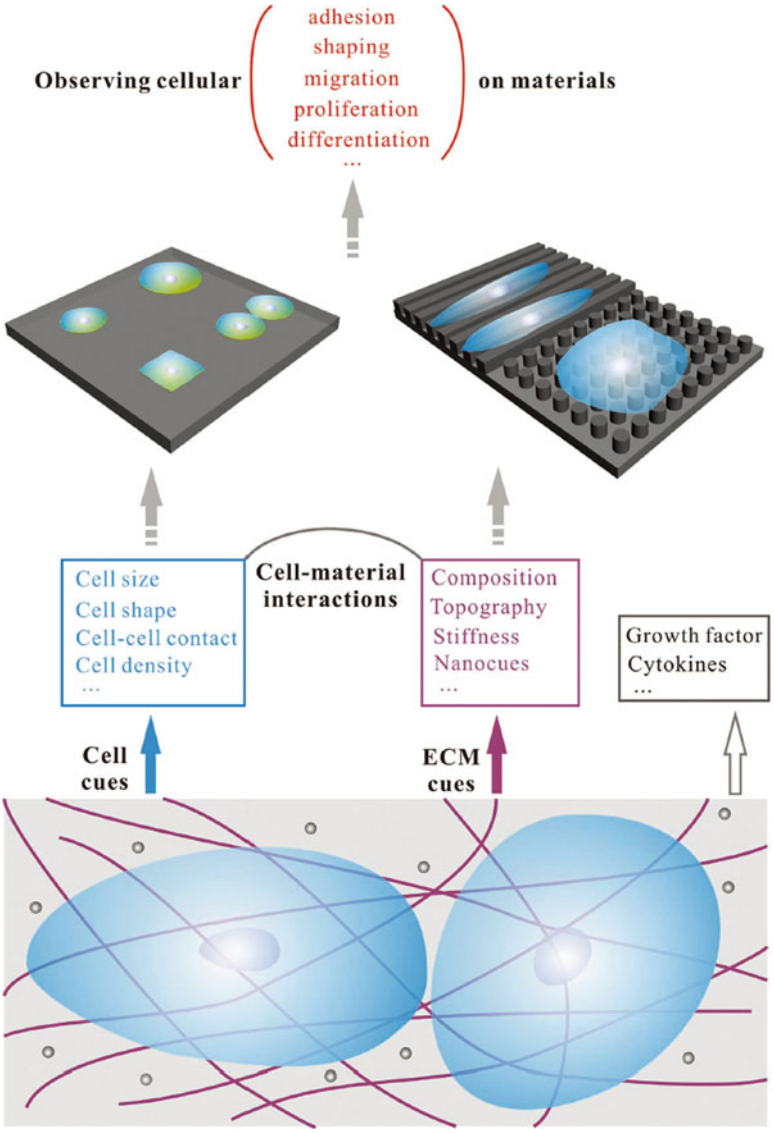

Fig. 1.5 Schematic presentation of the interfacial interactions. Cell behaviors are significantly influenced by the surface properties of the biomaterials and growth factors (Reprinted from [85] with permission. Copyright 2013 Wiley)

1.3.1 The Interactions of Biomaterial Surfaces with Proteins and Cells

After being placed in a biological milieu containing cells, the first molecules reaching to the biomaterial surface are water and salt ions, followed by proteins, and eventually cells come into contact (Fig. 1.6) [26]. The adsorption of proteins on surfaces is a unique phenomenon of major physiological and toxicological significance. Protein adsorption is the first step in many biological processes, for instance,

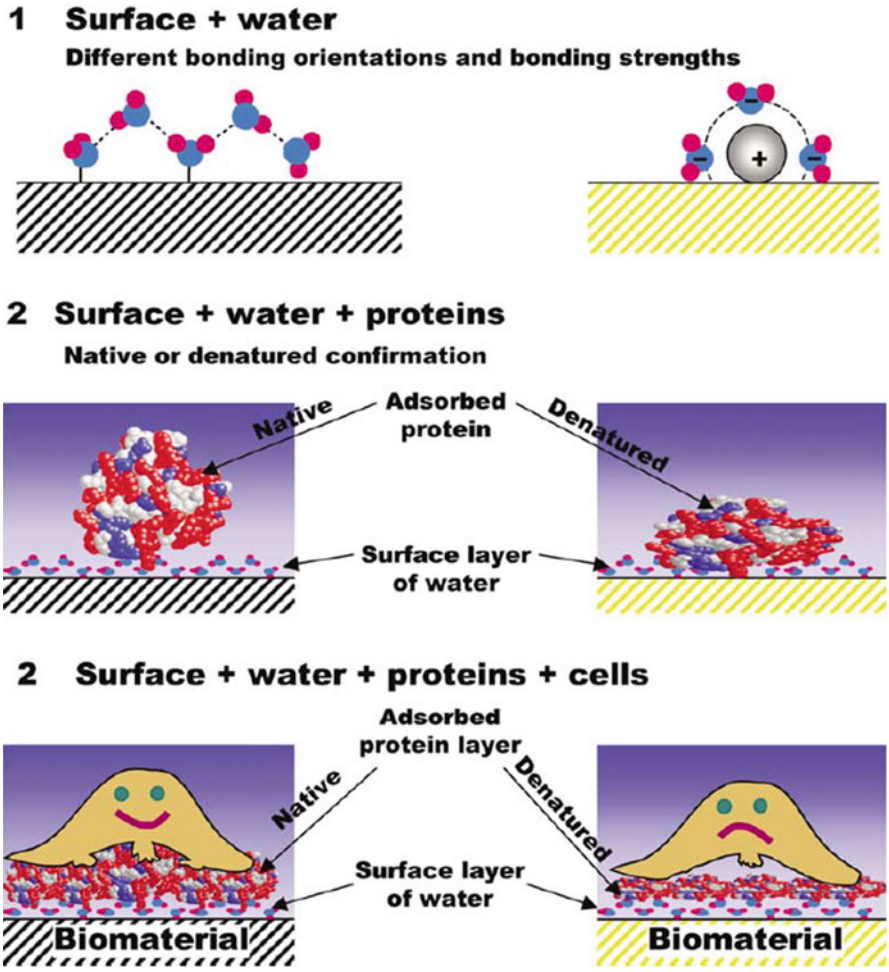

Fig. 1.6 Schematic illustration of the successive events following after implantation of a medical implant. The first molecules to reach the surface are water molecules (ns time scale). Then, protein adsorption starting on the micro- to millisecond time scale and continuing for much longer time. Eventually cells reach the surface (Reprinted from [26] with permission. Copyright 2013 Elsevier)

transmembrane signaling or the blood coagulation cascade [86–88]. Protein adsorption on artificial tissue scaffolds is the key factor for a proper tissue response [89]. Moreover, the contact of biomedical implants with blood stream may cause protein adsorption and may further result in thrombosis [90, 91].

Because of their complex structure, proteins typically exhibit different affinities in different regions of their surface depending on the local composition of amino acid residues. Proteins adsorbed on the biomaterial surface/interface are resulting from attractive coulomb and van der Waals interactions, hydrogen bonding, and the entropy gain of solvent molecules or counterion release. Protein adsorption on biomaterial surface is influenced by many factors such as environment (e.g., pH, temperature, and ion concentration), protein types, and biomaterial surface properties [92, 93]. Generally, proteins direct their hydrophobic patches to the hydrophobic surfaces [94]. Analogously, proteins tend to expose their positively or negatively charged regions to the oppositely charged biomaterial surfaces/interfaces [95]. Thus, proteins prefer to adhere more strongly to high surface tension than to low surface tension, to nonpolar than to polar, and to charged than to uncharged substrates [92]. General experimental finding suggests that in most cases the nonpolar surfaces destabilize proteins and thereby facilitate conformational reorientations, leading to strong surface-protein interactions. Upon adsorption to a solid surface/interface, proteins undergo conformation changes in order to make the free energy minimum [92]. It can be expected that the protein's biological functions are affected by the conformational changes upon adsorption. Indeed, some types of proteins or peptides exhibit their functions only after adsorption [96, 97].

When cells arrive, they "see" a protein-covered surface. It is widely recognized that adsorbed ECM proteins assist in specific cell adhesion and spreading through integrin binding and regulate other subsequent signaling events [33] including proliferation, differentiation [98], motility [99–101], gene expression, and survival. Woo et al. observed that the selectively enhanced protein (e.g., Fn and Vn) adsorption on nano-fibrous PLA scaffolds could enhance osteoblastic cell attachment [102]. Deng et al. found that the adhesion and migration behaviors of vascular smooth muscle cells (VSMCs) on salt-etched polyelectrolyte multilayers [100] and poly(hydroxyethyl methacrylate) (PHEMA) [103] and poly(ethylene glycol) (PEG) [99] brushes are modulated by Fn adsorption. Besides, the protein adsorption and cell behaviors are influenced by the surface properties (e.g., surface rigidity, modulus, charge, topology, roughness, and chemical compositions) [104, 105], environmental factors (e.g., pH, temperature, and ion concentration) [106, 107], and the cell types [108, 109].

1.3.2 Mediation of Cell Migration by Gradient Biomaterials

Cell migration in vivo is a very important and normal process in both physiological and pathological aspects. For example, during embryonic development in mammals, cells migrate beneath the ectoderm to create a different germ layer, and this

targeted cell translocation is required for proper tissue formation [110]. Upon wound occurrence, the fibroblasts and inflammatory cells migrate into the temporarily formed clots. Meanwhile, the epidermal cells migrate and proliferate to cover the surface [111]. Cells in vivo migrate in response to diverse gradients of stimuli including physical, chemical, and signal gradients. Physical gradients occur naturally in bone structure and are defined as the gradual change in a physical property such as porosity, stiffness, and topology [112]. The dense cortical bone is located at the outer layer of the bone, inside which is the low-density trabecular bone. The pore size decreases from inside to outside. These structures can provide excellent permeability and desired mechanical support [112]. The cell migration in vivo is widely recognized as the gradients of ECM proteins, growth factors, and other signaling molecules. Inspired by these natural phenomena, gradient biomaterials have been created to investigate the cell migration in vitro.

Therefore, various techniques including "top-down" and "bottom-up" have been developed to prepare gradient surfaces [114]. The "top-down" approach is usually used to introduce active sites for further functionalization on an inert *s*urface without reactive group. This method modifies the surface gradually via external sources such as corona discharge [115], ultraviolet irradiation [116, 117], plasma [118, 119], chemical degradation [120, 121], and so on to change the surface properties. For example, Han et al. developed gradient poly(sodium 4-styrenesulfonate) (PSS)/poly(diallyldimethylammonium) chloride (PDADMAC) multilayers with a gradually changed swelling ratio by using a salt-etched method [122]. The "bottom-up" technology is mostly used to introduce species of functional molecules onto surfaces with an adjustable grafting density, chain length, and mobility [123–125]. The gradient surfaces of materials can be obtained by time and spatially controlled reactions or by reactions in a gradient concentration of molecules. For instance, Ren et al. fabricated a molecular weight gradient of poly(2-hydroxyethyl methacrylate) (PHEMA) brushes with a thickness ranging from 3 to 30 nm and slopes of 0.8–3.2 nm/mm by using surface-initiated atom transfer radical polymerization (ATRP) and a dynamically controlled reaction process [126].

Since they are more similar to the situation in vivo and also have the potential application of inducing cell migration in the tissue regeneration process, the gradients in a 3D matrix are more important. However, the "top-down" and "bottom-up" are only used for fabricating the gradient surface on 2D surface, but are not suitable in a 3D matrix owing to their relative complicated structure. There are only a few technologies that have been successfully applied in a 3D matrix (e.g., porous scaffolds and hydrogels) [127, 128]. For example, Woodfield et al. fabricated a pore-size gradient using a novel 3D fiber deposition technique [127]. DeLong et al. developed hydrogels with a basic fibroblast growth factor (bFGF) gradient by diffusing two types of hydrogel precursor solutions (PEG-conjugated bFGF solution and only PEG solution) in a gradient maker [69]. Cells were observed to align on hydrogels modified with a bFGF gradient in the direction of increasing tethered bFGF concentration as early as 24 h after seeding [69]. Oh et al. fabricated a surface area gradient porous polycaprolactone (PCL)/Pluronic F127 cylindrical scaffold by a centrifugation method (Fig. 1.7a) [113]. The cylindrical scaffolds exhibit gradually increasing

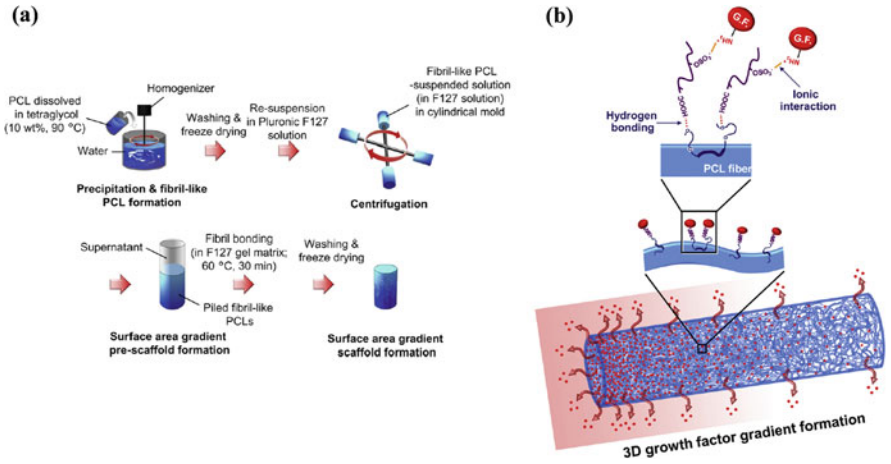

Fig. 1.7 (**a**) Schematic diagram showing the fabrication process of the surface area gradient porous scaffold by a centrifugation method. (**b**) Schematic diagrams of the successive binding of heparin and growth factor onto the fibril surface of PCL/F127 cylindrical scaffold and the formation of 3D growth factor gradient on the scaffold (Reprinted from [113] with permission. Copyright 2011 Elsevier)

surface areas along the longitudinal direction. Then, growth factors are immobilized via heparin binding to produce scaffolds with gradually increasing concentration of growth factors from the top position (near to rotation center) to the bottom position (bottom of the centrifuge tube, far to the rotation center) (Fig. 1.7b) [113]. The released amount of growth factor from the cylindrical scaffold gradually decreased along the longitudinal direction (from the bottom of the centrifuge tube to the top of the centrifuge tube) in a sustained manner for up to 35 days, which can allow for a minutely controlled spatial distribution of growth factors in a 3D environment (Fig. 1.7b) [113].

1.3.3 Influence of Biomaterial Surface on Stem Cell Fate

The promise of cellular therapy and tissue regeneration depends strongly on the cells used and the cell-biomaterial interaction in vitro and in vivo [129, 130]. However, the lack of available donor cell sources limits its ultimate clinical applicability. Stem cells (SCs) like mesenchymal stem cells (MSCs) are chosen for cell therapy due to their pluripotent nature and self-renewal capacity (Fig. 1.8). Control over their differentiation to a lineage of choice in an efficient and scalable manner is critical for the ultimate clinical success of cellular therapeutics [131, 132]. Surface modification to biomaterials can directly influence on stem cell behavior by altering surface interactions and microenvironment architecture and ultimately manipulating the signal transduction pathways in stem cells [133–135]. Diverse factors can

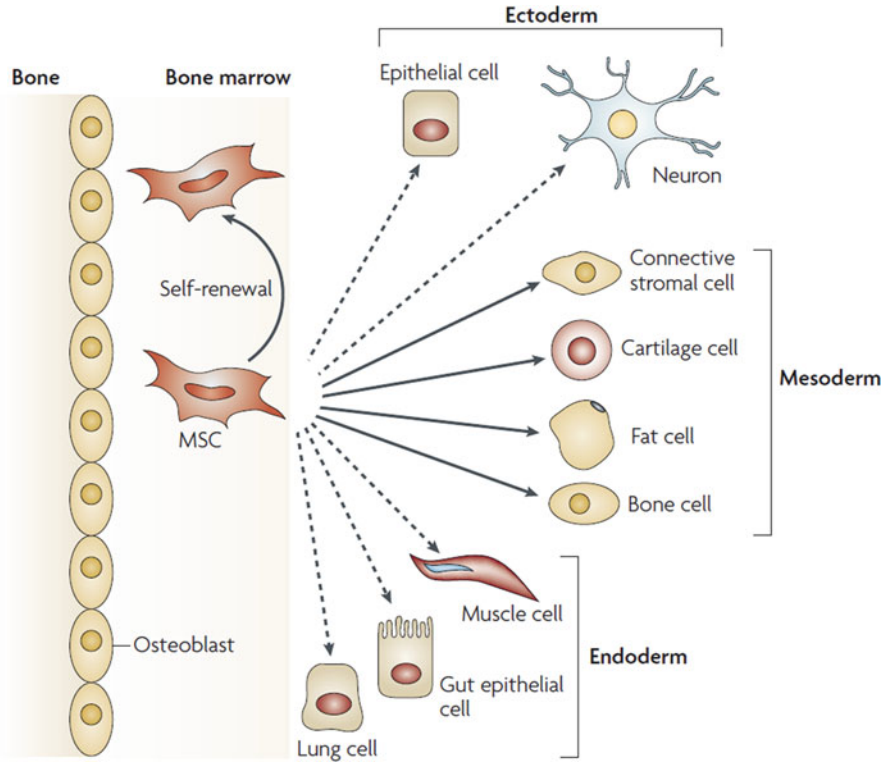

Fig. 1.8 The multipotentiality of MSCs. The ability of mesenchymal stem cells (MSCs) in the bone marrow cavity to self-renew (*curved arrow*) and to differentiate (*straight*, *solid arrows*) toward the mesodermal lineage (Reprinted from [137] with permission. Copyright 2008 Nature Publishing Group)

contribute to overall stem cell fates (i.e., differentiation into specific lineages), including the mechanical properties (e.g., elasticity or rigidity and stiffness), chemical and biological signals, and surface pattern [133–136].

The physical interactions between cells and the elasticity of substrates can influence on stem cell fates, although genetic or molecular mediators have been considered to be the controlling factors [138, 139]. Recently, numerous studies have proved that the elasticity of cell culture substrates defines the lineage commitment of stem cells [24, 28, 140–143]. It was observed that the stem cells tend to differentiate into specific tissue lineages when they are cultured on materials with similar elasticity to those tissues [24, 28, 140–143]. For example, soft cell culture materials guide mesenchymal stem cells (MSCs) into neuronal differentiation regardless of the use of induction medium [24, 144–146]. However, the MSCs tend to osteoblast differentiation when they are cultured on stiff substrates [147, 148]. In addition to the physical properties, stem cell differentiation can be directly mediated by presenting appropriate biological [37, 149] or chemical factors [150, 151] in their

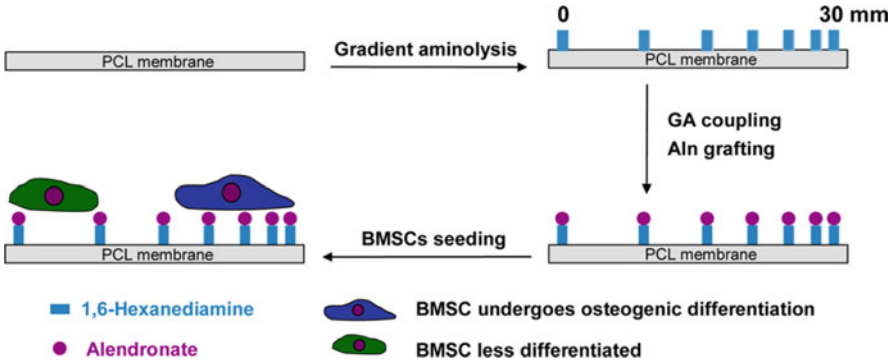

Fig. 1.9 Schematic diagram of aminolysis and Aln immobilization on a PCL membrane and influence on the differentiation of BMSCs in a gradient manner (Reprinted from [155] with permission. Copyright 2012 American Chemical Society)

microenvironment. For example, activin A has been demonstrated to promote the differentiation of stem cell-derived embryoid body (EB) toward the endoderm germ layer [152]. The use of retinoic acid and activin A can successfully enhance in vitro differentiation of mouse embryonic stem cells (mESCs) into α-, β-, γ-, and δ-cells, all of which are pancreatic endocrine cells [153]. Dexamethasone [154], β-glycerol phosphate [154], alendronate (Aln) [155, 156], and BMP [157, 158] can promote in vitro differentiation of mESCs into cartilage. Therefore, chemical and biological molecules have been used to modify the biomaterial surface to control the stem cell differentiation. More recently, these chemical and biological molecules are directly incorporated within the scaffold structure or into the scaffold biomaterial in a variety of ways. For example, soluble growth factors can be directly incorporated or encapsulated during the scaffold fabrication process [159, 160]. Another commonly used method is simple physical adsorption of chemical or biological molecules on the biomaterial or scaffold surface. Carstens et al. reported that human BMP-2 (rhBMP-2)-adsorbed collagen sponges show in situ osteogenesis in a craniofacial mandibular defect [161]. Compared to the above approaches, covalent conjugation of chemical or bioactive molecules to the biomaterials provides a more reproducible and controlled way since both ligand amount and ligand density can be controlled. Arginine-glycine-aspartic (RGD) peptide molecules are covalently conjugated to PEG chains using the widely used N-hydroxysuccinimidyl-ester (NHS) molecules [162]. The high density of RGD molecules-conjugated PEG hydrogel enhances osteogenic differentiation of MSCs [163]. Aln molecules are covalently attached onto the aminolyzed PCL membrane in a gradient manner via the coupling reaction between the derived aldehyde groups and -NH_2 groups (Fig. 1.9) [155]. The BMSCs show gradient osteogenic differentiation on the Aln-grafted gradient surface with a stronger tendency on the high density of Aln molecules (Fig. 1.9) [155].

1.4 Regenerations of Some Clinic-Targeted Tissues

Due to the poor regenerative capacity of tissues in vivo, the repair of tissue defects is always a great challenge in surgery therapy [164]. Tissue engineering combines the principles and technologies of bioengineering, medicine, and biology to repair or regenerate tissues by using the building blocks of native tissues, including cells, growth factors, and scaffolds, providing a promising approach for tissue repair and regeneration [165, 166]. Here, regeneration of some clinic-targeted tissues such as cartilage, skin, blood vessels, and cardiovascular is described briefly.

1.4.1 Cartilage Regeneration

Osteoarthritis, which is mainly caused by cartilage destruction, affects approximately 27 million adults in the United States [167]. Cartilage has limited capacity of self-repair due to its lack of vascularity, resulting in poor replicative capacity of chondrocytes, the main cell type in cartilage. The limited capacity of damaged cartilage to regenerate and the potential morbidity associated with implanting or transferring bone and cartilage make cartilage regeneration an attractive alternative. Therefore, the cartilage tissue engineering aims to create biologically compatible cartilage constructs, which are composed of certain cell types seeded within biomaterial scaffolds. Tissue-engineered cartilage contains a variety of components, such as various constituent cell types, biomimetic scaffolds, inductive bioactive factors, and genes.

The cells seeded into the scaffolds are responsible for the synthesis and metabolism of ECM. Initially, chondrocyte is used in cell-based therapy for repairing cartilage lesions, which is the principal cell type found in cartilage [168]. However, the availability of chondrocytes (e.g., adult chondrocytes and juvenile chondrocytes) is limited. Pluripotent stem cells such as ESCs are attractive options for tissue regeneration because of their potential for indefinite self-renewal and ability to differentiate into multiple tissue types [169, 170]. Although most of the pluripotent stem cells may be a viable treatment solution for cartilage regeneration, their undifferentiated nature and tendency to grow without restraint may lead to concern of tumor formation [171]. Mesenchymal stem cells (MSCs), another type of the pluripotent stem cells, have minimal tumorigenic capacity and thereby are of great promise for regenerating cartilage. MSCs have the ability to differentiate into various cell lineages including adipocytes, osteoblasts, chondrocytes, and myocytes [172]. Therefore, MSCs are an ideal option for cartilage regeneration because of their available and accessible supply and their capacity for considerable expansion and differentiation.

Cells must be seeded on a 3D scaffold that retains the seeded cells and provides mechanical support to aid in the development of cartilage over time. Thus, mainly four types of scaffolds including protein-based polymers, carbohydrate-based

polymers, synthetic polymers, and composite polymers are applied in cartilage tissue engineering [62]. Inspired by nature, the protein-based polymers such as fibrin, gelatin, and collagen have been widely used in bioengineered scaffolds. For example, collagen is the major component of ECM and can be used as a scaffold that could retain cell phenotypes. Being seeded with autologous chondrocytes in collagen type I-based scaffold, the obtained construct was implanted in 21 patients with grade III chondral defects of the distal femur [173]. The patients treated with these scaffold materials have significantly lower pain scores [173]. Hyaluronan, alginate, chitosan, and agarose are typical examples of carbohydrates and have been used as hydrogel scaffolds. They have a strong ability to adsorb and maintain water, which is similar to the properties of cartilage ECM. In one study, significant improvement in function and relief of pain was seen in cartilage defect patients being treated with hyaluronic acid-based scaffolds [174]. Synthetic polymers such as PLA, PCL, and PLGA are the most common materials used in cartilage regeneration. Previous work has demonstrated that a synthetic polymer-based scaffold containing PLGA and calcium sulfate could enhance the growth of cartilage and bone [175].

In contrast to scaffolds, cells and growth factors are used to stimulate cell growth, enhance chondrogenesis, and augment the management of cartilage defects. The five main groups of growth factors used in cartilage regeneration are transforming growth factor-β superfamily, fibroblast growth factor family, insulin-like growth factor, platelet-derived growth factor, and platelet-rich plasma [176]. Recently, a composite construct comprising of bone marrow mesenchymal stem cells (BMSCs), plasmid DNA encoding transforming growth factor-β1 (pDNA-TGF-β1), fibrin gel, and poly(lactide-co-glycolide) (PLGA) sponge was designed and employed to repair articular cartilage defects (Fig. 1.10a) [46]. To improve the gene transfection efficiency, a cationized chitosan derivative N,N,N-trimethyl chitosan chloride (TMC) was employed as the vector (Fig. 1.10a) [46]. In comparison with BMSCs or TMC/pDNA-TGF-β1 constructs, both the cartilage and subchondral bone were perfectly regenerated and integrated with the host tissues in the BMSC/TMC/pDNA-TGF-β1 composite constructs (Fig. 1.10b) [46]. These composite constructs have great potential for in situ cartilage regeneration.

1.4.2 Skin Regeneration

Skin, the largest organ of human body, plays a significant role in protecting the body against outside environment. It mainly consists of the epidermis, dermis, and hypodermis [178]. Severe acute and chronic wounds on the skin such as burns, abrasions, lesions, and ulcers may result in significant disability or even death. Because of the antigenicity of donor tissue and the limitation of donor sources, skin grafts have been a challenging task for surgeons, limiting their wide application [179, 180]. Therefore, various models for skin epidermis and dermis reconstruction have been developed to enhance skin cell growth during wound healing. Many new approaches

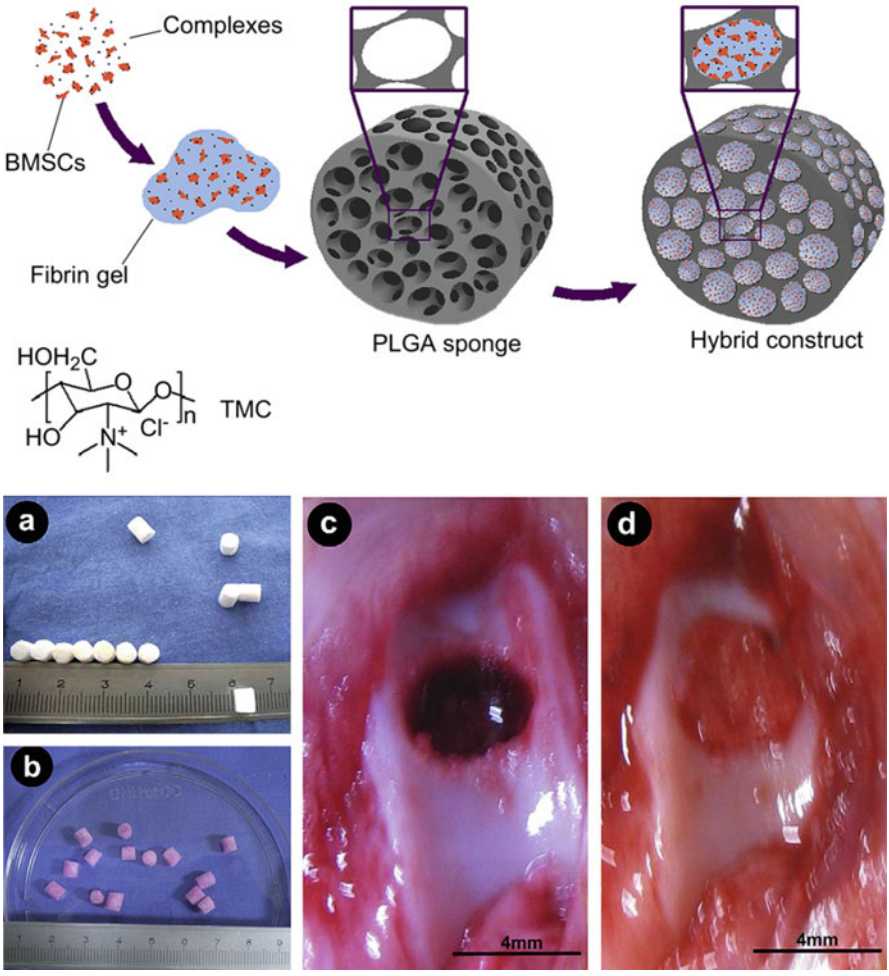

Fig. 1.10 (**a**) Schematic illustration of the fabrication procedures of the composite construct by filling BMSCs, TMC/DNA complexes, and fibrin gel into a PLGA sponge and chemical structure of TMC. pDNA-TGF-β1 was used in the in vivo experiment. (**b**) The macroscopic shape of (*a*) PLGA sponges and (*b*) PLGA sponges/fibrin gel/BMSCs/(TMC/pDNA-TGF-β1) constructs. (*c*) A full-thickness trauma was created on the articular cartilage with a diameter × depth of 4 × 4 mm, which was subsequently implanted with a composite construct (*d*) (Reprinted from [46] with permission. Copyright 2010 Elsevier)

(e.g., physical and pharmacological methods) have been explored to improve human skin cell growth [181, 182]. Tissue engineering is emerging as an effective method for developing skin substitutes and ameliorating the healing process.

To simulate the in vivo environment, a series of natural materials including silk, collagen, fibrin, and sugar are preferred for tissue-engineering applications. For

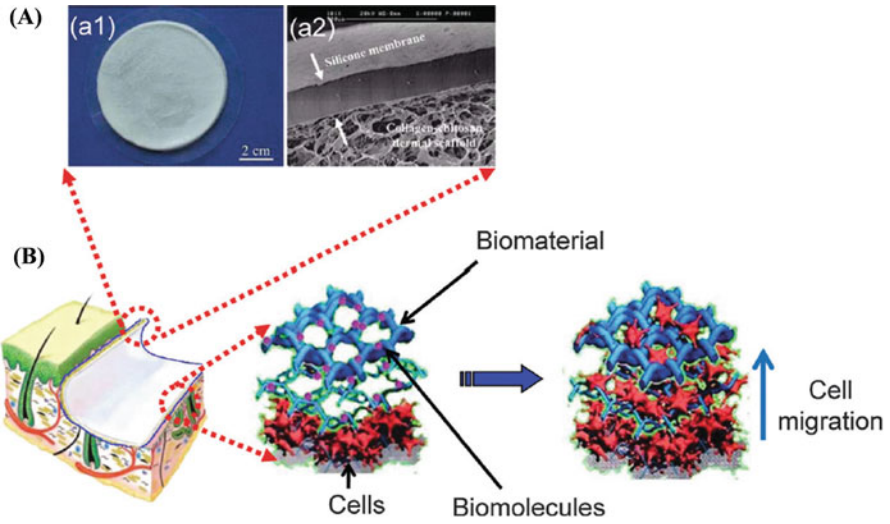

Fig. 1.11 (**a**) Macroscopic appearance (*a1*) and microstructure (*a2*) of the bilayer dermal equivalent (BDE) (Reprinted from [177] with permission. Copyright 2007 Springer). (**b**) Schematic presentation of functionalized BDE. The released biomacromolecules from the matrixes enhance the migration of host cells (Reprinted from [2] with permission. Copyright 2015 The Royal Society of Chemistry)

example, collagen is the main structural protein in vertebrates and the most useful biomaterial in bioengineering. A collagen/chitosan porous scaffold is fabricated for skin tissue engineering by a freeze-drying method, which serves as a potential candidate for dermal equivalent with enhanced biostability and good biocompatibility [180]. Besides the natural materials, the synthetic polymers are widely used in skin repair as well. For instance, PCL containing collagen is used to construct tissue-engineered skin substitutes [183]. Moreover, a biodegradable hybrid mesh composed of synthetic PLGA and collagen is used for skin tissue engineering, in which fibroblasts are cultured to obtain a construct. After it is implanted in the back of nude mice for 2 weeks, dermal tissues are formed, which became epithelialized 4 weeks [184]. Growth factors such as vascular endothelial growth factor (VEGF), TGF-β1, TGF-β2, and platelet-derived growth factor (PDGF) and higher levels of TGF-β3 enhance cell proliferation and stimulate angiogenesis. Therefore, incorporation of appropriate growth factors in artificial skin scaffolds will enhance host intake and minimize scarring [185]. Shi et al. fabricated a bilayer dermal equivalent (BDE) by combining collagen/chitosan porous scaffold with a silicone membrane, whose macroscopic shape and microstructure are illustrated in Fig. 1.11a [177]. The regenerated dermis can support the transplantation and survival of thick skin. This dermal equivalent can be further functionalized by incorporating TMC/pDNA-VEGF complexes, which enhance the migration of host cells (Fig. 1.11b) [2, 186].

1.4.3 Nerve Regeneration

Nerve regeneration remains a great challenge. For example, the incidence of peripheral nerve injury (PNI) is between 13 and 23 per 100,000 persons per year in the developed countries, resulting in partial or total loss of motion, sensory, and autonomic function in the involved segments of the body [187]. About 300,000 people are affected by PNI annually in Europe alone [188, 189]. Although the peripheral nervous system has great potential for axonal regeneration after injury, spontaneous peripheral nerve repair is always incomplete with poor functional recovery [190]. A number of medical therapies has been undertaken for hundreds years with the intention of improving outcomes [191, 192]. The most common used methods for current clinical treatment involve the end-to-end anastomosis and utilization of autografts. However, both of these procedures have their drawbacks and often ineffective because of the gap length between the injured nerves, formation of neuromas, and shortage of donor sources. Therefore, these ineffective therapies and limited availability of donor nerves motivate the development of artificial biodegradable nerve grafts.

Since the regeneration of damaged nerves is a complicated biological process that requires multiple signals to facilitate neurocyte survival and stimulate neurite growth, artificial nerve grafts should ideally possess several functionalities, for example, a favorable environment for regenerating axons and enhancing cellular growth and migration and offering the guidance and protection abilities from the surrounding tissues [194]. Furthermore, nerve grafts must possess sufficient mechanical strength for suturing to the nerve stumps and suitable biodegradation properties [195, 196]. Thus, natural biomaterials [197] (e.g., collagen, chitosan, fibrinogen, and alginate) and synthetic polymers [198, 199] (e.g., aliphatic polyesters) are common materials used for production of nerve grafts. To improve the biological performance of artificial grafts, several additional functionalities including topographical guidance, electrical activity, and neurotrophic activity have been introduced into the devices. Topography plays a fundamental role in nerve repair [200]. Electrospinning is widely used to develop aligned topography that supports cell adhesion and regulates the growth of neurons [201]. Besides, electrical stimulation is closely related to nerve regeneration as well [202]. Thus, electrically conducting polymers such as polypyrrole (PPY) and its derivatives are widely used in nerve repair because of their biocompatibility and conductivity [203]. Xu et al. fabricated a conducting composite nerve conduit with PPY and PDLLA, which was used to repair a rat sciatic nerve defect. It performs similarly to the golden standard of autologous graft [204]. Furthermore, trophic elements such as neurotrophic agents (e.g., acetylcholine [205], laminin-derived peptides including IKVAV and YIGSR [206, 207], and nerve growth factor (NGF) [208]) and Schwann cells [209] have frequently been combined with artificial conduits. Schmidt et al. fabricated a neural conduit with submicrometer-scale features, electrical conductivity, and neurotrophic activity by coating PPY onto the PLGA nanofibers with chemical immobilization of NGF onto the surface of the fibers [210]. The NGF-immobilized

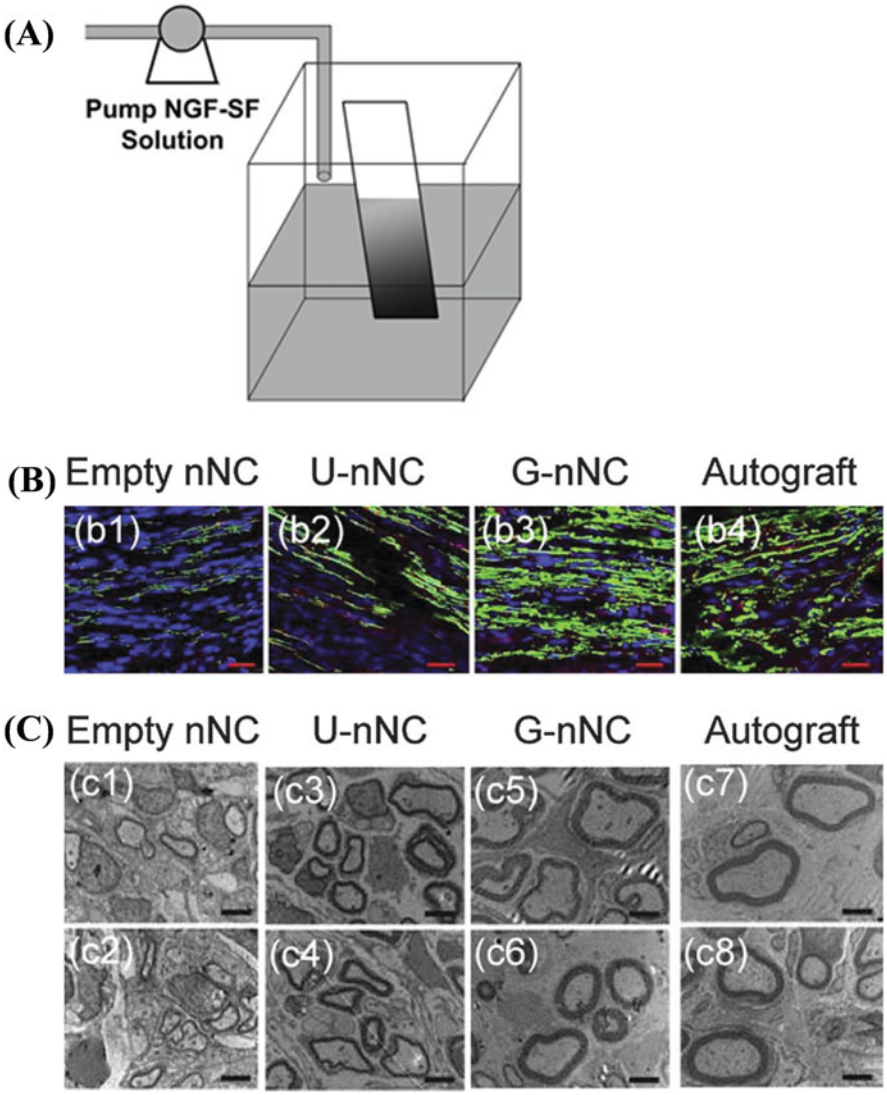

Fig. 1.12 (**a**) Schematic of the immobilization of nerve growth factor (NGF) gradients within membranes or conduits. (**b**) Axons regeneration 12 weeks after implantation. (*b1*) Empty nNC, (*b2*) uniform nNC, (*b3*) gradient nNC, and (*b4*) autograft. (**c**) TEM images of ultrathin sections showing myelinated axons at the middle and distal portion 12 weeks after implantation. (*c1* and *c2*) Empty nNC, (*c3* and *c4*) uniform nNC, (*c5* and *c6*) gradient nNC, and (*c7* and *c8*) autograft (Reprinted from [193] with permission. Copyright 2013 Elsevier)

PPY-coated PLGA fibers facilitate PC12 neurite formation and neurite growth [210]. Poly(caprolactone)-block-poly(L-lactic acid-co-e-caprolactone) (PCLA) nanofibrous nerve conduits immobilized with an NGF gradient by combining the differential adsorption duration of NGF and silk fibroin coating are fabricated (Fig. 1.12a) [193]. A rat sciatic nerve defect model is used to evaluate the efficacy of the NGF gradient-immobilized nanofibrous nerve conduits (nNCs) in vivo. After 12 weeks implantation, the NGF gradient-immobilized nNCs achieve positive results with morphological and functional improvements, which are similar to autografts, and better than empty and uniform NGF-immobilized nNCs (Fig. 1.12b) [193].

1.4.4 Regeneration of Blood Vessels

The blood vessels are composed of endothelial cells (ECs) that are in contact with the blood, vascular smooth muscle cells (VSMCs) that cover the ECs as well as form the middle layer, and the fibroblasts and matrix that form the vessels' outer layer [211, 212]. These layers of cells play a vital role in repairing, remodeling, and maintaining the blood vessels following an injury. Lack of vascularization is still a major issue for successful tissue engineering therapies. The formation of new blood capillaries is essential to alleviate the symptoms by supplying the necessary nutrients and oxygen to and removing waste products from cells. To date, there are different strategies are under investigation in order to develop a functional blood vessel. These strategies are mainly classified as tissue-engineered cell-seeded scaffolds or bioactive, cell-free approaches.

Tissue-engineered cell-seeded scaffolds have been intensively studied in order to replace a vein or artery. Thus, many functional materials have been developed including synthetic and natural biomaterials [212, 213]. One approach to generate the functional implants is the culture of cell-seeded scaffolds under defined and highly physiological conditions in a bioreactor system prior to implantation [214, 215]. One of these is the generation of native ECM sheets produced by smooth muscle cells (SMCs) from another species [216] or from human induced-pluripotent stem cell-derived SMCs [215]. After the engineered vessels are decellularized, the grafts are seeded with endothelial cells of the graft recipient. However, when aiming to generate a graft for bypass surgery, it takes a rather long time to produce autologous tissue-engineered implants.

Another focus on regeneration of blood vessels is scaffold functionalization with chemokines and growth factors. Angiogenic growth factors are major cues of vascularization [217]. In particular, VEGF stimulates cells to produce matrix metalloproteinases and enhances the proliferation and migration of ECs toward the interstitium to sprout new vascular networks [218]. Thus, angiogenic matrixes have been developed to deliver locally angiogenic growth factors or their encoding DNA. For example, dextran sulfate and chitosan polyelectrolyte complexes loaded with VEGF are embedded into tissue engineering scaffolds. The encapsulation of

VEGF enhances its efficiency by protection and controlled release from the scaffolds, sustaining cell infiltration and organization and stimulating blood vessel formation [219]. However, it is a major challenge for the growth factors-loaded scaffolds in terms of controllable release and bioactivity preservation for a longer period of time [220]. Thus, scaffolds carrying DNA-encoding angiogenesis factors represent an alternative, which act as bioreactors for the local production of tissue-inductive factors [221]. Mao et al. fabricated a collagen scaffold containing plasmid DNA encoding VEGF, which show faster angiogenesis in the in vivo experiments [222]. Although certain genes can be introduced into vascular cells to enhance their survival and proliferation, the manipulation may elicit the oncogenic worry. Previous works reported that long-lasting blood vessels can be formed in mice by co-implantation of human umbilical vein endothelial cells (HUVECs) and 10T1/2 mesenchymal precursor cells in a three-dimensional fibronectin type I collagen gel [223]. This method can bypass the need for risky genetic manipulation.

1.4.5 Cardiovascular Engineering

Cardiovascular diseases (CVDs) including coronary heart disease, rheumatic heart disease, congenital heart disease, myocardial infarction, and strokes are the leading cause of death in the world [224]. According to the estimation of the World Health Organization, the number of deaths shows an increase from 17.3 million in 2008 to 23.3 million by 2030 [225]. Various new therapies and risk-reducing strategies to prevent CVDs are performed to treat many patients suffering from these diseases. However, to date, there are no effective therapies to fully cure the CVDs because of an insufficient number of organ donors [226, 227]. The regenerative strategies such as cell-based therapies and scaffold-based therapies have a promising potential for recovering severe cardiovascular disease.

One focus in the field of regenerative medicine is the generation and development of functional biomaterials. These materials should be bioactive (e.g., releasing drugs, proteins, growth factors, and ECM components) and suitable mechanical functionality. Enormous efforts have been paid to generate and design biomaterials for cardiovascular tissue engineering (Fig. 1.13) [228, 229]. The biomimetic materials can mimic ECM architecture and provide potentially controllable in vivo-like microenvironments for cells [230]. Therefore, various biomimetic materials are developed for myocardial repair, cardiac patch generation, and heart valve tissue engineering [227, 228]. Hydrogels are commonly used in cardiovascular engineering, which can be made of PEG [231], chitosan [232, 233], fibrin [234], collagen [235], and alginate [236]. Kraehenbuehl et al. fabricated a PEG-vinyl sulfone hydrogel through Michael addition reaction in situ for cross-linking [237]. Loaded with cells and bioactive factors, these PEG-based hydrogels were used to preserve the contractile function of cardiomyocytes and resulted in decreased infarct sizes [237]. Electrospinning is another widely used method for creating fiber-containing and highly porous scaffolds in cardiovascular engineering application [238].

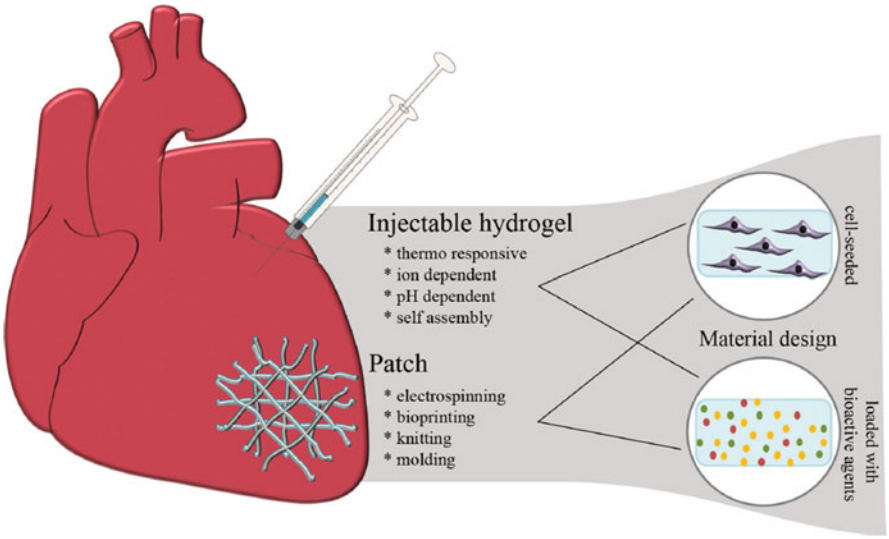

Fig. 1.13 Biomaterials for cardiac applications. Injectable hydrogels and/or cardiac patches are used as treatment options for cardiac damage. Both materials can either be cell-seeded or loaded with bioactive molecules such as RNA, small molecules, growth factors, or proteins (Reprinted from [228] with permission. Copyright 2013 Wiley)

Nanofibrous scaffolds of electrospun PCL exhibit comparable mechanical properties like the native myocardium [239] and have been shown to be beneficial for cardiac applications [240].

Another focus in the field of regenerative medicine is cell-based therapy, which has been clinically performed by the direct injection of dissociated cells [241]. This strategy avoids problems that may be related to synthetic materials, such as inflammation, stenosis, and infection, allowing for the complete graft integration and increase of the patency rate. The cell sources of cell therapy used for cardiovascular disease are mainly ESCs, induced pluripotent stem cells (iPSCs), and autologous cells [224, 227, 228]. ESCs and iPSCs are attractive for cardiovascular disease due to their ability to differentiate into beating cardiomyocytes easily by some certain methods [242, 243], while other human stem and progenitor cells can hardly do [228]. Autologous cells such as bone marrow- and peripheral blood-derived cells are under clinical trials for cardiovascular disease [244]. Although various cell injection therapies are now clinically performed and some therapies cause modest therapeutic effects, the efficacies are found to be unable to reach the level as clinicians expected [245–248]. Furthermore, it is a big issue for the cell injection therapy in terms of cell retention in the target tissue, since the injected cells are largely washed out or died [249, 250].

Some studies are focused on fabrication of completely biological tissue-engineered vascular grafts without the use of scaffolds. Thus, the cell-sheet-based technology have been developed, which consists of the in vitro growing of cells in

the culture medium containing ascorbic acid to generate a large production of ECM [251]. After a certain maturation period of time, the cell sheets are detached from the culture flasks using various technologies [252, 253]. For example, the cell sheet engineering using a unique temperature-responsive culture surface, which is covalently grafted with a temperature-responsive polymers such as poly(N-isopropylacrylamide) (PNIPAm), has been originally developed [252–255]. Three-dimensional tissues can be easily prepared by layering cell sheets, and the cells within sheets can be effectively delivered without cell loss due to the ability to preserve their own ECM [252, 253]. Kondoh et al. observed that the transplantation of skeletal myoblast cell sheets improves the cardiac performance and prolongs the life span of animals significantly, associating with the reorganization of the cytoskeletal proteins of host cardiac tissue and the reduction of myocardial fibrosis [256].

The use of bioreactors is advantageous when generating a tissue-engineered heart valve in vitro, which mimics the biophysical signals (e.g., various forces such as strain, pressure, torsion, or flow in tissues) presenting in the native organophysiological environment [224, 228]. For instance, the additional pulsatile flow bioreactor in a porous scaffold improves ECM production by vascular cells [257]. The pulsatile flow bioreactor also shows an increased collagen and elastin production and a significantly improved recellularization of the heart valve [258, 259].

References

1. Suh H. Tissue restoration, tissue engineering and regenerative medicine. Yonsei Med J. 2000;41:681.
2. Li Q, Ma L, Gao CY. Biomaterials for in situ tissue regeneration: development and perspectives. J Mater Chem B. 2015;3:8921.
3. Badylak SF, Nerem RM. Progress in tissue engineering and regenerative medicine. Proc Natl Acad Sci U S A. 2010;107:3285.
4. Langer R, Vacanti JP. Tissue engineering. Science. 1993;260:920.
5. Marston WA. A bioengineered human dermal equivalent for the treatment of chronic non-healing diabetic foot ulcer. Expert Rev Med Device. 2014;1:21.
6. Langer R. Perspectives and challenges in tissue engineering and regenerative medicine. Adv Mater. 2009;21:3235.
7. Ko IK, Lee SJ, Atala A, Yoo JJ. In situ tissue regeneration through host stem cell recruitment. Exp Mol Med. 2012;45:e57.
8. Shen Y, Dai L, Li X, Liang R, Guan G, Zhang Z, et al. Epidermal stem cells cultured on collagen-modified chitin membrane induce in situ tissue regeneration of full-thickness skin defects in mice. Plos One. 2014;9:e87557.
9. Hollister SJ. Porous scaffold design for tissue engineering. Nat Mater. 2005;4:518.
10. Slaughter BV, Khurshid SS, Fisher OZ, Khademhosseini A, Peppas NA. Hydrogels in regenerative medicine. Adv Mater. 2009;21:3307.
11. Chen B, Jones RR, Mi S, Foster J, Alcock SG, Hamley IW, et al. The mechanical properties of amniotic membrane influence its effect as a biomaterial for ocular surface repair. Soft Matter. 2012;8:8379.
12. Nakamura T. Regeneration of peripheral nerve on PGA-C tube and in situ tissue engineering. J Clin Anesth. 2013;33:507.

13. Wei G, Jin Q, Giannobile WV, Ma PX. The enhancement of osteogenesis by nano-fibrous scaffolds incorporating rhBMP-7 nanospheres. Biomaterials. 2007;28:2087.
14. Lei N, Dong C, Suo J, Peng Z, Feng S, Qi Y, et al. Physicochemical characterization and biocompatibility in vitro of biphasic calcium phosphate/polyvinyl alcohol scaffolds prepared by freeze-drying method for bone tissue engineering applications. Colloid Surf. 2012;B100:169.
15. Ji C, Annabi N, Hosseinkhani M, Sivaloganathan S, Dehghani F. Fabrication of poly-DL-lactide/polyethylene glycol scaffolds using the gas foaming technique, bioactive electrospun scaffolds delivering growth factors and genes for tissue engineering applications. Acta Biomater. 2012;8:570.
16. Ji W, Sun Y, Yang F, van den Beucken JJJP, Fan M, Chen Z, et al. Bioactive electrospun scaffolds delivering growth factors and genes for tissue engineering applications. Pharm Res. 2011;28:1259.
17. Mano JF. Designing biomaterials for tissue engineering based on the deconstruction of the native cellular environment. Mater Lett. 2015;141:198–202.
18. Kawaguchi Y, Huang CY, Wu YR, Yan Q, Pan CC, Zhao Y, et al. Influence of polarity on carrier transport in semipolar (2021xAF) and (202xAF1) multiple-quantum-well light-emitting diodes. Appl Phys Lett. 2012;100:231110.
19. Pérez RA, Won JE, Knowles JC, Kim HW. Naturally and synthetic smart composite biomaterials for tissue regeneration. Adv Drug Deliv Rev. 2013;65:471.
20. Liu X, Ma L, Mao Z, Gao C. Chitosan-based biomaterials for tissue repair and regeneration. Adv Polym Sci. 2011;244:81.
21. Maekawa T. Polymeric scaffolds in tissue engineering application: a review. Int J Polym Sci. 2011;2011:609.
22. Sowmya S, Bumgardener JD, Chennazhi KP, Nair SV, Jayakumar R. Role of nanostructured biopolymers and bioceramics in enamel, dentin and periodontal tissue regeneration. Prog Polym Sci. 2013;38:1748.
23. Zhang W, Xu B, Zhang Y, Luo Y. Evaluation of extracellular matrix-based nerve conduits for long-gap peripheral nerve repair in a goat model. J Biomater Tissue Eng. 2014;4:1063.
24. Engler AJ, Sen S, Sweeney HL, Discher DE. Matrix elasticity directs stem cell lineage specification. Cell. 2006;126:677.
25. Benoit DS, Schwartz MP, Durney AR, Anseth KS. Small functional groups for controlled differentiation of hydrogel-encapsulated human mesenchymal stem cells. Nat Mater. 2008;7:816.
26. Kasemo B. Biological surface science. Surf Sci. 2002;500:656.
27. Redey SA, Nardin M. Behavior of human osteoblastic cells on stoichiometric hydroxyapatite and type A carbonate apatite: role of surface energy. J Biomed Mater Res. 2000;50:353.
28. Mei Y, Saha K, Bogatyrev SR, Yang J, Hook AL, Kalcioglu ZI, et al. Combinatorial development of biomaterials for clonal growth of human pluripotent stem cells. Nat Mater. 2010;9:768.
29. Brunette D, Chehroudi B. The effects of the surface topography of micromachined titanium substrata on cell behavior in vitro and in vivo. J Biomech Eng. 1999;121:49.
30. Fuchs E, Tumbar T, Guasch G. Socializing with the neighbors: stem cells and their niche. Cell. 2004;116:769.
31. Wilson CJ, Clegg RE, Leavesley DI, Pearcy MJ. Mediation of biomaterial-cell interactions by adsorbed proteins: a review. Tissue Eng. 2005;11:1.
32. Ratner BD. The blood compatibility catastrophe. J Biomed Mater Res. 1993;27:283.
33. Mazzucotelli J, Klein-Soyer C, Beretz A, Brisson C, Archipoff G, Cazenave J. Endothelial cell seeding: coating Dacron and expanded polytetrafluoroethylene vascular grafts with a biological glue allows adhesion and growth of human saphenous vein endothelial cells. Int J Artif Organs. 1991;14:482.
34. Watt FM, Driskell RR. The therapeutic potential of stem cells. Philos Trans R Soc B. 2010;365:155.

35. Lane SW, Williams DA, Watt FM. Modulating the stem cell niche for tissue regeneration. Nat Biotechnol. 2014;32:795.
36. Bianco P, Robey PG. Stem cells in tissue engineering. Nature. 2001;414:118.
37. Watt FM, Huck WT. Role of the extracellular matrix in regulating stem cell fate. Nat Rev Mol Cell Biol. 2013;14:467.
38. Hall PA, Watt FM. Stem cells: the generation and maintenance of cellular diversity. Development. 1989;106:619.
39. Williams CK, Segarra M, Sierra MDLL, Sainson RC, Tosato G, Harris AL. Regulation of CXCR4 by the Notch ligand delta-like 4 in endothelial cells. Cancer Res. 2008;68:1889.
40. Lu B, Atala A. Small molecules and small molecule drugs in regenerative medicine. Drug Discov Today. 2014;19:801.
41. Lampe KJ, Heilshorn SC. Building stem cell niches from the molecule up through engineered peptide materials. Neurosci Lett. 2012;519:138.
42. Lee JS, Go DH, Bae JW, Lee SJ, Park KD. Heparin conjugated polymeric micelle for long-term delivery of basic fibroblast growth factor. J Control Release. 2007;117:204.
43. Discher DE, Eisenberg A. Polymer vesicles. Science. 2002;297:967.
44. Jiang Y, Chen J, Deng C, Suuronen EJ, Zhong Z. Click hydrogels, microgels and nanogels: emerging platforms for drug delivery and tissue engineering. Biomaterials. 2014;35:4969.
45. Choi DH, Park CH, Kim IH, Chun HJ, Park K, Han DK. Fabrication of core–shell microcapsules using PLGA and alginate for dual growth factor delivery system. J Control Release. 2010;147:193.
46. Wang W, Li B, Li Y, Jiang Y, Ouyang H, Gao C. In vivo restoration of full-thickness cartilage defects by poly(lactide-co-glycolide) sponges filled with fibrin gel, bone marrow mesenchymal stem cells and DNA complexes. Biomaterials. 2010;31:5953.
47. Wang W, Li B, Yang J, Xin L, Li Y, Yin H, Qi Y, Jiang Y, Ouyang H, Gao C. The restoration of full-thickness cartilage defects with BMSCs and TGF-beta 1 loaded PLGA/fibrin gel constructs. Biomaterials. 2010;31:8964.
48. Koutsopoulos S, Unsworth LD, Nagai Y, Zhang S. Controlled release of functional proteins through designer self-assembling peptide nanofiber hydrogel scaffold. Proc Natl Acad Sci U S A. 2009;106:4623.
49. Nugroho RWN, Odelius K, Höglund A, Albertsson AC. Highlighting the importance of surface grafting in combination with a layer-by-layer approach for fabricating advanced 3D poly(L-lactide) microsphere scaffolds. Chem Mater. 2016;28:3298.
50. Lee H, Yang S, Kim S, Kim GH. A scaffold with a bio-mimetically designed micro/nanofibrous structure using decellularized extracellular matrix. RSC Adv. 2016;6:29697.
51. Wei G, Ma PX. Structure and properties of nano-hydroxyapatite/polymer composite scaffolds for bone tissue engineering. Biomaterials. 2004;25:4749.
52. Loh QL, Choong C. Three-dimensional scaffolds for tissue engineering applications: role of porosity and pore size. Tissue Eng Part B Rev. 2013;19:485.
53. Ma T, Li Y, Yang ST, Kniss DA. Effects of pore size in 3-D fibrous matrix on human trophoblast tissue development. Biotechnol Bioeng. 2000;70:606.
54. Ikeda R, Fujioka H, Nagura I, Kokubu T, Toyokawa N, Inui A, et al. The effect of porosity and mechanical property of a synthetic polymer scaffold on repair of osteochondral defects. Int Orthop. 2009;33:821.
55. Liu Y, Ma L, Gao C. Facile fabrication of the glutaraldehyde cross-linked collagen/chitosan porous scaffold for skin tissue engineering. Mater Sci Eng C. 2012;32:2361.
56. Lee SB, Kim YH, Chong MS, Hong SH, Lee YM. Study of gelatin-containing artificial skin V: fabrication of gelatin scaffolds using a salt-leaching method. Biomaterials. 2005;26:1961.
57. Wang M, Ma L, Li D, Jiang P, Gao C. Preparation of polycaprolactone microspheres-aggregated scaffold with ultra big pores and fuzzy sphere surface by a one-step phase separation method. J Biomed Mater Res A. 2013;101:3219.
58. Wu X, Liu Y, Li X, Wen P, Zhang Y, Long Y, et al. Preparation of aligned porous gelatin scaffolds by unidirectional freeze-drying method. Acta Biomater. 2010;6:1167.

59. Zhu X, Cui W, Li X, Jin Y. Electrospun fibrous mats with high porosity as potential scaffolds for skin tissue engineering. Biomacromolecules. 2008;9:1795.
60. Yeong W, Sudarmadji N, Yu H, Chua C, Leong K, Venkatraman S, et al. Porous polycaprolactone scaffold for cardiac tissue engineering fabricated by selective laser sintering. Acta Biomater. 2010;6:2028.
61. Cox SC, Thornby JA, Gibbons GJ, Williams MA, Mallick KK. 3D printing of porous hydroxyapatite scaffolds intended for use in bone tissue engineering applications. Mater Sci Eng C. 2015;47:237.
62. Dhandayuthapani B, Yoshida Y, Maekawa T, Kumar DS. Polymeric scaffolds in tissue engineering application: a review. Int J Polym Sci. 2011;2011:2011.
63. Wichterle O, Lim D. Hydrophilic gels for biological use. Nature. 1960;185:117.
64. Van Vlierberghe S, Dubruel P, Schacht E. Biopolymer-based hydrogels as scaffolds for tissue engineering applications: a review. Biomacromolecules. 2011;12:1387.
65. Peppas N, Bures P, Leobandung W, Ichikawa H. Hydrogels in pharmaceutical formulations. Eur J Pharm Biopharm. 2000;50:27.
66. Hoffman AS. Hydrogels for biomedical applications. Adv Drug Deliv Rev. 2012;64:18.
67. Mahoney MJ, Anseth KS. Three-dimensional growth and function of neural tissue in degradable polyethylene glycol hydrogels. Biomaterials. 2006;27:2265.
68. Clapper JD, Pearce ME, Guymon CA, Salem AK. Biotinylated biodegradable nanotemplated hydrogel networks for cell interactive applications. Biomacromolecules. 2008;9:1188.
69. DeLong SA, Moon JJ, West JL. Covalently immobilized gradients of bFGF on hydrogel scaffolds for directed cell migration. Biomaterials. 2005;26:3227.
70. Anjum F, Lienemann PS, Metzger S, Biernaskie J, Kallos MS, Ehrbar M. Enzyme responsive GAG-based natural-synthetic hybrid hydrogel for tunable growth factor delivery and stem cell differentiation. Biomaterials. 2016;87:104.
71. Mosiewicz KA, Kolb L, van der Vlies AJ, Martino MM, Lienemann PS, Hubbell JA, et al. In situ cell manipulation through enzymatic hydrogel photopatterning. Nat Mater. 2013;12:1072.
72. Wegst UG, Bai H, Saiz E, Tomsia AP, Ritchie RO. Bioinspired structural materials. Nat Mater. 2015;14:23.
73. Singh M, Sandhu B, Scurto A, Berkland C, Detamore MS. Microsphere-based scaffolds for cartilage tissue engineering: using subcritical CO_2 as a sintering agent. Acta Biomater. 2010;6:137.
74. Lin K, Xia L, Gan J, Zhang Z, Chen H, Jiang X, et al. Tailoring the nanostructured surfaces of hydroxyapatite bioceramics to promote protein adsorption, osteoblast growth, and osteogenic differentiation. ACS Appl Mater Interf. 2013;5:8008.
75. Schnepp ZA, Gonzalez-McQuire R, Mann S. Hybrid biocomposites based on calcium phosphate mineralization of self-assembled supramolecular hydrogels. Adv Mater. 2006;18:1869.
76. Watanabe J, Akashi M. Novel biomineralization for hydrogels: electrophoresis approach accelerates hydroxyapatite formation in hydrogels. Biomacromolecules. 2006;7:3008.
77. Kato T. Polymer/calcium carbonate layered thin-film composites. Adv Mater. 2000;12:1543.
78. Li YQ, Yu T, Yang TY, Zheng LX, Liao K. Bio-inspired nacre-like composite films based on graphene with superior mechanical, electrical, and biocompatible properties. Adv Mater. 2012;24:3426.
79. Hartgerink JD, Beniash E, Stupp SI. Self-assembly and mineralization of peptide-amphiphile nanofibers. Science. 2001;294:1684.
80. Chen L, Ballarini R, Kahn H, Heuer A. Bioinspired micro-composite structure. J Mater Res. 2007;22:124.
81. Deville S, Saiz E, Nalla RK, Tomsia AP. Freezing as a path to build complex composites. Science. 2006;311:515.
82. Lewis JA. Direct ink writing of 3D functional materials. Adv Funct Mater. 2006;16:2193.
83. Pham TA, Kim DP, Lim TW, Park SH, Yang DY, Lee KS. Three-dimensional SiCN ceramic microstructures via nano-stereolithography of inorganic polymer photoresists. Adv Funct Mater. 2006;16:1235.

84. Ortiz C, Boyce MC. Bioinspired structural materials. Science. 2008;319:1053.
85. Yao X, Peng R, Ding J. Cell-material interactions revealed via material techniques of surface patterning. Adv Mater. 2013;25:5257.
86. Hinderliter A, Almeida PF, Creutz CE, Biltonen RL. Domain formation in a fluid mixed lipid bilayer modulated through binding of the C2 protein motif. Biochemistry. 2001;40:4181.
87. Hinderliter A, Biltonen RL, Almeida PF. Lipid modulation of protein-induced membrane domains as a mechanism for controlling signal transduction. Biochemistry. 2004;43:7102.
88. Horbett TA, Brash JL. Proteins at interfaces II, ACS symposium series. 1995. p. 548.
89. Vogel V, Baneyx G. The tissue engineering puzzle: a molecular perspective. Annu Rev Biomed Eng. 2003;5:441.
90. Walker RK, Krishnaswamy S. The activation of prothrombin by the prothrombinase complex. The contribution of the substrate-membrane interaction to catalysis. J Biol Chem. 1994;269:27441.
91. Malmsten M, Muller D, Lassen B. Sequential adsorption of human serum albumin (HSA), immunoglobulin G (IgG), and fibrinogen (Fgn) at HMDSO plasma polymer surfaces. J Colliod Interf Sci. 1997;193:88.
92. Rabe M, Verdes D, Seeger S. Understanding protein adsorption phenomena at solid surfaces. Adv Colloid Interf. 2011;162:87.
93. Vogler EA. Protein adsorption in three dimensions. Biomaterials. 2012;33:1201.
94. Means GE, Ampon K. Protein immobilization by adsorption of a hydrophobic amidine protein derivative to a hydrophobic surface, US. 1989.
95. Aramesh M, Shimoni O, Ostrikov K, Prawer S, Cervenka J. Surface charge effects in protein adsorption on nanodiamonds. Nanoscale. 2015;7:5726.
96. Hlady V, Buijs J. Protein adsorption on solid surfaces. Curr Opin Biotechnol. 1996;7:72–7.
97. Hollmann O, Steitz R, Czeslik C. Structure and dynamics of α-lactalbumin adsorbed at a charged brush interface. Phys Chem Phys. 2008;10:1448.
98. Miron RJ, Bosshardt D, Hedbom E, Zhang Y, Haenni B, Buser D, et al. Adsorption of enamel matrix proteins to a bovine-derived bone grafting material and its regulation of cell adhesion, proliferation, and differentiation. J Periodontol. 2012;83:936.
99. Sun M, Deng J, Tang Z, Wu J, Li D, Chen H, et al. A correlation study of protein adsorption and cell behaviors on substrates with different densities of PEG chains. Colloid Surf B. 2014;122:134.
100. Deng J, Sun M, Wang S, Han L, Mao Z, Li D, et al. Adsorption of fibronectin on salt-etched polyelectrolyte multilayers and its roles in mediating the adhesion and migration of vascular smooth muscle cells. Macromol Biosci. 2015;15:241.
101. Sun M, Deng J, Gao C. The correlation between fibronectin adsorption and attachment of vascular cells on heparinized polycaprolactone membrane. J Colloid Interf Sci. 2015;448:231.
102. Saranya N, Saravanan S, Moorthi A, Ramyakrishna B, Selvamurugan N. Enhanced osteoblast adhesion on polymeric nano-scaffolds for bone tissue engineering. J Biomed Nanotechnol. 2011;7:238.
103. Deng J, Ren T, Zhu J, Mao Z, Gao C. Adsorption of plasma proteins and fibronectin on poly (hydroxylethyl methacrylate) brushes of different thickness and their relationship with adhesion and migration of vascular smooth muscle cells. Regen Biomater. 2014;1:17.
104. Zheng W, Zhang W, Jiang X. Precise control of cell adhesion by combination of surface chemistry and soft lithography. Adv Healthc Mater. 2013;2:95.
105. Brandl F, Sommer F, Goepferich A. Rational design of hydrogels for tissue engineering: impact of physical factors on cell behavior. Biomaterials. 2007;28:134.
106. Le Moullac G, Haffner P. Environmental factors affecting immune responses in Crustacea. Aquaculture. 2000;191:121.
107. Thiery JP, Duband JL, Tucker GC. Cell migration in the vertebrate embryo: role of cell adhesion and tissue environment in pattern formation. Annu Rev Cell Biol. 1985;1:91.
108. Humphries MJ, Akiyama SK, Komoriya A, Olden K, Yamada KM. Identification of an alternatively spliced site in human plasma fibronectin that mediates cell type-specific adhesion. J Cell Biol. 1986;103:2637.

109. Knittel T, Aurisch S, Neubauer K, Eichhorst S, Ramadori G. Cell-type-specific expression of neural cell adhesion molecule (N-CAM) in Ito cells of rat liver. Up-regulation during in vitro activation and in hepatic tissue repair. Am J Pathol. 1996;149:449.
110. Gunawan RC, Silvestre J, Gaskins HR, Kenis PJ, Leckband DE. Cell migration and polarity on microfabricated gradients of extracellular matrix proteins. Langmuir. 2006;22:4250.
111. Martin P. Wound healing – aiming for perfect skin regeneration. Science. 1997;276:75.
112. Lin S, Sangaj N, Razafiarison T, Zhang C, Varghese S. Influence of physical properties of biomaterials on cellular behavior. Pharm Res. 2011;28:1422.
113. Oh SH, Kim TH, Lee JH. Creating growth factor gradients in three dimensional porous matrix by centrifugation and surface immobilization. Biomaterials. 2011;32:8254.
114. Wu J, Mao Z, Tan H, Han L, Ren T, Gao C. Gradient biomaterials and their influences on cell migration. Interf Focus. 2012;2:337.
115. Shin YN, Kim BS, Ahn HH, Lee JH. Adhesion comparison of human bone marrow stem cells on a gradient wettable surface prepared by corona treatment. Appl Surf Sci. 2008;255:293.
116. Gijsman P, Meijers G, Vitarelli G. Comparison of the UV-degradation chemistry of polypropylene, polyethylene, polyamide 6 and polybutylene terephthalate. Polym Degrad Stab. 1999;65:433.
117. Li B, Ma Y, Wang S, Moran PM. A technique for preparing protein gradients on polymeric surfaces: effects on PC12 pheochromocytoma cells. Biomaterials. 2005;26:1487.
118. Whittle JD. A method for the deposition of controllable chemical gradients. Chem Commun. 2003;14:1766.
119. Spijker HT, Bos R, Oeveren WV, Vries JD, Busscher HJ. Protein adsorption on gradient surfaces on polyethylene prepared in a shielded gas plasma. Colloid Surf B. 1999;15:89.
120. Zhu Y, Gao C, He T, Shen J. Immobilization of biomacromolecules onto aminolyzed poly(L-lactic acid) toward acceleration of endothelium regeneration. Tissue Eng. 2004;10:53.
121. Zhu Y, Gao C, He T, Shen J. Endothelium regeneration on luminal surface of polyurethane vascular scaffold modified with diamine and covalently grafted with gelatin. Biomaterials. 2004;25:423.
122. Han L, Mao Z, Wu J, Guo Y, Ren T, Gao C. Directional cell migration through cell–cell interaction on polyelectrolyte multilayers with swelling gradients. Biomaterials. 2013;34:975.
123. Xi Y, Zhiqiang W, Yugui J, Xi Z. Surface gradient material: from superhydrophobicity to superhydrophilicity. Langmuir. 2006;22:4483.
124. Li LH, Zhu Y, Li B, Gao C. Fabrication of thermoresponsive polymer gradients for study of cell adhesion and detachment. Langmuir. 2008;24:13632.
125. Morgenthaler S, Lee S, Stefan Zürcher A, Spencer ND. A simple, reproducible approach to the preparation of surface-chemical gradients. Langmuir. 2003;19:10459.
126. Ren T, Mao Z, Guo J, Gao C. Directional migration of vascular smooth muscle cells guided by a molecule weight gradient of poly (2-hydroxyethyl methacrylate) brushes. Langmuir. 2013;29:6386.
127. Woodfield T, Blitterswijk CV, Wijn JD, Sims T, Hollander A, Riesle J. Polymer scaffolds fabricated with pore-size gradients as a model for studying the zonal organization within tissue-engineered cartilage constructs. Tissue Eng. 2005;11:1297.
128. Oh SH, Park IK, Kim JM, Lee JH. In vitro and in vivo characteristics of PCL scaffolds with pore size gradient fabricated by a centrifugation method. Biomaterials. 2007;28:1664.
129. Hong WK, Long LY, Bin Z, Chao ZH. Cellular therapy and myocardial tissue engineering: the role of adult stem and progenitor cells. Eur J Cardio-Thorac. 2006;30:770.
130. Wertheim JA, Baptista PM, Alejandro SG. Cellular therapy and bioartificial approaches to liver replacement. Curr Opin Organ Transplant. 2012;17:235.
131. Wei X, Yang X, Han Z, Qu F, Shao L, Shi Y. Mesenchymal stem cells: a new trend for cell therapy. Acta Pharmacol Sin. 2013;34:747.
132. Robinton DA, Daley GQ. The promise of induced pluripotent stem cells in research and therapy. Nature. 2012;481:295.

133. Trappmann B, Gautrot JE, Connelly JT, Strange DG, Li Y, Oyen ML, et al. Extracellular-matrix tethering regulates stem-cell fate. Nat Mater. 2012;11:642.
134. Dalby MJ, Gadegaard N, Oreffo RO. Harnessing nanotopography and integrin-matrix interactions to influence stem cell fate. Nat Mater. 2014;13:558.
135. Lee J, Abdeen AA, Zhang D, Kilian KA. Directing stem cell fate on hydrogel substrates by controlling cell geometry, matrix mechanics and adhesion ligand composition. Biomaterials. 2013;34:8140.
136. Khetan S, Guvendiren M, Legant WR, Cohen DM, Chen CS, Burdick JA. Degradation-mediated cellular traction directs stem cell fate in covalently cross-linked three-dimensional hydrogels. Nat Mater. 2013;12:458.
137. Uccelli A, Moretta L, Pistoia V. Mesenchymal stem cells in health and disease. Nat Rev Immunol. 2008;8:726.
138. Guilak F, Cohen DM, Estes BT, Gimble JM, Liedtke W, Chen CS. Control of stem cell fate by physical interactions with the extracellular matrix. Cell Stem Cell. 2009;5:17.
139. Rowlands AS, George PA, Cooper-White JJ. Directing osteogenic and myogenic differentiation of MSCs: interplay of stiffness and adhesive ligand presentation. Am J Physiol Cell Physiol. 2008;295:C1037.
140. Banerjee A, Arha M, Choudhary S, Ashton RS, Bhatia SR, Schaffer DV, et al. The influence of hydrogel modulus on the proliferation and differentiation of encapsulated neural stem cells. Biomaterials. 2009;30:4695.
141. Winer JP, Janmey PA, McCormick ME, Funaki M. Bone marrow-derived human mesenchymal stem cells become quiescent on soft substrates but remain responsive to chemical or mechanical stimuli. Tissue Eng Part A. 2008;15:147.
142. Chowdhury F, Na S, Li D, Poh Y-C, Tanaka TS, Wang F, et al. Material properties of the cell dictate stress-induced spreading and differentiation in embryonic stem cells. Nat Mater. 2010;9:82.
143. Li L, Davidovich AE, Schloss JM, Chippada U, Schloss RR, Langrana NA, et al. Neural lineage differentiation of embryonic stem cells within alginate microbeads. Biomaterials. 2011;32:4489.
144. Pek YS, Wan AC, Ying JY. The effect of matrix stiffness on mesenchymal stem cell differentiation in a 3D thixotropic gel. Biomaterials. 2010;31:385.
145. Saha K, Keung AJ, Irwin EF, Li Y, Little L, Schaffer DV, et al. Substrate modulus directs neural stem cell behavior. Biophys J. 2008;95:4426.
146. Lanniel M, Huq E, Allen S, Buttery L, Williams PM, Alexander MR. Substrate induced differentiation of human mesenchymal stem cells on hydrogels with modified surface chemistry and controlled modulus. Soft Matter. 2011;7:6501.
147. Reilly GC, Engler AJ. Intrinsic extracellular matrix properties regulate stem cell differentiation. J Biomech. 2010;43:55.
148. Stevens MM, George JH. Exploring and engineering the cell surface interface. Science. 2005;310:1135.
149. Brizzi MF, Tarone G, Defilippi P. Extracellular matrix, integrins, and growth factors as tailors of the stem cell niche. Curr Opin Cell Biol. 2012;24:645.
150. Li W, Li K, Wei W, Ding S. Chemical approaches to stem cell biology and therapeutics. Cell Stem Cell. 2013;13:270.
151. Li W, Jiang K, Ding S. Concise review: a chemical approach to control cell fate and function. Stem Cells. 2012;30:61.
152. Rippon HJ, Polak JM, Qin M, Bishop AE. Derivation of distal lung epithelial progenitors from murine embryonic stem cells using a novel three-step differentiation protocol. Stem Cells. 2006;24:1389.
153. Nakanishi M, Hamazaki TS, Komazaki S, Okochi H, Asashima M. Pancreatic tissue formation from murine embryonic stem cells in vitro. Differentiation. 2007;75:1.
154. Pittenger MF, Mackay AM, Beck SC, Jaiswal RK, Douglas R, Mosca JD, et al. Multilineage potential of adult human mesenchymal stem cells. Science. 1999;284:143.

155. Zhu Y, Mao Z, Gao C. Control over the gradient differentiation of rat BMSCs on a PCL membrane with surface-immobilized alendronate gradient. Biomacromolecules. 2013;14:342.
156. Fu L, Tang T, Miao Y, Zhang S, Qu Z, Dai K. Stimulation of osteogenic differentiation and inhibition of adipogenic differentiation in bone marrow stromal cells by alendronate via ERK and JNK activation. Bone. 2008;43:40.
157. Kaur G, Valarmathi MT, Potts JD, Jabbari E, Sabo-Attwood T, Wang Q. Regulation of osteogenic differentiation of rat bone marrow stromal cells on 2D nanorod substrates. Biomaterials. 2010;31:1732.
158. Zhang Q, Tan K, Zhang Y, Ye Z, Tan W-S, Lang M. In situ controlled release of rhBMP-2 in gelatin-coated 3D porous poly(ε-caprolactone) scaffolds for homogeneous bone tissue formation. Biomacromolecules. 2013;15:84.
159. Jansen J, Vehof J, Ruhe P, Kroeze-Deutman H, Kuboki Y, Takita H, et al. Growth factor-loaded scaffolds for bone engineering. J Control Release. 2005;101:127.
160. Richardson TP, Peters MC, Ennett AB, Mooney DJ. Polymeric system for dual growth factor delivery. Nat Biotechnol. 2001;19:1029.
161. Carstens MH, Chin M, Li XJ. In situ osteogenesis: regeneration of 10-cm mandibular defect in porcine model using recombinant human bone morphogenetic protein-2 (rhBMP-2) and Helistat absorbable collagen sponge. J Craniofac Surg. 2005;16:1033.
162. Dawson E, Mapili G, Erickson K, Taqvi S, Roy K. Biomaterials for stem cell differentiation. Adv Drug Deliv Rev. 2008;60:215–28.
163. Yang F, Williams CG, Wang D-a, Lee H, Manson PN, Elisseeff J. The effect of incorporating RGD adhesive peptide in polyethylene glycol diacrylate hydrogel on osteogenesis of bone marrow stromal cells. Biomaterials. 2005;26:5991.
164. Jackson DW, Scheer MJ, Simon TM. Cartilage substitutes: overview of basic science and treatment options. J Am Acad Dermatol. 2001;9:37.
165. Levenberg S, Langer R. Advances in tissue engineering. Curr Top Dev Biol. 2004;61:113.
166. Vacanti CA. History of tissue engineering and a glimpse into its future. Tissue Eng. 2006;12:1137.
167. Helmick CG, Felson DT, Lawrence RC, Gabriel S, Hirsch R, Kwoh CK, et al. Estimates of the prevalence of arthritis and other rheumatic conditions in the United States. Arthritis Rheumatol. 2008;58:15.
168. Johnson K, Zhu S, Tremblay MS, Payette JN, Wang J, Bouchez LC, et al. A stem cell–based approach to cartilage repair. Science. 2012;336:717.
169. de Peppo GM, Marcos-Campos I, Kahler DJ, Alsalman D, Shang L, Vunjak-Novakovic G, et al. Engineering bone tissue substitutes from human induced pluripotent stem cells. Proc Natl Acad Sci U S A. 2013;110:8680.
170. Diekman BO, Christoforou N, Willard VP, Sun H, Sanchez-Adams J, Leong KW, et al. Cartilage tissue engineering using differentiated and purified induced pluripotent stem cells. Proc Natl Acad Sci U S A. 2012;109:19172.
171. Wei ST, Lee EH, Cao T. Potential of human embryonic stem cells in cartilage tissue engineering and regenerative medicine. Stem Cell Rev. 2011;7:544.
172. Tuan RS. Stemming cartilage degeneration: adult mesenchymal stem cells as a cell source for articular cartilage tissue engineering. Arthritis Rheumatol. 2006;54:3075.
173. Crawford DC, Heveran CM, Cannon WD, Li FF, Potter HG. An autologous cartilage tissue implant neocart for treatment of grade III chondral injury to the distal femur: prospective clinical safety trial at 2 years. Am J Sport Med. 2009;37:1334.
174. Gobbi A, Kon E, Berruto M, Francisco R, Filardo G, Marcacci M. Patellofemoral full-thickness chondral defects treated with hyalograft-C a clinical, arthroscopic, and histologic review. Am J Sport Med. 2006;34:1763.
175. Williams RJ, Gamradt SC. Articular cartilage repair using a resorbable matrix scaffold. Instr Course Lect. 2008;57:563–71.
176. Tuan RS, Chen AF, Klatt BA. Cartilage regeneration. J Am Acad Dermatol. 2013;21:303.
177. Shi Y, Ma L, Zhou J, Mao Z, Gao C. Collagen/chitosan-silicone membrane bilayer scaffold as a dermal equivalent. Polym Adv Technol. 2005;16:789.

178. Böttcher-Haberzeth S, Biedermann T, Reichmann E. Tissue engineering of skin. Burns. 2010;36:450.
179. Boyce ST. Design principles for composition and performance of cultured skin substitutes. Burns. 2001;27:523.
180. Ma L, Gao C, Mao Z, Zhou J, Shen J, Hu X, et al. Collagen/chitosan porous scaffolds with improved biostability for skin tissue engineering. Biomaterials. 2003;24:4833.
181. Dainiak MB, Allan IU, Savina IN, Cornelio L, James ES, James SL, et al. Gelatin–fibrinogen cryogel dermal matrices for wound repair: preparation, optimisation and in vitro study. Biomaterials. 2010;31:67.
182. Priya SG, Jungvid H, Kumar A. Skin tissue engineering for tissue repair and regeneration. Tissue Eng Part B Rev. 2008;14:105.
183. Dai N-T, Williamson M, Khammo N, Adams E, Coombes A. Composite cell support membranes based on collagen and polycaprolactone for tissue engineering of skin. Biomaterials. 2004;25:4263.
184. Chen G, Sato T, Ohgushi H, Ushida T, Tateishi T, Tanaka J. Culturing of skin fibroblasts in a thin PLGA–collagen hybrid mesh. Biomaterials. 2005;26:2559.
185. Naoshi Kinoshita MD, PhD MTM, Rodrigo Hamuy MD, PhD MNM, Nakamura-Kurashige T, Matsuu-Matsuyama M, et al. The usefulness of basic fibroblast growth factor for radiation-exposed tissue. Wound Repair Regen. 2012;20:91.
186. Rui G, Xu S, Ma L, Huang A, Gao C. Enhanced angiogenesis of gene-activated dermal equivalent for treatment of full thickness incisional wounds in a porcine model. Biomaterials. 2010;31:7308.
187. Li R, Liu Z, Pan Y, Chen L, Zhang Z, Lu L. Peripheral nerve injuries treatment: a systematic review. Cell Biochem Biophys. 2014;68:449–54.
188. Federici T, Boulis N. Gene therapy for peripheral nervous system diseases. Curr Gene Ther. 2007;7:239.
189. Kemp SW, Syed S, Walsh SK, Zochodne DW, Midha R. Collagen nerve conduits promote enhanced axonal regeneration, Schwann cell association, and neovascularization compared to silicone conduits. Tissue Eng Part A. 2009;15:1975.
190. Gu X, Ding F, Williams DF. Neural tissue engineering options for peripheral nerve regeneration. Biomaterials. 2014;35:6143.
191. Artico M, Cervoni L, Nucci F, Giuffré R. Birthday of peripheral nervous system surgery: the contribution of Gabriele Ferrara (1543–1627). Neurosurgery. 1996;39:380.
192. Battiston B, Papalia I, Tos P, Geuna S. Peripheral nerve repair and regeneration research: a historical note. Int Rev Neurobiol. 2009;87:1.
193. Tang S, Zhu J, Xu Y, Xiang AP, Mei HJ, Quan D. The effects of gradients of nerve growth factor immobilized PCLA scaffolds on neurite outgrowth in vitro and peripheral nerve regeneration in rats. Biomaterials. 2013;34:7086.
194. Zu A. Autologen nerventransplantaten, alternatives to autologous nerve grafts. Handchir Mikrochir Plast Chir. 2004;36:1.
195. Huang YC, Huang YY. Biomaterials and strategies for nerve regeneration. Artif Organs. 2006;30:514.
196. Yoshii S, Oka M. Collagen filaments as a scaffold for nerve regeneration. J Biomed Mater Res. 2001;56:400.
197. Khaing ZZ, Schmidt CE. Advances in natural biomaterials for nerve tissue repair. Neurosci Lett. 2012;519:103.
198. Meek MF, Coert JH. US food and drug administration/conformit Europe-approved absorbable nerve conduits for clinical repair of peripheral and cranial nerves. Ann Plast Surg. 2008;60:110.
199. Kehoe S, Zhang X, Boyd D. FDA approved guidance conduits and wraps for peripheral nerve injury: a review of materials and efficacy. Injury. 2012;43:553.
200. Spivey EC, Khaing ZZ, Shear JB, Schmidt CE. The fundamental role of subcellular topography in peripheral nerve repair therapies. Biomaterials. 2012;33:4264.

201. Wang HB, Mullins ME, Cregg JM, Hurtado A, Oudega M, Trombley MT, et al. Creation of highly aligned electrospun poly-L-lactic acid fibers for nerve regeneration applications. J Neural Eng. 2008;6:016001.
202. Syed N. Jullien G. Electrically stimulating nerve regeneration. 2006. Google Patents.
203. Lee JY, Bashur CA, Goldstein AS, Schmidt CE. Polypyrrole-coated electrospun PLGA nanofibers for neural tissue applications. Biomaterials. 2009;30:4325.
204. Xu H, Holzwarth JM, Yan Y, Xu P, Zheng H, Yin Y, et al. Conductive PPY/PDLLA conduit for peripheral nerve regeneration. Biomaterials. 2014;35:225.
205. Xing D, Ma L, Gao C. Synthesis of poly(ester-carbonate) with a pendant acetylcholine analog for promoting neurite growth. Acta Biomater. 2014;10:4127.
206. Xing D, Ma L, Gao C. Synthesis of functionalized poly(ester carbonate) with laminin-derived peptide for promoting neurite outgrowth of PC12 cells. Macromol Biosci. 2014;14:1429.
207. Callahan LAS, Xie S, Barker IA, Zheng J, Reneker DH, Dove AP, et al. Directed differentiation and neurite extension of mouse embryonic stem cell on aligned poly (lactide) nanofibers functionalized with YIGSR peptide. Biomaterials. 2013;34:9089.
208. Chung T-W, Yang M-C, Tseng C-C, Sheu S-H, Wang S-S, Huang Y-Y, et al. Promoting regeneration of peripheral nerves in-vivo using new PCL-NGF/Tirofiban nerve conduits. Biomaterials. 2011;32:734.
209. Frostick SP, Yin Q, Kemp GJ. Schwann cells, neurotrophic factors, and peripheral nerve regeneration. Microsurgery. 1998;18:397.
210. Lee JY, Bashur CA, Milroy CA, Forciniti L, Goldstein AS, Schmidt CE. Nerve growth factor-immobilized electrically conducting fibrous scaffolds for potential use in neural engineering applications. IEEE Trans Nanobioscience. 2012;11:15.
211. Vara DS, Salacinski HJ, Kannan RY, Bordenave L, Hamilton G, Seifalian AM. Cardiovascular tissue engineering: state of the art. Pathol Biol. 2005;53:599.
212. Nemeno-Guanzon JG, Lee S, Berg JR, Jo YH, Yeo JE, Nam BM, et al. Trends in tissue engineering for blood vessels. Biomed Res Int. 2012;2012:215.
213. He S, Xia T, Wang H, Wei L, Luo X, Li X. Multiple release of polyplexes of plasmids VEGF and bFGF from electrospun fibrous scaffolds towards regeneration of mature blood vessels. Acta Biomater. 2012;8:2659.
214. Quint C, Kondo Y, Manson RJ, Lawson JH, Dardik A, Niklason LE. Decellularized tissue-engineered blood vessel as an arterial conduit. Proc Natl Acad Sci U S A. 2011;108:9214.
215. Sundaram S, One J, Siewert J, Teodosescu S, Zhao L, Dimitrievska S, et al. Tissue-engineered vascular grafts created from human induced pluripotent stem cells. Stem Cell Transl Med. 2014;3:1535.
216. Quint C, Arief M, Muto A, Dardik A, Niklason LE. Allogeneic human tissue-engineered blood vessel. J Vasc Surg. 2012;55:790–8.
217. Banfi A, von Degenfeld G, Blau HM. Critical role of microenvironmental factors in angiogenesis. Curr Atheroscler Rep. 2005;7:227.
218. Hoeben A, Landuyt B, Highley MS, Wildiers H, Van Oosterom AT, De Bruijn EA. Vascular endothelial growth factor and angiogenesis. Pharmacol Rev. 2004;56:549.
219. Des Rieux A, Ucakar B, Mupendwa BPK, Colau D, Feron O, Carmeliet P, et al. 3D systems delivering VEGF to promote angiogenesis for tissue engineering. J Control Release. 2011;150:272.
220. Hadjiargyrou M, Chiu JB. Enhanced composite electrospun nanofiber scaffolds for use in drug delivery. Expert Opin Drug Deliv. 2008;5:1093.
221. Jang J-H, Shea LD. Controllable delivery of non-viral DNA from porous scaffolds. J Control Release. 2003;86:157.
222. Mao Z, Shi H, Guo R, Ma L, Gao C, Han C, et al. Enhanced angiogenesis of porous collagen scaffolds by incorporation of TMC/DNA complexes encoding vascular endothelial growth factor. Acta Biomater. 2009;5:2983.
223. Koike N, Fukumura D, Gralla O, Au P, Schechner JS, Jain RK. Tissue engineering: creation of long-lasting blood vessels. Nature. 2004;428:138.

224. Catto V, Farè S, Freddi G, Tanzi MC. Vascular tissue engineering: recent advances in small diameter blood vessel regeneration. ISRN Vasc Med. 2014;2014:923030.
225. Organization WH http://www.whoint/mediacentre/factsheets/fs317/en/index
226. Patra C, Boccaccini AR, Engel FB. Vascularisation for cardiac tissue engineering: the extracellular matrix. Thromb Haemost. 2015;113:532.
227. Haraguchi Y, Shimizu T, Yamato M, Okano T. Concise review: cell therapy and tissue engineering for cardiovascular disease. Stem Cell Transl Med. 2012;1:136.
228. Hinderer S, Brauchle E, Schenke-Layland K. Generation and assessment of functional biomaterial scaffolds for applications in cardiovascular tissue engineering and regenerative medicine. Adv Healthc Mater. 2015;4:2326.
229. Jaganathan SK, Supriyanto E, Murugesan S, Balaji A, Asokan MK. Biomaterials in cardiovascular research: applications and clinical implications. Biomed Res Int. 2014;2014:459465.
230. Kim TG, Shin H, Lim DW. Biomimetic scaffolds for tissue engineering. Adv Funct Mater. 2012;22:2446.
231. Habib M, Shapira-Schweitzer K, Caspi O, Gepstein A, Arbel G, Aronson D, et al. A combined cell therapy and in-situ tissue-engineering approach for myocardial repair. Biomaterials. 2011;32:7514.
232. Wang H, Shi J, Wang Y, Yin Y, Wang L, Liu J, et al. Promotion of cardiac differentiation of brown adipose derived stem cells by chitosan hydrogel for repair after myocardial infarction. Biomaterials. 2014;35:3986.
233. Liu Z, Wang H, Wang Y, Lin Q, Yao A, Cao F, et al. The influence of chitosan hydrogel on stem cell engraftment, survival and homing in the ischemic myocardial microenvironment. Biomaterials. 2012;33:3093.
234. Zhang X, Wang H, Ma X, Adila A, Wang B, Liu F, et al. Preservation of the cardiac function in infarcted rat hearts by the transplantation of adipose-derived stem cells with injectable fibrin scaffolds. Exp Biol Med. 2010;235:1505.
235. Parenteau-Bareil R, Gauvin R, Berthod F. Collagen-based biomaterials for tissue engineering applications. Materials. 2010;3:1863.
236. Leor J, Cohen S. Myocardial tissue engineering: creating a muscle patch for a wounded heart. Ann N Y Acad Sci. 2004;1015:312.
237. Kraehenbuehl TP, Zammaretti P, Van der Vlies AJ, Schoenmakers RG, Lutolf MP, Jaconi ME, et al. Three-dimensional extracellular matrix-directed cardioprogenitor differentiation: systematic modulation of a synthetic cell-responsive PEG-hydrogel. Biomaterials. 2008;29:2757.
238. Kumbar S, James R, Nukavarapu S, Laurencin C. Electrospun nanofiber scaffolds: engineering soft tissues. Biomed Mater. 2008;3:034002.
239. Ayaz HGŞ, Perets A, Ayaz H, Gilroy KD, Govindaraj M, Brookstein D, et al. Textile-templated electrospun anisotropic scaffolds for regenerative cardiac tissue engineering. Biomaterials. 2014;35:854.
240. Shin M, Ishii O, Sueda T, Vacanti J. Contractile cardiac grafts using a novel nanofibrous mesh. Biomaterials. 2004;25:3717.
241. Menasché P, Hagège AA, Scorsin M, Pouzet B, Desnos M, Duboc D, et al. Myoblast transplantation for heart failure. Lancet. 2001;357:279.
242. Takahashi K, Tanabe K, Ohnuki M, Narita M, Ichisaka T, Tomoda K, et al. Induction of pluripotent stem cells from adult human fibroblasts by defined factors. Cell. 2007;131:861.
243. Kehat I, Kenyagin-Karsenti D, Snir M, Segev H, Amit M, Gepstein A, et al. Human embryonic stem cells can differentiate into myocytes with structural and functional properties of cardiomyocytes. J Clin Invest. 2001;108:407.
244. Alaiti MA, Ishikawa M, Costa MA. Bone marrow and circulating stem/progenitor cells for regenerative cardiovascular therapy. Transl Res. 2010;156:112.
245. Soejitno A, Wihandani DM, Kuswardhani R. Clinical applications of stem cell therapy for regenerating the heart. Acta Med Indones. 2010;42:243.
246. Abdel-Latif A, Bolli R, Tleyjeh IM, Montori VM, Perin EC, Hornung CA, et al. Adult bone marrow–derived cells for cardiac repair: a systematic review and meta-analysis. Arch Intern Med. 2007;167:989.

247. Lipinski MJ, Biondi-Zoccai GG, Abbate A, Khianey R, Sheiban I, Bartunek J, et al. Impact of intracoronary cell therapy on left ventricular function in the setting of acute myocardial infarction: a collaborative systematic review and meta-analysis of controlled clinical trials. J Am Coll Cardiol. 2007;50:1761.
248. Martin-Rendon E, Brunskill SJ, Hyde CJ, Stanworth SJ, Mathur A, Watt SM. Autologous bone marrow stem cells to treat acute myocardial infarction: a systematic review. Eur Heart J. 2008;29:1807.
249. Zhang M, Methot D, Poppa V, Fujio Y, Walsh K, Murry CE. Cardiomyocyte grafting for cardiac repair: graft cell death and anti-death strategies. J Mol Cell Cardiol. 2001;33:907.
250. Hofmann M, Wollert KC, Meyer GP, Menke A, Arseniev L, Hertenstein B, et al. Monitoring of bone marrow cell homing into the infarcted human myocardium. Circulation. 2005;111:2198.
251. Peck M, Gebhart D, Dusserre N, Mcallister TN, L'Heureux N. The evolution of vascular tissue engineering and current state of the art. Cells Tissues Organs. 2011;195:144.
252. Masuda S, Shimizu T, Yamato M, Okano T. Cell sheet engineering for heart tissue repair. Methods Mol Biol. 2008;60:277.
253. Matsuda N, Shimizu T, Yamato M, Okano T. Tissue engineering based on cell sheet technology. Adv Mater. 2007;19:3089.
254. Yamada N, Okano T, Sakai H, Karikusa F, Sawasaki Y, Sakurai Y. Thermo-responsive polymeric surface: control of attachment and detachment of cultured cells. Makromo Chem Rapid Commun. 2003;11:571.
255. Okano T, Yamada N, Sakai H, Sakurai Y. A novel recovery system for cultured cells using plasma-treated polystyrene dishes grafted with poly(N-isopropylacrylamide). J Biomed Mater Res. 1993;27:1243.
256. Kondoh H, Sawa Y, Miyagawa S, Sakakida-Kitagawa S, Memon IA, Kawaguchi N, et al. Longer preservation of cardiac performance by sheet-shaped myoblast implantation in dilated cardiomyopathic hamsters. Cardiovasc Res. 2006;69:466.
257. Sodian R, Hoerstrup SP, Sperling JS, Daebritz SH, Martin DP, Schoen FJ, et al. Tissue engineering of heart valves: in vitro experiences. Ann Thorac Surg. 2000;70:140.
258. Schenkelayland K, Opitz F, Gross M, Döring C, Halbhuber KJ, Schirrmeister F, et al. Complete dynamic repopulation of decellularized heart valves by application of defined physical signals-an in vitro study. Cardiovasc Res. 2003;60:497.
259. Berry JL, Steen JA, Williams JK, Jordan JE, Atala A, Yoo JJ. Bioreactors for development of tissue engineered heart valves. Ann Biomed Eng. 2010;38:3272.

Part I
Structural Scaffolds and Bio-activation

Chapter 2
Polymeric and Biomimetic ECM Scaffolds for Tissue Engineering

Guoping Chen and Naoki Kawazoe

2.1 Introduction

Polymeric and biomimetic scaffolds have been a broad application in tissue engineering to control cell functions and to provide temporary support for the regeneration of functional new tissues and organs [1–3]. The scaffolds can be prepared from biodegradable polymers, either synthetic or naturally derived. The most frequently used biodegradable synthetic polymers for tissue engineering are aliphatic polyesters such as poly(glycolic acid) (PGA), poly(lactic acid) (PLA), poly(lactic acid-co-glycolic acid) (PLGA) and poly(ε-caprolactone) (PCL). Naturally derived polymers are produced from living organisms and can be categorized as proteins, polysaccharides, polyhydroxyalkanoates and polynucleotides. The first two categories are usually used to prepare porous scaffolds, which are usually modified or cross-linked to control their degradation to support cell culture and tissue formation. Acellular matrices are also very useful scaffolds for tissue engineering because of their similarity to the in vivo microenvironments [4].

Scaffolds can be prepared by many methods such as particle leaching [5], freeze-drying [6], phase separation [7], gas foaming [8], electrospinning [9], fiber bonding [10] and 3D printing [11]. The nano- and microstructures of scaffolds can be tailored for specific tissue engineering applications. The physical and biochemical properties of scaffolds for tissue engineering can affect the functions of cells cultured in vitro or in vivo. Porous scaffolds with a variety of nano- and microstructure, mechanical property and biochemical composition have been prepared by these methods.

Scaffold properties have diverse influences on cell functions. The pore structure of scaffolds can affect the cell behaviors such as distribution, migration, assembly

G. Chen (✉) • N. Kawazoe
International Center for Materials Nanoarchitectonics, National Institute for Materials Science, 1-1 Namiki, Tsukuba, Ibaraki 305-0044, Japan
e-mail: Guoping.CHEN@nims.go.jp

© Springer Science+Business Media Singapore 2016

C. Gao (ed.), *Polymeric Biomaterials for Tissue Regeneration*,
DOI 10.1007/978-981-10-2293-7_2

and tissue formation. Open pore structure of scaffolds is the premise to enable homogeneous cell seeding and homogenous tissue formation. Scaffolds with isotropic and open pore structure enable a homogeneous distribution of cells and formation of a homogenous tissue.

Chemical composition of scaffolds can also greatly affect cell functions. Cell adhesion and spreading are usually more promoted by the use of naturally derived polymer scaffolds compared with synthetic polymer scaffolds. Cells in normal tissue are surrounded with ECM which serve as a substrate to modulate cell behaviors. ECM of normal tissue have multiple components such as collagen, laminin, aggrecan, hyaluronic acid and fibronectin. Scaffolds with a chemical composition similar to that of normal tissue ECM should benefit cell proliferation and tissue formation [12]. This chapter introduces the methods to prepare polymer porous scaffolds with well-controlled microporous structures, cell-derived biomimetic ECM scaffolds and hybrid scaffolds of biodegradable synthetic polymers and naturally derived polymers.

2.2 Scaffolds Prepared with Ice Particulates

Scaffolds used for tissue engineering should have an adequate microporous structure for enabling cellular penetration into the construct to obtain a desirable cell distribution [13, 14]. Although a number of three-dimensional porous scaffolds have been developed from various types of biodegradable polymers, their pore structures need to be improved to make their surface pores open and bulk pores interconnected. When porous scaffolds are used for cell seeding and 3D cell culture, cells are easily allocated and distributed in the peripheral areas which results in nonhomogeneous cell distribution and partial tissue formation in the outermost peripheral layers of the scaffolds. Open structure of surface pores is desirable to guarantee smooth entry of cells into the pores during cell seeding [15]. Meanwhile pore interconnectivity is required to allow cells to penetrate from the surface pores into the bulk pores to reach all the pores throughout the scaffolds.

There are a few methods that have been developed for controlling various aspects of the pore structures, such as pore size, porosity and interconnectivity of the scaffolds [6, 16, 17]. Among these methods, the porogen-leaching method offers many advantages for the easy manipulation and control of pore size and porosity. In this method, the porogen materials can leave replica pores after leaching. Selection of porogen materials is important to decide the pore structures. Isolated particles of porogen materials result in the formation of isolated pores, a situation which is not desirable for tissue engineering scaffolds. To improve pore interconnectivity, the porogen materials are bonded before mixing them with polymer matrix [18, 19]. However, the bonded porogen materials require organic solvents for leaching and the residual solvents are toxic to cells. Mixing of polymer solution with the bonded porogen materials becomes difficult if the polymer solution has a high viscosity. To

overcome these problems, an approach using pre-prepared ice particulates as a porogen material has been developed [20–22].

In the pre-prepared ice particulate method, ice particulates are at first prepared. Ice particulates can be easily prepared by spraying or injecting water into liquid nitrogen through a sprayer or capillary. Ice particulates formed by spraying method are spherical. Their diameters can be controlled by the spraying speed. The ice particulates can be sieved by sieves with different mesh pores under low temperatures to obtain ice particulates with desired diameters. Subsequently the pre-prepared ice particulates are homogenously mixed with polymer solution. The mixing temperature is set at a temperature where the ice particulates do not melt and polymer solution does not freeze. Finally the mixture is frozen and freeze-dried to form porous structures. Ice particulates can be easily and completely removed by freeze-drying. The porous scaffolds are cross-linked after freeze-drying if the polymers are water soluble. During the preparation procedures, pre-prepared ice particulates not only work as porogens to control the pore size and porosity but also work as nuclei to initiate the formation of new ice crystals during freezing process if polymer aqueous solution is used. Pore structure is decided by both pre-prepared ice particulates and newly formed ice crystals. The newly formed ice crystals can increase the pore interconnectivity if they grow from the pre-prepared ice particulates.

Collagen porous scaffolds have been prepared by the pre-prepared ice particulate method [22]. At first, an aqueous collagen solution and ice particulates are prepared. An aqueous solution of collagen at a concentration of 2 % (w/v) is prepared by dissolving porcine type I collagen in a mixture solution of ethanol and acetic acid (10:90 v/v, pH 3.0) at 4 °C. The ethanol and acetic acid mixture solution is used to decrease the freezing temperature of the collagen aqueous solution. The collagen aqueous solution does not freeze at −4 °C, guaranteeing homogeneous mixing with the ice particulates. Ice particulates are prepared by spraying water into liquid nitrogen using a sprayer. The ice particulates are sieved at −15 °C by sieves with mesh pores of 150, 250, 355, 425 and 500 μm to obtain ice particulates having diameters of 150–250, 250–355, 355–425 and 425–500 μm. Subsequently, the 2 % (w/v) aqueous collagen solution is mixed with the sieved ice particulates at a ratio of 50:50 (v/w). Before mixing, the collagen solution and the ice particulates are moved to a −4 °C low-temperature chamber for 6 h to balance their temperatures. Finally, the four sets of mixtures are frozen and freeze-dried. The freeze-dried constructs are cross-linked with glutaraldehyde vapor by placing them in a closed box with 20 mL of a 25 % aqueous glutaraldehyde solution at 37 °C. After cross-linking, the constructs are washed and immersed in 0.1 M aqueous glycine solution to block the unreacted aldehyde groups. After washing, the collagen porous scaffolds are obtained.

Gross appearance and microstructures of the collagen porous scaffolds are shown in Fig. 2.1. The collagen porous scaffolds have large spherical pores and small pores. The small pores surround the large spherical pores and are located on the walls of large pores. The large spherical pores are evenly distributed and well stacked. The small pores on the walls of large pores connect the large pores, making the scaffold well interconnected. The size and density of large pores are dependent on the size and ratio of ice particulates used to prepare the scaffolds because they are the negative replicas of the ice particulates. The small pores are the negative

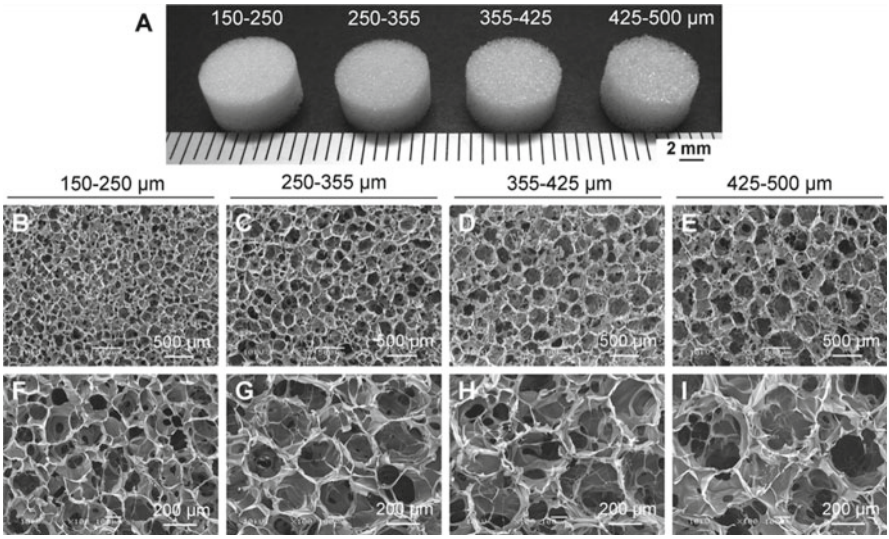

Fig. 2.1 Gross appearances (**a**) and SEM images (**b**–**i**) of the cross sections of four types of collagen porous scaffolds prepared with ice particulates having diameter ranges of 150–250 (**b**, **f**), 250–355 (**c**, **g**), 355–425 (**d**, **h**) and 425–500 μm (**e**, **i**) at low (**b**–**e**) and high (**f**–**i**) magnifications (Adapted from Ref. [22] with permission from Elsevier)

replicas of ice crystals that are formed during freezing, which size is dependent upon the freezing temperature. When the collagen porous scaffolds are used for culture of bovine articular chondrocytes, cells can be easily seeded and homogenously distributed throughout the scaffolds. The homogenous cell distribution in the four types of collagen porous scaffolds should be due to the good interconnectivity of the scaffolds. The interconnectivity among the spherical large pores facilitates the smooth delivery of cells in the scaffolds to each corner of the scaffolds.

The ratio of ice particulates and collagen concentration has some influence on the pore structure and mechanical property of collagen porous scaffolds. When collagen porous scaffolds prepared with 25, 50 and 75 (v/w) % ice particulates having a diameter from 335 to 425 μm are compared, the large spherical pores in scaffolds prepared with 25 (v/w) % ice particulates are sparsely distributed. When 75 % ice particulates are used, some collapsed large pores are observed. With a high ratio of ice particulates, the collagen aqueous solution filling the spaces between the spherical ice particulates decreases and the collagen matrix surrounding the large pores decreases. In addition, mixing of the ice particulates and the collagen aqueous solution becomes difficult when the ice particulate ratio is high. The collapsed large pores can be due to the less dense collagen matrix and incomplete mixing. Collagen scaffolds prepared with 50 (w/v) % ice particulates have the most homogenous pore structure.

The effect of the collagen concentration on the pore structure is investigated by fixing the ice particulate ratio at 50 % (w/v) and changing the collagen concentration from 1 % to 3 % (w/v). Collapsed large pores are observed in the collagen scaffolds prepared with 1 % and 3 % collagen aqueous solutions. The collapsed large pores in collagen scaffolds prepared with the 1 % collagen aqueous solution may be because of the low concentration which results in a less dense collagen matrix surrounding the large pores. The case involving the 3 % collagen aqueous solution may be due to incomplete mixing because the 3 % collagen solution is too viscous. The collagen scaffold prepared with the 2 % collagen solution has the most homogeneous pore structure.

When collagen concentration is fixed at 2 % and the ratio of ice particulates is changed, the Young's modulus of collagen porous scaffolds increases in the following order: 75 % <25 % <50 %. The collagen porous scaffolds prepared with 50 % ice particulates have the highest Young's modulus. The difference in the mechanical properties is mainly ascribed to the different pore structures. The spherical pores formed by ice particulates are thought to resist mechanical loading, therefore reinforcing the collagen scaffolds. The high mechanical strength of the collagen scaffold prepared with 50 % ice particulates should be due to the most appropriate packing of the large spherical pores and appropriate filling of the collagen matrix between the large spherical pores. The low mechanical strength of the collagen scaffold prepared with 75 % ice particulates may be due to the partially collapsed large pore structure. When the ratio of ice particulates is fixed at 50 (w/v)%, the Young's modulus increases as the collagen concentration increases. A dense collagen matrix surrounding the large pores can be formed to reinforce the scaffolds when the collagen concentration increases.

The ice particulate method has also been used to prepare porous scaffolds of gelatin and HA/collagen scaffolds [23, 24]. This method is applicable for all of the biodegradable polymers, especially for naturally derived polymers. Most of the naturally derived polymers are water soluble. There are many advantages of pre-prepared ice particulate method for scaffold preparation of naturally derived polymers because the method is proceeded at low temperature and no organic solvent is used. The method is good for incorporation of growth factors in the porous scaffolds while maintaining their bioactivities.

The method can also be used for scaffold preparation of biodegradable synthetic polymers [25]. Synthetic polymers are dissolved in organic solvents that have a much lower freezing temperature than the melting temperature of the ice particulates. The temperature of biodegradable polymers can be decreased to avoid melting of ice particulates during mixing of synthetic polymer solution and the pre-prepared ice particulates. Freezing of the mixture can induce phase separation of synthetic polymer solution among the ice particulates, resulting in the formation of microporous wall after freeze-drying. However, the mechanical property of biodegradable synthetic polymer scaffolds prepared by this method is much lower than the scaffolds prepared by normal porogen-leaching method using salt particles or sugar particles as a porogen material.

2.3 Funnel-Like Porous Scaffolds and Micropatterned Porous Scaffolds

To make the scaffold surface pores open, a method by using embossing ice particulates as a template has been developed [26]. The method is similar to the abovementioned ice particulate method. The ice particulates are formed on a surface and then used as a template to prepare porous scaffolds. As a general procedure, water droplets are at first formed on a thin film by spraying or injecting water or applying moisture on a hydrophobic surface. The size of the water droplets can be controlled by the number of spraying times, injected water volume or the moisture application time. Embossing ice particulates are formed after freezing the water droplets. And then the embossing ice particulates are used as a template to prepare porous scaffolds. The freezing, freeze-drying, cross-linking and washing steps during scaffold preparation are the same as those of the abovementioned procedures of pre-prepared ice particulate method. An aqueous solution of naturally derived polymers is eluted onto the embossing ice particulates and the construct is frozen. The frozen construct is freeze-dried to remove the embossing ice particulates and ice crystals newly formed during freezing. Porous scaffolds having open surface pore structures are prepared after cross-linking and washing.

The method has been used to prepare porous scaffolds of collagen, chitosan, hyaluronic acid and glycosaminoglycan collagen that have open surface pore structures [26–29]. The porous scaffolds have large open pores on their surfaces and small pores underlying the large surface pores. Such structure is similar to a funnel and therefore the porous scaffolds are referred as funnel-like porous scaffolds. The morphology, size and density of large surface pores are dependent on the embossing ice particulates because they are the negative replicas of the embossing ice particulates. The small pores are the negative replicas of ice crystals that are newly formed during freezing. The size of small pores is dependent on the freezing temperature as mentioned above.

The embossing ice particulate method can be used to prepare micropatterned pore structures in porous scaffolds [30]. In such an application, the embossing ice particulates are micropatterned. Micropatterned ice particulates or ice lines are at first prepared and used as templates to prepare the micropatterned porous scaffolds. The micropatterned ice particulates or ice lines are prepared by ejecting water droplets through a dispensing machine at a low temperature. By designing an ejection program, the micropatterns can be tethered. Figure 2.2a–h shows some micropatterns of ice particulates and the respective micropatterned collagen porous scaffolds. The micropatterned pore layers can be stacked to construct collagen porous scaffolds with 3D micropatterned pores (Fig. 2.2i, j).

To prepare the 3D micropatterned pore structures, polymer solution is eluted on the micropatterned ice particulates that is formed on a film (first layer of ice particulates) and frozen. The frozen polymer solution on the first layer of micropatterned ice particulates is used to prepare the second layer of micropatterned ice particulates (second layer of ice particulates) instead of the film. Polymer solution is eluted on the second layer of ice particulates and frozen. By repeating the procedure, polymer

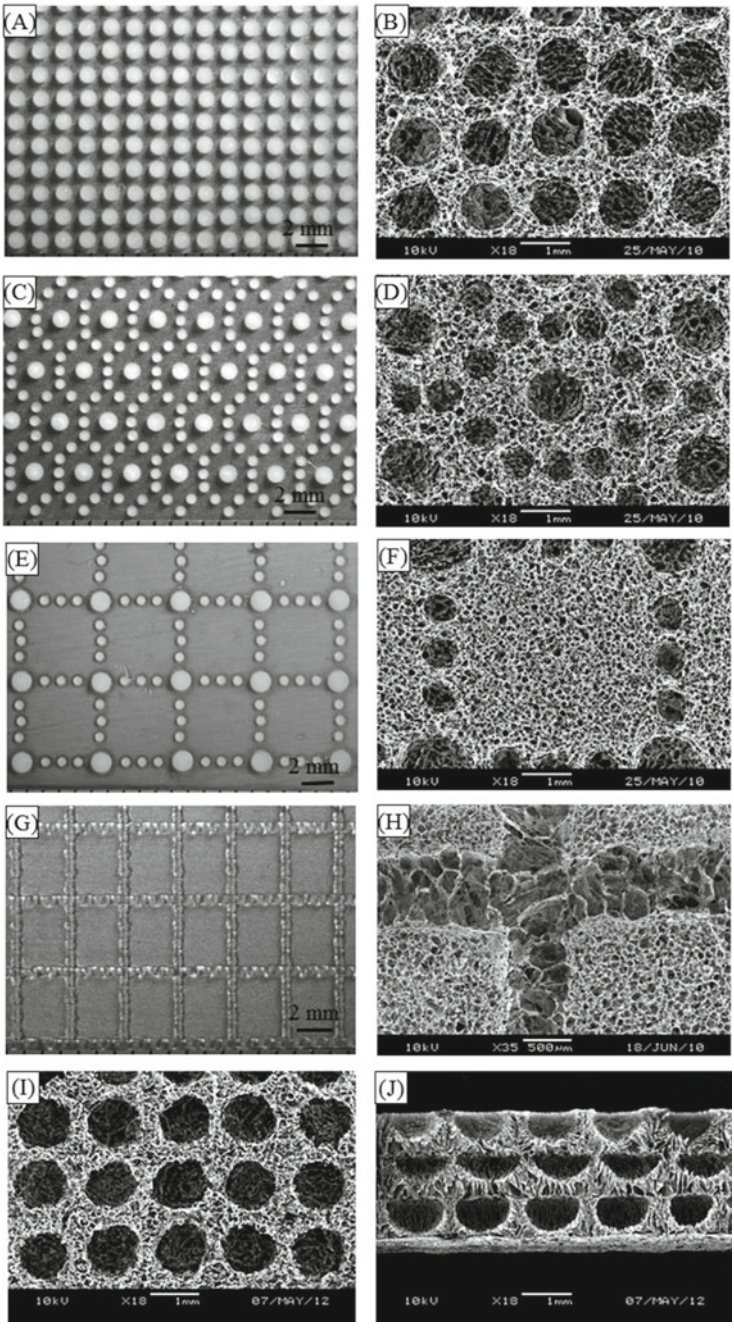

Fig. 2.2 Light microscopy images of four types of ice micropattern templates (**a**, **c**, **e**, **g**) and SEM images of collagen porous scaffolds with one layer of micropatterned pores that are prepared with the respective ice micropattern templates (**b**, **d**, **f**, **h**) and of a collagen sponge with three-dimensional micropatterned pores that is prepared with ice micropattern template shown in (**a**) (**i** top surface, **j** cross section) (Adapted from Ref. [30] with permission from John Wiley and Sons)

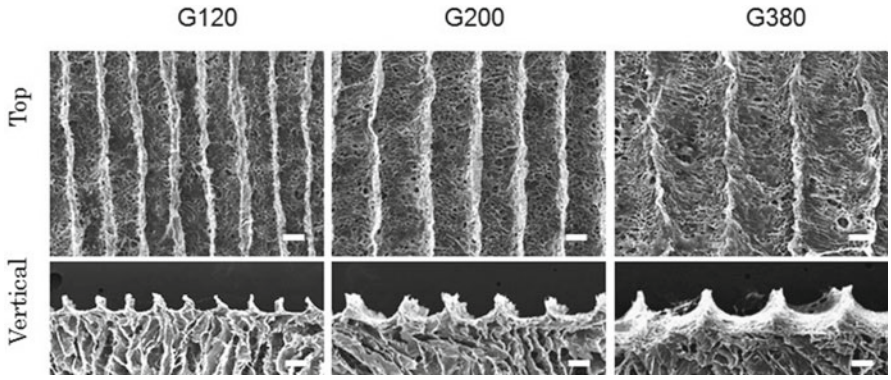

Fig. 2.3 SEM images of microgrooved collagen porous scaffolds with mean microgroove widths of 120, 200 and 380 μm. Upper images show the top view and lower images show the vertical cross-sectional view of different scaffolds. Scale bar = 100 μm (Adapted from Ref. [31] with permission from Elsevier)

matrix embedded with multilayers of micropatterned ice particulates can be obtained. After freeze-drying, cross-linking and washing, polymer porous scaffolds with 3D micropatterned pore structures are prepared. Collagen porous scaffolds with 3D micropatterned pore structures are shown in Fig. 2.2i, j. The cross section SEM image shows the stacked 3D pore structure.

Microgrooved collagen porous scaffolds have been prepared with this method by using micropatterned ice lines as a template [31]. By controlling the width of ice lines, three types of collagen porous scaffolds with microgroove width of 120, 200 and 380 μm are prepared (Fig. 2.3). They are referred as G120, G200 and G380. The microgrooved porous scaffolds have aligned concave microgrooves that exhibit semicircular shape in cross sections.

The collagen microgroove porous scaffolds have been used for culture of L6 skeletal myoblasts for skeletal muscle tissue engineering. Figure 2.4 shows cell aggregation and cell bundle formation in the G200 scaffolds. The width of microgrooves has some effects on cell orientation and cell bundle formation. Scaffolds with wide microgrooves (G200 and G380) enable the formation of discrete cell bundles after 14 days of culture. Scaffolds with narrow microgrooves (G120) result in the formation of some cell bundles in microgrooves and mostly cellular flakes covering most of the area of scaffolds. Staining of myosin heavy chain (MHC) shows that well-aligned myotubes are formed in G200 and G380, while in G120 some myotubes are aligned in microgrooves and other myotubes in cellular flakes have random orientation.

Furthermore the embossing ice particulate method can be used to micropattern bioactive molecules in 3D porous polymer scaffolds. As an example, collagen porous scaffolds with micropatterned fibronectin, VEGF and NGF have been prepared by the method [32, 33]. In this case, a collagen aqueous solution containing the bioactive molecules other than pure water is used to prepare the micropatterned ice lines. The ice micropatterns of the mixture of collagen/bioactive molecules are used to prepare collagen porous scaffolds having micropatterns of bioactive molecules. Not

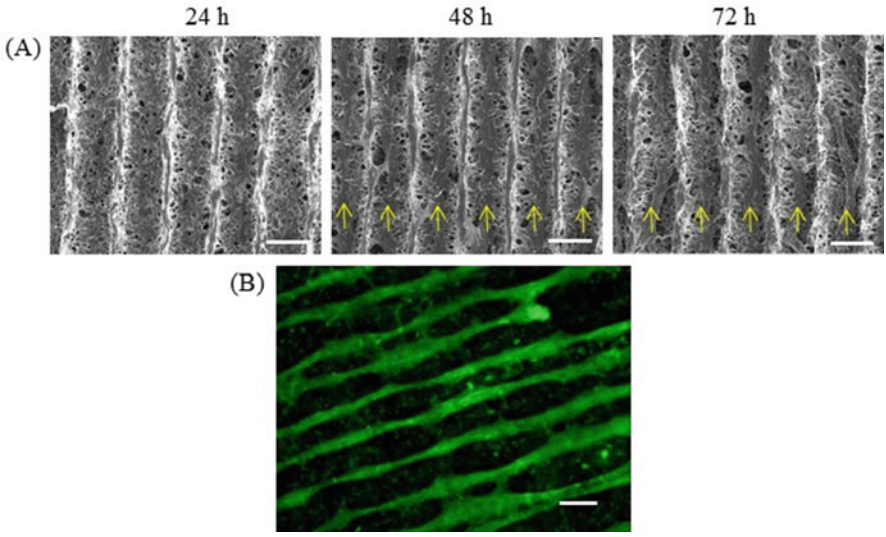

Fig. 2.4 SEM images of cells that are cultured in the microgrooved collagen porous scaffolds having a mean microgroove width 200 μm for 24, 48 and 72 h (**a**) and fluorescence micrograph of cell bundle formation in the scaffolds after culture for 14 days. Cell seeding concentration is 2.0×10^6/ml. Myoblasts are visualized using F-actin staining. Scale bar = 200 mm (Adapted from Ref. [31] with permission from Elsevier)

only single bioactive molecule but also a few types of bioactive molecules can be co-micropatterned in the porous scaffolds. The bioactive molecules can be mixed and micropatterned together or the bioactive molecules can be micropatterned separately to construct the porous scaffolds having co-micropatterns of a few types of bioactive molecules. Collagen porous scaffolds with micropatterned NGF and VEGF show stimulative effects on the regeneration of neural network and capillary network, respectively.

2.4 Biomimetic ECM Scaffolds

Extracellular matrices (ECM) are a complex network composed of a variety of proteins and proteoglycans. ECM play a very important role in regulation of cell functions. ECM derived from decellularized tissues has been widely explored as a source of biological scaffolds for tissue engineering. Acellular ECM has been prepared by decellularization of tissues and organs, such as the small intestinal submucosa, heart valve, blood vessel, skin, nerve, tendon, ligament, urinary bladder, vocal fold, amniotic membrane, heart, liver and lung [4]. The ECM scaffolds obtained from decellularized tissues and organs offer the advantage of maintaining the structures of the respective tissues and organs. However they suffer from problems of autologous tissue/organ scarcity, host responses and pathogen transfer when allogeneic and xenogeneic tissues and organs are used.

The cell culture method has been used as an alternate way to make ECM scaffolds. Cell-derived ECM has been used to make various scaffolds for tissue engineering applications [34–36]. Cultured cells offer several advantages of pathogen-free and availability over the decellularization of tissues and organs. Recently a method using 3D cell culture has been developed to construct cell-derived ECM porous scaffolds [37, 38]. The method is based on 3D cell culture in a selectively removable template. At first cells are cultured in a template. The cells proliferate and excrete their own extracellular matrices. Subsequently the cellular components are removed by decellularization after the cells have excreted enough amount of extracellular matrices. Finally the templates are selectively removed, while the extracellular matrices are remained. After cross-linking, ECM scaffolds are obtained.

The method has been used to prepare ECM scaffolds from human bone marrow mesenchymal stem cells (MSC), human articular chondrocytes and human dermal fibroblasts by using PLGA mesh as a template [38]. The ECM scaffolds from MSC (ECM-M), chondrocytes (ECM-C) and fibroblasts (ECM-F) have a mesh-like

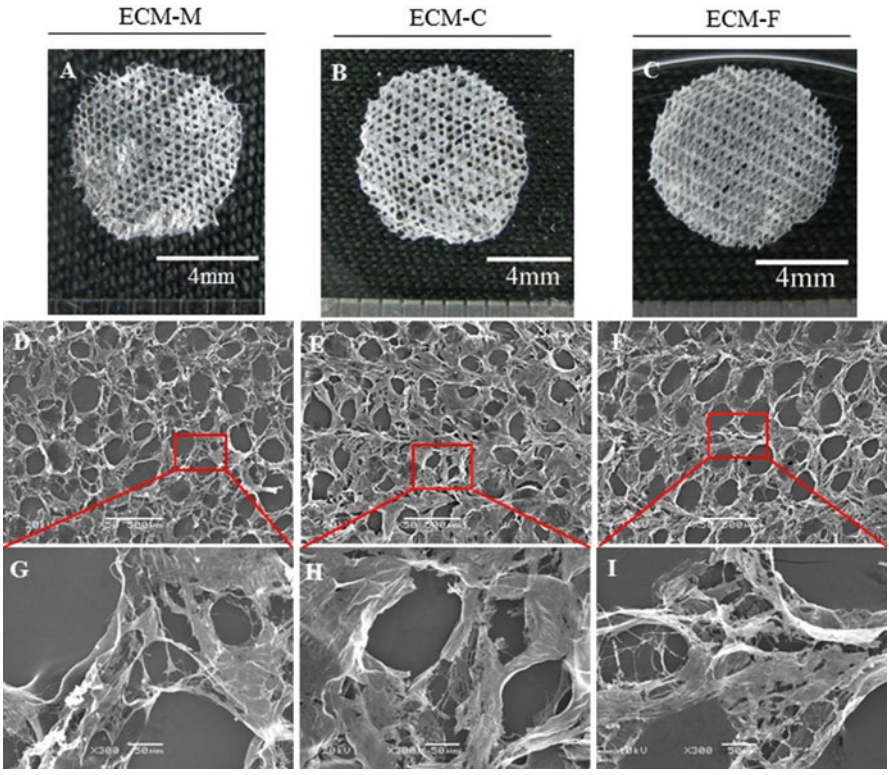

Fig. 2.5 Gross appearance (**a**–**c**) and SEM images (**d**–**i**) of ECM porous scaffolds prepared from MSC (**a**, **d**, **g**), chondrocytes (**b**, **e**, **h**) and fibroblasts (**c**, **f**, **i**). Scale bar = 500 μm in (**d**–**f**) and 50 μm in (**g**–**i**) (Adapted from Ref. [37] with permission from Elsevier)

appearance similar to that of the PLGA mesh template (Fig. 2.5). The ECM scaffolds have different composition that is dependent on the cell type and culture condition.

Furthermore the method has been used to prepare ECM scaffolds that can mimic the dynamic ECM change during stem cell differentiation. For example, chondrogenesis involves a cascade of strictly regulated events, including condensation of MSC, chondrogenic differentiation and maturation of chondrocytes. Accompanying with the progression of chondrogenesis, ECM composition and structure are remodeling and changing. At the early stage, ECM rich in collagen I and fibronectin are secreted and gradually replaced by collage II and aggrecan-rich ECM as the chondrogenesis proceeds in vivo. When cartilage becomes mature, more cartilage-specific ECM are accumulated by surrounding differentiated chondrocytes. The method has been used to prepare 3D scaffold mimicking ECM remodeling during chondrogenesis progression [39].

Stem cell-stage ECM scaffold (SC-ECM scaffold), early-stage chondrogenesis-mimicking ECM scaffold (CE-ECM scaffold) and late-stage chondrogenesis-mimicking ECM scaffold (CL-ECM scaffold) have been prepared from MSC that are cultured in growth medium or chondrogenic induction medium and controlled at different chondrogenesis stages (Fig. 2.6). The ECM scaffolds are defined as "stepwise chondrogenesis-mimicking ECM scaffolds." The alteration of composition of these ECM scaffolds shows different effects on the chondrogenic differentiation of MSC. These stepwise chondrogenesis-mimicking ECM scaffold should not only provide a good in vitro model for investigation of cell-matrix interactions during cartilage tissue development but also provide important information for the design and preparation of tissue engineering scaffolds.

2.5 Hybrid Porous Scaffolds

Porous scaffolds of biodegradable synthetic polymers and naturally derived polymers have their respective advantages and problems. Porous scaffolds prepared from synthetic biodegradable polymers such as PGA, poly(L-lactic acid) (PLLA), PLGA and PCL have relatively strong mechanical strength. Their degradation can be controlled by crystallinity, molecular weight and copolymer ratio of the polymers. However, synthetic polymer scaffolds are devoid of cell recognition signals and their hydrophobic surface property hinders smooth cell seeding. On the other hand, naturally derived polymers such as collagen, gelatin and hyaluronic acid have the advantages of specific cell interactions and hydrophilicity, while their mechanical property is inferior to synthetic polymer scaffolds. Biodegradable synthetic polymers and naturally derived polymers have hybridized to prepare their hybrid scaffolds to combine the advantageous properties of both types of polymers and overcome their drawbacks [40, 41]. One type of hybridization is to form microsponges of naturally derived polymers in the void spaces or opening of a porous skeleton of biodegradable synthetic polymers [42–45]. The void space or opening of biodegradable synthetic polymer porous skeleton is filled with microsponges of

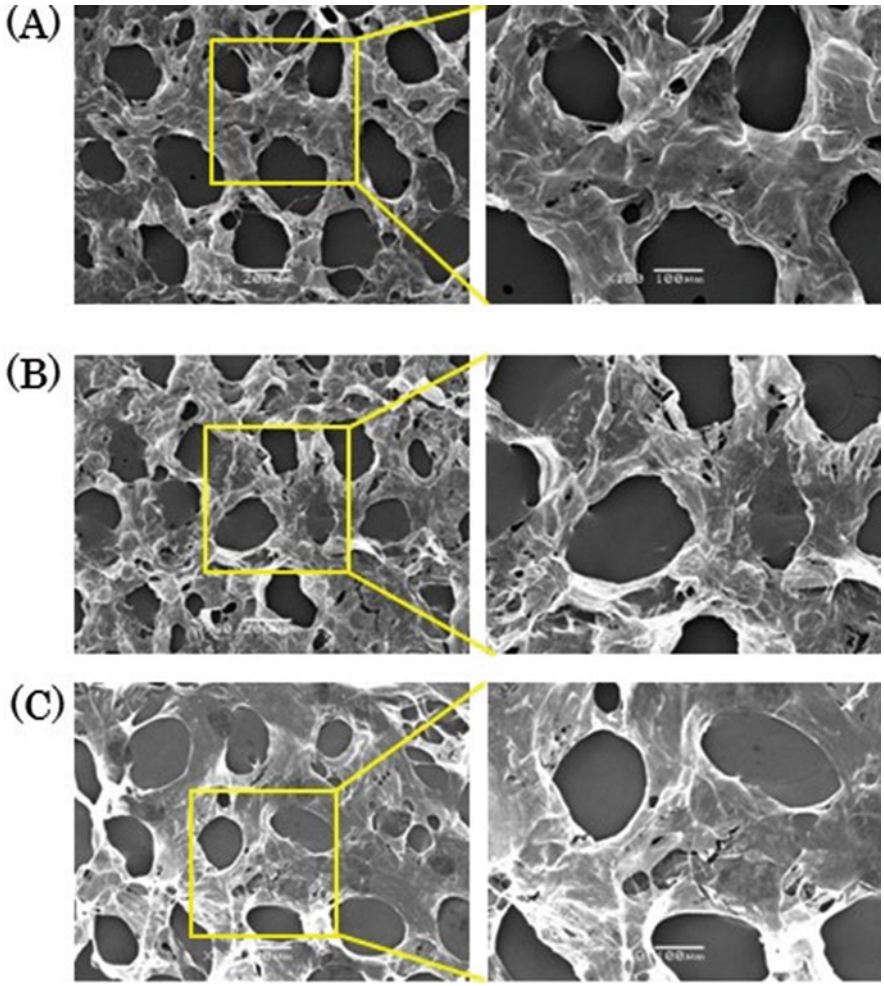

Fig. 2.6 SEM images of ECM porous scaffolds prepared from cells at stem cell stage (**a**), early stage of chondrogenesis (**b**) and late stage of chondrogenesis (**c**) at low and high magnifications (Adapted from Ref. [39] with permission from Elsevier)

naturally derived polymers. The pore surface of biodegradable polymer porous skeleton is also coated with naturally derived polymers. When the hybrid scaffolds are used for 3D cell culture, cells only contact and interact with naturally derived polymers. The porous skeleton of biodegradable polymers serves as a mechanical skeleton to provide necessary mechanical strength to support the whole scaffolds. Another type of hybridization is to construct naturally derived polymer porous structures in the open space of a cup, cage, or cylinder of biodegradable synthetic polymers [46, 47]. All the hybrid porous scaffolds have high mechanical strength, good cell interaction and surface hydrophilicity.

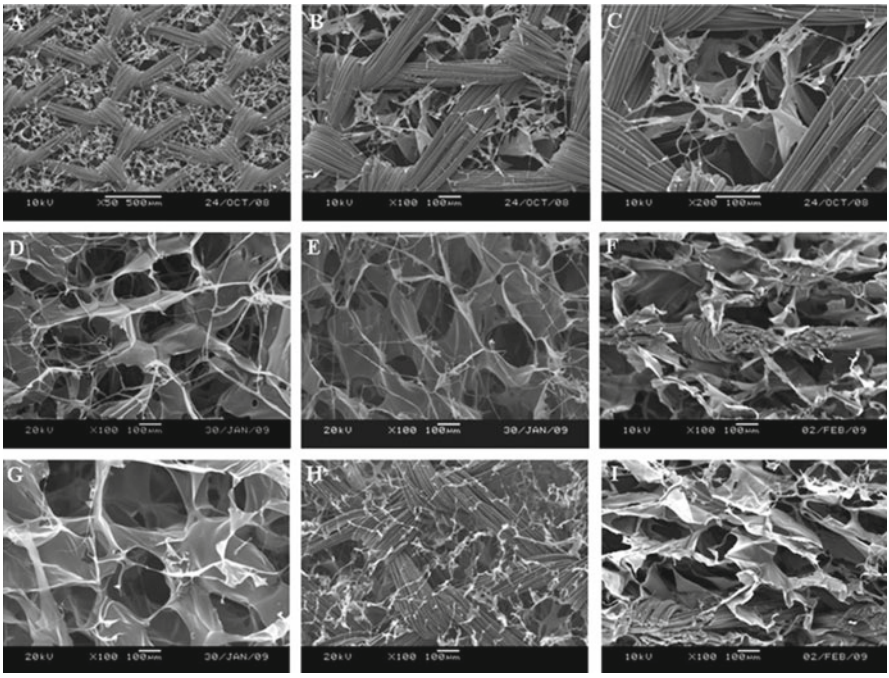

Fig. 2.7 SEM observation of THIN, SEMI and SANDWICH PLGA-collagen hybrid scaffolds. (**a**–**c**) top view of the THIN scaffolds; (**d**, **g**) top view of the SANDWICH and SEMI scaffolds, respectively; (**e**, **h**) bottom view of the SANDWICH and SEMI scaffolds, respectively; (**f**, **i**) cross-sectional view of the SANDWICH and SEMI scaffolds, respectively (Adapted from Ref. [40] with permission from Elsevier)

As a typical example of hybrid scaffolds, PLGA-collagen hybrid mesh can be prepared by introducing collagen microsponges in the interstices of a PLGA knitted mesh [44, 45]. Collagen sponge can also be formed on one side of the PLGA knitted mesh or both sides of the PLGA knitted mesh to construct semi-type or sandwich-type PLGA-collagen hybrid scaffolds (Fig. 2.7) [48].

The semi-type and sandwich-type PLGA-collagen hybrid scaffolds have been used for culture of bovine articular chondrocytes for cartilage tissue engineering (Fig. 2.8). Both hybrid scaffolds show a spatially even cell distribution, natural chondrocyte morphology, abundant cartilaginous extracellular matrix deposition and excellent biodegradation in vivo. The histological structure and mechanical properties of the engineered cartilage using the semi-type and sandwich-type hybrid scaffolds match the native bovine articular cartilage. The hybrid scaffolds are useful for tissue engineering and regenerative medicine.

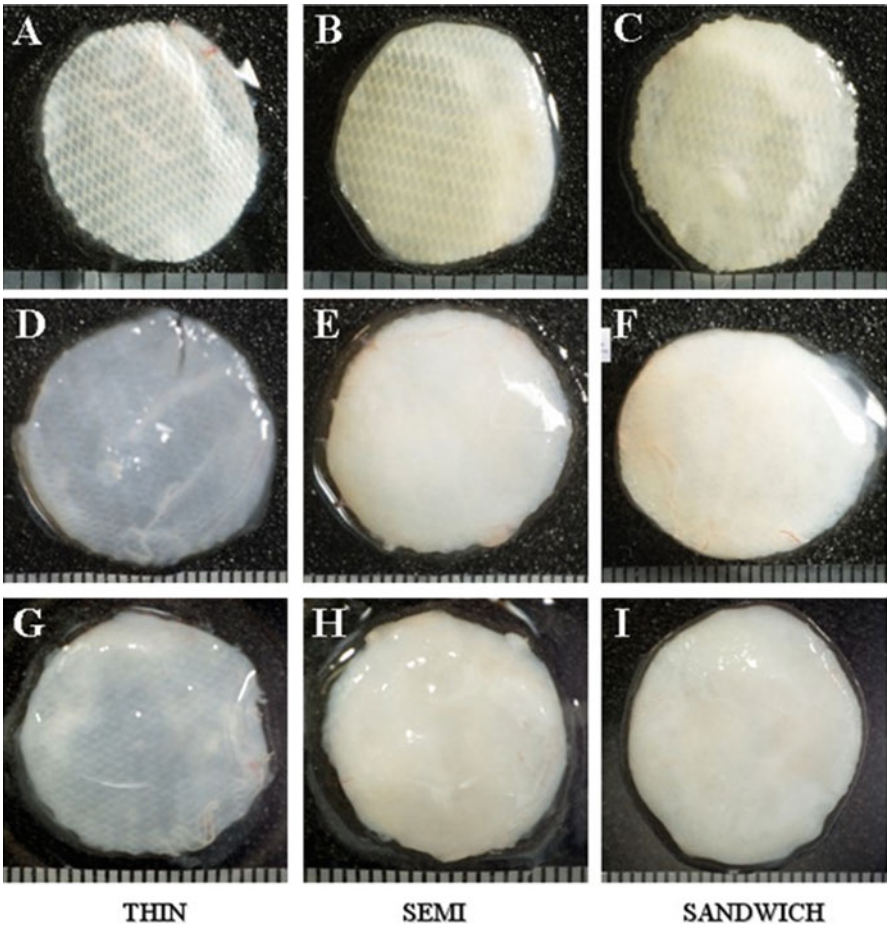

Fig. 2.8 Gross view of the implants of chondrocyte-seeded scaffolds after 2, 4 and 8 weeks implantation. (**a**, **d**, **g**) THIN scaffold; (**b**, **e**, **h**) SEMI scaffold; (**d**, **f**, **i**) SANDWICH scaffold (Adapted from Ref. [40] with permission from Elsevier)

2.6 Summary

Porous scaffolds can be prepared from varieties of biodegradable polymers and extracellular matrices. Their composition can be controlled by combining a few types of polymers and matrices. They can also be hybridized to overcome the drawbacks of single polymers. Their microporous structures can be controlled by using different fabrication methods. Pre-prepared ice particulate method and embossing ice particulate method can well control the micropore structures and introduce micropatterns in the scaffolds. Cell-derived ECM scaffolds not only mimic the cellular microenvironment but also mimic the dynamics of ECM remolding during

stem cell differentiation or tissue development. The polymer porous scaffolds and biomimetic ECM scaffolds can be widely used for engineering of various types of tissue and organs.

Acknowledgement This work was supported by the World Premier International Research Center Initiative on Materials Nanoarchitectonics (WPI-MANA) and JSPS KAKENHI Grant Number 15H03027.

References

1. Oberpenning F, Meng J, Yoo JJ, Atala A. Nat Biotechnol. 1999;17:149–55.
2. Engelmayr GC, Cheng M, Bettinger CJ, Borenstein JT, Langer R, Freed LE. Nat Mater. 2008;7:1003–10.
3. Lu H, Kawazoe N, Kitajima T, Myoken Y, Tomita M, Umezawa A, Chen G, Ito Y. Biomaterials. 2012;33:6140–6.
4. Hoshiba T, Lu H, Kawazoe N, Chen G. Expert Opin Biol Ther. 2010;10:1717–28.
5. Mikos AG, Thorsen AJ, Czerwonka LA, Bao Y, Langer R, Winslow DN, Vacanti JP. Polymer. 1994;35:1068–77.
6. Zhang HF, Hussain I, Brust M, Butler MF, Rannard SP, Cooper AI. Nat Mater. 2005;4:787–93.
7. Yang F, Murugan R, Ramakrishna S, Wang X, Ma YX, Wang S. Biomaterials. 2004;25:1891–900.
8. Harris LD, Kim BS, Mooney DJ. J Biomed Mater Res. 1998;42:396–402.
9. Meng W, Kim SY, Yuan J, Kim JC, Kwon OH, Kawazoe N, Chen G, Ito Y, Kang IK. J Biomater Sci Polym Ed. 2007;18:81–94.
10. Mikos AG, Bao Y, Cima LG, Ingber DE, Vacanti JP, Langer R. J Biomed Mater Res. 1993;27:183–9.
11. Sun W, Starly B, Darling A, Gomez C. Biotechnol Appl Biochem. 2004;39:49–58.
12. Benders KEM, Van Weeren PR, Badylak SF, Saris DBF, Dhert WJA, Malda J. Trends Biotechnol. 2013;31:169–76.
13. Silva M, Cyster LA, Barry JJA, Yang XB, Oreffo ROC, Grant DM, Scotchford CA, Howdle SM, Shakesheff KM, Rose F. Biomaterials. 2006;27:5909–17.
14. Woodfield TBF, Malda J, De Wijn J, Peters F, Riesle J, Van Blitterswijk CA. Biomaterials. 2004;25:4149–61.
15. Murphy CM, Haugh MG, O'brien FJ. Biomaterials. 2010;31:461–6.
16. Yoon JJ, Kim JH, Park TG. Biomaterials. 2003;24:2323–9.
17. Hou QP, Grijpma DW, Feijen J. Biomaterials. 2003;24:1937–47.
18. Choi SW, Xie JW, Xia YN. Adv Mater. 2009;21:2997–3001.
19. Chen VJ, Ma PX. Biomaterials. 2004;25:2065–73.
20. Zhang Q, Lu H, Kawazoe N, Chen G. J Bioact Compat Polym. 2013;28:426–38.
21. Zhang Q, Lu H, Kawazoe N, Chen G. Mater Lett. 2013;107:280–3.
22. Zhang Q, Lu H, Kawazoe N, Chen G. Acta Biomater. 2014;10:2005–13.
23. Chen S, Zhang Q, Nakamoto T, Kawazoe N, Chen G. Tissue Eng Part C Methods. 2016;22:189–98.
24. Chen S, Zhang Q, Kawazoe N, Chen G. RSC Adv. 2015;5:94405–10.
25. Chen G, Ushida T, Tateishi T. Biomaterials. 2001;22:2563–7.
26. Ko YG, Kawazoe N, Tateishi T, Chen G. J Bioact Compat Polym. 2010;25:360–73.
27. Ko YG, Kawazoe N, Tateishi T, Chen G. J Biomed Mater Res Part B Appl Biomater. 2010;93B:341–50.
28. Ko YG, Oh HH, Kawazoe N, Tateishi T, Chen G. J Biomater Sci Polym Ed. 2011;22:123–38.

29. Ko YG, Grice S, Kawazoe N, Tateishi T, Chen G. Macromol Biosci. 2010;10:860–71.
30. Oh HH, Ko YG, Lu H, Kawazoe N, Chen G. Adv Mater. 2012;24:4311–6.
31. Chen S, Nakamoto T, Kawazoe N, Chen G. Biomaterials. 2015;73:23–31.
32. Oh HH, Lu H, Kawazoe N, Chen G. J Biomater Sci Polym Ed. 2012;23:2185–95.
33. Oh HH, Lu H, Kawazoe N, Chen G. Biotechnol Prog. 2012;28:773–9.
34. Choi KH, Choi BH, Park SR, Kim BJ, Min BH. Biomaterials. 2010;31:5355–65.
35. Liao JH, Guo XA, Grande-Allen KJ, Kasper FK, Mikos AG. Biomaterials. 2010;31:8911–20.
36. Wolchok JC, Tresco PA. Biomaterials. 2010;31:9595–603.
37. Lu H, Hoshiba T, Kawazoe N, Chen G. Biomaterials. 2011;32:2489–99.
38. Lu H, Hoshiba T, Kawazoe N, Koda I, Song MH, Chen G. Biomaterials. 2011;32:9658–66.
39. Cai R, Nakamoto T, Kawazoe N, Chen G. Biomaterials. 2015;52:199–207.
40. Chen G, Ushida T, Tateishi T. Adv Mater. 2000;12:455–7.
41. Chen G, Ushida T, Tateishi T. Macromol Biosci. 2002;2:67–77.
42. Chen G, Ushida T, Tateishi T. Chem Commun. 2000;1505–6.
43. Chen G, Sato T, Ohgushi H, Ushida T, Tateishi T, Tanaka J. Biomaterials. 2005;26:2559–66.
44. Chen G, Sato T, Ushida T, Hirochika R, Shirasaki Y, Ochiai N, Tateishi T. J Biomed Mater Res A. 2003;67A:1170–80.
45. Chen G, Sato T, Ushida T, Ochiai N, Tateishi T. Tissue Eng. 2004;10:323–30.
46. He X, Lu H, Kawazoe N, Tateishi T, Chen G. Tissue Eng Part C Methods. 2010;16:329–38.
47. Kawazoe N, Inoue C, Tateishi T, Chen G. Biotechnol Prog. 2010;26:819–26.
48. Dai W, Kawazoe N, Lin X, Dong J, Chen G. Biomaterials. 2010;31:2141–52.

Chapter 3
Bioactive Hydrogels and Their Applications in Regenerative Medicine

Xiaolei Nie, Yon Jin Chuah, and Dongan Wang

3.1 Bioactive Hydrogel Gelation Mechanism

Hydrogel is the composition of cross-linked hydrophilic polymers [60] that has the capability of holding a large amount of water. Bioactive hydrogels possess unique functional groups that could enhance the functionality of the scaffolds such as cell adhesion, biodegradability and chemical release. To date, many existing distinctive cross-linking systems have been established to facilitate the formation of hydrogels which can be classified into physical, chemical and biological cross-linking.

3.1.1 Physical Cross-Linking

The mechanism of physical cross-linking comprises of either self-assembling or ionic cross-linking. Self-assembly is the programmed cross-linking under the outside stimuli (e.g. temperature and pH) by physical forces. For instance, thermoresponsive hydrogel involves the change of temperature to trigger the gelling behaviour without the use of any external stimulus. One of the established examples is poloxamer, now popularly known as Pluronic® or Synperonic® PE [25, 26], and is commonly utilised as antifoaming operators, wetting specialists, dispersants, thickeners and emulsifiers. This is achieved through the process of hydrophobic-driven gelation whereby a hydrophobic region is coupled to a hydrophilic segment and creates a polymer amphiphile. These amphiphiles are water soluble at low temperature, but the hydrophobic regions will aggregate when the temperature rises thus resulting in gelation [49]. Pluronic® or Synperonic® PE is a copolymer of

X. Nie • Y.J. Chuah • D. Wang (✉)
School of Chemical and Biomedical Engineering, Nanyang Technological University, Singapore, Singapore
e-mail: xnie002@e.ntu.edu.sg; ychuah001@e.ntu.edu.sg; dawang@ntu.edu.sg

© Springer Science+Business Media Singapore 2016

C. Gao (ed.), *Polymeric Biomaterials for Tissue Regeneration*,
DOI 10.1007/978-981-10-2293-7_3

polyethylene glycol (PEG) and poly(propylene oxide) (PPO) with a triblock unit of PEG-PPO-PEG, where PEG is hydrophilic and PPO is hydrophobic. This copolymer will form micelles in an aqueous solution with hydrophilic heads facing towards the outside arrangement and the hydrophobic tails towards the inward side of the micelles. When temperature rises, the micelles will start to aggregate and eventually result in the gelation of the materials [28].

Another example for physical gelation is ionic cross-linking which involves the electrostatic attraction between oppositely charged ions within the polymer chains. Usually, this application involves the use of divalent cations (e.g. Ca^{2+}, Ba^{2+}) and anions (e.g. β-glycerophosphate) to facilitate the formation of hydrogel [8]. For instance, alginate forms a hydrogel in the vicinity of calcium divalent cations. In this framework, the two carboxylic groups on various chains of polymers are associated together by the divalent cations because of the electrostatic strengths between inverse charges [1]. The gelation completes within minutes. The rate of the gelation could likewise be slowed down by low temperature (e.g. 4 °C) or anions that coexist in the arrangement (e.g. SO_4^{2-} in arrangement) which both result in lower gelation speed as contrasted to Cl^-.

3.1.2 Chemical Cross-Linking

Hydrogel formation with chemical cross-linking includes photo-cross-linking, Michael reaction, disulphide formation, Schiff's base reaction and click reaction. Photo-cross-linking is achieved with light exposure (e.g. UV light) to initiate the reaction. This is achieved by incorporating a photoinitiator into the framework of polymer which the exposure of light will generate free radicals by rearrangement, fragmentation or energy transfer. This formation of free radical is later followed by the propagation step of polymerisation to facilitate the formation of hydrogel [50].

Other types of chemical cross-linking mainly involve the incorporation of functional groups in the polymer chains. For instance, Michael addition occurs with the involvement of both thiol groups and methacrylate/acrylate or vinyl groups [19]. Disulphide formation requires the reaction between two thiols [30]. Schiff's base reactions involve the reaction between aldehyde and amine groups. With the dehydration of one water molecule in a condensation reaction, carbon nitrogen double bond is formed [49]. Click chemistry portrays the class of gelation instrument that can accomplish high specificity and exact spatiotemporal control whereby a particular impetus is exploited and the polymer chains are correspondingly modified [43]. However, the click chemistry mechanism requires usage of heavy metal, which leads to the toxicity of the hydrogel scaffold.

3.1.3 Biological Cross-Linking

Biological cross-linking usually involves enzyme-mediated reaction and molecular recognition and the use of bioactive particles. One such example of cross-linking is through the use of enzymes. By understanding the kinetics of the enzymes, it is utilised to catalyse the gelation development process. For instance, horseradish peroxidase is a protein with the presence of hydrogen peroxide that oxidises phenols to initiate carbon-oxygen (C-O) bond or carbon-carbon (C-C) bond between the two phenols [33].

Another major biological cross-linking approach is biomolecular recognition. Recognition and signalling molecules, such as antigen and antibody, transmembrane proteins and ligands are essential and abundant in organisms to perform basic life functions. Takashi Miyata et al. has reported a framework embracing immunoglobulin G (IgG) as the antigen and antibody [47] whereby IgGs facilitate the aggregation of monomers and consequently result in the gelation of the hydrogel.

Each of these gelation systems has its pros and cons. For instance, physical cross-linking approaches are feeble, while chemical cross-linking approaches are stronger mechanically. In the case of chemical cross-linking approach, it frequently involves chemicals that bring negative effects to the cells. For biological cross-linking, the use of bioactive particles is prone to denaturation or degradation and thus can be unstable. The pros and cons of each gelation system are illustrated in Table 3.1 and the schematic graph are shown in Fig. 3.1.

3.2 Methodology to Incorporate Bioactive Factors into the Hydrogels

Hydrogel is often custom designed as a vehicle of cells, drugs and bioactive molecules. In regenerative medicine, hydrogel is often used to deliver cells to the desired site. Numerous studies have incorporated bioactive molecules to either mimic the native tissue environment or to provide signal to the encapsulated cells so as to enhance the process of tissue regeneration.

The bioactive elements can be incorporated into the hydrogel platforms in different approaches. Similar to the gelation system, these approaches can be classified into physical, chemical and biological approaches. Physical methodologies include basic blending and physical forces. Blending the bioactive factors directly into the hydrogel is a straightforward approach but often meets with issues such as a burst discharge of the bioactive factors while a more managed and controllable discharge is desired. To achieve a much controllable discharge of bioactive factors, the interaction of hydrophobic strengths or the electrostatic forces between two elements can be tailored. Although this approach is only applicable to charged particles, many biological particles are charged, for instance, human growth hormone [54] and siRNA [31]. These particles are negatively charged and result in a more stable

Table 3.1 Different cross-linking mechanisms and their respective advantages and disadvantages

Cross-linking mechanism		Pros	Cons
Physical	Self-assembly	No external chemicals involved; reversible; reacting to external stimuli like pH, temperature and presence of ions	Mechanically weak
	Ionic cross-linking		Charged loaded drugs may interfere with the cross-linking
Chemical	Photo-cross-linking	Spatiotemporal control on gelation based upon the direction, location and timing of the light and the photoinitiator	Extra light source and photoinitiators are required
	Michael addition	High specificity; controllable gelation kinetics	Potentially toxic chemicals involved
	Disulphide formation		
	Click chemistry		
	Schiff's base reaction	Mild gelation	Low specificity due to the abundance of amine groups in various growth factors and extracellular matrix
Biological	Enzymatic cross-linking	High specificity	Requirement on suitable conditions for enzyme to be active; due to the catalyst nature of enzymes, it remains active after cross-linking which leads to other side effects
	Biomolecule recognition		Could be mechanically weak due to rapid degradation

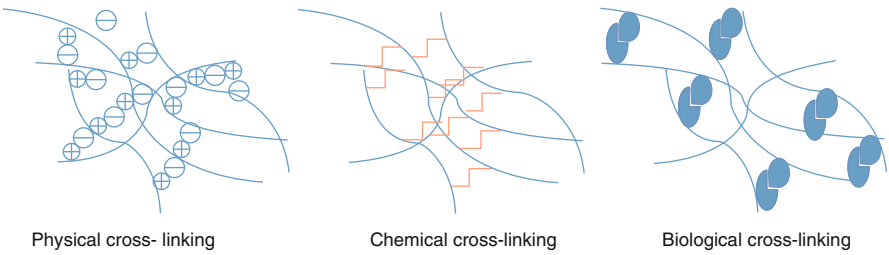

Fig. 3.1 Graphical illustration of physical, chemical and biological cross-linking mechanism

and controllable discharge of the bioactive factors with reduced starting burst. The release profile could be controlled by the charge density of the hydrogel; its discharge rate can be adjusted by varying the pH. A more extreme pH leads to a higher discharging rate.

Chemical approaches involving covalent bonding between the bioactive factors and hydrogel usually require the components to have a functional group, such as carboxylic group, amine group or thiol group. For instance, doxorubicin, a widely

used anticancer drug, contains an amine group which can be incorporated into a hydrogel containing polyphosphazene to achieve a more spatiotemporally controlled release with minimal toxicity [10]. This method is in large advantage especially when compared with the physical approach since it is applicable to hydrophobic particles too. However, it is of concern that after the covalent bonding, the bioactivity of the particles is lost due to the loss of a functional group.

Biological methodologies comprise of two sections; either the consolidation depends on the bioactivity of the particles that structures the hydrogel or the discharging of the therapeutics is reliant on the natural properties of the framework.

On one hand, to incorporate bioactive factors in to the hydrogel scaffold, natural binding processes are adopted, which means the fuse could likewise be because of the affinity between two organic recognition particles, including acknowledgement between two single strands of DNAs [64] and tying between two chains of peptides or proteins [72]. By means of this strategy, a maintained discharge is accomplished because of the larger binding energy between the hydrogel and the bioactive components and in the meantime, the binding capacity is better maintained. However, this present technique's discharge profile is still a burst at the beginning and reaches plateau later, where the distinction is that the underlying burst is not as intense as the straightforward blending. It is basically a milder discharge taking after the same pattern. Hence it is better that a fully controlled discharge could be accomplished. Thus on demand discharge is widely studied.

The fully controllable release is achieved by the hydrogel that will be debased based on the cell expansion status or the in vivo environment around the hydrogel. To make the debasement course of hydrogels match the cell multiplication profile, natural particles are embedded into the hydrogel system. Ordinarily cleavable locales will be fastened to the hydrogel polymers. The purported cleavage site is the substrates to specific compounds discharged by the cell in the expansion process. Accordingly, when the cells multiply abundant enough, it debases the hydrogels, and the bioactive element is further discharged to bolster the development of cells. This kind of framework is greatly valuable as a result of its responsive property to certain outside stimuli. For instance, a synthetic insulin-emitting vehicle is utilising this sort of scaffold. Numerous strategies have been used to make the hydrogel sensitive to glucose. One compound used is called glucose oxidase which can process glucose into gluconic acid [29]. As a result, the pH surrounding the hydrogel decreases and the degradation process is accelerated. Not only glucose oxidase but also concanavalin A [4] and phenylboronic acid [32] are adopted in integrating glucose-responsive hydrogel. Other than glucose, numerous different signs have been investigated to empower the arrival of bioactive factors, for example, mechanical signals [35], light [73], antigens [13] and electric field [48].

From the above examination, it is clear that each of the bioactive factor incorporation strategies has its own strengths and weaknesses. They are summarised in Table 3.2. Subsequently, to realise the best bioactive discharge impact, a combinational hydrogel is researched. An established model of combinational hydrogel is a hydrogel containing nanoparticles or microspheres within the framework. Through

Table 3.2 Summary of advantages and disadvantages of various bioactive factor incorporation methods in hydrogel

Incorporation method		Advantages	Disadvantages
Physical	Simple mixing	Straightforward	Initial burst
	Electrostatic force	Controlled release	Only applicable to ionic or polar molecules
	Ionic force		
Chemical	Covalent link	Sustained release	Potential damage to the function of bioactive factors
Biological	Incorporation	Sustained release	Hydrogels are to be synthesised or modified to improve the affinity with bioactive factors
	Release	Controlled release	Risks due to the application of external stimuli

this complexation, the therapeutics could be discharged in a prolonged and controlled way simultaneously.

3.3 Function of Bioactive Hydrogels

The motivation behind such a variety of strategies to manufacture the hydrogel-based scaffolds and join diverse sorts of bioactive factors into the framework is its application. The bioactive hydrogels could be utilised to direct cell destiny, and in turn cells could coordinate the hydrogel's "destiny". This interactive relationship mimics the genuine tissues well. Accordingly, bioactive hydrogels are helpful in drug delivery and tissue engineering and numerous different territories, for example, biological glue and production of integral cell sheets which could improve medicine and benefit the patients.

3.3.1 Bioactive Hydrogel Directs Cell Fate

It is generally realised that cell destinies are influenced by the situations encompassing the cells. The environment could influence the cells' multiplication, differentiation, apoptosis, migration and secretion [14]. The examination of bioactive hydrogel in coordinating cell destinies began from the two-dimensional level, essentially in a petri dish, on a culture plate or on the surface of the hydrogels. Step by step, the examination began to concentrate on the three-dimensional stereoscopic hydrogel system which is altogether different from the 2D condition yet is quite nearly mimicking the genuine in vivo environment.

3.3.1.1 Bioactive Hydrogel Directs Cell Fate in 2D Environment

Naturally derived hydrogels are bioactive; they suit the advancement of cells. However, they might incite immunology impacts. And the batch-to-batch variation is large. Moreover, the control from the researcher is imprecise. Synthetic materials are definitely controlled by the researcher. However numerous synthetic materials do not have the favour of the cells. In this manner, adhesive ligand structures are consolidated into the engineered hydrogel framework to build the bond and affinity between cells and hydrogels [11]. For instance, a peptide grouping found in common adhesive proteins, such as fibrin, collagen and laminin – arginine-glycine-aspartic acid (RGD) tripeptide – is joined into the hydrogel system to enhance its cell adhesion [57]. Cells can be categorised into anchorage-dependent and non-anchorage-dependent cells. Both of them actually tend to attach to a surface; while the anchorage-dependent cells can survive only if they are attached to a surface [40], the non-anchorage-dependent cells are still able to survive without attaching to a surface, and attachment to a surface initiates differentiation of the cell lineage. Other than cell adhesion, ligands' density and dispersion pattern in hydrogel-based platform also influence the expansion, apoptosis, migration [34] and morphology of cells [53]. A higher ligand density is more suitable for the attachment of cells. Normally a more adhesive surface is more suitable for the proliferation of cells. However, if the surface is too cell adhesive, the cell migration is diminished and thus the cell proliferation is prohibited.

The stiffness and elasticity are well known to be influential to the differentiation of cells. Generally speaking, a harder material is more suitable for the differentiation of stem cells into osteogenic cells [21]. On the other end, a softer material is more suitable for the differentiation of stem cells into endothelial cells and smooth muscle cells [58]. Those materials with a medial range of stiffness are more suitable for the differentiation into skeletal muscle cells, myogenic muscle cells, chondrocytes and neural cells [20]. The scope of stiffness that is suitable for the cell to develop is a few kilopascals. From a more general perspective, a relative stiffer surface is more suitable for the attachment of cells [13] and hence affects the movement of cells along the gradient towards a stiffer surface [39].

Other than the density of the ligands and the solidness of the material, a more delegate control on cell destiny could be accomplished by controlling the pattern of the ligands or the topology of the ligands. One basic shape is the square zone. As indicated by Ingber et al., a square island with edge length under 10 μm is not suitable for the living of cells, while a square island with edge length more than 25 μm is most favourable for the proliferation of cells [7]. On the top of size, the shape of the adhesive points assumes an indispensable part too. Channels or nano-gratings are more suitable for the differentiation into neural cells or muscle cells which need an alignment to be functioning [9], and micro- or nano-pit surfaces at a suitable size in a rectangle or square shape are proper for the differentiation into osteoblasts [12].

With the effectiveness of the hydrogel influencing the cell destiny on a surface, three-dimensional spaces which are more like in vivo conditions are the focus of research currently.

3.3.1.2 Bioactive Hydrogel Directs Cell Fate in 3D Environment

Based on the experience in directing cell fate on a surface plane, cell-adhesive proteins or peptide sequences are incorporated into the spatial hydrogel network to improve the affinity to the cells. The same sequences found effective on a plane are adopted in the spatial network and still reported as effective [75]. Peptides, as a biochemical signal grafted in the hydrogel, can be manipulated to vary the cell material interaction property of the network. Stiffness is also found to be able to direct the cell differentiation in three-dimensional spatial environments similar to the stiffness study on a plane. It is found that 2.5 kPa induces the differentiation to adipose cells while 110 kPa induces the differentiation towards osteogenic direction [27]. The scale of the pressure is much larger than in a surface environment. Nevertheless, the trend is the same, meaning a tougher material is more inductive towards the osteogenesis, while a softer environment is more towards the softer tissues, such as adipose tissues.

When the hydrogels are fabricated, the expected cell adhesion or stiffness properties are presented at the beginning, but gradually the control on these properties is lost due to the degeneration of the peptides or hydrogels. Therefore, research is conducted to add in temporal control on the system. Photopolymerisation is one method [17]. The light needs to be applied manually. Although this method is able to generate locally specific control of gelation or hardening of the scaffold material, however the process is not reversible and the material can only become tougher than before. Thus, later a photodegradable compartment is added to the system. Hence, a photoreversible system is fabricated [15]. Like the controlling of chemical signals, the incorporation of photodegradable molecules decreases the cross-linking density upon the application of light [22]. Via the incorporation of photo-cross-linker and photodegradable molecules, a dynamic hydrogel is invented. This is more influential in cell differentiation induction than a static system. According to Young and Engler, the increasing of stiffness during a period of 300 h, which matches the natural development process of a mesoderm to myocardium, results in a more successful differentiation than any static network [74].

3.3.2 Stimuli-Responsive Hydrogel

Bioactive hydrogels can interact with the cells. It is not just the hydrogels that can coordinate the cells' destiny; additionally, the cells can decide the "destiny" of the hydrogel, that is, the degradation profile. As a result, a stimuli-responsive hydrogel is achieved to release cells or bioactive factors on target on time.

When a hydrogel is inside a biological environment, it naturally degrades by hydrolysis. To control the degradation profile is important because when the degradation profile is optimised, the cells' expansion is best regulated. If the degradation rate is too quick, the hydrogel loses its capacity as scaffold, while if the degradation is too slow, it hinders the recovery of tissues. This capacity is acknowledged by the

insertion of biological particles into the hydrogel framework. Those natural particles are substrates to matrix metalloproteinases (MMPs) or collagenases which are abundantly secreted by proliferating cells [42]. Accordingly, when cells multiply, the hydrogels can degrade correspondingly and give space to the expansion of cells. One of the substrates is the bis-cysteine peptide sequence CGPQGIWGQGCR; it is utilised by Jordan S. Miller et al. to encourage the blood vessel invasion. These peptide sequences are incorporated into PEG hydrogels along a line where the endothelial cells are easier to intrude by digesting the peptide sequence and forming in blood vessels [46].

3.3.2.1 Drug Delivery Vehicles

MMP substrates are likewise helpful to discharge therapeutics like growth factors, which ought to coordinate the multiplication status of cells, based on the proliferation status of cells [38]. For example, a modified VEGF growth factor is incorporated into a fibrin-based scaffold by a research team in Zurich University; upon the degradation of fibrin by plasmin, the VEGF is released and induces angiogenesis [18]. Other than a discharge profile corresponding to a cell development profile, other controlled deliveries of medications on target are likewise in need. The arrival of medications in response to pH is valuable in the treatment for cancers. Around cancer cells, the pH is lower [55]. Therefore, the hydrogels that degrade much faster under acidic conditions are great delivery vehicles for medications hostile to cancer to minimise side effects. As a rule, the hydrogel perfect to be the medication delivery vehicle ought to have the capacity to discharge drugs at a particular site with a controlled rate.

Different from the fancy delivery vehicles mentioned in the previous paragraph, a fundamental delivery vehicle is a covering for the therapeutics to prevent the damage from the cruel environment in the stomach [62], since oral administration is practically the most convenient method for dosing. Without a shell, numerous medications will be degenerated in the extreme acidic condition in the stomach and lose their capacity. Alginate is one of such a material which can resist the low-pH condition. The assurance on medications and a maintained discharge are relied upon hydrogel vehicles. This is helpful in the delivery of medications that should be taken persistently. The use of managed discharge can diminish the recurrence of dosage and provide convenience to patients [63].

3.3.2.2 Cell Delivery Vehicles

A bioactive hydrogel-based scaffold is helpful in the delivery of medications as well as cells. These vehicles are generally utilised as a part of tissue engineering. The alleged tissue engineering is to convey right cells into the right site to recover the harm on tissues or organs. The advantage of cells on a scaffold compared with cells

without a scaffold is the reduction on cell migration and immune response as well as improvement on cell viability.

Factors to be considered in fabrication of hydrogels for tissue engineering is cell adhesion, bioactive factor delivery and degradation profile. This could be accomplished by incorporation of cell-adhesive peptide sequence, bioactive factors and catalyst-cleavable moieties. These days, the clinically accessible tissue engineering items include the skin, cartilage and cornea.

3.3.3 Other Functions

In the previous part, it is discussed that good hydrogels need to have the property of cell adhesion. However, in some unique utilisation of hydrogels, it is non-cell adhesion that is a profitable property. This sort of material is utilised as adhesion evasion after the surgery to avoid entanglements. It can likewise be utilised to treat urinary incontinence [2].

The three-dimensional hydrogel system is not just successful in conveying medications and cells. It has in vitro application also. It can be utilised as a testing model. As examined beforehand, the cell status on a plane is altogether different from that in a stereo space. However, the genuine environment in a living organism is a stereo space. This clarifies why numerous therapeutics are effective in the in vitro test yet comes up ineffective in the animal test. Thus to enhance the effectiveness of the drug testing process, three-dimensional in vitro cell cluster models are invented. The model comprises of a hydrogel scaffold and the objective cells dwelling in the scaffold.

As discussed in the first section, some hydrogels can gel spontaneously or under certain stimuli. This kind of phase change from solution to colloid is helpful as a bio-glue to seal the sutures after surgery. In addition, this phase change is utilised to produce intact cell sheet. The poly N-isopropylacrylamide (PNIPAm) is utilised as it is able to change from hydrophilic to hydrophobic under different temperatures. In this way, researchers have created clinically applicable cornea and treat visual deficiency [51].

3.4 Classical Example: Polyethylene Glycol (PEG)

PEG is a gold standard hydrogel in tissue engineering. Because of nomenclature, it is also called poly(ethylene oxide) (PEO). PEG is a prevalently studied synthetic polymer in the tissue engineering field. To compensate the weaknesses of a PEG as a synthetic material, including absence of cell attachment and lack of control on degradation rate, modifications on PEG are made.

3.4.1 Cell Adhesion

PEG is a very hydrophilic polymer, which is not most favoured by cells. The material that is most suitable for the attachment of cells is moderately hydrophobic in those hydrophilic materials. It is demonstrated by the low viability of anchorage-dependent cells inside PEG hydrogels [6]. The natural extracellular matrix (ECM) is the best model to be imitated to accomplish cell adhesion. The ECM is for the most part composed of proteins and glycosaminoglycans (GAGs); a few GAGs can connect to some serine-rich proteins to form proteoglycans (PGs) [68]. Among the proteins, collagen, elastin, fibrin and laminin are the most plenteous and common ones. Collagen is a moderately intense molecule and maintains the structure of ECM, while elastin gives flexibility to the ECM. Fibrin and laminin are cell-adhesive molecules. And GAGs are likewise partially taking the mechanical loadings on the ECM and all the more vitally they permit the pass and reservation of supplements and signal particles [68].

To mimic the cell-adhesive natural ECM, the peptide sequences isolated from the ECM proteins have been incorporated to the hydrogel. The common sequences are RGD [44], KQAGDV [23], REDV [69] and PHSRN [70] from fibrin; YIGSR [70], IKVAV [67], PDGSR [67], LRE [70], LRGDN [67] and IKLLI [67] from laminin; GFOGER [45] from collagen; and VAPG [76] from elastin. In these peptides, RGD is the most broadly utilised and thoroughly studied on in light of the easy isolation and early revelation of the peptide. RGD could be connected to the PEG hydrogel by most of the beforehand specified strategies, including photo-cross-linking, Michael addition, click chemistry and enzymatic cross-linking [16]. When a chemical strategy is used, the PEG is added with an acrylate group so that there are chemical groups to react. There are two types of RGD; one is linear and the other is cyclic. It is found that the cyclic RGD has better cell-adhesive function than linear RGD, which is because it is a better imitation to native RGD structure. It improves the cell adhesion more than 200 times contrasted to its linear form [24].

3.4.2 Degradation Profile

To make the hydrogel framework degrade coordinating the development profile of cells, which is another property of the regular ECM, biologically active particles are mixed inside the hydrogel polymers. When PEG is first invented, the enzyme-sensitive molecules have not been discovered. Alteration has been made on PEG hydrogel to make it hydrolytically more degradable. It is accomplished by photopolymerisation of PEG diacrylate cross-linked with ester bond [52] and polyester compartment like polylactic acid (PLA) or polyglycolic acid (PGA) [5]. This kind of degradation is fast but is still linear, which does not coordinate the expansion profile of cells. Cells expand fast when the cell density is low but reaches saturation after several generations of duplication. Along with the study on natural tissue

regeneration and development process, it is found that there are biological particles in the extracellular matrix that could be cleaved by the matrix metalloproteinases (MMPs), plasmin and elastase secreted by the regenerating or stem cells in proliferation. Digestion of the ECM opens more space for proliferation and generation of new tissue [65]. Thusly the substrates in this process are fused into the hydrogels. The substrates include GPQG-IAGQ [41] (the "-" line represents the cleavage site), GPQG-IWGQ [36], APG-L [71] and L-GPA [37], which are sensitive to MMPs, and YK-NRD [56] and VR-N [71], which are sensitive to plasmin.

When both cell-adhesive molecule and enzyme substrates are incorporated into a hydrogel, a cell adhesion-varying hydrogel is fabricated by consolidation of a CPENFFRGD peptide sequence, where the PENFF is cleavable by MMP and RGD is a cell-adhesive peptide. In this way, the cell attachment is diminished continuously with the degradation of the gel. This is exhibited as powerful in coordinating stem cells' differentiation into chondrocytes [59].

3.4.3 Recognition of Bioactive Molecules

The GAGs in natural ECM are repositories and paths for signal particles. Hence the ability to carry growth factors is another foundation criterion of a good framework. To unite the growth factors tightly to the hydrogel-based scaffolds, the growth factors are modified with functional groups, such as thiol, acryl or azide [77]. Simultaneously, the PEG is modified with functional groups as well so that the growth factors can be covalently linked to the polymer by Michael addition [66]. Chemical incorporation method undertakes the risk of denaturation of bioactivity of the molecules. Therefore, biological incorporation method is researched to carry growth factors in the hydrogel-based scaffolds. The heparin is a biologically active molecule that is incorporated by carboxyl/amine conjugation and is able to recognise growth factors [61]. Other than heparin, those cell-adhesive peptides are also binding sites for growth factors.

3.4.4 Other Applications of PEG

Other than the standard bioactivity of hydrogel, PEG has some unique applications. West et al. have reported the fruitful design of PEG conveying nitrogen monoxide. The PEG hydrogel conveys nucleophiles that can complex with NO [3]. NO can diminish platelet gathering and expands blood vessels. This hydrogel is helpful in the treatment for thrombosis and restenosis.

Because of the high hydrophilicity of PEG, the hydrogel is not favoured by the cells for attachment. Therefore, PEG could be used as a space filler to avoid tissue adhesion after surgery or to treat urine incontinence.

3.5 Bioactive Hydrogel Design Strategy

From the previous content, it is clear that the bioactive hydrogels are very useful and have wide applications in drug delivery and tissue engineering. This section is going to give some design guidelines to help the researchers in designing and fabricating their own bioactive hydrogels fulfilling their goals.

3.5.1 Molecular Design

When the hydrogels are designed, the primary outline is on the molecular formula of the polymer chain. Much the same as in proteins, the primary structure, i.e. the arrangement of the amino acid sequence, decides the secondary and tertiary structures. Similarly, designing on hydrogels' molecular structures determines the functions of the hydrogels. There are two principle classes of procedures. One is top-down design. The other is bottom-up design.

The *top-down* design is to unite the particles having the expected properties or capacities into the hydrogels. As a result, the hydrogels possess the expected property as well. These molecules are generally harvested from the microenvironment around the cells. A typical example is the beforehand mentioned cell-adhesive peptides and proteinase-cleavable peptides.

In turn, the *bottom-up* configuration is to outline the hydrogel synthetically block by block. This is based on the comprehension of the molecular formula of bioactive molecules. Despite the fact that it might confront a synthesis efficiency issue, there is accurate control on the molecules. Typical examples are similar to the copolymer or tripolymer of different monomer pieces in the Pluronic® or Synperonic® PE.

3.5.2 Property Design

Generally, when chemical cross-linking approaches are utilised to gel up the hydrogel, the mechanical property of the gel is strong. When the cross-linking mechanism is physical, the mechanical property is weak. Biological cross-linking's mechanical strength has a wider range; however, the consistency is relinquished.

Cell-adhesive peptide consolidation can enhance cell affinity. The stiffness, ligand density and ligand distribution pattern can control cell spreading, adhesion and the migration orientation. The topology of the substrate materials, density of ligands and stiffness are able to incite differentiation of undeveloped cells. The joining of enzyme-cleavable moieties can accomplish cell expansion coordinating the degradation rate of scaffolds or discharge profiles of growth factors. The ionic, biological molecules and pH-sensitive hydrogels are helpful in outlining on target discharge or controlled delivery of the therapeutics in light of homeostasis status.

References

1. Augst A, Kong H, Mooney D. Alginate hydrogels as biomaterials. Macromol Biosci 2016;6(8):623–33. Science Citation Index, EBSCOhost, viewed 25 January 2016.
2. Bent A, Foote J, Siegel S, Faerber G, Chao R, Gormley E. Collagen implant for treating stress urinary incontinence in women with urethral hypermobility. J Urol 2016;166(4):1354–57. Science Citation Index, EBSCOhost, viewed 16 March 2016.
3. Bohl K, West J. Nitric oxide-generating polymers reduce platelet adhesion and smooth muscle cell proliferation. Biomaterials. 2000;21(22):2273–8. MEDLINE, EBSCOhost, viewed 14 March 2016.
4. Brownlee M, Cerami A. A glucose-controlled insulin-delivery system: semisynthetic insulin bound to lectin. Science. 1979;4423:1190. JSTOR Journals, EBSCOhost, viewed 3 February 2016.
5. Burdick J, Mason M, Hinman A, Thorne K, Anseth K. Research article: delivery of osteoinductive growth factors from degradable PEG hydrogels influences osteoblast differentiation and mineralization. J Control Release. 2002;83:53–63. ScienceDirect, EBSCOhost, viewed 14 March 2016.
6. Cai W. Engineering in translational medicine. [Electronic Resource], n.p.: London: Springer London: Imprint: Springer, 2014., NTU Library Catalogue, EBSCOhost, viewed 14 March 2016.
7. Chen C, Mrksich M, Huang S, Whitesides G, Ingber D. Geometric control of cell life and death. Science. 1997;5317:1425. JSTOR Journals, EBSCOhost, viewed 6 February 2016.
8. Chenite A, Chaput C, Wang D, Combes C, Buschmann M, Hoemann C, Leroux J, Atkinson B, Binette F, Selmani A. Novel injectable neutral solutions of chitosan form biodegradable gels in situ. Biomaterials. 2000;21:2155–61. ScienceDirect, EBSCOhost, viewed 25 January 2016.
9. Choi C, Hagvall S, Wu B, Dunn J, Beygui R, Kim C. Cell interaction with three-dimensional sharp-tip nanotopography. 2007;9, eScholarship, EBSCOhost, viewed 6 February 2016.
10. Chun C, Lee S, Kim C, Hong K, Kim S, Yang H, Song S. Doxorubicin – polyphosphazene conjugate hydrogels for locally controlled delivery of cancer therapeutics. Biomaterials. 2009;30:4752–62. ScienceDirect, EBSCOhost, viewed 1 February 2016.
11. Cushing M, Anseth K. Hydrogel cell cultures. Science. 2007;5828:1133. JSTOR Journals, EBSCOhost, viewed 4 February 2016.
12. Dalby M, Gadegaard N, Tare R, Andar A, Riehle M, Herzyk P, Wilkinson C, Oreffo R. The control of human mesenchymal cell differentiation using nanoscale symmetry and disorder. Nat Mater. 2007;6(12):997–1003. MEDLINE, EBSCOhost, viewed 6 February 2016.
13. Discher D, Janmey P, Wang Y. Tissue cells feel and respond to the stiffness of their substrate. Science. 2005;5751:1139. Expanded Academic ASAP, EBSCOhost, viewed 5 February 2016.
14. DeForest C, Anseth K. Advances in bioactive hydrogels to probe and direct cell fate. Ann Rev Chem Biomol Eng. 2012;3:421–44. MEDLINE, EBSCOhost, viewed 4 February 2016.
15. DeForest C, Tirrell D. A photoreversible protein-patterning approach for guiding stem cell fate in three-dimensional gels. Nat Mater. 2015;14(5):523–31. MEDLINE, EBSCOhost, viewed 14 March 2016.
16. DeLong S, Gobin A, West J. Covalent immobilization of RGDS on hydrogel surfaces to direct cell alignment and migration. J Control Release. 2005;109:139–48. Proceedings of the Twelfth International Symposium on Recent Advances in Drug Delivery Systems, ScienceDirect, EBSCOhost, viewed 14March2016.
17. Drury J, Mooney D. Review: hydrogels for tissue engineering: scaffold design variables and applications. Biomaterials. 2003;24:4337–51. Synthesis of Biomimetic Polymers, ScienceDirect, EBSCOhost, viewed 14 March 2016.
18. Ehrbar M, Djonov V, Schnell C, Tschanz S, Martiny-Baron G, Schenk U, Wood J, Burri P, Hubbell J, Zisch, A. Cell-demanded liberation of VEGF(121) from fibrin implants induces local and controlled blood vessel growth. Circ Res 2016;94(8):1124–32. Science Citation Index, EBSCOhost, viewed 15 March 2016.

19. Elbert D, Pratt A, Lutolf M, Halstenberg S, Hubbell J. Protein delivery from materials formed by self-selective conjugate addition reactions. J Control Release. 2001;76:11–25. ScienceDirect, EBSCOhost, viewed 25 January2016.
20. Engler A, Griffin M, Sen S, Bönnemann C, Sweeney H, Discher D. Myotubes differentiate optimally on substrates with tissue-like stiffness: pathological implications for soft or stiff microenvironments. J Cell Biol. 2004;6:877. JSTOR Journals, EBSCOhost, viewed 5 February 2016.
21. Engler A, Sen S, Sweeney H, Discher D. Matrix elasticity directs stem cell lineage specification. Cell. 2006;126(4):677–89. MEDLINE, EBSCOhost, viewed 5 February 2016.
22. Fan W, Tong X, Yan Q, Fu S, Zhao Y. Photodegradable and size-tunable single-chain nanoparticles prepared from a single main-chain coumarin-containing polymer precursor. Chem Commun 2016;50(88):13492–94. Science Citation Index, EBSCOhost, viewed 14 March 2016.
23. Girotti A, Reguera J, Rodríguez-Cabello J, Arias F, Alonso M, Matestera A. Design and bioproduction of a recombinant multi(bio)functional elastin-like protein polymer containing cell adhesion sequences for tissue engineering purposes. J Mater Sci Mater Med. 2004;15(4):479–89. MEDLINE, EBSCOhost, viewed 14 March 2016.
24. Haubner R, Schmitt W, Holzemann G, Goodman S, Jonczyk A, Kessler H. Cyclic RGD peptides containing beta-turn mimetics. J Am Chem Soc. 1996;34:7881. Expanded Academic ASAP, EBSCOhost, viewed 14 March 2016.
25. http://worldaccount.basf.com/wa/NAFTA~en_US/Catalog/ChemicalsNAFTA/pi/BASF/Brand/pluronic. Viewed 22 January 2016.
26. http://www.crodaindustrialchemicals.com/home.aspx?d=content&s=131&r=185&p=6724. Viewed 22 January 2016
27. Huebsch N, Arany P, Mao A, Shvartsman D, Ali O, Bencherif S, Rivera-Feliciano J, Mooney D. Harnessing traction-mediated manipulation of the cell/matrix interface to control stem-cell fate. Nat Mater 2016;9(6):518–26. Science Citation Index, EBSCOhost, viewed 14 March 2016.
28. Huynh C, Nguyen M, Lee D. Injectable block copolymer hydrogels: achievements and future challenges for biomedical applications. Macromol 2016;44(17):6629–36. Science Citation Index, EBSCOhost, viewed 25 January 2016.
29. Ishihara K, Kobayashi M, Ishimaru N, Shinohara I. Glucose induced permeation control of insulin through a complex membrane consisting of immobilized glucose oxidase and a poly(amine). Polym J. 1984;16(8):625–31. J-STAGE, EBSCOhost, viewed 3 February 2016.
30. Kast C, Bernkop-Schnürch A. Thiolated polymers—thiomers: development and in vitro evaluation of chitosan–thioglycolic acid conjugates. Biomaterials. 2001;22:2345–52. ScienceDirect, EBSCOhost, viewed 25 January 2016.
31. Kim Y, Park M, Song S. Injectable polyplex hydrogel for localized and long-term delivery of siRNA. Acs Nano 2016;6(7):5757–66. Science Citation Index, EBSCOhost, viewed 27 January 2016.
32. Kitano S, Koyama Y, Kataoka K, Okano T, Sakurai Y. A novel drug delivery system utilizing a glucose responsive polymer complex between poly (vinyl alcohol) and poly (N-vinyl-2-pyrrolidone) with a phenylboronic acid moiety. J Control Release. 1992;19:161–70. ScienceDirect, EBSCOhost, viewed 3 February 2016.
33. Kobayashi S, Uyama H, Kimura S. Enzymatic polymerization. Chem Rev. 2001;12:3793. Academic OneFile, EBSCOhost, viewed 25 January 2016.
34. Koo L, Irvine D, Mayes A, Lauffenburger D, Griffith L. Co-regulation of cell adhesion by nanoscale RGD organization and mechanical stimulus. J Cell Sci. 2002;115(Pt 7):1423–33. MEDLINE, EBSCOhost, viewed 5 February 2016.
35. Lee K, Peters M, Mooney D. Controlled drug delivery from polymers by mechanical signals. Adv Mater 2016;13(11):837–+.Science Citation Index, EBSCOhost, viewed 3 February 2016.

36. Lee S, Miller J, Moon J, West J. Proteolytically degradable hydrogels with a fluorogenic substrate for studies of cellular proteolytic activity and migration. Biotechnol Prog 2016;21(6):1736–41. Science Citation Index, EBSCOhost, viewed 14 March 2016.
37. Lee S, Moon J, Miller J, West J. Poly(ethylene glycol) hydrogels conjugated with a collagenase-sensitive fluorogenic substrate to visualize collagenase activity during three-dimensional cell migration. Biomaterials. 2007;28:3163–70. ScienceDirect, EBSCOhost, viewed 14 March 2016.
38. Leslie-Barbick J, Moon J, West J. Covalently-immobilized vascular endothelial growth factor promotes endothelial cell tubulogenesis in poly(ethylene glycol) diacrylate hydrogels. J Biomater Sci Polym Ed. 2009;20(12):1763–79. MEDLINE, EBSCOhost, viewed 14 March 2016.
39. Lo C, Wang H, Dembo M, Wang Y. Cell movement is guided by the rigidity of the substrate. Biophys J. 2000;79:144–52. ScienceDirect, EBSCOhost, viewed 5 February 2016.
40. Lüdemann I, Pörtner R, Schaefer C, Schick K, Srámkova K, Reher K, Neumaier M, Franěk F, Märkl H. Improvement of the culture stability of non-anchorage-dependent animal cells grown in serum-free media through immobilization. Cytotechnology. 1995;19(2):111–24. MEDLINE, EBSCOhost, viewed 4February 2016.
41. Lutolf M, Lauer-Fields J, Schmoekel H, Metters A, Weber F, Fields G, Hubbell J. Synthetic matrix metalloproteinase-sensitive hydrogels for the conduction of tissue regeneration: engineering cell-invasion characteristics. Proc Natl Acad Sci USA. 2003;9:5413. JSTOR Journals, EBSCOhost, viewed 14 March 2016.
42. Lutolf M, Raeber G, Zisch A, Tirelli N, Hubbell J.Cell-responsive synthetic hydrogels. Adv Mater 2016;15(11):888–+. Science Citation Index, EBSCOhost, viewed 14 March 2016.
43. Malkoch M, Vestberg R, Gupta N, Mespouille L, Dubois P, Mason A, Hedrick J, Liao Q, Frank C, Kingsbury K, Hawker C. Synthesis of well-defined hydrogel networks using click chemistry. Chem Commun (Cambridge, England). 2006;26:2774–6. MEDLINE, EBSCOhost, viewed 25 January 2016.
44. Mann B, Tsai A, Scott-Burden T, West J. Modification of surfaces with cell adhesion peptides alters extracellular matrix deposition. Biomaterials. 1999;20:2281–6. ScienceDirect, EBSCOhost, viewed 14 March 2016.
45. Mann B, Schmedlen R, West J. Tethered-TGF-b increases extracellular matrix production of vascular smooth muscle cells. Biomater-Guildford. 2001;22(5):439–44. British Library Document Supply Centre Inside Serials & Conference Proceedings, EBSCOhost, viewed 14 March 2016.
46. Miller J, Shen C, Legant W, Baranski J, Blakely B, Chen C. Bioactive hydrogels made from step-growth derived PEG – peptide macromers. Biomaterials. 2010;31:3736–43. ScienceDirect, EBSCO*host*, viewed 1 April 2016.
47. Miyata T, Asami N, Uragami T. A reversibly antigen-responsive hydrogel. Nature. 1999;6738:766. Academic OneFile, EBSCOhost, viewed 26 January 2016.
48. Murdan S. Electro-responsive drug delivery from hydrogels. J Control Release 2016;92(1–2):1–17. Science Citation Index, EBSCOhost, viewed 3 February 2016.
49. Nguyen M, Alsberg E. Bioactive factor delivery strategies from engineered polymer hydrogels for therapeutic medicine. Prog Polymer Sci 2016;39, Topical Issue on Biomaterials, pp. 1235–65, ScienceDirect, EBSCOhost, viewed 25 January 2016.
50. Nguyen K, West J. Photopolymerizable hydrogels for tissue engineering applications. Biomaterials. 2002;23:4307–14. Injectable Polymeric Biomaterials, ScienceDirect, EBSCOhost, viewed 25 January 2016.
51. Nishida K, Hayashida Y, Yamamoto K, Maeda N, Nagai S, Kikuchi A, Tano Y, Okano T, Watanabe H, Adachi E, Watanabe K, Yamato M. Corneal reconstruction with tissue-engineered cell sheets composed of autologous oral mucosal epithelium. N Engl J Med. 2004;12:1187. Expanded Academic ASAP, EBSCOhost, viewed 14 March 2016.
52. Nuttelman C, Rice M, Rydholm A, Salinas C, Shah D, Anseth K. Macromolecular monomers for the synthesis of hydrogel niches and their application in cell encapsulation and tissue engineering. Prog Polymer Sci 2016;33(2):167–79. Science Citation Index, EBSCOhost, viewed 14 March 2016.

53. Palecek S, Loftus J, Ginsberg M, Lauffenburger D, Horwitz A. Integrin-ligand binding properties govern cell migration speed through cell-substratum adhesiveness. Nature. 1997;6616:537. Expanded Academic ASAP, EBSCOhost, viewed 5 February 2016.
54. Park M, Chun C, Ahn S, Ki M, Cho C, Song S. Cationic and thermosensitive protamine conjugated gels for enhancing sustained human growth hormone delivery. Biomaterials. 2010;31:1349–59. ScienceDirect, EBSCOhost, viewed 27 January 2016.
55. Patra S, Roy E, Karfa P, Kumar S, Madhuri R, Sharma P. Dual-responsive polymer coated superparamagnetic nanoparticle for targeted drug delivery and hyperthermia treatment. ACS Appl Mater Interfaces. 2015;7(17):9235. Supplemental Index, EBSCOhost, viewed 14 March 2016.
56. Pratt A, Weber F, Schmoekel H, Muller R, Hubbell J. Synthetic extracellular matrices for in situ tissue engineering. Biotechnol Bioeng 2016;86(1):27–36. Science Citation Index, EBSCOhost, viewed 14 March 2016.
57. Ruoslahti E, Pierschbacher M. New perspectives in cell adhesion: RGD and integrins. Science. 1987;4826:491. JSTOR Journals, EBSCOhost, viewed 4 February 2016.
58. Saha K, Keung A, Irwin E, Li Y, Little L, Schaffer D, Healy K. Substrate modulus directs neural stem cell behavior. Biophys J. 2008;95:4426–38. ScienceDirect, EBSCOhost, viewed 5 February 2016.
59. Salinas C, Anseth K. The enhancement of chondrogenic differentiation of human mesenchymal stem cells by enzymatically regulated RGD functionalities. Biomaterials. 2008;29:2370–7. ScienceDirect, EBSCOhost, viewed 14 March 2016.
60. Seliktar D. Designing cell-compatible hydrogels for biomedical applications. Science (New York, NY). 2012;336(6085):1124–8. MEDLINE, EBSCOhost, viewed 20 January 2016.
61. Seliktar D, Zisch A, Lutolf M, Wrana J, Hubbell J. MMP-2 sensitive, VEGF-bearing bioactive hydrogels for promotion of vascular healing. J Biomed Mater Research Part A 2016;68A(4);704–16. Science Citation Index, EBSCOhost, viewed 14 March 2016.
62. Sharpe L, Daily A, Horava S, Peppas N. Therapeutic applications of hydrogels in oral drug delivery. Expert Opin Drug Delivery 2016;11(6):901–15. Science Citation Index, EBSCOhost, viewed 14 March 2016.
63. Singla A, Garg A, Aggarwal D. Paclitaxel and its formulations. Int J Pharm. 2002;235:179–92. ScienceDirect, EBSCOhost, viewed 1 February 2016.
64. Soontornworajit B, Zhou J, Shaw M, Fan T, Wang Y. Hydrogel functionalization with DNA aptamers for sustained PDGF-BB release. Chem Commun (Cambridge, England). 2010;46(11):1857–9. MEDLINE, EBSCOhost, viewed 2 February 2016.
65. Sternlicht M, Werb Z. How matrix metalloproteinases regulate cell behavior. Ann Rev Cell Dev Biol. 2001;17(1):463. Academic Search Premier, EBSCOhost, viewed 14March 2016.
66. Tallawi M, Rosellini E, Barbani N, Cascone M, Rai R, Saint-Pierre G, Boccaccini A. Strategies for the chemical and biological functionalization of scaffolds for cardiac tissue engineering: a review. J R Soc Interf R Soc. 2015;12(108):20150254. MEDLINE, EBSCOhost, viewed 14 March 2016.
67. Tsang V, Chen A, Cho L, Jadin K, Sah R, DeLong S, West J, Bhatia S. Fabrication of 3D hepatic tissues by additive photopatterning of cellular hydrogels. FASEB J 2007;3. AGRIS, EBSCOhost, viewed 14 March 2016.
68. Uzman A. Molecular cell biology (4th edition). Biochem Mol Biol Educ. 2001;29(3):126–8. British Library Document Supply Centre Inside Serials & Conference Proceedings, EBSCOhost, viewed 14 March 2016.
69. Weber L, Hayda K, Haskins K, Anseth K. The effects of cell-matrix interactions on encapsulated b-cell function within hydrogels functionalized with matrix-derived adhesive peptides. Biomater-Guildford. 2007;28(19):3004–11. British Library Document Supply Centre Inside Serials & Conference Proceedings, EBSCOhost, viewed 14 March 2016.
70. Weber L, Anseth K. Hydrogel encapsulation environments functionalized with extracellular matrix interactions increase islet insulin secretion. Matrix Biol. 2008;27:667–73. ScienceDirect, EBSCOhost, viewed 14 March 2016.

71. West J, Hubbell J. Polymeric biomaterials with degradation sites for proteases involved in cell migration. Macromol 2016;32(1):241–4. Science Citation Index, EBSCOhost, viewed 14 March 2016.
72. Xun W, Wu D, Li Z, Wang H, Huang F, Cheng S, Zhang X, Zhuo R. Peptide-functionalized thermo-sensitive hydrogels for sustained drug delivery. Macromol Biosci. 2009;9(12):1219–26. MEDLINE, EBSCOhost, viewed 2 February 2016.
73. Yan B, Boyer J, Habault D, BrandaN, Zhao Y. Near infrared light triggered release of biomacromolecules from hydrogels loaded with upconversion nanoparticles. J Am Chem Soc 2016;134(40):16558–61. Science Citation Index, EBSCOhost, viewed 3 February 2016.
74. Young J, Engler A. Hydrogels with time-dependent material properties enhance cardiomyocyte differentiation in vitro. Biomaterials. 2011;32:1002–9. ScienceDirect, EBSCOhost, viewed 14 March 2016.
75. Zhou M, Smith A, Das A, Hodson N, Collins R, Ulijn R, Gough J. Self-assembled peptide-based hydrogels as scaffolds for anchorage-dependent cells. Biomaterials. 2009;30:2523–30. ScienceDirect, EBSCOhost, viewed 14 March 2016.
76. Zhu J. Review: bioactive modification of poly(ethylene glycol) hydrogels for tissue engineering. Biomaterials. 2010;31:4639–56. ScienceDirect, EBSCOhost, viewed 14 March 2016.
77. Zhu J, Marchant R. Design properties of hydrogel tissue-engineering scaffolds. Expert Rev Med Devices. 2011;8(5):607–26. MEDLINE, EBSCOhost, viewed 14 March 2011.

Chapter 4
Multilayer Microcapsules with Tailored Structures and Properties as Delivery Carriers for Drugs and Growth Factors

Weijun Tong and Changyou Gao

4.1 Introductions

Hollow capsules are of great interest due to their potential applications and fundamental importance as new colloidal structures in areas such as medicine, catalysis, cosmetics, as well as biotechnology [1]. One of the promising methods which can fabricate hollow capsules with tailored structures and functions is the layer-by-layer (LbL) assembly [2, 3] of multilayer films onto colloidal particles, followed by core removal (Fig. 4.1) [4, 5]. Through this method, the capsules with well-controlled size and shape, finely tuned wall thickness, and variable wall compositions have been obtained [6]. The LbL microcapsules with integrated multifunctionality have high capacity for loading of a wide range of substances and sensitive response to diverse stimuli and thus are highly attractive for the biorelated applications [7–9]. At the beginning, the studies of LbL multilayer capsules are mainly focused on the fabrication and basic physicochemical properties [6]. However, the past decade has witnessed a rapid increase of researches concerning their functionalization and applications, particularly in the biomedical fields such as drug delivery [10]. In this chapter, we first focus on the recent progress of the LbL microcapsules in our lab with respect to manipulation of their properties by chemical cross-linking and fabrication of the microcapsules based on new driving forces, the capsules with subcompartments, and the capsules which can transform their shape. Then, we will discuss the potential applications of LbL capsules as drug delivery carriers, emphasizing on the new encapsulation methods developed in our lab, the surface modification of smaller particles, as well as the deformation and recovery behavior of microcapsules passing through a model capillary vessel. Finally, the loading of

W. Tong (✉) • C. Gao
MOE Key Laboratory of Macromolecular Synthesis and Functionalization, Department of Polymer Science and Engineering, Zhejiang University, Hangzhou 310027, China
e-mail: tongwj@zju.edu.cn

© Springer Science+Business Media Singapore 2016

C. Gao (ed.), *Polymeric Biomaterials for Tissue Regeneration*,
DOI 10.1007/978-981-10-2293-7_4

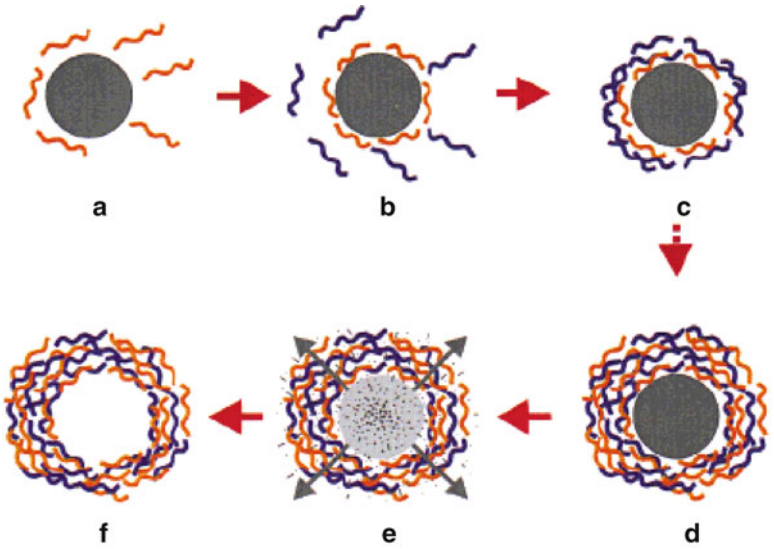

Fig. 4.1 Schematic illustration of the polyelectrolyte deposition process and of subsequent core decomposition (Reprinted with permission from Ref. [5]. Copyright 1998 by Wiley-VCH)

growth factors into multilayer capsules and their incorporation into scaffolds are discussed.

4.2 Multilayer Microcapsules with Tailored Structures, Properties, and Functions

4.2.1 Cross-Linking to Tailor the Properties of Microcapsules

The electrostatic interaction is first used for the fabrication of LbL microcapsules. Although it is generally strong enough to hold the integrity of the microcapsules, in some cases cross-linking is still necessary for the capsules to survive through harsh conditions such as high ionic strength, extreme pH, and strong polar organic solvent [11, 12]. Moreover, cross-linking also can effectively manipulate the permeability and mechanical strength of the capsules. [11, 13]. For the multilayer films and capsules based on hydrogen bonding, further stabilization is also required for biomedical applications since most of them will be disassembled at physiological conditions [14, 15]. Many methods have been developed to cross-link the multilayer films and capsules, such as carbodiimide chemistry [16–18], UV irradiation [13], as well as thermal cross-linking [19]. More recently, disulfide [20, 21] and click chemistry [22–28] have also been proved effective for cross-linking the hydrogen-bonded multilayers and microcapsules.

The above mentioned techniques are exclusively based on a reaction between the functional groups of the two components in the multilayers. We demonstrated that the multilayer microcapsules assembled from poly(allylamine hydrochloride) (PAH) and poly(styrene sulfonate) (PSS) could be considerably stabilized by cross-linking of only the PAH component with glutaraldehyde (GA) [29]. After cross-linking, the capsule wall was apparently thicker and with higher folds. The capsules were quite stable in 0.1 M NaOH even after 24 h. The elasticity modulus (680 MPa) of the capsule walls was doubled compared with that of the control. Furthermore, the permeability of the capsule walls was also greatly reduced after cross-linking. We further applied this method to the poly(ethylenimine) (PEI) and poly(acrylic acid) (PAA) weak polyelectrolyte microcapsules [30]. The cross-linked microcapsules can maintain their macroscopic topology at extreme low or high pH while reorganizing their localized microstructure to enable selective permeation or rejection of macromolecules at lower (< pH 4) and higher pH (> pH 6), respectively. Thus, it is possible to produce capsules that are dual-pH responsive and stable over a broad pH range.

4.2.2 Capsules Directly Assembled Based on Non-electrostatic Interactions

Different driving forces can endow the microcapsules with different physicochemical structures, stimuli response, and thereby their functionality and applicability. At the beginning, the electrostatic interaction was the first driving forces for the LbL assembly [4, 5, 31]; thus the building blocks were mainly charged species. Then hydrogen bonding has been employed for the assembly of microcapsules. Recently, the multilayer hollow microcapsules based on other non-electrostatic interactions such as covalent bonding, host-guest interaction, and bio-specific interactions have been fabricated, which show unique properties.

Covalent LbL-assembled microcapsule is stable enough to withstand the long-time etching of strong polar organic solvent [32]. We recently fabricated a new structure of microcapsules with high modulus and high stability through the covalent LbL assembly (Fig. 4.2) [33]. Aminosilanized SiO_2 microparticles were used as templates. Poly(glycidyl methacrylate) (PGMA) and PAH were alternately immobilized onto the particle surfaces through a coupling reaction between the epoxides and the amines. Thus, a highly cross-linked structure was produced in this process. The templates were removed by HF etching, resulting in hollow microcapsules. The microcapsules are stable in extreme pHs and elevated temperature. Using the method of osmotic-induced invagination [34, 35], the elastic modulus of the microcapsule walls without any treatments was found to be as high as 910 MPa, which is quite stable even under acid and base treatment.

The reaction between amine and aldehyde is fast and efficient in aqueous solution at room temperature; based on this reaction, single polyelectrolyte component

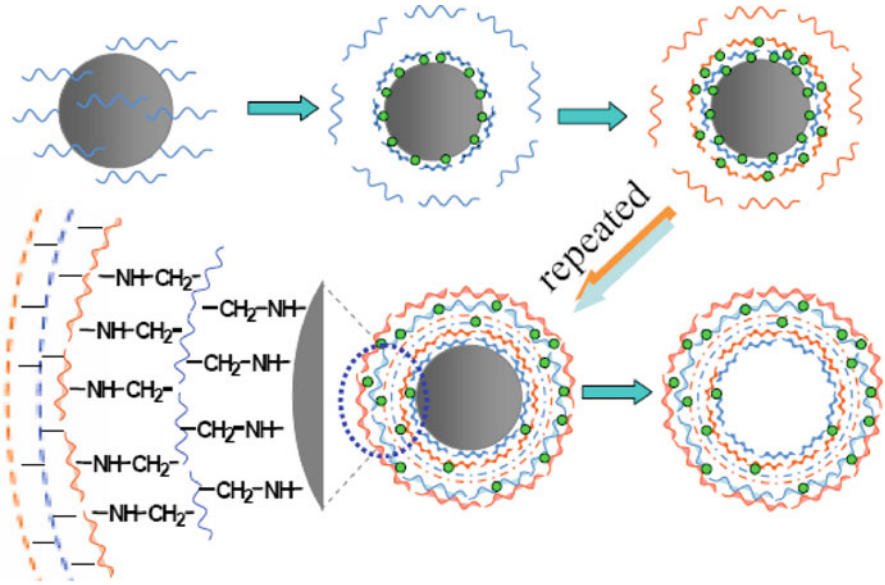

Fig. 4.2 Schematic illustration of the process of direct covalent LbL assembly on a silica particle and fabrication of a hollow capsule by etching out the template core. The *blue lines* represent PGMA, the *red lines* represent PAH, and the *green dots* represent the covalent linkage between layers (Reprinted with permission from Ref. [33]. Copyright 2007 by Wiley-VCH)

multilayers and microcapsules can be fabricated through direct covalent assembly of PAH with GA [36]. The structure and the cutoff molecular weight of the capsule walls are dependent on the molecular weight of used polymers [37]. This method can be applied not only on biomacromolecules with amine groups such as polypeptides and proteins but also on polysaccharides, because GA also can readily react with hydroxyl groups at very mild conditions.

However, the main drawback of the abovementioned methods is that the obtained capsules may largely lose their stimuli-responsive properties due to the uncontrollable covalent reactions [36, 37]. One solution to this problem is to carefully control the content of reactive groups in polymer chains, leading to a controllable reaction degree and a number of functional groups [38]. Bovine serum albumin (BSA) is a kind of biocompatible and biodegradable natural protein. It has a high content of aspartic and glutamic acids, lysine, and arginine [39, 40]. Only the amine groups of lysine can be cross-linked by GA [41], while the other amino acids with free carboxylic groups still exist, which can induce the pH response of the resultant capsules. We recently demonstrated that [42] BSA hollow capsules could be obtained by covalent assembly of BSA and GA on a template followed by core removal. The capsules possessed reversible pH-responsive permeability, which can be used to encapsulate macromolecules.

Host-guest interaction is another type of driving forces frequently employed in supramolecular chemistry. It is known that the host-guest interaction is readily

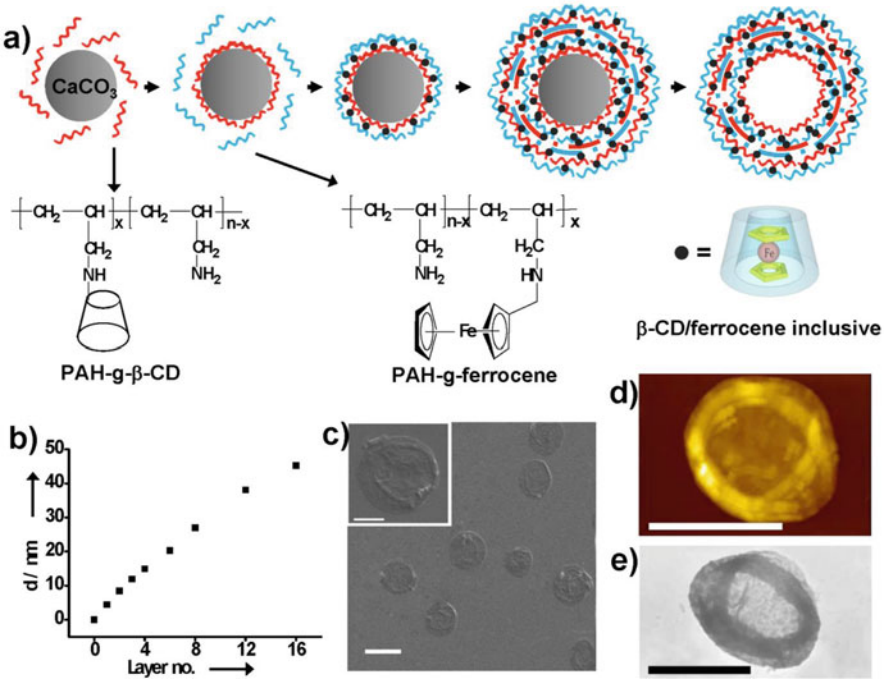

Fig. 4.3 Fabrication process and structure characterization of host-guest microcapsules. (**a**) LbL assembly of same polyelectrolyte on carbonate particles to obtain hollow microcapsules using host-guest interaction. The chemical structure of PAH-g-β-CD, PAH-g-ferrocene, and β-CD/ferrocene inclusive are shown in the second row. (**b**) The thickness of the PAH-g-β-CD/PAH-g-ferrocene multilayers assembled on silicon wafer as a function of layer no. (**c**) SEM, (**d**) SFM, and (**e**) TEM images of the prepared (PAH-g-β-CD/PAH-g-ferrocene)3 microcapsules, respectively; bar is 5 μm. Inset in (**c**) is a higher magnification image of one capsule; bar is 2 μm (Reprinted with permission from Ref. [43]. Copyright 2008, American Chemical Society)

mediated by the host and guest molecules with respect to their matching degree and concentration. If charge interaction is further introduced, multi-responsive microcapsules can thus be expected. According to this design, multilayer microcapsules were fabricated by using the interaction between β-cyclodextrin (β-CD) and ferrocene grafted to a weak polyelectrolyte PAH, which can further introduce charge interaction into the capsule walls (Fig. 4.3) [43]. The microcapsules that consist of PAH-g-β-CD and PAH-g-ferrocene indeed show multi-responsiveness to environmental stimuli. For example, they swell and shrink at low and high pH, respectively. Incubation in a salt or β-CD solution can also mediate their swelling and shrinking behaviors. With these smart features, the microcapsules can serve as reservoirs for drugs, DNAs, enzymes, and so on.

The specific interactions between complementary DNA bases are stable enough under physiological conditions in nature, which can be used for the assembly of multilayer films and capsules [44]. Moreover, carbohydrate-protein interaction,

which is a combination of multiple hydrogen bonding and hydrophobic interactions and participates in a wide variety of biological events [45–47], is also quite stable at physiological conditions. Therefore, this interaction can be used to assemble microcapsules which simultaneously possess good stability and responsiveness to external stimulus due to its non-covalent nature. Concanavalin A (Con A) can specifically bind to polysaccharides such as dextran and glycogen [48–50]; thus it can be utilized to fabricate thin films with them through lectin-carbohydrate interactions [51–53]. These films can respond to glucose [50, 53]. Recently, the hollow capsules assembled by Con A and glycogen through LbL method were also obtained. They are stable at physiological pH range due to the relatively strong multiple hydrogen bonding but still can respond to glucose [54]. The sequential multilayer film growth proceeds successfully on both planar and curved substrates when the Con A molecules adopt confirmation of tetramers or more complicated aggregates. The obtained capsules show layer-number-dependent shell shrinkage, distortion, and densification. The capsules are stable in a pH range of 6–9 and show specific responses to glucose, mannose, fructose, and dextran. Triggered by these stimuli, the preloaded cargoes in the capsules can be released.

4.2.3 Capsules with Subcompartments

The multi-compartmental micro- and nanostructures can be loaded with multiple cargoes and mimic the structure of cells; thus they have received tremendous attention recently [55–58]. Hollow capsules with subcompartments are ideal models which resemble the structure of cells. By combining of other techniques, diverse LbL capsules with different subcompartments have been obtained [59]. The subcompartments can be incorporated through two different ways: wall decoration and interior loading.

Kreft et al. first reported the LbL microcapsules with a shell-in-shell structure for integrated and spatially confined enzymatic reactions [60]. De Geest et al. reported the assembly of multilayers on big hydrogel particles (hundreds of microns) in which tens of hollow LbL microcapsules or microparticles are loaded [57, 61]. Recently, Caruso group incorporated intact liposomes into LbL capsule walls or inside capsules to prepare “capsosomes,” which can be then employed as enzymatic reactors and delivery vehicles for hydrophobic cargoes [62–66].

Alternatively, polymeric micelles also can be incorporated into the walls or interiors of LbL capsules as the subcompartments. The micelles possess advantages of sustained release of hydrophobic substances. In particular, polymeric micelles possess a unique core/shell structure and relatively good stability [67]. Thus the micelle-incorporated microcapsules combine the advantages of both micro- and nanostructures. Polymeric micelles can be loaded into the shell through alternating assembly of poly(styrene-b-acrylic acid) (PS-b-PAA) micelles and oppositely charged polyelectrolyte on templates [68]. After core removal, the as-prepared microcapsules show extraordinary stability in concentrated HCl (37 %) and 0.1 M

NaOH. This extraordinary stability against highly acidic or alkaline conditions is possibly due to the hydrophobic interaction between PS cores of the micelles and hydrogen bonding of the PAA chains in adjacent layers and PAH chains. The incorporation of polymeric micelles in LbL capsule interiors has been presented by Li et al. [69] as well as Tong et al. [70]. In the latter method [70], LbL assembly was conducted on $CaCO_3$ microparticles pre-doped with PS-b-PAA micelles, resulting in encapsulation of micelles after core removal. The micelles inside the capsules can form a chain and network-like structure with more micelles near the capsule walls. Hydrophobic drugs as such can be loaded into the hydrophobic cores of micelles, while the negatively charged PAA corona of the micelles can result in spontaneous deposition [71–75] of water-soluble and positively charged drugs. The apparent concentrations of hydrophobic and water soluble are much higher than that of the feeding values. Therefore, capsules with this synergetic feature show their great promise in loading of drugs with different physicochemical properties.

4.2.4 Shape Transformation of Capsules

The smart capsule systems are of high attraction due to their ability to respond to the alteration of environment conditions. LbL-assembled capsules can change their structure and properties intelligently in response to various stimuli. But most of the intelligence of the hollow structures results from controllable swelling and shrinking, accompanying with permeability change [76]. Less concern is paid to shape transformation of the hollow structures, which is only observed in vesicles and hollow silica spheres previously [77–83]. Recently, single-component microcapsules were fabricated in our lab by an in situ reaction of reactive hydrophobic low-molecular-weight molecules with corresponding PE-doped $CaCO_3$ microparticles, followed by core removal [84, 85].

The first example is the capsules made of ferrocenecarboxaldehyde (Fc-CHO) and PAH-doped CaCO3 microparticles [84]. This single-component microcapsule is stabilized by hydrophobic aggregation of Fc moieties. Due to the redox properties of Fc, the PAH-Fc microcapsules can reversibly swell and shrink in response to oxidation and reduction. At the same time, the permeability also can be changed reversibly. PAH-pyrene (Py) microcapsules also can be fabricated through the reaction of pyrenecarboxaldehyde with the doped PAH [85]. When this kind of capsules is incubated in acidic solution, one-dimensional nanotubes (1D-NTs) or nanorods (1D-NRs) are protruded from the microcapsules. The 1D-NTs keep growing with incubation time and eventually form a network. Meanwhile, the microcapsules are degraded gradually and disappear completely after 144 h (Fig. 4.4). The micelles assembled from PAH-Py polymers treated at similar conditions also can be transformed into one-dimensional structures. The one-dimensional nanotubes are formed by 1-pyrenecarboxaldehyde with ordered π-π stacking and exhibit a helical structure and anisotropic property. The final nanostructures are determined by the different hydrolysis rate of Schiff base at different pH values. The linear PAH also can

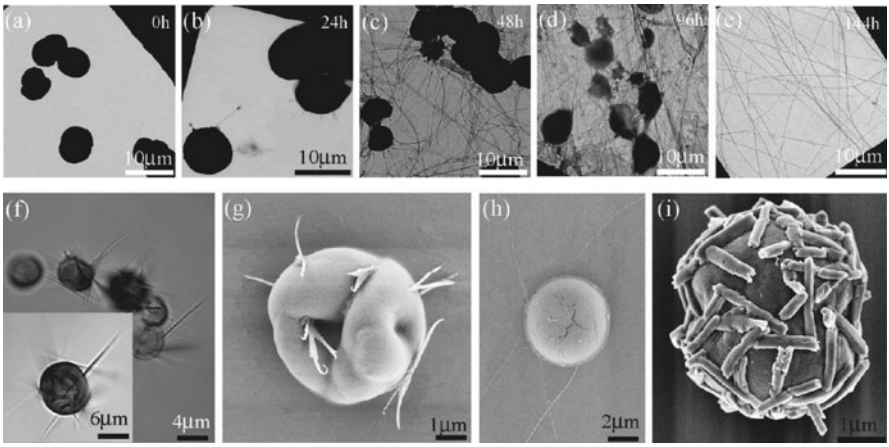

Fig. 4.4 TEM images showing the process of nanotube protruding from the PAH-Py microcapsules incubated in pH 0 HCl for 0, 24, 48, 96, and 144 h, respectively. (**f**) Optical images (inset, a higher magnification) showing the protruded nanotubes from the PAH-Py microcapsules incubated in pH 0 HCl for 30 h. SEM images of a microcapsule with nanotubes after treatment in pH 0 HCl for (**g**) 30 h and (**h**) 72 h, respectively. (**i**) SEM image of a microcapsule with nanorods after treatment in pH 2 HCl for 1 h (Reprinted with permission from Ref. [85]. Copyright 2011, American Chemical Society)

guide the building-up process especially for the nanotubes. Through this mechanism, hollow capsules budded with nanotubes or nanorods mimicking the cellular protrusion of filopodia are successfully fabricated by controlling the incubation time in solutions with different pH (Fig. 4.4).

By chemical cross-linking and surface modification, 1D-NR growth state from the PAH-Py microcapsules can be well controlled [86]. The 1D-NRs also can grow in the LbL-assembled capsules in a controllable manner [87]. For this purpose, PSS/PAH multilayers were assembled on the surface of $CaCO_3$ (PAH-Py) microparticles, yielding PAH-Py and (PSS/PAH)n double-shell capsules. By incubation of the obtained capsules in pH 2 solution, the 1D-NRs grow within the PSS/PAH multilayer capsules in three dimensions. The fluorescence emission intensity of Py NRs inside the capsules can be tuned by a charge-transfer pair. This novel composite structure with PAH-Py NRs inside PE multilayer microcapsules provides a creative strategy for in situ nanomaterials fabrication, illuminating the trend for controllable properties and functions of smart nanodevices. The modulation of the protrusion of NRs also can be achieved by addition of small molecules such as 1-pyrenesulfonic acid sodium salt ($PySO_3Na$) [88], demonstrating the tunable properties of such kind of nanostructures.

Inspired by the above results, PAH-Py NRs consisting of a Py-CHO core and PAH shell can be prepared by surface grafting of PAH onto Py-CHO NRs [89]. After coated with PAH, The NRs become more curved and flexible as a result of partial loss of Py-CHO from the NRs. The PAH-Py NRs with a hydrophilic and charged PAH layer can be suspended stably in water for at least 3 months. Because

of the charge attraction and coordination effect of amino groups, Au NPs can be either adsorbed or in situ synthesized on the PAH-Py NR surface. The initial fluorescence emission of Py is largely remained due to the excellent isolation effect of PAH, which avoids direct contact between Py and the Au NPs. Using the similar process, other hybrid organic-inorganic functional nanomaterials with controlled physicochemical structures can be synthesized, such as tetraphenylethylene (TPE) nanoparticles [90]. TPE-substituted poly(allylamine hydrochloride) (PAH-g-TPE) was synthesized by a Schiff base reaction between PAH and TPE-CHO. The PAH-g-TPE forms micelles in water at pH 6, which are further transformed into pure TPE-CHO nanoparticles (NPs) with a diameter of ~300 nm after incubation in a solution of low pH value. In contrast, only amorphous precipitates are obtained when TPE-CHO methanol solution is incubated in water. The aggregation-induced emission feature of the TPE molecule is completely retained in the TPE NPs, which can be internalized into cells and show blue fluorescence. Formation mechanism of the TPE NPs is proposed by taking into account the guidance effect of linear and charged PAH molecules and the propeller-stacking manner between the TPE-CHO molecules.

4.3 Microcapsules as Drug Delivery Carriers

The LbL-assembled capsules with tailored structures and functions are versatile platforms for encapsulation, storage, and delivery of diverse substances. Thus the LbL-assembled capsules are ideal advanced drug carriers for the delivery of diverse drugs and growth factors. There are already several excellent reviews which summarized the very recent progress in this field [21, 91–99]. The following sections will mainly focus on the recent contributions of our lab to this field.

4.3.1 Controlled Loading Through Spontaneous Deposition

Many applications of the multilayer capsules must face a challenge of efficient loading of the desired substances. This is particularly difficult for loading of low-molecular-weight and water-soluble substances because small molecules can freely diffuse through the capsule walls [100]. We developed the “spontaneous deposition” method, which is based on a mechanism of high affinity of the preloaded substances in the capsules with the cargoes that will be loaded. Gao et al. first found that positively charged molecules such as dextran labeled with tetramethylrhodamine isothiocyanate (TRITC-dextran) could deposit into the aged “hollow” microcapsules templated on melamine formaldehyde (MF) particles with a large amount [71]. The strong fluorescence emitted from the interior of capsules could prove the existence of considerable high concentration of dextran in the capsule interiors (the so-called spontaneous deposition) (Fig. 4.5a). Many other water-soluble substances

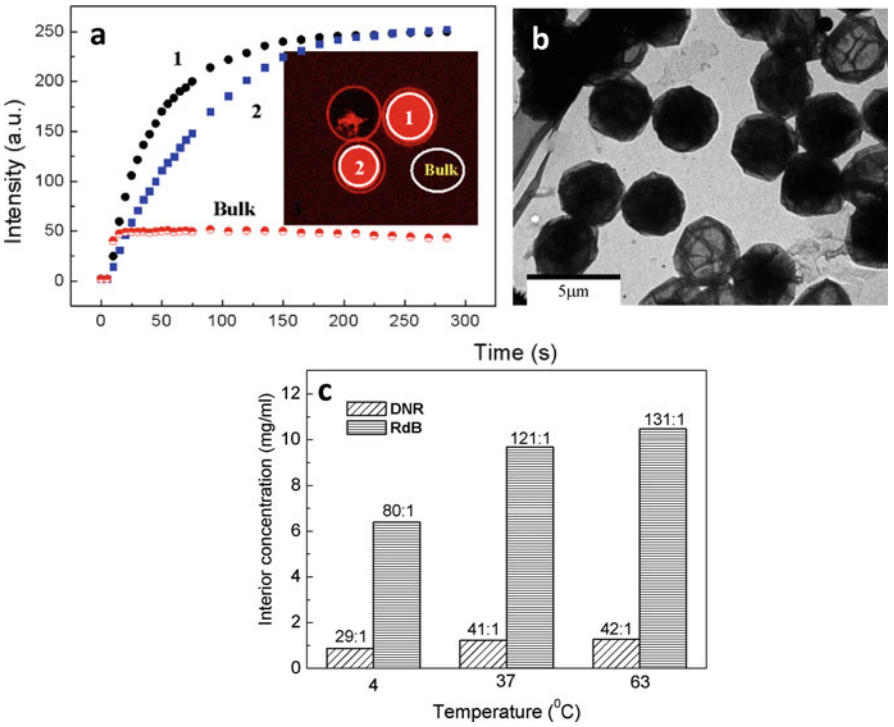

Fig. 4.5 (**a**) Fluorescence intensity averaged from inside the *circles* as a function of incubation time. TRITC-dextran (Mw ~65 kDa) and preformed MF-(PSS/PAH)5 capsules were used. (**b**) TEM images of daunorubicin (DNR) deposited MF-(PSS/PAH)5 capsules. (**c**) DNR and rhodamine B (*RdB*) concentrations in the capsule interior as a function of temperature. MF-(PSS/PAH)4(PSS/PDADMAC)5 capsules were used for DNR with a feeding concentration of 30 mg/ml and MF-(PSS/PAH)5 capsules for RdB, 80 mg/ml. The *numbers* in the figure represent the concentration ratios of capsule interior and bulk. *PDADMAC* = poly(diallyldimethylammonium chloride) (Reprinted with permission from Ref. [73]. Copyright 2005 by Wiley-VCH)

with positive charges such as polyelectrolytes [71], proteins [71], enzymes [72], and low-molecular-weight dyes and anticancer drugs (Fig. 4.5b, c) [73] can be spontaneously deposited with a large quantity. Moreover, the deposition still occurs even if the molecules have very few positive charges such as the TRITC-dextran (Fig. 4.5a), which gets positive charges from a few pendent TRITC groups. The driving force for this phenomenon is the electrostatic interaction between the negatively charged complex (PSS/MF) within the capsule interior and the loaded molecules. The PSS/MF complex is formed by the dissociated PSS from the very initial layer and the positively charged MF degradation product.

The spontaneously deposited low-molecular-weight drugs in the LbL microcapsules templated on MF colloidal particles can be released in a sustained manner [73, 74]. The amount of the loaded drugs can be controlled through changing the feeding concentration of the drugs, temperature, as well as salt concentration. This tailorable

deposition behavior is crucial for control release applications. The loaded drugs can be released in a sustained manner. The release profile can be tuned by changing the interaction between the drugs and the PSS/MF complex. The presence of anticancer drug-loaded capsules can effectively kill HL-60 cells, a kind of human leukemia cell [73].

For better control of the spontaneous deposition property, the capsules can be preloaded with charged polyelectrolyte using a polyelectrolyte-doped template [75, 101–104]. At higher drug feeding concentration and higher salt concentration, large amount of daunorubicin (DNR) and DOX can be loaded [75, 103]. The drug concentration within the microcapsules is hundreds of times higher than the feeding concentration. The drug can be released from the capsules through a diffusion-controlled release mechanism at the initial stage (4 h). The in vitro experiments demonstrate that the encapsulated drug can effectively induce the apoptosis of HepG2 tumor cells. The encapsulated DOX also has better efficacy than that of the free drug in terms of tumor inhibition in a 4-week in vivo culture period [104].

Nonetheless, challenge is still remained to better maintain the drugs inside the capsules and then control their release profile. Previous studies demonstrate that poly(diallyldimethylammonium chloride) (PDADMAC)/PSS capsules with PSS as the outmost layer can shrink dramatically at elevated temperature [105, 106], resulting in a thicker and denser capsule wall. So dextran (Mw from 10 to 70 kDa) can be effectively encapsulated with a slightly higher concentration than the feeding value [107]. The loading of water-soluble small molecular drugs also can be achieved using this method [108]. In our recent work [109], spontaneous deposition and heat-induced shrinkage were combined to fabricate a drug carrier system, showing a high drug loading efficiency and more controllable release profile. Through this strategy, photosensitizers also can be encapsulated, and most of them are stably retained for a long time and protected by capsule wall against reductive enzyme [110].

4.3.2 LbL Assembly on Smaller Particles for Targeting

Most of the LbL capsules have a diameter of a few micrometers, which are too large for intravenous injection. One possible solution is to assemble multilayers on particles with a smaller size. De Koker et al. have reviewed the progress of LbL assembly on ultrasmall (sub-100 nm) particles, which are mainly gold NPs [98]. In our lab, surface modification of biodegradable and nontoxic polyester, poly(lactide-co-glycolide) (PLGA) NPs with a size around 200–300 nm using LbL assembly have been extensively investigated. PLGA is one of the commonly used polymers for drug delivery [111, 112]. These particles with such a size can be injected into the blood vessel and may accumulate in cancerous tissues through the well-known enhanced permeability and retention (EPR) effect. Modification of NP surface with targeting molecules can enhance the drug concentration in the targeted organs or tissues and reduce the dosage and toxic side effects. In order to effectively immobilize the ligands, the NPs should possess enough number of active groups and are

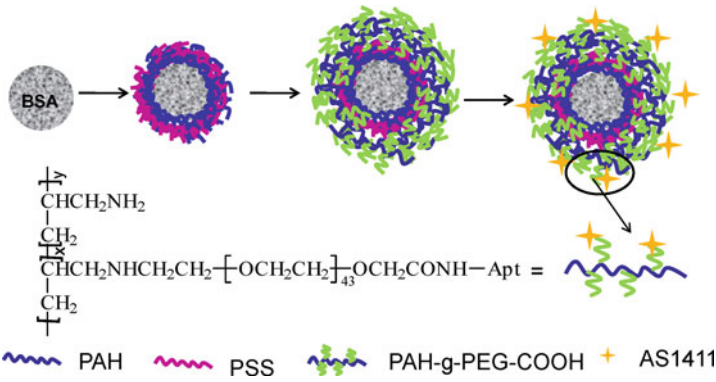

Fig. 4.6 Schematic illustration to show the preparation process of BSA nanoparticles coated with PAH/PSS multilayers and coupled with aptamer AS1411 (Reprinted with permission from Ref. [116]. Copyright 2012 by RSC)

stable enough for following reactions. The LbL assembly can endow the NPs with uniform surface charge density, numerous active groups, and excellent stability in various mediums. For example, PAA/PEI and chitosan (CS)/alginate (CS/ALG) can be used to build multilayers on the PLGA NPs for further immobilization of PEG and folic acid aiming at long-time circulation and targeting [113, 114]. The surface charge and the thickness of the assembled multilayers can greatly influence the release profile of loaded dyes [115]. The surface with negative charges or PEG also can reduce protein adsorption, whereas surface modified with folic acid can enhance the NP uptake by human hepatoma cells.

The multilayers also can be assembled on the NPs before drug loading, and then different drugs can be loaded into the preformed multilayer-coated particles for different applications. In our recent work [116], BSA NPs with a size about 200 nm were coated with PAH/PSS multilayers, onto which a layer of PAH-g-PEG-COOH was further adsorbed. By carbodiimide chemistry, aptamer-AS1411 molecules were immobilized (Fig. 4.6). Aptamer-AS1411 can target to overexpressed nucleolin on cancer cell membrane [117, 118]. The PEGylated multilayer-coated BSA NPs have enhanced colloidal stability even in serum-containing medium [119]. DOX can be effectively loaded into the preformed BSA NPs through electrostatic interaction between negative charges in BSA and positive charges in DOX. The encapsulation efficiency (98.6 %) and loading percentage (9 %) are both very high. The loaded drugs can be released faster at pH 5.5 than at pH 7.4. In vitro cell culture demonstrates that the as-prepared BSA NPs can specifically bind to liver cancer cells, leading to higher cellular uptake and cytotoxicity.

4.3.3 Capsules Squeeze Through a Confined Capillary

Compared with their nanometer-sized counterparts, the LbL microcapsules can be fabricated in an easier way [120]. However, microcapsules are difficult for intravenous injection. But in human blood, the circulation cells have a size of several microns. One example is red blood cell (RBC), which has extreme reversible deformability under physiological flow, so that it can easily pass through the smallest blood capillary vessel (~3 μm). One can imagine that if the capsules have proper shape and flexibility, they may easily squeeze through narrow capillary as natural RBC. This kind of capsules may have great potential applications as drug carriers. The deformability of polymeric microparticles (mainly hydrogel microparticles) with different shapes and sizes through a narrow constriction has been studied under flow conditions. For example, RBC-mimicking particles, which are flexible enough to flow through narrow glass capillaries and able to recover to discoidal shape, have been successfully fabricated [121]. Hayashi et al. demonstrated that 3.5 μm biconcave disk-shaped particles fabricated by electrospraying of cellulose derivative polymers can maintain RBC-like shape after filtrated through a membrane with a pore size of 1 μm [122]. Haghgooie et al. synthesized PEG hydrogel particles with different shapes including disks, rings, crosses, and S-shapes and demonstrated the modes of particles' passage through poly(dimethyl siloxane) (PDMS) channels [123]. However, little is known about the deformation behaviors of multilayer microcapsules with a size similar to RBC under flow in a smaller microchannel [124], although the static deformation behaviors have been systematically studied under the press of a colloidal probe [125] or osmotic pressure [34, 35].

Recently, the deformability of multilayer microcapsules under flow in a confined microchannel was studied in our lab (Fig. 4.7) [126]. The influences of capsule size, wall thickness, cross-linking, and the filling of PSS inside on the deformation and recovery behaviors of the capsules were systematically investigated. The recovery ability of capsules is dependent on the deformation extent but not mechanical strength. The squeezed hollow microcapsules can recover their original spherical shape when the deformation extent is smaller than 16 %, whereas permanent physical deformation takes place at a larger deformation extent such as 34 %. In a sharp contrast, all the intact capsules prefilled with PSS can recover their original shape even when the deformation extent is as large as 47 %. The spontaneously loaded dyes can be well maintained after the deformation and recovery process. It is the first time to disclose the alteration of drug amount in multilayer microcapsules after flowing through a constriction.

Furthermore, the RBC-like multilayer microcapsules also have been successfully fabricated by templating on $Ca(OH)_2$ particles with an RBC-like shape through covalent LbL method. The capsules can preserve their RBC-like morphology well in water after template removal. When the RBC-like capsules (6.7 μm) are trapped in a microcapillary with a smaller size (5 μm), they deform only in the areas in contact with the capillary wall. After they are forced to pass through, 90 % of the RBC-like capsules recover their original discoidal shape. By assembling additional

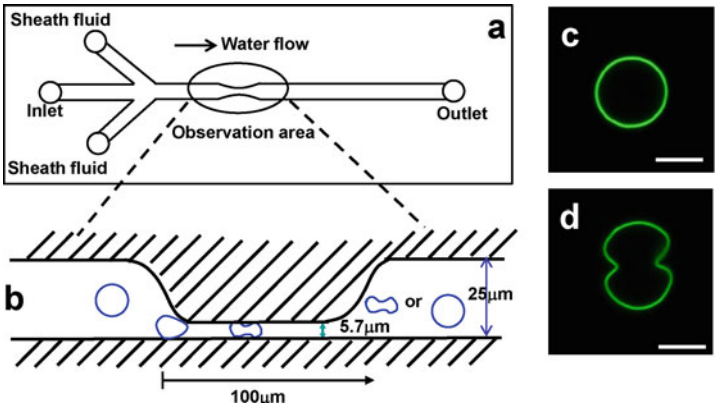

Fig. 4.7 Scheme drawing to show the structure of the microchannel device by (**a**) *top view* and (**b**) *side view*. CLSM images of the 6.8 μm (**c**) and 8.6 μm (**d**) (PAH/PSS)5 microcapsules after being squeezed through the microchannel with a height of 5.7 μm. The former can recover its original spherical shape (**c**), while the latter keeps its deformed shape (**d**) (Adapted with permission from Ref. [126]. Copyright 2012, American Chemical Society)

hemoglobin layers on the RBC-like capsules, they can be endowed with oxygen-binding and release capacity [127].

Yet this is only the first step toward the fabrication of RBC-mimicking multilayer capsules. Nonetheless, the current results are important not only for understanding of capsule properties but also for their practical applications as drug delivery carriers. For example, the capsules for injection application should have a smaller size, soft wall structure, and RBC-like shape, while those for embolization should have a stiff wall which can clog the blood vessels with higher efficiency.

4.3.4 Anisotropic Capsules Interact with Cells

As drug carriers, multilayer capsules should interact with different cells and may be internalized, which is of practical important for delivery of cargoes into cells. Thus their interactions with cells draw much attention recently. It is well known that the physicochemical properties of colloidal particles can strongly influence their interactions with biological systems [128, 129]. Especially, the small differences on their physicochemical characteristics may strongly influence the interactions between particles and cells and further affect their cellular uptake, intracellular distribution, and ultimate cellular fate [130]. Recently, the shape of particles has been found to play a crucial role in the interactions between cells and particles and is regarded as a new important parameter for designing materials to realize specific biological functions [131, 132]. Smith and coworkers [133] demonstrated that the polystyrene particles with three shapes (spheres, prolate ellipsoids, and oblate ellipsoids) could manipulate different attachment and internalization of macrophages. Mitragotri and

coworkers [134] found that compared with rods, the spherical polystyrene particles with identical total volumes exhibited significant perinuclear accumulation. When ovalbumin is used as a model antigen conjugated to particle surfaces, the regulation of immune response could be achieved by changing sizes and shapes of nanoparticles. [135]. Moreover, in a model microvascular network, elongated particles exhibited higher adhesion and binding probability than spheres [136, 137]. In an in vivo experiment, the hydrogel microparticles mimicking the shape of red blood cells could possess the increased blood circulation and enhanced adhesion ability [138].

Polyelectrolyte multilayer microcapsules with tailored structures and properties have gained much interest in biomedical field especially for drug loading and release [10, 91–99]. However, researches about the interactions between anisotropic polyelectrolyte microcapsules and cells are rare [139, 140], and the mechanism of shape-induced difference in interactions between capsules and cells needs further investigation. For example, Caruso and coworkers [139] reported the fabrication of rod-shaped hydrogel capsules with tunable aspect ratios by a templating method. With increasing of the aspect ratios, slower and less cellular internalization of capsules was observed. Kharlampieva and coworkers [140] obtained polymer capsules with hemispherical geometry by drying poly(N-vinyl pyrrolidone)/tannic acid (PVPON/TA)n multilayer capsules and found that compared with their spherical and cubic counterparts, the hemispherical capsules are taken up in a greater extent. However, the mechanism behind is not very clear.

More recently, bowl-like microcapsules were fabricated by osmotic-induced invagination of microcapsule in concentrated PSS solution [141]. Both the bowl-like and spherical capsules maintained their colloidal stability and shape in cell culture medium up to 7 days. The bowl-like microcapsules could be internalized with a faster rate and higher number by SMCs and macrophages than their spherical counterparts. Preferential attachment onto the cell membrane from the bend side and easier enwrapping by cell membranes are likely the major reasons enabling the uptake of the bowl-like capsules in priority than their spherical counterparts. Such results may help people to understand the role of capsule shape in the interaction with cells and provide useful guidance for further design of more efficient carriers.

4.4 Microcapsules as Growth Factor Carriers and Their Incorporation into Scaffold

Spatial- and temporal-controlled delivery of growth factors is crucial for the efficient repair upon tissue injury or failure in tissue engineering. But delivery of growth factors to the site of tissue regeneration is challenging since these proteins have short half-lives, high molecular weight, and slow tissue penetration. Thus the generally used strategy to enhance in vivo efficacy of growth factors is the use of growth factor-loaded delivery systems, which release growth factors in a controlled way. Due to the tailored structures, multiple functionalities, as well as controlled

permeability, the multilayer capsules are promising candidates as growth factor carriers.

Several methods have been successfully developed to load different growth factors into multilayer capsules. Akashi and coworkers first developed biodegradable multilayer capsules to encapsulate basic fibroblast growth factor (bFGF) as a cytokine release carrier [142]. The multilayer capsules were fabricated via the layer-by-layer (LbL) assembly of chitosan and dextran sulfate. The bFGF was encapsulated into the capsules by reversibly controlling the capsule permeability. At pH < 8.0, the capsule shell was non-permeable for macromolecules. However, FITC-dextran with a molecular weight as high as 250 kDa could easily penetrate the capsules at pH > 8.0. Using the pH-controlled reversible shell permeability, bFGF was successfully encapsulated into the capsules. Release of the encapsulated bFGF was sustained over 70 h. Due to the local and sustained release of bFGF, mouse L929 fibroblast cells proliferated well for 2 weeks. Antipina and coworker used a coprecipitation-based layer-by-layer encapsulation method to load bFGF into the microcapsules [143]. In this method, bFGF was first protected by heparin and bovine serum albumin and then coprecipitated into $CaCO_3$ microparticles. Low cytotoxic and biodegradable polyelectrolytes dextran sulfate and poly-L-arginine were used for capsule shell assembly on the $CaCO_3$ microparticles. The encapsulation efficiency was greatly influenced by the shell thickness. Under optimized conditions, a maximum encapsulation efficiency of 42 % could be achieved. The controlled release of FGF2 from the microcapsules was helpful to enhance the proliferation of L929 cells. De Geest and coworkers introduced a postloading approach by engineering the capsules in such a way that they acted as growth factor-binding "microsponges" [144]. In this method, $CaCO_3$ microparticles doped with heparin were first fabricated by a coprecipitation method. Subsequently, these microparticles were coated with heparin/poly-L-arginine multilayers, followed by decomposition of the $CaCO_3$ core. In this way, hollow capsules were obtained with heparin both as membrane component and being suspended in their hollow void. Heparin is well known to have a high affinity for several growth factors. Therefore the engineered microcapsules with high heparin content will enhance their growth factor-binding capacity. Transforming growth factor-beta 1 (TGF-beta 1) could be loaded and released from such kind of heparin-engineered microcapsules without affecting its biological activity. The growth factor-loaded multilayer capsules could be easily incorporated within a gelatin tissue engineering scaffold without affecting the properties of this scaffold.

Benkirane-Jessel and coworkers first demonstrated that a hydrogel scaffold incorporated with the growth factor-loaded multilayer capsules could induce bone formation in vivo [145]. In this research, bone morphogenetic proteins (BMP_2) and TGF-beta 1 were assembled into the shell of biodegradable multilayer microcapsules. The stem cells were differentiated into bone cells when cocultured with growth factor-loaded multilayer capsules. More importantly, when such kind of capsules were integrated with alginate gel and implanted into mice, inducing bone formation in vivo was observed. The in vivo results demonstrate the promising

application potential of multilayer microcapsules as growth factor carriers in the field of tissue engineering and regenerative medicine.

4.5 Conclusions and Outlooks

The LbL assembly technique is a highly versatile and powerful platform for the fabrication of capsules with tailored structures and functions. They have already shown their great promise of applications in many areas, especially in the field of controlled release. Recently, much attention has been paid on the multilayer capsules assembled by new driving forces and those with highly sophisticated structures for biomedical applications, such as drug and growth factor carriers, as highlighted in this chapter.

Although the significant advances have been made in this area, there are still some key obstacles which should be overcome. First, for the real practical applications of multilayer capsules, rapid, scalable, and efficient new preparation methods should be developed. One recent example is the microcapsule preparation technique utilizing a fluidized bed for the LbL assembly of polymers [146]. The properties of obtained microcapsules are in close agreement with conventionally prepared LbL capsules. The technique provides a new way to rapidly generate microcapsules, while being also amenable to scale-up and mass production. Furthermore, a fully flow-based technique using tangential flow filtration (TFF) for LbL assembly on particles was developed. [147]. Multilayered particles and capsules with size ranging from micrometers to submicrometers can be assembled on different templates using diverse polymers. The well-controlled, integrated, and automatable nature of the TFF LbL system provides significant progress of the practical applications of LbL systems. Second, the in vivo behaviors of LbL capsules such as degradation and toxicity are largely unexplored. For intravenous injection, the LbL capsules are required to circulate in the bloodstream and have good hemocompatibility. Several recent researches have shown that coating of blood-compatible multilayers on the ultrasmall (~20 nm) [148, 149] and submicron (~500 nm) [150] particles is beneficial to obtain injectable capsule drug delivery systems. Therefore, particles with a submicron size are attractive for preparation of LbL capsules, which may accumulate in cancerous tissues through EPR effect.

The LbL capsules with tailed structures and functions can be loaded with both drugs and imaging agents within a single system to form theranostic carriers, which can selectively accumulate in diseased tissues and simultaneously report their biochemical and morphological characteristics. At the same time, the synergistic carriers which carry chemo-, radio-, and gene therapeutics can enhance the treatment efficacy [151, 152].

For successful tissue regeneration, it is extremely important to provide cells with a local environment using biomaterials which enable them to proliferate and differentiate efficiently and correctly, resulting in cell-induced tissue regeneration. For this purpose, capsules or spheres can be integrated into different scaffolds to provide

for prolonged, site-specific delivery of loaded growth factors, drugs, as well as other bioactive species. The capsules should be well designed with properly controlled release profile as well as surface properties, so that they can act as an integral part of the porous three-dimensional scaffolds, and their incorporation does not significantly affect the scaffold properties but can release their cargoes to meet the needs of cells.

The researches and applications of LbL multilayer capsules are highly multidisciplinary. With the efforts afforded by the experts from fields of chemistry, materials science, mechanical engineering, biology, and so on, the abovementioned obstacles will be overcome sooner or later, and more achievements in this field can be expected in the future.

Acknowledgments The research is financially supported by the Natural Science Foundation of China (51120135001 and 21374101, 21174130, 20804036), Ph.D. Programs Foundation of the Ministry of Education of China (20110101130005), and Zhejiang Provincial Natural Science Foundation of China (Y4110064).

References

1. Caruso F. Hollow capsule processing through colloidal templating and self-assembly. Chem Eur J. 2000;6:413–9.
2. Decher G, Hong JD. Buildup of ultrathin multilayer films by a self-assembly process.1. Consecutive adsorption of anionic and cationic bipolar amphiphiles on charged surfaces. Makromol Chem Macromol Symp. 1991;46:321–7.
3. Decher G. Fuzzy nanoassemblies: toward layered polymeric multicomposites. Science. 1997;277:1232–7.
4. Caruso F, Caruso RA, Mohwald H. Nanoengineering of inorganic and hybrid hollow spheres by colloidal templating. Science. 1998;282:1111–4.
5. Donath E, Sukhorukov GB, Caruso F, Davis SA, Mohwald H. Novel hollow polymer shells by colloid-templated assembly of polyelectrolytes. Angew Chem Int Ed. 1998;37:2202–5.
6. Peyratout CS, Dahne L. Tailor-made polyelectrolyte microcapsules: from multilayers to smart containers. Angew Chem Int Ed. 2004;43:3762–83.
7. Tong WJ, Gao CY. Multilayer microcapsules with tailored structures for bio-related applications. J Mater Chem. 2008;18:3799–812.
8. Sukhorukov GB, Rogach AL, Garstka M, Springer S, Parak WJ, Munoz-Javier A, Kreft O, Skirtach AG, Susha AS, Ramaye Y, Palankar R, Winterhalter M. Multifunctionalized polymer microcapsules: novel tools for biological and pharmacological applications. Small. 2007;3:944–55.
9. Sukhorukov GB, Mohwald H. Multifunctional cargo systems for biotechnology. Trends Biotechnol. 2007;25:93–8.
10. Tong WJ, Song XX, Gao CY. Layer-by-layer assembly of microcapsules and their biomedical applications. Chem Soc Rev. 2012;41(18):6103–24.
11. Pastoriza-Santos I, Scholer B, Caruso F. Core-shell colloids and hollow polyelectrolyte capsules based on diazoresins. Adv Funct Mater. 2001;11:122–8.
12. Mauser T, Dejugnat C, Sukhorukov GB. Reversible ph-dependent properties of multilayer microcapsules made of weak polyelectrolytes. Macromol Rapid Commun. 2004;25:1781–5.
13. Zhu HG, McShane MJ. Macromolecule encapsulation in diazoresin-based hollow polyelectrolyte microcapsules. Langmuir. 2005;21:424–30.

14. Sukhishvili SA, Granick S. Layered, erasable, ultrathin polymer films. J Am Chem Soc. 2000;122:9550–1.
15. Sukhishvili SA, Granick S. Layered, erasable polymer multilayers formed by hydrogen-bonded sequential self-assembly. Macromolecules. 2002;35:301–10.
16. Yang SY, Rubner MF. Micropatterning of polymer thin films with ph-sensitive and cross-linkable hydrogen-bonded polyelectrolyte multilayers. J Am Chem Soc. 2002;124:2100–1.
17. Yang SY, Lee D, Cohen RE, Rubner MF. Bioinert solution-cross-linked hydrogen-bonded multilayers on colloidal particles. Langmuir. 2004;20:5978–81.
18. Kozlovskaya V, Ok S, Sousa A, Libera M, Sukhishvili SA. Hydrogen-bonded polymer capsules formed by layer-by-layer self-assembly. Macromolecules. 2003;36:8590–2.
19. Tong WJ, Gao CY. Stable microcapsules assembled stepwise from weak polyelectrolytes followed by thermal crosslinking. Polym Adv Technol. 2005;16:827–33.
20. Zelikin AN, Quinn JF, Caruso F. Disulfide cross-linked polymer capsules: En route to biodeconstructible systems. Biomacromolecules. 2006;7:27–30.
21. Such GK, Johnston APR, Caruso F. Engineered hydrogen-bonded polymer multilayers: from assembly to biomedical applications. Chem Soc Rev. 2011;40:19–29.
22. Connal LA, Kinnane CR, Zelikin AN, Caruso F. Stabilization and functionalization of polymer multilayers and capsules via thiol-ene click chemistry. Chem Mater. 2009;21:576–8.
23. Kinnane CR, Such GK, Antequera-Garcia G, Yan Y, Dodds SJ, Liz-Marzan LM, Caruso F. Low-fouling poly(n-vinyl pyrrolidone) capsules with engineered degradable properties. Biomacromolecules. 2009;10:2839–46.
24. Ochs CJ, Such GK, Yan Y, van Koeverden MP, Caruso F. Biodegradable click capsules with engineered drug-loaded multilayers. ACS Nano. 2010;4:1653–63.
25. Leung MKM, Such GK, Johnston APR, Biswas DP, Zhu ZY, Yan Y, Lutz JF, Caruso F. Assembly and degradation of low-fouling click-functionalized poly(ethylene glycol)-based multilayer films and capsules. Small. 2011;7:1075–85.
26. Ng SL, Such GK, Johnston APR, Antequera-Garcia G, Caruso F. Controlled release of DNA from poly(vinylpyrrolidone) capsules using cleavable linkers. Biomaterials. 2011;32:6277–84.
27. Ochs CJ, Such GK, Caruso F. Modular assembly of layer-by-layer capsules with tailored degradation profiles. Langmuir. 2011;27:1275–80.
28. Liang K, Such GK, Zhu ZY, Yan Y, Lomas H, Caruso F. Charge-shifting click capsules with dual-responsive cargo release mechanisms. Adv Mater. 2011;23:H273–7.
29. Tong WJ, Gao CY, Mohwald H. Manipulating the properties of polyelectrolyte microcapsules by glutaraldehyde cross-linking. Chem Mater. 2005;17:4610–6.
30. Tong WJ, Gao CY, Mohwald H. Stable weak polyelectrolyte microcapsules with ph-responsive permeability. Macromolecules. 2006;39:335–40.
31. Sukhorukov GB, Donath E, Lichtenfeld H, Knippel E, Knippel M, Budde A, Mohwald H. Layer-by-layer self assembly of polyelectrolytes on colloidal particles. Colloids Surf A Physicochem Eng Asp. 1998;137:253–66.
32. Zhang YJ, Yang SG, Guan Y, Cao WX, Xu J. Fabrication of stable hollow capsules by covalent layer-by-layer self-assembly. Macromolecules. 2003;36:4238–40.
33. Feng ZQ, Wang ZP, Gao CY, Shen JC. Direct covalent assembly to fabricate microcapsules with ultrathin walls and high mechanical strength. Adv Mater. 2007;19:3687–91.
34. Gao C, Donath E, Moya S, Dudnik V, Mohwald H. Elasticity of hollow polyelectrolyte capsules prepared by the layer-by-layer technique. Eur Phys J E. 2001;5:21–7.
35. Gao CY, Leporatti S, Moya S, Donath E, Mohwald H. Stability and mechanical properties of polyelectrolyte capsules obtained by stepwise assembly of poly(styrenesulfonate sodium salt) and poly(diallyldimethyl ammonium) chloride onto melamine resin particles. Langmuir. 2001;17:3491–5.
36. Tong WJ, Gao CY, Mohwald H. Single polyelectrolyte microcapsules fabricated by glutaraldehyde-mediated covalent layer-by-layer assembly. Macromol Rapid Commun. 2006;27:2078–83.

37. Tong WJ, Gao CY, Mohwald H. Poly(ethyleneimine) microcapsules: glutaraldehyde-mediated assembly and the influence of molecular weight on their properties. Polym Adv Technol. 2008;19:817–23.
38. Such GK, Tjipto E, Postma A, Johnston APR, Caruso F. Ultrathin, responsive polymer click capsules. Nano Lett. 2007;7:1706–10.
39. Peters T. Serum-albumin. Adv Protein Chem. 1985;37:161–245.
40. Carter DC, Ho JX. Structure of serum-albumin. Adv Protein Chem. 1994;45:153–203.
41. Rubino OP, Kowalsky R, Swarbrick J. Albumin microspheres as a drug-delivery system – relation among turbidity ratio, degree of cross-linking, and drug-release. Pharm Res. 1993;10:1059–65.
42. Tong WJ, Gao CY, Moehwald H. Ph-responsive protein microcapsules fabricated via glutaraldehyde mediated covalent layer-by-layer assembly. Colloid Polym Sci. 2008;286:1103–9.
43. Wang ZP, Feng ZQ, Gao CY. Stepwise assembly of the same polyelectrolytes using host-guest interaction to obtain microcapsules with multiresponsive properties. Chem Mater. 2008;20:4194–9.
44. Johnston APR, Read ES, Caruso F. DNA multilayer films on planar and colloidal supports: sequential assembly of like-charged polyelectrolytes. Nano Lett. 2005;5:953–6.
45. Quiocho FA. Carbohydrate-binding proteins – tertiary structures and protein-sugar interactions. Annu Rev Biochem. 1986;55:287–315.
46. Lee YC, Lee RT. Carbohydrate-protein interactions – basis of glycobiology. Acc Chem Res. 1995;28:321–7.
47. Nelson RM, Venot A, Bevilacqua MP, Linhardt RJ, Stamenkovic I. Carbohydrate-protein interactions in vascular biology. Annu Rev Cell Dev Biol. 1995;11:601–31.
48. Lis H, Sharon N. Lectins: carbohydrate-specific proteins that mediate cellular recognition. Chem Rev. 1998;98:637–74.
49. Becker JW, Reeke GN, Cunningham BA, Edelman GM. New evidence on location of saccharide-binding site of concanavalin-a. Nature. 1976;259:406–9.
50. Goldstein IJ, Hollerman CE, Smith EE. Protein-carbohydrate interaction. 2. Inhibition studies on interaction of concanavalin a with polysaccharides. Biochemistry. 1965;4:876–83.
51. Lvov Y, Ariga K, Ichinose I, Kunitake T. Layer-by-layer architectures of concanavalin a by means of electrostatic and biospecific interactions. J Chem Soc-Chem Commun. 1995;2313–2314.
52. Lvov Y, Ariga K, Ichinose I, Kunitake T. Molecular film assembly via layer-by-layer adsorption of oppositely charged macromolecules (linear polymer, protein and clay) and concanavalin a and glycogen. Thin Solid Films. 1996;284:797–801.
53. Sato K, Imoto Y, Sugama J, Seki S, Inoue H, Odagiri T, Hoshi T, Anzai J. Sugar-induced disintegration of layer-by-layer assemblies composed of concanavalin a and glycogen. Langmuir. 2005;21:797–9.
54. Zhu Y, Tong WJ, Gao CY. Molecular-engineered polymeric microcapsules assembled from concanavalin a and glycogen with specific responses to carbohydrates. Soft Matter. 2011;7:5805–15.
55. Walker SA, Kennedy MT, Zasadzinski JA. Encapsulation of bilayer vesicles by self-assembly. Nature. 1997;387:61–4.
56. Lutz JF, Laschewsky A. Multicompartment micelles: has the long-standing dream become a reality? Macromol Chem Phys. 2005;206:813–7.
57. De Geest BG, De Koker S, Immesoete K, Demeester J, De Smedt SC, Hennink WE. Self-exploding beads releasing microcarriers. Adv Mater. 2008;20:3687–91.
58. Zhang Y, Ruder WC, Leduc PR. Artificial cells: building bioinspired systems using small-scale biology. Trends Biotechnol. 2008;26:14–20.
59. Delcea M, Yashchenok A, Videnova K, Kreft O, Mohwald H, Skirtach AG. Multicompartmental micro- and nanocapsules: hierarchy and applications in biosciences. Macromol Biosci. 2010;10:465–74.

60. Kreft O, Prevot M, Mohwald H, Sukhorukov GB. Shell-in-shell microcapsules: a novel tool for integrated, spatially confined enzymatic reactions. Angew Chem Int Ed. 2007;46:5605–8.
61. De Geest BG, McShane MJ, Demeester J, De Smedt SC, Hennink WE. Microcapsules ejecting nanosized species into the environment. J Am Chem Soc. 2008;130:14480–2.
62. Stadler B, Chandrawati R, Price AD, Chong SF, Breheney K, Postma A, Connal LA, Zelikin AN, Caruso F. A microreactor with thousands of subcompartments: enzyme-loaded liposomes within polymer capsules. Angew Chem Int Ed. 2009;48:4359–62.
63. Hosta-Rigau L, Stadler B, Yan Y, Nice EC, Heath JK, Albericio F, Caruso F. Capsosomes with multilayered subcompartments: assembly and loading with hydrophobic cargo. Adv Funct Mater. 2010;20:59–66.
64. Chandrawati R, Stadler B, Postma A, Connal LA, Chong SF, Zelikin AN, Caruso F. Cholesterol-mediated anchoring of enzyme-loaded liposomes within disulfide-stabilized polymer carrier capsules. Biomaterials. 2009;30:5988–98.
65. Hosta-Rigau L, Chung SF, Postma A, Chandrawati R, Stadler B, Caruso F. Capsosomes with "free-floating" liposomal subcompartments. Adv Mater. 2011;23:4082–7.
66. Stadler B, Chandrawati R, Goldie K, Caruso F. Capsosomes: subcompartmentalizing polyelectrolyte capsules using liposomes. Langmuir. 2009;25:6725–32.
67. Gohy JF. Block copolymer micelles. In: Block copolymers ii. Berlin: Springer; 2005. p. 65–136.
68. Zhu Y, Tong WJ, Gao CY, Mohwald H. Assembly of polymeric micelles into hollow microcapsules with extraordinary stability against extreme ph conditions. Langmuir. 2008;24:7810–6.
69. Li XD, Lu T, Zhang JX, Xu JJ, Hu QL, Zhao SF, Shen JC. A study of properties of "micelle-enhanced" polyelectrolyte capsules: structure, encapsulation and in vitro release. Acta Biomater. 2009;5:2122–31.
70. Tong WJ, Zhu Y, Wang ZP, Gao CY, Mohwald H. Micelles-encapsulated microcapsules for sequential loading of hydrophobic and water-soluble drugs. Macromol Rapid Commun. 2010;31:1015–9.
71. Gao CY, Donath E, Mohwald H, Shen JC. Spontaneous deposition of water-soluble substances into microcapsules: phenomenon, mechanism, and application. Angew Chem Int Ed. 2002;41:3789–93.
72. Gao CY, Liu XY, Shen JC, Mohwald H. Spontaneous deposition of horseradish peroxidase into polyelectrolyte multilayer capsules to improve its activity and stability. Chem Commun. 2002;1928–29.
73. Liu XY, Gao CY, Shen JC, Mohwald H. Multilayer microcapsules as anti-cancer drug delivery vehicle: deposition, sustained release, and in vitro bioactivity. Macromol Biosci. 2005;5:1209–19.
74. Mao ZW, Ma L, Gao CY, Shen JC. Preformed microcapsules for loading and sustained release of ciprofloxacin hydrochloride. J Control Release. 2005;104:193–202.
75. Zhao QH, Zhang SA, Tong WJ, Gao CY, Shen JC. Polyelectrolyte microcapsules templated on poly(styrene sulfonate)-doped caco3 particles for loading and sustained release of daunorubicin and doxorubicin. Eur Polym J. 2006;42:3341–51.
76. He Q, Song WX, Moehwald H, Li JB. Hydrothermal-induced structure transformation of polyelectrolyte multilayers: from nanotubes to capsules. Langmuir. 2008;24:5508–13.
77. Wang JG, Xiao Q, Zhou HJ, Sun PC, Yuan ZY, Li BH, Ding DT, Shi AC, Chen TH. Budded, mesoporous silica hollow spheres: hierarchical structure controlled by kinetic self-assembly. Adv Mater. 2006;18:3284–8.
78. Yu K, Zhang L, Eisenberg A. Novel morphologies of "crew-cut" aggregates of amphiphilic diblock copolymers in dilute solution. Langmuir. 1996;12:5980–4.
79. Tung PH, Kuo SW, Chan SC, Hsu CH, Wang CF, Chang FC. Micellization and the surface hydrophobicity of amphiphilic poly(vinylphenol)-block-polystyrene block copolymers. Macromol Chem Phys. 2007;208:1823–31.

80. Sha K, Li D, Li Y, Zhang B, Wang J. The chemoenzymatic synthesis of a novel cbabc-type pentablock copolymer and its self-assembled “crew-cut” aggregation. Macromolecules. 2007;41:361–71.
81. Menger FM, Seredyuk VA. Internally catalyzed separation of adhered lipid membranes. J Am Chem Soc. 2003;125:11800–1.
82. Zhou YF, Yan DY. Real-time membrane fission of giant polymer vesicles. Angew Chem Int Ed. 2005;44:3223–6.
83. Zhou YF, Yan DY. Real-time membrane fusion of giant polymer vesicles. J Am Chem Soc. 2005;127:10468–9.
84. Wang ZP, Mohwald H, Gao CY. Preparation and redox-controlled reversible response of ferrocene-modified poly(allylamine hydrochloride) microcapsules. Langmuir. 2011;27:1286–91.
85. Wang ZP, Mohwald H, Gao CY. Nanotubes protruding from poly(allylamine hydrochloride)-graft-pyrene microcapsules. ACS Nano. 2011;5:3930–6.
86. Wang ZP, Xie Y, Gao CY. Repeated protrusion of fluorescent pyrene nanorods on the surface of crosslinked poly(allylamine hydrochloride) microcapsules. RSC Adv. 2012;2:11354–8.
87. Wang ZP, Liu MY, Xie Y, Gao CY. In situ fabrication of pyrene derivative nanorods inside polyelectrolytes microcapsules with tunable fluorescent properties. J Mater Chem. 2012;22:2855–8.
88. Guan EJ, Wang TX, Wang ZP, Gao CY. Modulating the nanorods protrusion from poly(allylamine hydrochloride)-g-pyrene microcapsules by 1-pyrenesulfonic acid sodium salt. J Colloid Interface Sci. 2013;405:10–6.
89. Wang ZP, Skirtach AG, Xie Y, Liu MY, Mohwald H, Gao CY. Core-shell poly(allyamine hydrochloride)-pyrene nanorods decorated with gold nanoparticles. Chem Mater. 2011;23:4741–7.
90. Wang TX, Cai YB, Wang ZP, Guan EJ, Yu DH, Qin AJ, Sun JZ, Tang BZ, Gao CY. Decomposition-assembly of tetraphenylethylene nanoparticles with uniform size and aggregation-induced emission property. Macromol Rapid Commun. 2012;33:1584–9.
91. De Geest BG, De Koker S, Sukhorukov GB, Kreft O, Parak WJ, Skirtach AG, Demeester J, De Smedt SC, Hennink WE. Polyelectrolyte microcapsules for biomedical applications. Soft Matter. 2009;5:282–91.
92. De Geest BG, Sukhorukov GB, Mohwald H. The pros and cons of polyelectrolyte capsules in drug delivery. Expert Opin Drug Deliv. 2009;6:613–24.
93. Johnston APR, Such GK, Ng SL, Caruso F. Challenges facing colloidal delivery systems: from synthesis to the clinic. Curr Opin Colloid Interface Sci. 2011;16:171–81.
94. Johnston APR, Such GK, Caruso F. Triggering release of encapsulated cargo. Angew Chem Int Ed. 2010;49:2664–6.
95. De Cock LJ, De Koker S, De Geest BG, Grooten J, Vervaet C, Remon JP, Sukhorukov GB, Antipina MN. Polymeric multilayer capsules in drug delivery. Angew Chem Int Ed. 2010;49:6954–73.
96. Yan Y, Such GK, Johnston APR, Lomas H, Caruso F. Toward therapeutic delivery with layer-by-layer engineered particles. ACS Nano. 2011;5:4252–7.
97. De Koker S, Lambrecht BN, Willart MA, van Kooyk Y, Grooten J, Vervaet C, Remon JP, De Geest BG. Designing polymeric particles for antigen delivery. Chem Soc Rev. 2011;40:320–39.
98. De Koker S, Hoogenboom R, De Geest BG. Polymeric multilayer capsules for drug delivery. Chem Soc Rev. 2012;41:2867–84.
99. Ariga K, McShane M, Lvov YM, Ji QM, Hill JP. Layer-by-layer assembly for drug delivery and related applications. Expert Opin Drug Deliv. 2011;8:633–44.
100. Sukhorukov GB, Brumen M, Donath E, Mohwald H. Hollow polyelectrolyte shells: exclusion of polymers and donnan equilibrium. J Phys Chem B. 1999;103:6434–40.
101. Tong WJ, Dong WF, Gao CY, Mohwald H. Charge-controlled permeability of polyelectrolyte microcapsules. J Phys Chem B. 2005;109:13159–65.

102. Tong WJ, Song HQ, Gao CY, Mohwald H. Equilibrium distribution of permeants in polyelectrolyte microcapsules filled with negatively charged polyelectrolyte: the influence of ionic strength and solvent polarity. J Phys Chem B. 2006;110:12905–9.
103. Zhao QH, Mao ZW, Gao CY, Shen JC. Assembly of multilayer microcapsules on caco3 particles from biocompatible polysaccharides. J Biomater Sci Polym Ed. 2006;17:997–1014.
104. Zhao QH, Han BS, Wang ZH, Gao CY, Peng CH, Shen JC. Hollow chitosan-alginate multilayer microcapsules as drug delivery vehicle: doxorubicin loading and in vitro and in vivo studies. Nanomed Nanotechnol Biol Med. 2007;3:63–74.
105. Kohler K, Shchukin DG, Mohwald H, Sukhorukov GB. Thermal behavior of polyelectrolyte multilayer microcapsules. 1. The effect of odd and even layer number. J Phys Chem B. 2005;109:18250–9.
106. Kohler K, Mohwald H, Sukhorukov GB. Thermal behavior of polyelectrolyte multilayer microcapsules: 2. Insight into molecular mechanisms for the pdadmac/pss system. J Phys Chem B. 2006;110:24002–10.
107. Sadasivan S, Kohler K, Sukhorukov GB. Fabrication of organized porphyrin-nanotube-attached heat-sensitive polyelectrolyte capsules. Adv Funct Mater. 2006;16:2083–8.
108. Song WX, He Q, Mohwald H, Yang Y, Li JB. Smart polyelectrolyte microcapsules as carriers for water-soluble small molecular drug. J Control Release. 2009;139:160–6.
109. Tong WJ, She SP, Xie LL, Gao CY. High efficient loading and controlled release of low-molecular-weight drugs by combination of spontaneous deposition and heat-induced shrinkage of multilayer capsules. Soft Matter. 2011;7:8258–65.
110. Han YY, Bu J, Zhang YY, Tong WJ, Gao CY. Encapsulation of photosensitizer into multilayer microcapsules by combination of spontaneous deposition and heat-induced shrinkage for photodynamic therapy. Macromol Biosci. 2012;12:1436–42.
111. Hans ML, Lowman AM. Biodegradable nanoparticles for drug delivery and targeting. Curr Opin Solid State Mater Sci. 2002;6:319–27.
112. Uhrich KE, Cannizzaro SM, Langer RS, Shakesheff KM. Polymeric systems for controlled drug release. Chem Rev. 1999;99:3181–98.
113. Zhou J, Romero G, Rojas E, Ma L, Moya S, Gao CY. Layer by layer chitosan/alginate coatings on poly(lactide-co-glycolide) nanoparticles for antifouling protection and folic acid binding to achieve selective cell targeting. J Colloid Interface Sci. 2010;345:241–7.
114. Zhou J, Romero G, Rojas E, Moya S, Ma L, Gao CY. Folic acid modified poly(lactide-co-glycolide) nanoparticles, layer-by-layer surface engineered for targeted delivery. Macromol Chem Phys. 2010;211:404–11.
115. Zhou J, Moya S, Ma L, Gao CY, Shen JC. Polyelectrolyte coated plga nanoparticles: templation and release behavior. Macromol Biosci. 2009;9:326–35.
116. Xie L, Tong W, Yu D, Xu J, Li J, Gao C. Bovine serum albumin nanoparticles modified with multilayers and aptamers for ph-responsive and targeted anti-cancer drug delivery. J Mater Chem. 2012;22:6053–60.
117. Kim JK, Choi KJ, Lee M, Jo MH, Kim S. Molecular imaging of a cancer-targeting theragnostics probe using a nucleolin aptamer- and microrna-221 molecular beacon-conjugated nanoparticle. Biomaterials. 2012;33:207–17.
118. Iwasaki H, Nabeshima K, Nishio J, Jimi S, Aoki M, Koga K, Hamasaki M, Hayashi H, Mogi A. Pathology of soft-tissue tumors: daily diagnosis, molecular cytogenetics and experimental approach. Pathol Int. 2009;59:501–21.
119. Xie LL, Tong WJ, Xu JQ, Gao CY. Multilayers and poly(allylamine hydrochloride)-graft-poly(ethylene glycol) (pah-g-peg) modified bovine serum albumin nanoparticles: improved stability and ph-responsive drug delivery. Chin J Polym Sci. 2012;30:719–26.
120. Schneider G, Decher G. Functional core/shell nanoparticles via layer-by-layer assembly. Investigation of the experimental parameters for controlling particle aggregation and for enhancing dispersion stability. Langmuir. 2008;24:1778–89.

121. Doshi N, Zahr AS, Bhaskar S, Lahann J, Mitragotri S. Red blood cell-mimicking synthetic biomaterial particles. Proc Natl Acad Sci U S A. 2009;106:21495–9.
122. Hayashi K, Ono K, Suzuki H, Sawada M, Moriya M, Sakamoto W, Yogo T. Electrosprayed synthesis of red-blood-cell-like particles with dual modality for magnetic resonance and fluorescence imaging. Small. 2010;6:2384–91.
123. Haghgooie R, Toner M, Doyle PS. Squishy non-spherical hydrogel microparticles. Macromol Rapid Commun. 2010;31:128–34.
124. Prevot M, Cordeiro AL, Sukhorukov GB, Lvov Y, Besser RS, Mohwald H. Design of a microfluidic system to investigate the mechanical properties of layer-by-layer fabricated capsules. Macromol Mater Eng. 2003;288:915–9.
125. Dubreuil F, Elsner N, Fery A. Elastic properties of polyelectrolyte capsules studied by atomic-force microscopy and ricm. Eur Phys J E. 2003;12:215–21.
126. She S, Xu C, Yin X, Tong W, Gao C. Shape deformation and recovery of multilayer microcapsules after being squeezed through a microchannel. Langmuir. 2012;28:5010–6.
127. She S, Li Q, Shan B, Tong W, Gao C. Fabrication of red-blood-cell-like polyelectrolyte microcapsules and their deformation and recovery behavior through a microcapillary. Adv Mater. 2013;5814–8
128. Toy R, Peiris PM, Ghaghada KB, Karathanasis E. Shaping cancer nanomedicine: the effect of particle shape on the in vivo journey of nanoparticles. Nanomedicine. 2014;9:121–34.
129. Albanese A, Tang PS, Chan WC. The effect of nanoparticle size, shape, and surface chemistry on biological systems. Annu Rev Biomed Eng. 2012;14:1–16.
130. Nel AE, Maedler L, Velegol D, Xia T, Hoek EMV, Somasundaran P, Klaessig F, Castranova V, Thompson M. Understanding biophysicochemical interactions at the nano-bio interface. Nat Mater. 2009;8:543–57.
131. Huang X, Teng X, Chen D, Tang F, He J. The effect of the shape of mesoporous silica nanoparticles on cellular uptake and cell function. Biomaterials. 2010;31:438–48.
132. Alexander JF, Kozlovskaya V, Chen J, Kuncewicz T, Kharlampieva E, Godin B. Cubical shape enhances the interaction of layer-by-layer polymeric particles with breast cancer cells. Adv Healthc Mater. 2015;4:2657–66.
133. Sharma G, Valenta DT, Altman Y, Harvey S, Xie H, Mitragotri S, Smith JW. Polymer particle shape independently influences binding and internalization by macrophages. J Control Release. 2010;147:408–12.
134. Kolhar P, Mitragotri S. Polymer microparticles exhibit size and shape dependent accumulation around the nucleus after endocytosis. Adv Funct Mater. 2012;22:3759–64.
135. Kumar S, Anselmo AC, Banerjee A, Zakrewsky M, Mitragotri S. Shape and size-dependent immune response to antigen-carrying nanoparticles. J Control Release. 2015;220:141–8.
136. Doshi N, Prabhakarpandian B, Rea-Ramsey A, Pant K, Sundaram S, Mitragotri S. Flow and adhesion of drug carriers in blood vessels depend on their shape: a study using model synthetic microvascular networks. J Control Release. 2010;146:196–200.
137. Shah S, Liu Y, Hu W, Gao J. Modeling particle shape-dependent dynamics in nanomedicine. J Nanosci Nanotechnol. 2011;11:919–28.
138. Merkel TJ, Jones SW, Herlihy KP, Kersey FR, Shields AR, Napier M, Luft JC, Wu H, Zamboni WC, Wang AZ, Bear JE, DeSimone JM. Using mechanobiological mimicry of Red blood cells to extend circulation times of hydrogel microparticles. Proc Natl Acad Sci U S A. 2011;108:586–91.
139. Shimoni O, Yan Y, Wang Y, Caruso F. Shape-dependent cellular processing of polyelectrolyte capsules. ACS Nano. 2013;7:522–30.
140. Chen J, Kozlovskaya V, Goins A, Campos-Gomez J, Saeed M, Kharlampieva E. Biocompatible shaped particles from dried multilayer polymer capsules. Biomacromolecules. 2013;14:3830–41.
141. Li HY, Zhang WB, Tong WJ, Gao CY. Enhanced cellular uptake of bowl-like microcapsules. ACS Appl Mater Interfaces. 2016;8:11210–4.

142. Itoh Y, Matsusaki M, Kida T, Akashi M. Locally controlled release of basic fibroblast growth factor from multilayered capsules. Biomacromolecules. 2008;9(8):2202–6.
143. She Z, Wang CX, Li J, Sukhorukov GB, Antipina MN. Encapsulation of basic fibroblast growth factor by polyelectrolyte multilayer microcapsules and its controlled release for enhancing cell proliferation. Biomacromolecules. 2012;13(7):2174–80.
144. De Cock LJ, De Wever O, Van Vlierberghe S, Vanderleyden E, Dubruel P, De Vos F, Vervaet C, Remon JP, De Geest BG. Engineered (hep/pARG)(2) polyelectrolyte capsules for sustained release of bioactive TGF-beta 1. Soft Matter. 2012;8(4):1146–54.
145. Facca S, Cortez C, Mendoza-Palomares C, Messadeq N, Dierich A, Johnston APR, Mainard D, Voegel JC, Caruso F, Benkirane-Jessel N. Active multilayered capsules for in vivo bone formation. Proc Natl Acad Sci U S A. 2010;107(8):3406–11.
146. Richardson JJ, Teng D, Bjornmalm M, Gunawan ST, Guo J, Cui JW, Franks GV, Caruso F. Fluidized bed layer-by-layer microcapsule formation. Langmuir. 2014;30(33):10028–34.
147. Bjornmalm M, Roozmand A, Noi KF, Guo JL, Cui JW, Richardson JJ, Caruso F. Flow-based assembly of layer-by-layer capsules through tangential flow filtration. Langmuir. 2015;31(33):9054–60.
148. Poon Z, Chang D, Zhao XY, Hammond PT. Layer-by-layer nanoparticles with a ph-sheddable layer for in vivo targeting of tumor hypoxia. ACS Nano. 2011;5:4284–92.
149. Poon Z, Lee JB, Morton SW, Hammond PT. Controlling in vivo stability and biodistribution in electrostatically assembled nanoparticles for systemic delivery. Nano Lett. 2011;11:2096–103.
150. Yu L, Gao YG, Yue XL, Liu SQ, Dai ZF. Novel hollow microcapsules based on iron-heparin complex multilayers. Langmuir. 2008;24:13723–9.
151. Chen X, Gambhir SS, Cheon J. Theranostic nanomedicine. Acc Chem Res. 2011;44:841.
152. Lammers T, Aime S, Hennink WE, Storm G, Kiessling F. Theranostic nanomedicine. Acc Chem Res. 2011;44:1029–38.

Part II
Biomaterials Surfaces/Interfaces and Bio-interactions

Chapter 5
Interactions of Biomaterial Surfaces with Proteins and Cells

Zhonglin Lyu, Qian Yu, and Hong Chen

The interactions of material surfaces with proteins and cells play a vital role in various biological phenomena and determine the ultimate biofunctionality of a given material in contact with a given biological environment [1]. The effects of surface topography and roughness (especially at the nanometer scale) on protein and cell behavior have attracted increasing attention since topographic features may have dimensions similar to those of proteins and cell membrane receptors [2, 3]. For example, gold nanoparticle layers (GNPLs) consist of nanoparticle aggregates with a distribution of sizes and three-dimensional micro- and nano-sized porous structures [4–9]. GNPLs hold great promise in biomedical applications, for example, biosensors and tissue engineering, due to their large surface-to-volume ratio, efficient electron transfer, good stability, and high loading capacity [7, 10, 11]. Formation of GNPL on material surfaces is usually achieved by reduction of tetrachloroauric (III) acid either through surface-bonded reducing groups or reducing agents [4, 5, 10, 12]. For example, Zhang and coworkers used the Si-H reducing group in the residual curing agent (silicone resin solution) in poly(dimethylsiloxane) (PDMS) matrix to reduce $HAuCl_4$ in the preparation of a PDMS-gold nanoparticle composite film. Wang and coworkers have also reported a method for fabricating PDMS-GNPs films [10]. In another report, chitosan, used as a reducing and stabilizing agent, was coated on PDMS; the coated PDMS was then immersed in $HAuCl_4$ solution to form a layer of GNPs [12]. In our research, stable GNPL were prepared on a variety of materials via a facile and low-cost glucose reduction method [4, 5]. The applications of GNPL for control of protein adsorption and regulation of cell behavior are discussed in the following sections.

Z. Lyu • Q. Yu • H. Chen (✉)
State and Local Joint Engineering Laboratory for Novel Functional Polymeric Materials, College of Chemistry, Chemical Engineering and Materials Science, Soochow University, Suzhou 215123, China
e-mail: chenh@suda.edu.cn

© Springer Science+Business Media Singapore 2016

C. Gao (ed.), *Polymeric Biomaterials for Tissue Regeneration*,
DOI 10.1007/978-981-10-2293-7_5

5.1 Control of Protein Adsorption

The interaction of biomaterials with proteins is of crucial importance in various applications including biochips [13], biosensors [14], medical device coatings [15], and drug delivery [16]. Controlling the adsorption of proteins (e.g., antibodies, enzymes) on material surfaces and conserving their activity are essential in the design of functional surfaces [17]. In this section, protein adsorption on GNPL-modified enzyme-linked immunosorbent assay (ELISA) plates is discussed in detail. The combined effects of the micro-/nano-structures of the GNPL and the chemistry of polymer brushes grafted on GNPL on protein adsorption are highlighted in this discussion.

5.1.1 Protein Adsorption on GNPL-Modified ELISA Plates

ELISA is widely used in clinical diagnosis due to its relative simplicity, low cost, and high sensitivity [18, 19]. A major limitation is low binding affinity of antigens and antibodies; in addition, the accessibility of adsorbed proteins on a standard "two-dimensional" microplate surface for the recognition and binding of antigens and antibodies may be limited [20]. To improve accessibility and sensitivity, we have investigated modification of ELISA plates with GNPL to give surfaces that may be described as "three dimensional" [4].

GNPL exhibits three-dimensional porous structures that are composed of gold nanoparticle aggregates with thickness in the micrometer range. By adjusting the volume of the plating solution in the wells, a series of GNPLs with different porosity rates were obtained. With increasing solution volume, the micro- and nano-sized porous structures became more densely aggregated and the porosity value decreased gradually (Fig. 5.1) [4]. It was found that the quantity of proteins (lysozyme (LYZ), human serum albumin (HSA), and fibrinogen (Fg), used as model proteins of different size) adsorbed on GNPL-modified ELISA plates increased significantly with increasing solution volume; e.g., for GNPL prepared with the highest solution volume, the adsorbed quantities of LYZ, HSA, and Fg were, respectively, 2.76-, 2.34-, and 3.26-fold higher than on the unmodified plate. Moreover, due to the micro- and nano-structures of the GNPL, the activity of LYZ absorbed on GNPL was found to be at least 2.65-fold higher than on the unmodified plate. The GNPL-modified plate was shown to amplify the ELISA signals for carcinoembryonic antigen (CEA) and antithrombin (AT) and to increase the limits of detection (LOD) of these antigens significantly. Useful ELISA signals were obtained on GNPL-modified plates when the quantity of CEA was above 2 ng/well; in contrast, no useful signal was obtained on the pristine high-binding ELISA plate even for quantities greater than 10 ng/well. The LOD for AT in buffer solution with GNPL-modified plate was two orders of magnitude lower than for the unmodified plate.

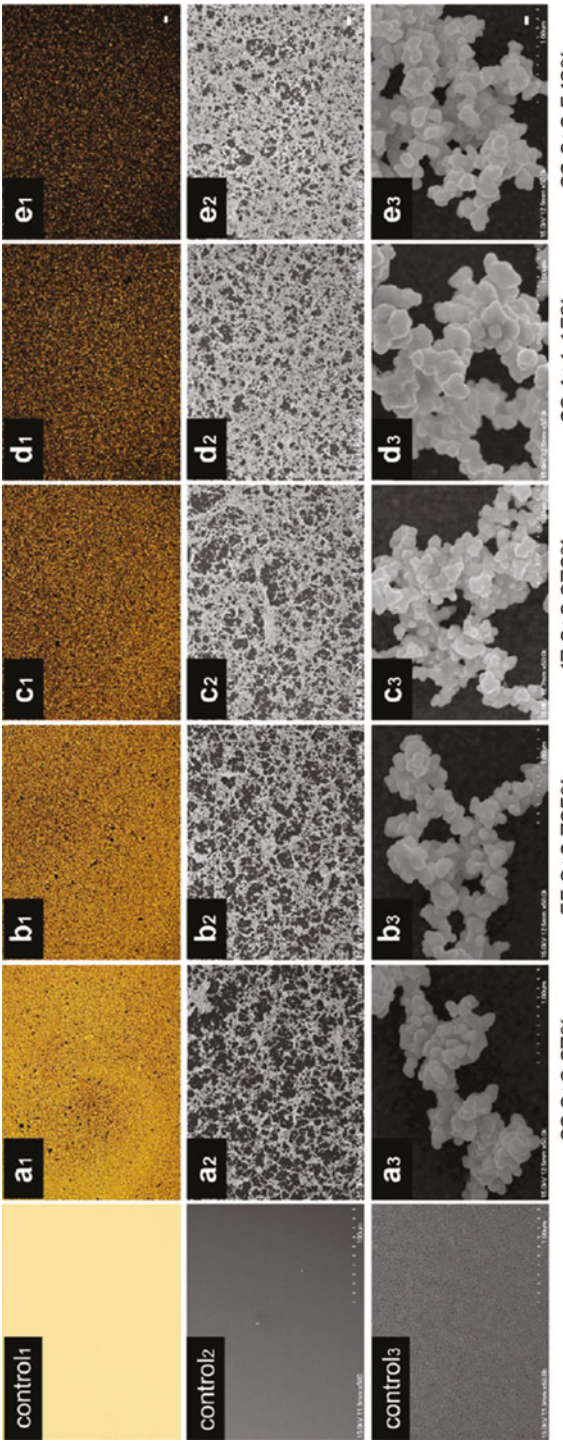

Fig. 5.1 Characterization of unmodified (control) and GNPL-modified ELISA plates. The volumes of plating solution for GNPL a-e were 50, 100, 150, 200, and 250 μL, respectively. *a1–e1* are visible light micrographs (bar: 100 μm); *a2–e2* are field emission scanning electron microscopy (FESEM) images (*bar*: 10 μm); *a3–e3* are high-magnification FESEM images (*bar*: 100 nm); the numbers under the columns are the respective porosity values for GNPL *a–e* (Reprinted from Ref. [4] with permission. Copyright 2011 American Chemical Society)

To overcome the limitation of indirect ELISA to selectively bind a specific target from a multi-protein fluid such as serum or plasma, we proposed a GNPL-based ELISA in sandwich format [5]. Sandwich ELISA is widely used in various commercially available kits. In "traditional" sandwich ELISA, the captured (adsorbed) antibody (Ab) binds to the ELISA plate by physical adsorption, resulting in random orientation of the Ab molecules and thus in decreased performance. We hypothesized that an optimum orientation of Ab on the ELISA plate by covalent attachment might improve performance [21]. Accordingly we immobilized goat anti-rabbit IgG (IgG-alkaline phosphatase (ALP)) on GNPL using 1-ethyl-3-(3-dimethylaminopropyl) carbodiimide hydrochloride (EDC)/N-hydroxysuccinimide (NHS) conjugation chemistry. We showed that the activity of IgG covalently immobilized on the GNPL plate was 61 % higher than that of IgG physically adsorbed on the unmodified plate.

This result may be attributed, in part, to the improved binding efficiency of the GNPL-modified, compared to the unmodified, ELISA plate; more importantly, the GNPL-modified plate may favor an Ab orientation that facilitates the binding of the IgG substrate to the enzyme. The GNPL-modified ELISA plate showed a lower LOD and higher sensitivity for rabbit IgG in buffer and CEA in plasma. For IgG in buffer, the detection limit of the GNPL-modified ELISA was 0.0512 ng/mL, two orders of magnitude lower than that of the unmodified plate (1.28 ng/mL). For CEA in plasma, the GNPL-modified plate gave a stronger ELISA signal than the unmodified, high-binding ELISA plate as indicated by the deeper color. This was especially true for CEA concentrations greater than 8 ng/mL. The LOD for the GNPL-modified ELISA plate was 2 ng/mL compared to 4 ng/mL for a typical commercial ELISA kit (Linc-Bio Co.).

5.1.2 Controlling Protein Adsorption on GNPL Modified with Hydrophilic Polymer Brushes

Surfaces with micro-/nano-structures adsorb greater quantities of protein than smooth surfaces on a nominal area basis. On the other hand, surfaces modified with hydrophilic polymers such as poly[oligo(ethylene glycol) methacrylate] (POEGMA) tend to resist nonspecific protein adsorption [6, 8]. It was of interest, therefore, to investigate the combined effects of micro-/nano-structures and hydrophilic polymers on protein adsorption. GNPL were modified with POEGMA by surface-initiated atom transfer radical polymerization (SI-ATRP) [6, 8]. Protein adsorption was measured using radiolabeled protein. It was found for human serum albumin (HSA, one of the most abundant proteins in the body) that adsorption on the GNPL surface was about 5.8-fold higher than on smooth Au (sAu) (Fig. 5.2). After modification with POEGMA, adsorption was reduced by about 97 %. Adsorption on GNPL-POEGMA and sAu-POEGMA was similar (Fig. 5.2) indicating the strong protein resistance of POEGMA.

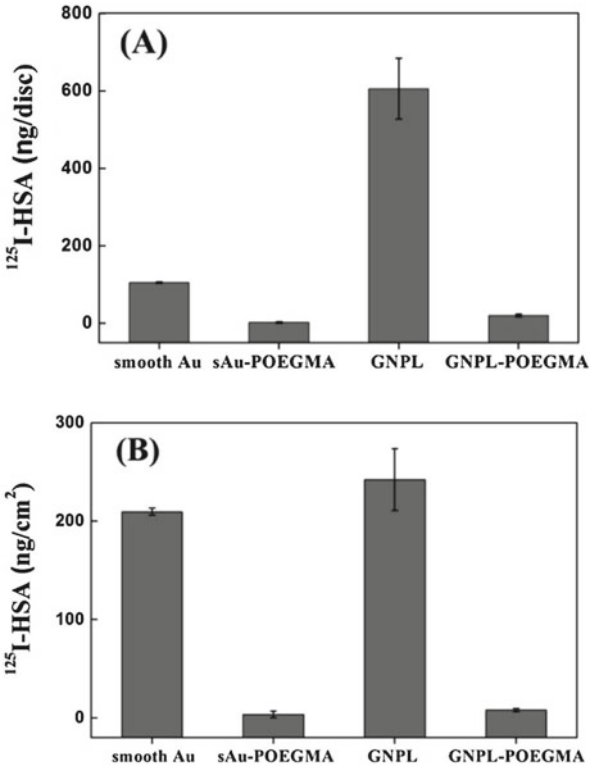

Fig. 5.2 The adsorption of 1mg/mL HSA measured using ^{125}I radiolabeling method, as expressed in (**A**) nanograms/disc or (**B**) nanograms/cm^2. (Data are means ± SD (n = 3)) (Reprinted from Ref. [8] with permission. Copyright 2012 American Chemical Society)

5.2 Regulation of Cell Behavior

It has been demonstrated that the surfaces on which cells reside and interact in vivo are rough and are composed of diverse three-dimensional micro-/nano-structures which are essential in maintaining cellular functions [22]. For example, extracellular matrix (ECM) and the inner surfaces of blood vessels are rough, with topographical features that affect protein adsorption and cellular responses [23, 24]. Lensen et al. found that poly(ethylene glycol) (PEG) hydrogel surfaces, which are intrinsically cell repellent, support the growth of L929 cells after introducing micro-/nano-topographical features in the surface [25]. Nano-topography has been shown to regulate the properties and behavior of human embryonic stem cells (hESCs), including cell morphology, adhesion, proliferation, and self-renewal [24]. Cardiovascular stents with micro-/nano-topographical surfaces were also found to endothelialize more effectively than those with smooth surfaces [26]. Also nanostructured surfaces modified with cell-specific ligands were significantly more efficient in the capture and isolation of circulating tumor cells [27, 28].

5.2.1 *Maintaining the Pluripotency of ESCs on GNPLs with Nanoscale Surface Roughness*

The influence of surface nanoscale features on the function of ESCs is attracting increasing attention because the features resemble those of the natural ECM where cells reside and interact [29]. Using photolithography Chen and coworkers prepared glass substrates with patterned surface roughness features of 70 and 150 nm and investigated the behavior of hESCs on these surfaces. They found that smooth glass was conducive to maintaining the self-renewal and pluripotency of hESCs in long-term culture; in contrast, the nanorough surfaces promoted spontaneous differentiation and loss of pluripotency [24]. In general, however, the influence of sub-microscale and microscale roughness on the maintenance of ESC pluripotency has not been much explored and remains unclear.

To address this question, we investigated the influence of surface roughness from nano- to submicro- to micro-scale on the maintenance of mouse ESC (mESC) pluripotency in long-term culture under feeder-free conditions [7]. GNPLs with nano-, sub-micro-, and micro-scale roughness were prepared by adjusting the volume of the gold plating solution (designated GL-1, GL-2, GL-3, GL-4, and GL-5 with increasing surface roughness). Undifferentiated ESCs can express the Oct-4 gene, which is essential for maintaining the cells in the undifferentiated state. Decreases in Oct-4 immunoreactivity signify cell differentiation. The majority of mESCs seeded on sAu, GL-1, and GL-2, whose surface roughness is less than 392 nm, retained their "stemness" after culture for 3 and 7 days, as shown by expression of the Oct-4 gene (Fig. 5.3a). In contrast, the pluripotency of cells cultured on GL-3, GL-4, and GL-5, with surface roughness greater than 573 nm, decreased from day 3; loss of pluripotency was greater after 7 days, particularly on microrough GL-5 (Fig. 5.3b). These results are consistent with data from quantitative polymerase chain reaction (qPCR) analysis of Oct-4 expression: no significant loss of Oct-4 gene expression was observed in cells grown on nanorough GL-1 (~84 %) compared with those on sAu. In contrast, Oct-4 gene expression decreased strongly on GL-3 (~73 %) and GL-5 (~52 %), with roughness greater than 573 nm. In sum these results show that sAu and GNPLs with low sub-microscale roughness (Rq less than 392 nm) supported very well the long-term pluripotency of mESC. However, GNPLs with sub-microscale surface roughness (Rq) greater than 573 nm and microscale surface roughness of 1,205 nm decreased the pluripotency of the cells and accelerated their spontaneous differentiation, especially on microrough GNPL.

The signaling cascades engaged in topological sensing by mESCs were investigated by analyzing the expression of proteins related to E-cadherin-mediated cell-cell adhesion and the formation of integrin-mediated focal adhesions (FAs). It was found that mESCs cultured on sAu and nanorough GNPL (Rq, 106 nm) tended to form larger colonies with cells tightly connected with each other than cells on microrough GNPL. Also the cells maintained much stronger expression of E-cadherin than cells on microrough GNPL. In contrast, the ability of the cells cultured on microrough GNPL to form colonies was significantly decreased, and cells

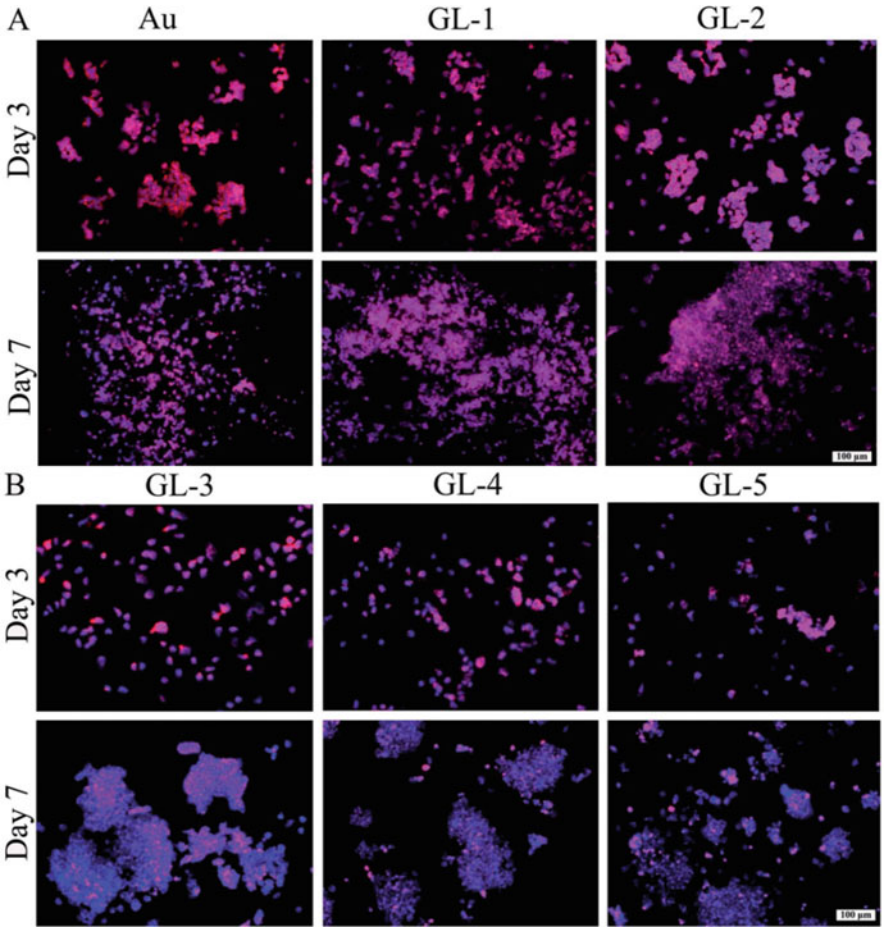

Fig. 5.3 Immunofluorescence images of mESCs cultured for 3 and 7 days on various surfaces. The cells were co-stained for Oct-4 (*red*) and nuclei (DAPI; *blue*). Undifferentiated mESCs were positively immuno-labeled for Oct-4 and were stained *red*. DAPI (*blue* counterstain) labels all cells in the population; therefore, differentiated cell types appear *blue*. (**a**) *Au*, *GL-1*, and *GL-2*; (**b**) *GL-3*, *GL-4*, and *GL-5*. *Bar*, 100 μm (Reprinted from Ref. [7] with permission. Copyright 2014 Royal Society of Chemistry)

were distributed randomly with much weaker expression of E-cadherin (Fig. 5.4a, b). In addition, β-catenin was expressed exclusively in cells cultured on sAu and nanorough GNPLs, indicating the presence of strong adherens junctions that support E-cadherin-mediated cell-cell adhesions in mESC colonies. In comparison, the cells cultured on microrough GNPL showed much weaker expression of β-catenin (Fig. 5.4c). In focal adhesion (FA) analysis, mESCs exhibited much stronger expression of vinculin (a FA protein) on sAu and nanorough GNPL than on microrough GNPL. These results suggest that nanorough GNPL is conducive to the formation

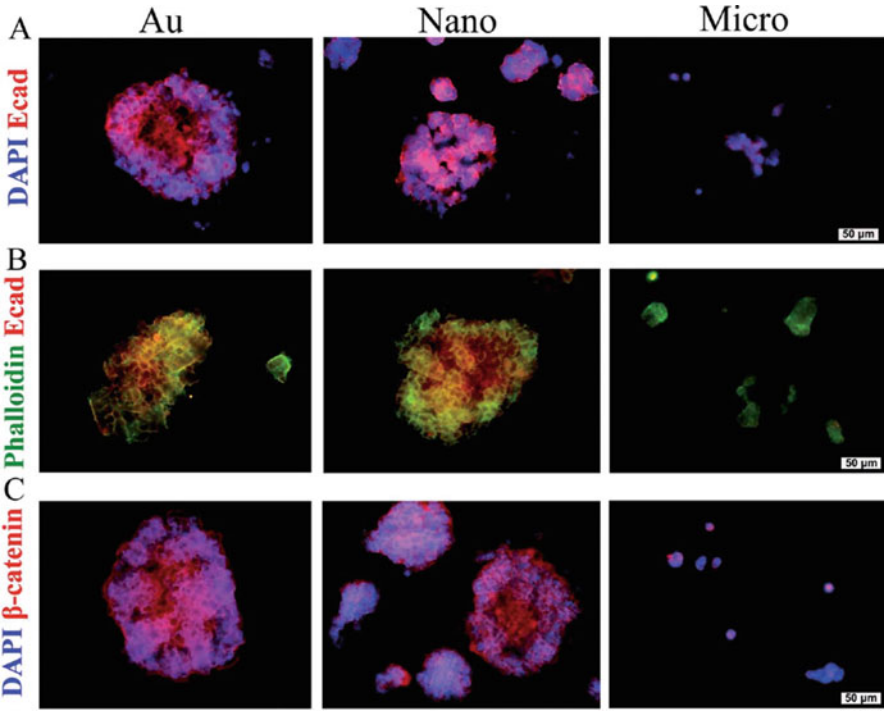

Fig. 5.4 Immunofluorescence images of mESCs on smooth Au and GNPLs with nanoscale and microscale surface roughness after culture for 3 days. (**a**) Cells co-stained for nuclei (*DAPI*, *blue*) and E-cadherin (*red*); (**b**) cells co-stained for cytoskeleton (phalloidin, *green*) and E-cadherin (*red*); (**c**) cells co-stained for nuclei (*DAPI*, *blue*) and *β-catenin* (*red*). *Bar*, 50 μm (Reprinted from Ref. [7] with permission. Copyright 2014 Royal Society of Chemistry)

of FAs in mESCs, while microrough GNPL strongly inhibits FA formation, possibly resulting in faster spontaneous differentiation of the mESCs.

5.2.2 Controlling Cell Behavior on GNPL Grafted with Protein-Resistant Polymers

Despite much effort devoted to the investigation of the interactions between topography and cell behavior, cellular responses to topography are not well understood and results are contradictory in different experimental systems [30]. Many studies have shown that topographical surfaces increase cell adhesion and cell proliferation by affecting the distribution of ECM proteins adsorbed from the cell culture medium [31, 32] and by increasing protein adsorption [33]. Others believe that cellular responses do not rely only on the cell adhesion proteins or ligands in the local environment, that the topographical structure of the surface itself is important, and that

protein adsorption alone does not determine cell behavior. For example, on a surface patterned with grooves overlaid with an orthogonal fibronectin pattern, osteoblasts were aligned predominantly with the grooves, regardless of the distribution of fibronectin (Fn), implying that the topography influenced the cell behavior independently of protein adsorption [34]. Dalby and coworkers showed that cell adhesion was quite different on 10 nm and 50 nm nanoscale islands on poly(n-butyl methacrylate)/poly(styrene) blend films [35].

To investigate the role of surface topology independent of other factors on cell behavior, we modified GNPL with POEGMA using SI-ATRP to obtain a topological surface having minimal protein adsorption [8]. Cell adhesion experiments were carried out using two cell types, human L02 hepatocytes and human hepatocellular carcinoma BEL-7402 cells. The cell density on GNPL was higher than on sAu, and after modification with POEGMA cell adhesion was reduced on both surfaces. However, whereas cell adhesion was greatly decreased on sAu, it was reduced by only ~50 % for GNPL-POEGMA, and the density on GNPL-POEGMA was an order of magnitude higher than on sAu-POEGMA. L02 and BEL-7402 adhesion on sAu-POEGMA was lower by 92.8 % and 97.7 %, respectively, compared to sAu. For GNPL-POEGMA surface, the decrease in adhesion compared to GNPL was only 51.5 % for L02 and 38.4 % for BEL-7402 cells. These data showed that surface topography is an important determinant of cell adhesion on protein-resistant POEGMA surfaces.

The combined effects of topography and protein resistance on cell-surface interactions were also investigated. Cell spreading was evaluated using fluorescent staining with Alexa Fluor 488 phalloidin (Fig. 5.5a, c). Spreading occurred on the sAu and GNPL surfaces. On the POEGMA-modified surfaces, cell spreading appeared to be constrained to some extent based on the spherical shape of the cells. However, spreading was quite different on the GNPL-POEGMA and sAu-POEGMA surfaces, as shown in the confocal microscopy images (Fig. 5.5 insets). Cells on GNPL-POEGMA showed small lamelipodia and short cell filopodia (Fig. 5.5a4, c4), whereas cells on sAu-POEGMA did not (Fig. 5.5a2, c2). Similar trends were found in SEM images (Fig. 5.5b, d). These results demonstrate that although cell spreading on protein-resistant surfaces was constrained, presumably because of the lack of adsorbed proteins, the cells on topographical surfaces were more firmly attached compared to those on smooth surfaces. In general, it was concluded that topography is more important than protein-resistant polymers for cell adhesion on a protein-resistant surface.

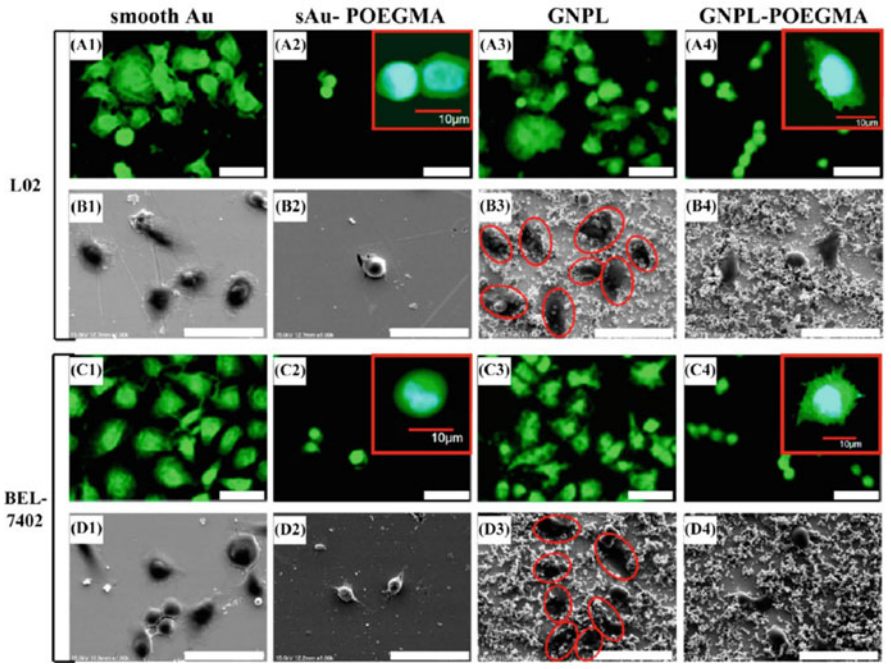

Fig. 5.5 Fluorescence and SEM images of L02 and BEL-7402 cells on different surfaces. Spread cells on the GNPL surface are indicated by *red ovals* in B3 and D3. The *scale bar* in all images is 50 μm. The shape and filopodia of the cells on POEGMA-modified surfaces were observed by confocal microscopy and are shown as *insets* in *A2*, *A4*, *C2*, and *C4* (scale bar 10 μm) (Reprinted from Ref. 8 with permission. Copyright 2012 American Chemical Society)

5.2.3 Controlling Cell Behavior on GNPL Modified with Cell-Binding Ligands

As well as surface topography, surface chemical modification has been shown to be effective in regulating cell behavior [36, 37]. To promote specific interactions between cells and material surfaces, cell-binding ligands such as arginine-glycine-aspartic acid (RGD) peptide have often been used [38, 39]. However, nonspecific adsorption of serum proteins can interfere with specific cell-ligand interactions. To avoid nonspecific adsorption of serum proteins, Causa and coworkers investigated cell-specific interactions with surfaces in serum-free medium [39]. However, serum contains many proteins and hormones that are vital for the maintenance of cell function. Therefore studies under serum-free conditions cannot accurately reflect cell-specific interactions. To address this issue, we used protein-resistant polymer brushes (POEGMA) to modify GNPL via SI-ATRP and further modified the POEGMA with glycine-arginine-glycine-aspartic acid-tyrosine (GRGDY) peptide, a typical ligand that binds integrins and triggers specific cell responses [6]. It was found that the cell density on sAu was significantly higher than on GNPL (Fig. 5.6),

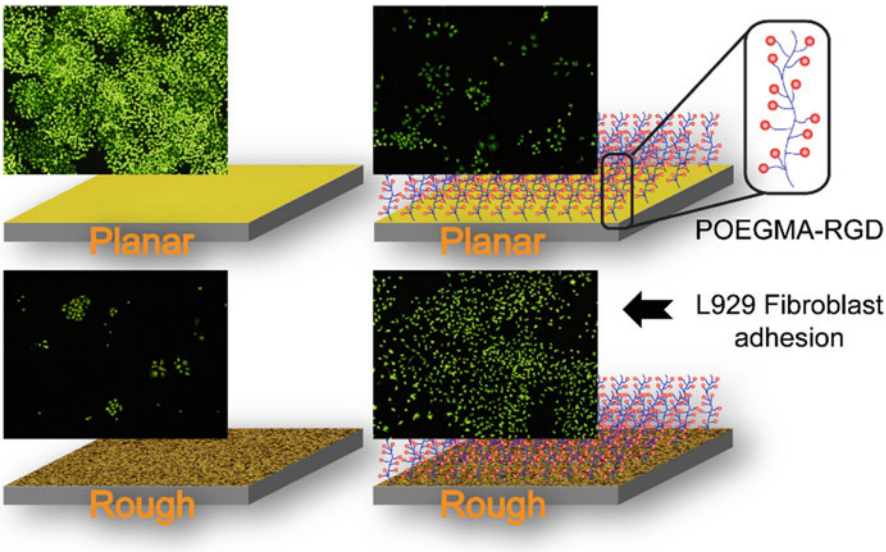

Fig. 5.6 Regulating the behavior of L929 fibroblasts on GNPL modified with POEGMA and cell-binding ligand GRGDY (Reprinted from Ref. [6] with permission. Copyright 2012 Wiley-VCH)

suggesting that L929 fibroblasts prefer to adhere and proliferate on smooth surfaces. This observation is consistent with previously reported research [40]. We speculated that GNPL surface alters the native conformations of the adsorbed cell-adhesive proteins [41], thereby resulting in poor recognition and binding between the membrane integrins of L929 and those proteins. Hence, it is difficult for L929 cells to form mature focal adhesions on GNPL surfaces thereby further hindering cell adhesion, spreading, and proliferation.

The cell densities on all of the surfaces modified with POEGMA were significantly reduced and most adherent cells did not spread. A few cells aggregated to form small clusters, indicating that the surfaces were unfavorable for cell adhesion. However, after modification with GRGDY peptide, the cellular responses were totally reversed. The specific binding between cells and GRGDY greatly improved cell adhesion (Fig. 5.6). Cell densities on the GNPL-POEGMA-GRGDY surface were at least 131 ± 13 cells/mm^2 at 120 h. This value was much higher than on the unmodified and POEGMA-modified GNPLs and even higher than on sAu after the same treatment. Thus, it appeared that although the increased surface roughness was unfavorable for the adhesion of L929 cells, the much higher surface-to-volume ratio of the GNPL surface resulted in a higher density of surface immobilized molecules, and the enhanced specific interactions between cells and GRGDY peptides counteracted the negative effect of the roughness, resulting in improved cell adhesion and proliferation.

The cell density on GNPL with lower surface roughness (GNPL (a)) was higher than on the two GNPLs with higher surface roughness (GNPL (c) and GNPL (b);

roughness: GNPL (c) > GNPL (b)), and it was the only GNPL that supported cell growth. It appears that surface roughness and cell-specific binding, having opposite effects, reached an optimal balance on GNPL (a). The densities of GRGDY peptide on GNPL (b) and (c) were higher than on GNPL (a) due to their higher surface-to-volume ratios. However, according to a study reported by Mann and West, a very high density of cell-binding ligands immobilized on surfaces is unfavorable for the proliferation of certain mesenchymal-derived cell types [42]. A similar phenomenon was observed by Bellis and coworkers [43, 44]. In our work [6], although the cell density on sAu-POEGMA-GRGDY surface also increased to 83 ± 8 cells/mm^2, it was still lower than on unmodified Au surface (310 ± 25 mm^2) (Fig. 5.6). This could be due to lower specific binding on the modified sAu surface compared to the modified GNPL surface; in addition, the POEGMA spacer reduced the adsorption of serum proteins including that of cell-adhesive proteins such as Fn.

5.2.4 Capture of Circulating Cancer Cells Using Aptamer-Modified GNPL

The measurement and analysis of circulating tumor cells (CTCs) can be regarded as a "liquid biopsy" of the tumor, providing insight into tumor biology in the critical window where intervention could actually make a difference [45]. However, CTCs are present in extremely low numbers in the bloodstream: typically one CTC cell per 10^5–10^7 normal blood cells [46]. Therefore enrichment of CTCs is a prerequisite for CTC analysis. Over the past few decades, a diverse suite of technologies have been developed for isolating and counting CTCs in patient blood samples [47, 48]. The known enhancement of cell-surface interactions, including cell adhesion, by micro-/nano-structuring can [49] be exploited for the enrichment and separation of CTCs. Aptamers (APTs), which may be considered as nucleic acid forms of traditional antibodies, can be designed to have specific affinity for given cell types. Moreover, APTs have been designed as efficient diagnostic probes for tumors both in vitro and in vivo [50]. Based on this knowledge, we modified GNPLs, first with POEGMA as an antifouling spacer using SI-ATRP; TD05 APT with high specific affinity for Ramos cells was then linked to the terminal hydroxyl groups of POEGMA by N,N'-disuccinimidyl carbonate (DSC) activation to give Au-POEGMA-APT and GNPL-POEGMA-APT surfaces. The B leukemia CTC cell, Ramos cell, was selected as a target to study the selective capture ability of cell-specific APT-modified GNPLs of varying surface roughness (designated GNPL1, GNPL2, and GNPL3 with increasing surface roughness) in cell mixtures containing Ramos and CEM cells (CL1014, T cell line, human ALL) under serum-containing cell culture conditions [9].

The number of Ramos cells on the APT-modified GNPL surfaces increased with increasing surface roughness while the CEM cell number decreased, albeit slowly. The density of Ramos cells on the sAu, GNPL1, GNPL2, and GNPL3 surfaces

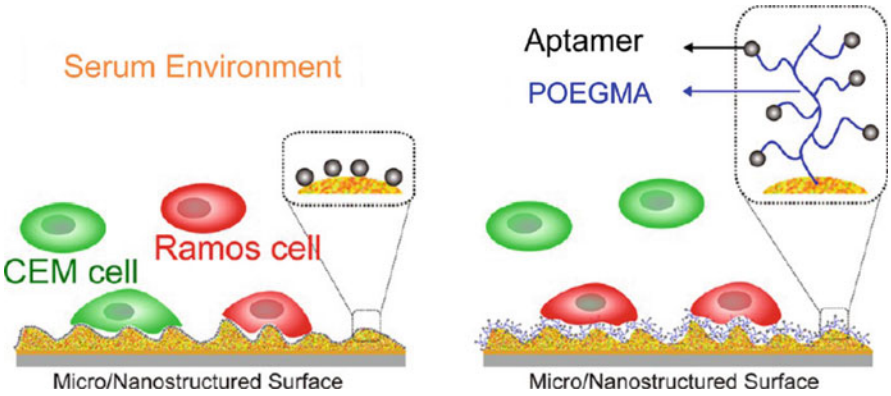

Fig. 5.7 Selective capture of Ramos cells in serum-containing conditions on GNPL surface modified with POEGMA and APT (Reprinted from Ref. [9] with permission. Copyright 2013 American Chemical Society)

were, respectively, 1.3-, 1.9-, 1.9-, and 2.2-fold greater than those of CEM cells. In contrast, after aptamer modification, the proportion of Ramos cells increased significantly with increasing surface roughness, with densities on the sAu, GNPL1, GNPL2, and GNPL3 surfaces, respectively, 2.2-, 2.8-, 3.0-, and 2.7-fold greater than those of CEM cells. We concluded that in serum-containing conditions, the roughness of the GNPLs enhanced the selectivity of the APT for Ramos cells. However, compared with serum-free conditions, the selectivity was still much weaker.

Serum is a highly complex fluid that contains many types of proteins which adsorb to surfaces nonspecifically and may "hide" the surface-immobilized APT to some extent, thereby further inhibiting the binding of cell receptors to the immobilized APT. This effect may be responsible, in large part, for the observed decrease in selectivity in serum compared to buffer. To improve the Ramos selectivity of the APT-modified surfaces in serum-containing conditions, we introduced POEGMA as a protein-resistant element. After POEGMA modification, the numbers of cells on Au-POEGMA and GNPL(1–3)-POEGMA were significantly reduced compared to the unmodified surfaces in serum-containing conditions. In addition, there was no observable difference in the numbers of Ramos and CEM cells. With the introduction of APT on the POEGMA, the density of Ramos cells increased significantly, whereas the density of CEM cells did not change. The density of Ramos cells on the four (sAu, GNPL1, GNPL2, and GNPL3) POEGMA surfaces modified with APT were, respectively, 0.9-, 1.5-, 3.5-, and 6.6-fold greater than those of CEM (Fig. 5.7).

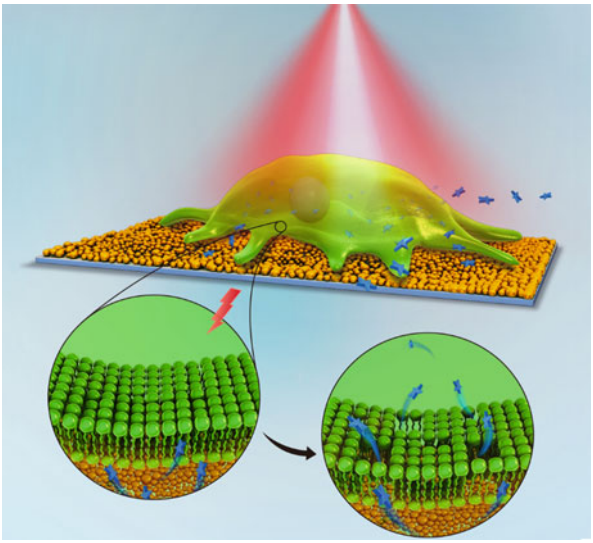

Fig. 5.8 A novel platform for macromolecular delivery into cells using gold nanoparticle layers via the photoporation effect

5.2.5 Macromolecular Delivery to Cells Using GNPL via the Photoporation Effect

Gold nanoparticle (GNP)-mediated photoporation has garnered increasing attention as a promising approach for macromolecular delivery to living cells [51, 52]. When exposed to laser light of particular wavelengths, the membrane-associated GNPs convert the absorbed laser energy into heat, leading to increased membrane permeability and the transport of normally cell-impermeable macromolecules directly into the cytosol [53]. Additionally, by tuning the laser energy, the size of the pores created in the cell membrane by the GNPs can be varied, allowing control of the quantity and size of the molecules delivered [54]. Compared with traditional photoporation, in which cell membrane permeability is achieved by focusing high-intensity femtosecond (fs) laser pulses onto individual cells, GNP-mediated photoporation can be achieved at a lower laser energy with unfocused laser light that can irradiate a large number of cells, leading to greatly increased throughput [51]. Moreover, GNPs have superior chemical and biological properties including easy surface modification for molecular attachment and improved biocompatibility. Although effective, this method relies on complex and expensive equipment to generate laser light in short pulses [54]. Moreover, concerns remain because the extreme heating of the GNPs during irradiation may cause them to distort and fragment, resulting in high cytotoxicity [55, 56]. To solve these problems, we developed a new platform for macromolecular delivery that retains the photothermal properties of GNPs while avoiding the side effects caused by their entry into the cells. Instead of free GNPs, we used GNPLs as the photoporation "reagent." GNPLs, composed of numerous GNPs with nano- and micro-topography, provide multiple sites for contact between cell membranes and the GNPs. We therefore hypothesized that GNPLs

may serve as a novel and versatile macromolecular delivery platform upon irradiation with continuous-wave (CW) laser light (Fig. 5.8) [57].

We first tried delivery of dextran to cells using this approach. Tetramethylrhodamine isothiocyanate (TRITC)-labeled dextran (red fluorescence), with a molecular weight of 4.4 kDa, was used as a model macromolecule and HeLa cells as model cells. It was found that without laser irradiation, dextran did not enter the cells efficiently; no red fluorescence was observed. Strong red fluorescence began to be observed at 3.2 $W \cdot cm^{-2}$/45 s, and the fluorescence intensity increased further at 5.1 $W \cdot cm^{-2}$/30 s. Decrease in irradiation time to 20 s at 5.1 $W \cdot cm^{-2}$ failed to give high fluorescence intensity. The delivery efficiency in presence of sAu under those conditions was much lower. To further demonstrate the efficient delivery of TRITC-dextran to HeLa cells, we obtained confocal microscopy images using the Z-stack mode to view the distribution of TRITC-dextran. Scans were taken from top to bottom of the cell membrane. The images indicated that macromolecules entered the interior of the cells and were not merely attached to the cell membrane. Moreover, cell viability experiments demonstrated that vitality was maintained under these conditions.

Plasmid DNA (pDNA) is a commonly used gene carrier and its efficient delivery to living cells is essential for gene therapy. However, due to its large size and the necessity for transport into the nucleus, transfection is more difficult with pDNA than with dextran or RNA. In our work, the applicability of GNPL-laser irradiation for the delivery of pDNA encoding green fluorescent protein (GFP), a widely used pDNA model that can easily transfect HeLa cells, was assessed. Lipofectamine 2000 (Lipo2000) complexed with pDNA was used as a standard cell transfection agent (positive control) because Lipo2000 is a widely used, commercially available transfection reagent for delivery of pDNA and RNA into cells [58]. It was found that under irradiation conditions 3.2 $W \cdot cm^{-2}$/45 s and 5.1 $W \cdot cm^{-2}$/30 s, virtually 100 % of the HeLa cells gave a green fluorescence signal, suggesting the successful delivery and expression of pDNA in the cells. These results are in line with data from flow cytometry. Compared with 3.2 $W \cdot cm^{-2}$/45 s, the transfection efficiency at 5.1 $W \cdot cm^{-2}$/30 s was significantly higher; the cells showed stronger green fluorescence, similar to that obtained using Lipo2000. These results show that under laser irradiation, our platform based on GNPLs achieved direct and efficient delivery of pDNA to HeLa cells without compromising cell viability. Moreover, the transfection efficiency of this vector-free system was comparable to that of Lipo2000.

Gene delivery to different cell types has resulted in advances in the understanding of gene function and the development of genetic therapies. Although Lipo2000 is effective for the transfection of many cell types, it is ineffective for the transfection of hard-to-transfect cell types such as primary cells including mouse embryonic fibroblasts (mEFs) used widely in stem cell research. Therefore we investigated the delivery of pDNA to hard-to-transfect mEFs. It was shown that pDNA was delivered to and expressed in mEFs under irradiation conditions of 3.2 $W \cdot cm^{-2}$/45 s with a transfection efficiency of approximately 39 %, much higher than the ~19 % using Lipo2000 ($p < 0.001$). At 5.1 $W \cdot cm^{-2}$/30 s, the transfection efficiency was further enhanced to 53 % ($p < 0.001$, vs Lipo2000), and the fluorescence intensity was much higher than for Lipo2000 ($p < 0.001$). In addition, cell viability both

immediately after and 24 h after laser irradiation was higher than 95 % under both conditions. These data demonstrate that this system is effective for the pDNA transfection of hard-to-transfect cell types with an efficiency much higher than for Lipo2000 alone.

5.3 Summary and Outlook

Gold nanoparticle layers, as a representative material with surface topological structures, have a direct influence on protein adsorption/activity and cell behavior including adhesion, spreading, proliferation, and differentiation. Compared to smooth gold surfaces, GNPLs, due to their "three-dimensional" structure, offer better access for the binding of biomacromolecules such as proteins, antigens, and antibodies and favor the maintenance of their conformation and bioactivity, thereby improving cell adhesion further. In combination with protein-resistant polymers and specific ligands for certain types of proteins or cells, modified GNPL can selectively bind certain proteins and cells from protein and cell mixtures, including the highly complex environment of serum. In addition, under laser irradiation, GNPLs can serve as a novel and efficient platform for the delivery of various macromolecules to different cell types including hard-to-transfect cell types. It is concluded that GNPLs hold great promise in many biomedical fields such as protein detection, regulation of cell behavior, capture of circulating cancer cells, and macromolecular delivery to living cells.

Acknowledgments This work was supported by the National Natural Science Foundation of China (21334004, 21404076) and the Natural Science Foundation of Jiangsu Province (BK20140316). We thank Prof. John Brash for the helpful discussion.

References

1. Yuan L, Yu Q, Li D, Chen H. Surface modification to control protein/surface interactions. Macromol Biosci. 2011;11:1031–40.
2. Gittens RA, McLachlan T, Olivares-Navarrete R, Cai Y, Berner S, Tannenbaum R, Schwartz Z, Sandhage KH, Boyan BD. The effects of combined micron-/submicron-scale surface roughness and nanoscale features on cell proliferation and differentiation. Biomaterials. 2011;32:3395–403.
3. Chen W, Weng S, Zhang F, Allen S, Li X, Bao L, Lam RH, Macoska JA, Merajver SD, Fu J. Nanoroughened surfaces for efficient capture of circulating tumor cells without using capture antibodies. ACS Nano. 2012;7:566–75.
4. Zhou F, Yuan L, Wang H, Li D, Chen H. Gold nanoparticle layer: a promising platform for ultra-sensitive cancer detection. Langmuir. 2011;27:2155–8.
5. Zhou F, Wang M, Yuan L, Cheng Z, Wu Z, Chen H. Sensitive sandwich ELISA based on a gold nanoparticle layer for cancer detection. Analyst. 2012;137:1779–84.

6. Zhou F, Li D, Wu Z, Song B, Yuan L, Chen H. Enhancing specific binding of L929 fibroblasts: effects of multi-scale topography of GRGDY peptide modified surfaces. Macromol Biosci. 2012;12:1391–400.
7. Lyu Z, Wang H, Wang Y, Ding K, Liu H, Yuan L, Shi X, Wang M, Wang Y, Chen H. Maintaining the pluripotency of mouse embryonic stem cells on gold nanoparticle layers with nanoscale but not microscale surface roughness. Nanoscale. 2014;6:6959–69.
8. Shi X, Wang Y, Li D, Yuan L, Zhou F, Wang Y, Song B, Wu Z, Chen H, Brash JL. Cell adhesion on a POEGMA-modified topographical surface. Langmuir. 2012;28:17011–8.
9. Wang Y, Zhou F, Liu X, Yuan L, Li D, Wang Y, Chen H. Aptamer-modified micro/nanostructured surfaces: efficient capture of Ramos cells in serum environment. ACS Appl Mater Interfaces. 2013;5:3816–23.
10. Zhang Q, Xu J-J, Liu Y, Chen H-Y. In-situ synthesis of poly (dimethylsiloxane)–gold nanoparticles composite films and its application in microfluidic systems. Lab Chip. 2008;8:352–7.
11. Bai H-J, Shao M-L, Gou H-L, Xu J-J, Chen H-Y. Patterned Au/poly (dimethylsiloxane) substrate fabricated by chemical plating coupled with electrochemical etching for cell patterning. Langmuir. 2009;25:10402–7.
12. Wang B, Chen K, Jiang S, Reincke F, Tong W, Wang D, Gao C. Chitosan-mediated synthesis of gold nanoparticles on patterned poly (dimethylsiloxane) surfaces. Biomacromolecules. 2006;7:1203–9.
13. Drummond TG, Hill MG, Barton JK. Electrochemical DNA sensors. Nat Biotechnol. 2003;21:1192–9.
14. Nam J-M, Thaxton CS, Mirkin CA. Nanoparticle-based bio-bar codes for the ultrasensitive detection of proteins. Science. 2003;301:1884–6.
15. Webster TJ, Schadler LS, Siegel RW, Bizios R. Mechanisms of enhanced osteoblast adhesion on nanophase alumina involve vitronectin. Tissue Eng. 2001;7:291–301.
16. Brigger I, Dubernet C, Couvreur P. Nanoparticles in cancer therapy and diagnosis. Adv Drug Deliv Rev. 2002;54:631–51.
17. Roach P, Farrar D, Perry CC. Surface tailoring for controlled protein adsorption: effect of topography at the nanometer scale and chemistry. J Am Chem Soc. 2006;128:3939–45.
18. Eteshola E, Leckband D. Development and characterization of an ELISA assay in PDMS microfluidic channels. Sensor Actuat B-Chem. 2001;72:129–33.
19. Jia C-P, Zhong X-Q, Hua B, Liu M-Y, Jing F-X, Lou X-H, Yao S-H, Xiang J-Q, Jin Q-H, Zhao J-L. Nano-ELISA for highly sensitive protein detection. Biosens Bioelectro. 2009;24:2836–41.
20. Park J-S, Cho MK, Lee EJ, Ahn K-Y, Lee KE, Jung JH, Cho Y, Han S-S, Kim YK, Lee J. A highly sensitive and selective diagnostic assay based on virus nanoparticles. Nat Nanotechnol. 2009;4:259–64.
21. Dixit CK, Vashist SK, O'Neill FT, O'Reilly B, MacCraith BD, O'Kennedy R. Development of a high sensitivity rapid sandwich ELISA procedure and its comparison with the conventional approach. Anal Chem. 2010;82:7049–52.
22. Ross AM, Jiang Z, Bastmeyer M, Lahann J. Physical aspects of cell culture substrates: topography, roughness, and elasticity. Small. 2012;8:336–55.
23. Dolatshahi-Pirouz A, Jensen T, Kraft DC, Foss M, Kingshott P, Hansen JL, Larsen AN, Chevallier J, Besenbacher F. Fibronectin adsorption, cell adhesion, and proliferation on nanostructured tantalum surfaces. ACS Nano. 2010;4:2874–82.
24. Chen W, Villa-Diaz LG, Sun Y, Weng S, Kim JK, Lam RH, Han L, Fan R, Krebsbach PH, Fu J. Nanotopography influences adhesion, spreading, and self-renewal of human embryonic stem cells. ACS Nano. 2012;6:4094–103.
25. Schulte VA, Díez M, Möller M, Lensen MC. Surface topography induces fibroblast adhesion on intrinsically nonadhesive poly (ethylene glycol) substrates. Biomacromolecules. 2009;10:2795–801.
26. Loya MC, Brammer KS, Choi C, Chen L-H, Jin S. Plasma-induced nanopillars on bare metal coronary stent surface for enhanced endothelialization. Acta Biomater. 2010;6:4589–95.

27. Chen L, Liu X, Su B, Li J, Jiang L, Han D, Wang S. Aptamer-mediated efficient capture and release of T lymphocytes on nanostructured surfaces. Adv Mater. 2011;23:4376–80.
28. Sekine J, Luo SC, Wang S, Zhu B, Tseng HR, Yu H. Functionalized conducting polymer nanodots for enhanced cell capturing: the synergistic effect of capture agents and nanostructures. Adv Mater. 2011;23:4788–92.
29. Lee MR, Kwon KW, Jung H, Kim HN, Suh KY, Kim K, Kim K-S. Direct differentiation of human embryonic stem cells into selective neurons on nanoscale ridge/groove pattern arrays. Biomaterials. 2010;31:4360–6.
30. Cretel E, Pierres A, Benoliel A-M, Bongrand P. How cells feel their environment: a focus on early dynamic events. Cell Mole Bioeng. 2008;1:5–14.
31. Chen H, Song W, Zhou F, Wu Z, Huang H, Zhang J, Lin Q, Yang B. The effect of surface microtopography of poly (dimethylsiloxane) on protein adsorption, platelet and cell adhesion. Colloid Surf B. 2009;71:275–81.
32. Yamamoto S, Tanaka M, Sunami H, Arai K, Takayama A, Yamashita S, Morita Y, Shimomura M. Relationship between adsorbed fibronectin and cell adhesion on a honeycomb-patterned film. Surf Sci. 2006;600:3785–91.
33. Rechendorff K, Hovgaard MB, Foss M, Zhdanov V, Besenbacher F. Enhancement of protein adsorption induced by surface roughness. Langmuir. 2006;22:10885–8.
34. Charest JL, Eliason MT, García AJ, King WP. Combined microscale mechanical topography and chemical patterns on polymer cell culture substrates. Biomaterials. 2006;27:2487–94.
35. Dalby M, Riehle M, Johnstone H, Affrossman S, Curtis A. Nonadhesive nanotopography: fibroblast response to poly (nbutyl methacrylate)-poly (styrene) demixed surface features. J Biomed Mater Res A. 2003;67:1025–32.
36. Marcon L, Spriet C, Coffinier Y, Galopin E, Rosnoblet C, Szunerits S, Héliot L, Angrand P-O, Boukherroub R. Cell adhesion properties on chemically micropatterned boron-doped diamond surfaces. Langmuir. 2010;26:15065–9.
37. Lagunas A, Comelles J, Martínez E, Samitier J. Universal chemical gradient platforms using poly (methyl methacrylate) based on the biotin− streptavidin interaction for biological applications. Langmuir. 2010;26:14154–61.
38. Li B, Chen J, Wang JHC. RGD peptide-conjugated poly (dimethylsiloxane) promotes adhesion, proliferation, and collagen secretion of human fibroblasts. J Biomed Mater Res A. 2006;79:989–98.
39. Causa F, Battista E, Della Moglie R, Guarnieri D, Iannone M, Netti PA. Surface investigation on biomimetic materials to control cell adhesion: the case of RGD conjugation on PCL. Langmuir. 2010;26:9875–84.
40. Kunzler TP, Drobek T, Schuler M, Spencer ND. Systematic study of osteoblast and fibroblast response to roughness by means of surface-morphology gradients. Biomaterials. 2007;28:2175–82.
41. Lord M, Cousins B, Doherty P, Whitelock J, Simmons A, Williams R, Milthorpe B. The effect of silica nanoparticulate coatings on serum protein adsorption and cellular response. Biomaterials. 2006;27:4856–62.
42. Mann BK, West JL. Cell adhesion peptides alter smooth muscle cell adhesion, proliferation, migration, and matrix protein synthesis on modified surfaces and in polymer scaffolds. J Biomed Mater Res. 2002;60:86–93.
43. Sawyer A, Weeks D, Kelpke S, McCracken MS, Bellis S. The effect of the addition of a polyglutamate motif to RGD on peptide tethering to hydroxyapatite and the promotion of mesenchymal stem cell adhesion. Biomaterials. 2005;26:7046–56.
44. Sawyer AA, Hennessy KM, Bellis SL. The effect of adsorbed serum proteins, RGD and proteoglycan-binding peptides on the adhesion of mesenchymal stem cells to hydroxyapatite. Biomaterials. 2007;28:383–92.
45. Wang S, Liu K, Liu J, Yu ZTF, Xu X, Zhao L, Lee T, Lee EK, Reiss J, Lee YK. Highly efficient capture of circulating tumor cells by using nanostructured silicon substrates with integrated chaotic micromixers. Angew Chem Int Edit. 2011;50:3084–8.

46. Alunni-Fabbroni M, Sandri MT. Circulating tumour cells in clinical practice: methods of detection and possible characterization. Methods. 2010;50:289–97.
47. Nagrath S, Sequist LV, Maheswaran S, Bell DW, Irimia D, Ulkus L, Smith MR, Kwak EL, Digumarthy S, Muzikansky A. Isolation of rare circulating tumour cells in cancer patients by microchip technology. Nature. 2007;450:1235–9.
48. Adams AA, Okagbare PI, Feng J, Hupert ML, Patterson D, Göttert J, McCarley RL, Nikitopoulos D, Murphy MC, Soper SA. Highly efficient circulating tumor cell isolation from whole blood and label-free enumeration using polymer-based microfluidics with an integrated conductivity sensor. J Am Chem Soc. 2008;130:8633–41.
49. Fischer KE, Alemán BJ, Tao SL, Daniels RH, Li EM, Bünger MD, Nagaraj G, Singh P, Zettl A, Desai TA. Biomimetic nanowire coatings for next generation adhesive drug delivery systems. Nano Lett. 2009;9:716–20.
50. Medley CD, Bamrungsap S, Tan W, Smith JE. Aptamer-conjugated nanoparticles for cancer cell detection. Anal Chem. 2011;83:727–34.
51. Qin Z, Bischof JC. Thermophysical and biological responses of gold nanoparticle laser heating. Chem Soc Rev. 2012;41:1191–217.
52. Sapsford KE, Algar WR, Berti L, Gemmill KB, Casey BJ, Oh E, Stewart MH, Medintz IL. Functionalizing nanoparticles with biological molecules: developing chemistries that facilitate nanotechnology. Chem Rev. 2013;113:1904–2074.
53. Delcea M, Sternberg N, Yashchenok AM, Georgieva R, Bäumler H, Möhwald H, Skirtach AG. Nanoplasmonics for dual-molecule release through nanopores in the membrane of red blood cells. ACS Nano. 2012;6:4169–80.
54. Xiong R, Raemdonck K, Peynshaert K, Lentacker I, De Cock I, Demeester J, De Smedt SC, Skirtach AG, Braeckmans K. Comparison of gold nanoparticle mediated photoporation: vapor nanobubbles outperform direct heating for delivering macromolecules in live cells. ACS Nano. 2014;8:6288–96.
55. Vogel A, Noack J, Hüttman G, Paltauf G. Mechanisms of femtosecond laser nanosurgery of cells and tissues. Appl Phys B. 2005;81:1015–47.
56. Baumgart J, Humbert L, Boulais É, Lachaine R, Lebrun J-J, Meunier M. Off-resonance plasmonic enhanced femtosecond laser optoporation and transfection of cancer cells. Biomaterials. 2012;33:2345–50.
57. Lyu Z, Zhou F, Liu Q, Xue H, Yu Q, Chen H. A universal platform for macromolecular deliveryinto cells using gold nanoparticle layers via the photoporation effect. Adv Funct Mater. 2016;26:5787–95.
58. Katas H, Alpar HO. Development and characterisation of chitosan nanoparticles for siRNA delivery. J Control Release. 2006;115:216–25.

Chapter 6
Surface Modification of Tissue Engineering Scaffolds

Feng Wen, Charles Chau Sang Lau, Jing Lim, Yanwan Liao, Swee Hin Teoh, and Mark Seow Khoon Chong

6.1 Introduction

A wide range of biomaterials, both synthetic and biologically derived, are used widely in biomedical applications, including utility as scaffolds in tissue engineering. These materials are largely selected on their bulk properties, such as mechanical strength and degradation properties, in order to meet basic requirements on strength [1, 2]. However, host responses are largely mediated by interactions with the material surface [3], and there emerges a need to tailor these surface properties to elicit appropriate biological responses, while retaining the bulk properties on which the materials were selected [4]. To meet these needs, much research has been dedicated towards the development of surface modification technologies. This chapter discusses the common technologies being used, as well as the methods employed to characterise the modified surfaces.

6.2 Surface Modification Techniques

6.2.1 Physical Surface Modification

Physical surface modification refers to the process that applies physical methods to change the physical properties (e.g. roughness and wettability), biochemical properties (e.g. biochemical components, functional groups and/or the distribution of them) and/or topographic structure (e.g. lattice structure, pore size and micropatterns) of the surface. Through the physical, biochemical or topographic cues

F. Wen • C.C.S. Lau • J. Lim • Y. Liao • S.H. Teoh • M.S.K. Chong (✉)
Nanyang Technological University, Singapore, Singapore
e-mail: markchong@ntu.edu.sg

© Springer Science+Business Media Singapore 2016

C. Gao (ed.), *Polymeric Biomaterials for Tissue Regeneration*,
DOI 10.1007/978-981-10-2293-7_6

given by these modification methods, the adhesion, proliferation, alignment and intracellular physiological activities of cells on modified surface can be controlled. More recently, physical modification methods have been used to elicit antimicrobial effects [5, 6] and even retard blood coagulation [7–9].

6.2.1.1 Topographical Engineering

Scaffolds in tissue engineering are analogous to the extracellular matrix (ECM) in that they provide the mechanical substrate for cell growth. Besides structural support, it has become evident that physical cues, in the form of topographical microstructures, are capable of guiding cell alignment and migration in the microenvironment [10, 11]. This phenomenon was described in as early as 1912 by Harrison in the direction of cell motion on spider web and was later defined as "contact guidance" by Weiss [12]. More recent work has focused on the biological effects of these geometrical cues. Fibroblasts seeded on quartz slides with parallel ridge-groove structure, for example, showed alignment and elongation along the direction of gratings, giving a typical example for contact guidance. In addition, this trend was more significant on substrate with increasing groove depth [13]. In another study on PMMA substrate with a similar pattern, a larger depth and width were found to be more effective in restricting the lateral movement of fibroblasts across groove structures, while a smaller width was more effective in restricting the longitudinal movement along the ridges [14]. Two theories have been raised to explain these phenomena: (1) patterning of focal adhesions and (2) filopodial sensing [15, 16]. Focal adhesions are multi-protein complexes mechanically linking intracellular actin to extracellular substrates via integrin-ligand bundles. By influencing the integrin-matrix interactions, integrin clustering [17] and integrin spacing can be adjusted. Thus, the geometry and distribution of surface topographical features can control cell adhesion to substrate and then guide cell elongation and migration [18–21]. Additionally, focal adhesions serve as biochemical signal sensors to allow transmembrane signal transduction, such as focal adhesion kinase pathways, by activation of integrin receptors [22–24]. Topographic cues also have mechanical effects on cells by causing deformation of cytoskeleton and adjusting intracellular tension. Subsequent transduction of both the biochemical signals and mechanical signals may modulate transcription factors and influence cell physiological activities, not only cell motility but also cell apoptosis [25], proliferation and differentiation [26–29]. Ceballos et al. reported significantly improved in vivo peripheral nerve regeneration in collagen tubes filled with aligned collagen gel compared to randomly aligned control tubes [30]. In another nerve regeneration study, up-regulation of neural markers at mRNA and protein levels was observed in human mesenchymal stem cells (hMSCs) on aligned poly(ε-caprolactone) (PCL) nanofibre scaffold when compared with that on polystyrene (PS) plate, indicating an enhanced commitment of MSCs into neural cells [31].

In order to modify the topographical structure of tissue engineering scaffold, materials are either added onto substrate surface by methods like nanofibre coating

[32] and plasma deposition [33] or ablated by methods like chemical etching and laser corrosion [34]. Additionally, mechanical techniques like stretching may also be applied to polymer materials to avoid weight loss and change in material composition while creating new microstructures. After uniaxial stretching, for example, oriented ridge-groove structures are observed on polycaprolactone (PCL) films and successfully guided human bone marrow MSC elongation and alignment with a preferential orientation approximately parallel to the ridges. The elongation and alignment of MSC could be observed from 12 h post seeding and lasted as long as 15 days [35]. More specifically, altered cell morphology, cytoskeletonal reorientation and nucleus elongation were pointed out in a following study, and increased expression of myogenic genes in MSCs was observed with an increasing time length of cell culture on stretched PCL film [35]. The topographical features of stretched PCL films can be further controlled by alkaline hydrolysis [36] and augmented with femtosecond laser microperforation to create secondary microfeatures [37]. Small concaved features formed at the edge of ridges after soaking in aqueous NaOH solution for longer than 10 days that developed into parallel grooves across the ridges and finally split the ridges into small parallel islands after 30 days of soaking. With declined ridge height and aspect ratio between ridges and grooves that resulted from hydrolysis, the guidance effect on MSC alignment and elongation may be tailored. For applications in vascular tissue engineering, MSCs and human umbilical vein endothelial cells (HUVECs) were separately seeded on each face of stretched PCL film. Aligned through holes on the film created by direct laser microperforation facilitate myoendothelial communications between tunica media and intima, consequently enhancing heterotypic cell-cell contacts across PCL film and cell ingrowth into the film.

6.2.1.2 Wettability Engineering

Wettability refers to the interaction at the two-phase interface between fluid and solid. Solid surface with a greater wettability is more favourable for the fluid to spread over or adhere to it, so that the contact angle between solid-fluid interface and vapour-fluid interface is smaller. In tissue engineering study, wettability presents as one of the primary concerns in scaffold material design for its influence on initial cell attachment and migration on scaffold via adsorption of proteins from culture medium in vitro or from extracellular fluid in vivo and then binding to cell adhesion molecules on cell surface. The preferable range of wettability varies according to the kind of cells. For example, the optimal cell adhesion of foetal rat skin fibroblast was achieved on polymer films with a water contact angle of around 70° [38], but a more hydrophilic surface with a water contact angle between 20 and 40° was more suitable for cell attachment of NIH 3T3 fibroblasts [39]. However, raw biomaterials exhibit certain water contact angle that may not fall into the preferable range for cell growth, which reveals the necessity of modification. Despite the biodegradability and feasibility to fabricate into tissue engineering scaffold with varied shape design, electrospun PCL fibre is a hydrophobic material with a water

contact angle of 123.3 ± 10.8°. By adding a poly(vinyl phosphonic acid-co-acrylic acid) (PVPA) coating layer, PCL scaffold has turned to be hydrophilic with the water contact angle dropped to 43.3 ± 1.2°. After 14 days in vitro culture, osteoblasts on this PCL/PVPA scaffold generated a better-defined cytoskeleton than those on uncoated PCL scaffold, indicating a better cell spreading due to improved wettability of PCL fibre [40]. Although high hydrophobicity is usually not suitable for cell attachment and migration, hydrophilic biomaterials like poly(ethylene glycol) (PEG) hydrogel may lack the stability to maintain its mechanical strength as well as shape due to fast degradation. Thus, instead of altering the bulk properties of the material, surface modification is employed as a superior approach to partially improve material wettability.

Alkaline hydrolysis is one of the mature techniques to modify surface wettability for polyester biomaterials such as PCL [41], PLA [42] and PLGA [43, 44] and already has been applied in industry. After treatment with alkaline agent (usually mild NaOH solution), the ester bonds on the surface of polyester materials break and form carboxyl and hydroxyl. Such oxygen-containing polar groups have stronger electric attraction to water molecules; as a result, the material surface shows a higher hydrophilicity and thus a higher percentage of attachment of specific cell types. Another technique is to modify the surface roughness. Based on the Wenzel equation, the increase in roughness of solid surface can either increase the hydrophilicity in a hydrophilic system in which the water contact angle is smaller than 90° or increase the hydrophobicity in a hydrophobic system where the water contact angle is larger than 90°. Thus, by changing the surface roughness, the wettability of biomaterials can be optimised for a better cytocompatibility. Extreme ultraviolet (EUV) irradiation is another approach for roughness optimisation for polymeric materials. For instance, polytetrafluoroethylene (PTFE) is a hydrophobic polymer material widely used in tissue regeneration studies. This material has inherently low surface energy, which makes it largely chemically inert and ideally suited for passive, structural applications. Unfortunately, this also renders the surface incompatible for cellular attachment and vulnerable to pathologic states, such as denudation of vascular graft surfaces. To modify the extremely stable PTFE surface, EUV irradiation in the presence of nitrogen gas was used to increase surface roughness. The average surface roughness of EUV-treated polymer samples increased by up to four times as compared to that of the pristine control, resulted in enhanced hydrophobicity of PTFE and significantly improved the adhesion and morphology of L929 fibroblasts [45]. Nanofibre deposition or nanoparticle deposition onto the surface of biomaterials is another approach to change surface roughness. On poly(lactic acid) (PLA) films incorporated with magnetic nanoparticles, enhanced adhesion and proliferation of cardiac-like rat myoblasts H9c2 was found on the film with the highest amount of embedded nanoparticles and hence the largest surface roughness with the largest water contact angle [46]. It is noteworthy that in this study, with the increase of surface roughness, film surface turned from being hydrophilic to hydrophobic, which looks contrary to abovementioned conclusion from the Wenzel equation. This is because surface wettability is influenced by complex factors including not

only the roughness but also other aspects like electrical and chemical nature, which should also be taken into account at the design of material surface.

Novel techniques for surface roughening are still under exploration. Borrowing ideas from micromanipulation, carving the surface of polymer materials or moving polymer chains at a microlevel and even nano-level high precision for surface modification may be realised under atomic force microscope (AFM) or scanning tunnelling microscope (STM) with manipulator and tip of scanning probe. However, the feasibility of such techniques is very limited due to high cost and high requirement on operation. Particularly, only the polymer material with a conductive surface or a conductive coating can be processed under STM, which sets another obstacle to practical application of micromanipulation.

6.2.1.3 Physical Deposition

Physical deposition is one of the methods to produce a functional coating layer on substrate material so as to grant the material with more desirable properties. In particular, bioactive components including inorganic particles, synthetic polymer, lipid, polysaccharide, peptides, protein as well as its ligand [47, 48] are deposited onto scaffold materials for enhanced initial cell attachment and proliferation or to regulate intracellular protein synthesis and induce cell differentiation [49]. For the combination of functional materials with substrates, weak forces such as van der Waals forces, hydrogen bond force and electrostatic attraction force are formed during deposition. Compared to chemical conjugation, physical modification is less stable, leading to gradual loss of the coating layer [50]. On the other hand, physical deposition has a broader application with the multitude of materials as substrate or as coating layer regardless of their chemical composition. Based on the existing form of coating materials, physical deposition can be classified into solution deposition and vapour deposition.

Solution deposition methods may be further subcategorised into immersion and adsorption, casting, dip coating and electrophoretic deposition. These methods are based on allowing the substrate to contact and adsorb the functional molecules dissolved in a liquid phase, followed by removal of the solvent by evaporation. Immersion and adsorption are the simplest methods by which substrate stands in a solution and spontaneously adsorbs the functional molecules uniformly dispersed in this solution. In applied electric field, deposition of coating molecules can be accelerated by electrophoretic motion of these molecules in solution towards the substrate placed at a corresponding electrode. This technique for physical deposition is named as electrophoretic deposition. Besides, the thickness of coating layer is determined by the time length of deposition and/or electric field strength. The technique as casting for modification of smooth and flat surface is developed from the same principle as immersion. Other than a static contact between substrate and solution, solution containing functional molecules is sprayed onto the substrate and subsequently spreads over the surface at high-speed spinning and thereby forms a thin liquid layer that leaves the functional molecules as a film covering the substrate

after evaporation. The thickness of this coating film is controllable depending on both the speed of centrifuging and the viscosity of the solution. Dip coating is another low-cost technique for deposition on monolithic three-dimensional scaffolds. The process is completed by partially or fully inserting the substrate into coating solution followed by removal from the solution. In addition, this process can be repeated to obtain multiple coating layers, which is named as "layer-by-layer" fabrication. Unlike simple immersing or spin casting, dip coating enables oriented alignment of coating layers formed by amphiphilic molecules like phospholipid and further affects surface properties of scaffold materials. Amphiphilic molecules refer to the kind of molecules that possesses both hydrophilic groups and lipophilic groups. In a solution, these molecules float on the surface of the solvent, keep the part of the molecule compatible with the solvent under liquid level and expose the other part above liquid level. Through different operating procedures consisted of dipping and removing, specific moieties on the amphiphilic molecules can be connected to the substrate surface or the previous coating layer. Especially on polymer substrates, entrapment of coating molecules in the surface may occur at the same time with physical adsorption due to the space created at swelling of polymers in the solvent, resulting in added amount of coating molecules deposited on polymer substrate [51].

Physical vapour deposition (PVD) is a surface coating method in which the coating material is vaporised in a cell at high temperature and vacuum state or filled with gaseous plasma. The vapour is subsequently transported to the substrate surface and condenses to generate a thin film on it. Based on the methods applied to generate and deposit material, PVD is further classified into vacuum evaporation deposition [52], sputtering deposition [53, 54], pulsed laser deposition [55, 56], electron beam deposition [57] and cathodic arc deposition [58]. In surface modification on synthetic polymer tissue engineering scaffold, the method applied is mainly the sputtering deposition. In order to create gaseous coating material, inert gas (typically argon) is transferred into plasma and accelerated under high-voltage electric field. Bombardment from this high-energy plasma at cathodic target frees coating molecules from solid source into a vapour phase through momentum transfer. These active molecules deposit on all surfaces inside a chamber to release energy and rebuild thermodynamic equilibrium, therefore forming a thin film on the substrate surface. Compared to evaporation deposition, sputtering deposition is superior in surface coating using materials with very high melting points and forming a more sturdy coating on the substrate.

6.2.2 Chemical Modification

While biomaterials are primarily selected on their bulk properties, host responses are largely governed by cell-material surface interactions. It follows that synthetic materials, ranging from polymers to ceramics and metals, usually lack appropriate biological surface cues to elicit or direct desirable cellular and tissue responses such

Table 6.1 Physical and chemical surface modification methods

Methods	References
Radiation (electron beam and gamma)	[62, 63]
Plasma (RF, microwave, acoustic, corona discharge)	[64–66]
Photo (UV and visible sources)	[67]
Ion beam (sputtering, etching, implantation)	[68, 69]
Gas phase deposition	[60, 70, 71]
Silanisation	[72]
Coating (with or without covalent bonding)	[73, 74]
Chemical reaction (oxidation, reduction, hydrolysis, aminolysis)	[59, 75, 76]

as adhesion, proliferation and immune response [1, 59–61]. To this end, chemical surface modifications may be performed to introduce biochemical cues onto material surfaces, while retaining the existing bulk material properties. These modification methods are summarised in Table 6.1, of which plasma-, gamma-, UV-, hydrolysis- and aminolysis-induced chemical modifications are the most common and are discussed in further detail.

6.2.2.1 Plasma-Induced Modification

Plasma-induced modification is an extremely useful method enabling selective creation of chemistry and topography on the surface of a biomaterial with excellent retention of bulk characteristics for specific biomedical applications [77–80]. Plasma, the fourth state of matter after solid, liquid and gas, is typically generated by applying high voltages to gases, under which the gas molecules or atoms will be ionised by the electrical discharge and therefore split up into electrons and ions [81]. The effectiveness of the ionisation process is dependent on operating parameters such as gas flow rate, pressure and constituents, as well as the distance between the discharge electrodes. Plasma can be further characterised with an energy distribution in the range 10–20 eV which is effective to modify surface chemistry of the substrate in plasma. The interaction between ionised gas species with surfaces of substrate contacted in plasma could produce tailored physical and chemical modifications on substrate surface through ionic activity in plasma and functionalities (functional groups or free radicals) formation on the surface. As described above, in physical modification, the bombardment of ionic species powered by an electrical field can increase substrate surface roughness and promote interfacial adhesion of depositions [78]. Additionally, chemical modification can be achieved by controlling the (1) functional groups or free radicals which are generated on substrate surfaces by interaction between charged particles and surface molecules of the substrate and [64] (2) desirable monomer polymerisation and deposition on the surface of the substrate [82]. The functionalities formation on substrate surfaces may be altered by proper selection of the nature of the gaseous medium in plasma. Plasma generated

in oxygen, ammonia and carbon dioxide gases can be used to introduce functionalities such as hydroperoxide, amino and carboxylic groups on substrate surface, respectively. Additionally, inert gases such as argon lead to the generation of free radicals on the polymer backbone, which are transformed into hydroperoxide bridges in the presence of oxygen and water vapour [1, 83]. Biomaterials with functionalities formation on their surface are either directly used for biomedical applications or continuously conjugated with following various desirable molecules for specific biomedical applications while those functionalities will be used as anchorage points. It has been reported that polyethylene (PE) surfaces exposed to ammonia plasma [84] resulted in surface amination, providing functional groups for the subsequent conjugation of functional biomolecules on the surface [85], typically involving polymerisation with spacers. Together, control of plasma parameters and conjugants provides great versatility in the tailoring and customisation of surfaces of biomaterials. It is important to note here the process of plasma surface modification often leads to the formation of a layer of polymer on the surface and is coupled with physical alterations to the topography (discussed above in the preceding section) [1, 86, 87].

Poly(caprolactone) (PCL) and poly(lactide-co-caprolactone) (PLCL) have been used as bioresorbable polymers in numerous medical devices as well as for tissue engineering applications. Biomolecules were conjugated on their surfaces to optimise their performances through plasma-induced surface modification [1, 64]. In these studies, monomeric acrylic acid was polymerised on the surface of PCL and PLCL as spacer for the conjugation of biomolecules. The exposure of the PCL and PLCL membranes under argon/oxygen plasma resulted in the formation of peroxide and hydroperoxide groups, which were used to initiate the addition polymerisation of acrylic acid by decomposition of hydroperoxides under UV irradiation. The degree of polymerisation of acrylic acid on membrane surfaces is considerably influenced by the plasma exposure parameters, such as plasma power, pressure, exposure time and the reaction conditions involving monomer concentration and reaction time. Collagen and Jagged-1 peptides were immobilised on PCL and PLCL surface through carbodiimide route, respectively.

These technologies may be readily adapted towards other biomolecules, in order to tailor specific responses. Hyaluronic acid (HA), for example, is a nontoxic and water-soluble polymer which is extensively used for biomedical applications [88]. It is largely considered to be nonimmunogenic, enzymatically degradable and relatively nonadhesive to cells and proteins. Additionally, HA is involved in several physiological processes, including angiogenesis, extracellular matrix homeostasis, wound healing and the mediation of long-term inflammation. This versatile nature of HA has led to many studies not only on the preparation of HA alone but also on the subsequent usage for surface modification of biomaterials for specific medical applications. While HA can be applied as a physical coating, they get displaced easily, and covalent bonding of HA is necessary for use in biomedical applications. For example, HA covalently bonded on polydimethylsiloxane surface through oxygen plasma surface modification resulted in the decrease in the protein adsorption and significant cell growth and neural differentiation [86].

In performing plasma modifications, several parameters may be controlled in order to maximise polymerisation yield. Plasma treatment time, for example, significantly influences the formation of free radicals, and titration may be performed to establish the optimum plasma treatment time required for maximal free radical generation. Overexposure may also lead to the loss of free radicals that are otherwise responsible for peroxidation during exposure to oxygen [64, 89]. Additionally, the polymerisation conditions, such as spacer-monomer concentration, have profound impact on the yield of polymerisation. Without UV irradiation (typically at elevated temperatures), the yield initially increases with monomer concentration, reaches a maximum and then tends to decrease beyond a critical concentration [65], whereby extensive autocatalysis leads to homopolymerisation of the solution phase. In contrast, with UV irradiation and controlled temperatures, the yield typically increases continuously with the increase of the monomer concentration [90].

6.2.2.2 Ultraviolet (UV)-Induced Modification

UV irradiation is a simple, efficient and economic method used for surface modification of biomaterials [91, 92]. UV light is generally classified in four sub-bands: UVA (315–400 nm); UVB (280–315 nm); UVC (100–280 nm); and EUV (10–124 nm). At wavelengths from 180 to 400 nm, UV light provides sufficient energy to disrupt molecular bonds on biomaterial surfaces, leading to a series of photophysical, thermal and photochemical processes. However, this influence is often not limited only to surface layer of the material but potentially alters the material bulk properties [93]. Therefore, initiators are commonly used, which can reduce the dosage of UV irradiation in the surface modification process [80, 94, 95].

Surface modification of HDPE (high-density polyethylene) membranes has been performed through UV light irradiation with photosensitive compounds [95]. In this study, HDPE was treated with selected active compounds and a photo-initiator under 254 nm UV excitation. Results showed surface chemistry of HDPE was modified through functional moieties conjugated on its surface via specific bonds, resulting in changes to the surface properties of HDPE, as demonstrated by the increased wettability of the previously hydrophobic HDPE surface.

In another example of UV-induced surface modification, polyethylene terephthalate (PET) films were functionalised through conjugation with both RGD peptide and galactose ligands to enhance cell adhesion and functions synergistically [80]. The combination of plasma and UV irradiation was used in this study. PET films were first irradiated in argon plasma with power output of 40 W for 1 min and then exposed to air for 10 min to induce the formation of peroxides and hydroperoxides on its surface. In order to achieve high yield of polymerisation, degassing of acrylic acid solution was done by argon bubbling to thoroughly remove oxygen before subsequent UV-induced polymerisation of acrylic acid. Alternatively, this step could be replaced by the addition of some agents such as sodium periodate, which helps in oxygen depletion to ensure polymerisation efficiently. Exposure to UV (365 nm) was then performed to initiate the formation of a poly(acrylic acid)

(PAAc) on the PET surface. Subsequently, RGD peptide and galactose ligands were immobilised on the pAAc layer using carbodiimide chemistry. Results showed that pAAc was successfully grafted on the surface of PET film, with carboxyl-group density of 78.57 nmol/cm^2 available for subsequent conjugation of RGD peptides and galactose ligands.

More recently, extreme UV (EUV) radiation has been used as a source of high-energy ultraviolet radiation. The main advantage of the EUV irradiation is preservation of bulk properties of irradiated material due to its photon energy which is capable of breaking more molecular bonds at the upper surface of the material as compared to common UV light [96]. For the same reason, however, EUV radiation propagates only in vacuum, and hence, irradiation of materials in gaseous environment requires a special arrangement. Similar to plasma etching, EUV radiation is also used to produce nano-/micro-sized pattern on the surface of polymers [97].

6.2.2.3 Gamma-Induced Modification

Gamma radiation is an extremely high-frequency electromagnetic radiation and therefore comprises high-energy photons (above 110 keV). Gamma-induced modification is a well-established technique to modify biomaterial properties by gamma ray irradiation-induced modifications (grafting, cross-linking or gel formation). Cobalt-60 and cesium-137 are common sources used in gamma-induced modifications. This technique has been intensively used for applications in the medical field for surface modification of materials to control blood-material interactions and conjugation of molecules in polymeric matrices to form specific chemical moieties or drug carriers. The major advantages of gamma-induced modification are as follows: (1) Due to its high-energy nature, initiators are not required in the process. Therefore, the purity of products may be maintained, as free radicals are formed on the polymer/monomer backbone. (2) Deep penetration of gamma rays through the polymer matrix enables rapid and uniform generation of free radicals and therefore could initiate the modification process throughout the entire material. (3) The gamma-induced modification can be performed at room temperatures. (4) It generates less environmental pollution than chemical methods. Several studies have been devoted to the development of biomaterials based on the radiation surface modification process [62, 98–101].

As described above, surface chemistry is critical in mediating host and cellular responses. Additionally, functional groups on the surface can be exploited as chemically reactive sites for coupling other function molecules for specific biomedical applications. In this context, gamma irradiation may be useful for the introduction of functional moieties to the material surface. For example, polystyrene (PS) is a typically inert polymer which lacks functional groups. Exposure to gamma radiation yielded carbonyl and ether functional groups on the surface. Carbonyl groups were presented below the top few molecular layers of ester. Unsaturated carbonyl/acid groups formed a higher proportion of the total carbonyls with increasing depth, and the extent of interior oxidation was linear with gamma dosage [56]. One of the main challenges in designing blood-contacting biomaterials lies in the need to prevent

thrombus formation. Proper tailoring of the biomaterial surface is aimed at reducing the adsorption of clot-initiating proteins and the adhesion of platelets. In one study, polyethylene glycol methacrylate (PEG-MA) with different molecular weights was conjugated on the surface of PE films by gamma irradiation, and results showed less adsorption of proteins and adhesion of platelets on PE film surfaces after modification [102]. The degree of grafting is found to be strongly dependent on the reaction conditions, as well as the storage time and temperature of the irradiated film prior to the reaction. Additionally, reaction temperatures can be controlled to keep segmental mobility low such that the free radicals that are produced during the irradiation remain trapped within the matrix.

6.2.2.4 Hydrolysis- and Aminolysis-Induced Modification

Many polyesters such as poly(lactic-glycolic acid) (PLGA), PET, poly(ester urethane) (PU), poly(L-lactic acid) (PLLA) and PCL have been used for wide biomedical applications such as drug delivery and medical devices due to their well controllable degradation rate and mechanical properties [76, 103–105]. As mentioned above, surface modification of these polymers is necessary to improve their biocompatibility. Among those surface modification methods available, wet-chemical methods of hydrolysis and aminolysis are used most frequently due to their (1) simple steps, (2) ease of control (3) and scalability to three-dimensional structures. Through hydrolysis and aminolysis, carboxylic acid and amine groups could be produced on the surface of polymer in a highly controlled manner, with minimal erosion.

Hydrolysis of polyesters can be driven by either acidic or basic conditions [75]. However, under acidic conditions, hydrolysis of esters is achieved via electrophilic attack by hydrogen ions on the carbonyl oxygen which requires very strongly acidic conditions and may target the bulk material, instead of being limited to surface hydrolysis. In contrast, under basic conditions, hydrolysis is achieved by nucleophilic attack by hydroxide ions on the carbonyl carbon, which is surface-oriented and results in less bulk hydrolysis. For example, aminolysis is driven by nucleophilic attack on the carbonyl carbon to generate a positively charged tetrahedral intermediate. Aminolysis may be performed either in basic solutions or in an aprotic, polar solvent. Unlike base hydrolysis, the overall activation energy for the aminolysis is low and even negative in organic solvents, resulting in reduced or inverse dependence of aminolysis on the reaction temperature. It has been previously reported that aminolysis rates typically reach a plateau at pH values just above the pKa of the amine in aqueous solutions [106].

In an attempt to improve endothelialisation of PCL scaffold surfaces, aminolysis was performed to create amino groups on the PCL film surface through reaction surface of PCL with 1,6-hexanediamine [103]. It was found that the amount of amino groups generated on the PCL film surface increased with 1,6-hexanediamine concentrations (0–14 %) and also with exposure duration, reaching a maximum value at 1 h. Incubation beyond that resulted in a decrease in free amine groups,

possibly due to auto-polymerisation with terminal carboxyl groups or degradation of the superficial layer. The exposed amino groups could subsequently be used as anchor sites for the conjugation of protein such as gelatin, chitosan and collagen. The follow-up endothelial cell culture proved that the cell attachment and proliferation ratios were obviously improved, and the cells showed a similar morphology to those cultured on tissue culture polystyrene surfaces.

6.3 Techniques for Analysing Modified Surfaces

Analysing the surface properties of a modified material is essential in determining whether the surface modification is successful and whether the modified surface can satisfy the requirements of its intended application [107, 108]. There are various techniques to analyse and characterise the surface properties of a material, and they are broadly categorised into physical, chemical and biological techniques based on the nature of the information being sought. In brief, physical techniques focus on the surface tension and surface topography, chemical techniques provide information on the chemical structure and chemical composition of the surface, and biological techniques assess the biocompatibility and cellular responses on the surface. The most common techniques used in the characterisation of polymeric biomaterial surfaces for tissue engineering applications are summarised in Table 6.2 and presented in the following sections.

6.3.1 Physical Characterisation

6.3.1.1 Contact Angle Measurement

Since a polymeric biomaterial is likely to be employed in an aqueous environment, it is important to study the interaction between water and the surface of the material, also known as its wettability. This reactivity of water with material surface is central in molecular self-association of water at the interface, leading to the formation of water structure that governs the selective adsorption of proteins on the material surface [109]. The wettability of a surface is typically determined by placing a drop of liquid onto the surface and measuring the contact angle – the angle between the liquid-vapour interface and the solid surface. The contact angle θ is related to the surface tensions at the liquid-vapour, solid-vapour and solid-liquid interfaces (represented by γ_{LV}, γ_{SV} and γ_{SL}) in Young's equation given in Fig. 6.1a [110, 111]. In general, a stronger attraction between the liquid and the surface leads to a lower contact angle. For biomaterials, water is typically used as the probe liquid. Surfaces with a contact angle of more than 90° are generally defined as hydrophobic (Fig. 6.1b), whereas surfaces with a contact angle of less than 90° are generally defined as hydrophilic (Fig. 6.1c). In surface modification experiments, comparing the

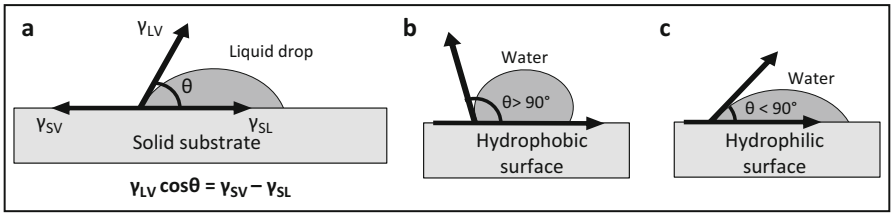

Fig 6.1 Schematic representation of (**a**) the relation between the contact angle θ and the surface tensions at the three interfaces, (**b**) a drop of water on a hydrophobic surface and (**c**) a drop of water on a hydrophilic surface [110, 111]

contact angle value before the modification with the value after the modification can determine the effectiveness of the modification process.

Contact angle measurements are typically done on a goniometer, an instrument used for precise measurements of angles. A modern goniometer is equipped with a camera and a software where the researcher can define the solid-liquid interface (also known as drop baseline) and set the fitting method to fit the drop shape. Beside static measurements, dynamic contact angle measurements can also be performed to enhance sensitivity. Dynamic techniques include increasing and decreasing the drop volume and tilting the surface to determine the advancing and receding contact angles. While contact angle measurement is valuable for assessing surface wettability, it is not reliable for heterogeneous surfaces where the wettability differs at various parts of the sample and porous samples where the drop is absorbed into the material [112]. Contact angle measurements also do not offer information on the surface chemistry and topography changes after surface modification. Hence, other characterisation techniques are often performed in addition to contact angle measurements to provide a full evaluation on the effectiveness of a surface modification process.

6.3.1.2 Scanning Electron Microscopy (SEM)

Information on the surface morphology and topography of a polymeric biomaterial can be obtained by various microscopic techniques, depending on the dimension of the surface, the desired lateral resolution, the depth of the surface and the sample environment. While optical microscopy is the easiest to use and least invasive among the techniques, its lateral resolution is limited to the wavelength of light, which is around 300 nm. Hence SEM, which reveals surface features at nanometre lateral resolutions, is often the preferred technique to visualise the surface topography of a biomaterial [111, 113]. In SEM, a beam of electrons is directed onto the sample under vacuum, and the resultant interaction between the electrons and the sample surface causes an emission of secondary electrons, which are collected by the detector to produce an electron micrograph [114]. Samples that are not electrically conductive need to be sputter-coated with a thin metallic coating to prevent

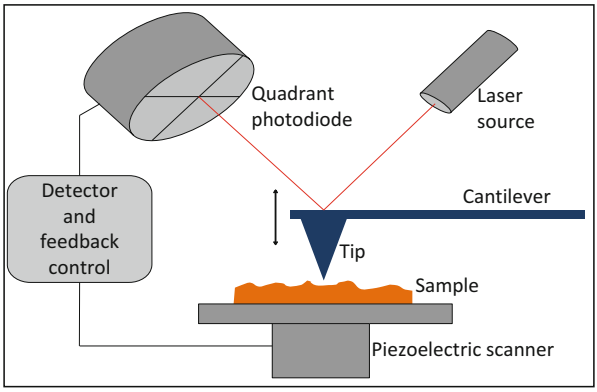

Fig. 6.2 Schematic representation of the working principle of AFM

electrical charging (the accumulation of electrons) on the sample. As the analysis takes place under vacuum to prevent scattering of electrons by air molecules, samples containing cells and biological tissues have to be fixed and dried to ensure that the biological components remain stable in vacuum [115]. Some samples, such as hydrated polymers and surfaces modified with adsorbed molecules, may not be suitable for SEM due to their instability in vacuum. As the SEM operates in a dry environment, the information obtained may not truly represent the actual surface topography in physiological conditions. Nevertheless, the ease of operation and the ease of interpreting the images make SEM one of the most universal techniques to analyse surface topography of a biomaterial at the nanometre scale.

6.3.1.3 Atomic Force or Scanning Force Microscopy (AFM or SFM)

AFM offers high resolution both in width and depth at the sample surface and is capable of detecting surface features of several nanometres in depth or height, unlike SEM where the resolution in depth is limited to microscale. In fact, AFM can be used to resolve molecules or even single atoms adsorbed on a smooth surface, and its sensitivity allows researchers to obtain images of delicate biological features [111, 116]. An AFM consists of a sharp tip attached to a flexible microscale cantilever (Fig. 6.2). When the tip is scanned across the sample surface, attractive and repulsive forces between the tip and sample cause the cantilever to deflect vertically. The deflection is detected by a photodiode via a laser beam reflected off the top of the cantilever, and the signal is processed into a topographical image. Depending on the scan mode, a constant force or constant height between the tip and the sample is maintained by a feedback loop, which controls the movement of the piezoelectric scanner holding the sample [117, 118].

Depending on the sample's properties and the application, the AFM can be operated in a number of modes. One frequently used mode is the contact mode, where the tip is in constant contact with the sample. While the contact mode offers the

highest resolution, the shear forces applied by the tip may damage soft samples and surfaces with weakly adsorbed molecules. Another frequently used mode is the tapping mode, where the cantilever is oscillating above the moving sample and the changes in amplitude and phase are tracked. Since the tip is not in contact with the sample, the tapping mode is suitable for soft samples. Besides high resolutions, other advantages of the AFM include its ability to operate in a variety of environments including air and aqueous solutions, its ability to measure interaction forces between a surface and adsorbed molecules and its ability to measure electrical properties (e.g. charge density) of a surface. On the other hand, limiting characteristics of the AFM are a much slower scanning speed, small scanning area (less than 100 μm wide), sample damage or sample movement caused by shear forces from the tip and probe damage caused by hard samples with steep features.

6.3.2 Chemical Characterisation

6.3.2.1 Attenuated Total Reflectance Fourier Transform Infrared Spectroscopy (FTIR)

The surface chemistry of polymeric biomaterials can be investigated by various spectroscopic techniques, and ATR-FTIR is one spectroscopic technique that is widely employed. The principle behind Fourier transform infrared spectroscopy (FTIR) is that various organic functional groups absorb light at specific wavelengths in the infrared (IR) spectrum that are characteristic of their vibrational modes [119]. Hence, FTIR allows quantitative determination of a sample's chemical composition and is a powerful tool to track the chemical changes that occur in a chemical reaction. FTIR is typically performed by passing a beam of IR light through a solid sample blended with a salt transparent to IR or a liquid sample sandwiched between two salt discs. However, since most polymeric biomaterials are opaque to IR light and cannot be homogeneously blended with salt, they are analysed in the attenuated total reflection mode, where the surface of the sample is pressed onto an inorganic crystal (e.g. ZnSe or Ge) and a beam of IR light is directed towards the crystal-sample interface. Despite total reflection at the interface, the incident IR beam penetrates the sample in the form of an evanescent wave. After the sample absorbs light at specific wavelengths, the reflected beam leaves the crystal and is converted to an IR spectrum by the FTIR system [120, 121]. While the ATR-FTIR is fast and easy to use, it is not a very surface-specific technique because the probe depth ranges from several hundred nanometres to several micrometres. In contrast, a layer of immobilised molecules (e.g. proteins) on a surface may only be several to tens of nanometres thick. For polymeric biomaterials, the bulk phase's IR absorption may mask the peaks of the immobilised molecules, making it impossible to detect the presence of the immobilised molecules [108]. Because of this reason, ATR-FTIR is limited to the analysis of homogeneous samples or thin layers of organic molecules on inorganic substrates, where the IR absorptions of the inorganic phase do not overlap with that of the organic molecules.

6.3.2.2 X-Ray Photoelectron Spectroscopy (XPS)

XPS is a more powerful and more surface-specific technique than ATR-FTIR for analysing the surface chemical composition of polymeric biomaterial, with a sampling depth of less than 10 nm [108]. In XPS, soft X-rays are directed onto the sample to excite the electrons in the atoms, causing the electrons at the surface of the sample to eject. The quantity of the ejected electrons is measured as a function of the incident energy by the photoelectron spectrometer. As each chemical element has a characteristic spectrum, the overall spectrum can be used to quantitatively determine the elemental composition of the sample surface. Although the incident X-ray can penetrate far into the sample surface, only the electrons within 10 nm of the surface can leave the sample without obstruction [113, 122]. This explains the high surface specificity of XPS. The sampling depth and surface sensitivity can be further controlled by changing the angle between incident X-ray and the sample surface. As XPS is surface specific, it is a useful tool to detect the presence of immobilised molecules on the surface of a modified biomaterial. For example, protein molecules grafted onto an aliphatic polymer can be detected and quantified by the N1 peaks, since nitrogen atoms are present in the protein molecules but not in the polymer [123] (Fig 6.3). Besides elemental quantification, chemical state information can also be obtained from XPS, as the chemical environment around an atom can influence the binding energy of the ejected electrons and cause a chemical shift. One example is carbon, which exhibits different binding energy in various functional groups. As a result, the chemical shift of the C1 peak can be used to identify certain functional groups [124]. However, one major limitation of XPS is its inability to detect hydrogen or helium, which can lead to inaccurate information on the elemental composition of a hydrogen-containing sample. While XPS is sensitive, it requires a vacuum environment to prevent scattering of ejected electrons by gas molecules. This means that, similar to SEM, XPS is only suitable for dry samples and may not be suitable for surfaces with adsorbed molecules. In addition, caution has to be taken for polymers and biomolecules as they can degrade under X-ray radiation, leading to altered chemical properties.

6.3.2.3 Time-of-Flight Secondary Ion Mass Spectroscopy (TOF-SIMS)

TOF-SIMS or simply SIMS is a spectroscopy technique for obtaining information on the chemical composition of a solid surface. With a sampling depth of 1–2 nm, it has an even higher surface specificity than XPS. Originally developed for the analysis of inorganic materials, SIMS has progressed into a versatile tool for the analysis of organic molecules, biomolecules and polymers, and it has an advantage over XPS for being able to identify hydrogen [108, 113, 123]. In SIMS, a beam of energetic primary ions, usually argon or gallium, is directed

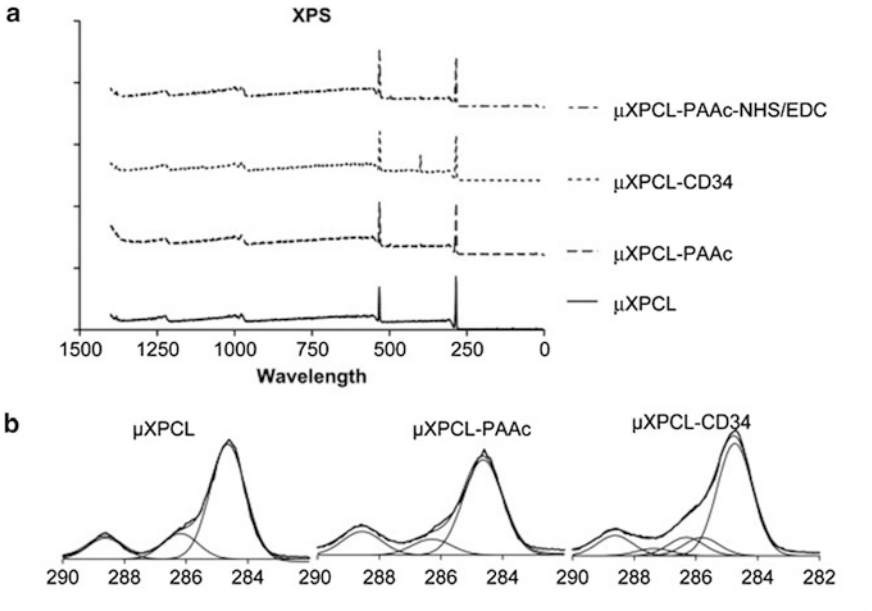

Atomic Ratio (%)					
Binding Energy (eV)	-C-H ~284.6	-C-O ~286.2	-O-C=O ~288.6	-C-N ~285.8	-O-C-N ~287.4
Pristine	71.2	15.8	13.0	-	-
μXPCL-PAAc	70.7	11.8	17.5	-	-
μXPCL-CD34	63.7	10.4	11.5	10.3	4.1

Fig. 6.3 XPS survey of material surfaces. (**a**) XPS can be used to obtain a wide survey spectra of material surfaces. Here, polycaprolactone (*PCL*) films were modified with polyacrylic acid (*pAAc*) to allow conjugation of a protein (CD34 antibody), as identified by the peak at 286.4 eV. (**b**) Relative intensity of the deconvoluted C1S spectra can also be used to show increase in carboxyl groups following PAAc engraftment, followed by introduction of peptide groups following CD34 antibody conjugation (Reprinted with permission from Chong et al. [77], with permission from Elsevier)

onto the sample surface, generating a collision cascade where the primary ions transfer energy to the sample. The collision causes atoms and molecules to sputter from the sample surface. A small portion of the sputtered particles are ionised to produce secondary ions, which are accelerated to the same kinetic energy via an electric field and then made to travel the same distance in a field-free drift region before reaching the detector. As the speed of the ions depends on their masses, the time of flight of an ion provides information on its mass and eventually its identity. As each chemical structure has its characteristic mass spectrum, analysis of the final spectrum can provide significant information on the chemical composition of the sample surface [125, 126]. TOF-SIMS can be operated in

two modes – static and dynamic. Static TOF-SIMS scans the sample surface with a low-energy primary ion beam to produce a static analysis of the topmost layer of the sample. Dynamic TOF-SIMS uses a high-energy primary ion beam to erode the sample surface continuously and record the real-time signal simultaneously, producing a depth profile of the chemical compositions layer by layer into the bulk. While SIMS is highly sensitive for surface analysis, it can also be sensitive to contamination. Common contaminants include plasticisers found in plastic containers and silicones found in double-sized tape used to secure samples [123]. Because of this reason, SIMS samples should be stored in aluminium foil or clean glass containers. Like SEM and XPS, SIMS is performed in a high-vacuum environment, so samples should be dry and stable in vacuum. Another limitation of SIMS is the huge quantity of data generated, as every pixel of a two-dimensional image contains a full mass spectrum. Analysis of the data can be extremely time-consuming and complicated if one does not know the sample well. To simplify data analysis and maximise the amount of meaningful information, computational multivariate analysis methods are developed to process TOF-SIMS images [127].

Table 6.2 Most common techniques for characterising polymeric biomaterial surfaces

Technique	Category	Probe	Information	Requirement
Contact angle	Physical	Liquid drop	Surface energy	Clean, homogeneous, nonporous surface
Scanning electron microscopy (SEM)	Physical	Electrons	Surface topography	Vacuum, conductive sample surface
Atomic force microscopy (AFM)	Physical	Cantilever	Surface topography, composition, roughness	
Attenuated total reflectance Fourier transform infrared spectroscopy (FTIR)	Chemical	Infrared light	Surface composition, binding state	Bulk phase having no overlapping IR absorption with surface molecules
X-ray photoelectron spectroscopy (XPS)	Chemical	X-ray/electrons	Chemical composition, binding state	Vacuum, separate elemental analysis for hydrogen
Time-of-flight secondary ion mass spectroscopy (TOF-SIMS)	Chemical	Ions	Surface composition	Vacuum, samples stored in aluminium foil or clean glass containers

6.4 Characterisation of Biocompatibility

Having discussed the physical and chemical characterisation methods, this section focuses on the biological characterisation of surface-modified biomaterials. In general, the ISO 10993 provides an extensive set of guidelines to evaluate the safety and efficacy of devices and may be applied towards material testing. It also provides an opportunity for the investigator to better understand the safety and efficacy profiles of the material used, which may be helpful in the eventual translation of the material into clinics. Many of these tests are contextual and need to be appropriately selected for use in specific applications. The ISO 10993-13, for example, deals with material interactions with blood and provides the basis for selection and design of appropriate tests for blood-contacting surfaces, such as engineered blood vessels. It is, however, beyond the scope of this chapter to describe each section in detail; the ISO 10993-5 provides basic guidelines for cytocompatibility testing and will be the focus of discussion. At this point, it should be noted, for eventual translation into the market, that the European Committee (EC) adopts this standard and makes it part of their technical review; where additional requirements are required, the adopted version has a prefix "EN". It may be useful to conform to the more stringent requirements in the standard issued by the EC.

6.4.1 ISO10993-5: Tests for In Vitro Cytotoxicity

The ISO 10993-5 deals primarily with the evaluation of cytotoxicity or, more accurately in this case, the lack thereof. Broadly, it involves exposing test cells to the material, either directly or indirectly, followed by evaluation of viability. Some tests available for such evaluations are listed in Table 6.3.

In general, a numerical grade of >2 in qualitative scoring is considered cytotoxic. For qualitative testing, reduction of cell viability by >30 % shall indicate cytotoxic effects. Under these conditions, significant considerations shall be given to the surface modification procedure, which could include but is not limited to (1) use of cross-linking agents, (2) chemical alteration of biomaterial molecular structure and (3) surface-modified coating chemistry and its cytotoxicity effects.

At this point, it is critical to highlight that the evaluation of cytocompatibility alone is not a direct measure of surface modification efficacy (except where the

Table 6.3 Summary of cytotoxicity tests and their corresponding cell lines

Test name	Suitable cell lines
Neutral red uptake	BALB/c 3T3 cells, clone 31 CRB 9005
Colony-forming cytotoxicity	V79
MTT cytotoxicity	L-929
XTT cytotoxicity	L-929

Referenced from ISO 10993-5:2009, Annexes A–D. Copyright remains with ISO

modification is performed specifically to improve cytocompatibility). It does, however, provide important indications on the safety profile of the surface coating process, in order to flag out unexpected cytotoxic events arising from the modification process.

6.4.1.1 Direct Contact

Direct contact methods involve the direct exposure of cells to the material surface, followed by evaluation of cell viability. One important test requirement would be to ensure that there is at least one flat surface (no specific requirement on roughness is provided). In addition, if the biomaterial is meant to be used sterile, then it shall be sterilised accordingly before testing is done. Otherwise, the basic principles of aseptic handling during testing shall apply. The selection of cell lines to be used for testing shall, in principle, follows the requirements of the standard. However, concession is also given to situations where a specific response to a selected cell line is desired; in this case, cell line reproducibility and accuracy of response need to be demonstrated. Testing the material involves culturing the cells to subconfluency on standard plates and subsequently placing the material directly on the cells. Cell viability is then tracked over multiple days and may also be morphologically observed under microscope. Important test requirements are that appropriate experimental controls (both positive and negative) should be included and that the biomaterial shall only cover one-tenth of the exposed surface area of the cell layer.

Determination of cytotoxicity may be performed using qualitative and quantitative measurements although it is preferred that quantitative measurements are taken. If qualitative measurements are taken, the following table (Table 6.4) provides the guidelines to which cytotoxicity shall be measured.

6.4.1.2 Exposure to Liquid Extracts

This process involves the incubation of the modified material in an extraction fluid medium, to which the cells are subsequently exposed. Extraction conditions generally follow the principle of simulating or exaggerating clinical use conditions without causing significant changes in the biomaterial. For this purpose, the extraction vehicle can be culture medium, physiological saline or any other justifiable medium. Importantly, to fulfil the requirements of the standard, the extraction vehicle(s) should allow extraction of polar and nonpolar elements.

The extraction conditions shall be conducted without causing significant changes in the biomaterial and therefore should be chosen carefully. Generally, normal cell culture condition of 37 °C for a period of 24 ± 2 h is applied. However, raised temperatures and durations of extraction may be applied provided that the chemistry of the biomaterial is unaffected, and the intended use of the biomaterial justifies the extraction conditions. Additionally, in situations where the cumulative contact of the biomaterial is less than 4 h, and is in contact with intact skin or mucosa surfaces, the extraction times shall be at least 4 h.

Table 6.4 Reactivity grades for direct contact test

Grade	Reactivity	Description of reactivity zone
0	None	No detectable zone around or under specimen
1	Slight	Some malformed or degenerated cells under specimen
2	Mild	Zone limited to area under specimen
3	Moderate	Zone extending specimen size up to 10 cm
4	Severe	Zone extending farther than 10 cm beyond specimen

Adapted from ISO 10993-5:2009, section 8.5. Copyright remains with ISO

6.4.1.3 Indirect Contact

Indirect methods are concerned with measuring the leachables from a material. Two methods are most commonly performed. In the agar diffusion method, selected cell lines are grown to subconfluency, and 0.5–2 % mass percent of melted agar is casted over the cells, with a fresh culture medium change. The sample is then placed on top of the agar, followed by a predefined period of incubation (24–74 h) before evaluation. In the filter diffusion method, a surfactant-free filter of pore size 0.45 μm is used. Briefly, an aliquot of a continuously stirred cell suspension is added onto the surfactant-free filter and incubated until subconfluency is achieved. The filters are then transferred onto a layer of solidified agar (cell side facing down) before the biomaterial is placed onto the acellular side of the filter (top side).

6.5 Conclusion

Surface modification of biomaterials allows for retention of desirable bulk properties, while directing favourable biological reactions. In this chapter, common surface modification methods were discussed. Additionally, methods of characterising the material surfaces were summarised. Evaluation should be performed in accordance with existing standards, in order to facilitate eventual clinical translation. Thorough understanding of the available modalities to modify and characterise material surfaces will be integral for the appropriate design of tissue engineering scaffolds.

References

1. Cheng Z, Teoh S-H. Surface modification of ultra thin poly (ε-caprolactone) films using acrylic acid and collagen. Biomaterials. 2004;25(11):1991–2001. doi:http://dx.doi.org/10.1016/j.biomaterials.2003.08.038.

2. Huebsch N, Mooney DJ. Inspiration and application in the evolution of biomaterials. Nature. 2009;462(7272):426–32.
3. Gupta B. Radiation effects on polymers for biological use, Advances in polymer science, vol. 162. Berlin: Springer; 2003. doi:10.1007/3-540-45668-6.
4. Mitragotri S, Lahann J. Physical approaches to biomaterial design. Nat Mater. 2009;8(1):15–23.
5. Erakovic S, Jankovic A, Tsui GC, Tang C-Y, Miskovic-Stankovic V, Stevanovic T. Novel bioactive antimicrobial lignin containing coatings on titanium obtained by electrophoretic deposition. Int J Mol Sci. 2014;15(7):12294–322.
6. Gour N, Ngo KX, Vebert-Nardin C. Anti-infectious surfaces achieved by polymer modification. Macromol Mater Eng. 2014;299(6):648–68.
7. Ren X, Feng Y, Guo J, Wang H, Li Q, Yang J, Hao X, Lv J, Ma N, Li W. Surface modification and endothelialization of biomaterials as potential scaffolds for vascular tissue engineering applications. Chem Soc Rev. 2015;44(15):5680–742.
8. Rudolph A, Teske M, Illner S, Kiefel V, Sternberg K, Grabow N, Wree A, Hovakimyan M. Surface modification of biodegradable polymers towards better biocompatibility and lower thrombogenicity. PLoS One. 2015;10(12):e0142075. doi:10.1371/journal.pone.0142075.
9. Milleret V, Hefti T, Hall H, Vogel V, Eberli D. Influence of the fiber diameter and surface roughness of electrospun vascular grafts on blood activation. Acta Biomater. 2012;8(12):4349–56. doi:http://dx.doi.org/10.1016/j.actbio.2012.07.032.
10. Provenzano PP, Inman DR, Eliceiri KW, Trier SM, Keely PJ. Contact guidance mediated three-dimensional cell migration is regulated by Rho/ROCK-dependent matrix reorganization. Biophys J. 2008;95(11):5374–84.
11. Flemming R, Murphy C, Abrams G, Goodman S, Nealey P. Effects of synthetic micro- and nano-structured surfaces on cell behavior. Biomaterials. 1999;20(6):573–88.
12. Zhou F, Yuan L, Huang H, Chen H. Phenomenon of “contact guidance” on the surface with nano-micro-groove-like pattern and cell physiological effects. Chin Sci Bull. 2009;54(18):3200–5. doi:10.1007/s11434-009-0366-1.
13. Britland S, Morgan H, Wojiak-Stodart B, Riehle M, Curtis A, Wilkinson C. Synergistic and hierarchical adhesive and topographic guidance of BHK cells. Exp Cell Res. 1996;228(2):313–25. doi:http://dx.doi.org/10.1006/excr.1996.0331.
14. Sun F, Casse D, Van Kan JA, Ge R, Watt F. Geometric control of fibroblast growth on proton beam-micromachined scaffolds. Tissue Eng. 2004;10(1–2):267–72.
15. Driscoll MK, Sun X, Guven C, Fourkas JT, Losert W. Contact guidance of amoeboid cells via nanotopography. ACS Nano. 2014;8(4):3546–3555. doi:10.1021/nn406637c.
16. Bettinger CJ, Langer R, Borenstein JT. Engineering substrate topography at the micro- and nanoscale to control cell function. Angew Chem Int Ed Engl. 2009;48(30):5406–15. doi:10.1002/anie.200805179.
17. Biggs MJP, Richards RG, Gadegaard N, Wilkinson CDW, Dalby MJ. The effects of nanoscale pits on primary human osteoblast adhesion formation and cellular spreading. J Mater Sci: Mater Med. 2007.;18(2):399–404. doi:10.1007/s10856-006-0705-6.
18. Dalby MJ, Gadegaard N, Oreffo ROC. Harnessing nanotopography and integrin-matrix interactions to influence stem cell fate. Nat Mater. 2014;13(6):558–69. doi:10.1038/nmat3980.
19. Cavalcanti-Adam EA, Volberg T, Micoulet A, Kessler H, Geiger B, Spatz JP. Cell spreading and focal adhesion dynamics are regulated by spacing of integrin ligands. Biophys J. 2007;92(8):2964–74. doi:10.1529/biophysj.106.089730.
20. Yim EK, Darling EM, Kulangara K, Guilak F, Leong KW. Nanotopography-induced changes in focal adhesions, cytoskeletal organization, and mechanical properties of human mesenchymal stem cells. Biomaterials. 2010;31(6):1299–306. doi:10.1016/j.biomaterials.2009.10.037.
21. Decuzzi P, Ferrari M. Modulating cellular adhesion through nanotopography. Biomaterials. 2010;31(1):173–9. doi:http://dx.doi.org/10.1016/j.biomaterials.2009.09.018.

22. Goodman SL, Sims PA, Albrecht RM. Three-dimensional extracellular matrix textured biomaterials. Biomaterials. 1996;17(21):2087–95. doi:http://dx.doi.org/10.1016/0142-9612(96)00016-6.
23. Ozaki I, Hamajima H, Matsuhashi S, Mizuta T. Regulation of TGF-β1-induced proapoptotic signaling by growth factor receptors and extracellular matrix receptor integrins in the liver. Front Physiol. 2011;2. doi:10.3389/fphys.2011.00078.
24. Teo BKK, Wong ST, Lim CK, Kung TYS, Yap CH, Ramagopal Y, Romer LH, Yim EKF. Nanotopography modulates mechanotransduction of stem cells and induces differentiation through focal adhesion kinase. ACS Nano. 2013;7(6):4785–98. doi:10.1021/nn304966z.
25. Cao H, Marcy G, Goh ELK, Wang F, Wang J, Chew SY. The effects of nanofiber topography on astrocyte behavior and gene silencing efficiency. Macromol Biosci. 2012;12(5):666–74.
26. Tsimbouri PM, Murawski K, Hamilton G, Herzyk P, Oreffo ROC, Gadegaard N, Dalby MJ. A genomics approach in determining nanotopographical effects on MSC phenotype. Biomaterials. 2013;34(9):2177–84. doi:http://dx.doi.org/10.1016/j.biomaterials.2012.12.019.
27. McMurray RJ, Gadegaard N, Tsimbouri PM, Burgess KV, McNamara LE, Tare R, Murawski K, Kingham E, Oreffo ROC, Dalby MJ. Nanoscale surfaces for the long-term maintenance of mesenchymal stem cell phenotype and multipotency. Nat Mater. 2011;10(8):637–44. doi:http://www.nature.com/nmat/journal/v10/n8/abs/nmat3058.html#supplementary-information.
28. Chen W, Villa-Diaz LG, Sun Y, Weng S, Kim JK, Lam RHW, Han L, Fan R, Krebsbach PH, Fu J. Nanotopography influences adhesion, spreading, and self-renewal of human embryonic stem cells. ACS Nano. 2012;6(5):4094–103. doi:10.1021/nn3004923.
29. Chew SY, Low WC. Scaffold-based approach to direct stem cell neural and cardiovascular differentiation: an analysis of physical and biochemical effects. J Biomed Mater Res A. 2011;97(3):355–74.
30. Ceballos D, Navarro X, Dubey N, Wendelschafer-Crabb G, Kennedy WR, Tranquillo RT. Magnetically aligned collagen gel filling a collagen nerve guide improves peripheral nerve regeneration. Exp Neurol. 1999;158(2):290–300. doi:http://dx.doi.org/10.1006/exnr.1999.7111.
31. Chew SY, Mi RF, Hoke A, Leong KW. Aligned protein-polymer composite fibers enhance nerve regeneration: a potential tissue-engineering platform. Adv Funct Mater. 2007;17(8):1288–96. doi:10.1002/adfm.200600441.
32. Chen F, Lee CN, Teoh SH. Nanofibrous modification on ultra-thin poly(e-caprolactone) membrane via electrospinning. Mater Sci Eng C. 2007, March;27(2):325–32. ISSN 0928–4931, http://dx.doi.org/10.1016/j.msec.2006.05.004.
33. Flamm DL, Auciello O, d'Agostino R. Plasma deposition, treatment, and etching of polymers: the treatment and etching of polymers. New York: Elsevier; 2012.
34. Tiaw KS, Goh SW, Hong M, Wang Z, Lan B, Teoh SH. Laser surface modification of poly(epsilon-caprolactone) (PCL) membrane for tissue engineering applications. Biomaterials. 2005;26(7):763–9. doi:10.1016/j.biomaterials.2004.03.010.
35. Wang ZY, Teo EY, Chong MS, Zhang QY, Lim J, Zhang ZY, Hong MH, Thian ES, Chan JK, Teoh SH. Biomimetic three-dimensional anisotropic geometries by uniaxial stretch of poly(epsilon-caprolactone) films for mesenchymal stem cell proliferation, alignment, and myogenic differentiation. Tissue Eng Part C Methods. 2013;19(7):538–49. doi:10.1089/ten.TEC.2012.0472.
36. Wang ZY, Lim J, Ho YS, Zhang QY, Chong MS, Tang M, Hong MH, Chan JK, Teoh SH, Thian ES. Biomimetic three-dimensional anisotropic geometries by uniaxial stretching of poly(epsilon-caprolactone) films: degradation and mesenchymal stem cell responses. J Biomed Mater Res A. 2014;102(7):2197–207. doi:10.1002/jbm.a.34899.
37. Wang Z, Du Z, Chan JKY, Teoh SH, Thian ES, Hong M. Direct laser microperforation of bioresponsive surface-patterned films with through-hole arrays for vascular tissue-engineering application. ACS Biomater Sci Eng. 2015;1(12):1239–49. doi:10.1021/acsbiomaterials.5b00455.

38. Tamada Y, Ikada Y. Fibroblast growth on polymer surfaces and biosynthesis of collagen. J Biomed Mater Res. 1994;28(7):783–9. doi:10.1002/jbm.820280705.
39. Webb K, Hlady V, Tresco PA. Relative importance of surface wettability and charged functional groups on NIH 3T3 fibroblast attachment, spreading, and cytoskeletal organization. J Biomed Mater Res. 1998;41(3):422.
40. Bassi A, Gough J, Zakikhani M, Downes S. The chemical and physical properties of poly (ε-caprolactone) scaffolds functionalised with poly (vinyl phosphonic acid-co-acrylic acid). J Tissue Eng. 2011;2(1):31–8.
41. Wong W, Yeo A, Sju E, Teoh S. Modifications in surface characteristics and pore morphology of PCL-TCP scaffolds under varying alkaline treatment conditions. J Biomed Mater Res A. 2010 Jun 15;93(4):1358–67. doi: 10.1002/jbm.a.32633.
42. Wang Y-Q, Cai J-Y. Enhanced cell affinity of poly(l-lactic acid) modified by base hydrolysis: wettability and surface roughness at nanometer scale. Curr Appl Phys. 2007;7(Supplement 1):e108–11. doi:http://dx.doi.org/10.1016/j.cap.2006.11.027.
43. Park G, Park K, Webster T. NaOH-treated PLGA scaffolds allow for greater articular chondrocyte functions. In: Bioengineering conference, 2004. Proceedings of the IEEE 30th Annual Northeast, 2004. IEEE, pp 148–9.
44. Nam YS, Yoon JJ, Lee JG, Park TG. Adhesion behaviours of hepatocytes cultured onto biodegradable polymer surface modified by alkali hydrolysis process. J Biomater Sci Polym Ed. 1999;10(11):1145–58.
45. Ahad IU, Butruk B, Ayele M, Budner B, Bartnik A, Fiedorowicz H, Ciach T, Brabazon D. Extreme ultraviolet (EUV) surface modification of polytetrafluoroethylene (PTFE) for control of biocompatibility. Nucl Instrum Methods Phys Res B: Beam Interact Mater Atoms. 2015;364:98–107. doi:http://dx.doi.org/10.1016/j.nimb.2015.08.093.
46. Ventrelli L, Fujie T, Turco SD, Basta G, Mazzolai B, Mattoli V. Influence of nanoparticle-embedded polymeric surfaces on cellular adhesion, proliferation, and differentiation. J Biomed Mater Res A. 2014;102(8):2652–61.
47. Pan H, Zheng Q, Yang S, Guo X. Effects of functionalization of PLGA-[Asp-PEG]n copolymer surfaces with Arg-Gly-Asp peptides, hydroxyapatite nanoparticles, and BMP-2-derived peptides on cell behavior in vitro. J Biomed Mater Res A. 2014;102(12):4526–35. doi:10.1002/jbm.a.35129.
48. Jaganathan SK, Balaji A, Vellayappan MV, Subramanian AP, John AA, Asokan MK, Supriyanto E. Review: radiation-induced surface modification of polymers for biomaterial application. J Mater Sci. 2015;50(5):2007–18.
49. Hersel U, Dahmen C, Kessler H. RGD modified polymers: biomaterials for stimulated cell adhesion and beyond. Biomaterials. 2003;24(24):4385–415. doi:http://dx.doi.org/10.1016/S0142-9612(03)00343-0.
50. Katti DS, Vasita R, Shanmugam K. Improved biomaterials for tissue engineering applications: surface modification of polymers. Curr Top Med Chem. 2008;8(4):341–53.
51. Xie Z, Buschle-Diller G, DeInnocentes P, Bird RC. Electrospun poly (D, L)-lactide nonwoven mats for biomedical application: surface area shrinkage and surface entrapment. J Appl Polym Sci. 2011;122(2):1219–25.
52. Duran H, Ogura K, Nakao K, Vianna SD, Usui H, Advincula RC, Knoll W. High-vacuum vapor deposition and in situ monitoring of N-carboxy anhydride benzyl glutamate polymerization. Langmuir. 2009;25(18):10711–8.
53. Shtansky DV, Grigoryan AS, Toporkova AK, Arkhipov AV, Sheveyko AN, Kiryukhantsev-Korneev PV. Modification of polytetrafluoroethylene implants by depositing TiCaPCON films with and without stem cells. Surf Coat Technol. 2011;206(6):1188–95. doi:http://dx.doi.org/10.1016/j.surfcoat.2011.08.029.
54. Ryu GH, Yang W-S, Roh H-W, Lee I-S, Kim JK, Lee GH, Lee DH, Park BJ, Lee MS, Park J-C. Plasma surface modification of poly (d,l-lactic-co-glycolic acid) (65/35) film for tissue engineering. Surf Coat Technol. 2005;193(1–3):60–4. doi:http://dx.doi.org/10.1016/j.surfcoat.2004.07.062.

55. Murcia-López S, Fàbrega C, Monllor-Satoca D, Hernández-Alonso MD, Penelas-Pérez G, Morata A, Morante JR, Andreu T. Tailoring multilayered BiVO4 photoanodes by pulsed laser deposition for water splitting. ACS Appl Mater Interfaces. 2016;8(6):4076–85. doi:10.1021/acsami.5b11698.
56. Johnson S. Pulsed laser deposition of hydroxyapatite thin films. Atlanta: Georgia Institute of Technology; 2005.
57. Hamdi M, Ektessabi A-I. Calcium phosphate coatings: a comparative study between simultaneous vapor deposition and electron beam deposition techniques. Surf Coat Technol. 2006;201(6):3123–8.
58. Chang Y-Y, Yang S-J, Wang D-Y. Characterization of TiCr (C, N)/amorphous carbon coatings synthesized by a cathodic arc deposition process. Thin Solid Films. 2007;515(11):4722–6.
59. Du Y, Han R, Wen F, Ng San San S, Xia L, Wohland T, Leo HL, Yu H. Synthetic sandwich culture of 3D hepatocyte monolayer. Biomaterials. 2008;29(3):290–301. doi:10.1016/j.biomaterials.2007.09.016.
60. Yang ZL, Wang J, Luo RF, Maitz MF, Jing FJ, Sun H, Huang N. The covalent immobilization of heparin to pulsed-plasma polymeric allylamine films on 316L stainless steel and the resulting effects on hemocompatibility. Biomaterials. 2010;31(8):2072–83. doi:10.1016/j.biomaterials.2009.11.091.
61. Xie YT, Zhai WY, Chen L, Chang J, Zheng XB, Ding CX. Preparation and in vitro evaluation of plasma-sprayed Mg2SiO4 coating on titanium alloy. Acta Biomater. 2009;5(6):2331–7. doi:10.1016/j.actbio.2009.03.003.
62. Yang F, Li X, Cheng M, Gong Y, Zhao N, Zhang X, Yang Y. Performance modification of chitosan membranes induced by gamma irradiation. J Biomater Appl. 2002;16(3):215–26. doi:10.1106/088532802021176.
63. Schulze A, Maitz MF, Zimmermann R, Marquardt B, Fischer M, Werner C, Went M, Thomas I. Permanent surface modification by electron-beam-induced grafting of hydrophilic polymers to PVDF membranes. RSC Adv. 2013;3(44):22518–26. doi:10.1039/C3RA43659D.
64. Wen F, Wong HK, Tay CY, Yu H, Li H, Yu T, Tijore A, Boey FYC, Venkatraman SS, Tan LP. Induction of myogenic differentiation of human mesenchymal stem cells cultured on notch agonist (Jagged-1) modified biodegradable scaffold surface. ACS Appl Mater Interfaces. 2014;6(3):1652–61. doi:10.1021/am4045635.
65. Gupta B, Hilborn JG, Bisson I, Frey P. Plasma-induced graft polymerization of acrylic acid onto poly(ethylene terephthalate) films. J Appl Polym Sci. 2001;81(12):2993–3001. doi:10.1002/app.1749.
66. Kim S-W. Surface modification of polypropylene in an impulse corona discharge. Kor J Chem Eng. 1996;13(1):97–100. doi:10.1007/bf02705895.
67. Ul Ahad I, Bartnik A, Fiedorowicz H, Kostecki J, Korczyc B, Ciach T, Brabazon D. Surface modification of polymers for biocompatibility via exposure to extreme ultraviolet radiation. J Biomed Mater Res A. 2014;102(9):3298–310. doi:10.1002/jbm.a.34958.
68. Ensinger W, Müller HR. Surface modification and coating of powders by ion beam techniques. Mater Sci Eng A. 1994;188(1–2):335–40. doi:http://dx.doi.org/10.1016/0921-5093(94)90389-1.
69. Shen ZG, Lee CH, Wu C, Jiang DY, Yang SZ. Material surface modification by pulsed ion beam. J Mater Sci. 1990;25(7):3139–41. doi:10.1007/bf00587663.
70. Saini G, Sautter K, Hild FE, Pauley J, Linford MR. Two-silane chemical vapor deposition treatment of polymer (nylon) and oxide surfaces that yields hydrophobic (and superhydrophobic), abrasion-resistant thin films. J Vac Sci Technol A. 2008;26(5):1224–34. doi:http://dx.doi.org/10.1116/1.2953699.
71. Shafi HZ, Khan Z, Yang R, Gleason KK. Surface modification of reverse osmosis membranes with zwitterionic coating for improved resistance to fouling. Desalination. 2015;362:93–103. doi:http://dx.doi.org/10.1016/j.desal.2015.02.009.
72. Yu H, Lui YS, Xiong S, Leong WS, Wen F, Nurkahfianto H, Rana S, Leong DT, Ng KW, Tan LP. Insights into the role of focal adhesion modulation in myogenic differentiation of human mesenchymal stem cells. Stem Cells Dev. 2013;22(1):136–47. doi:10.1089/scd.2012.0160.

73. Engler AJ, Sen S, Sweeney HL, Discher DE. Matrix elasticity directs stem cell lineage specification. Cell. 2006;126(4):677–89. doi:10.1016/j.cell.2006.06.044.
74. Özçam AE, Efimenko K, Spontak RJ, Fischer DA, Genzer J. Multipurpose polymeric coating for functionalizing inert polymer surfaces. ACS Appl Mater Interfaces. 2016;8(8):5694–705. doi:10.1021/acsami.5b12216.
75. Chong MSK, Lee CN, Teoh SH. Characterization of smooth muscle cells on poly(ε-caprolactone) films. Mater Sci Eng C. 2007;27(2):309–12. doi:http://dx.doi.org/10.1016/j.msec.2006.03.008.
76. Wen F, Chang S, Toh YC, Teoh SH, Yu H. Development of poly (lactic-co-glycolic acid)-collagen scaffolds for tissue engineering. Mater Sci Eng C. 2007;27(2):285–92.
77. Chong MSK, Chan J, Choolani M, Lee C-N, Teoh S-H. Development of cell-selective films for layered co-culturing of vascular progenitor cells. Biomaterials. 2009;30(12):2241–51.
78. Laschke MW, Augustin VA, Sahin F, Anschütz D, Metzger W, Scheuer C, Bischoff M, Aktas C, Menger MD. Surface modification by plasma etching impairs early vascularization and tissue incorporation of porous polyethylene (Medpor®) implants. J Biomed Mat Res Part B Appl Biomater. 2015;n/a-n/a. doi:10.1002/jbm.b.33528
79. Moraczewski K, Rytlewski P, Malinowski R, Zenkiewicz M. Comparison of some effects of modification of a polylactide surface layer by chemical, plasma, and laser methods. Appl Surf Sci. 2015;346(0):11–7. doi:http://dx.doi.org/10.1016/j.apsusc.2015.03.202.
80. Du Y, S-m C, Han R, Chang S, Tang H, Yu H. 3D hepatocyte monolayer on hybrid RGD/galactose substratum. Biomaterials. 2006;27(33):5669–80.
81. Khelifa F, Ershov S, Habibi Y, Snyders R, Dubois P. Free-radical-induced grafting from plasma polymer surfaces. Chem Rev. 2016;116(6):3975–4005. doi:10.1021/acs.chemrev.5b00634.
82. Löpez GP, Ratner BD, Tidwell CD, Haycox CL, Rapoza RJ, Horbett TA. Glow discharge plasma deposition of tetraethylene glycol dimethyl ether for fouling-resistant biomaterial surfaces. J Biomed Mater Res. 1992;26(4):415–39. doi:10.1002/jbm.820260402.
83. Cai EZ, Teo EY, Jing L, Koh YP, Qian TS, Wen F, Lee JWK, Hing ECH, Yap YL, Lee H, Lee CN, Teoh S-H, Lim J, Lim TC. Bio-conjugated polycaprolactone membranes: a novel wound dressing. Arch Plast Surg. 2014;41(6):638–46.
84. Holmes S, Schwartz P. Amination of ultra-high strength polyethylene using ammonia plasma. Compos Sci Technol. 1990;38(1):1–21. doi:http://dx.doi.org/10.1016/0266-3538(90)90068-G.
85. Hayat U, Tinsley AM, Calder MR, Clarke DJ. ESCA investigation of low-temperature ammonia plasma-treated polyethylene substrate for immobilization of protein. Biomaterials. 1992;13(11):801–6. doi:http://dx.doi.org/10.1016/0142-9612(92)90022-G.
86. Yue Z, Liu X, Molino PJ, Wallace GG. Bio-functionalisation of polydimethylsiloxane with hyaluronic acid and hyaluronic acid – collagen conjugate for neural interfacing. Biomaterials. 2011;32(21):4714–24. doi:10.1016/j.biomaterials.2011.03.032.
87. Chong MSK, Teoh S-H, Teo EY, Zhang Z-Y, Lee CN, Koh S, Choolani M, Chan J. Beyond cell capture: antibody conjugation improves hemocompatibility for vascular tissue engineering applications. Tissue Eng Part A. 2010;16(8):2485–95.
88. Ruiz A, Rathnam KR, Masters KS. Effect of hyaluronic acid incorporation method on the stability and biological properties of polyurethane-hyaluronic acid biomaterials. J Mater Sci Mater Med. 2014;25(2):487–98. doi:10.1007/s10856-013-5092-1.
89. Suzuki M, Kishida A, Iwata H, Ikada Y. Graft copolymerization of acrylamide onto a polyethylene surface pretreated with glow discharge. Macromolecules. 1986;19(7):1804–8. doi:10.1021/ma00161a005.
90. Cheng Z, Teoh S-H. Surface modification of ultra thin poly ([var epsilon]-caprolactone) films using acrylic acid and collagen. Biomaterials. 2004;25(11):1991–2001. doi:10.1016/j.biomaterials.2003.08.038.

91. Schnyder B, Lippert T, Kötz R, Wokaun A, Graubner V-M, Nuyken O. UV-irradiation induced modification of PDMS films investigated by XPS and spectroscopic ellipsometry. Surf Sci. 2003;532–535:1067–71. doi:http://dx.doi.org/10.1016/S0039-6028(03)00148-1.
92. Praschak D, Bahners T, Schollmeyer E. PET surface modifications by treatment with monochromatic excimer UV lamps. Appl Phys A. 1998;66(1):69–75. doi:10.1007/s003390050639.
93. Eve S, Mohr J. Study of the surface modification of the PMMA by UV-radiation. Procedia Eng. 2009;1(1):237–40. doi:http://dx.doi.org/10.1016/j.proeng.2009.06.056.
94. Cho J-D, Kim S-G, Hong J-W. Surface modification of polypropylene sheets by UV-radiation grafting polymerization. J Appl Polym Sci. 2006;99(4):1446–61. doi:10.1002/app.22631.
95. Daniloska V, Blazevska-Gilev J, Dimova V, Fajgar R, Tomovska R. UV light induced surface modification of HDPE films with bioactive compounds. Appl Surf Sci. 2010;256(7):2276–83. doi:http://dx.doi.org/10.1016/j.apsusc.2009.10.052.
96. Bartnik A, Lisowski W, Sobczak J, Wachulak P, Budner B, Korczyc B, Fiedorowicz H. Simultaneous treatment of polymer surface by EUV radiation and ionized nitrogen. Appl Phys A. 2012;109(1):39–43. doi:10.1007/s00339-012-7243-5.
97. Reisinger B, Fahrner M, Frischauf I, Yakunin S, Svorcik V, Fiedorowicz H, Bartnik A, Romanin C, Heitz J. EUV micropatterning for biocompatibility control of PET. Appl Phys A. 2010;100(2):511–6. doi:10.1007/s00339-010-5845-3.
98. Rahman N, Sato N, Sugiyama M, Hidaka Y, Okabe H, Hara K. The effect of hot DMSO treatment on the gamma]-ray-induced grafting of acrylamide onto PET films. Polym J. 2014;46(7):412–21. doi:http://dx.doi.org/10.1038/pj.2014.12.
99. Cunha L, Coutinho FMB, Teixeira VG, Jesus EFO, Gomes AS. Surface modification of styrene-divinylbenzene copolymers by polyacrylamide grafting via gamma irradiation. Polym Bull. 2008;61(3):319–30. doi:10.1007/s00289-008-0962-2.
100. Velo-Gala I, López-Peñalver JJ, Sánchez-Polo M, Rivera-Utrilla J. Surface modifications of activated carbon by gamma irradiation. Carbon. 2014;67:236–49. doi:http://dx.doi.org/10.1016/j.carbon.2013.09.087.
101. Onyiriuka EC, Hersh LS, Hertl W. Surface modification of polystyrene by gamma-radiation. Appl Spectrosc. 1990;44(5):808–11.
102. Kwon OH, Nho YC, Park KD, Kim YH. Graft copolymerization of polyethylene glycol methacrylate onto polyethylene film and its blood compatibility. J Appl Polym Sci. 1999;71(4):631–41. doi:10.1002/(SICI)1097-4628(19990124)71:4<631::AID-APP15>3.0.CO;2-G.
103. Zhu Y, Gao C, Liu X, Shen J. Surface modification of polycaprolactone membrane via aminolysis and biomacromolecule immobilization for promoting cytocompatibility of human endothelial cells. Biomacromolecules. 2002;3(6):1312–9. doi:10.1021/bm020074y.
104. Liu Y, He T, Gao C. Surface modification of poly(ethylene terephthalate) via hydrolysis and layer-by-layer assembly of chitosan and chondroitin sulfate to construct cytocompatible layer for human endothelial cells. Colloids Surf B Biointerfaces. 2005;46(2):117–26. doi:http://dx.doi.org/10.1016/j.colsurfb.2005.09.005.
105. Wen F, Chang S, Toh YC, Arooz T, Zhuo L, Teoh SH, Yu H. Development of dual-compartment perfusion bioreactor for serial coculture of hepatocytes and stellate cells in poly(lactic-co-glycolic acid)-collagen scaffolds. J Biomed Mater Res B Appl Biomater. 2008;87B(1):154–62. doi:10.1002/jbm.b.31086.
106. Croll TI, O'Connor AJ, Stevens GW, Cooper-White JJ. Controllable surface modification of poly(lactic-co-glycolic acid) (PLGA) by hydrolysis or aminolysis I: physical, chemical, and theoretical aspects. Biomacromolecules. 2004;5(2):463–73. doi:10.1021/bm0343040.
107. Stamm M. Polymer surface and interface characterization techniques. In: Stamm M, editor. Polymer surfaces and interfaces: characterization, modification and applications. Berlin/Heidelberg: Springer; 2008. p. 1–16. doi:10.1007/978-3-540-73865-7_1.
108. Ma Z, Mao Z, Gao C. Surface modification and property analysis of biomedical polymers used for tissue engineering. Colloids Surf B-Biointerfaces. 2007;60(2):137–57. doi:10.1016/j.colsurfb.2007.06.019.
109. Vogler EA. Structure and reactivity of water at biomaterial surfaces. Adv Colloid Interface Sci. 1998;74:69–117.

110. Grundke K. Characterization of polymer surfaces by wetting and electrokinetic measurements – contact angle, interfacial tension, zeta potential. In: Stamm M, editor. Polymer surfaces and interfaces: characterization, modification and applications. Berlin/Heidelberg: Springer; 2008. p. 103–38. doi:10.1007/978-3-540-73865-7_6.
111. Murthy NS. Techniques for analyzing biomaterial surface structure, morphology and topography. In: Surface modification of biomaterials. Woodhead Publishing; 2011. pp 232–55. doi:http://dx.doi.org/10.1533/9780857090768.2.232.
112. Hawker MJ, Pegalajar-Jurado A, Fisher ER. Innovative applications of surface wettability measurements for plasma-modified three-dimensional porous polymeric materials: a review. Plasma Processes Polym. 2015;12(9):846–63. doi:10.1002/ppap.201500035.
113. Merrett K, Cornelius RM, McClung WG, Unsworth LD, Sheardown H. Surface analysis methods for characterizing polymeric biomaterials. J Biomater Sci-Polym Ed. 2002;13(6):593–621. doi:10.1163/156856202320269111.
114. Smith KCA, Oatley CW. The scanning electron microscope and its fields of application. Br J Appl Phys. 1955;6(11):391.
115. Russell SD, Daghlian CP. Scanning electron microscopic observations on deembedded biological tissue sections: comparison of different fixatives and embedding materials. J Electron Microsc Tech. 1985;2(5):489–95. doi:10.1002/jemt.1060020511.
116. Variola F. Atomic force microscopy in biomaterials surface science. Phys Chem Chem Phys. 2015;17(5):2950–9. doi:10.1039/c4cp04427d.
117. Eaton P, West P. Atomic force microscopy. Oxford: Oxford University Press; 2010.
118. Siedlecki CA, Marchant RE. Atomic force microscopy for characterization of the biomaterial interface. Biomaterials. 1998;19(4–5):441–54. doi:10.1016/s0142-9612(97)00222-6.
119. Müller M. Vibrational spectroscopic and optical methods. In: Stamm M, editor. Polymer surfaces and interfaces: characterization, modification and applications. Berlin/Heidelberg: Springer; 2008. p. 47–70. doi:10.1007/978-3-540-73865-7_3.
120. Barbucci R, Casolaro M, Magnani A. Characterization of biomaterial surfaces: ATR-FTIR, potentiometric and calorimetric analysis. Clin Mater. 1992;11(1–4):37–51. doi:http://dx.doi.org/10.1016/0267-6605(92)90028-R.
121. Chittur KK. FTIR/ATR for protein adsorption to biomaterial surfaces. Biomaterials. 1998;19(4–5):357–69. doi:http://dx.doi.org/10.1016/S0142-9612(97)00223-8.
122. Pleul D, Simon F. X-ray photoelectron spectroscopy. In: Stamm M, editor. Polymer surfaces and interfaces: characterization, modification and applications. Berlin/Heidelberg: Springer; 2008. p. 71–89. doi:10.1007/978-3-540-73865-7_4.
123. Yang J, Alexander MR. Techniques for analysing biomaterial surface chemistry. In: Surface modification of biomaterials. Woodhead Publishing; 2011. pp 205–32. doi:http://dx.doi.org/10.1533/9780857090768.2.205.
124. Ratner BD, Castner DG. Electron spectroscopy for chemical analysis. In: Surface analysis – the principal techniques. Wiley; 2009. pp 47–112. doi:10.1002/9780470721582.ch3.
125. Pleul D, Simon F. Time-of-flight secondary ion mass spectrometry. In: Stamm M, editor. Polymer surfaces and interfaces: characterization, modification and applications. Berlin/Heidelberg: Springer; 2008. p. 91–102. doi:10.1007/978-3-540-73865-7_5.
126. Vickerman JC. Molecular surface mass spectrometry by SIMS. In: Surface analysis – the principal techniques. Wiley; 2009. pp 113–205. doi:10.1002/9780470721582.ch4.
127. Tyler BJ, Rayal G, Castner DG. Multivariate analysis strategies for processing ToF-SIMS images of biomaterials. Biomaterials. 2007;28(15):2412–23. doi:10.1016/j.biomaterials.2007.02.002.

Chapter 7
Gradient Biomaterials and Their Impact on Cell Migration

Zhengwei Mao, Shan Yu, Tanchen Ren, and Changyou Gao

7.1 Introduction

Regenerative medicine is the process of regenerating cells and extracellular matrix to restore the normal functions of tissues. An important step is to recruit nearby somatic or stem cells to wound sites with the assistance of biomaterials [1]. Within this process, cell migration, especially directionally moving toward the wound site under the guidance of spatiotemporal signals, plays a paramount role [2]. Therefore, it is very important to study the cell migration behavior with the presence of physical, chemical, and biological cues to get in-depth understanding of tissue regeneration process and thereby provide guidance principles for designing advanced biomaterials.

Cells migrate in response to gradients of stimuli such as dissolved chemoattractants (chemotaxis) or surface-attached molecules (haptotaxis) as well as biophysical contact cues (durotaxis or mechanotaxis) in vivo [3, 4]. Ramón Cajal (1892) first proposed that gradients of attractive molecules could guide growing axons to their targets [5]. Since then, in vivo gradients of chemical signals have been proved to exist, and their roles in guiding the translocation of cells have been widely recognized.

The "gradient biomaterials" offer an ideal model, enabling the studies of cell behaviors in a complicate and precisely regulated microenvironment. Over the past 20 years, a lot of techniques have been developed to generate spatiotemporal gradients and advanced functional biomaterials [6, 7]. The gradient biomaterials have been adopted to systematically study the cell responses to biomaterials including cell adhesion, distribution, and alignment [8]. Recently, cell migration induced by

Z. Mao (✉) • S. Yu • T. Ren • C. Gao (✉)
MOE Key Laboratory of Macromolecular Synthesis and Functionalization, Department of Polymer Science and Engineering, Zhejiang University, Hangzhou 310027, China
e-mail: zwmao@zju.edu.cn; cygao@zju.edu.cn

© Springer Science+Business Media Singapore 2016

C. Gao (ed.), *Polymeric Biomaterials for Tissue Regeneration*,
DOI 10.1007/978-981-10-2293-7_7

gradient biomaterials [9] and their potential applications in tissue regeneration [10, 11] are attracting more and more attentions.

In this chapter, we focus on the design of the gradient biomaterials and their impact on cell migration. Firstly, the knowledge obtained from nature: biological gradients existing in vivo and their influences on cell migration will be introduced. Methodologies for preparing the gradient materials will be summarized, followed by the directed migration behaviors of cells. Finally, the chapter concludes with current challenges and future perspectives.

7.2 Cell Migration

Cell migration in vivo is a very significant process on both physiological and pathological aspects. During embryonic development in mammal, cells migrate beneath ectoderm to create different germ layers, which are required for proper tissue formation [12]. Cell migration is also prominent in numerous processes in adults, such as morphogenesis, angiogenesis, wound healing, immune response, and tumor metastasis [13, 14]. For example, when wound occurs, immune cells and subsequently fibroblasts invade into the temporarily formed clots to fill the defect under the guidance of inflammatory factors. Meanwhile, the epidermal cells proliferate and migrate to cover the surface [13]. In metastasis, tumor cells detach from the original tumor tissue, invade into blood and lymphatic systems, and subsequently settle down into a new site.

More importantly, undesired cell migration will cause diseases or improper regeneration of tissues such as atherosclerosis, a chronic inflammatory disease of arterial wall [15]. During atherosclerosis, endothelium, composed of endothelial cells (ECs), is damaged, and subsequent migration of vascular smooth muscle cells (SMCs), which naturally move much faster than ECs to the impaired vessels, is stimulated by various inflammatory factors [16], leading to further damage of the vasculature. In-stent restenosis (ISR), a particular refractory form of neointimal hyperplasia [17], is another example. Stent implantation has become the main method to treat coronary artery diseases. However, the implantation may induce a series of pathological processes such as thrombosis and abnormal release of cytokines. These pathological events subsequently trigger the migration and proliferation of SMCs and thereby induce ISR [18]. Therefore, it is of great importance to understand the mechanism of cell migration especially under correct physiological conditions.

7.2.1 The Biological Processes of Cell Migration

The migration of single cell is the best-studied model of cell movement in vitro, and the newly developed fluorescent tagging technology also makes it possible to visualize the cell migration in vivo [19–21]. Cell migration is a complex process

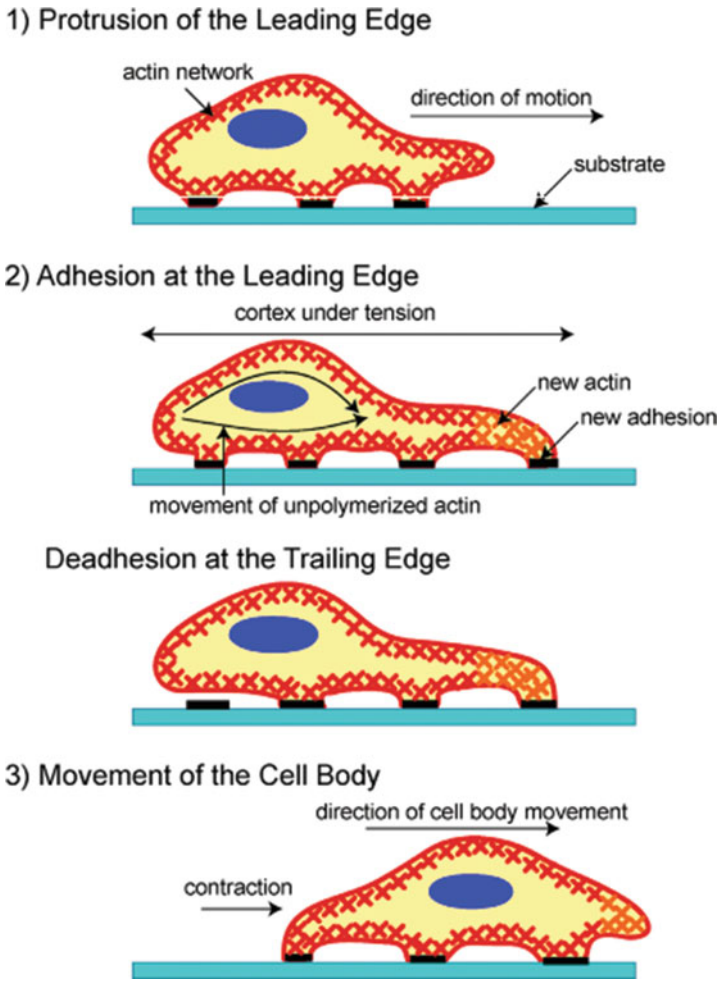

Fig. 7.1 A schematic of the three stages of cell movement: after determining its direction of motion, the cell extends a protrusion in this direction by actin polymerization at the leading edge. It then adheres its leading edge to the surface where it is moving and de-adheres at the cell body and rear. Finally, it pulls the whole cell body forward by contraction force generated on the cell body and rear of the cell (Reprinted from [22] with permission. Copyright Ivyspring International Publisher)

requiring work cooperation of cytoskeleton, membrane, and signaling systems (Fig. 7.1) [22]. Responding to the external topographic or chemical stimuli, cells protrude their leading edge [23]. The directional extension of active membrane, including both lamellipodia (sheetlike protrusions) and filopodia (spikelike protrusions), brings on attachment and thus traction force to the substrate, resulting in a counter-force on the cell to promote cell migration [24]. The contraction of cytoskeleton filaments pulls the cell body toward the leading edge, with a consequent release of attachment at the rear to allow the tail to retract, then the cell moves forward. All

these steps involve the assembly and disassembly of the cytoskeleton filaments, especially actin fibers, producing forward movement of cells. Herein, moderate adhesion strength provided by the supporting matrix is essential for dynamic cell protrusion and contraction [25].

The cell migration process also involves the spatiotemporal transition of intracellular signaling, such as focal adhesion kinase (FAK), mitogen-activated protein kinases (MAPKs), and Rho GTPases [20, 26–28]. Rho family GTPases, including Cdc42, Rac, and Rho, act as molecular switches of actin polymerization, actomyosin contraction, and cell mobility. Cdc42 and Rac regulate actin polymerization and membrane protrusion, while Rho generates the contraction and retraction forces required in the cell body and at the rear [29]. MAPKs, including ERK, p38MAPK, and JNK, can promote cell migration by regulating actin dynamics. For example, ERK1 and ERK2 can phosphorylate MLCK and increase MLC phosphorylation to enhance cell migration [30–32]. In addition, many downstream signal molecules participate in the migration process. For example, the Ser/Thr kinase p65PAK controls focal adhesion turnover since the integrin adhesion complexes should be dynamically changed, allowing the cells to adhere and pass [33].

Collective migration is the second principal mode of cell movement [34, 35]. This mode differs from single cell migration since cells remain connected as they move, resulting in migrating cohorts and varying degrees of tissue organization [36, 37]. Collective migration of cohesive cell groups in vivo is particularly prevalent during embryogenesis and drives the formation of many complex tissues and organs.

Collective cell migration can be defined by three hallmarks. Firstly, the cells remain physically and functionally connected because the cell-cell junctions are well preserved during movement [38, 39]. Secondly, multicellular polarity and organization of the actin networks generate traction and protrusion forces for migration and maintain cell-cell junctions. Thirdly, in most modes of collective migration, moving cells structurally modify the tissue along the migration path, leading to the modification of ECM [40]. Depending on the context, collective movement can occur by two-dimensional sheet migration across a planar surface or by multicellular strands or groups moving through a three-dimensional scaffold.

7.2.2 Gradient Signals In Vivo

Although cells have different migration patterns, they migrate in response to diverse gradients of stimuli in vivo. They are surrounded by extracellular matrix (ECM), which is a complex network consisting of proteins, polysaccharides, and signaling molecules. Physical cues such as pore size, topography, and stiffness as well as chemical cues including the composition of ECM and concentration of signal molecules are the main guiding cues for cell migration in vivo, inducing cell polarity and thus controlling the migration rate and direction.

7.2.2.1 Physical Gradients and Their Influence on Cell Migration

Physical gradients are defined as the gradual varying physical properties such as porosity, stiffness, and morphology. Native bones have physical gradients. The dense cortical bone locates in the outer layer and low-density "trabecular" bone locates inside. The pore size decreases from inside to outside. Such structures provide great permeability and excellent mechanical support [41]. Particularly, the mechanical strength or modulus is inversely dependent on the porosity and the pore volume [42]. Therefore, the bimodal structure of bone (cortical and cancellous) gives rise to the gradient of mechanical properties in the nature bone. In addition to the porosity, the bone stiffness and elasticity can also be determined by the variability of mineralization or mineral density, cell type, and cytokine gradient features [43]. The compression strength differs from 133 MPa in midfemoral to 6.8 MPa in proximal femoral, while the modulus of elasticity decreases from 17 to 0.4 GPa [44]. Teeth also contain gradients in composition and mineral density, which give rise to gradients in mechanical properties [45].

Cells can guide their movement by probing the substrate rigidity. Endothelial cells (ECs) and smooth muscle cells (SMCs) can move into tumor tissues due to higher stiffness inside, leading to fast angiogenesis. Fibroblasts also can move into scar tissues because of its higher stiffness and speed up the wound healing process [46].

As shown in Fig. 7.2 [47], increase in substrate stiffness can cause an increase in traction force, which would then pull the region forward and trigger a bias in movement direction and an increase in spreading. Such force-induced cytoskeletal contractility was also suggested by studies that adopted magnetic twisting force or dragging force onto integrin-bound beads. The cells responded by increasing the resistive forces and/or reinforcing the integrin-cytoskeleton linkages [48, 49]. Based

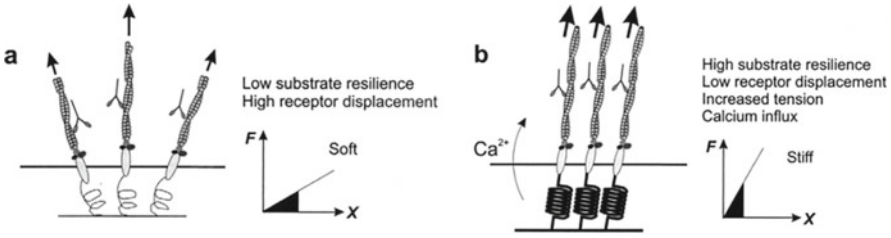

Fig. 7.2 Model for the signal detection of substrate stiffness. The initial probing forces are generated by actin-myosin interactions associated with cell-substrate adhesion sites. (**a**) On a soft substrate, the receptor-ligand complex is mobile and the tension at the anchorage site is weak. With a given energy input (*black area* under the force-displacement graph), the complex can move over a long distance (*x-axis*). (**b**) On a stiff substrate, equivalent energy consumption (shown as an equivalent *black area* under the force-displacement graph) causes a higher tension (*y-axis*) and lower displacement of the receptor-ligand complex (*x-axis*). The increase in tension may induce an influx of extracellular calcium through the stress-activated channels (Reprinted from [47] with permission. Copyright 2000 The Biophysical Society)

on these observations, Sheetz et al. speculated that stiffness of the ECM might function as an environmental cue to orient the direction of cell movement [50].

It is unclear how cells actually translate substrate rigidity into downstream responses. One possibility is that cells can directly sense the distance of receptor movement as a result of exerted probing forces. Alternatively, the rigidity of the substrate could be determined by monitoring the magnitude of counterforces upon the consumption of a given amount of energy. On the stiff substrate, strong mechanical feedback from the substrate occurs after a small receptor displacement. Because elastic energy is the integration of forces along the distance, with the same amount of energy consumption, the soft substrate can generate only a weaker mechanical feedback but a larger displacement. The stronger mechanical feedback on stiff substrate may then lead to the activation of stress-sensitive ion channels [51] or conformational changes of other tension-sensitive proteins. These responses in turn may regulate the extent of protein tyrosine phosphorylation, the stability of focal adhesions, and the strength of contractile forces [52]. Therefore, an effective navigating system emerges, in which cells send out local protrusions to probe the mechanical properties nearby. Those receiving strong feedback from the environment are amplified and become the primary leading edge, whereas those receiving weak feedback become unstable and may be further weakened because of the reorganization of the cytoskeleton. These coordinated responses would be a powerful means to direct cell movement in response to mechanical gradient [47]. By utility of step-rigidity micropost arrays, cells are proved to sense substrate rigidity locally to induce an asymmetrical intracellular traction force distribution to contribute to durotaxis [53].

7.2.2.2 Chemical Gradients

There are two main styles of chemical gradients in nature in living body. One is the biomolecules bound in extracellular matrix, including chemokines, hormones, and proteins. The dominating proteins are ECM proteins such as collagen, fibronectin (Fn), and laminin and growth factors such as fibroblast growth factor family (FGFs), vascular epidermal growth factor (VEGF), and so on. They can initiate multiple intracellular signaling pathways after binding to the receptors on cell surface, regulating various cell responses. For example, bone morphogenetic protein (BMP) concentration gradient in zebrafish is responsible for guiding bone formation [54–56]. Semaphoring Sema 2a concentration gradient is also known for guiding neuron outgrowth [57]. Expression of laminin-2 decreases from the base of the villus to the top in the epithelium of the small intestine, while the expression of laminin-1 increases. Stem cells are guided by this signal gradient and proliferate and undergo differentiation while moving upward to the tip of the villus in vivo. The other kinds of gradients are made of soluble biomolecules, formed through diffusion and convection (larger molecules) when they are released from the cells and the matrix [58, 59]. The cells respond to the gradients in a diffusion speed and distance-dependent manner [60]. Tumor cells, for example, are known to secrete an array of chemokines (e.g., IL8, CCL21, SDF-1α) and growth factors (e.g., EGF) to form a tight control

of their microenvironments and to enhance their ability to migrate to a distant site [61, 62]. Immune cells are another kind of cells that utilize molecular gradients within their surrounding as guidance cues to migrate [63, 64]. Dendritic cells, for instance, are known to migrate up lymphoidal chemokine gradients (CCL21 and CCL19) toward lymphatic vessels [65].

The second example of the molecular gradient formation is the oxygen concentration or pH gradient as a result of cellular metabolic activities [66–69]. Tumor cells have a high metabolic rate and thus a high oxygen consumption rate. Tumor cells initially grow with a mature vascular structure until the tumor body reaches a critical size, where the cells in the center become hypoxic due to limited oxygen supply from their surrounding tissues by diffusion. As a result, an oxygen concentration gradient with the highest concentration at the tumor edge is generated. In a vascularized tumor, blood vessels are oxygen suppliers to the tumor cells. Due to tumor metabolic activities, there is an oxygen and pH gradient adjacent to the blood vessel. As a result, tumor cells can sense the oxygen concentration gradient and pH gradient and then move toward blood vessels, which is a key step of tumor metastasis [61, 66]. In contrast, endothelial cells migrate toward the acidic end of an extracellular pH gradient, because cell membrane protrusion stability and actin–integrin adhesion complex formation are increased in acidic pH, which could contribute to the preferential polarization toward acidic pH and favor directional cell migration [70].

These two kinds of gradients also coordinate with each other to complete biological activities. For example, during angiogenesis, the soluble VEGF gradient increases the vessel caliber, while the gradient of matrix-bound VEGF promotes the vessel branch sprouting [71].

7.2.3 Possible Mechanism of Gradient-Dominated Cell Migration

In nature, an object always travels randomly in an environment without an asymmetric cue, which has been recognized as Brownian movement. In an anisotropic system, a driving force is imposed to the object due to the asymmetric interactions with surrounding environment. The directional transport of liquid and particles based on the gradients of surface energy has been reported [7, 72].

The first response of cells to the gradient is to polarize, by redistributing chemosensory signaling receptors on their surface [73–75]. Chan et al. reported that the cells reoriented and positioned toward the direction of higher ligand density when they were seeded on a ligand density gradient [76]. Arnold and Hirschfeld-Warneken et al. prepared an RGD density gradient to control the spatial distribution of integrin receptors on cell membrane, leading to the cell polarization and subsequent migration [77, 78]. Directional cell migration can be achieved when cellular polarization is kept in one direction due to the presence of the external gradient signaling.

Another explanation of gradient-guided cell migration is attributed to the adhesiveness between the cell and the underlying substrate. Cells attach to the substrate stronger at one end. The imbalance of adhesive force leads to forward movement toward the direction of increasing adhesiveness. The rear of the cells contracts to diminish the cellular polarization extent, and the movement is paused until the cells polarize again [73, 74]. Smith et al. found that the cells move faster on the gradient with a larger slope, but had no difference in cell polarization [79]. So the increase of migration speed is attributed to the higher frequency of cellular polarization, gradient recognition, and/or more stable polarization state.

7.3 Methods to Prepare Gradient Biomaterials

Since cells migrate in response to signal gradients in vivo, it would be of interest to prepare gradient biomaterials to mimic the signal and study material–cell interactions and/or guide cell directional movement for tissue regeneration. So far many methods have been developed to prepare gradient biomaterials. Although 3D gradient biomaterials are more important in application, however, their preparation methods and structures are relatively more complicate and difficult to control precisely. More importantly, it is much more difficult to elucidate the cell responses in 3D gradient biomaterials, which is not favorable to discuss the biological effect of gradient biomaterials and subsequently optimize their structure. Thus most efforts are focused on the development of 2D gradient.

There are two categories of techniques for producing gradient surfaces: "bottom-up" and "top-down." The former technique constructs patterns by continuously introducing building blocks on the surface, such as silane, thiol, and macromolecules without destroying the bulk materials [80]. The latter one is deconstruction and modification of surfaces gradually via external stimuli such as light, electron, plasma, etching solution, and so on [81]. As a result, the structures and properties of the surface will be altered.

Besides these technologies that are initially designed for the modification of material surface, another category of technologies has been developed to construct gradients in 3D matrix.

7.3.1 Bottom-Up Approaches

The bottom-up technologies are valid for various functional molecules and are feasible to control their grafting density, chain length, and spatial organization. By changing the chemical structures, the surface properties can be gradually switched from hydrophilic to hydrophobic [82], from soft to rigid, and from cell resistant to cell adhesive [83]. The gradient surfaces can be prepared based on kinetic and spatial controlled reaction (Fig. 7.3).

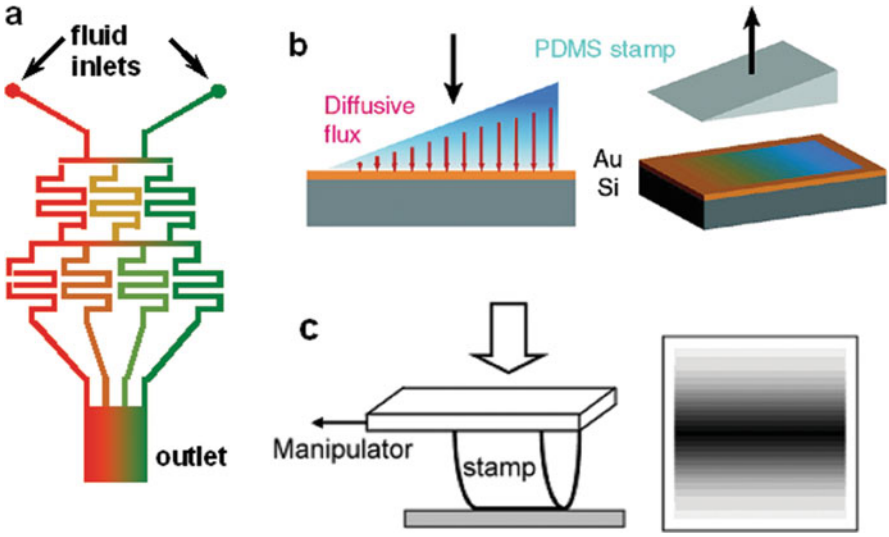

Fig. 7.3 (**a**) Schematic design of a representative gradient-generating microfluidic network. Solutions containing different chemicals are introduced from the *top* inlets and allowed to flow through the network. When all the branches are recombined, a concentration gradient is established across the outlet channel (Reprinted from [84] with permission. Copyright 2001 American Chemical Society). (**b**) Thiol diffuses into the stamp from an ink pad. It leaves the stamp because of adsorption to the gold surface and creates a partially covered surface (Reprinted from [85] with permission. Copyright 2005 American Chemical Society). (**c**) Symmetrical lateral gradients are generated using hemicylindrical stamps. The contact area increases under increased compression. The *darker areas* indicate the more hydrophobic region where the contact time is longer. The sketch is not to scale (Reprinted from [86] with permission. Copyright 2003 American Chemical Society)

7.3.1.1 Infusion

By gradually elevating or lowering the solution level, surfaces can be decorated with organic monolayer with a gradient pattern [87, 88]. The method is so simple and convenient that neither special instrument nor rigorous condition is required. Furthermore, it is feasible to generate gradients of a variety of chemical functionalities on the millimeter to centimeter scale. By controlling the injection speed, the position on the gradient corresponds directly to the immersion time. The slope of the gradient also can be tuned by adjusting the injection speed: higher infusion speed will make a smaller slope [89]. Also, the slopes and the lengths of the gradients can be tailored by changing the feeding concentration [90]. The concentration of molecules or the molecular weight of polymers on the gradient decreases linearly with its maximum at the bottom end which reacts for the longest time. Yu et al. fabricated a gradient from superhydrophobicity to superhydrophilicity by slowly adding the $HS(CH_2)_{11}CH_3$ solution to the container holding the gold substrate and then backfilling $HS(CH_2)_{10}CH_2OH$ [91]. In a further step, the gradients can be backfilled either in a contrary direction (head-to-tail method) or by fully immersing it

into the complementary solution (full immersion method). Obviously, the head-to-tail method produces a steeper gradient [92].

7.3.1.2 Diffusion

The molecular diffusion and transportation can be achieved in solution, vapor, or gel. The chemical gradient pattern is generated by imprinting the molecules onto the surface. Chaudhury et al. evaporated silane molecules, which were deposited more on the substrate end closer to the vapor source, and achieved the silane density gradient [93]. The steepness of the gradient can be easily adjusted by controlling the diffusion time, the silane molecules, and environment conditions such as humidity and temperature [94–96]. Mougin et al. prepared a thiol concentration gradient by diffusing into a gel matrix and then transferred the gradient to gold substrates [97, 98].

Claussen et al. presented a straightforward experimental method for fabrication of a gradient in mechanical properties on the centimeter scale based on a poly(dimethyl siloxane) (PDMS) system. Compositional gradients are realized by using three syringe pumps feeding different prepolymers capable to undergo thermal cross-linking. Within the gradient samples, the stiffness between the hard and soft part can be varied up to a factor of four. This method can be expanded to other polyaddition systems including polyurethanes and others based on photopolymerizable acrylates and thiol-ene click chemistry [99–101]. However, there is a common problem called “fingering” when two diffusion streams meet. As a result, an inhomogeneity will inevitably exist in the direction perpendicular to the gradient [83].

7.3.1.3 Microfluidic Lithography (μFL)

Microfluidic system offers a simple and fast way of generating dynamic chemical gradients of growth factors, ECM proteins, enzymes, drugs, or other functional molecules (Fig. 7.3a). Gradient patterns are formed by injecting multiple solutions simultaneously into a channel network, after which the fluid streams repeatedly split, mix, recombine, and branch. Finally, a chemical gradient is established in a single large channel that is perpendicular to the flow and combines all individual branches of fluids. By designing the microchannel network, the slope and shape of the gradients are precisely controlled [84, 102]. Gunawan et al. injected laminin and collagen solutions into a microfluidic system where the streams containing the highest concentration of laminin or collagen were in the farthest channel, respectively [12]. Finally, a concentration gradient with laminin and collagen in converse direction was formed. The microfluidic system also can be used to generate physical gradients. For example, a roughness gradient was fabricated on a silicon wafer after etching by an HF concentration gradient generated by microfluidic assay. By mixing solutions of unifunctional monomers and bifunctional monomers in the microchannels and irradiated under the UV light, a stiffness gradient is created [103]. The

two-dimensional channel system limits itself to continuous patterns within relative small size. To overcome this limitation, 3D microfluidic technique is developed using several layers of interconnecting channels [104]. It provides a unique platform to generate complicate and discontinuous gradients and incorporates multiple biomolecules on one gradient [105].

7.3.1.4 Lithography Techniques

The microcontact printing (μCP), developed by Whitesides and his coworkers, has been widely used for generating self-assembled monolayers (SAMs) for its versatility and highly accurate in nanoscale. Recently, a series of technologies have been developed based on μCP, such as decal transfer microlithography (DTM) [106], nanotransfer printing (nTP) [97], and metal transfer printing (MTP) [107, 108]. Kraus et al. produced a chemical gradient by the mass transfer microcontact printing because the ink mass transported to the substrate was controlled by the thickness of the stamp (Fig. 7.3b) [85]. Jeon et al. found that the surface density of octadecyltrichlorosilane (OTS) was increased by prolongation of the reaction time [109]. Inspired by Jeon's finding, Choi et al. developed a method to prepare chemical gradients by changing the contact time. Gradually or stepwisely increasing the pressure upon the half ball-shaped elastic stamp results in the increase of contact area and correspondingly decreases the contact time from the center to the edge. Subsequently, density gradients of OTS were generated. The gradient length and slope were easily tuned by the radius and curvature of the elastic stamp (Fig. 7.3c) [86]. Lang et al. prepared a microfluidic network into a silicon wafer to deliver protein solutions containing different concentrations of an axonal guidance molecule ephrinA5 onto a silicone stamp. In a subsequent μCP step, the protein was transferred onto a polystyrene culture dish. In this way, stepwise substrate-bound concentration gradients of ephrinA5 were fabricated, spanning a total distance of 320 μm [110]. Although the patterns generated by μCP are complex and facile, the μCP technologies are limited to planar surface [104].

A series of surface patterning techniques which utilize an ultrasharp scanning tip (or an array of tips in some examples) have been developed for the fabrication of 3D nanostructures on surfaces. For example, Zheng et al. developed dip-pen nanodisplacement lithography (DNL), a high-resolution, program controllable, solution-free, and diffusion-limited lithography tool for construction of molecules on a surface at the nanometer scale [104, 111]. Briefly, an AFM tip inked with initiator molecules ω-mercaptoundecyl bromoisobutyrate (MUDBr) was used to shave Au surfaces which had been modified with an inert SAM of 16-mercaptohexadecanoic acid (MHA) at a contact mode. At high load (typically larger than 100 nN), MHA molecules were removed by the tip, where simultaneously MUDBr molecules were transferred onto the same area of Au surface. Finally, poly(2-(methacryloyloxy)ethyl-trimethylammonium chloride) (PMETAC) brushes were prepared via SI-ATRP method (Fig. 7.4a, b). This technique can be used to project a 2D feature density array into a 3D surface morphology with polymer brushes

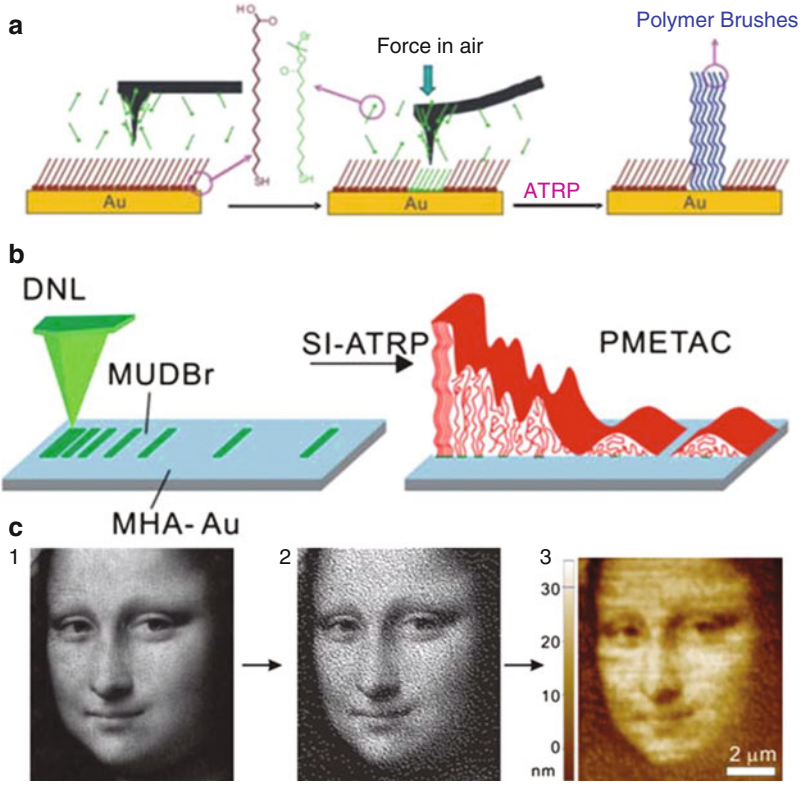

Fig. 7.4 3D PMETAC brushes fabricated by DNL. (**a**) Schematic illustration of the DNL process. (**b**) Schematic illustration of obtained nanopatterning of polymer brushes. (**c**) 3D Mona Lisa portrait fabricated by the feature density method. *1* Grayscale image of Mona Lisa's face. (*2*) Bitmap image converted from (*1*). (*3*) AFM topographic view of PMETAC brushes fabricated with DNL and SI-ATRP using (*2*) as guild map (Reprinted from [112] with permission. Copyright 2011 WILEY-VCH Verlag GmbH)

[112]. For instance, the authors fabricated polymer gradients of different shapes. A grayscale image with gradual change of brightness was first converted into a bitmap image, where the density of white/black pixels is proportional to the brightness/darkness. Then the bitmap was used as a blueprint for DNL patterning, yielding an initiator pattern comprising arrays of initiator nanodots. After SI-ATRP, PMETAC brushes were grown from the as-made initiator "bitmap" to generate a Mona Lisa's face (Fig. 7.4c).

7.3.1.5 Electrochemical Method

The isoelectric focusing (IEF) technology has been used to develop a concentration gradient of charged molecules and then transferred to a desired substrate [113]. In the IEF technique, the ampholytes migrate directionally due to the presence of the

electric field. For instance, positively charged polylysine accumulates around the cathode and forms a concentration gradient accordingly. The gradient can be transferred to a substrate with the assistant of soaked PDMS stamp. This method can be applied to various polyelectrolytes including proteins, peptides, and polysaccharides. The slope of the gradients can be adjusted by both electrical field and pH value which determines the charge property of the molecules [114].

Electrochemical techniques based on the oxidation–reduction reaction have also been used to prepare thiol gradients immobilized on the gold surface. By applying an external electric field, the thiols are reduced and detached from the substrate on the region close to the cathode, whereas the thiols are oxidized and remained onto the substrate on the region close to the anode [76, 115].

7.3.2 Top-Down Technologies

The top-down approaches are widely used to introduce active sites on inert surface. For the inert materials without reactive groups, such as polyethylene (PE), polytetrafluoroethylene (PTFE), and polyesters, surface modifications can be performed under high-energy sources such as plasma, corona, and UV light (Fig. 7.5). They provide a destructive process on the surfaces and generate a lot of reactive residues. Chemical gradients can be prepared by spatially altering the exposure time or the power of the energy sources.

7.3.2.1 Plasma Treatment

The plasma changes substrate by bombarding the surface with high-energy particulates such as electrons, atoms, ions, and radicals. The etching extent is gradually reduced by partly shielding off the reactive particles. Spijker et al. generated a gradient surface by using an aluminum shield on the sample, with its slope conveniently tunable by changing the distance between the mask and the sample [116]. Mangindaan et al. created a wettability gradient on hydrophobic polypropylene film by plasma treatment under a mask [119]. Various functional groups such as amino groups, carboxyl groups, hydroxyl groups, and sulfonic acid groups can be introduced onto the substrate by applying nitrogen, ammonia, oxygen, and sulfur dioxide plasma, respectively [120, 121]. Polymer gradients can also be created on the surface under a shield during plasma polymerization process [122].

7.3.2.2 Corona Discharge

The corona discharge treatment is a relative simple and cheap technology to generate gradient on the surfaces, as the samples are treated in air instead of in vacuum during the plasma treatment. Lee et al. adopted this technology to create various

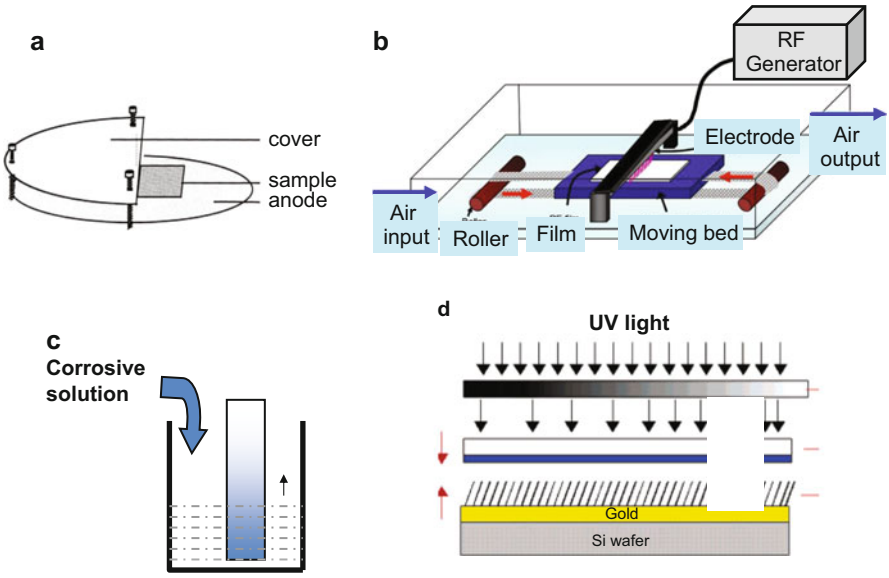

Fig. 7.5 (**a**) Schematic presentation (*side view*) of the glow-discharge reactor chamber, with the electrodes, sample cover, and sample position (Reprinted from [116] with permission. Copyright 1999 Elsevier Science B.V.) (**b**) Schematic diagram of apparatus for preparation of a gradient on PE surfaces by corona discharge (Reprinted from [117] with permission. Copyright 2008 Elsevier B.V.) (**c**) Scheme of the preparation process of the gradient by a chemical degradation method. (**d**) Remote photocatalytic oxidation of a thiol SAM under a gradient of UV illumination (Reprinted from [118] with permission. Copyright 2007 American Chemical Society)

gradient surfaces [117, 123–126]. For example, polymer sheets were placed under a knife-type electrode which was connected to a radio-frequency generator. Carbon radicals were produced on the polymer surfaces, forming hydroperoxides, and then decomposed into polar oxygen-based groups such as hydroxyl, ether, aldehyde, and carboxylic acid group [124]. Gradients with increasing density of functional groups can be produced by gradually enhancing power while moving the sample with a motorized drive [127]. The radicals also can serve as initiators to trigger the surface-initiated polymerization and active sites to immobilize proteins and peptides [128, 129].

7.3.2.3 UV Irradiation

Peroxides can be generated on the surfaces under strong UV irradiation [130]. Bin et al. produced a gradient with increasing density of carboxyl groups by slowly moving the photomask between a UV lamp and polymer substrates [131, 132]. This process is efficient and simple which only requires a light source. Besides, multi-component can be immobilized simultaneously. Photolithography is another example using light to prepare gradient materials [72, 118, 133]. For instance, the

substrate is firstly covered with a thiol or silane self-assembled monolayer (SAM) and then irradiated by a UV light to destroy the organic layer. Blondiaux et al. developed a technique by combining a mask with grayscale gradient and titanium dioxide (TiO_2) remote photocatalytic lithography [118]. The TiO_2 layer was placed under the mask and the region exposed to UV irradiation produced radicals, which diffused vertically and thus locally degraded the organic SAM on the gold surface underneath. As a result, a chemical gradient was created with tunable shape and length dependent on the masks.

7.3.2.4 Wet Chemistry Etching

This method was normally applied to the degradable polymers such as polyesters. Gao et al. developed an aminolysis technology to introduce amino groups on the surface of polyesters, which act as active sites for further functionalization [134–137]. Using this method, polymers are degraded progressively by continuously immersing into the reactive solution or injecting the reactive solution into a tube containing the substrates via a microinjection pump [138]. Tan et al. used this technology to construct an amine density gradient on poly(L-lactic acid) (PLLA) film [139, 140]. Besides polyesters, the wet chemistry can also be applied to etch the polyelectrolyte multilayers which are assembled by the alternative adsorption of polycations and polyanions via electrostatic attraction. Generally, etching the multilayers in a salt solution with a critical high ionic strength will reorganize the charge and structure of the multilayers, leading to swell, soften, and even dissolve of the multilayers [141, 142]. The chemical composition and related structure of the modified multilayers are determined by the salt concentration, which provides a simple method to generate gradient multilayers. Han et al. post-treated the polyelectrolytes multilayers in a gradient NaCl solution with a concentration ranging from 3 to 5 M, yielding the gradient multilayers with a similar chemistry composition and surface charge but gradually changed swelling ratio [143].

However, the top-down technologies in general are limited to the types of functional surfaces generated and unsuitable to process surfaces with unstable biomacromolecules such as ECM proteins and growth factors. Thus, recently the bottom-up methods are more widely used or adopted to further functionalize the surfaces after introduction of active sites on inert surfaces by the top-down approaches.

7.3.3 3D Gradient Generation Technologies

The gradients in a 3D matrix are more important because they are more similar to the situation in vivo and have the potential application of inducing cell migration in the tissue regeneration process. However, the “top-down” and the “bottom-up” technologies are usually applied to manufacture gradients on material surfaces, not suitable or at least needing major modification in a 3D matrix. Up to present, only

limited technologies have been developed to generate 3D gradients in porous scaffolds or hydrogels.

Several techniques have been developed for fabricating physical gradient with gradually changing pore size or porosity in scaffolds, to mimic the graded tissue morphology in vivo [85, 86, 109]. For example, Tampieri et al. developed a multiple and differentiated impregnation procedure to prepare porosity-gradient HA scaffolds [42]. Roy et al. [144] and Woodfield et al. [145] used a 3D printing technology to create polymer scaffolds with gradually changing porosity and pore size, respectively. Oh et al. developed a centrifugation method to fabricate a polycaprolactone (PCL) scaffold with gradually increasing pore size and porosity along a cylindrical axis via directional phase separation [146]. Additionally, gradients with gradually changing microstructure can be fabricated using a temperature gradient, based on the heat-induced phase separation [147, 148]. Polyurethane copolymers with different block compositions are also good candidates for this method, resulted in diverse microphase separation and gradient of microstructure [149].

It is relatively easier to prepare 3D chemical gradients in hydrogels due to their similarity to the solutions. Delong et al. prepared hydrogels with a bFGF gradient by diffusing two types of hydrogel precursor solutions (with/without bFGF) [150]. In brief, the PEG solution with bFGF was persistently injected into a container having PEG solution without bFGF. The two solutions were mixed together and finally pumped into a mold where they were exposed to UV light to cross-link the polymer network and stabilize the gradient [8, 151]. Microfluidic and diffusion technologies can also be applied to fabricate gradient hydrogels [10–14, 154]. The 3D stiffness gradient can be generated by spatially controlling the cross-linking degree. Wong et al. prepared polyacrylamide hydrogels with gradually changing modulus by applying a photomask with a grayscale gradient to control the polymerization degree under a UV light [155]. Hansen et al. fabricated arrays of 84 polymer gradients on a single glass microscope slide by inkjet printing, allowing a combination of high-throughput and true combinatorial methods. The gradual change of composition within the polymer gradients is achieved by using two different monomers and a cross-linker [156].

In contrast to hydrogels, preparation of gradients in porous scaffolds is a bit more difficult and usually not precisely controllable. Charu et al. put a droplet of EDC-activated protein solution under fibrin scaffolds. Along with the protein solution diffused upward to the top, a protein concentration gradient was generated and covalently immobilized within the 3D scaffolds. This kind of diffusion-based method offers good control of gradient slopes by changing reaction time and can be extended to conjugate a variety of proteins on different materials [139]. Oh et al. prepared PCL/Pluronic F127 scaffolds with gradually increasing growth factor density from top to bottom by centrifugation of fibril-like PCL and subsequent surface immobilization of growth factors (Fig. 7.6) [157]. Several kinds of growth factors such as VEGF165, BMP-7, and transforming growth factor-β2 (TGF-β2) were immobilized on the surfaces via heparin binding and reached a density gradient due to gradually increasing surface area along the longitudinal direction. The released amount of VEGF165 from the cylindrical scaffolds gradually decreased along the

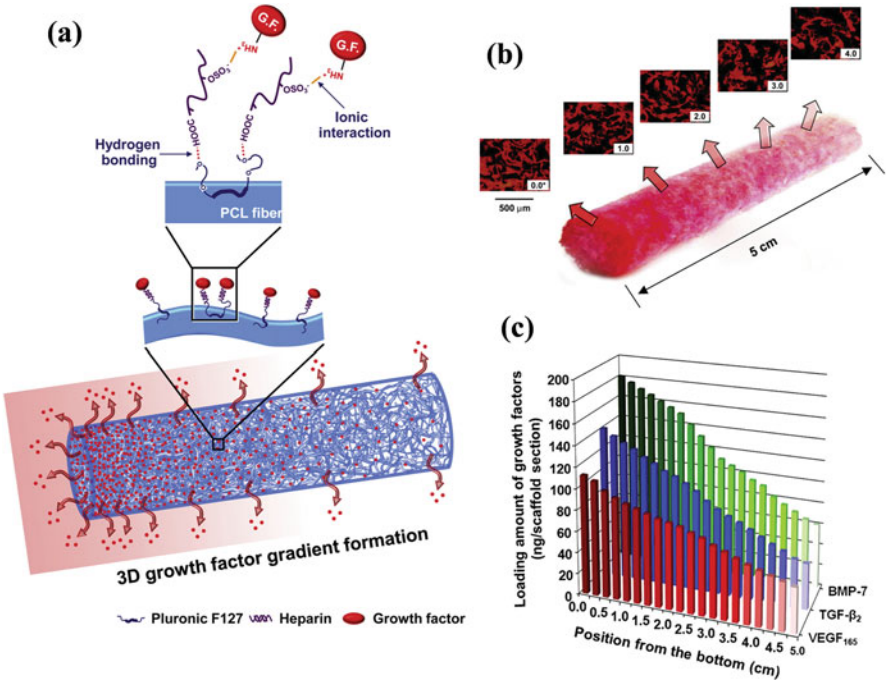

Fig. 7.6 (**a**) Schematic diagrams of the successive binding of heparin and growth factor onto the fibril surface of the PCL/F127 cylindrical scaffold and the formation of 3D growth factor gradient on the scaffold. (**b**) Gross appearance and fluorescence microscopy images showing the rhodamine-labeled VEGF165 gradient along the longitudinal direction of the PCL/F127 cylindrical scaffold. The VEGF165 immobilized on the cylindrical scaffold is expressed as a *red color*. **c** Loading amount of growth factors (BMP-7, TGF-β2, and VEGF165) immobilized onto the PCL/F127/heparin scaffold sections. The scaffolds show the gradually decreasing concentration of growth factors along the longitudinal direction from the *bottom* position to the *top* position (growth factor concentration gradient scaffolds) (Reprinted from [157] with permission. Copyright 2011 Elsevier Ltd)

longitudinal direction in a sustained manner, which allows for a controlled spatial distribution of growth factors in a 3D environment. Barry et al. used plasma-induced polymerization method to deposit a thicker layer of polymer on the scaffold periphery than that in the scaffold core, leading to functional scaffolds containing a gradient [158].

7.4 Influences of Gradient Biomaterials on Cell Migration

Gradient materials are widely considered as an engine to drive orient movement of objects such as droplets, particles, and living cells [159, 160]. Whitesides et al. presented the first study of a gradient of surface free energy, which drives water drop to move uphill. The motion of water droplet was the result of an imbalance in the

forces due to surface tension acting on the liquid-solid contact line on the two opposite sides ("uphill" or "downhill") of the drop [93]. Although many investigations are taken to correlate cell responses such as adhesion, proliferation, differentiation, and migration [161–163] to the physical and chemical cues, much less studies have been carried out to elucidate the cell migration patterns on gradient materials. According to the forms of gradients, there are in general two categories of gradients: (1) simple gradients with one dominating signal and one direction and (2) complicate gradients with several signals and/or several directions.

7.4.1 The Effect of Simple Gradients on Cell Migration

The simple gradients can be divided into two categories as well: (1) physical gradients with gradually changing physical properties including modulus and topography and (2) chemical gradients with the spatially changing chemical compositions including the density and species of the functional molecules.

7.4.1.1 Physical Gradients

Matrix stiffness has been found to have a severe influence on cell adhesion and mobility. Nadia et al. found that cells attached to a rigid substrate exhibited better defined cytoskeleton and filament structure [103]. Pelham et al. confirmed that cells exhibited higher lamellipodia activity and motility on soft surface due to the destabilized adhesion [164]. Cheung et al. used microfluidic-based lithography to pattern cell-adhesive hydrogel substrates with micro-variations in stiffness. The micropatterns are generated by feeding PEG-fibrinogen and various amounts of poly(ethylene glycol diacrylate) (PEGDA) into the microfluidic channel. Human foreskin fibroblasts respond to the patterned stiffness heterogeneity by migrating toward the stiffer regions along the discrete stiffness gradients [165]. Hopp et al. gradually immersed poly(allylamine hydrochloride)/poly(acrylic acid) (PAH/PAA) polyelectrolyte multilayers into 1-ethyl-3-(3-dimethylaminopropyl) carbodiimide (EDC) solution and obtained the gradient multilayers which had an elastic modulus ranging from 0.5 MPa at the non-cross-linked end to 110 MPa at the end of the substrate cross-linked for 4 h. Human dermal fibroblasts attach better to the stiffer regions of the gradient initially and subsequently a higher proliferation rate and stronger cytoskeletal development [166]. Thus, the stiffness gradient is expected to guide cell migration [155, 167]. Vascular smooth muscle cells were found to undergo direct migration on a radial gradient-compliant substrate from soft to stiff regions, leading to accumulation of cells in the stiff regions after 24 h.

Keller et al. prepared photosensitive multilayers and then a continuous surface gradient of modulus by photo-cross-linking. A7r5 smooth muscle cells exhibited the greater sensitivity to both shallow and steep modulus gradients by elongating and orienting along the shallow gradient and durotaxing up the steep gradient.

U2OS osteoblast-like cells only spread and adhered well to the stiffer part of the gradient, but did not show obvious directional migration along the gradient [168]. Kuo et al. casted polyacrylamide gels on a stiff support with controlled topography, resulting in a thin gel layer of variable height. The topographical profiles projected a stiffness map onto the gel, resulting in controlled linear and nonlinear 2D stiffness gradients. Fibroblasts, which migrate toward stiffer substrates, accumulated in areas with a gel thickness below 15 μm [169].

Lo et al. studied the mechanism of cell response [47, 170]. Focal adhesion kinase (FAK) plays an important role in mechanical stimulation. For an equal amount of energy, the counterforce provided by the soft substrate is smaller compared to the rigid one. The stronger feedback makes cell adhere stronger and spread better on the tough region. Thus, cells migrate directionally through dynamic detecting the imbalance in forces from the front to the back [51]. Besides, cell-cell interaction also plays an important role in cell migration. Han et al. post-treated the polyelectrolyte multilayers in a gradient NaCl solution with a concentration ranging from 3 to 5 M, yielding the gradient multilayers with a similar chemistry composition but gradually changing swelling ratio [143]. Compared to the random migration with a lower speed at a smaller cell density, the vascular smooth muscle cells migrated directionally to the low hydration side with higher modulus at an appropriate cell density (~$1.5 \times 10^4/cm^2$) under the assistance of cell-cell interactions. The cell migration rates on the gradient surface were significantly larger than those on the corresponding uniform surfaces with the similar chemical structure and mechanical property. Both the gradient cues and cell-cell interaction address important influences on the directional cell migration (Fig. 7.7).

Topography, the configuration of a surface, can largely affect the cell migration behaviors. Kim et al. created a model substrate of anisotropic micro- and nanotopographic pattern arrays with variable local density using UV-assisted capillary force lithography (CFL). They found that fibroblasts attached on the denser pattern areas aligned and elongated stronger along the direction of ridges, while those on the sparser areas showed a biphasic dependence of the migration speed on the pattern density. In addition, cells responded to local variations in topography by altering morphology and preferably migrating along the direction of grooves, i.e., direction of pattern and increasing pattern density [171, 172]. Mak et al. created microchannels with gradually narrowing spaces to study the metastasis process of cancer cells penetrating tight spaces within the ECM and during intravasation and extravasation through the vascular wall. The highly metastatic breast cancer cells (MDA-MB-231) showed a more invasive nature since 87 % of the cells migrated into the spatially confining region. In contrast, most of the non-metastatic breast epithelial cells (MCF-10A) (75 %) were turning around by repolarization [173].

Han et al. prepared multilayers with gradually changing stiffness on air-plasma-treated poly(dimethylsiloxane) membranes, with the pattern direction parallel to the gradient. The synergetic effects of the surface topography and swelling gradient can effectively guide the unidirectional migration of single smooth muscle cells without impairment of their migration rate [174, 175].

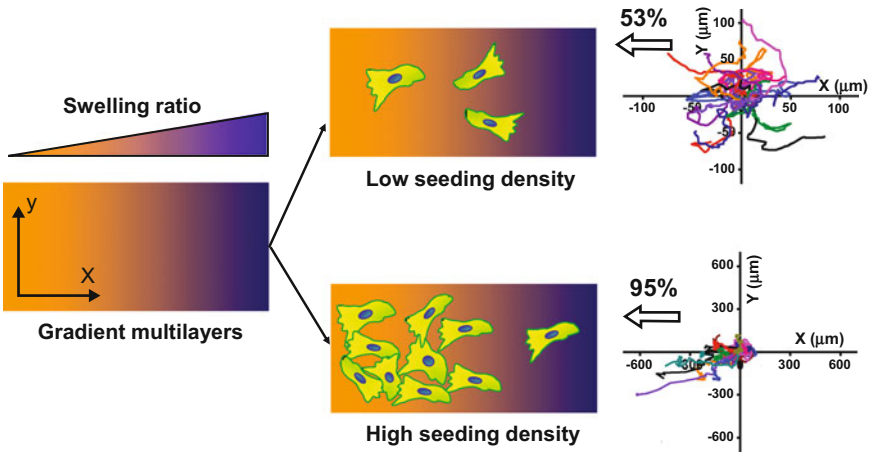

Fig. 7.7 Schematic illustration of cell migration on gradient PSS/PDADMAC PEMs with gradually changing swelling ratio at different cell density (Reprinted with permission from [143] Copyright 2012, Elsevier Ltd)

7.4.1.2 Chemical Gradients

Since gradients of extracellular matrix proteins, growth factors, and other signaling molecules have already been acknowledged in vivo, many chemical gradients are created and used to study their influences on cell migration behaviors in vitro. Gradients of synthetic polymers in terms of density, chain length, and chemical composition are constructed, in order to provide gradually alteration of hydrophilicity, charge, and eventually cell responses on different positions. Many gradients can efficiently regulate cell adhesion, elongation, and polarization; they are in general not effective enough to guide directional cell migration.

The gradients of biological molecules have a stronger influence on cell migration, depending on both the absolute concentration and the slope of the concentration gradient [176]. As there are two kinds of chemical gradients in vivo, i.e., one bound to ECM and the other soluble, the gradient materials are also divided into two categories:

1. Immobilized gradients

The immobilized gradients can be further divided into three subcategories: synthetic molecules, ECM proteins (including related peptides), and growth factors. Zelzer et al. presented a new diffusion-controlled method to easily prepare chemical gradients by plasma polymerization. Surface chemical gradients from hydrophobic plasma-polymerized hexane to a more hydrophilic plasma-polymerized allylamine, with a water contact angle range of 60–93° over a length of 8 mm, were formed on glass coverslips. Fibroblasts adhered and proliferated preferentially on hydrophilic end, showing a gradual decrease of cell density toward the hydrophobic end [177]. Wu et al. prepared surfaces with various densities of methoxy poly(ethylene glycol)

(mPEG) brushes to modulate the cell adhesion force: cell adhesion force gradually decreases on the surfaces with a higher mPEG density. The migration rate of vascular smooth muscle cells increased initially and then decreased along with the increase of mPEG grafting mass. The fastest rate appeared on the mPEG brushes with moderate grafting mass of 300–500 ng/cm^2 [25]. Ren et al. prepared hydrophilic poly(2-hydroxyethyl methacrylate) (PHEMA) brushes with a gradient increase of the molecular weight, which provided a precise control over the density of hydrophilic units along the gradient. The gradients were proved to provide a gradient of cell adhesion force, which in turn tuned the directional cell migration [178].

Collagen is one of the major proteins in ECM, which can significantly improve the cell adhesion and spreading. Fibronectin and laminin are able to mediate the communication and movement of cells. These proteins have certain structure domains which can bind to the corresponding receptors on cell plasma membrane. For example, both collagen and fibronectin contain the peptide sequence of RGD (Arg-Gly-Asp), which can bind to integrin subfamily, a kind of transmembrane receptors [179, 180]. The specific interaction between the integrin and the receptors conveys the external stimuli and transition into cells. Rajagopalan et al. studied the effect of Fn and RGD on spreading and motility of fibroblasts [181]. Although the migration speed is similar, fibroblasts on Fn-modified surface have higher traction force that is directly related to the size of focal adhesion, indicating that Fn has a higher affinity toward fibroblasts. Thus, ECM protein density gradients are supposed to carry the increasing strength of signal, making the cells polarized and subsequently directional migration. Smith et al. prepared fibronectin density gradients on gold surface to increase the migration speed of bovine aortic endothelial cells along the gradient direction [182]. The same group also reported that human microvascular endothelial cells (hMEC) migrated faster on a fibronectin gradient with a larger slope in the range of 0.34–1.23 ng Fn/mm^3 [79]. Gunawan et al. created linear density gradients of laminin by the microfluidic method. Rat IEC-6 intestinal crypt-like cells migrated up the gradients with similar rate compared to that on the same local laminin concentration on uniform surface. However, cell directedness decreased significantly at high laminin densities [12]. Cai et al. prepared a collagen gradient on PLLA surface. Endothelial cells on the gradient areas with low and moderate collagen surface densities displayed a strong motility tendency, whereas the cells grew on the gradient area with a high collagen density demonstrating a reverse response to the collagen gradient. The results suggest that cell motility is regulated by the collagen gradient in a surface-density-dependent manner [183]. Yu et al. prepared an amino group density gradient on poly(e-caprolactone) (PCL) membrane surface by a gradient aminolysis method, which was transferred into gelatin density gradient by covalent linking with glutaraldehyde. The resulted gelatin density gradient ranged from 0.49 to 1.57 μg/cm^2 on the PCL membrane. Human vein endothelial cells showed preferred orientation and directional migration toward the gradient direction with an enhanced gelatin density at the proper position (gelatin density), forwarding a new step toward the preparation of applicable gradient biomaterials in tissue regeneration [184].

Usually, a peptide with a functional amino acid sequence of specific proteins can be used as an alternative in gradient preparation because of its high stability and low molecular weight [185]. Adams et al. placed chick embryo dorsal root ganglia (DRG) in the middle of a grid pattern containing gradients of IKVAV peptide, the functional sequence in laminin. DRG growth cones followed a peptide path to the perpendicularly oriented gradients, and most of the growth cones could turn and climb up the gradients [186]. Delong et al. cultured human dermal fibroblasts on hydrogels with surface gradients of RGD peptide and found that the cells aligned with the gradients and tended to migrate up the gradients [8]. Guarnieri et al. also demonstrated that mouse fibroblasts prefer to migrate to the direction of an RGD gradient on hydrogel surfaces with higher migration rate than that on uniform RGD surfaces and increased along with slope of the RGD density gradient [187]. Hirschfeld-Warneken et al. found that cells elongated along the ligand density gradient with a larger distance [78]. The migration speed of a single cell in response to a linear ligand density gradient on a solid substrate as a function of gradient slope was theoretically predicted based on a 1D continuum viscoelastic model. The model predicts a biphasic dependence of cell migration speed on gradient slope, with a maximum speed at an intermediate gradient slope [188].

Besides ECM proteins and their derived peptides, various growth factors are used to prepare gradients and study their effect on cell migration. DeLong et al. synthesized hydrogels with bFGF density gradients and observed that smooth muscle cells migrated directionally up the gradients toward increasing bFGF concentration [150]. Liu et al. found the density gradient of VEGF can induce the directional migration of endothelial cells. This guidance effect is further enhanced on the combinational gradients of VEGF and FN [189]. Masters et al. found that keratinocytes exhibited almost tenfold directional migration on an optimal concentration at EGF gradient compared to that on EGF free surfaces. Immobilization of IGF-1 (insulin-like growth factor 1) gradients also accelerated and directed keratinocytes migration; however, no difference in migration was found when combining EGF and IGF-1 gradients [190].

2. Gradients of soluble factors

Soluble factor concentration gradients which are commonly existed in natural 3D environment are also widely used to guide cell migration. For example, Frevert et al. developed a gradient of interleukin-8 (IL-8). Single neutrophils preferably migrated to the direction of higher concentration of IL-8 at the local concentration up to 200 ng/mL [191]. Besides, bFGF, stromal cell-derived factor-1 alpha (SDF-1α), EGF, and VEGF are also used as chemotactic agents [150, 192–194]. Wang et al. found that metastatic breast cancer cells could migrate up EGF gradient of nonlinear polynomial profile toward a higher EGF concentration [195]. However, there are some factors that can inhibit the cell mobility such as transforming growth factor β-1 (TGF β-1) [196] and angiotensin 1 [197].

7.4.2 The Effect of Complicate Gradients on Cell Migration

Besides the simple gradients with one dominating factor and/or one direction, there are always more complicate gradients exist in nature and generated on biomaterials. As expected, these gradients may have different impact on cell migration compared to their simpler counterparts. Study of the cell motility on a complicate gradient will provide insight into the complex physiological environment that guides and directs cell migration.

7.4.2.1 Gradients with Complicate Shape

Kidoaki et al. developed custom designed equipment for reduction projection-type photolithographic microelasticity patterning. By using the system, they prepared microelasticity-patterned gels with square hard domains within a softer surrounding gel. The jump in elasticity across the boundary was adjusted by regulating the photo-gelation conditions by varying the photoirradiation power and duration, and the boundary width was regulated by controlling the focus on reduction-projected images of photomasks (Fig. 7.8) [198]. The effects of the elasticity jump and boundary width were assessed systematically. As a result, the conditions required to induce mechanotaxis were found to be a jump in elasticity of a certain threshold magnitude (30–40 kPa) and a sufficiently narrow width of the elasticity boundary (50 μm), comparable to the adhesion area of a single cell. On the other hand, smaller boundary conditions of 3–20 kPa/50 μm did not induce mechanotaxis. Levchenko et al. presented a 2D topographically patterned substrate of variable local densities and anisotropy in a single substrate as a platform for studying the organization and migration of adherent cells. The patterns were fabricated by UV-assisted capillary force lithography, which provides a simple and efficient way to construct micropatterns with controlled geometry over a large area. They demonstrated that fibroblasts can recognize the topographic pattern density gradient, resulting in directional migration toward the denser area. The cell shape and velocity were largely dependent on the degree of the local anisotropy of the substrate, indicating that cells could integrate orthogonally directed mechanical cues on the scale comparable to that of the sizes of the native ECM networks [172]. The same group prepared a mountain-like fibronectin density gradient and found that Chinese hamster ovary (CHO) cells moved from both edges toward the center areas of the gradient with a higher fibronectin surface density [199].

7.4.2.2 Gradients with Complicate Signals

Several gradient signals with synergetic or opposite guidance on cell migration may merge together. Therefore, it would be interesting and also important to know how cell moves under such a complicate environment. Hale et al. designed a

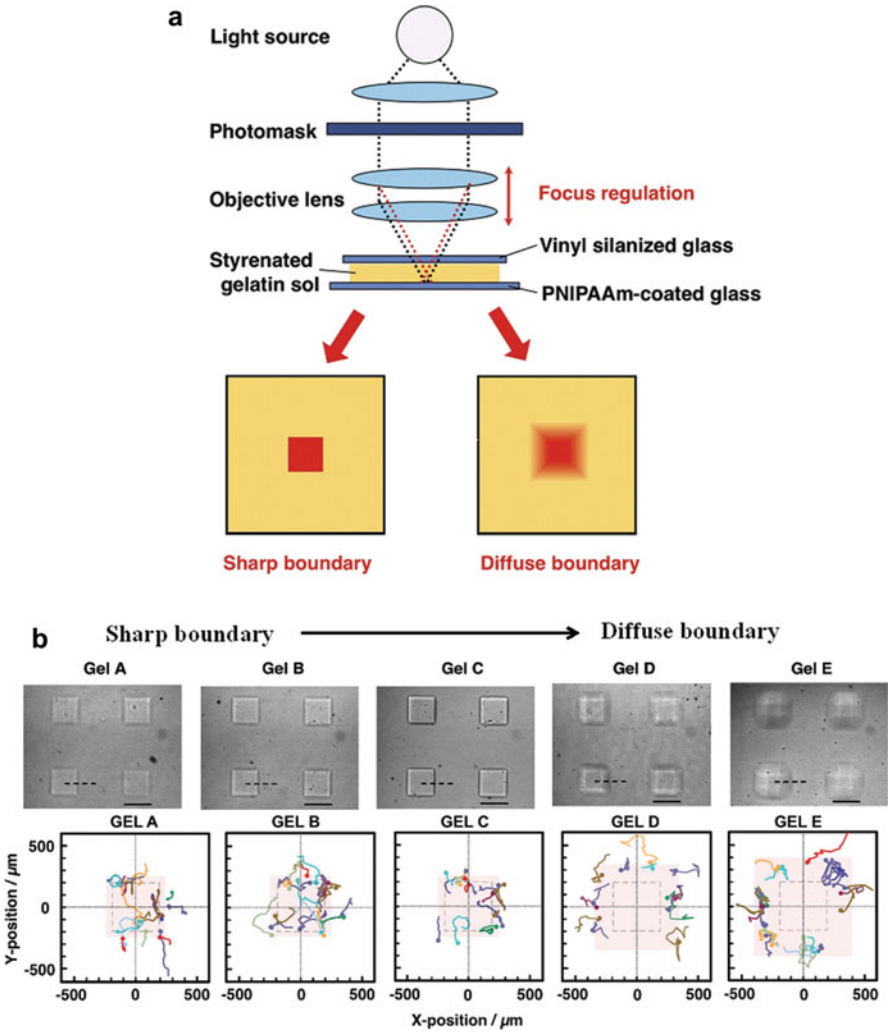

Fig. 7.8 (**a**) Schematic representation of the reduction projection-type photolithographic micro-elasticity patterning of styrenated gelatin gel. The resulting gel sample is attached to the *top* of vinyl-silanized glass, and photomask patterns are copied on the *bottom* of the gel surface covered with PNIPAAm-coated glass. The boundary conditions of the elasticity gradient can be controlled by raising the lens position and focusing out from the gel surface. (**b**) *Upper photos*: phase-contrast microscopic images of micropatterned *square* hard domains with elasticity gradients of different boundary conditions. *Lower graphs* show cell trajectories observed around elasticity boundaries with different gradient conditions. The starting positions of each trajectory are indicated by a dot (Reprinted from [198] with permission. Copyright 2011 Elsevier Ltd)

polyacrylamide hydrogel with a 100 μm interfacial region where the chemical and mechanical properties were gradually varied in opposing directions: the stiffer side has a low collagen concentration, whereas the softer side has a high collagen concentration. The mouse fibroblasts either migrated preferentially toward the high collagen density and soft side on the gradient or remained on the high collagen density region, suggesting that chemical gradient is more powerful than stiffness gradient in directing fibroblasts' movement [200]. Rao et al. studied cell movement in response to an epidermal growth factor (EGF) gradient in a gradually tapered space, imposing mechanical stresses. The chemoattractant drives cell migration into the narrow confines of the tapered channels, while the mechanical gradient clearly alters the migration of cells. PC-3 cells, a prostate cancer cell line, prefer to enter the channels from the wider to the narrow end. In contrast, PNT1A cells, a normal prostate epithelial cell, do not like to enter. The results indicate that the impact of physical stress on cell migration patterns may be cell type specific [201]. Mao et al. developed a special microfluidic device which has six channels, each with separate inlets for cell seeding and cytokine infusion. This device enables the competitive recruitment of cells that are simultaneously exposed to multiple cytokine gradients under real-time imaging, to identify the most chemotactic factors on bone marrow mesenchymal stem cells [202].

Wu et al. designed a PEG density gradient surface to drive the directional cell migration through the continuously increasing cell adhesion force along the reduced mPEG density axis, together with striped patterns at the same direction. The cells elongated along the direction of the stripes and the gradient and were separated by spacing stripes grafted with dense mPEG brushes. The cell orientation guided by striped patterns and polarization imitated by the chemical gradient have a synergetic effect on cell movement, leading to a more effective directional migration [203]. Ren et al. developed complementary density gradients consist of hydrophilic PHEMA brushes and cell anchoring peptides: both gradients provide the same direction guidance on cell migration, leading to fivefold increase of cell mobility and very high directionality [204].

7.4.3 Cell Migration in 3D Matrix and Possible Application in Tissue Regeneration

The cell migration behaviors as a function of gradients in 3D scaffolds and hydrogels have also been demonstrated. Dodla et al. cast dorsal root ganglia in agarose gels and prepared laminin gradient by photochemistry after diffusion. The presence of laminin gradients significantly enhanced the rate of neurite extension from the cells [205]. Moore et al. prepared PHEMA gels containing concentration gradients of NGF and neurotrophin 3 (NT-3), which were immobilized during photo-crosslinking of the PHEMA [206]. Dorsal root ganglia cells only showed extended neurites along gradients of both factors rather than the ones with one factor alone,

suggesting a synergistic effect. Musoke-Zawedde et al. used UV light micropatterning to fabricate RGD peptide density gradients in hyaluronan gels. The gradients were able to guide neurite outgrowth from primary neural cells [207].

Tampieri et al. [42] prepared ceramic scaffolds containing a gradient in porosity and applied them for rabbit femur defects repair. New bone formation was accelerated in the scaffolds at the region with higher porosity. Roy et al. [144] implanted polymer/ceramic composite scaffolds containing porosity gradient in rabbit calvarial defects. More new bone formation was observed in the high porosity zones than in the low porosity zones. Hoffman et al. [208] demonstrated that silk scaffolds containing pore size gradients have better performance to induce formation of a tissue with a graded morphology. Oh et al. studied the cell/tissue responses to the scaffolds with a pore size/porosity gradient in vitro and in vivo. The chondrocytes and osteoblasts prefer to migrate in large pore/high porosity part, while the fibroblasts prefer to proliferate in smaller pores/lower porosity part of the scaffolds in vitro. The best bone formation was found from midrange pore/porosity scaffolds after implantation into rabbit calvarial defects [146]. Based on electrospinning technique, Sundararaghavan et al. prepared gradients of increasing stiffness and RGD peptides' density along the thickness of fibrous HA scaffolds. The chick aortic arch explants had significantly greater cell infiltration into the scaffolds toward increasing RGD density gradient than that in the scaffolds with uniform RGD distribution [209].

7.5 Conclusions and Future Perspectives

Various top-down and bottom-up technologies have been developed to produce 2D and 3D gradient materials with gradually changing physical, chemical, and biological properties, mimicking the microenvironments in vivo and proving the possibility to guide cell directional migration in vitro. Complicate gradients consist of multiple signal gradients, and/or complicate gradient shapes have also been prepared to mimic the real environment in vivo. The majority of the current literatures are focused on single cell/cell sheet migration on planar gradient surfaces. It is of importance to study the migration behaviors of cells encapsulated in 3D matrix, more closely mimicking the situation in vivo. The gradients in 3D scaffolds or gels are somewhat more complicate to fabricate and characterize. More importantly, measuring the migration of cells (usually a group of cells rather than single cell or cell sheet) encapsulated in 3D matrix is also more challenging.

Selective cell migration plays an essential role in many physiological processes. Undesired cell migration at the wrong time or place can lead to serious problems [15, 210]. For example, after nerve damage, Schwann cells (SCs), the principle glial cells that support the survival and function of neurons in the peripheral nervous system [211], are required to migrate out and form a tunnel which is able to lead damaged neuron to sprout and grow, thus guiding the regeneration of nerves [212]. However, fibroblasts in the connective tissue around usually have stronger mobility

and form scar tissues by secreting collagen-based ECM after injury [213]. This will impede the migration of Schwann cells and thus regeneration of functional nerve tissue [214, 215]. Therefore, it is very important to design gradient biomaterials that are able to specifically guide the directional migration of cells required in tissue regeneration.

Last but not the least, material synthesis techniques should be sufficiently advanced to create physiologically relevant gradient materials to fit complex spatio-temporal phenomena such as tissue morphogenesis. Smart biomaterials incorporated with multiple gradient cues inside scaffolds, which mimic the timely cellular and structural characteristics of native tissues, could then be created for the regeneration of tissues having complex and multi-types of cells.

References

1. Godwin, Brockes. Regeneration, tissue injury and the immune response. J Anat. 2006;209:423–32.
2. Jagur-Grodzinski. Polymers for tissue engineering, medical devices, and regenerative medicine. Concise general review of recent studies. Polym Adv Technol. 2006;17:395–418.
3. Redd, et al. Imaging macrophage chemotaxis in vivo: studies of microtubule function in zebrafish wound inflammation. Cell Motil Cytoskeleton. 2006;63:415–22.
4. Cara, et al. Role of p38 mitogen-activated protein kinase in chemokine-induced emigration and chemotaxis in vivo. J Immunol. 2001;167:6552–8.
5. Cajal. La Rétine des Vertébrés. Cellule. 1892;9:119–257.
6. Keenan, Folch. Biomolecular gradients in cell culture systems. Lab Chip. 2008;8:34–57.
7. Genzer, Bhat. Surface-bound soft matter gradients. Langmuir. 2008;24:2294–317.
8. DeLong, et al. Covalent immobilization of RGDS on hydrogel surfaces to direct cell alignment and migration. J Control Release. 2005;109:139–48.
9. Chung, et al. Microfluidic platforms for studies of angiogenesis, cell migration, and cell-cell interactions. Ann Biomed Eng. 2010;38:1164–77.
10. Mimura, et al. A novel exogenous concentration-gradient collagen scaffold augments full-thickness articular cartilage repair. Osteoarthritis Cartilage. 2008;16:1083–91.
11. Singh, et al. Strategies and applications for incorporating physical and chemical signal gradients in tissue engineering. Tissue Eng B-Rev. 2008;14:341–66.
12. Gunawan, et al. Cell migration and polarity on microfabricated gradients of extracellular matrix proteins. Langmuir. 2006;22:4250–8.
13. Martin. Wound healing – aiming for perfect skin regeneration. Science. 1997;276:75–81.
14. Bernstein, Liotta. Molecular mediators of interactions with extracellular matrix components in metastasis and angiogenesis. Curr Opin Oncol. 1994;6:106–13.
15. Ceradini, et al. Progenitor cell trafficking is regulated by hypoxic gradients through HIF-1 induction of SDF-1. Nat Med. 2004;10:858–64.
16. Tedgui, Mallat. Cytokines in atherosclerosis: pathogenic and regulatory pathways. Physiol Rev. 2006;86:515–81.
17. Casscells. Migration of smooth muscle and endothelial cells. Critical events in restenosis. Circulation. 1992;86:723–9.
18. Galis, et al. Targeted disruption of the matrix metalloproteinase-9 gene impairs smooth muscle cell migration and geometrical arterial remodeling. Circ Res. 2002;91:852–9.
19. Ahmed, et al. GFP expression in the mammary gland for imaging of mammary tumor cells in transgenic mice. Cancer Res. 2002;62:7166–9.

20. Ridley AJ, et al. Cell migration: integrating signals from front to back. Science. 2003;302:1704–9.
21. Friedl, Weigelin. Interstitial leukocyte migration and immune function. Nat Immunol. 2008;9:960–9.
22. Ananthakrishnan, Ehrlicher. The forces behind cell movement. Int J Biol Sci. 2007;3:303–17.
23. Raftopoulou, Hall. Cell migration: Rho GTPases lead the way. Dev Biol. 2004;265:23–32.
24. Mitchison, Cramer. Actin-based cell motility and cell locomotion. Cell. 1996;84:371–9.
25. Wu, et al. Controlling the migration behaviors of vascular smooth muscle cells by methoxy poly(ethylene glycol) brushes of different molecular weight and density. Biomaterials. 2012;33:810–20.
26. Wehrle-Haller, Imhof. Actin, microtubules and focal adhesion dynamics during cell migration. Int J Biochem Cell Biol. 2003;35:39–50.
27. Hall. Rho GTPases and the control of cell behaviour. Biochem Soc Trans. 2005;33:891–5.
28. Wong, et al. Signal transduction in neuronal migration: roles of GTPase activating proteins and the small GTPase Cdc42 in the slit-robo pathway. Cell. 2001;107:209–21.
29. Manabe, et al. GIT1 functions in a motile, multi-molecular signaling complex that regulates protrusive activity and cell migration. J Cell Sci. 2002;115:1497–510.
30. Klemke, et al. Regulation of cell motility by mitogen-activated protein kinase. J Cell Biol. 1997;137:481–92.
31. Cheresh, et al. Regulation of cell contraction and membrane ruffling by distinct signals in migratory cells. J Cell Biol. 1999;146:1107–16.
32. Nguyen, et al. Myosin light chain kinase functions downstream of Ras/ERK to promote migration of urokinase-type plasminogen activator-stimulated cells in an integrin-selective manner. J Cell Biol. 1999;146:149–64.
33. Obermeier, et al. PAK promotes morphological changes by acting upstream of Rac. Embo J. 1998;17:4328–39.
34. Vaughan, Trinkaus. Movements of epithelial cell sheets in vitro. J Cell Sci. 1966;1:407–13.
35. Friedl, et al. Collective cell migration in morphogenesis and cancer. Int J Dev Biol. 2004;48:441–9.
36. Friedl. Prespecification and plasticity: shifting mechanisms of cell migration. Curr Opin Cell Biol. 2004;16:14–23.
37. Montell. Morphogenetic cell movements: diversity from modular mechanical properties. Science. 2008;322:1502–5.
38. Carmona-Fontaine, et al. Contact inhibition of locomotion in vivo controls neural crest directional migration. Nature. 2008;456:957–61.
39. Friedl, Wolf. Proteolytic interstitial cell migration: a five-step process. Cancer Metastasis Rev. 2009;28:129–35.
40. Friedl, Gilmour. Collective cell migration in morphogenesis, regeneration and cancer. Nat Rev Mol Cell Biol. 2009;10:445–57.
41. Lin, et al. Influence of physical properties of biomaterials on cellular behavior. Pharm Res. 2011;28:1422–30.
42. Tampieri, et al. Porosity-graded hydroxyapatite ceramics to replace natural bone. Biomaterials. 2001;22:1365–70.
43. Karageorgiou, Kaplan. Porosity of 3D biomaterial scaffolds and osteogenesis. Biomaterials. 2005;26:5474–91.
44. Cullinane, Einhorn. Biomechanics of bone. Princ Bone Biol. 2002;1:17–32.
45. Ho, et al. The tooth attachment mechanism defined by structure, chemical composition and mechanical properties of collagen fibers in the periodontium. Biomaterials. 2007;28:5238–45.
46. Lange, Fabry. Cell and tissue mechanics in cell migration. Exp Cell Res. 2013;319:2418–23.

47. Lo, et al. Cell movement is guided by the rigidity of the substrate. Biophys J. 2000;79:144–52.
48. Wang, et al. Mechanotransduction across the cell-surface and through the cytoskeleton. Science. 1993;260:1124–7.
49. Choquet, et al. Extracellular matrix rigidity causes strengthening of integrin-cytoskeleton linkages. Cell. 1997;88:39–48.
50. Sheetz, et al. Cell migration: regulation of force on extracellular-matrix-integrin complexes. Trends Cell Biol. 1998;8:51–4.
51. Lee, et al. Regulation of cell movement is mediated by stretch-activated calcium channels. Nature. 1999;400:382–6.
52. Pelham, Wang. High resolution detection of mechanical forces exerted by locomoting fibroblasts on the substrate. Mol Biol Cell. 1999;10:935–45.
53. Breckenridge, et al. Substrates with engineered step changes in rigidity induce traction force polarity and durotaxis. Cel Mol Bioeng. 2014;7:26–34.
54. Myers, et al. Bmp activity gradient regulates convergent extension during zebrafish gastrulation. Dev Biol. 2002;243:81–98.
55. Jones, Smith. Establishment of a BMP-4 morphogen gradient by long-range inhibition. Dev Biol. 1998;194:12–7.
56. Piccolo, et al. The head inducer Cerberus is a multifunctional antagonist of nodal, BMP and Wnt signals. Nature. 1999;397:707–10.
57. Isbister, et al. Gradient steepness influences the pathfinding decisions of neuronal growth cones in vivo. J Neurosci. 2003;23:193–202.
58. Zhou, et al. Nutrient gradients in engineered cartilage: metabolic kinetics measurement and mass transfer modeling. Biotechnol Bioeng. 2008;101:408–21.
59. Swartz, Fleury. Interstitial flow and its effects in soft tissues. Annu Rev Biomed Eng. 2007;9:229–56.
60. Luhmann, Hall. Cell guidance by 3D-gradients in hydrogel matrices: importance for biomedical applications. Materials. 2009;2:1058–83.
61. Kim, Wu. Microfluidics for mammalian cell chemotaxis. Ann Biomed Eng. 2012;40:1316–27.
62. Roussos, et al. Chemotaxis in cancer. Nat Rev Cancer. 2011;11:573–87.
63. Herzmark, et al. Bound attractant at the leading vs. the trailing edge determines chemotactic prowess. Proc Natl Acad Sci U S A. 2007;104:13349–54.
64. Servant, et al. Polarization of chemoattractant receptor signaling during neutrophil chemotaxis. Science. 2000;287:1037–40.
65. Haessler, et al. Dendritic cell chemotaxis in 3D under defined chemokine gradients reveals differential response to ligands CCL21 and CCL19. Proc Natl Acad Sci U S A. 2011;108:5614–9.
66. Carmeliet, Jain. Angiogenesis in cancer and other diseases. Nature. 2000;407:249–57.
67. Choi, et al. Phosphorescent nanoparticles for quantitative measurements of oxygen profiles in vitro and in vivo. Biomaterials. 2012;33:2710–22.
68. Helmlinger, et al. Interstitial pH and pO(2) gradients in solid tumors in vivo: high-resolution measurements reveal a lack of correlation. Nat Med. 1997;3:177–82.
69. Verbridge, et al. Oxygen-controlled three-dimensional cultures to analyze tumor angiogenesis. Tissue Eng Part A. 2010;16:2133–41.
70. Paradise, et al. Directional cell migration in an extracellular pH gradient: a model study with an engineered cell line and primary microvascular endothelial cells. Exp Cell Res. 2013;319:487–97.
71. Ruhrberg, et al. Spatially restricted patterning cues provided by heparin-binding VEGF-A control blood vessel branching morphogenesis. Genes Dev. 2002;16:2684–98.
72. Ito, et al. The movement of a water droplet on a gradient surface prepared by photodegradation. Langmuir. 2007;23:1845–50.
73. Singer, Kupfer. The directed migration of eukaryotic cells. Annu Rev Cell Biol. 1986;2:337–65.
74. Lauffenburger, Horwitz. Cell migration: a physically integrated molecular process. Cell. 1996;84:359–69.

75. Sullivan, et al. Asymmetric distribution of the chemotactic peptide receptor on polymorphonuclear leukocytes. J Cell Biol. 1984;99:1461–7.
76. Chan, Yousaf. A photo-electroactive surface strategy for immobilizing ligands in patterns and gradients for studies of cell polarization. Mol Biosyst. 2008;4:746–53.
77. Arnold, et al. Induction of cell polarization and migration by a gradient of nanoscale variations in adhesive ligand spacing. Nano Lett. 2008;8:2063–9.
78. Hirschfeld-Warneken, et al. Cell adhesion and polarisation on molecularly defined spacing gradient surfaces of cyclic RGDfK peptide patches. Eur J Cell Biol. 2008;87:743–50.
79. Smith, et al. Directed cell migration on fibronectin gradients: effect of gradient slope. Exp Cell Res. 2006;312:2424–32.
80. Tu, Tirrell. Bottom-up design of biomimetic assemblies. Adv Drug Deliv Rev. 2004;56:1537–63.
81. Morgenthaler, et al. Surface-chemical and -morphological gradients. Soft Matter. 2008;4:419–34.
82. Wang, et al. Tunable wettability and rewritable wettability gradient from superhydrophilicity to superhydrophobicity. Langmuir. 2010;26:12203–8.
83. Riepl, et al. Molecular gradients: an efficient approach for optimizing the surface properties of biomaterials and biochips. Langmuir. 2005;21:1042–50.
84. Dertinger, et al. Generation of gradients having complex shapes using microfluidic networks. Anal Chem. 2001;73:1240–6.
85. Kraus, et al. Printing chemical gradients. Langmuir. 2005;21:7796–804.
86. Choi, Newby. Micrometer-scaled gradient surfaces generated using contact printing of octadecyltrichlorosilane. Langmuir. 2003;19:7427–35.
87. Tomlinson, Genzer. Formation of grafted macromolecular assemblies with a gradual variation of molecular weight on solid substrates. Macromolecules. 2003;36:3449–51.
88. Matyjaszewski, et al. Polymers at interfaces: using atom transfer radical polymerization in the controlled growth of homopolymers and block copolymers from silicon surfaces in the absence of untethered sacrificial initiator. Macromolecules. 1999;32:8716–24.
89. Li, et al. Fabrication of thermoresponsive polymer gradients for study of cell adhesion and detachment. Langmuir. 2008;24:13632–9.
90. Venkataraman, et al. Order and composition of methyl-carboxyl and methyl-hydroxyl surface-chemical gradients. Langmuir. 2006;22:4184–9.
91. Yu, et al. Surface gradient material: from superhydrophobicity to superhydrophilicity. Langmuir. 2006;22:4483–6.
92. Morgenthaler, et al. A simple, reproducible approach to the preparation of surface-chemical gradients. Langmuir. 2003;19:10459–62.
93. Chaudhury, Whitesides. How to make water run uphill. Science. 1992;256:1539–41.
94. Zhao. A combinatorial approach to study solvent-induced self-assembly of mixed poly(methyl methacrylate)/polystyrene brushes on planar silica substrates: effect of relative grafting density. Langmuir. 2004;20:11748–55.
95. Wu, et al. Combinatorial study of the mushroom-to-brush crossover in surface anchored polyacrylamide. J Am Chem Soc. 2002;124:9394–5.
96. Genzer, et al. Formation mechanisms and properties of semifluorinated molecular gradients on silica surfaces. Langmuir. 2006;22:8532–41.
97. Liedberg, Tengvall. Molecular gradients of omega-substituted alkanethiols on gold – preparation and characterization. Langmuir. 1995;11:3821–7.
98. Mougin, et al. Construction of a tethered poly(ethylene glycol) surface gradient for studies of cell adhesion kinetics. Langmuir. 2005;21:4809–12.
99. Karpiak, et al. Density gradient multilayer polymerization for creating complex tissue. Adv Mater. 2012;24:1466–70.
100. Claussen, et al. Learning from nature: synthesis and characterization of longitudinal polymer gradient materials inspired by mussel byssus threads. Macromol Rapid Commun. 2012;33:206–11.

101. Cai, et al. Lubricated biodegradable polymer networks for regulating nerve cell behavior and fabricating nerve conduits with a compositional gradient. Biomacromolecules. 2012;13:358–68.
102. Irimia, et al. Universal microfluidic gradient generator. Anal Chem. 2006;78:3472–7.
103. Zaari, et al. Photopolymerization in microfluidic gradient generators: microscale control of substrate compliance to manipulate cell response. Adv Mater. 2004;16:2133–7.
104. Chiu, et al. Patterned deposition of cells and proteins onto surfaces by using three-dimensional microfluidic systems. Proc Natl Acad Sci U S A. 2000;97:2408–13.
105. Wigenius, et al. Limits to nanopatterning of fluids on surfaces in soft lithography. Adv Funct Mater. 2008;18:2563–71.
106. Childs, Nuzzo. Decal transfer microlithography: a new soft-lithographic patterning method. J Am Chem Soc. 2002;124:13583–96.
107. Wang, et al. Metal transfer printing and its application in organic field-effect transistor fabrication. Adv Mater. 2003;15:1009–12.
108. Bhangale, et al. Biologically active protein gradients via microstamping. Adv Mater. 2005;17:809–13.
109. Jeon, et al. Structure and stability of patterned self-assembled films of octadecyltrichlorosilane formed by contact printing. Langmuir. 1997;13:3382–91.
110. Lang, et al. Growth cone response to ephrin gradients produced by microfluidic networks. Anal Bioanal Chem. 2008;390:809–16.
111. Liu, et al. Programming nanostructures of polymer brushes by dip-pen nanodisplacement lithography (DNL). Nanoscale. 2010;2:2614–8.
112. Zhou, et al. Fabrication of arbitrary three-dimensional polymer structures by rational control of the spacing between nanobrushes. Angew Chem-Int Ed. 2011;50:6506–10.
113. Righetti, Bossi. Isoelectric focusing in immobilized pH gradients: an update. J Chromatogr B. 1997;699:77–89.
114. Venkateswar, et al. An electrophoretic method for microstamping biomolecule gradients. Biomed Microdevices. 2000;2:255–64.
115. Plummer, et al. Electrochemically derived gradients of the extracellular matrix protein fibronectin on gold. Langmuir. 2003;19:7528–36.
116. Spijker, et al. Protein adsorption on gradient surfaces on polyethylene prepared in a shielded gas plasma. Colloids Surf B-Biointerfaces. 1999;15:89–97.
117. Shin, et al. Adhesion comparison of human bone marrow stem cells on a gradient wettable surface prepared by corona treatment. Appl Surf Sci. 2008;255:293–6.
118. Blondiaux, et al. Fabrication of multiscale surface-chemical gradients by means of photocatalytic lithography. Langmuir. 2007;23:3489–94.
119. Mangindaan, et al. Experimental and numerical modeling of the controllable wettability gradient on poly(propylene) created by SF6 plasma. Plasma Processes Polym. 2010;7:754–65.
120. Pitt. Fabrication of a continuous wettability gradient by radio-frequency plasma discharge. J Colloid Interface Sci. 1989;133:223–7.
121. Golander, Pitt. Characterization of hydrophobicity gradients prepared by means of radio-frequency plasma discharge. Biomaterials. 1990;11:32–5.
122. Whittle, et al. A method for the deposition of controllable chemical gradients. Chem Commun. 2003;9:1766–7.
123. Lee, et al. Interaction of different types of cells on polymer surfaces with wettability gradient. J Colloid Interface Sci. 1998;205:323–30.
124. Lee, et al. Platelet adhesion onto chargeable functional group gradient surfaces. J Biomed Mater Res. 1998;40:180–6.
125. Khang, et al. The effect of fluid shear stress on endothelial cell adhesiveness to modified polyurethane surfaces. Korea Polym J. 2000;8:179–85.
126. Kim, et al. Gradient polymer surfaces for biomedical applications. Prog Polym Sci. 2008;33:138–64.
127. Lee, Lee. A wettability gradient as a tool to study protein adsorption and cell-adhesion on polymer surfaces. J Biomater Sci-Polym Ed. 1993;4:467–81.

128. Kim, et al. First preparation of biotinylated gradient polyethylene surface to bind photoactive caged streptavidin. Langmuir. 2005;21:4066–70.
129. Lee, et al. Preparation and characterization of functional-group gradient surfaces. J Polym Sci A-Polym Chem. 1994;32:1569–79.
130. Gijsman, et al. Comparison of the UV-degradation chemistry of polypropylene, polyethylene, polyamide 6 and polybutylene terephthalate. Polym Degrad Stab. 1999;65:433–41.
131. Li, et al. A technique for preparing protein gradients on polymeric surfaces: effects on PC12 pheochromocytoma cells. Biomaterials. 2005;26:1487–95.
132. Li, et al. Influence of carboxyl group density on neuron cell attachment and differentiation behavior: gradient-guided neurite outgrowth. Biomaterials. 2005;26:4956–63.
133. Ding, et al. Spatial variation of the charge and sulfur oxidation state in a surface gradient affects plasma protein adsorption. Langmuir. 2010;26:12140–6.
134. Zhu, et al. Immobilization of biomacromolecules onto aminolyzed poly(L-lactic acid) toward acceleration of endothelium regeneration. Tissue Eng. 2004;10:53–61.
135. Zhu, et al. Endothelium regeneration on luminal surface of polyurethane vascular scaffold modified with diamine and covalently grafted with gelatin. Biomaterials. 2004;25:423–30.
136. Zhu, et al. Endothelial cell functions in vitro cultured on poly(L-lactic acid) membranes modified with different methods. J Biomed Mater Res A. 2004;69A:436–43.
137. Li, et al. PCL film surfaces conjugated with P(DMAEMA)/gelatin complexes for improving cell immobilization and gene transfection. Bioconjug Chem. 2011;22:1842–51.
138. Uedayukoshi, Matsuda. Cellular-responses on a wettability gradient surface with continuous variations in surface compositions of carbonate and hydroxyl-groups. Langmuir. 1995;11:4135–40.
139. Tan, et al. Microscale control over collagen gradient on poly(L-lactide) membrane surface for manipulating chondrocyte distribution. Colloids Surf B-Biointerfaces. 2008;67:210–5.
140. Wu, et al. Covalently immobilized gelatin gradients within three-dimensional porous scaffolds. Chin Sci Bull. 2009;54:3174–80.
141. Han, et al. Modulating the structure and properties of poly(sodium 4-styrenesulfonate)/poly(diallyldimethylammonium chloride) multilayers with concentrated salt solutions. Langmuir. 2012;28:193–9.
142. Kunzler, et al. Systematic study of osteoblast and fibroblast response to roughness by means of surface-morphology gradients. Biomaterials. 2007;28:2175–82.
143. Han, et al. Directional cell migration through cell-cell interaction on polyelectrolyte multilayers with swelling gradients. Biomaterials. 2013;34:975–84.
144. Roy, et al. Performance of degradable composite bone repair products made via three-dimensional fabrication techniques. J Biomed Mater Res A. 2003;66A:283–91.
145. Woodfield, et al. Polymer scaffolds fabricated with pore-size gradients as a model for studying the zonal organization within tissue-engineered cartilage constructs. Tissue Eng. 2005;11:1297–311.
146. Oh, et al. In vitro and in vivo characteristics of PCL scaffolds with pore size gradient fabricated by a centrifugation method. Biomaterials. 2007;28:1664–71.
147. Meredith. Advances in combinatorial and high-throughput screening of biofunctional polymers for gene delivery, tissue engineering and anti-fouling coatings. J Mater Chem. 2009;19:34–45.
148. Meredith, et al. Combinatorial characterization of cell interactions with polymer surfaces. J Biomed Mater Res A. 2003;66A:483–90.
149. Sormana, Meredith. High-throughput discovery of structure-mechanical property relationships for segmented poly(urethane-urea)s. Macromolecules. 2004;37:2186–95.
150. DeLong, et al. Covalently immobilized gradients of bFGF on hydrogel scaffolds for directed cell migration. Biomaterials. 2005;26:3227–34.
151. Kapur, Shoichet. Immobilized concentration gradients of nerve growth factor guide neurite outgrowth. J Biomed Mater Res A. 2004;68A:235–43.
152. Wong, et al. Partitioning microfluidic channels with hydrogel to construct tunable 3-D cellular microenvironments. Biomaterials. 2008;29:1853–61.

153. Guarnieri, et al. Engineering of covalently immobilized gradients of RGD peptides on hydrogel scaffolds: effect on cell behaviour. Macromol Symp. 2008;266:36–40.
154. Luo, Shoichet. A photolabile hydrogel for guided three-dimensional cell growth and migration. Nat Mater. 2004;3:249–53.
155. Wong, et al. Directed movement of vascular smooth muscle cells on gradient-compliant hydrogels. Langmuir. 2003;19:1908–13.
156. Hansen, et al. Fabrication of arrays of polymer gradients using inkjet printing. Macromol Rapid Commun. 2012;33:1114–8.
157. Oh, et al. Creating growth factor gradients in three dimensional porous matrix by centrifugation and surface immobilization. Biomaterials. 2011;32:8254–60.
158. Barry, et al. Using a core-sheath distribution of surface chemistry through 3D tissue engineering scaffolds to control cell ingress. Adv Mater. 2006;18:1406–10.
159. Macner, et al. Condensation on surface energy gradient shifts drop size distribution toward small drops. Langmuir. 2014;30:1788–98.
160. Hernandez, et al. Chemical gradients on graphene to drive droplet motion. ACS Nano. 2013;7:4746–55.
161. Maheshwari, et al. Cell adhesion and motility depend on nanoscale RGD clustering. J Cell Sci. 2000;113:1677–86.
162. Bhat, et al. Tailoring cell adhesion using surface-grafted polymer gradient assemblies. Adv Mater. 2005;17:2802–7.
163. Borkenhagen, et al. Three-dimensional extracellular matrix engineering in the nervous system. J Biomed Mater Res. 1998;40:392–400.
164. Pelham, Wang. Cell locomotion and focal adhesions are regulated by substrate flexibility. Proc Natl Acad Sci U S A. 1997;94:13661–5.
165. Cheung, et al. Microscale control of stiffness in a cell-adhesive substrate using microfluidics-based lithography. Angew Chem-Int Ed. 2009;48:7188–92.
166. Hopp, et al. The influence of substrate stiffness gradients on primary human dermal fibroblasts. Biomaterials. 2013;34:5070–7.
167. Liang, et al. Dynamic changes in focal adhesion kinase during cell migration induced by bFGF and the significance. Sheng Li Xue Bao: [Acta Physiologica Sinica]. 2004;56:509–14.
168. Martinez, et al. Cell durotaxis on polyelectrolyte multilayers with photogenerated gradients of modulus. Biomacromolecules. 2013;14:1311–20.
169. Kuo, et al. Complex stiffness gradient substrates for studying mechanotactic cell migration. Adv Mater. 2012;24:6059–64.
170. Wang, et al. Focal adhesion kinase is involved in mechanosensing during fibroblast migration. Proc Natl Acad Sci U S A. 2001;98:11295–300.
171. Kim, et al. Mechanosensitivity of fibroblast cell shape and movement to anisotropic substratum topography gradients. Biomaterials. 2009;30:5433–44.
172. Kim, et al. Guided cell migration on microtextured substrates with variable local density and anisotropy. Adv Funct Mater. 2009;19:1579–86.
173. Mak, et al. Microfabricated physical spatial gradients for investigating cell migration and invasion dynamics. PLoS ONE. 2011;6:e20825.
174. Han, et al. Unidirectional migration of single smooth muscle cells under the synergetic effects of gradient swelling cue and parallel groove patterns. Colloids Surf B-Biointerfaces. 2013;111:1–6.
175. Han, et al. Polyelectrolyte multilayer patterns created by capillary force and their impact on cell migration. Chin J Chem. 2014;32:66–72.
176. Peret, Murphy. Controllable soluble protein concentration gradients in hydrogel networks. Adv Funct Mater. 2008;18:3410–7.
177. Zelzer, et al. Investigation of cell-surface interactions using chemical gradients formed from plasma polymers. Biomaterials. 2008;29:172–84.

178. Ren, et al. Directional migration of vascular smooth muscle cells guided by a molecule weight gradient of poly(2-hydroxyethyl methacrylate) brushes. Langmuir. 2013;29:6386–95.
179. Zhu, Evans. Analysis of the roles of RGD-binding integrins, alpha(4)/alpha(9) integrins, alpha(6) integrins, and CD9 in the interaction of the fertilin beta (ADAM2) disintegrin domain with the mouse egg membrane. Biol Reprod. 2002;66:1193–202.
180. Chan, et al. In vitro and in vivo consequences of Vla-2 expression on rhabdomyosarcoma cells. Science. 1991;251:1600–2.
181. Rajagopalan, et al. Direct comparison of the spread area, contractility, and migration of balb/c 3T3 fibroblasts adhered to fibronectin- and RGD-modified substrata. Biophys J. 2004;87:2818–27.
182. Smith, et al. Measurement of cell migration on surface-bound fibronectin gradients. Langmuir. 2004;20:8279–86.
183. Cai, et al. Regulation of endothelial cells migration on poly(D, L-lactic acid) films immobilized with collagen gradients. Colloids Surf B-Biointerfaces. 2010;79:291–7.
184. Yu, et al. Preparation of gelatin density gradient on poly(epsilon-caprolactone) membrane and its influence on adhesion and migration of endothelial cells. J Colloid Interface Sci. 2015;451:177–83.
185. Wu, et al. Gradient biomaterials and their influences on cell migration. Interface Focus. 2012;2:337–55.
186. Adams, et al. Growth cones turn and migrate up an immobilized gradient of the laminin IKVAV peptide. J Neurobiol. 2005;62:134–47.
187. Guarnieri, et al. Covalently immobilized RGD gradient on PEG hydrogel scaffold influences cell migration parameters. Acta Biomater. 2010;6:2532–9.
188. Sarvestani, Jabbari. Analysis of cell locomotion on ligand gradient substrates. Biotechnol Bioeng. 2009;103:424–9.
189. Liu, et al. Endothelial cell migration on surface-density gradients of fibronectin, VEGF, or both proteins. Langmuir. 2007;23:11168–73.
190. Stefonek-Puccinelli, Masters. Co-immobilization of gradient-patterned growth factors for directed cell migration. Ann Biomed Eng. 2008;36:2121–33.
191. Frevert, et al. Measurement of cell migration in response to an evolving radial chemokine gradient triggered by a microvalve. Lab Chip. 2006;6:849–56.
192. Bernal, et al. L-selectin and SDF-1 enhance the migration of mouse and human cardiac mesoangioblasts. Cell Death Differ. 2012;19:345–55.
193. Cornejo, et al. Effect of NRG1, GDNF, EGF and NGF in the migration of a Schwann cell precursor line. Neurochem Res. 2010;35:1643–51.
194. de Simone, et al. NGF promotes microglial migration through the activation of its high affinity receptor: modulation by TGF-beta. J Neuroimmunol. 2007;190:53–60.
195. Wang, et al. Differential effects of EGF gradient profiles on MDA-MB-231 breast cancer cell chemotaxis. Exp Cell Res. 2004;300:180–9.
196. Sutton, et al. The response of endothelial-cells to Tgf-beta-1 is dependent upon cell-shape, proliferative state and the nature of the substratum. J Cell Sci. 1991;99:777–87.
197. Ennett, Mooney. Tissue engineering strategies for in vivo neovascularisation. Expert Opin Biol Ther. 2002;2:805–18.
198. Kawano, Kidoaki. Elasticity boundary conditions required for cell mechanotaxis on microelastically-patterned gels. Biomaterials. 2011;32:2725–33.
199. Park, et al. Simple haptotactic gradient generation within a triangular microfluidic channel. Lab Chip. 2010;10:2130–8.
200. Hale, et al. Cell migration at the interface of a dual chemical-mechanical gradient. ACS Appl Mater Interfaces. 2010;2:2317–24.
201. Rao, et al. The migration of cancer cells in gradually varying chemical gradients and mechanical constraints. Micromachines. 2014;5:13–26.

202. Mendelson, et al. Competitive stem cell recruitment by multiple cytotactic cues dagger. Lab Chip. 2013;13:1156–64.
203. Wu, et al. Directional migration of vascular smooth muscle cells guided by synergetic surface gradient and chemical pattern of poly(ethylene glycol) brushes. J Bioact Compat Polym. 2013;28:605–20.
204. Ren, et al. Complementary density gradient of poly(hydroxyethyl methacrylate) and YIGSR selectively guides migration of endotheliocytes. Biomacromolecules. 2014;15:2256–64.
205. Dodla, Bellamkonda. Anisotropic scaffolds facilitate enhanced neurite extension in vitro. J Biomed Mater Res A. 2006;78A:213–21.
206. Moore, et al. Immobilized concentration gradients of neurotrophic factors guide neurite outgrowth of primary neurons in macroporous scaffolds. Tissue Eng. 2006;12:267–78.
207. Musoke-Zawedde, Shoichet. Anisotropic three-dimensional peptide channels guide neurite outgrowth within a biodegradable hydrogel matrix. Biomed Mater. 2006;1:162–9.
208. Hofmann, et al. Control of in vitro tissue-engineered bone-like structures using human mesenchymal stem cells and porous silk scaffolds. Biomaterials. 2007;28:1152–62.
209. Sundararaghavan, Burdick. Gradients with depth in electrospun fibrous scaffolds for directed cell behavior. Biomacromolecules. 2011;12:2344–50.
210. Kunkel, Butcher. Chemokines and the tissue-specific migration of lymphocytes. Immunity. 2002;16:1–4.
211. Taniuchi, et al. Induction of nerve growth-factor receptor in Schwann-cells after axotomy. Proc Natl Acad Sci U S A. 1986;83:4094–8.
212. Fields, Stevens-Graham. Neuroscience – new insights into neuron-glia communication. Science. 2002;298:556–62.
213. Richard, et al. Endoneurial fibroblast-like cells. J Neuropathol Exp Neurol. 2012;71:938–47.
214. Atkins, et al. Scarring impedes regeneration at sites of peripheral nerve repair. Neuroreport. 2006;17:1245–9.
215. Dreesmann, et al. Nerve fibroblast impact on Schwann cell behavior. Eur J Cell Biol. 2009;88:285–300.

Chapter 8
Stem Cell Differentiation Mediated by Biomaterials/Surfaces

Hongyan He and Changsheng Liu

8.1 Introduction

As one of the greatest discoveries in the biomedical field over the last century, stem cells have the remarkable potential to develop into different cell/tissue types in the body under the proper conditions during early life and growth [1, 2]. In addition, stem cells are capable of serving as a sort of internal regenerating/repair system in many tissues, dividing essentially without limit to replenish other cells as long as the person or animal is still alive [3]. Because of these unique capabilities, stem cells have absorbed a great interest for regenerative medicine and tissue engineering [4, 5]. Typically, stem cells are divided into embryonic stem cells (ESCs) and adult stem cells (ASCs). ESCs are pluripotent stem cells derived from the inner cell mass of blastocysts and able to differentiate to generate primitive ectoderm, which ultimately differentiates into all derivatives of the three primary germ layers: ectoderm, endoderm, and mesoderm [6, 7]. Meanwhile, ASCs are multipotent cells derived from adult somatic tissues with the potential to differentiate into many specific cell types [8]. In comparison with ASCs, ESCs can generate all cell types in the body and have long-term self-renewal capacity. In other words, ESCs are capable of propagating themselves indefinitely in an undifferentiated state under defined conditions and generating almost all mature cell phenotypes [9], allowing ESCs as useful resources for basic research and clinical applications[7]. Recently, human ESCs have been produced and approved for use in a very small number of early clinical trials. However, ESC research still needs to face the challenges including ethical considerations, safety issue of ESCs, and a higher risk of tumorigenicity [10].

With the development of cell biology and biotechnologies, many researchers have tended to develop ASC-based therapies for regenerative medicine and

H. He • C. Liu (✉)
School of Material Science and Engineering, East China University of Science and Technology, Shanghai, China
e-mail: liucs@ecust.edu.cn

© Springer Science+Business Media Singapore 2016

C. Gao (ed.), *Polymeric Biomaterials for Tissue Regeneration*,
DOI 10.1007/978-981-10-2293-7_8

tissue-engineered applications. Generally, ASCs can be isolated from several sources including the body itself (i.e., the brain, bone marrow, blood vessels, and other organs and tissues), amniotic fluid, pluripotent stem cells, and other ASCs [11]. Over the last decade, it has become essential to better understand how to direct the differentiation fates of stem cells into a specific stromal lineage. However, the uncontrolled and inefficient proliferative and differentiation behaviors of stem cells are still the significant challenges for medical uses. Since the stem cell fate is strongly determined by the characteristics of the microenvironment in vitro, the biomaterial/surface constructs in two-dimensional or three-dimensional (3D) artificial structures could offer the several biological, mechanical, and chemical cues to modulate the cellular proliferation and most importantly lineage particular differentiation. Besides these regulation cues, adding growth components existing in the ECM also holds the potential for guiding the stem cell fate in vitro. Therefore, this chapter aims to provide an update on the influencing cues that are being explored to govern stem cell fate, with a focus on the differentiation of bone-marrow-derived MSCs. The factors discussed here include topography, porosity and pore size, stiffness, hierarchy structure, chemical properties, and genetic factors. The emphasis of discussion will be placed on the influence of these factors to govern stem cell fate. The successful strategies and the mechanisms to control stem cells fate are highlighted for regenerative medicine and tissue engineering.

8.2 Mesenchymal Stem Cells and Alternatives

Mesenchymal stem cells (MSCs), or marrow stromal cell, are the most popular types of ASCs for medical research and clinical uses. These types of stem cells are usually isolated from the bone marrow and also derived from non-marrow tissues, such as the placenta, umbilical cord blood, adipose tissue, adult muscle, corneal stroma, or the dental pulp of deciduous baby teeth [12, 13]. MSCs are multipotent stromal cells that can differentiate into a variety of cell types, including osteoblasts, chondrocytes, myocytes, and adipocytes [8, 14]. Numerous studies have demonstrated that MSCs have great differentiation capacity and immunomodulatory functions [15]. For cell-based therapies, MSCs indeed display several advantages over embryonic or induced pluripotent stem cells: easier isolation via autologous ways, don't require rigorous conditions in vitro, and a low risk of tumorigenicity [16]. Summing up the increasing research activities over the last decade, MSCs have the clinic perspectives to replace cell tissues that have been damaged or destroyed in treating cancers, neurological disorder, autoimmune disease, and orthopedic applications [17, 18].

8.3 Biomaterials as an Artificial Extracellular Matrix

8.3.1 Extracellular Matrix

The integration of material science and molecular cell biology has shed new light to the interaction and communications between cells and materials, from a more extensive and profound perspective [19–21]. Over the past decades, scientists have noticed the bidirectional relations between cells and materials. Cells can alter the physical or chemical properties of materials through secreting cytokines or other chemical cues. In addition, surrounding materials (especially the surface of materials) can determine the temporal and spatial coordination of numerous cell fates by inducing a myriad of signals [19, 22]. Particularly, in the field of tissue engineering or regenerative medicine, it is of great interest to utilize the close interaction between cells and materials to design materials that may facilitate the ingrowth and differentiation of cells or induce morphogenesis in constructed tissues. Among all materials, extracellular matrix (ECM) can serve as the best candidate due to its high similarity to original organs or tissues, biocompatibility, and bioactivities. The main advantage of ECM as a scaffolding material is its realization for so-called constructive remodeling, that is, it supports and encourages specific tissue formation at the implantation site rather than forming inferior and less functional scar tissue [23].

Naturally, extracellular matrix is a combination of macromolecules that are synthesized and secreted by cells [24]. Such macromolecules are usually distributed on the surface of cells or around different cells, comprising a delicate and complicated network to support and connect the tissue structure and adjust the physiological behaviors among cells. Typically, extracellular matrix could be classified into three groups: glycosaminoglycans, structural proteins, and adhesives (shown in Fig. 8.1) [24]. Glycosaminoglycans or proteoglycan can form hydrogels, encapsulating various matrix components. Structural proteins, such as collagen and elastin, can ensure the strength and flexibility of ECM. Meanwhile, the adhesives including fibronectin and laminin can promote the adhesion of cells onto ECM.

ECM provides the foremost function as structural support to cells; it also bestows an optimized environment by providing sites for cell adhesion, creating soluble factor gradients, and forming interfaces between different cell types within a tissue. Take an example, three-dimensional ECMs in tissue engineering are employed to construct new natural tissues from isolated cells (i.e., stem cells). The ECMs encapsulating stem cells can facilitate the inflow of nutrients and ensure the mechanical stability of the local environment for the seeded cells to form specific gene expression [25].

Many researchers have revealed that tissue formation, function, and regeneration depend on the interaction of numerous individual cell fate processes, each of which is induced by an array of signals originating from the extracellular environment. Thus, the cell fate processes would be directed or guided by controlling the ECMs surrounding each cell and comprising the molecular signals. The important components in ECMs include (i) insoluble natural matrix molecule (collagen, laminin,

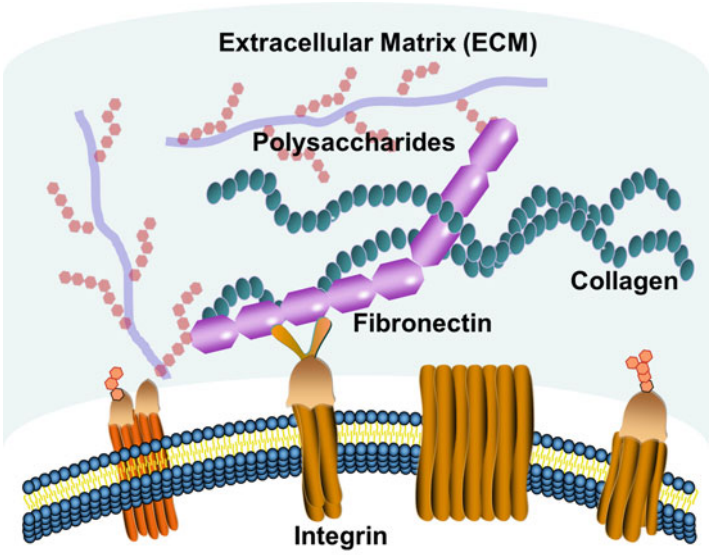

Fig. 8.1 Schematic structure of extracellular matrix

elastin, or fibronectin), (ii) soluble macromolecules (growth factors, chemokines, and cytokines), and (iii) proteins on surfaces of neighboring cells (cadherins) [19]. The ultimate fate of a cell to proliferate, differentiate, migrate, apoptose, or perform other specific functions is a coordinated response to the molecular interactions with these ECM components. Take stem cell as an example, cell fate is influenced by such coordinated interaction of soluble factors, extracellular matrix, and signals from neighboring cells. Specific binding of signal molecules with cell surface receptors induces complex intracellular signaling pathways with subsequent effects on gene expression, self-renewal, morphogenesis, and differentiation [25].

8.3.2 Natural ECM and Artificial ECM

According to the material sources, extracellular matrix could be classified into two categories: naturally derived ones and synthetic ECMs [26]. Take a natural example, collagens are purified protein components separated from animal or human tissues. Such biologically derived materials can be desired carriers to embed cells and then be grafted into tissue defects or induce regeneration and remodeling due to potential advantages of specific cell interactions. Since natural ECM-derived biomaterials are

highly biocompatible, a number of them have been already approved by FDA for clinical applications. Apart from the compatibility, naturally derived ones still preserve inherent properties of biological recognition originating from the animal source, such as receptor-binding ligands and susceptibility to cell-triggered proteolytic degradation and remodeling. Those cell-recognizable receptors are able to improve integrin-dependent interaction, and some of them (i.e., carbohydrates) can act as the specific ligands to recognize the surface molecules of the cells (e.g., galactose, a specific ligand for asialoglycoprotein receptor on hepatocytes) [27]. However, there still exist limitations for natural ECM-derived materials. First, the quality of the natural products depends on the animal source and the manufacturing process. They might have instable properties and suffer from batch-to-batch variations. The quantities of the natural ECM materials are not enough to meet the application needs because of the complexities associated with purification. Secondly, the natural ECM-derived materials cannot meet the mechanical requirements for some specific clinical applications. Commonly, such materials show lower mechanical strength and are only suitable for soft-tissue repairing. Moreover, natural biomaterials might have potential risks in immunogenicity issues and pathogen transmission.

In order to solve those issues above, synthetic biomaterials are designed and prepared to meet the requirements chemically and biologically. The past few years have witnessed the rapid development of synthesized biomaterials as artificial extracellular matrix for biomedical applications and clinical use. Compared to naturally derived ones, synthetic biomaterials can be manufactured reproducibly on a large scale and have great flexibility in tuning their microstructure, mechanical properties, and physiological properties. However, synthetic materials show poor capability of cell recognition in general. Therefore, the biomaterials as artificial ECMs for engineering tissues have to follow several criterions. The materials should facilitate the localization and delivery of imbedded cells to the specific sites in the body, while maintaining the structural stability. Moreover, the material should possess molecular cues, mimicking different aspects of natural extracellular matrix and guiding the cell behaviors. To achieve these favorable effects, different functional components should be introduced on/into the artificial ECMs. The most important components could be integrin-dependent ligands (i.e., collagen, laminin, or fibronectin), cell–cell adhesion molecules (i.e., cadherins or ICAM), binding sites for growth factor proteins (i.e., bone morphogenetic protein-2 (BMP-2), HGF, and VEGF), or small molecules (i.e., drugs or hormones), which allows the easy accessibility to cells and ligands for endocytosis.

Nowadays, a wide range of synthesized materials have been developed to mimic extracellular matrix with many functions including cellular 3D architecture, mechanical integrity to the new tissue, and the space for the diffusion of nutrients and metabolites. In general, such biomaterials could be divided into synthesized hydrogels, degradable polymers, or polypeptides and recombinant artificial ECM.

8.3.2.1 Synthesized Hydrogels

Typically, synthesized hydrogels have similar characteristics with natural ECM in biocompatibility and suitability for cells to survive. These useful materials have already gained much attention in the field of biological application and clinical use. The cross-linked and hydrophilic polymers with controllable microstructures can be beneficial for tissue-like viscoelasticity, oxygen transportation, and nutrient flow. Rape et al. [28] have prepared light-modulated hyaluronic acid hydrogels that enable imposition of mutually independent and spatially continuous gradients of ligand density and substrate stiffness, which facilitated the MSCs for mechanosensitive differentiation. Another study from Yosi Navaro [29] reveals that modification of matrix stiffness will have great influence on the ability of cultured stem cells to proliferate, survive, and differentiate into mature cells.

In particular, when cells are encapsulated in 3D hydrogels, the whole biomaterial is highly similar to extracellular matrix in our body. It has been reported that photopolymerizable polyethylene glycol (PEG) derivatives have been used as tissue engineering scaffolds for synthetic ECM analogs by Brenda K. Mann and his colleagues [30]. The materials highly resembled the natural ECMs and demonstrated the excellent performance for biocompatibility. However, most synthesized hydrogels lack essential biological cues to induce favorable cell behaviors and cannot be biodegradable. Therefore, a number of biological sites are incorporated in the hydrogels, such as cell adhesion ligands, proteolytic susceptible ligands, and growth factors. Meanwhile, proteolytically degradable peptides or enzymatic degradable groups are also introduced to improve the degradability. As reported by Elena Cambria, sortase-mediated ligation was used to conjugate human epidermal growth factor grafted to a GGG ligation motif (GGG-EGF) to PEG hydrogels containing the sortase LPRTG substrate, promoting biological activity [31]. It is noted that the cell-containing hydrogels must be prepared under mild conditions so as not to cause the loss in cell viability or subsequent cell behaviors such as cell adhesion, migration, and differentiation.

8.3.2.2 Degradable Polymers

Degradable polymers are also widely used as artificial ECMs. Since the physical and chemical properties of biodegradable polymers can be easily turned by controlling the synthesized conditions, or choosing the functional monomers, the degradable polymers can be designed to match the requirements of many medical applications. Compared to other materials, degradable polymers can be easily modified on surfaces for further functionalization through grafting or anchoring.

Polyesters are one of the degradable polymers that are commonly employed as artificial ECMs, including polyglycolic acid (PGA), poly(L-lactic acid) (PLLA), and copolymers of poly(lactic-co-glycolic acid) (PLGA). All of these materials have already been approved by FDA for various biomedical applications and clinical use.

The ester bonds in the polymers enable them to degrade through hydrolysis, and the degradation rate could also be adjusted by changing the number of ester bonds during synthesis process. Meanwhile, polyesters have better mechanical strength than hydrogels or naturally derived ECMs and thus can be applied in hard-tissue repairing. For instance, nanofibrous PLLA scaffolds have been reported to show the similarity to the structure of natural collagen fibers and create a more favorable microenvironment for cells to survive [32]. Besides the advantages above, typical degradable polymers further need the introduction of biomedical cues stimulating or responding to the cells. Therefore, growth factors or bioactive domains have been incorporated into/onto polymers to endow the materials with the ability to recapitulate natural ECMs. For instance, RGD peptides (three letters which stand for arginine, glycine, and aspartic acid, respectively) are widely employed in the modification of polymers to promote cell adhesion, since the surface density, spatial arrangement, as well as integrin affinity and selectivity of RGD peptide influenced cell responses like adhesion and migration [33].

Amino acid-based polymers are also degradable polymers employed as artificial extracellular matrix. With the development of the synthesized poly(amino acid), such new biomaterials have been increasingly used for medical uses in recent years. Compared to other polymers that need further modification or functionalization for biomedical cues, amino acid-based polymers naturally preserve the ability to build the interactions with cells. It is worth noting that certain manipulations on subsequent cell behaviors could be achieved by precisely determining the amino acid orders and well-defined molecular architecture. For example, Girotti and co-workers incorporated elastin domains, lysines, and fibronectin CS5 domains containing well-known cell attachment sequence REDV into one single polymer, promoting cell proliferation activity, angiogenesis, and other bioactivities of interest for tissue growing, repairing, and healing [34]. Yihua Loo and his group reported a novel peptide bioinks for 3D printing in tissue repairing applications [35]. The artificial ECM contained lysine hexapeptides, which could self-assemble into stable, nanofibrous three-dimensional hydrogels with excellent stiffness of up to 40 kPa. These biocompatible scaffolds supported the three-dimensional culture of human stem cells and differentiation of primary cells into organotypic (gastrointestinal and skin) structures.

8.3.2.3 Recombinant Artificial ECM

Hydrogels and degradable polymers have showed unique properties although there are some mechanical limitations. Most inorganic materials such as ceramics possess great mechanical property, but are limited in terms of fragility, poor degradability, and lack of bioactive sites. Recently, recombinant artificial ECM materials have been developed to combine the advantages of degradable polymers, natural saccharides, and even inorganic materials. For example, sericin loaded electrospun nanofibrous composite scaffold composing cationic gelatin, hyaluronan and chondroitin

sulfate, and selected glycosaminoglycans (GAGs) was developed to mimic the extracellular microenvironment for dermal tissue applications [36]. Within the composite, the gelatin functioned as the structural support and hyaluronan, chondroitin sulfate, and GAGs as naturally derived ECM composites for cell adhesion and proliferation, while sericin served as promoter for subsequent differentiation of hMSCs. Moreover, it was revealed that the electrospun scaffold with multiple compositions could promote epithelial differentiation of hMSC in terms of several protein markers and gene expression of some dermal proteins.

With the deep understanding about the signals and the underlying pathways regulating stem cell fate, adult stem cells have been demonstrated the residence within specific extracellular regulatory microenvironments, consisting of a complex mixture of soluble and insoluble, short- and long-range ECM signals. These multiple, local environmental cues are integrated by cells that respond by choosing self-renewal or a pathway of differentiation. Synthesized artificial ECMs could facilitate the formation of damaged tissues, homeostasis, and regeneration by offering suitable stem cell niches for stem cells to differentiate to favorable lineages. As we can see, great emphasis could be placed on the precise control of stem cell fate through the careful regulation of synthesized artificial ECM materials. The design of synthetic materials mimicking natural stem cell microenvironments may be a potentially powerful tool to understand and control stem cell function. A great number of artificial ECMs have been developed to explore the interaction between the materials and stem cell fate control. Synthetic extracellular matrix either made of hyaluronic acid (HA) [37] and gelatin or HA hydrogels [38] showed the improved differentiation of MSCs and superior integration of the repair tissue. Kraehenbuehl's group also demonstrated that the synthetic 3D ECM based on metalloproteinase-sensitive PEGs could direct differentiation of pluripotent cardioprogenitors [39].

With certain biological cues incorporated into the materials, together with the stem cells, the artificial ECMs could mimic the natural ECM while possessing better performance in mechanical and degradable properties, reproducible large-scale production, and good processability. Therefore, great challenges still remain in the control over dynamics and spatial organization of presentation of multiple signals due to the intricate and complicated structure of natural ECMs. As to the signals, the number of molecules that may have great impact on the cell behaviors is still underexploited. As for the materials, novel materials that have better spatial and hierarchical orders are still needed to upgrade the current materials. Hopefully, with the joint efforts from the scientists of different fields, new generation of artificial ECMs will soon appear and bring benefits to tissue engineering and regenerative medicine.

8.4 The Influence of Biomaterials/Surfaces on Stem Cell Differentiation

8.4.1 Surface Topography

Cell interactions with the surrounding ECM play an important role in regulating cellular behaviors. It has widely appreciated that the properties of this cell–ECM interface – chief of all is surface topography – must mimic those of native ECM to appropriately guide cell function. Recent advances in biomaterial surface engineering have shown that surface biomechanical, spatial, and topographical properties can elicit control over fundamental biological processes such as cell shape, proliferation [40, 41], and differentiation [42–44]. The modification of topology is critical in controlling cellular functions by designing surfaces as well as creating different topological cues to control cell adhesion and hence differentiation.

8.4.1.1 Surface Structure and Two-Dimensional Organization

Currently, several surface topographical cues in scaffolds with 2D structure, such as surface roughness or various kinds of micro-/nanoscale topographies of materials, have been shown in vitro or in vivo to guide marrow stem cell differentiation toward osteogenesis and sustain bone ingrowth. For example, Ana et al. [45] prepared surface roughness gradients of average roughness (Ra) varying from the submicron to the micrometer range (~0.5–4.7 μm) and mean distance between peaks (RS_m) gradually varying from ~214 μm to 33 μm. Their study demonstrated optimal surface roughness (Ra ~2.1–3.1 μm/RS_m ~71.1 down to 48.1 μm) promoting faster osteogenic commitment and the strongest osteogenic expression. It has also been suggested from in vivo studies that controlling surface roughness is one of the most important parameters governing osteointegration [46]. In that regard, roughness topography may mimic the physical cues left by osteoclast activity on bone surface morphology during bone resorption [47]. Furthermore, the surface roughness increases the surface area of the implant material, allowing greater initial matrix deposition and earlier bone ingrowth [48].

Apart from surface roughness, there are a variety of micro- or submicro-surface topologies. Liu and his group [49] reported that biomaterial microtopography induced indirect mechanotransduction and thus osteoblast differentiation. As shown in Fig. 8.2, Seo et al. [50] upregulated the osteogenic differentiation of mMSC by culturing on the tailor-made micropit (tMP, 3×3 mm^2) surfaces that enhanced focal adhesion (FA) and actin polymerization (AP) of the cells. As shown in Fig. 8.2c, the cell on the flat surface was spread with broad lamellipodium and little traction force. On the contrary, the cell on the tMP surface significantly shrank and had a relatively strong traction force in the central direction which is important for signaling activation correlated with the cell differentiation. Wang et al. [51] investigated the effects

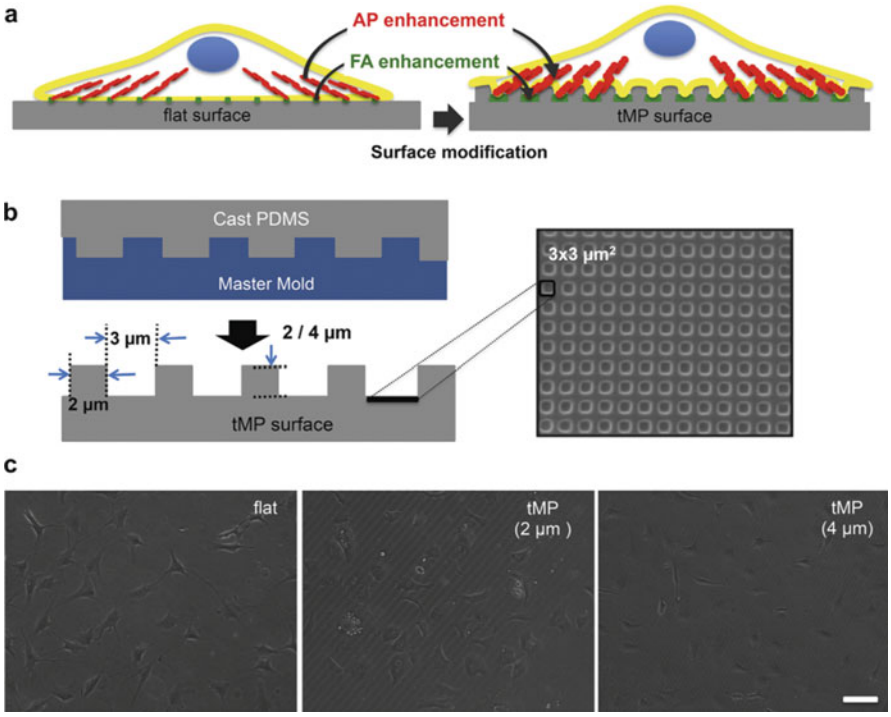

Fig. 8.2 (**a**) Schematic showing the strategy of the tMP bioactive surfaces which are intended to enhance focal adhesion (FA) and actin polymerization (AP) by the surface modification; (**b**) schematic showing preparation of the tMP surfaces which are intended to enhance FA and AP; (**c**) phase contrast images of cells cultured on the prepared substrates 24 h after seeding [50] (Copyright 2013 Elsevier Ltd.)

of grooved topography on the differentiation of MSCs into osteoblasts, adipocytes, and myoblasts regarding the late markers. In their study, a series of submicron-grooved surfaces with groove-to-ridge ratio of 1 to 1 (groove width/depth (nm), 450/100,450/350, 900/100, and 900/550) was fabricated; the result of differentiation of MSCs into different lineages, especially osteogenesis, is that the two deep-grooved substrates (450/350 and 900/550) were increased to a level compared to that on the flat surface and significantly higher than those on the shallow surfaces (450/100 and 900/100).

These methods of controlling cell attachment, shape, and then differentiation by surface topography have shown that MSCs have the remarkable ability to switch between becoming fat and bone cells based just on their ability to spread on a surface and contract against it. Well-spread cells express calcifying bone proteins common in osteoblasts in a manner that is dependent on the cell's ability to apply traction to the material. On the other hand, poorly spread cells develop large lipid deposits typical of adipocytes and are limited in their spreading and tension generation. Besides traction force, another distinct impact of these micropit-/micron-grooved

substrates on cell behavior is the formation of focal adhesions and F-actin. Several studies indicated that micropit- or submicron-grooved substrates enhanced the formation of actin filaments and focal contacts compared with plain surfaces and the enhancement was positively correlated with pit/groove depth [52]. It has been suggested that the formation of both focal adhesions and F-actin is correlated to the differentiation of MSCs [53–55].

8.4.1.2 Designing Surface Topology for the Third Dimension

Inspired by these previous investigations in 2D biomaterials, surface topology in 3D scaffold with hierarchical structures and its distribution should also have direct or indirect effects on osteoblast maturation as well as MSC osteogenic differentiation, presenting different effects from 2D surface. Due to the restriction and difficulties of fabrication of surface topologies with uniform distribution and different morphologies on the highly interconnected hole wall of the 3D material, majority of existing surface modification in metal or polymer materials stayed in 2D level rather than in 3D scaffold. Thus, subsequent smart designs should incorporate 3D structures, which more closely mimic native ECM and may guide cell shape and differentiation to improve the generative function of an engineered tissue.

To mimic the hierarchical porous architecture and specific biological cues of natural bone, Tang et al. [56] developed a trimodal macro-/micro-/nanoporous scaffold (Fig. 8.3). Comparing with the BMS (2D MBG), the TMS (3D MBG) exhibited inspiring properties in terms of osteoconductivity, osteoinductivity, recombinant human BMP-2 (rhBMP-2) delivery, and biodegradability.

Gwendolen et al. [57] analyzed the reason why stem cells are liable to differentiate on substrate in 3D microenvironment. The cell "feels" the structural properties of the biomaterial surrounding it depending strongly on biomaterial structure. As shown in Fig. 8.4, a microporous foam, where the pore size greatly exceeds the cell, effectively presents a flat or slightly curved substrate to the cell as it adheres to a strut (Fig. 8.4a, top). By only attaching its basal surface to the material, mechanotransduction mechanisms of the cell may be similar to those already elucidated on planar substrates where large forces are observed on stiff strut materials (Fig. 8.4b, large arrows). Intriguingly, micropatterns that induce cell curvature on surfaces as well as micropores of varying size within a scaffold appear to directly regulate force production in stem cells, indicating that there may exist a gradual transition from a highly tensed, spread cell to a low-tension, more rounded cell that contacts the material in all dimensions (Fig. 8.4a, b, bottom). If the pore size is too large that the cell can only spread on a strut of the scaffold in a manner similar to planar materials, the cell's environment is then dominated by the scaffold's stiff mechanical properties and forces are large (big arrows). On the other hand, when porosity is small and the cell can attach in three dimensions, the force developed will be smaller (smaller arrows), more likely resulting in differentiation.

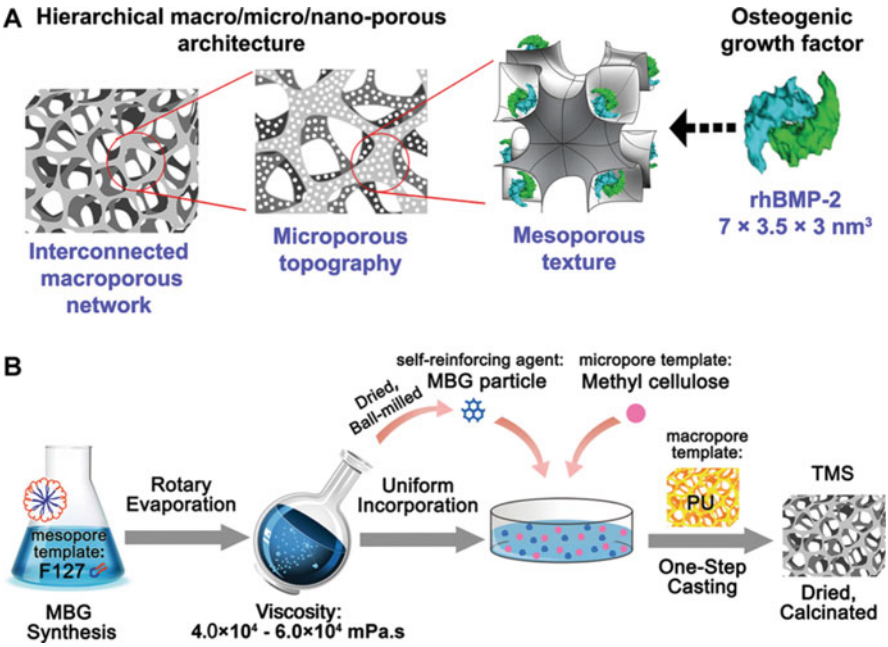

Fig. 8.3 (**a**) Design of trimodal macro-/micro-/nanoporous scaffold loaded with rhBMP-2; (**b**) schematic illustration of preparing trimodal MBG scaffold (TMS) [56] (Copyright © 2015 Acta Materialia, Inc. Published by Elsevier Ltd.)

8.4.1.3 Regulation of Stem Cells by Surface Nanotopography

As discussed earlier, the microenvironment that cells contact with can be a potent regulator of adhesion and differentiation. In addition to macroscale surface topology, cells also have the ability to sense nanoscale geometric cues from their environment. Recent findings show that mammalian cells do respond to nanoscale features on synthetic surfaces [58, 59]. In respect of stem cell adhesion, Yim et al. [60] demonstrated that nanotopography alone can upregulate the neuronal markers of hMSCs. Another group has also demonstrated the important roles of topography in one-dimensional and three-dimensional cell migration [61]. Yim et al. [53] designed a type of nanotopography as shown in Fig. 8.5 that modulated cell behavior by changing the integrin clustering and focal adhesion (FA) assembly, leading to changes in cytoskeletal organization and cell mechanical properties.

In terms of stem cell differentiation, one impressive report from Dalby et al. [62] demonstrates that the use of nanoscale disorder with a diameter of 120 nm is able to induce hMSCs to produce bone mineral and osteogenic differentiation in vitro, in the absence of osteogenic supplements. This approach of scaffold materials stimulating stem cell differentiation had similar efficiency to that of stem cells cultured with osteogenic media. Zhao et al. designed a series of hierarchical micro-/nanotextured topographies (MNTs) combined with micropitted and nanotube topography

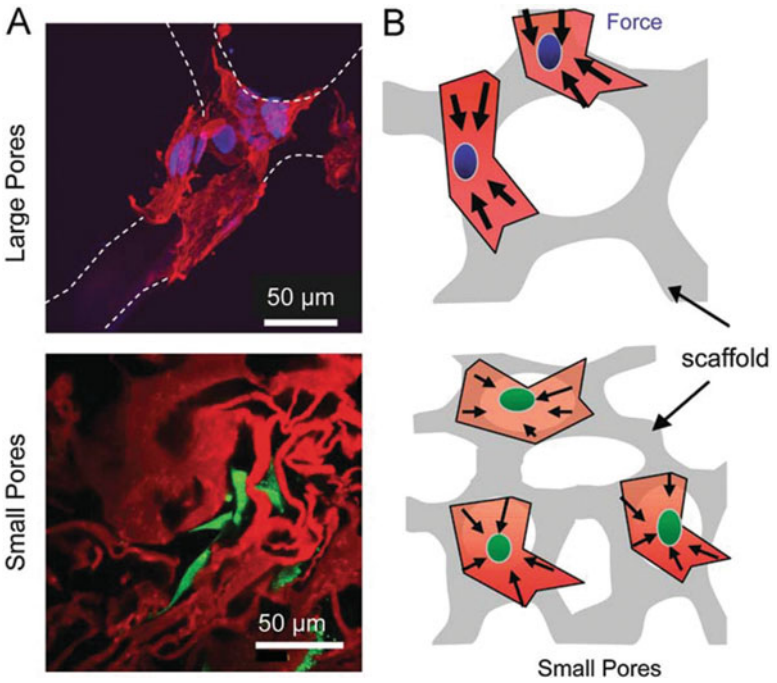

Fig. 8.4 3D Scaffold parameters influence stem cell contractility and differentiation [57] (Copyright 2009 Elsevier Ltd.)

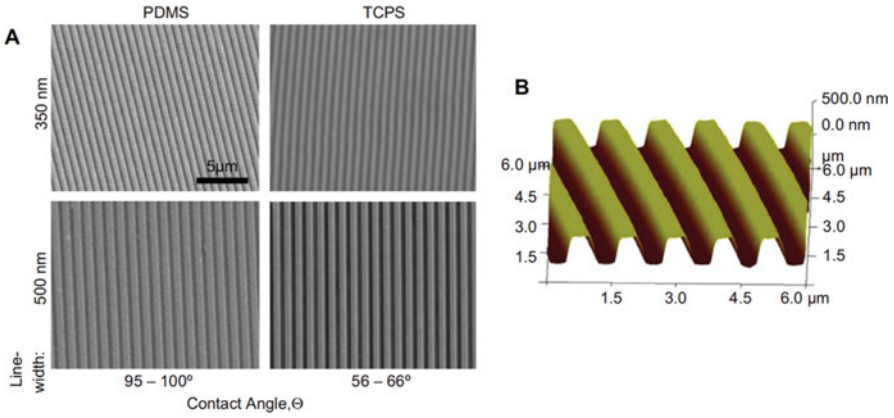

Fig. 8.5 (**a**) Scanning electron micrographs of gratings with 350 nm linewidth and 700 nm pitch (350 nm gratings) and 500 nm linewidth and 1 mm pitch (500 nm gratings); (**b**) atomic force micrograph (AFM) of 350 nm gratings on TCPS [53] (Copyright 2009 Elsevier Ltd.)

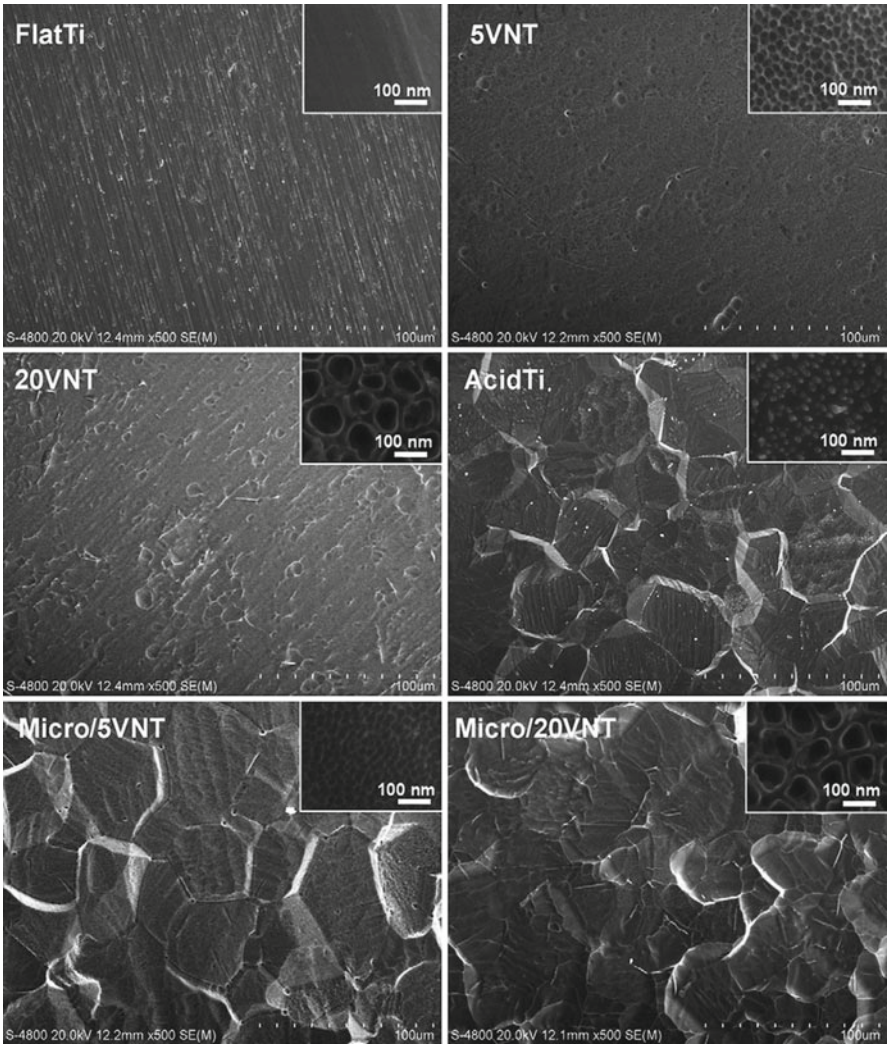

Fig. 8.6 SEM pictures showing the morphology of the fabricated samples [49] (Copyright 2014 Elsevier Ltd.)

(as shown in Fig. 8.6). They provided that the combined topography was more similar to the extracellular matrix (ECM) of natural bone and exhibited more pronounced effects on MSC osteogenic differentiation as well as osteoblast maturation [63, 64].

The micro- and nanoscale surface topographical modification is widely applied to enhance properties of biomaterials and regulate cell osteogenic differentiation. The underlying mechanism is also widely explored. Liu et al. [49] propose that the surface topography modulates cell differentiation via mechanotransduction of direct

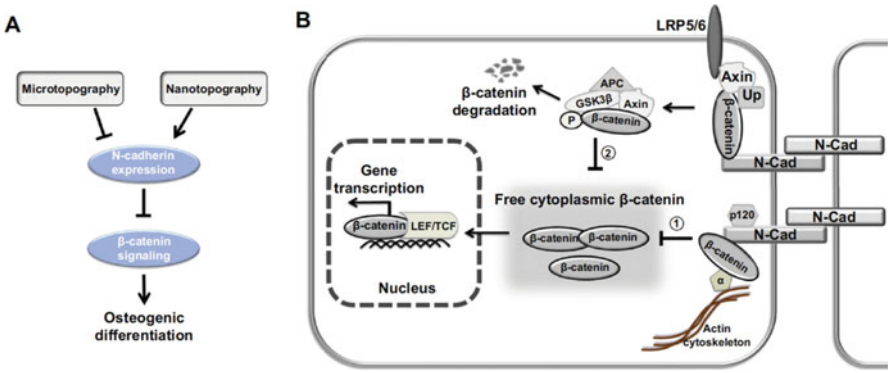

Fig. 8.7 Illustration of the detailed N-cadherin/β-catenin signaling in the micro-/nanotopography-induced mechanotransduction [63] (Copyright 2011 Elsevier Ltd.)

and indirect. As shown in Fig. 8.7, N-cadherin may be important in the process of topography inducing indirect mechanotransduction as well as regulating the β-catenin signaling. In Fig. 8.7a, the microtopography downregulates the N-cadherin expression leading to higher β-catenin signaling and consequently osteoblast differentiation, whereas the nanotopography significantly upregulates the N-cadherin expression resulting in reduced β-catenin signaling activity and thus depressed differentiation. As shown in Fig. 8.7b, N-cadherin can cut down the β-catenin at the cell–cell adhesion site and interact with the Wnt coreceptor LRP5/6. Inhibiting the Wnt/β-catenin signaling results in negative regulation of the β-catenin.

In this regard, the control of surface topography in engineered constructs has proven to be a valuable tool in guiding the commitment and development of stem cells. Importantly, the ability to modulating variety of surface topologies that, through physical as well as molecular interactions, enable undirected or directed control of stem cell behavior may further enhance our capabilities in engineering functional tissue substitutes. By controlling the nanotopography and microtopography of tissue engineering scaffolds in two/three dimensions, we may further improve the regulation of stem cell fate in bio-artificial systems. Such significant advances shown in these in vitro studies emphasize the importance of a multidisciplinary approach for the use of stem cells in the development of engineered tissue substitutes and may lead to enhanced biomaterial clinical performance.

8.4.2 Porosity and Pore Size

Porosity is a parameter that refers to the fraction of the gel volume filled with liquid phase, which is the volume of voids around matrix scaffold molecules per unit volume of the gel. Pore size is a very different parameter, which, unlike porosity, directly refers to geometry of pores. Cell adhesion and motility depend on the size

of the pores, rather than porosity. Mean pore size has correlation with porosity for many synthetic polymers of simple composition. However, for natural polymers like collagenous gels, there is no direct correlation, since the diameter of collagen fibrils can vary from few nanometers to a few hundred nanometers [65].

Porosities of scaffolds are the prerequisite for permeability in vitro and in vivo. Scaffold matrices act mostly as media for fluid flow, diffusion, and cell migration [66]. Permeability of ECM defines accessibility of small molecules (nutrients, hormones, and oxygen), large molecules (e.g., function of basement membranes), cell processes (e.g., axons), or cells (vascularization). Permeability of ECM to cell migration is important for regenerative processes. Poor permeability for cells, such as in scarred tissues, results in poor regeneration. Therefore, permeability for fluid flows and molecular diffusion is important for cell survival, since low permeability may result in lack of nutrients and ischemia.

Interconnected porous structures provide nutrients to the cells growing into the pores and allow for optimal interaction of the scaffold with cells. The aspects that are taken under consideration include pore size, size distribution, porous morphology, interconnectivity, and surface area-to-volume ratio [67]. Each of these factors influences biological response, notably, cell migration, proliferation, and thus tissue regeneration. Substrate porosity seems to be an important factor as it can vary the length between two adjacent anchoring points, to which cell can adhere [68]. According to the IUPAC, the porous size of dense materials is classified into three different types: micropores (<2 nm), mesopores (2–50 nm), and macropores (>50 nm). Nevertheless, for tissue engineering, a slightly different description of the pore sizes is commonly applied. In the following part, we will adopt the nomenclature used by biomaterial scientists to describe the pore sizes of tissue engineering scaffolds, which classify pore sizes as macropores (>50 μm), micropores (0.1–50 μm), and mesopores (2–50 nm). Therefore, we will distinguish these three different types of pores throughout this section and will not consider the pore ranges established by IUPAC.

8.4.2.1 Macropores

Scaffold macroporosity plays a critical role in the regeneration of damaged tissues, allowing cell penetration, which is essential for the later integration with the host tissue and increases the chances for key processes to take place, including tissue matrix and blood vessel ingrowth. It is generally acknowledged that the optimum pore size for scaffolds lies in the range between 100 and 400 μm [69]. Specifically, macropore size determines the efficiency at which cells seed into the scaffold. Small pores prevent the cells from penetrating the scaffold, while large pores prevent cell attachment due to a reduced area and, therefore, available ligand density [70]. The scaffold should have an adequate porosity in terms of the magnitude of the porosity, the pore size distribution, and its interconnectivity. This also will allow cell ingrowth and vascularization and promote metabolite transport. A scaffold with an open and

interconnected pore network and a high degree of porosity (>90 %) is ideal for the scaffold to interact and integrate with the host tissue [71].

Macroporous scaffolds were observed to be potentially promising toward wound healing in relation to nonporous. Porous hydroxyapatite (HAp) scaffolds fabricated by additive manufacturing methods indicated significant bone formation when the pore diameter was in the range of ~400–1200 and ~300–800 μm [72]. As mentioned before, the extent of bone ingrowth was observed to depend on pore size. Pores of diameter ~20–50 μm are expected to provide favorable functionality from the viewpoint of physiological liquid exchange, while pores of diameter ~100–350 μm are suitable for cell colonization and vascularization, leading to penetration of tissue into the biomaterial structure [73]. This size range facilitated migration of cells in porous scaffolds and was appropriate for increased bone regeneration.

The degree of macropore interconnectivity is considered to be critically important in a manner similar to pore size. In biodegradable porous ceramics, the degree of interconnectivity was noted to be seemingly more important than the pore size, while in nonbiodegradable materials, interconnectivity and pore size were observed to be equally important. Under in vivo conditions, the penetration of cells and chondroid tissue formation inside macropores occurred when the interconnectivity dimensions were greater than ~20 μm, while mineralized bone formation occurred when the interconnectivity size exceeded 50 μm [74]. The interconnectivity of pores ensures availability of higher surface area for enhanced cell adhesion and proliferation.

The range of the optimum macropore size differs with different materials. For example, the effect of 3D silk fibroin scaffolds on cell proliferation and migration of human foreskin fibroblast showed that pore sizes of 200–250 μm and porosity of approximately 86 % enabled better cell proliferation [75]. However, cell proliferation of these scaffolds with smaller pore sizes of 100–150 μm can be improved by having higher porosity of approximately 91 %. Hence, by altering the pore size, porosity, or both parameters, the cell viability and proliferation can be enhanced [76]. Besides affecting the cell proliferation capability, it has been shown that the amount of ECM produced, that is, the amount of GAG secretion, and the expression of collagen gene markers are also affected by the pore size of scaffolds [77]. The study by Lien et al. demonstrated that chondrocytes showed preferential proliferation and ECM production for scaffolds with pore sizes between 250 and 500 μm [78]. This pore size range was observed to be capable of maintaining the phenotype of cells, while pores ranging from 50 to 200 μm resulted in cell dedifferentiation [79]. Thus, the role of porosity and interconnectivity in scaffolds is also to facilitate cell migration within the porous structure such that cell growth is enabled while overcrowding is avoided.

Therefore, for bone tissue engineering, the optimal pore size for osteoblast activity in tissue-engineered scaffolds is still controversial. In general, scaffolds with pore sizes of about 20–1500 μm have been used. Akay et al. studied the behavior of osteoblasts in polyHIPE polymer (PHP), a type of highly porous polymeric foam [80]. The osteoblasts were shown to populate more in smaller pores (40 μm) when they were grown in scaffolds with different pore sizes, but larger pore sizes (100

μm) facilitated cell migration. However, the different pore sizes did not have any effect on the extent of mineralization or cell penetration depth. Collagen–GAG (CG) scaffolds were also studied to determine its optimal pore size for bone tissue engineering purposes and the effect of pore size on a preosteoblastic cell line, MC3T3-E1 [81]. From the results, optimal cell proliferation and infiltration were found in CG scaffolds with mean pore sizes greater than 300 μm. In addition, the ability of larger pores to facilitate cell infiltration was shown to override the beneficial effect of greater initial cell attachment surface areas provided by smaller pores. Hence, this study supported previous reports that suggested the importance of having pore sizes greater than 300 μm for osteogenesis to occur. However, it should be noted that cell differentiation is also dependent on the cell type, scaffold material, and fabrication conditions.

The pore size has also been shown to have an effect on the proliferation and differentiation of cells for cartilage tissue engineering. Adipose stem cells were seeded on PCL scaffolds prepared with different pore sizes (100, 200, and 400 μm) and were placed under chondrogenic differentiation conditions for 21 days. The results showed that proliferation was higher for the 100 and 200 μm pore sizes, whereas cells tended to agglomerate in the 400 μm pore size scaffolds. Nevertheless, proteoglycan production as well as chondrogenic markers was significantly higher for the 400 μm pore size scaffolds compared to the 100 and 200 μm pore sizes [82]. Cell aggregation and cell–cell contact are known to be the most significant step for chondrogenic differentiation. Hence, the higher pore size allows the allocation of higher number of cells in the pores, which tend to agglomerate once they encounter other cells in the bigger pores showing higher markers of chondrogenesis. In the smaller pores, the number of cells is more limited and therefore preferentially attaches to the substrates rather than surrounding cells since there is no proper space to accommodate more cells.

Another effective system to determine the optimum pore size is through the use of gradient scaffolds. In general, results show a cell-dependent behavior, presenting osteoblast and chondrocytes preferentially in the bigger pore sizes after 56 days, whereas fibroblasts are mainly present in the smaller ones [83]. Furthermore, adipose stem cells grown in the gradient pore size (90–400 μm) scaffolds were shown to have the highest chondrogenic differentiation but lowest proliferation in the biggest pore size (400 μm) [84]. This further confirms the previous hypothesis, showing that when cells encounter bigger pore sizes, enough number of cells can be allocated to allow the cell–cell contact and hence present higher markers of chondrogenic differentiation.

8.4.2.2 Micropores

While macropores with pore sizes and pore interconnections in the range of hundreds of microns are relevant for cells to migrate and proliferate, micropores with pore sizes in a smaller range also play pivotal roles in tissue engineering. These pores are usually few microns in size and are involved mainly on the initial

adsorption of proteins on the surface of the materials. Cells interact with biomaterials through cell–protein interactions through the transmembrane proteins. Therefore, it is believed that the increase in protein concentration may significantly affect cell fate. Besides the ability to adsorb proteins, these small-sized pores are also known to allow the regulation of cell behavior, playing key roles in directing stem cell fate.

The role of macroporosity has been mainly associated with the ability of a scaffold to allow proper bone ingrowth and bone regeneration, while having in general slight effects on cell proliferation and differentiation. Nevertheless, the porosity in the range of nanometers up to several microns has tremendous effects on the ability of cells to proliferate and differentiate and hence plays a key role in the overall bone regeneration. Not only it is able to regulate the phenotype of cells to induce higher cell mineralization but also increase the protein adsorption, which in turn can increase the osteoinductive capacity of a material.

Microporosity can be incorporated into ceramic and polymeric scaffolds with different techniques. For example, a microporous foam material, wherein the pore size greatly exceeds the cell, displays a slightly curved substrate to the cell. As the basal surface of the cell attaches to the material, mechanotransduction mechanisms may be similar to those already elucidated on planar substrates. Microscopic pores of about cell size lead to a low-tension, more grounded cell contacts with the material in all dimensions. There may exist a gradual transition from first variant to the last for intermediate pore sizes [85].

Surface microporosity of a material plays a very important role on cell behavior. The influence of pore sizes on cell behavior was determined by culturing MG-63 osteoblast-like cells on polycarbonate membranes designed with different pore sizes. Lee et al. [86] have reported that the cells spread and adhered better on membranes with smaller micropores (0.2 μm diameter) than on those with larger micropores (3.0–8.0 μm). Moreover, the cells cultured on larger micropores produced increased levels of ALP and osteocalcin. In another study, the different microporosity and topography of CDHA materials (total porosity of 35 vol.%, pores by 5 μm) were partially responsible for the different patterns of proliferation and differentiation observed for osteoblast cells [87]. Materials with smaller CDHA crystals stimulated differentiation, whereas those with bigger crystals enhanced proliferation.

Habibovic et al. performed an elegant experiment to determine the role of microporosity in two families of chemically identical porous ceramics: HAp and biphasic calcium phosphate (BCP) [88]. Sintering temperatures between 1100 and 1200 °C allowed modifying the microporosity (within a pore diameter range of 2 μm) while not altering their macroporosity (249 ± 38 μm). The results showed that the implantation into the back muscles of Dutch milk goats for 6 and 12 weeks allowed bone formation in the presence of micropores but failed when the amount of micropores remained low (HAp sintered at 1250 °C). The higher amount of adsorbed/entrapped proteins in the microporous walls enhanced bone formation [89], which was essential to provide the biomaterial with osteoinductive capacity. It is thus speculated that the microporosity modifies the dynamic interface of materials and consequently triggers the differentiation of relevant cells toward the osteogenic lineages. It has been pointed out that a higher microporosity was inherently linked with a higher

specific surface area and hence could cause a major dissolution of ions [88]. The higher ion dissolution would facilitate the apatite formation in vivo, causing the coprecipitation of endogenous proteins (e.g., BMPs) that could in turn trigger the differentiation of recruited undifferentiated cells toward the osteogenic lineage [90]. Another hypothesis suggested that the inflammatory response triggered after the implantation of a biomaterial, which causes the release of cytokines that promote the differentiation of circulating MSCs into osteoblasts, would induce osteoinductivity [91]. In experiments by Peyton et al. [92], on MSC motility in 3D PEG scaffolds, pore diameter has been varied from 7 to 17 μm (i.e., from significantly smaller than the spherical cell diameter to approximately cell diameter). Cell speed is the highest compared to larger pores, but net displacement of the cells within matrix is maximal for intermediate pore sizes, probably because of difficulty in finding straight way in the large-pore scaffold.

Micropores also play a key role in controlling protein adsorption as well as cell–material interactions. Nevertheless, these pores may also be efficient systems for the loading and release of specific biological molecules with regenerative potential. These pores which are usually in the range of tens of microns have been shown to be ideal for growth factor allocation that has enhanced bone regeneration [93]. These promotions in bone regeneration by micropores have been collectedly defined as an "initial micropore acceleration" at the early stage of regeneration [56, 94]. Combining previous literatures with the results, Tang et al. speculated several possible reasons for this acceleration as follows. By providing a larger surface area, the microporosities could facilitate the coprecipitation of endogenous cytokines and growth factor, which indirectly stimulate stem cell recruitment to the defect site [95]. After then, surfaces with microporous topologies could significantly enhance biomineralization and were beneficial for protein adsorption and cell attachment. During cartilage formation, newly formed collagen fibers mineralized and wrapped in the micropores forming tight interlock between the material and tissue, resulting in a bone/scaffold composite with no "dead space." Due to this "initial micropore acceleration," the healing progresses of trimodal macro-/micro-/nanoporous and bimodal macro-/microporous scaffolds were in ahead of bimodal macro-/nanoporous scaffolds.

8.4.2.3 Mesopores/Nano-pores

Mesoporous materials refer to as mesostructured materials or simply mesophases and belong to the class of nanomaterials, whose properties can be tuned at the nanometrical scale. Specifically, according to IUPAC nomenclature, mesoporous materials refer to materials with pore sizes ranging within 2–50 nm. These materials are generally obtained by coupling a sol–gel method that is very effective to prepare glasses and ceramics at room temperature, with a supramolecular self-assembling process. This particular approach is possible by taking advantage of hydrophobic/hydrophilic features of some molecules (i.e., surfactants) to prepare supramolecular aggregates (micelle). The first successful synthesis of pure-silica mesostructured

materials was performed in the early 1990s, when surfactants as structure-directing agents were used by Mobil Oil researchers [96]. Since then, many classes of mesoporous materials with different pore features have been synthesized.

With regard to the biomedical field, mesoporous materials, being characterized by an ordered texture of nano-sized pores, can easily host drug molecules and, therefore, are good candidates for designing and producing systems for controlled drug delivery. In addition, the silanol groups located on the walls of silica mesoporous materials may not only be useful to functionalize the walls for enhancing the drug adsorption ability of the materials, but can also react with biological fluids to produce HAp or apatite-like nanocrystals [97]. In vitro bioactivity studies, carried out by soaking SBA-15, MCM-41, and MCM-48 in SBF, revealed that an apatite-like layer was formed on the surface of SBA-15 and MCM-48 materials after 30 and 60 days of immersion, respectively [98]. This behavior is quite surprising as these mesophases, being constituted by pure silica, should not exhibit bioactive properties. In fact, according to Hench's definition of bioactivity [99], bioactive mechanisms can occur only if particular ion exchange phenomena take place between the material and surrounding fluids. On the other hand, it is obvious that mesoporous materials are nontraditional materials and, therefore, their mesoporous texture can impart them unexpected and fascinating properties. MCM-41 also exhibited a bioactive behavior when its walls were doped with phosphorus or by adding small quantities of bioactive glasses.

MBG scaffolds exhibited greatly enhanced bone-forming properties, when compared with traditional bioactive glass (BG) scaffold of the same composition [100]. Besides its higher surface area and pore volume, the effects of mesopores reported by literatures are described. Drug release studies by using gentamicin have been reported [101]. The drug uptake ability of MBG scaffolds was over twofold higher than that of the BG scaffold; in addition, as far as drug delivery is concerned, during the whole release period in SBF, gentamicin was delivered from the MBG scaffold at a much lower release rate when compared with that from BG scaffolds.

Since entrapment in mesopores has turned out to be a promising strategy in the fields of enzymatic biocatalysis, biosensors, etc., some researchers have reported that the mesoporous support with comparable porous size to the protein molecule is beneficial for higher loading, preserved activity, and sustained release. Motivated by these previous investigations, Tang et al. [56] proposed the concept of "size-matched mesoporous entrapment" for rhBMP-2 delivery and endeavored to investigate the possibility of matching the mesoporous dimension with the size of rhBMP-2 molecule ($7 \times 3.5 \times 3$ nm^3) to achieve a desirable immobilization and further realize optimal bone regeneration by cooperation of multiscale structure and rhBMP-2.

Cells respond to their surrounding structure and with nanostructures exhibit unique proliferative and differentiation properties. Since the early 1970s, bioactive glasses are known to be able to chemically bond to living bone without the formation of fibrous tissue around the implant due to the growth of a bone-like apatite layer on its surface [102, 103]. It was demonstrated that HAp formation on the sol–gel glass surface is related both to the structure and to the composition of the material, whereas melt-derived bioactive glasses show a direct dependence only

from the composition. An increase of the pore volume and specific area (up to 200 m^2/g) in sol–gel glasses highly accelerates the deposition of HAp, thus enhancing the bonding of the material to the bone tissue [104]. Ordered mesoporous silica possess a very high surface area and an ordered system of generally open mesopores but are not properly suitable as filling materials for bone repair because of their almost complete lack of bioactivity [105]. Some authors reported a weak bioactive behavior of SBA-15 and MCM-48, but only after relevant times of contact with biological fluids (>30 days) [106]. On the contrary, MBGs belonging to the SiO_2–CaO–P_2O_5 ternary system were found to exhibit a faster and higher bioactivity also in comparison with sol–gel glasses, thanks to their textural and structural properties (specific surface area up to 500 m^2/g) [107]. Therefore, considering their superior bioactivity, MBGs may be a very promising material for bone tissue regeneration and exhibit the potential of mediate the fate of stem cells by immobilization of growth factors and its inherent osteoinductive properties.

8.4.3 Surface Stiffness

Matrix stiffness is an important regulator of cellular responses (such as migration, proliferation, and collagen deposition) mediating interface integration. As cells lay down extracellular matrix (mainly collagen) within a cell sheet or biomaterial sheet scaffold during in vitro culture or in vivo post-implantation, matrix density and stiffness increase. Increasing matrix stiffness would, in turn, be expected to affect the integration process by regulating critical cell behavior. It has been suggested that identification of variations in matrix stiffness could provide a useful tool for assessing interface integrity at step-off edges during cartilage repair [108].

Cell behavior and mechanical properties of the extracellular environment are intimately related. Cells can translate the stiffness of the microenvironments to which they are attached into biological signals (mechanotransduction) by a series of transmembrane receptors. These receptors comprise an intracellular domain (interacting with cytoplasmic proteins including the cytoskeleton) and an extracellular domain that specifically binds to adhesion partners. Tension forces expose active sites in these receptors with kinase activity, which allow the transformation of mechanical stimulation in chemical signals [109].

Matrix stiffness has been shown to play an important role in cell survival, proliferation, and differentiation. For example, the stiffness of different matrices (0.1–1 kPa, 8–17 kPa, and 25–40 kPa) on which native mesenchymal stem cells were cultured was demonstrated to determine the lineage of the cells during differentiation (neurogenic, myogenic, and osteogenic, respectively) in vitro [110]. These experiments show that mechanical properties of the ECM induce not only cell spreading and changes in cell morphology but also stimulate or repress the synthesis of specific transcription factors, inducing the establishment of special phenotypes concordant with the organ where the cells come from or defining their fate in the case of stem cell differentiation.

Stiffness of the adjacent tissue affects stem cell fate in vivo when the cell exits its niche and starts to participate in regenerative process [111–113]. Stem cells tend to proliferate, migrate toward the injured site, and differentiate to the relevant cell type, adoptive to stiffness of the substrate. Stiffness of ECM has been shown to be crucial for the maintenance of satellite stem cells in vivo [112]. Collagen VI has been proved to be the major regulator of stiffness in the stem cell niche in this case. For instance, experimental models that allow control over physical properties of ECM such as stiffness typically employ small adhesion molecules (i.e., short peptides) instead of natural full-size multi-domain matrix molecules. Short peptides immobilized on abnormally stiff surfaces are also a standard approach to study the effect of spatial placement of epitopes. Biologically relevant full-size ECM adhesion molecules, such as niche-specific laminin isoforms, fibronectin, or vitronectin, are often immobilized on flat and abnormally stiff plastic or glass surfaces [85].

To date several hundreds of research papers are dedicated to dependence of stem cell fate on stiffness of their substrates in vitro. Similar results are obtained with different materials used as substrates: MSCs tend to differentiate to the cell type relevant to stiffness of the substrate as long as the other parameters (such as different substrate geometries or adhesion ligands) are not limiting for cell attachment and spreading [114]. These elastic materials include polyacrylamide gels, PEG hydrogels, or HA gels. MSCs are cultured on substrates of different stiffness in differentiation media specific for the particular cell lineage, and the expression of specific cell markers is monitored.

Briefly, the MSCs differentiate into neuronal or glial cells on the soft matrices that resemble soft brain tissue [115]. They differentiate into adipocytes on twofold stiffer substrates [68], into myoblasts on tenfold stiffer substrates [116], and into osteocytes on harder matrices that mimic premineralized bone [117]. MSC differentiation tendency with respect to substrate stiffness is summarized in Table 8.1.

MSCs have weaker cell adhesion to soft substrates, but anchor more strongly to stiff substrates. The level of adhesion strength correlates with commitment of the MSC to specific cell lineage. Suppression of adhesion strength for a cell on hard substrates imitates cell behavior on soft substrates in terms of the lineage marker expression. Alterations in the number, stability, and strength of the developing cell adhesions lead to reorganization of the cytoskeleton and change in cell morphology. On stiffer substrates stem cells tend to spread more and tend to assemble their cytoskeleton, such as building long actin–myosin stress fibers [43]. Majority of MSCs develop branched morphology with multiple filopodia on soft gels that mimic elasticity of the brain (0.1–1 kPa) [118]. MSCs acquire rather spheroid shape on matrices resembling adipose tissue (4 kPa) [68]. Spindle-shaped cells appear on stiffer matrices that mimic elasticity of striated muscle (8–17 kPa). Spreading on even more stiff matrices (25–40 kPa) yields polygonal MSCs similar in morphology to osteoblasts.

Also stiffer hydrogels generally promote acceleration of stem cell proliferation compared to softer gels. It has been established for human bone marrow stem cells on polyvinyl alcohol gels of 1–24 kPa stiffness [119] and for rat bone marrow stem cells on polyacrylamide (PAA) substrates of 6.1 kPa and 46.7 kPa [120]. The human

Table 8.1 Summary of MSC differentiation dependence on substrate stiffness [85]

Lineage	Matrix stiffness, *E*	Material	Testing method
Neurogenic	0.1–1 kPa	2D polyacrylamide gels, collagen coated	Nanoindentation using atomic force microscopy
	~1 kPa	2D polyvinyl alcohol hydrogel	Compression test
	1 kPa	3D type I collagen gel and hyaluronic acid gel	Compression test
	~1–2 kPa	2D gelatin–hydroxyphenylpropionic acid gel	Dynamic shear deformation 1 %, 1 Hz using rheometer
	6.1 kPa	2D polyacrylamide (PAA) gel	Compression test
Gliogenic	10 kPa	3D type I collagen gel and hyaluronic acid gel	Compression test
Vascular endothelial cells	2–3 kPa	3D polyethylene glycol dimethacrylate (PEGdma) nanofiber hydrogel	Tensile test
Adipogenic	2.5–5 kPa	3D alginate–agarose hydrogel with RGD	Compression test
	4 kPa	2D polyacrylamide (PAA) gel	Nanoindentation using atomic force microscopy
	L5 kPa, 6 kPa	2D polydimethylsiloxane (PDMS)	Tensile and macroscopic indentation tests
Myogenic	7–17 kPa	2D polyacrylamide (PAA) gels, collagen coated	Nanoindentation using atomic force microscopy
	12–15 kPa	3D polyethylene glycol dimethacrylate (PEGdma) nanofiber hydrogel	Tensile test
	~30 kPa	2D gelatin–hydroxyphenylpropionic acid gel	Dynamic shear deformation 1 %, 1 Hz using rheometer
	>9 kPa, 25 kPa, 80 kPa	2D polyacrylamide gel, coated with collagen, fibronectin	Dynamic mechanical analysis
Cardiomyocytes	45 and 65 kPa	3D thermosensitive hydrogel (PAA and HEMA-PTMC)	Tensile test
Osteogenic	11–30 kPa	3D alginate–agarose hydrogel with RGD	Compression test
	15–100 kPa	2D polydimethylsiloxane (PDMS)	Tensile and macroscopic indentation tests
	24 kPa	2D polyvinyl alcohol hydrogel	Compression test
	25–40 kPa	2D polyacrylamide gels, collagen coated	Nanoindentation using atomic force microscopy

(continued)

Table 8.1 (continued)

Lineage	Matrix stiffness, *E*	Material	Testing method
	30 kPa	2D polyacrylamide (PAA) gel	Nanoindentation using atomic force microscopy
	42 kPa	2D polyacrylamide (PAA) gel collagen coated	Tensile test
	46.7 kPa	2D polyacrylamide (PAA) gel	Compression test
	~60 kPa	2D gelatin–hydroxyphenylpropionic acid	Dynamic shear deformation 1 %, 1 Hz using rheometer
	80 kPa	2D polyacrylamide gel coated with collagen, fibronectin	Dynamic mechanical analysis
	190 kPa–3.1 MPa	2D polydimethylsiloxane (PDMS)	Nanoindentation

Copyright © 2015 Maria Akhmanova et al.

MSC proliferation rate increases up to tenfold with the increase of stiffness from 0.7 to 80 kPa on the polyacrylamide (PAA) substrates [121]. The murine embryonic stem cell (ESC) proliferation accelerates as stiffness increases from 41 kPa to 2.3 MPa on the polydimethylsiloxane (PDMS) substrates [122].

Cells are not only sensitive to ECM adhesion but also to its rigidity and elasticity. It was observed that there is an inverse correlation between matrix density or rigidity and cell migration. Discher and collaborators demonstrated the importance of matrix elasticity on stem cell fate [123]. Depending on the elasticity of the surface on which the MSCs were grown, they could differentiate into lineages that corresponded to the stiffness of the native environment which was resembled. For example, MSCs cultured on soft gels (0.1–1 kPa), to mimic brain elasticity, developed a neuronal morphology, with filopodia branching and spreading including expressing genes related to neuronal differentiation pattern. Furthermore, medium stiffness gels (8–17 kPa), which mimic striated muscle elasticity, promoted differentiation to myogenic cells, and the gels with the highest stiffness (25–40 kPa), to mimic bone elasticity, enhanced osteogenic differentiation.

A recent study based on an ECM composed of hyaluronan and fibronectin found that adult human dermal fibroblasts migrate faster on softer substrates and demonstrate more dynamic lamellipodial activity [124]. Perhaps more significantly, in addition to having an effect on the speed of migration, substrate stiffness has also been implicated in controlling the direction of cell movement. A previous report suggested that cells migrate preferentially toward stiffer surfaces, a phenomenon termed durotaxis [125].

As matrix stiffness is proved to affect significantly formation of focal adhesions, it is crucial to investigate the epitope cluster effect with respect to substrate stiffness. Stem cells express specific integrins, which connect cytoskeleton to the ECM. The level of cell surface integrins appears to be significantly lower on soft

substrates than that on stiff substrates [126]. Different types of integrins are responsible for adhesions at different stiffness levels. Thus, integrin α2 is upregulated in the course of osteogenic induction of MSCs on stiff matrices [127]. Integrin α5 is downregulated on soft gels, but its overexpression had no effect on cell spreading [128]. Activation of integrin α1 in bone marrow MSCs is induced by soft substrate to a significantly greater degree than by stiff substrate [126, 129]. α1-integrin signaling in the niche is involved in the maintenance of epidermal stem cells or neural stem/progenitors in a stem cell state. Proliferation of MSC is mediated by activation of integrin α1 and selectin. Later, we shall discuss in detail the biochemistry of integrin interaction with the specific matrix molecules.

Moreover, stiffer matrices made of the same material have lower pore size and permeability. Polymer substrates of the same stiffness but variable pore sizes can be produced [113]. It is important to note that solute permeability of the matrix is enhanced under dynamic deformations due to increased fluid flow [130]. Permeability for the cells also is affected by substrate stiffness and viscoelasticity, because cells can deform actively more pliable matrices to move through. These aspects are still to be investigated.

8.4.4 Chemical Properties

Incorporation of well-defined chemical properties into/onto biomaterials/scaffolds also enhances the adhesion and growth of stem cells and then directs specific differentiation to induce certain biological functions. Briefly, the cell–biomaterial interaction is a very complex process which involves many cytokines and ECM proteins. The surface chemical characteristics of biomaterials/scaffolds can affect the adsorption of such cytokines and ECM proteins, and this in turn influences the subsequent cellular response. Chemical properties of biomaterials, mainly including substrate elemental composition, surface functional groups, and biochemical functionalization, have significant influences on regulating stem cell activities. In this section, we will provide an interpretation of how the above chemical cues can affect stem cell response and direct stem cell fate in vitro.

8.4.4.1 Physiological Processes of Cell–Material Interaction

Understanding the mechanism of the physiological processes that control cell–biomaterial interaction is fundamental to investigate the influence of chemical properties on stem cell adhesion and phenotype. As the first step, adhesion of stem cells onto the biomaterial matrix is essential for its viability, proliferation, and differentiation. The adhesion of stem cells on biomaterials is primarily mediated by specific recognition and binding of cellular receptors on cell membrane to cytokines/ECM proteins adsorbed on the material surfaces. Among all the transmembrane receptors

in stem cells, integrins, a widely expressed family of heterodimeric receptors [131], have turned out to exert principal role in anchoring cells to ECM. By binding to its extracellular ligand, an Arg–Gly–Asp (RGD) peptide found in several ECM proteins, integrins can activate the formation of the focal adhesion (FA) complex and cytoskeleton reorganization in stem cell [132, 133]. Through integrin–ECM protein-mediated focal adhesions, stem cells are able to sense the underlying material substrate and react to its chemical properties (Fig. 8.8). For example, focal adhesion kinase (FAK) and vinculin are major players in the focal adhesion processes activated by integrin–fibronectin (Fn) interactions [134–136]. In particular, vinculin transduces integrin-mediated intracellular signaling molecules that promote cell migration [132, 137].

Importantly, it was testified that the initial adhesion and morphology of stem cells at the material surface can influence the subsequent long-term function of stem cell lineage [138]. Cell–material and cell–cell interactions activate specific intracellular signal pathways that regulate stem cell fate. Thus, the enhancement in early cellular response including adhesion and cytoskeleton changes is prerequisite to stimulating subsequent stem cell differentiation and, ultimately, to achieving a specific cell phenotype and certain biological functions. Specifically, many reports demonstrated that the substrate-induced intracellular FA formation and actin polymerization could stimulate the osteogenic differentiation of MSCs [139–142]. In the following, we will mainly discuss the effects of biomaterial chemical properties on MSC adhesion, viability, and osteogenic differentiation.

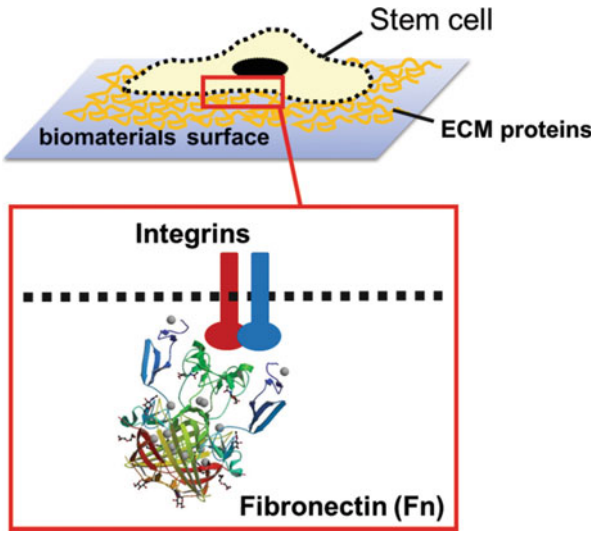

Fig. 8.8 Schematic illustration of the integrin function in cell–material interaction

8.4.4.2 Effects of Elemental Composition on Stem Cell Behaviors

The effects of chemical elemental characteristics on stem cell responses have been investigated extensively. It is noteworthy that some divalent ions have been found to participate in the bioprocess of cell adhesion [143]. Some functions of integrins are dependent on interaction with divalent cations such as calcium, magnesium, and manganese through a metal ion-dependent adhesion site (MIDAS) and MIDAS-like motives [143, 144]. Among divalent cations, magnesium increases the affinity of integrins for ligands including ECM in a millimolar concentration, while calcium reverses the increased affinity in some cases [143, 145]. Magnesium is a vital and widely used component for the bone substitutes. Zhang et al. [146] systematically studied the effects of the magnesium in calcium phosphate cement (CPC) on the initial responses and the ultimate differentiation of MSCs, as well as the mechanism involved. The magnesium precursor (MPC) consisted of Ca $(H_2PO_4)_2 \cdot H_2O$ and MgO in a molar ratio of 1:2 was incorporated into CPC to obtain the MPC-modified CPC (MCPC). By regulating the weight percentage of MPC in the range from 0 % to 20 % in MCPC, MCPC surfaces with different magnesium densities were obtained. The Fn adsorption and the availability of the cell-binding domains on the synthesized surfaces were determined by immunofluorescence staining and quartz crystal microbalance with dissipation (QCM-D) analysis. The attachment, morphology, focal adhesion formation, actin filament assembly, and the expression of integrin subunits of MSCs on different cements were assayed. The results indicated that the incorporation of certain content of MPC into CPC could not only enhance the adhesion and spread but also promote the osteogenic differentiation of MSCs in vitro. And the desirable efficacy was achieved on the 5MCPC (with 5 % MPC) with moderate proportion of Mg. As the schematic diagram (Fig. 8.9) shows, 5MCPCs were believed to effectively modulate the orientation of the adsorbed Fn for enhanced cell-binding affinity and upregulate the integrin α5β1 expression of MSCs. Based on these results, it can be inferred that the Mg element concentration had predominant effect on the interaction of Fn and integrin α5β1, which mediated the MCPC-induced enhanced cellular response in MSCs.

Besides, some research has shown that the existence of silicon may stimulate the proliferation of MSCs and activate cells to produce transforming growth factors (TGF). For example, Ding et al. found that the Si/Ca ratio of calcium silicate cements could modulate attachment and proliferation of MSCs [147]. Calcium silicate cements with a higher Si content promoted cell attachment and triggered greater total integrin, pFAK, and collagen type I expression compared to the cement with a higher Ca content. Integrin expression profiles changed accordingly, with higher levels of α2β1 and αvβ3 subintegrin in the cells on the Si-rich and Ca-rich cements, respectively, which were ascribed to the collagen-binding and Fn-binding subintegrin on human primary cells, respectively. Mitogen-activated protein kinase (MAPK)/extracellular regulated kinase (ERK) and MAPK/p38 signaling pathways were activated in MSCs cultured on these cement substrates, and their inhibition significantly attenuated cell adhesion, proliferation, and differentiation as assessed according to total DNA and alkaline phosphatase (ALP) activity. Si component of

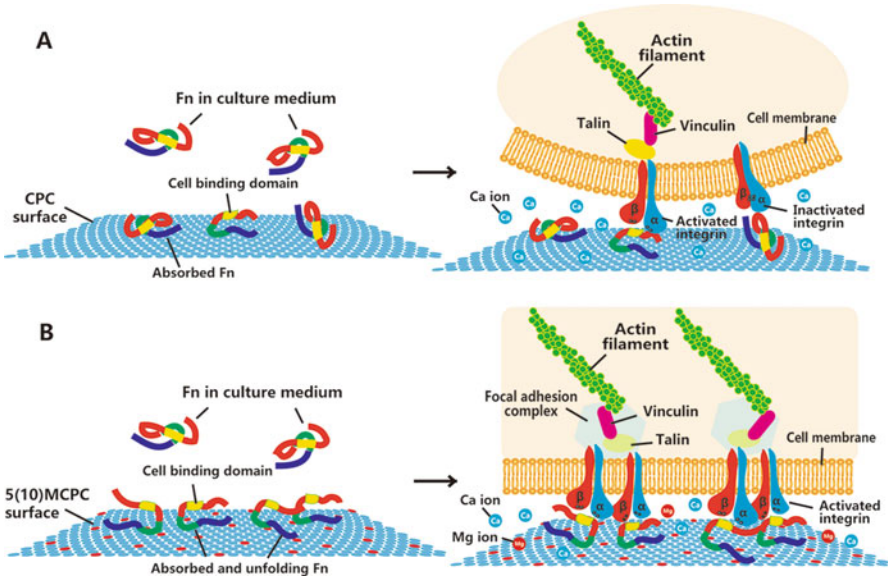

Fig. 8.9 Schematic diagram of the adsorption-induced changes in the structural orientation of the binding domain in Fn and the ensuing interaction between Fn and integrin α5β1 on (**a**) CPC and (**b**) 5(10)MCPC

calcium silicate materials can induce upregulation of MAPK/ERK and MAPK/p38 signaling pathway more effectively than Ca component.

8.4.4.3 Effects of Functional Groups on Stem Cell Behaviors

Many functional groups, for example, $–CH_3$, $–NH_2$, –SH, –OH, and –COOH, can influence the self-renewal and lineage commitment of MSCs directly or through interacting with specific ECM proteins. Using self-assembled monolayers (SAMs) of alkanethiols on gold as model surfaces, Keselowsky et al. [136] investigated the effects of surface chemistry on Fn adsorption, integrin binding, and cell adhesion. SAMs presenting terminal $–CH_3$, –OH, –COOH, and $–NH_2$ functionalities modulated adsorbed Fn conformation as determined through differences in the binding affinities of monoclonal antibodies raised against the central cell-binding domain ($–OH > –COOH = –NH_2 > –CH_3$). Binding of integrin α5β1 to adsorbed Fn was controlled by SAM surface chemistry in a manner consistent with antibody binding ($–OH > –COOH = –NH_2 > –CH_3$), whereas integrin αV binding followed the trend –COOH much greater than $–OH = –NH_2 = –CH_3$, demonstrating integrin α5β1 specificity for Fn adsorbed onto the NH_2 and OH SAMs. Cell adhesion strength to Fn-coated SAMs correlated with integrin α5β1 binding ($–OH > –COOH = –NH_2 > –CH_3$), and experiments with function-perturbing antibodies demonstrated that this receptor provides the dominant adhesion mechanism.

Curran et al. [148] examined the behavior of MSCs cultured on a range of silane-modified surfaces to determine the effects of the surface functional groups on the early differentiation potential of MSCs in vitro. Cells were cultured for 1 and 7 days in direct contact with glass which had been functionalized by surface treatment to provide a range of different surfaces, $–CH_3$-, $–NH_2$-, –SH-, –OH-, and –COOH-modified surfaces, and a clean glass reference (TAAB). Viable cell adhesion was quantified by lactate dehydrogenase assay, and morphology and viability were qualitatively evaluated using calcein AM, ethidium homodimer, cytoskeletal (F-actin), ECM (Fn and vitronectin), and Hoechst staining (nucleus). The expression of selected differentiation markers, collagen type II (chondrocytes), CBFA1 (bone transcription factor), collagen type I (MSC marker), and TGF-β3 (extracellular matrix production), was determined using real-time polymerase chain reaction. The expression of ornithine decarboxylase was evaluated as a marker of proliferation. Surfaces of the $–NH_2$ group demonstrated the greatest level of cell adhesion by the 7-day period, and mRNA expression profiles indicated osteogenic differentiation, increased CBFA1, and decreased collagen type II expression. Cells cultured in contact with the –COOH surfaces displayed different cell morphologies and Fn and vitronectin spatial distributions compared with the cells in contact with the $–NH_2$ surfaces, in addition to an increase in collagen type II expression, indicative of chondrogenic differentiation. The modifications to the surface chemistry of glass did affect cell behavior, in terms of viable cell adhesion, morphology, and profiles of mRNA expression, providing the means to alter the differentiation potential of the MSCs.

Using high internal phase emulsion (HIPE) templating method, Viswanathan et al. [149] fabricated a 3D scaffold with amphiphilic block copolymers, polystyrene-b-poly(ethylene oxide) (PS-PEO) and/or polystyrene-b-poly(acrylic acid) (PS-PAA), which exhibited both cell inert (PEO) and adhesive (PAA) domains. The results demonstrate how Fn and MSCs adhere in a domain-specific manner: an optimal balance between concentration and spatial distribution of PAA domains may be contributing toward the preferential adhesive behavior of the stem cells, which means not only the type but also the spatial distribution (pattern) of the functional groups directing the stem cell growth and fate.

8.4.4.4 Effects of Biochemical Functionalization on Stem Cell Behaviors

Another approach toward the control of stem cell behavior on biomaterials is the biochemical incorporation of adhesion-promoting oligopeptides or oligosaccharides. Stem cell adhesion to traditional biomaterials is based upon recognition of short peptides of ECM proteins from the body fluids adsorbing specifically or non-specifically to the material surface by the corresponding adhesion receptors, which means the cell–material interaction is indirect. As a more direct approach, several investigators have explored the covalent or physicochemical incorporation of adhesion-promoting oligopeptides and oligosaccharides onto the biomaterial surface.

Extensive research has been performed by anchoring oligopeptides representing the ECM-binding sites onto the biomaterial surfaces. The most commonly used peptide for surface modification is RGD, the signaling domain derived from fibronectin and laminin. A number of materials including glass [150], quartz [151], metal oxide [152], and polymers [153] have been modified with these peptides and characterized for cellular interaction with their surfaces. Different coupling techniques have also been employed to ensure covalent binding of the peptides to the surface of the materials. For example, the reactive moieties on the model surface, usually $–NH_2$, were chemically reacted with certain functional groups, usually –COOH, that are present within the bioactive peptide. A bifunctional cross-linker that has a long spacer arm can be used for the immobilization of the peptide to the surface, which can enable the immobilized peptide to move flexibly in the biological environment [151]. For polymer substrates lacking appropriate functional groups for a coupling reaction, a photochemical immobilization method [154] has been utilized to graft cell-binding peptides. In order to examine that any cellular responses to the modified substrates are mediated solely by the immobilized peptides, the experiment has often been performed under serum-free conditions.

Designing materials that can selectively interact with cell-binding peptides while minimizing nonspecific adsorption of ECM proteins is also challenging. Immobilization of poly(ethylene glycol) (PEG) [155] or its derivative [156] on the surface has been effective to limit cell adhesion. The interpenetrating polymer network (IPN) that consists of both the hydrophilic chain that can limit nonspecific adsorption of proteins and the reactive chain that allows for peptide immobilization may be desirable for this application [157]. With RGD covalently incorporated into poly(ethylene glycol) diacrylate (PEODA) hydrogel, Yang et al. [158] demonstrated that RGD-conjugated PEGDA hydrogel system promotes the osteogenesis of bone-marrow-derived MSCs. RGD-tethered hydrogel stimulated the production of bone marker proteins, such as ALP and osteocalcin, in a dose-dependent manner, with 2.5 mM being the optimal concentration.

Cao et al. [159] synthesized a series of charged or neutral oligopeptide motifs coupled with RGD using quartz substrates as the model. MSC behaviors on the modified surfaces with different charged oligopeptide motifs were studied. It was found that these different charged oligopeptide motifs coupled with RGD were biocompatible for cell proliferation and adhesion. Moreover, it was demonstrated that the positively charged oligopeptide motif could inhibit osteogenic differentiation, while the negatively charged and neutral oligopeptide motifs could enhance osteogenic differentiation in the presence of RGD.

Chien et al. [160] determined the effects of surface bioadhesive signals on self-renewal and osteogenic differentiation of MSCs using a low-fouling platform. Cell-resistant poly(carboxybetaine) hydrogel was conjugated with 5 μM or 5 mM of cell-adhesive RGD peptides in order to control the cells' affinity to the substrate. MSCs were cultured on the RGD-modified poly(carboxybetaine) hydrogel, and then the cells' states of stemness and osteogenic differentiation were evaluated. The MSCs formed 3D spheroids on the 5 μM RGD substrate while exhibiting spreading morphology on the 5 mM RGD substrate. Furthermore, MSCs on the 5 μM RGD

hydrogel maintained a better stemness phenotype, while the hMSCs on the 5 mM RGD hydrogel proliferated faster and underwent osteogenic differentiation. In conclusion, the stemness of hMSCs was best maintained on a low RGD surface, while osteogenic differentiation of hMSCs was enhanced on a high RGD surface. Wang et al. [161] investigated MSC behaviors on micro-/nanopatterns with RGD nanoarrays of nanospacings 46 and 95 nm and with micropans of side lengths 35 and 65 μm (four groups in total). The osteogenic and adipogenic differentiation of MSCs was conducted, and the potential effect of RGD nanospacing and the effect of cell-spreading size on cell differentiation were decoupled for the first time. The results reveal that RGD nanospacing, independent of cell-spreading size, acts as a strong regulator of cell tension and stem cell differentiation.

8.4.5 Multiscale Hierarchical Structure

Hierarchical structures were first proposed in 1994 in order to develop novel processing technologies to fabricate hierarchically structured materials with proper control on an industrial scale [162]. In 2005, Hollister proposed a clear definition stating hierarchical structure refers to the features at scales from the nanometer to millimeter that are able to determine how well the bioscaffold meets the conflicts between mechanical function and mass transport needs [163].

Almost all types of biomaterials, such as metals, polymers, ceramics, hybrids, and composites, can be machined into biomedical scaffolds for the purpose of tissue engineering. For example, by employing a liquid foaming method and subsequent chemical treatments, three-dimensionally hierarchical porous structures can be successfully achieved in titanium scaffolds with pore size ranging from the nanometer to micrometer scale. This scaffold also has a sufficient compressive strength to meet the requirements of implantation [164]. Woodard et al. revealed that the micropores in porous hierarchical HAp bone scaffolds are quite important to maintain the mechanical satiability of the scaffolds, as the newly formed bone in the scaffolds supported the load after a fracture. The mechanical failure stress was significantly less than that of the scaffolds with pure macropores. Furthermore, evidence also suggested that the bone could arrest crack propagation in hierarchical HAp scaffolds [165]. Practically, hierarchical bimodal or multimodal porous architectures with macro-, micro-, and nano-pores, simultaneously, are also important in modulating the permeability and compliance of polymeric scaffolds that favor various applications in tissue engineering.

8.4.5.1 Hierarchical Pore Size Structure

Actually, sol–gel glass scaffolds can be considered the precursors of the hierarchically structured macro-/mesoporous glass scaffolds [166]. In the last couple of years, some attempts for fabricating multiscale glass-based scaffolds have been

carried out by using properly mesostructured materials, in which the nanoporous size and arrangement can be carefully controlled and designed. The purpose of such scaffolds is twofold, as they combine the properties of traditional glass-derived scaffolds, i.e., mechanical support in the defect zone, bioactivity, favored osteointegration, and bone tissue regeneration, with the unique features supplied by mesoporous materials, such as enhanced bioactivity and controlled drug adsorption/release ability for drug therapy in situ.

Yun et al. [167] synthesized hierarchically porous 3D MBG scaffolds with good in vitro bioactivity by using a combination of sol–gel, double polymer templating, and rapid prototyping techniques. Li et al. [168] reported the synthesis of multiscale porous MBG scaffolds by using the block copolymer EO20PO70EO20 (P123) and a PU macroporous sponge as co-templates and demonstrated that a HAp layer was formed on the scaffold surface after soaking in SBF for 4 h. Zhu et al. [169] successfully prepared 3D porous MBG scaffolds by a combination of PU sponge and P123 surfactant as co-templates and evaporation-induced self-assembly (EISA) process. Apart from MBG, inorganic nanostructures based on calcium phosphates are also compounds of great interest in scaffold development since they are the major inorganic constituent (69 wt%) of naturally occurring mineralized bone.

Of special interests are the scaffolds that are able to present a bimodal pore size distribution, mainly having macropores for cell penetration and micropores for protein adsorption/delivery. Interestingly, the micropores also present some roles in the overall mechanical properties of scaffolds. For instance, HAp scaffolds were prepared with two different micropore sizes, mainly 5.96 and 16.2 μm, showing higher bending and compression strength in the presence of smaller micropores [93]. Microporous (54–80 vol.%) bioactive glass scaffolds with hierarchical porosity have been recently developed with the aim to satisfy the macroporosity needed for bone ingrowth while maintaining adequate mechanical properties (12–20 MPa) [93].

Inspired by the impressive property of natural bone, 3D hierarchical porous scaffolds have attracted significant attentions since they can provide transportation "highways" on various scales during osteo-regeneration and promote the innate regenerative mechanisms of the human body. In recent years, synthetic scaffolds with hierarchical macro-/micro- or macro-/nano-architectures are being rapidly developed and have evolved various biomaterials, including biodegradable polymers (tyrosine-derived polycarbonate, PLGA), ceramics (hydroxyapatite, bioglass, calcium carbonate), metals (stainless steel and titanium), etc. Numerous studies have concluded that interconnected macroporosity with diameter larger than 100 μm is a prerequisite for bone ingrowth, cellular infiltration, and nutrient/waste transportation [170]; and micro- and nano-topologies on the material surface play a critical role on cell attachment, biomineralization, and full-scale osteointegration in vivo. Based on these previous researches, Tang et al. [56] have successfully incorporated trimodal macro-/micro-/nanoscale structures into one scaffold to achieve optimal osteogenic properties.

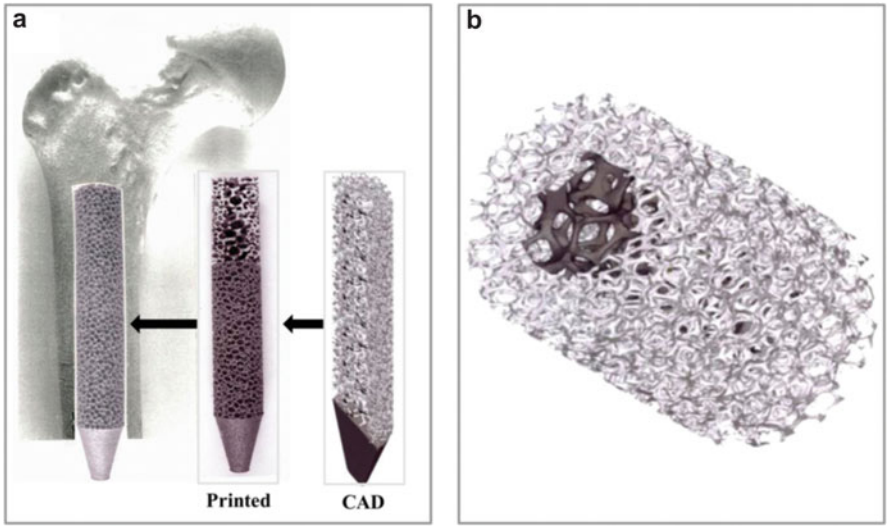

Fig. 8.10 (**a**) A conceptual view of intramedullary stem of Ti–6Al–4V foam built by EBM using the CAD model and (**b**) cylindrical foam with dense outer region and low-density inner core [172] (Copyright 2012 Lawrence E. Murr et al.)

8.4.5.2 Hierarchical Porosity Structure

Natural bone is a classic case of a functionally graded structure with an outer highly dense region (cortical bone) having an elastic modulus of ~18 GPa, the inner porous region (cancellous bone) having an elastic modulus of ~1 GPa, and the bone marrow cavity in the central region [171]. Thus, there is a gradual increase in porosity as well as modulus variation from cortical to cancellous transition, especially at the end of long bones. Thus, to replicate the architecture of natural bone, 3D scaffolds with graded porosity are preferred. In this context, Ti–6Al–4V rod was fabricated with central foam core (density ~0.6 g/cm^3) and outer foam structure with relatively higher density (~1.1 g/cm^3) as shown in Fig. 8.10 [172]. The inner and outer foam is characterized by a stiffness of 0.3 and 2.2 GPa, respectively. Also, a porous cylinder of Ti–6Al–4V alloy was fabricated using the electron beam melting (EBM) method, characterized by a lower-density inner foam, surrounded by a foam with relatively higher density (Fig. 8.10b). Generally, porous materials with a specific pore size facilitate growth of one particular cell. For example, pore sizes of ~5–15 μm were considered suitable for fibroblast, ~70–120 μm for chondrocytes, and ~100–400 μm for osteoblast ingrowth. In contrast, gradient porous materials can simultaneously repair and reconstruct two or more different tissues, since the different regions provide different microenvironments for multiple tissues.

8.4.5.3 Hierarchical Surface Structure

Cells are innately receptive of their surroundings, typically to a broad spectrum of feature sizes from the macro down to molecular level, between 100 μm and 10 nm. It is through an elaborate and dynamic feedback mechanism of signal transfer between the ECM and the cells that the behavior of the latter is coordinated into complex functional tissues. Hence, engineering these dynamic ECM mechanisms into biomaterials is the key to control cell behavior.

It is already circumstantiated that both micrometer- and nanometer-scale features of a material have marked influence on cell behavior. Additionally, materials organized on multiple length scales have better conformity to biological matrices than those with single-scale features and are, hence, more propitious for all kinds of biomedical applications. The effects of microscale surface topography on cellular responses have been investigated over the years. Currently, nanostructuring of surfaces has garnered immense interest in view of their structural similitude to the native ECM of cells. Undeniably, nanotopography plays a cardinal role in modulating cell functionality. Recent research by Gentile et al. manifests the potentiality of moderately rough nanostructured surfaces with large fractal dimensions in promoting stable cell adhesion, growth, and proliferation [173].

Literature is replete with evidences on topographic sensitivity of cells (i.e., interplay of cells with surface features) to nanoscale as well as micrometer-range features like grooves, ridges, and wells. Nanoscale alterations in topography evoke multifarious cell responses, including changes in cell adhesion, cell orientation, cell motility, surface antigen display, cytoskeletal condensation, activation of tyrosine kinases, and modulation of intracellular signaling pathways, which in turn coordinate transcriptional activity and gene expression. Notwithstanding the feature size, cell behavior is also administered by the nature of ordered topography (e.g., ridges, grooves, steps, pits, pillars, channels) and their symmetry (e.g., orthogonal or hexagonal packing).

In vivo, the basement membrane, composed of ECM components, is a complex network of pores, fibers, ridges, and other features of nanometer-sized dimensions. Topographical cues generated by the ECM, independent of biochemistry, have direct effects on cell behavior such as adhesion, migration, cytoskeletal arrangements, and differentiation. Cells are inherently sensitive to local microscale, mesoscale, and nanoscale topographic and molecular patterns in the ECM environment, a phenomenon called “contact guidance” [174]. The development of microfluidics and micro-/nanofabrication methods to analyze the cellular response to substrate topography has provided new insights into the interactions of cells with their microenvironments.

Grooves and pillars are the most common feature types employed in the study of the effects of surface structures on cells. The influence of groove patterns on the behavior of cell has been extensively investigated by using various cell types such as fibroblast, osteoblast, epithelial, myoblast, etc. A large number of studies revealed that cells tend to align to the long axis of the grooves. Kaiser et al. defined the role of groove/ridge dimensions on fibroblast cell migration [175]. They found that surface

structures significantly influenced cell orientation, migration direction, as well as migration speed in the directions parallel and perpendicular to the grooves/ridges in a surface structure-dependent way. Uttayarat et al. investigated the combination of flow shear stress and groove guidance on endothelial cell migration [176]. When flow direction was oriented parallel to microgrooves, the cells migrated along the microgrooves. When microgrooves were oriented perpendicular to the flow, most cells migrated orthogonal to the grooves and downstream with the flow. Lee et al. reported that the nanoscale ridge/groove pattern arrays alone can effectively and rapidly induce the differentiation of human embryonic stem cells into a neuronal lineage without the use of any differentiation-inducing agents, indicating the significant role of topography in determining cell fates [177].

The influence of pillar patterns on the behavior of cells has also been extensively studied. MSCs preferentially differentiated and osteosarcoma cancer cells increased their malignant transformation due to the micro-pillar geometry. In particular, the increase of pillar heights from 1 to 10 μm affected the in vitro adhesion and guides morphology of fibroblasts by laminin expression enhancement [178]. Furthermore, the spacing between 5 and 10 μm of pillars was shown to rearrange the actin cytoskeleton and govern fibroblast migration in vitro [179]. Nanotopography alone can induce the differentiation of MSCs into neuronal lineage and induced a more significant upregulation of neuronal markers compared to microtopography, highlighting the importance of feature size in topography-induced differentiation.

Other micro-/nano-sized features, such as nodes, pits, pores, and so forth, have been reported to influence the behavior of cells. The topography of the cell substratum plays an important role in regulating cellular behavior, and micro-/nanofabrication techniques provide useful tools for manipulating cells in both fundamental cell biology research and tissue engineering.

8.5 Delivery of Bioactive Agents

To enhance the interactions between the materials and host cells/tissues and direct the differentiation of MSCs, one of the useful strategies is the introduction of the bioactive components in extracellular matrix components within/onto the material structures. These components usually include ECM peptides/polypeptides, cytokines, growth factors, and DNAs. In the view of the osteoinductive potential, osteogenic growth factors such as fibroblast growth factor-2 (FGF-2), TGF-β2, and BMP-2 have been extensively used to improve the material osteoinductivity.

8.5.1 Growth Factors

Growth factors were initially discovered as a result of their ability to motivate continuous mitosis of quiescent cells in a nutritionally complete medium without serum. While nutrients and growth factors are both essential for mitosis, only

growth factors know how to initiate mitosis of quiescent cells. A variety of cellular processes need growth factors as regulatory agents. The biology of these factors differs from the classical hormones as neither their site(s) of synthesis nor site(s) of action is limited to defined tissues.

Growth factors are polypeptides that transmit signals to modulate cellular activities. It is known that growth factors play crucial roles in communication and information transfer between cells and their microenvironment [180]. Moreover, growth factors are soluble-secreted signaling polypeptides capable of instructing specific cellular responses in a biological environment. The specific cellular response trigged by growth factor signaling can result in a very wide range of cell actions, including cell survival, and control over migration, differentiation, or proliferation of a specific subset of cells. Prior to addressing strategic delivery of growth factors, understanding the biological functions and roles of these proteins in the extracellular matrix is first of all required because the extracellular matrix contains numerous components such as adhesive molecules, notch signaling molecules, traction-enabling adhesion molecules, and proteoglycan molecules to bind and modulate the activity of a number of growth factors. The signal transmission mechanism initiates with growth factor secretion by the producer cell. The growth factor instructs cell behavior through binding to specific transmembrane receptors on the target cells. The machinery that transduces the growth factor-binding signal to the cell nucleus involves a complex array of events involving cytoskeleton protein phosphorylation, ion fluxes, changes in metabolism, gene expression, protein synthesis, and ultimately an integrated biological response.

Growth factors differ from other oligo-/polypeptide molecules, such as insulin and hormones, in the mode of delivery and response elicited. Typically, growth factors do not act in an endocrine fashion; they exhibit short-range diffusion through the extracellular matrix and act locally owing to their short half-lives and slow diffusion [181]. The ability of a growth factor to deliver a particular message to a distinct subpopulation of cells is not exclusively determined by the identity of the growth factor and its ability to diffuse through the ECMs; it is also determined by the target cell number, the type of receptors, and the intracellular signal transduction subsequent to factor binding. The same growth factor can convey different instructions depending on the receptor type to which it binds and on the cell type to which it binds. Moreover, the same receptor can translate different messages depending on the intracellular transduction pathways. The ultimate response of a target cell to a particular soluble growth factor can also be governed by external factors, including the ability of the factors to bind to ECM, ECM degradation, and growth factor concentration and cell target location [182].

Growth factors are involved in the regulation of a variety of cellular processes and typically act as signaling molecules between cells [183]. They promote cell proliferation, differentiation, and maturation, which vary in growth factors. As a result, they play important roles in wound healing and tissue regeneration. However, most growth factors act in a diffusible manner and are generally unstable in a tissue environment. This prolonged retention is considered to maintain the activity of growth factors in cells or in their environment (i.e., the ECM or artificial implant scaffolds), until the repair process is initiated or even completed. Thus, many

attempts have been made to improve the performance of growth factors (e.g., their active period and stability). In addition, it is very important to add biofunctionality such as the regulation of cell functions to biomaterials used for artificial organs. Modification of growth factors for immobilization on or for high-affinity binding to cells or scaffold biomaterials has been performed by various researchers [184].

Most growth factors, which act in a diffusible manner, interact with their cognate receptor on the cell membrane and form a complex. This interaction induces phosphorylation of the receptor and triggers signal transduction in the cell. These complexes are then internalized, partially decomposed by lysosomes, and partially recycled to the cell membrane [185]. Thus, internalization of the receptor/growth factor complexes leads to the desensitization of cells (downregulation) and to the reduction of excessive responses and overstimulation. In contrast, some growth factors are known to act in a nondiffusible manner by being present at the cell surface (juxtacrine) or by associating with specific substances, such as the ECM (matricrine). The nondiffusible mechanism was elucidated by the discovery of cell membrane-bound growth factors in the 1990s, which include heparin-binding EGF-like (HB-EGF) growth factor, transforming growth factor-β (TGF-β), tumor necrosis factor-α (TNF-α), colony-stimulating factor 1 (CSF-1), and the c-kit ligand [186]. These growth factors are barely internalized even after binding to their receptors but exhibit long-term activity without downregulation. This point suggests the possibility of designing binding growth factors with specific activities.

There are several characteristic properties of growth factors. Many cell types can produce the same growth factor, and the same growth factor can act on many cell types (pleiotropism) with the same or different effects. Furthermore, different growth factors can share the same biological effect (redundancy). Growth factors can influence the secretion of other growth factors (antagonize or enhance). Growth factors are not stored as preformed molecules, but their secretion is a brief self-limited event and their synthesis is initiated by new gene transcription, transient transcriptional activation, and their mRNAs are unstable [187]. There are transient synthesis and rapid release with activity controlled by posttranscriptional mechanisms such as proteolytic release of an active product from an inactive precursor. Most cellular responses to growth factors require new mRNA and protein synthesis.

The availability of growth factors from the conditioned medium of cultured human cells, their expansion through recombinant technologies, and improved understanding of their functions and clinical applications has increased the need for pharmaceutical forms. Unfortunately, the short half-lives of growth factors, their relatively large size, slow tissue penetration, and their potential toxicity at systemic levels all leading to a long time for the tissue to respond obviate conventional routes of administration.

All vascularization processes involve a series of interactions among cytokines, growth factors, various types of cells, and enzymes. The onset of vascularization begins with the binding of biological agents to the surface receptors of endothelial or endothelial progenitor cells, and a resulting cascade of agents act in the subsequent processes of vascularization. Numerous growth factors involved in vasculogenesis, angiogenesis, and arteriogenesis have been identified and characterized, including

vascular endothelial growth factor (VEGF), fibroblast growth factor (FGF), placental growth factor (PIGF), hepatocyte growth factor (HGF), platelet-derived growth factor (PDGF), angiopoietin-1 and angiopoietin-2, insulin-like growth factor (IGF), granulocyte macrophage colony-stimulating factor (GM-CSF), and monocyte chemoattractant protein-1 (MCP-1). Growth factors are often chosen as drug candidates for rebuilding networks of blood vessels for therapeutic angiogenesis or for tissue engineering.

Members of the transforming growth factor-β (TGF-β) superfamily are secreted multifunctional growth factors that determine the development, maintenance, and regeneration of tissues and organs. Their importance in the development of multicellular organisms is clear from their presence in all vertebrates and invertebrate animals. On the basis of their phylogenetic and functional relationships, the TGF-β/bone morphogenetic proteins (BMPs) can be subdivided into four subgroups, which also highlight mechanistic differences in receptor binding and activation or the differences found in modulatory mechanisms [188]. These subgroups are the TGF-βs, the bone morphogenetic proteins (BMPs) and growth and differentiation factors (GDFs), activins/inhibins, and the so-called outsider subgroup.

8.5.2 Brief Introduction of BMPs

Bone morphogenetic proteins belong to the large transforming growth factor-beta (TGF-β) superfamily of structurally related signaling proteins which are disulfide-linked dimers composed of two 12–15 kD monomers. To date, more than 20 members have been identified in humans with varying functions during developmental and physiological processes [189] such as embryogenesis, skeletal formation, hematopoiesis, and neurogenesis. Among these growth factors, BMP-2, BMP-4, and BMP-7 (also called osteogenic protein-1) have been largely used as recombinant proteins for their ability to repair bone defects in different animal models [190, 191]. Liu et al. [192] have elucidated the exact mechanism by which BMPs affect MSCs. These proteins generate the transcription factor Smads by combining with type I or II serine/threonine receptor on the MSC membrane to activate 203 gene loci which control the osteoblast differentiation of MSCs.

BMP-2 is a FDA-approved growth factor and can induce ectopic bone and cartilage formation in adult vertebrates and is involved in central steps in early embryonal development. A cDNA encoding mature human BMP-2 could be efficiently expressed in *Escherichia coli*, and after renaturation a dimeric BMP-2 protein of Mr 26000 was prepared with a purity greater than 98 %. Fernando Lecanda et al. [193] have proved that BMP-2 has profound effects on the proliferation, the expression of most of the bone matrix proteins, and the mineralization of both relatively immature human bone marrow stromal preosteoblasts and mature human osteoblasts. However, combined with clinical challenges such as limited efficacy, excessive doses, side effects, and high costs, efforts have focused on improving BMP-2 half-life and/or sustaining and localizing its release [194].

8.5.3 Immobilization of Growth Factors

Growth factors typically act as signaling molecules to regulate a variety of cellular processes. For example, BMPs stimulate bone cell differentiation and improve the cell proliferation, whereas FGF and VEGF enhance angiogenesis. BMPs have been integrated onto/into the implantable materials to significantly enhance a wide variety of biological functions including stimulating osteogenesis and angiogenesis [195, 196]. Upregulation of BMP-2 has been observed during the first 3 weeks of osteogenesis [197]. Moreover, the growth factors released during the inflammatory phase have the potential of attracting undifferentiated mesenchymal stem cells to the injured site [198]. On the basis of these findings and the nature of BMP-2, this growth factor must be delivered in a sustained fashion that emulates the natural release profile of BMP-2 in vivo.

There are several methods for immobilizing biological molecules including BMPs on inorganic/organic surfaces. Physisorption is the easiest method of surface modification. The fundamental interacting force of physisorption is van der Waals force and the interaction energy is very weak. Therefore, the direct immobilization of growth factors by physisorption is easily disrupted by desorption, and the growth factors will diffuse into the surrounding medium, losing their ability to exert a sustained effect [199]. Moreover, the loading amount of bioactive agents with physisorption is limited, and there is an obvious burst release at the beginning stage. To improve the surface properties of a substrate, such as its appearance, adhesion, and wettability, the substrate surfaces can be modified or functionalized via coating growth factors with other materials. A variety of biomaterials including calcium phosphates, collagen gels, sponges, HA, dextran, and chitosan have been co-coated for prolonged and local release of BMPs.

Growth factors have also been chemically immobilized on surfaces by covalent bonding. Some linkers have also been used as intermediaries to chemically immobilized growth factors, including coupling agents and dopamine. Meanwhile, the covalent binding usually requires nonphysiological conditions and complex procedures [200]. Many researchers have also developed layer-by-layer self-assembly and biomimetic/electrochemical deposition approaches for immobilizing growth factors [201]. However, either time-consuming or poor controlling of the coating properties limits their applications. To achieve the high loading efficiency and maintain the biological stability of BMP-2, the immobilization techniques require the fast operation, mild conditions, as well as the well-controlled coating. Among different techniques, the electrostatic spray deposition (ESD) has shown a great potential for biomolecule incorporation onto/into metallic materials because of simple and low-cost, fast deposition rate and protein-friendly, well-controlled, and easy coating for complex geometries [202]. To date, this technology has been successfully applied to deposit many inorganic/organic materials on the metallic surfaces. Our group also used this technique to co-deposit BMP-2 and chitosan on metallic surface for enhancing the proliferation and osteogenic differentiation of bone MSCs [203].

Growth factors are often added to the scaffold surface via electrostatic interaction and ionic complexation, and the corresponding release depends on protein–surface interactions that are governed by surface charge, surface roughness, and surface energetics. For more sustained release, bioactive molecules can be physically encapsulated within the scaffolding material and in microparticles. Covalent immobilization methods must be assessed in terms of gradients, spatial distribution and density, conjugation efficiency, dose dependence, downstream signaling, heparin-/affinity-based delivery, dual delivery, and cleavable linkers [204]. For the purpose of this review, 100 % or less delivery over the course of 30 days is considered successful sustained release, based on the timescale required for repairing different tissues.

8.5.4 Influence of Ions on rhBMP-2 and Stem Cell Differentiation

8.5.4.1 The Influence of Various Ions on the Activity of rhBMP-2 to Induce the Osteogenic Differentiation

As has been discussed, rhBMP-2 is a widely used, potent osteogenic growth factor and can induce osteogenic differentiation of multipotent mesenchymal cells and induce bone formation in both animals and humans. Various matrices have been and are currently being adopted to carry recombinant human BMP-2 (rhBMP-2) [205–208]. However, due to the hydrogen/ionic/hydrophobic interaction with the substrates or the environmental factors such as pH, ionic strength, and temperature in vitro and in vivo, highly efficient delivery of rhBMP-2 remains a challenge till now. Therefore, fundamental understanding of the conformational behavior of rhBMP-2 during its application in vitro and in vivo would be very significant to the design and fabrication of the rhBMP-2-based orthopedic implants/scaffolds. Recent studies reveal that metal cations play a decisive role in the regulation of protein folding, conformation, stability, and bioactivity of protein. Zinc (Zn^{2+}), copper (Cu^{2+}), calcium (Ca^{2+}), magnesium (Mg^{2+}), manganese (Mn^{2+}), and strontium (Sr^{2+}) have been reported as modulators for protein conformation and biofunctions [209–211]. Thus, the interaction between cations and rhBMP-2 was systematically elucidated in this section.

Considering the fact that Ca^{2+} is the most pervasive component of the bone matrix/scaffold and is abundant in cell culture medium and the physiological environment, the "hormesis" phenomenon was observed for the influence of calcium on the bioactivity of rhBMP-2. Briefly, low concentration of Ca^{2+} (0.18 mM) enhanced rhBMP-2-induced osteogenic differentiation, while high Ca^{2+} concentration (>1.80 mM) exerted negative effect. In vivo ectopic bone formation exhibited similar trend. Further studies using circular dichroism spectroscopy and fluorescence spectroscopy, together with cell culture experiments, revealed that at low concentration, weak interaction of Ca^{2+} and rhBMP-2 slightly increased β-sheet/β-turn content and

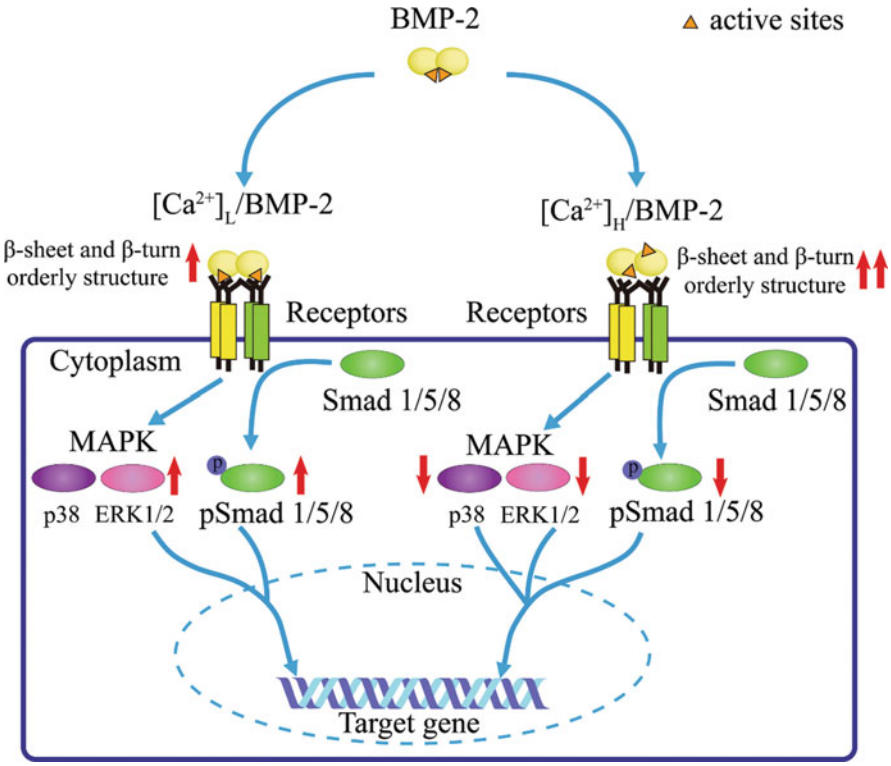

Fig. 8.11 Schematic depiction of the effect of Ca^{2+} on the conformation and bioactivity of rhBMP-2. Effect of Ca^{2+} on the rhBMP-2-induced osteogenic differentiation. Ca^{2+} ion at low concentration facilitated for the binding capacity of BMP-2 with its receptors on the cell membrane and thus enhanced Smad1/5/8 and MAPK signaling transduction, which further stimulated the expression of osteogenic marker genes and the ALP activity. Additionally, increasing Ca^{2+} attenuated the binding capacity to BMPRIA, downregulated the signaling transductions of Smad1/5/8 and MAP kinases, and consequently reduced the rhBMP-2-induced gene expression and ALP activity [212] (Copyright 2015 Changsheng Liu et al.)

facilitated recognition of BMP-2 and BMPRIA. But, high Ca^{2+} concentration (>1.8 mM) induced the formation of Ca–rhBMP-2 complex and markedly increased the content of β-sheet/β-turn, which led to inhibition binding of rhBMP-2 and BMPRIA and thus suppression of downstream Smad1/5/8, ERK1/2, and p38 mitogen-associated protein kinase signaling pathways (as shown in Fig. 8.11). Those results suggested osteogenic bioactivity of BMP-2 can be adjusted via extracellular Ca^{2+}, which should provide guide and assist for development of BMP-2-based materials for bone regeneration [212].

Strontium (Sr^{2+}) has pronounced effects on stimulating bone formation and inhibiting bone resorption in bone regeneration. The interaction between Sr^{2+} and rhBMP-2 was further discussed in this part. Sr^{2+} could bind recombinant human BMP-2 (rhBMP-2) rapidly, even in the presence of Ca^{2+} and Mg^{2+}, and inhibited rhBMP-2-induced osteogenic differentiation in vitro and osteogenetic efficiency

in vivo. Further studies demonstrated that Sr^{2+} treatment undermined the binding capacity of rhBMP-2 with its receptor BMPRIA and thus attenuated Smad1/5/8 phosphorylation without affecting their dephosphorylation in C2C12 cells. Furthermore, circular dichroism spectroscopy, fluorescence spectroscopy, and X-ray photoelectron spectroscopy all revealed that the inhibitory effect of Sr^{2+} on the rhBMP-2 osteogenic activity was associated with the formation of Sr–rhBMP-2 complex and ensuing enhancement of β-sheet structure (as shown in Fig. 8.12). Our work suggests the activity of rhBMP-2 to induce osteogenic differentiation was decreased by direct interaction with free Sr ions in solution, which should provide guidance and assistance for development of BMP-2-based materials for bone regeneration [213].

Moreover, magnesium is a vital and widely used component for the bone substitutes. Mg^{2+} plays a vital role to modulate the conformation and bioactivity of rhBMP-2. However, possibly due to the weak bonding of Mg^{2+} with rhBMP-2, low concentration of Mg^{2+} has no obvious effect on the osteogenic activity of rhBMP-2.

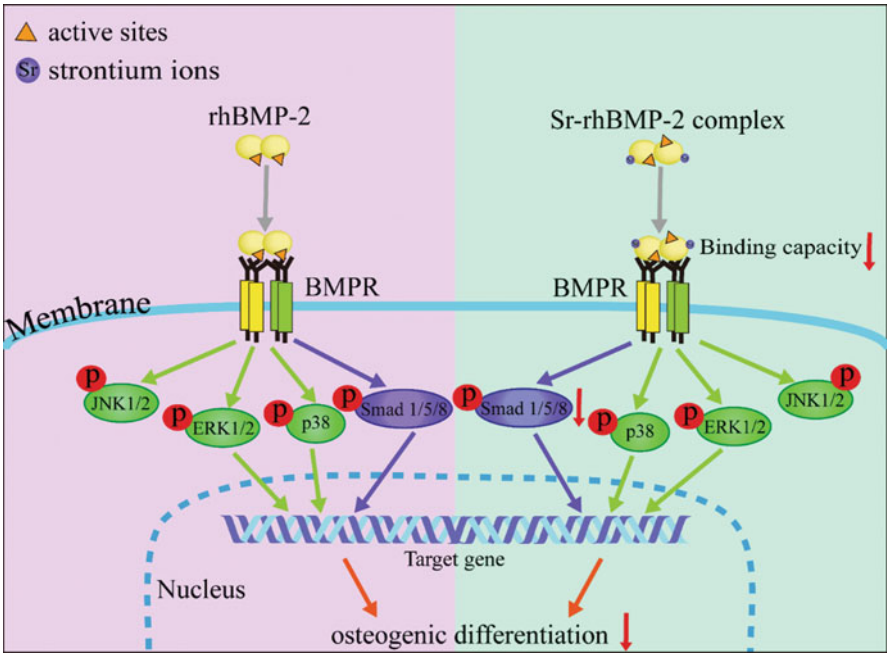

Fig. 8.12 Schematic depiction of the effect of Sr2+ on the conformation and bioactivity of rhBMP-2. Compared with free rhBMP-2, the Sr–rhBMP-2 complex, facilitated by the interaction of rhBMP-2 and Sr2+ ion, attenuated the binding capacity to BMPRIA, consequently downregulated the Smad signaling transduction cascades, and eventually reduced the rhBMP-2-induced osteogenic differentiation in vitro (including ALP activity and bone-related protein and gene expression) and osteogenetic efficiency in vivo [213] (Copyright © 2016 Acta Materialia, Inc. Published by Elsevier Ltd.)

However, those results mentioned above were analyzed using C2C12, a pluripotent skeletal muscle myogenic progenitor cell line, which can differentiate toward an osteoblastic lineage in the presence of BMP-2 and thus is considered as a useful model for analyzing both the common and specific signaling mechanisms of BMPs [214]. Although the rhBMP-2-induced ALP activity in rat mesenchymal stem cells showed a same trend, the influence of cations on the rhBMP-2 in stem cells is still unknown.

Furthermore, lithium (Li^+) ions, which are widely used as a long-term mood stabilizer in the treatment of depressive disorders, are known to affect embryonic development by altering cell fate determination and pattern formation. Li^+ activates the canonical Wnt signaling pathway through inhibition of the β-catenin degradation kinase and glycogen synthase kinase-3 (GSK3) to mimic the canonical WNT signaling. Analogous to WNT, lithium prevents GSK3-mediated phosphorylation of cytosolic transcription factor β-catenin and its subsequent degradation by the proteasome complex. Although stabilization of β-catenin in osteoblasts has been shown to promote bone mass accrual in a mouse model, several studies reported inhibitory effects of lithium supplements on the osteogenic differentiation of cultured mesenchymal stem cells. One possible explanation for these apparent contradictory findings might be that lithium affects the differentiation of osteoblast progenitors through additional signaling events, which independently or in concert with WNT signaling affect the bone resorption activities in vivo. In murine MC3T3-E1 preosteoblasts and a pluripotent mesenchymal cell line C2C12, lithium inhibits BMP-2 signaling to affect osteogenic differentiation on account to reduction of BMP-2-induced Smad1/5/8 phosphorylation without affecting their dephosphorylation. Additionally, in MC3T3-E1 cells, lithium attenuates BMP-2-induced osteogenic differentiation through GSK3 inhibition, while in C2C12 cells, these negative effects of lithium ions on BMP-2 signaling do not rely on GSK3 inhibition or activation of canonical WNT signaling [215].

8.5.4.2 Influence of Various Ions on the Osteogenic Differentiation of Stem Cells

Due to the excellent biocompatibility and bioactivity, CaP-based biomaterials have been attracting great attention in the bone regeneration. The dynamic dissolution/precipitation of CaP minerals from the mineralized matrices dictates the concentrations of Ca^{2+} and PO_4^{3-} in the extracellular milieu. The previous investigation has proposed the role for inorganic ions in stimulating osteogenic differentiation.

The response of osteoprogenitors to calcium (Ca^{2+}), which created an in vitro environment with high extracellular Ca^{2+}, is of primary interest for both normal bone homeostasis and the clinical field of bone regeneration. It reported that Ca^{2+} enhanced proliferation and morphological changes in human bone-marrow-derived mesenchymal stromal cells (hMSCs) with the upregulated expression level of osteogenic genes including ECM proteins (osteopontin, bone sialoprotein, and osteocalcin) and BMP-2. This means hMSCs will develop an osteoblastic phenotype due to

increased [Ca^{2+}] in the culture medium. Ca^{2+} is a ligand for several G-protein-coupled receptors (GPCRs) and can enter the cell via gap junction hemichannels or activate the Notch signaling pathway in the chick embryo during left–right organ asymmetry acquisition. The best described GPCR involved in Ca^{2+} sensing is the calcium-sensing receptor (CaSR), as well as metabotropic glutamate receptors (mGluRs), gamma-aminobutyric acid (GABA), GABAB, and GPRC6A. Furthermore, ion channels such as voltage-gated Ca^{2+} channels (VGCCs), acid-sensing ion channels (ASIC) – ASIC1a/ASIC1b – and human ether-à-go-go-related gene (HERG) K^+ channels open in response to variations in [Ca^{2+}]. The analysis of signal transduction pathways with GPCR agonists and antagonists, targeting the CaSR and mGluR1, respectively, suggests that these receptors are not involved in BMP-2 expression, but cannot exclude the possibility of an unknown GPCR mediating hMSC BMP-2 expression in response to [Ca^{2+}]. Type L voltage-gated calcium channels are involved in mediating the signaling pathway between extracellular Ca^{2+} and BMP-2 expression, but not exclusively. Moreover, in other cell lines such as osteoblasts, Ca^{2+} treatment results in phosphorylation of extracellular signal-regulated kinases 1 and 2 (ERK1/2), and ERK1/2 phosphorylation also occurred when MC3T3-E1 cells were treated with Ca^{2+}. In addition, biphasic CaP crystals failed to induce the expression of a characteristic set of genes in mouse embryonic fibroblasts when upstream activators of ERKs were blocked. In hMSCs, MEK1/2 activity is essential for the effect of Ca^{2+}, probably via Fos expression and AP-1 formation that in turn binds to the AP-1-binding domain of the BMP-2 promoter region [216].

Phosphate ions have generated excitement in the field of vascular biology due to an increased propensity for intravascular calcification with hyperphosphatemia seen in chronic renal disease. The mechanism behind phosphate-induced osteogenesis has been partially elucidated to involve the ubiquitous sodium phosphate cotransporter SLC20A1, adenosine signaling, and ERK1/2 phosphorylation. Extracellular PO_4^{3-} enters the cells through SLC20A1 and subsequently into the mitochondria, which serves as a substrate for ATP synthesis. ATP is then secreted and metabolized into adenosine, which subsequently promotes osteogenic differentiation of hMSCs through the A2b adenosine receptor via autocrine and/or paracrine signaling. Another possibility is that intracellular transport of calcium or phosphate ions inhibits negative regulators of the Smad signaling pathway such as Smad6 or Smad7 [217, 218].

Due to the pronounced effects for stimulating bone formation and inhibiting bone resorption, strontium (Sr^{2+}) has been incorporated into biomaterials/scaffolds to improve the bioactivity for bone regeneration applications [219–221]. It has reported that Sr^{2+} promotes osteoblast differentiation including upregulating expression of the endogenous BMP-2 [222] probably via calcium-sensing receptor (CaR)-dependent mechanism [223] or modulation of the Wnt/β-catenin [224] and MAPK pathways [225].

The further studies aimed to investigate the possible effects of strontium on MSCs and signaling pathways possibly involved. The increased phosphorylation of mitogen-activated protein kinase (MAPK) ERK1/2 and p38 was detected in strontium-treated MSCs. PD98059 and SB203580, selective inhibitors of ERK1/2

kinase and p38, attenuated the effect of strontium on osteogenesis. Furthermore, it was demonstrated that rat sarcoma (Ras) viral oncogene homolog, an upstream regulator of ERK1/2 and p38, was activated by strontium treatment and siRNA-mediated Ras knockdown inhibited strontium-stimulated expression of osteogenic markers. Finally, the transcriptional activity and phosphorylation level of runt-related transcription factor-2 (Runx2) were significantly increased in response to strontium treatment in MSCs. PD98059 and Ras siRNA inhibited the effect of strontium on Runx2 activation. Taken together, strontium can promote osteogenic differentiation of MSCs through activating the Ras/MAPK signaling pathway and the downstream transcription factor Runx2 [226].

Wnt/β-catenin signaling is involved in almost every aspect in embryonic development and plays a central role in bone development and homeostasis. β-Catenin signaling also plays an important role in regulating the commitment of the differentiation of pluripotent stem cell into osteoblast lineage during fracture healing. The canonical Wnt signaling could regulate osteogenesis of MSCs and improve the efficiency of bone tissue engineering. The in vivo data demonstrated the expression of β-catenin, and Frizzled receptor was significantly increased by strontium, thus transducing signals that activated the downstream osteogenic transcription factors and enhancing osteoblastic differentiation; on the other hand, strontium could also inhibit the expression of Wnt pathway inhibitors, prevent the degradation of β-catenin, and promote osteogenic differentiation.

8.5.5 Influences of Other Molecules on rhBMP-2 and Stem Cell Differentiation

8.5.5.1 Interactions Between GAG Sugars and BMP-2

Recent evidence suggests that BMP-2 kinetics can be improved by complexing the growth factor with glycosaminoglycan (GAG) sugars [226]. GAGs are long-chain compounds composed of repeating disaccharide units with a carboxyl group and one or more sulfates, in which one sugar is N-acetylgalactosamine or N-acetylglucosamine [227]. These highly anionic, linear polysaccharides form important constituents of the extracellular matrix and are noted for their ability to bind, stabilize, and protect various growth and adhesive factors [228]. Heparin, heparan sulfate (HS), keratan sulfate, dermatan sulfate, chondroitin sulfate, and hyaluronic acid are well known as endogenous GAGs.

Heparin, a hyper-sulfated glycosaminoglycan (GAG) sugar harvested from mast cell-rich tissues, has been investigated extensively and shown great promise in this regard. Heparin can bind to and modulate various extracellular molecules including growth factors, adhesion molecules, and receptors. Rainer Ruppert et al. [229] identified the basic N-terminal domains of dimeric BMP-2 as heparin-binding sites that are not obligatory for receptor activation but modulate its biological activity. Some studies have reported that heparin enhances the bioactivities of BMP-2 through

binding to and stabilizing BMP-2, protecting BMP-2 from degradation and inhibition by BMP antagonists [226, 230], or acting as a BMP-2 coreceptor by facilitating ligand-induced receptor hetero-oligomerization [231], thereby improving BMP-2 efficacy. In contrast, some researchers have found that heparin inhibits BMP-2 osteogenic bioactivity in vitro by binding to both BMP-2 and BMP receptor (BMPR) [232] or sequestering BMP-2 on the cell surface and mediating the internalization of BMP-2 [226]. In addition, Shin Kanzaki et al. [233] found that heparin decreased the phosphorylation of Smad1/5/8 after 0.5 h culture, while prolonged periods of culture with heparin enhanced the Smad phosphorylation in BMP-2-stimulated MC3T3 cells. These findings indicate biphasic effects of heparin on BMP-2 activity and suggest that heparin has complex effects on the BMP-2 osteogenic bioactivities. Thus, the mechanism by which heparin regulates bone metabolism induced by BMP-2 remains unclear.

Despite promising results, the use of heparin to augment BMP-2 therapy may pose unwanted effects due to heparin's affinity for a wide range of proteins. For instance, heparin's ability to interact and activate antithrombin III promotes its wide use in anticoagulant therapy [234]. As the fracture hematoma acts as a reservoir for cytokines and growth factors important for bone repair [235], the use of anticoagulant compounds like heparin may be counterproductive. Furthermore, heparin treatment is known to reduce bone density and has been linked to the development of osteoporosis [236] through its pro-osteoclastic actions in vitro [237] and in vivo [236].

Like heparin, HS is a GAG sugar with repeating disaccharide units of N-glucosamine and uronic acid. Importantly, however, HS is less sulfated (40–60 %) compared to heparin (>80 %) and has a greater variability in its sulfation pattern that is critical for binding specific signaling molecules [238]. This specificity is of major biomedical significance, because HS retains the advantageous bioactivity of heparin without the adverse effects associated with its pleiotropic protein affinity.

Dombrowski et al. [239] found that exogenous application of HS to cultures of primary rat MSCs could stimulate their proliferation, leading to increased expression of osteogenic markers and enhanced bone nodule formation. Studies from Bramono et al. [240] have demonstrated that marrow-derived HS (HS5) is an effective adjuvant of BMP-2 which sustains BMP-2-dependent osteogenic activity in a similar pattern to heparin and minimizes side effects by (i) prolonging BMP-2 half-life, (ii) reducing interactions between BMP-2 with its antagonist noggin, and (iii) modulating BMP-2 distribution on the cell surface. The sulfated polysaccharides could enhance the biological activity of both homodimers and heterodimers of BMPs by continuously serving the ligands to their signaling receptors expressed on cell membranes [226]. In addition, not only the total amounts of sulfur but also its position and/or structure is important to modify the stimulatory capacity of BMP activity.

Degat et al. [241] explored the binding capacity of synthetic heparin-like dextran derivatives to BMP-2. Affinity electrophoresis analysis provided evidence that carboxy-methylated dextran polymers grafted with high amounts of benzylamide groups (named DMCB) interact with BMP-2. In vitro, DMCB dose dependently

promoted osteoblast differentiation induced by BMP-2 in C2C12 myoblasts more efficiently than heparin. In rats in vivo, DMCB also stimulated ectopic calcification mediated by BMP-2. These data indicate that dextran-based polysaccharides prolong the half-life of the growth factor and promote its biological activity.

Dose-dependent effects on BMP bioactivity were observed in both sulfated chitosan and heparin. Compared with native heparin, 2-N,6-O-sulfated chitosan (26SCS) showed much stronger simultaneous effects on the BMP-2 bioactivity at low dose. Stimulated secreted noggin protein failed to block the function of BMP-2 in the presence of 26SCS. The BMP-2 ligand bound to its receptor was enhanced by low dose of 26SCS, whereas weakened by the increasing amounts of 26SCS. Furthermore, simultaneous administration of BMP-2 and 26SCS in vivo dose dependently induced larger amounts of ectopic bone formation compared with BMP-2 alone. These findings indicated that 26SCS could be used as the synergistic factor of BMP-2 for bone regeneration [242]. Buttner et al. [243] have reported that over-sulfated CS derivatives themselves are able to induce osteogenic differentiation of hMSC, probably independent of BMP-2 and TGF-β1 signaling, and offer therefore an interesting approach for the improvement of bone healing. The enzymatic disruption of HS and CS chains on cell surface proteoglycans alters BMP and Wnt activity so as to enhance the lineage commitment and osteogenic differentiation of hMSCs [244].

Hyaluronic acid is a long polysaccharide consisting of repeating disaccharide units of N-acetylglucosamine and d-glucuronic acid and a major component of extracellular matrix (ECM) proteins in mammalian tissues. Michinao Kawano et al. [245] found that HA enhanced BMP-2 osteogenic bioactivity in MG63 cells via downregulation of BMP-2 antagonists and ERK phosphorylation. Also Jungju Kim et al. [246] found that during bone regeneration in vivo, there was a synergetic effect of bone formation with HA-based hydrogel with hMSCs and BMP-2 in the histological and immunohistochemical analysis.

8.5.5.2 Dexamethasone/Ascorbic Acid/Glycerophosphate (DAG)

Dexamethasone (DEX)/ascorbic acid/glycerophosphate (DAG) and BMP-2 are potent agents in cell proliferation and differentiation pathways. Dexamethasone (DEX) is a synthetic glucocorticoid that has been used clinically as an anti-inflammatory drug, although long-term administration of DEX or other steroids may cause or exacerbate osteoporosis. However, DEX has also been used for decades to differentiate MSCs into adipogenic [8], chondrogenic [247], and osteogenic lineages [248]. DEX affected not only the proliferation rate but also the subpopulation composition of BMSCs and MuSCs and subsequently augmented their osteogenic capacity during osteogenic differentiation. During osteogenic induction by BMP-2, DEX also markedly affected cell proliferation in both BMSCs and MuSCs. In an in vivo ectopic bone formation model, bone formation in muscle-implanted scaffolds containing dexamethasone and BMP-2 was more than twofold

higher than that in scaffolds containing BMP-2 alone. These results suggest that DEX potently enhances the osteogenic capability of BMP-2 and may thus decrease the quantity of BMP-2 required for clinical application, thereby reducing the complications caused by excessive doses of BMP-2 [249].

In Langenbach and Handschel's review [250], it has been concluded that DEX induces Runx2 expression by FHL2-/β-catenin-mediated transcriptional activation and that DEX enhances Runx2 activity by upregulation of TAZ and MKP1. Ascorbic acid leads to the increased secretion of collagen type I (Col1), which in turn leads to increased Col1/α2β1 integrin-mediated intracellular signaling. The phosphate from β-Gly serves as a source for the phosphate in hydroxyapatite and in addition influences intracellular signaling molecules. Treatment with β-glycerophosphate can result in non-osteogenic dystrophic mineralization.

Marcus et al. [251] found that DAG induced collagen I secretion from MSCs, which was further increased by the combination of DAG + BMP-2. In comparison, the collagen scaffold and the control samples showed no significant influence on collagen I secretion of MSCs. DAG stimulation of MSCs led also to a steady but not significant increase of BMP-2 level. A DAG and more, a DAG+BMP-2, stimulation increased the number of mesenchymal cells (CD105+/CD73+). To be summarized, BMP-2 enhances DAG-induced osteogenic differentiation in mesenchymal bone marrow cells. Both agents interact in various ways and can modify osteoblastic bone formation.

8.5.5.3 Extracellular Antagonists of BMP-2

BMP antagonists were found in the Spemann organizer of Xenopus embryos as a molecule to inhibit BMP binding to their receptors. They are designated as noggin and chordin. After the first discovery of the BMP antagonists, numerous BMP antagonists, which are secretory proteins with cysteine arrangement structure, were found. The extracellular BMP antagonists represent a number of secreted peptides, which bind BMPs with high affinity and prevent their interaction with their specific receptors. Antagonists such as noggin, chordin, gremlin (Grem1), and twisted gastrulation-1 (Twsg1) have been shown to inhibit BMP action in a range of different cell types and developmental stage-specific contexts.

Noggin binds to BMP-2 and BMP-4 with high affinity and to BMP-6 and BMP-7 with low affinity to prevent further action of BMP action. Chao Chen's study [252] showed that noggin suppression significantly decreased human MSC metabolism and DNA content on days 3 and 6 and decreased total protein amount on day 14. Noggin suppression also reduced the expression levels of osteoblastic genes, ALP, integrin-binding sialoprotein (IBSP), muscle segment homeobox gene (MSX2), osteocalcin (OC), osteopontin (OPN), and runt-related transcription factor-2 (Runx2). Significantly decreased enzymatic ALP activity in noggin-suppressed group was evident. Moreover, noggin suppression decreased calcium deposits by BMP-2-induced osteoblasts. Collectively, this study showed that noggin suppression decreased viability and BMP-2-induced osteogenic differentiation of human

MSCs, suggesting that noggin is stimulatory to osteogenesis of human MSCs. It has also been reported that endogenous signaling by BMP-2 controls the differentiation of embryonic stem cells into this lineage. Treatment of embryonic stem cell cultures with BMP antagonist noggin blocks this form of differentiation and induces the appearance of a novel cell type that can give rise to neural precursors [253].

Chordin as well as noggin binds BMPs and modulates BMP action. Using fluorescent labeling, BMP-2 was found to be internalized in HeLa cells via a clathrin-dependent pathway, with noggin and Grem1 increasing BMP-2 uptake. By contrast, chordin decreased BMP-2 uptake, suggesting that BMP ligand and receptor interactions on the cell surface involve cooperative binding of BMP antagonists such as noggin and Grem1 as well as other proteins such as the endoglin CD105 coreceptor [254]. Francois NK Kwong et al. [255] demonstrated that chordin knockdown accelerated early osteogenesis of MSCs and led to increased deposition of mineral at late time points. The suppression of chordin led to an increase in the bioavailability of endogenously produced BMP-2 to drive the differentiation of osteoprogenitors.

Twisted gastrulation (TSG) is expressed in the lung, thymus, and kidney and binds to BMPs to inhibit BMP action in osteoblasts. The action of TSG may be determined in cell-specific manner. Recent studies using TSG overexpression system in stromal/preosteoblasts supported antagonistic activity of TSG on BMP signaling [256]. The mechanism for agonist activity of TSG is explained by indirect action: TSG promotes cleavage of co-associator chordin to enhance to BMP activity.

Gremlin is a glycoprotein that binds and antagonizes the actions of BMP-2, BMP-4, and BMP-7. Gremlin appears to activate the extracellular regulated kinase (ERK) pathway in endothelial and tumor cells and as a consequence to have direct cellular effects. Gremlin antagonizes BMP actions on the differentiation of marrow stromal cells and on osteoblastic function in vitro. Targeted osteoblast gremlin overexpression in vivo leads to spontaneous fractures and osteopenia. The reduction in bone volume is due to a decrease in osteoblast function and in number, confirming a possible effect of this BMP antagonist in the regulation of cell growth. Gremlin and other members of the differential screening-selected gene aberrative in neuroblastoma family, such as cerberus, coco, and sclerostin, inhibit BMP as well as Wnt activity, suggesting additional potential mechanisms of action for this group of BMP antagonists [256].

8.5.5.4 Interplay Between BMP-2 and Other Cytokines

Currently, commercially available recombinant human BMP-2 (rhBMP-2) is impregnated in an absorbable collagen sponge (ACS), which is used to retain rhBMP-2 at wound sites and to permit a slow release into the extracellular milieu. In the clinic, trauma, contamination, degradation of the ACS, and exogenous BMP-2 [257, 258] can trigger an exaggerated inflammatory environment, which is characterized by the recruitment of inflammatory cells and stem cells to the implantation

site and the secretion of various inflammatory cytokines in serum, such as TNF-α, IL-1β, IL-8, and IL-6 [259]. Recently, the use of anti-inflammatory drugs such as bone morphogenetic protein-binding peptide [260], triptolide-micelles [261], and corticosteroids [262] was proved to reduce the inflammatory response and subsequently enhance the osteoinductive capacity of BMP-2. These results indicate that the low osteoinductive efficacy of BMP-2 may be a result of the exaggerated inflammatory environment. Huang's group has reported that TNF-α/IL-1β- and BMP-2-activated p38 and ERK1/2 signaling have opposing roles that converge on Runx2 to regulate osteoblastic differentiation [263]. The elucidation of these mechanisms may hasten the development of new strategies and improve the osteoinductive efficacy of BMP-2 in the clinic to enhance osteoblastic differentiation and bone formation. Their recent studies have demonstrated that synergy between IL-6 and sIL-6R promotes the cell surface translocation of BMPRIA and maintains the stability of BMPRI A expression, leading to enhanced BMP-2-/ACS-induced bone regeneration [264].

In addition, the combined release of stromal cell-derived factor-1 (SDF-1) and BMP-2 enhanced the recruitment of osteogenic cells and angiogenesis, resulting in the synergistic effect on bone regeneration [265]. Kleinschmidt et al. [266] produced a mutant growth and differentiation factor-5 (GDF-5) protein BB-1 which enhanced heterotopic bone formation in mice. Rabbit radius defects treated with a BB-1-coated collagen carrier healed earlier and with increased bone volume compared to BMP-2 and GDF-5 according to in vivo micro-CT follow-up. While BMP-2 callus often remained spongy, BB-1 supported earlier corticalis and marrow cavity formation, showing no pseudojoint persistence like with GDF-5. Thus, by combining positive angiogenic and osteogenic features of GDF-5 and BMP-2, only BB-1 restored the natural bone architecture within 12 weeks, rendering this promising growth factor variant especially promising for long bone regeneration.

TGF-βs and FGF-2, FGF-4, and FGF-6 have been proven to be inducers of osteoblast proliferation (a higher extent for TGF-β and FGF-2) and inhibitors of ALP activity and osteoblast mineralization, indicating potential application for in vitro bone growth induction in bone tissue engineering. To determine how fibroblast growth factor-2 (FGF-2) affects the BMP signaling pathway during BMP-induced ectopic bone formation, Nakamura et al. [267] implanted type I collagen disks containing constant amounts of BMP-2 (5 μg) onto the back muscles of adult male mice and confirmed that low doses of FGF-2 increased ectopic bone formation in vivo and high doses inhibited bone formation. Northern and/or Western blots of recovered muscle from the in vivo experiment and treated muscle-derived primary culture cells from the in vitro experiment revealed that low doses of FGF-2, but not high doses, increased the expression of BMP receptor (BMPR)IB, phosphorylated Smad1, noggin, and osteocalcin. It is further indicated that low-dose FGF-2 may facilitate BMP-2-induced ectopic bone formation by altering the expression of BMPRs on the surface of bone-forming progenitor cells.

In a summary, there is accumulating evidence to demonstrate that stem cell fate could be regulated by the chemical/mechanical properties of matrix materials, topography, geometry and hierarchy structure, and genetic clues delivered. It is

obvious that stem cells have the ability to sense the microenvironment and give the response to the surroundings in a different manner. By well regulating the factors discussed above, the stem cell fates could be potentially directed to the desirable way for medical applications. However, the microenvironments surrounding the stem cells in vivo are integrated and complicated. Besides the factors we have discussed in this chapter, MSCs in vivo are also composed of microenvironmental cells that nurture stem cells and enable them to maintain tissue homeostasis, such as potential of hydrogen (pH), ionic concentration, cytokines secreted by immune cells, oxygen, and biomechanics introduced by implants. Numerous attempts have been made to reveal the interaction between the stem cells and microenvironment in vivo [268–270]. However, this field of research is still developing, but there is great promise that stem cell fate could be controlled by designing advanced biomaterials and intelligent surfaces, which are responsive to their environment to fulfill bone healing demands.

8.6 Future Perspectives

Nanotopography and micro-/nano-hierarchy structure have shown to offer important clues for controlling specific stem cell responses. Using these nanoscale features of biomaterials to guide stem cell fate holds great promise for bone repair and regeneration. Furthermore, micro-/nano-hierarchy structure could be designed on a single biomaterial to induce different stem cell responses by creating gradient pores, matching further scope for therapeutic applications. The main challenges in using these nanoscale features in the clinical applications are the precise control of nanostructures for large-scale production. Therefore, it is necessary to make more attempts for the feasible and affordable technologies for large-scale production.

The immobilization of growth factors (i.e., rhBMP-2) or other bioactive agents to biomaterials has been confirmed to be a successful strategy in directing stem cell differentiation. Many strategies have been applied for effectively immobilizing growth factors with sustained releasing, directing stem cell fate. However, further studies are required for successful clinical translation. A better control of the bioactivity, orientation, and spacing and stability of the growth factor must be defined to achieve the desired control of stem cell differentiation.

Another important issue is the long-term effects of biomaterials, the growth factors, and functional groups on the response of the stem cells/microenvironment in vivo. There is a great need to determine the better regulation of the inductive chemical clues for the desired response in a specific application. Since the cells other than stem cells in vivo would response to these material clues, further investigation needs to be done to ensure the wanted functionalities without negative effects in vivo.

Many studies have investigated the effect of different factors on stem cell behavior. However, it becomes a big challenge to take into account more factors and even all possible parameters for guiding the stem cell fate. Advanced technology and

more testing model systems need to develop for mimicking the microenvironments including stem cells, other surrounding cells, biomaterials, etc. All these knowledge and results allow us to better understand the intrinsic function and reparative properties of the stem cells and offer the great potential for more economical and clinically effective cell therapies for future medical applications.

References

1. Thomson JA, Itskovitz-Eldor J, Shapiro SS, et al. Blastocysts embryonic stem cell lines derived from human. Science. 1998;282(5391):1145–7.
2. Becker AJ, McCulloch EA, Till JE. Cytological demonstration of the clonal nature of spleen colonies derived from transplanted mouse marrow cells. Nature. 1963;197:452–4.
3. http://stemcells.nih.gov/staticresources/info/basics/.
4. Sundelacruza S, Kaplana DL. Stem cell- and scaffold-based tissue engineering approaches to osteochondral regenerative medicine. Semin Cell Dev Biol. 2009;20(6):646–55.
5. Dawson JI, Oreffo ROC. Bridging the regeneration gap: stem cells, biomaterials and clinical translation in bone tissue engineering. Arch Biochem Biophys. 2008;473:124–31.
6. Rao BM, Zandstra PW. Culture development for human embryonic stem cell propagation: molecular aspects and challenges. Curr Opin Biotechnol. 2005;16:568–76.
7. Moore KA, Lemischka IR. Stem cells and their niches. Science. 2006;311:1880–5.
8. Pittenger MF, Mackay AM, Beck SC, et al. Multilineage potential of adult human mesenchymal stem cells. Science. 1999;284(5411):143–7.
9. Ying QL, Nichols J, Chambers I, Smith A. BMP induction of Id proteins suppresses differentiation and sustains embryonic stem cell self-renewal in collaboration with STAT3. Cell. 2003;115(3):281–92.
10. Knoepfler PS. Deconstructing stem cell tumorigenicity: a roadmap to safe regenerative medicine. Stem Cells. 2009;27:1050–6.
11. Lodi D, Iannitti T, Palmieri B. Stem cells in clinical practice: applications and warnings. J Exp Clin Cancer Res. 2011;30(1):9.
12. Wang S, Qu X, Zhao R. Clinical applications of mesenchymal stem cells. J Hematol Oncol. 2012;5(19):1–9.
13. Branch MJ, Hashmani K, Dhillon P, et al. Mesenchymal stem cells in the human corneal limbal stroma. Invest Ophthalmol Vis Sci. 2012;53(9):5109–16.
14. Brighton CT, Hunt RM. Early histologic and ultrastructural changes in microvessels of periosteal callus. J Orthop Trauma. 1997;11(4):244–53.
15. Gebler A, Zabel O, Seliger B. The immunomodulatory capacity of mesenchymal stem cells. Trends Mol Med. 2012;18(2):128–34.
16. Zaman WS, Makpol S, Sathapan S, Chua KH. Long-term in vitro expansion of human adipose-derived stem cells showed low risk of tumourigenicity. J Tissue Eng Regen Med. 2014;8:67–76.
17. Murphy MB, Moncivais K, Caplan A. Mesenchymal stem cells: environmentally responsive therapeutics for regenerative medicine. Exp Mol Med. 2013;45:e54.
18. Tanna T, Sachan V. Mesenchymal stem cells: potential in treatment of neurodegenerative diseases. Curr Stem Cell Res Ther. 2014;9(6):513–21.
19. Lutolf MP, Hubbell JA. Synthetic biomaterials as instructive extracellular microenvironments for morphogenesis in tissue engineering. Nat Biotech. 2005;23(1):47–55.
20. Langer R, Tirrell DA. Designing materials for biology and medicine. Nature. 2004;428(6982):487–92.

21. Bao G, Suresh S. Cell and molecular mechanics of biological materials. Nat Mater. 2003;2(11):715–25.
22. Moghaddam MJ, Matsuda T. Molecular design of three-dimensional artificial extracellular matrix: photosensitive polymers containing cell adhesive peptide. J Polym Sci Part A: Polym Chem. 1993;31(6):1589–97.
23. Badylak SF. Xenogeneic extracellular matrix as a scaffold for tissue reconstruction. Transpl Immunol. 2004;12:367–77.
24. Freeman S. Biological science. 2nd ed. New Jersey: Pearson Prentice Hall. Inc; 2005.
25. Trappmann B, Gautrot JE, Connelly JT, et al. Extracellular-matrix tethering regulates stem-cell fate. Nat Mater. 2012;11(7):642–9.
26. Badylak SF, Freytes DO, Gilbert TW. Reprint of: extracellular matrix as a biological scaffold material: structure and function. Acta Biomater. 2015;23:S17–26.
27. Grazyna K, Victoria K-B. Galactose-specific receptors on liver cells. I. Hepatocyte and liver macrophage receptors differ in their membrane anchorage. Biochim Biophys Acta. 1985;847(1):108–14.
28. Rape AD, Zibinsky M, Murthy N, Kumar S. A synthetic hydrogel for the high-throughput study of cell-ECM interactions. Nat Commun. 2015;6:8129.
29. Navaro Y, Bleich-Kimelman N, Hazanov L, et al. Matrix stiffness determines the fate of nucleus pulposus–derived stem cells. Biomaterials. 2015;49:68–76.
30. Mann BK, Gobin AS, Tsai AT, et al. Smooth muscle cell growth in photopolymerized hydrogels with cell adhesive and proteolytically degradable domains: synthetic ECM analogs for tissue engineering. Biomaterials. 2001;22(22):3045–51.
31. Cambria E, Renggli K, Ahrens CC, et al. Covalent modification of synthetic hydrogels with bioactive proteins via sortase-mediated ligation. Biomacromolecules. 2015;16(8):2316–26.
32. Woo KM, Chen VJ, Ma PX. Nano-fibrous scaffolding architecture selectively enhances protein adsorption contributing to cell attachment. J Biomed Mater Res A. 2003;67(2):531–7.
33. Hersel U, Dahmen C, Kessler H. RGD modified polymers: biomaterials for stimulated cell adhesion and beyond. Biomaterials. 2003;24(24):4385–415.
34. Girotti A, Reguera J, Rodríguez-Cabello JC, et al. Design and bioproduction of a recombinant multi (bio) functional elastin-like protein polymer containing cell adhesion sequences for tissue engineering purposes. J Mater Sci Mater Med. 2004;15(4):479–84.
35. Loo Y, Lakshmanan A, Ni M, et al. Peptide bioink: self-assembling nanofibrous scaffolds for three-dimensional organotypic cultures. Nano Lett. 2015;15(10):6919–25.
36. Bhowmick S, Scharnweber D, Koul V. Co-cultivation of keratinocyte-human mesenchymal stem cell (hMSC) on sericin loaded electrospun nanofibrous composite scaffold (cationic gelatin/hyaluronan/chondroitin sulfate) stimulates epithelial differentiation in hMSCs: in vitro study. Biomaterials. 2016;88:83–96.
37. Liu Y, Shu XZ, Prestwich GD. Osteochondral defect repair with autologous bone marrow-derived mesenchymal stem cells in an injectable, in situ, cross-linked synthetic extracellular matrix. Tissue Eng. 2006;12(12):3405–16.
38. Khetan S, Guvendiren M, Legant WR, et al. Degradation-mediated cellular traction directs stem cell fate in covalently crosslinked three-dimensional hydrogels. Nat Mater. 2013;12(5):458–65.
39. Kraehenbuehl TP, Zammaretti P, Van der Vlies AJ, et al. Three-dimensional extracellular matrix-directed cardioprogenitor differentiation: systematic modulation of a synthetic cell-responsive PEG-hydrogel. Biomaterials. 2008;29(18):2757–66.
40. Geiger B, Bershadsky A, Pankov R, Yamada KM. Transmembrane crosstalk between the extracellular matrix cytoskeleton crosstalk. Nat Rev Mol Cell Biol. 2001;2:793–805.
41. Huang S, Ingber DE. The structural and mechanical complexity of cell-growth control. Nat Cell Biol. 1999;1:E131–8.
42. Reilly GC, Engler AJ. Intrinsic extracellular matrix properties regulate stem cell differentiation. J Biomech. 2010;43:55–62.
43. Discher DE, Mooney DJ, Zandstra PW. Growth factors, matrices, and forces combine and control stem cells. Science. 2009;324:1673–7.

44. Vogel V, Sheetz M. Local force and geometry sensing regulate cell functions. Nat Rev Mol Cell Biol. 2006;7:265–75.
45. Ana BF, Stefanie GL, Markus R, et al. Differential regulation of osteogenic differentiation of stem cells on surface roughness gradients. Biomaterials. 2014;35:9023–32.
46. Elias CN, Oshida Y, Lima JHC, Muller CA. Relationship between surface properties (roughness, wettability and morphology) of titanium and dental implant removal torque. J Mech Behav Biomed Mater. 2008;1(3):234–42.
47. Hefti T, Frischherz M, Spencer ND, et al. A comparison of osteoclast resorption pits on bone with titanium and zirconia surfaces. Biomaterials. 2010;31(28):7321–31.
48. Yeo A, Wong WJ, Khoo HH, Teoh SH. Surface modification of PCL-TCP scaffolds improve interfacial mechanical interlock and enhance early bone formation: an in vitro and in vivo characterization. J Biomed Mater Res A. 2010;92(1):311–21.
49. Liu Q, Wang W, Zhang L, et al. Involvement of N-cadherin/b-catenin interaction in the micro/nanotopography induced indirect mechanotransduction. Biomaterials. 2014;35:6206–18.
50. Seo C, Jeong H, Feng Y, et al. Micropit surfaces designed for accelerating osteogenic differentiation of murine mesenchymal stem cells via enhancing focal adhesion and actin polymerization. Biomaterials. 2014;35:2245–52.
51. Wang PY, Li WT, Yu J, Tsai WB. Modulation of osteogenic, adipogenic and myogenic differentiation of mesenchymal stem cells by submicron grooved topography. J Mater Sci Mater Med. 2012;23(12):3015–28.
52. Wang P-Y, Yu J, Lin J-H, Tsai W-B. Modulation of alignment, elongation and contraction of cardiomyocytes through a combination of nanotopography and rigidity of substrates. Acta Biomater. 2011;7:3285–93.
53. Yim EK, Darling EM, Kulangara K, et al. Nanotopography- induced changes in focal adhesions, cytoskeletal organization, and mechanical properties of human mesenchymal stem cells. Biomaterials. 2010;31:1299–306.
54. Kilian KA, Bugarija B, Lahn BT, Mrksich M. Geometric cues for directing the differentiation of mesenchymal stem cells. Proc Natl Acad Sci U S A. 2010;107:4872–7.
55. Salasznyk RM, Klees RF, Williams WA, et al. Focal adhesion kinase signaling pathways regulate the osteogenic differentiation of human mesenchymal stem cells. Exp Cell Res. 2007;313:22–37.
56. Tang W, Lin D, Yu YM, et al. Bioinspired trimodal macro/micro/nano-porous scaffolds loading rhBMP-2 for complete regeneration of critical size bone defect. Acta Biomater. 2016;32:309–23.
57. Gwendolen CR, Adam J. E. Intrinsic extracellular matrix properties regulate stem cell differentiation. J Biomech. 2010;43:55–62.
58. Dalby MJ, Gadegaard N, Riehle MO, et al. Investigating filopodia sensing using arrays of defined nano-pits down to 35 nm diameter in size. Int J Biochem Cell Biol. 2004;36(10):2005–15.
59. Yim EK, Reano RM, Pang SW, et al. Nanopattern induced changes in morphology and motility of smooth muscle cells. Biomaterials. 2005;26(26):5405–13.
60. Yim EK, Pang SW, Leong KW. Synthetic nanostructures inducing differentiation of human mesenchymal stem cells into neuronal lineage. Exp Cell Res. 2007;313(9):1820–9.
61. Doyle AD, Wang FW, Matsumoto K, Yamada KM. One-dimensional topography underlies three-dimensional fibrillar cell migration. J Cell Biol. 2009;184(4):481–90.
62. Dalby MJ, Gadegaard N, Tare R, et al. The control of human mesenchymal cell differentiation using nanoscale symmetry and disorder. Nat Mater. 2007;6:997–1003.
63. Zhao L, Liu L, Wu Z, et al. Effects of micropitted/nanotubular titania topographies on bone mesenchymal stem cell osteogenic differentiation. Biomaterials. 2012;33:2629–41.
64. Zhao L, Mei S, Chu PK, Zhang Y, Wu Z. The influence of hierarchical hybrid micro/nanotextured titanium surface with titania nanotubes on osteoblast functions. Biomaterials. 2010;31:5072–82.
65. Liu Y, Manjubala I, Roschger P, et al. Characteristics of mineral particles in the callus during fracture healing in a sheep model. Calcif Tissue Int. 2008;82:S69–70.
66. Ramanujan S, Pluen A, McKee TD, et al. Diffusion and convection in collagen gels: implications for transport in the tumor interstitium. Biophys J. 2002;83:1650–60.

67. Sabetrasekh R, Tiainen H, Lyngstadaas SP, et al. A novel ultra-porous titanium dioxide ceramic with excellent biocompatibility. J Biomater Appl. 2011;25(6):559–80.
68. Wen JH, Vincent LG, Fuhrmann A, et al. Interplay of matrix stiffness and protein tethering in stem cell differentiation engler. Nat Mater. 2014;13:979–87.
69. Cyster L, Grant D, Howdle S, et al. The influence of dispersant concentration on the pore morphology of hydroxyapatite ceramics for bone tissue engineering. Biomaterials. 2005;26:697–702.
70. Edwards SL, Werkmeister JA. Mechanical evaluation and cell response of woven polyetheretherketone scaffolds. J Biomed Mater Res A. 2012;100(12):3326–31.
71. Freyman TM, Yannas IV, Gibson LJ. Cellular materials as porous scaffolds for tissue engineering. Prog Mater Sci. 2001;46:273–82.
72. Kumara A, Nunea KC, Murra LE, Misra RDK. Biocompatibility and mechanical behavior of three-dimensional scaffolds for biomedical devices: process–structure–property paradigm. Int Mat Rev. 2016;16(1):20–40.
73. Sun T, Donoghue PS, Higginson JR, et al. The interactions of astrocytes and fibroblasts with defined pore structures in static and perfusion cultures. Biomaterials. 2011;32(8):2021–31.
74. Lu JX, Flautre B, Anselme K, et al. Role of interconnections in porous bioceramics on bone recolonization in vitro and in vivo. J Mater Sci Mater Med. 1999;10(2):111–20.
75. Mandal BB, Kundu SC. Cell proliferation and migration in silk fibroin 3D scaffolds. Biomaterials. 2009;30(15):2956–65.
76. Berger M, Probst F, Schwartz C, et al. A concept for scaffold-based tissue engineering in alveolar cleft osteoplasty. J Craniomaxillofac Surg. 2015;43(6):830–6.
77. Nam J, Johnson J, Lannutti JJ, Agarwala S. Modulation of embryonic mesenchymal progenitor cell differentiation via control over pure mechanical modulus in electrospun nanofibers. Acta Biomater. 2011;7(4):1516–24.
78. Lien SM, Ko LY, Huang TJ. Effect of pore size on ECM secretion and cell growth in gelatin scaffold for articular cartilage tissue engineering. Acta Biomater. 2009;5(2):670–9.
79. Loh QL, Choong C. Three-dimensional scaffolds for tissue engineering applications: role of porosity and pore size. Tissue Eng Part B Rev. 2013;19(6):485–502.
80. Akay G, Birch MA, Bokhari MA. Microcellular polyHIPE polymer supports osteoblast growth and bone formation in vitro. Biomaterials. 2004;25(18):3991–4000.
81. Ahn G, Kim Y, Lee S-W, et al. Effect of heterogeneous multi-layered gelatin scaffolds on the diffusion characteristics and cellular activities of preosteoblasts. Macromol Res. 2014;22:99–107.
82. Im GI, Ko JY, Lee JH. Chondrogenesis of adipose stem cells in a porous polymer scaffold: influence of the pore size. Cell Transplant. 2012;21(11):2397–405.
83. Carlier A, van Gastel N, Geris L, et al. Size does matter: an integrative in vivo-in silico approach for the treatment of critical size bone defects. PLoS Comput Biol. 2014;10(11):e1003888.
84. Mygind T, Stiehler M, Baatrup A, et al. Mesenchymal stem cell ingrowth and differentiation on coralline hydroxyapatite scaffolds. Biomaterials. 2007;28:1036–104.
85. Akhmanova M, Osidak E, Domogatsky S, et al. Physical, spatial, and molecular aspects of extracellular matrix of in vivo niches and artificial scaffolds relevant to stem cells research. Stem Cells Int. 2015;2015:167025.
86. Lee JH, Lee SJ, Khang G, Lee HB. Interaction of fibroblasts on polycarbonate membrane surfaces with different micropore sizes and hydrophilicity. J Biomater Sci Polym Ed. 1999;10(3):283–94.
87. Guo H, Su J, Wei J, Kong H, Liu C. Biocompatibility and osteogenicity of degradable Ca-deficient hydroxyapatite scaffolds from calcium phosphate cement for bone tissue engineering. Acta Biomater. 2009;5(1):268–78.
88. Habibovic P, Yuan H, van der Valk CM, et al. 3D microenvironment as essential element for osteoinduction by biomaterials. Biomaterials. 2005;26(17):3565–75.

89. Kruyt MC, Wilson CE, de Bruijn JD, et al. The effect of cell-based bone tissue engineering in a goat transverse process model. Biomaterials. 2006;27(29):5099–106.
90. Chan CK, Kumar TS, Liao S, et al. Biomimetic nanocomposites for bone graft applications. Nanomedicine (Lond). 2006;1(2):177–88.
91. Prall WC, Haasters F, Heggebö J, et al. Mesenchymal stem cells from osteoporotic patients feature impaired signal transduction but sustained osteoinduction in response to BMP-2 stimulation. Biochem Biophys Res Commun. 2013;440(4):617–22.
92. Peyton SR, Kalcioglu ZI, Cohen JC, et al. Marrow-derived stem cell motility in 3D synthetic scaffold is governed by geometry along with adhesivity and stiffness. Biotechnol Bioeng. 2011;108(5):1181–93.
93. Perez RA, Mestres G. Role of pore size and morphology in musculo-skeletal tissue regeneration. Mater Sci Eng C Mater Biol Appl. 2016;61:922–39.
94. Kim JS, Cha JK, Cho AR, et al. Acceleration of bone regeneration by BMP-2-loaded collagenated biphasic calcium phosphate in rabbit sinus. Clin Implant Dent Relat Res. 2015;17(6):1103–13.
95. Lan Levengood SK, Polak SJ, Poellmann MJ, et al. The effect of BMP-2 on micro- and macroscale osteointegration of biphasic calcium phosphate scaffolds with multiscale porosity. Acta Biomater. 2010;6(8):3283–91.
96. Yanagisawa T, Tsuneo S, Shimizu T, Kuroda K, Kato C. The preparation of alkyltrimethylammonium-kanemite complexes and their conversion to microporous materials. Bull Chem Soc Jpn. 1990;63:988–92.
97. Simovic S, Ghouchi-Eskandar N, Sinn AM, Losic D, Prestidge CA. Silica materials in drug delivery applications. Curr Drug Discov Technol. 2011;8(3):269–76.
98. Izquierdo-Barbaa I, Ruiz-Gonzálezb L, Doadrioa JC. Tissue regeneration: a new property of mesoporous materials. Solid State Sci. 2005;8:983–9.
99. Gough JE, Notingher I, Hench LL. Osteoblast attachment and mineralized nodule formation on rough and smooth 45S5 bioactive glass monoliths. J Biomed Mater Res A. 2004;68(4):640–50.
100. Yun HS, Kim SH, Khang D, et al. Biomimetic component coating on 3D scaffolds using high bioactivity of mesoporous bioactive ceramics. Int J Nanomed. 2011;6:2521–31.
101. Zhu Y, Kaskel S. Comparison of the in vitro bioactivity and drug release property of mesoporous bioactive glasses (MBGs) and bioactive glasses (BGs) scaffolds. Microporous Mesoporous Mater. 2009;118(1–3):176–82.
102. Termine JD, Eanes ED. Comparative chemistry of amorphous and apatitic calcium phosphate preparations. Calcif Tissue Res. 1972;10(3):171–97.
103. Xia W, Chang J. Preparation, in vitro bioactivity and drug release property of well-ordered mesoporous 58S bioactive glass. J Non-Cryst Solids. 2008;354(12):1338–41.
104. Kaur G, Pickrell G, Sriranganathan N, Kumar V, Homa D. Review and the state of the art: sol-gel and melt quenched bioactive glasses for tissue engineering. J Biomed Mater Res B Appl Biomater. 2015. doi:10.1002/jbm.b.33443.
105. Horcajada P, Ramila A, Boulahya K, et al. Bioactivity in ordered mesoporous materials. Solid State Sci. 2004;X6:1295–300.
106. Aghaeia H, Nourbakhshb AA, Karbasic S, et al. Investigation on bioactivity and cytotoxicity of mesoporous nano-composite MCM-48/hydroxyapatite for ibuprofen drug delivery. Ceram Int. 2014;40(5):7355–62.
107. Yan X, Deng H, Huang X, et al. Mesoporous bioactive glasses. I. Synthesis and structural characterization. J Non-Cryst Solids. 2015;10:3209–17.
108. Bae WC, Law AW, Amiel D, Sah RL. Sensitivity of indentation testing to step-off edges and interface integrity in cartilage repair. Ann Biomed Eng. 2004;32(3):360–9.
109. Zhang H, Landmann F, Zahreddine H, et al. A tension-induced mechanotransduction pathway promotes epithelial morphogenesis. Nature. 2011;471(7336):99–103.
110. Okolicsanyi RK, Griffiths LR, Haupt LM. Mesenchymal stem cells, neural lineage potential, heparan sulfate proteoglycans and the matrix. Dev Bio. 2014;388(1):1–10.

111. Eroshenko N, Ramachandran R, Yadavalli VK, Rao RR. Effect of substrate stiffness on early human embryonic stem cell differentiation. J Biol Eng. 2013;7(1):7.
112. Hosseinkhani M, Shirazi R, Rajaei F, et al. Engineering of the embryonic and adult stem cell niches. Iran Red Crescent Med J. 2013;15(2):83–92.
113. Zhao W, Li X, Liu X, Zhang N, Wen X. Effects of substrate stiffness on adipogenic and osteogenic differentiation of human mesenchymal stem cells. Mater Sci Eng C Mater Biol Appl. 2014;40:316–23.
114. Yilgor P, Sousa RA, Reis RL, et al. 3D plotted PCL scaffolds for stem cell based bone tissue engineering. Macromol Symp. 2008;269:92–9.
115. Her GJ, Wu HC, Chen MH, et al. Control of three-dimensional substrate stiffness to manipulate mesenchymal stem cell fate toward neuronal or glial lineages. Acta Biomater. 2013;9(2):5170–80.
116. Wang L-S, Boulaire J, Chan PPY, Chung JE, Kurisawa M. The role of stiffness of gelatin-hydroxyphenylpropionic acid hydrogels formed by enzyme-mediated crosslinking on the differentiation of human mesenchymal stem cell. Biomaterials. 2010;31(33):8608–16.
117. Wang P-Y, Tsai W-B, Voelcker NH. Screening of rat mesenchymal stem cell behaviour on polydimethylsiloxane stiffness gradients. Acta Biomater. 2012;8(2):519–30.
118. Flanagan LA, Ju YE, Marg B, et al. Janmey Neurite branching on deformable substrates. Neuroreport. 2002;13:2411–5.
119. Kim TH, An DB, Oh SH, et al. Creating stiffness gradient polyvinyl alcohol hydrogel using a simple gradual freezing-thawing method to investigate stem cell differentiation behaviors. Biomaterials. 2015;40:51–60.
120. Li Z, Gong Y, Sun S, et al. Differential regulation of stiffness, topography, and dimension of substrates in rat mesenchymal stem cells. Biomaterials. 2013;34(31):7616–25.
121. Rowlands AS, George PA, Cooper-White JJ. Directing osteogenic and myogenic differentiation of MSCs: interplay of stiffness and adhesive ligand presentation. Am J Physiol Cell Physiol. 2008;295(4):C1037–44.
122. Evans ND, Minelli C, Gentleman E, et al. Substrate stiffness affects early differentiation events in embryonic stem cells. Eur Cell Mater. 2009;18:1–13.
123. Tse JR, Engler AJ. Stiffness gradients mimicking in vivo tissue variation regulate mesenchymal stem cell fate. PLoS ONE. 2011;6(1):e15978.
124. Ghosh K, Pan Z, Guan E, et al. Cell adaptation to a physiologically relevant ECM mimic with different viscoelastic properties. Biomaterials. 2007;28(4):671–9.
125. Isenberg BC, Dimilla PA, Walker M, Kim S, Wong JY. Vascular smooth muscle cell durotaxis depends on substrate stiffness gradient strength. Biophys J. 2009;97(5):1313–22.
126. Du J, Chen X, Liang X, et al. Integrin activation and internalization on soft ECM as a mechanism of induction of stem cell differentiation by ECM elasticity. Proc Natl Acad Sci U S A. 2011;108(23):9466–71.
127. Shih YR, Tseng KF, Lai HY, Lin CH, Lee OK. Matrix stiffness regulation of integrin-mediated mechanotransduction during osteogenic differentiation of human mesenchymal stem cells. J Bone Miner Res. 2011;26(4):730–8.
128. Yeung T, Georges PC, Flanagan LA, et al. Effects of substrate stiffness on cell morphology, cytoskeletal structure, and adhesion. Cell Motil Cytoskeleton. 2005;60:24–34.
129. Jiang L, Sun Z, Chen X, et al. Cells sensing mechanical cues: stiffness influences the lifetime of cell-extracellular matrix interactions by affecting the loading rate. ACS Nano. 2016;10(1):207–17.
130. Albro MB, Chahine NO, Li R, et al. Dynamic loading of deformable porous media can induce active solute transport. J Biomech. 2008;41:3152–7.
131. García AJ. Get a grip: integrins in cell-biomaterial interactions. Biomaterials. 2005;26:7525–9.
132. Berrier AL, Yamada KM. Cell-matrix adhesion. J Cell Physiol. 2007;213:565–73.
133. Hynes RO. Integrins: bidirectional, allosteric signaling machines. Cell. 2002;110:673–87.

134. García AJ, Boettiger D. Integrin-fibronectin interactions at the cell-material interface: initial integrin binding and signaling. Biomaterials. 1999;20:2427–33.
135. Dumbauld DW, Michael KE, Hanks SK, García AJ. Focal adhesion kinase-dependent regulation of adhesive forces involves vinculin recruitment to focal adhesions. Biol Cell. 2010;102:203–13.
136. Keselowsky BG, Collard DM, Garcia AJ. Surface chemistry modulates fibronectin conformation and directs integrin binding and specificity to control cell adhesion. J Biomed Mater Res A. 2003;66:247–59.
137. Galbraith CG, Yamada KM, Sheetz MP. The relationship between force and focal complex development. J Cell Biol. 2002;159:695–705.
138. ter Brugge PJ, Torensma R, De Ruijter JE, Figdor CG, Jansen JA. Modulation of integrin expression on rat bone marrow cells by substrates with different surface characteristics. Tissue Eng. 2002;8:615–26.
139. Khang D, Kim SY, Liu-Snydera P, et al. Enhanced fibronectin adsorption on carbon nanotube/poly(carbonate) urethane: independent role of surface nano-roughness and associated surface energy. Biomaterials. 2007;28:4756–68.
140. Rodriguez JP, Gonzalez M, Rios S, Cambiazo V. Cytoskeletal organization of human mesenchymal stem cells (MSC) changes during their osteogenic differentiation. J Cell Biochem. 2004;93:721–31.
141. Engler AJ, Sen S, Sweeney HL, Discher DE. Matrix elasticity directs stem cell lineage specification. Cell. 2006;126:677–89.
142. Khang D, Choi J, Im YM, et al. Role of subnano-, nano and submicron-surface features on osteoblast differentiation of bone marrow mesenchymal stem cells. Biomaterials. 2012;33:5997–6007.
143. Leitinger B, McDowall A, Stanley P, Hogg N. The regulation of integrin function by Ca^{2+}. Biochim Biophys Acta. 2000;1498:91–8.
144. Baneres JL, Roquet F, Martin A, Parello J. A minimized human integrin alpha 5 beta 1 that retains ligand recognition. J Biol Chem. 2000;275:5888–903.
145. Grzesiak J, Davis G, Kirchhofer D, Pierschbacher M. Regulation of alpha 2 beta 1-mediated fibroblast migration on type I collagen by shifts in the concentrations of extracellular Mg^{2+} and Ca^{2+}. J Cell Biol. 1992;117(5):1109–17.
146. Zhang J, Ma XY, Lin D, et al. Magnesium modification of a calcium phosphate cement alters bone marrow stromal cell behavior via an integrin-mediated mechanism. Biomaterials. 2015;53:251–64.
147. Shie MY, Ding SJ. Integrin binding and MAPK signal pathways in primary cell responses to surface chemistry of calcium silicate cements. Biomaterials. 2013;34:6589–606.
148. Curran JM, Chen R, Hunt JA. Controlling the phenotype and function of mesenchymal stem cells in vitro by adhesion to silane-modified clean glass surfaces. Biomaterials. 2005;34:7057–67.
149. Viswanathan P, Chirasatitsin S, Ngamkham K, et al. Cell instructive microporous scaffolds through interface engineering. J Am Chem Soc. 2012;134(49):20103–9.
150. Dee KC, Anderson TT, Bizios R. Design and function of novel osteoblast-adhesive peptides for chemical modification of biomaterials. J Biomed Mater Res. 1998;40:371–7.
151. Rezania A, Johnson R, Lefkow AR, Healy KE. Bioactivation of metal oxide surfaces. 1. Surface characterization and cell response. Langmuir. 1999;15:6931–9.
152. Xiao S-J, Textir M, Spencer ND. Covalent attachment of cell-adhesive (Arg-Gly-Asp)-containing peptides to titanium surface. Langmuir. 1998;14:5507–16.
153. Massia SP, Hubbell JA. Covalently attached GRGD on polymer surfaces promotes biospecific adhesion of mammalian cells. Ann N Y Acad Sci. 1990;589:261–70.
154. Sugawara T, Matsuda T. Photochemical surface derivatization of a peptide containing Arg-Gly-Asp (RGD). J Biomed Mater Res. 1995;29:1047–52.
155. Houseman BT, Mrksich M. The microenvironment of immobilized Arg-Gly-Asp peptides is an important determinant of cell adhesion. Biomaterials. 2001;22:943–55.

156. Bearinger JP, Castner DG, Healy KE. Biomolecular modification of p(AAm-co-EG/AA) IPNs supports osteoblast adhesion and phenotypic expression. J Biomater Sci Polym Ed. 1998;9:629–52.
157. Kao WJ, Lee D, Schense JC, Hubbell JA. Fibronectin modulates macrophage adhesion and FBGC formation: the role of RGD, PHSRN, and PRRARV domains. J Biomed Mater Res. 2000;55:79–88.
158. Yang F, Williams CG, Wang DA, et al. The effect of incorporating RGD adhesive peptide in polyethylene glycol diacrylate hydrogel on osteogenesis of bone marrow stromal cells. Biomaterials. 2005;26(30):5991–8.
159. Cao FY, Yin WN, Fan JX, et al. Evaluating the effects of charged oligopeptide motifs coupled with rgd on osteogenic differentiation of mesenchymal stem cells. ACS Appl Mater Interfaces. 2015;7(12):6698–705.
160. Chien HW, Fu SW, Shih AY, Tsai WB. Modulation of the stemness and osteogenic differentiation of human mesenchymal stem cells by controlling RGD concentrations of poly(carboxybetaine) hydrogel. Biotech J. 2014;9(12):1613–23.
161. Wang X, Li SY, Yan C, Liu P, Ding JD. Fabrication of RGD micro/nanopattern and corresponding study of stem cell differentiation. Nano Lett. 2015;15(3):1457–67.
162. Brandt K, Wolff MF, Salikov V, et al. A novel method for a multi-level hierarchical composite with brick-and-mortar structure. Sci Rep. 2013;3:2322.
163. Thiagarajan G, Deshmukh K, Wang Y, et al. Nano finite element modeling of the mechanical behavior of biocomposites using multi-scale (virtual internal bond) material models. J Biomed Mater Res A. 2007;83(2):332–44.
164. Dhandayuthapani B, Yoshida Y, Maekawa T, Kuma DS. Polymeric scaffolds in tissue engineering application: a review. Int J Polym Sci. 2011. Article ID 290602. 19 pages.
165. Kim K, Yeatts A, Dean D, Fisher JP. Stereolithographic bone scaffold design parameters: osteogenic differentiation and signal expression. Tissue Eng Part B Rev. 2010;16(5):523–39.
166. Cabanas-Polo S, Philippart A, Boccardi E, et al. Facile production of porous bioactive glass scaffolds by the foam replica technique combined with sol-gel/electrophoretic deposition. Ceram Int. 2016;42(5):5772–7.
167. Yun HS, Kim SE, Hyeon YT. Design and preparation of bioactive glasses with hierarchical pore networks. Chem Commun. 2007;21:2139–41.
168. Li X, Wang X, Chen H, Shi J. Hierarchically porous bioactive glass scaffolds synthesized with a PUF and P123 cotemplated approach. Chem Mater. 2007;19(17):4322–6. doi:10.1021/cm0708564.
169. Zhu M, Zhang J, Zhou Y, et al. Preparation and characterization of magnetic mesoporous bioactive glass/carbon composite scaffolds. J Chem. 2013, 2013: Article ID 893479.
170. Dorozhkin SV. Biocomposites and hybrid biomaterials based on calcium orthophosphates. Biomatter. 2011;1(1):3–56.
171. Esen S, Bor ET, Bor S. Characterization of loose powder sintered porous titanium and Ti6Al4V alloy. Turkish J Eng Environ Sci. 2009;33:207–19.
172. Murr LE, Gaytan SM, Martinez E, Medina F, Wicker RB. Next generation orthopaedic implants by additive manufacturing using electron beam melting. Int J Biomate. 2012;2012:245727.
173. Mitra J, Tripathi G, Sharmaaand A, Basu B. Scaffolds for bone tissue engineering: role of surface patterning on osteoblast response. RSC Adv. 2013;3:11073–94.
174. Zheng W, Zhang W, Jiang X. Precise control of cell adhesion by combination of surface chemistry and soft lithography. Adv Healthc Mater. 2013;2(1):95–108.
175. Kim DH, Han K, Gupta K, et al. Mechanosensitivity of fibroblast cell shape and movement to anisotropic substratum topography gradients. Biomaterials. 2009;30(29):5433–44.
176. Uttayarat P, Chen M, Li M, et al. Microtopography and flow modulate the direction of endothelial cell migration. Am J Physiol Heart Circ Physiol. 2008;294(2):H1027–35.

177. Lee MR, Kwon KW, Jung H, et al. Direct differentiation of human embryonic stem cells into selective neurons on nanoscale ridge/groove pattern arrays. Biomaterials. 2010;31(15):4360–6.
178. Baker DW, Liu X, Weng H, Luo C, Tang L. Fibroblast/fibrocyte: surface interaction dictates tissue reactions to micropillar implants. Biomacromolecules. 2011;12(4):997–1005.
179. Ng CK, Yu KN. Proliferation of epithelial cells on PDMS substrates with micropillars fabricated with different curvature characteristics. Biointerphases. 2012;7:21.
180. Nimni ME. Polypeptide growth factors: targeted delivery systems. Biomaterials. 1997;18(18):1201–25.
181. Amsden B. Novel biodegradable polymers for local growth factor delivery. Eur J Pharm Biopharm. 2015;97(Pt B):318–28.
182. Lee K, Silva EA, Mooney DJ. Growth factor delivery-based tissue engineering: general approaches and a review of recent developments. J R Soc Interface. 2011;8(55):153–70.
183. Werner S, Grose R. Regulation of wound healing by growth factors and cytokines. Physiol Rev. 2003;83:835–70.
184. Xiao Y, Reis LA, Zhao Y, Radisic M. Modifications of collagen-based biomaterials with immobilized growth factors or peptides. Methods. 2015;84:44–52.
185. Tada S, Kitajima T, Ito Y. Design and synthesis of binding growth factors. Int J Mol Sci. 2012;13(5):6053–72.
186. Iwamoto R, Mekada E. Heparin-binding EGF-like growth factor: a juxtacrine growth factor. Cytokine Growth Factor Rev. 2000;11(4):335–44.
187. Pagès G, Pouysségur J. Transcriptional regulation of the vascular endothelial growth factor gene – a concert of activating factors. Cardiovasc Res. 2005;65(3):564–73.
188. Yadin D, Knaus P, Mueller TD. Structural insights into BMP receptors: specificity, activation and inhibition. Cytokine Growth Factor Rev. 2016;27:13–34.
189. Yoon BS, Lyons KM. Multiple functions of BMPs in chondrogenesis. J Cell Biochem. 2004;93:93–103.
190. Sellers RS, Peluso D, Morris EA. The effect of recombinant human bone morphogenetic protein-2 (rhBMP-2) on the healing of full-thickness defects of articular cartilage. J Bone Joint Surg Am. 1997;79:1452–63.
191. Louwerse RT, Heyligers IC, Klein-Nulend J, et al. Use of recombinant human osteogenic protein-1 for the repair of subchondral defects in articular cartilage in goats. J Biomed Mater Res. 2000;49:506–16.
192. Liu H, Peng H, Wu Y, et al. The promotion of bone regeneration by nanofibrous hydroxyapatite/chitosan scaffolds by effects on integrin-BMP/Smad signaling pathway in BMSCs. Biomaterials. 2013;34:4404–17.
193. Lecanda F, Avioli LV, Cheng S-L. Regulation of bone matrix protein expression and induction of differentiation of human osteoblasts and human bone marrow stromal cells by bone morphogenetic protein-2. J Cell Biochem. 1997;67:386–9.
194. Nauth A, Ristiniemi J, McKee MD, Schemitsch EH. Bone morphogenetic proteins in open fractures: past, present, future. Injury. 2009;40 Suppl 3:S27–31.
195. Kanczler JM, Oreffo ROC. Osteogenesis and angiogenesis: the potential for engineering bone. Eur Cells Mater. 2008;15:110–4.
196. La WG, Park S, Yoon HH. Delivery of a therapeutic protein for bone regeneration from a substrate coated with graphene oxide. Small. 2013;9(23):4051–60.
197. Dimitriou R, Tsiridis E, Giannoudis PV. Current concepts of molecular aspects of bone healing. Injury. 2005;36:1392–404.
198. Chappard D, Aguado E, Hure G, et al. The early remodeling phases around titanium implants: a histomorphometric assessment of bone quality in a 3 and 6 months study in sheep. Int J Oral Max Impl. 1999;14:189–96.
199. Hall J, Sorensen RG, Wozney JM, Wikesjo UM. Bone formation at rhBMP-2-coated titanium implants in the rat ectopic model. J Clin Periodontol. 2007;34:444–51.

200. Kim D, Herr AE. Protein immobilization techniques for microfluidic assays. Biomicrofluidics. 2013;7(4):41501. 1-47.
201. Hong J, Shah NJ, Drake AC, et al. Graphene multilayers as gates for multi-week sequential release of proteins from surfaces. ACS Nano. 2012;6(1):81–8.
202. Rosario C, Rodriguez-Evora M, Reyes R. Evaluation of nanostructure and microstructure of bone regenerated by BMP-2-porous scaffolds. Biomed Mater. 2015;103(9):2998–3011.
203. Qin J, He H, Zhang W, Chen F, Liu C. Effective incorporation of rhBMP-2 on implantable titanium disks with microstructures by using electrostatic spraying deposition. RSC Adv. 2016;6:51914–23.
204. Reed S, Wu B. Sustained growth factor delivery in tissue engineering applications. Ann Biomed Eng. 2014;42(7):1528–36.
205. Kang Y, Kim S, Khademhosseini A, Yang Y. Creation of bony microenvironment with CaP and cell-derived ECM to enhance human bone-marrow MSC behavior and delivery of BMP-2. Biomaterials. 2011;32:6119–30.
206. Jeon O, Song SJ, Kang SW, Putnam AJ, Kim BS. Enhancement of ectopic bone formation by bone morphogenetic protein-2 released from a heparin-conjugated poly(L-lactic-co-glycolic acid) scaffold. Biomaterials. 2007;28:2763–71.
207. Mercado AE, Ma J, He X, Jabbari E. Release characteristics and osteogenic activity of recombinant human bone morphogenetic protein-2 grafted to novel self-assembled poly(lactide-co-glycolide fumarate) nanoparticles. J Control Release. 2009;140:148–56.
208. Shen H, Hu X, Yang F, Bei J, Wang S. The bioactivity of rhBMP-2 immobilized poly(lactide-co-glycolide) scaffolds. Biomaterials. 2009;30:3150–7.
209. Hoang QQ, Sicheri F, Howard AJ, Yang DS. Bone recognition mechanism of porcine osteocalcin from crystal structure. Nature. 2003;425:977–80.
210. Mi L, Giarmarco MM, Shao Q, Jiang S. Divalent cation-mediated polysaccharide interactions with zwitterionic surfaces. Biomaterials. 2012;33:2001–6.
211. Zhang Y, Jiang T, Zheng Y, Zhou P. Interference of EGCG on the Zn(II)-induced conformational transition of silk fibroin as a model protein related to neurodegenerative diseases. Soft Matter. 2012;8:5543–9.
212. Zhang W, He H, Tian Y, et al. Calcium ion-induced formation of beta-sheet/-turn structure leading to alteration of osteogenic activity of bone morphogenetic protein-2. Sci Rep. 2015;5:12694–700.
213. Zhang W, Tian Y, He H, et al. Strontium attenuates rhBMP-2-induced osteogenic differentiation via formation of Sr-rhBMP-2 complex and suppression of Smad-dependent signaling pathway. Acta Biomater. 2016;33:290–300.
214. Lee K-S, Kim H-J, Li Q-L, et al. Runx2 is a common target of transforming growth factor β1 and bone morphogenetic protein 2, and cooperation between Runx2 and Smad5 induces osteoblast-specific gene expression in the pluripotent mesenchymal precursor cell line C2C12. Mol Cell Biol. 2000;20:8783–92.
215. Li J, Khavandgar Z, Lin S-H, Murshed M. Lithium chloride attenuates BMP-2 signaling and inhibits osteogenic differentiation through a novel WNT/GSK3- independent mechanism. Bone. 2011;48:321–31.
216. Barradas AM, Fernandes HA, Groen N, et al. A calcium-induced signaling cascade leading to osteogenic differentiation of human bone marrow-derived mesenchymal stromal cell. Biomaterials. 2012;33(11):3205–15.
217. Shih Y-RV, Hwang Y, Phadke A, et al. Calcium phosphate-bearing matrices induce osteogenic differentiation of stem cells through adenosine signaling. Proc Natl Acad Sci U S A. 2014;111:990–5.
218. Ren X, Bischoff D, Weisgerber DW, et al. Osteogenesis on nanoparticulate mineralized collagen scaffolds via autogenous activation of the canonical BMP receptor signaling pathway. Biomaterials. 2015;50:107–14.
219. Verberckmoes SC, De Broe ME, D'Haese PC. Dose-dependent effects of strontium on osteoblast function and mineralization. Kidney Int. 2003;64:534–43.

220. Xin Y, Jiang J, Huo K, Hu T, Chu PK. Bioactive SrTiO3 nanotube arrays: strontium delivery platform on Ti-based osteoporotic bone implants. ACS NANO. 2009;3:3228–34.
221. Andersen OZ, Offermanns V, Sillassen M, et al. Accelerated bone ingrowth by local delivery of strontium from surface functionalized titanium implants. Biomaterials. 2013;34:5883–90.
222. Zhao L, Wang H, Huo K, et al. The osteogenic activity of strontium loaded titania nanotube arrays on titanium substrates. Biomaterials. 2013;34:19–29.
223. Bonnelye E, Chabadel A, Saltel F, Jurdic P. Dual effect of strontium ranelate: stimulation of osteoblast differentiation and inhibition of osteoclast formation and resorption in vitro. Bone. 2008;42:129–38.
224. Yang F, Yang D, Tu J, Zheng Q, Cai L, Wang L. Strontium enhances osteogenic differentiation of mesenchymal stem cells and in vivo bone formation by activating Wnt/catenin signaling. Stem Cells. 2011;29:981–91.
225. Peng S, Zhou G, Luk KD, et al. Strontium promotes osteogenic differentiation of mesenchymal stem cells through the Ras/MAPK signaling pathway. Cell Physiol Biochem. 2009;23:165–74.
226. Takada T, Katagiri T, Ifuku M, et al. Sulfated polysaccharides enhance the biological activities of bone morphogenetic proteins. J Biol Chem. 2003;278:43229–35.
227. Bellows CG, Aubin JE, Heersche JN, Antosz ME. Mineralized bone nodules formed in vitro from enzymatically released rat calvaria cell populations. Calcif Tissue Int. 1986;38:143–54.
228. Rai B, Nurcombe V, Cool SM. Heparan sulfate-based treatments for regenerative medicine. Crit Rev Eukaryot Gene Expr. 2011;21:1–12.
229. Ruppert R, Hoffmann E, Sebald W. Human bone morphogenetic protein 2 contains a heparin-binding site which modifies its biological activity. Rur J Biochem. 1996;237:295–302.
230. Zhao B, Katagiri T, Toyoda H, et al. Heparin potentiates the in vivo ectopic bone formation induced by bone morphogenetic protein-2. J Biol Chem. 2006;281:23246–53.
231. Kuo WJ, Digman MA, Lander AD. Heparan sulfate acts as a bone morphogenetic protein coreceptor by facilitating ligand-induced receptor hetero-oligomerization. Mol Biol Cell. 2010;21:4028–41.
232. Kanzaki S, Takahashi T, Kanno T, et al. Heparin inhibits BMP-2 osteogenic bioactivity by binding to both BMP-2 and BMP receptor. J Cell Physiol. 2008;216:844–50.
233. Kanzaki S, Ariyoshi W, Takahashi T, et al. Dual effects of heparin on BMP-2-induced osteogenic activity in MC3T3-E1 cells. Pharmacol Rep. 2011;63:1222–30.
234. Atha DH, Stephens AW, Rosenberg RD. Evaluation of critical groups required for the binding of heparin to antithrombin. Proc Natl Acad Sci U S A. 1984;81(4):1030–4.
235. Park SH, Silva M, Bahk WJ, et al. Effect of repeated irrigation and debridement on fracture healing in an animal model. J Orthop Res. 2002;20(6):1197–204.
236. Muir JM, Andrew M, Hirsh J, et al. Histomorphometric analysis of the effects of standard heparin on trabecular bone in vivo. Blood. 1996;88(4):1314–20.
237. Goldhaber P. Heparin enhancement of factors stimulating bone resorption in tissue culture. Science. 1965;147:407–8.
238. Esko JD, Selleck SB. Order out of chaos: assembly of ligand binding sites in heparan sulfate. Annu Rev Biochem. 2002;71:435–71.
239. Dombroeski C, Song SJ, Chuan P, et al. Heparan sulfate mediates the proliferation and differentiation of rat mesenchymal stem cells. Stem Cells Dev. 2009;18(4):661–70.
240. Bramono DS, Murali S, Rai B, et al. Bone marrow-derived heparan sulfate potentiates the osteogenic activity of bone morphogenetic protein-2 (BMP-2). Bone. 2012;50(4):954–64.
241. Degat MC, Dubreucq G, Meunier A. Enhancement of the biological activity of BMP-2 by synthetic dextran derivatives. J Biomed Mater Res A. 2009;88A(1):174–83.
242. Zhou H, Qian J, Wang J, et al. Enhanced bioactivity of bone morphogenetic protein-2 with low dose of 2-N, 6-O-sulfated chitosan in vitro and in vivo. Biomaterials. 2009;30:1715–24.

243. Buttner M, Moller S, Keller M, et al. Over-sulfated chondroitin sulfate derivatives induce osteogenic differentiation of hMSC independent of BMP-2 and TGF-β1 signaling. J Cell Physiol. 2013;228(2):330–40.
244. Manton KJ, Leong DF, Cool SM, Nurcombe V. Disruption of heparan and chondroitin sulfate signaling enhances mesenchymal stem cell-derived osteogenic differentiation via bone morphogenetic protein signaling pathways. Stem Cells. 2007;25:2845–54.
245. Kawano M, Ariyoshi W, Iwanaga K, et al. Mechanism involved in enhancement of osteoblast differentiation by hyaluronic acid. Biochem Biophys Res Commun. 2011;405(4):575–80.
246. Kim J, Kim IS, Cho TH, et al. Bone regeneration using hyaluronic acid-based hydrogel with bone morphogenic protein-2 and human mesenchymal stem cells. Biomaterials. 2007;28(10):1830–7.
247. Derfoul A, Perkins GL, Hall DJ, Tuan RS. Glucocorticoids promote chondrogenic differentiation of adult human mesenchymal stem cells by enhancing expression of cartilage extracellular matrix genes. Stem Cells. 2006;24:1487–95.
248. Haynesworth SE, Goshima J, Goldberg VM, Caplan AI. Characterization of cells with osteogenic potential from human marrow. Bone. 1992;13:81–8.
249. Yuasa M, Yamada T, Taniyama T, et al. Dexamethasone enhances osteogenic differentiation of bone marrow- and muscle-derived stromal cells and augments ectopic bone formation induced by bone morphogenetic protein-2. PLoS ONE. 2015;10(2):e0116462.
250. Lanqenbach F, Handschel J. Effects of dexamethasone, ascorbic acid and β-glycerophosphate on the osteogenic differentiation of stem cells in vitro. Stem Cell Res Ther. 2013;4:117.
251. Marcus J, Johannes F, Wiebke D, et al. Dexamethasone modulates BMP-2 effects on mesenchymal stem cells in vitro. J Orthop Res. 2008;26(11):1440–8.
252. Chen C, Hasan U, Wang ZX, et al. Noggin suppression decreases BMP-2-induced osteogenesis of human bone marrow-derived mesenchymal stem cells in vitro. J Cell Biochem. 2012;113:3672–80.
253. Pera MF, Andrade J, Houssami S, et al. Regulation of human embryonic stem cell differentiation by BMP-2 and its antagonist noggin. J Cell Sci. 2004;117:1269–80.
254. Alborzinia H, Schmidt-Glenewinkel H, Ilkavets I, et al. Quantitative kinetics analysis of BMP2 uptake into cells and its modulation by BMP antagonists. J Cell Sci. 2013;126:117–27.
255. Kwong FN, Richardson SM, Evans CH. Chordin knockdown enhances the osteogenic differentiation of human mesenchymal stem cells. Arthritis Res Ther. 2008;10:R65.
256. Gazzerro E, Pereira RC, Jorgetti V, et al. Skeletal overexpression of gremlin impairs bone formation and causes osteopenia. Endocrinology. 2005;146:655–65.
257. Schett G. Effects of inflammatory and anti-inflammatory cytokines on the bone. Eur J Clin Invest. 2011;41:1361–6.
258. Ritting AW, Weber EW, Lee MC. Exaggerated inflammatory response and bony resorption from BMP-2 use in a pediatric forearm nonunion. J Hand Surg [Am]. 2012;37:316–21.
259. Robin BN, Chaput CD, Zeitouni S, et al. Cytokine-mediated inflammatory reaction following posterior cervical decompression and fusion associated with recombinant human bone morphogenetic protein-2: a case study. Spine (Phila Pa 1976). 2010;35:E1350–4.
260. Lee KB, Murray SS, Taghavi CE, et al. Bone morphogenetic protein-binding peptide reduces the inflammatory response to recombinant human bone morphogenetic protein-2 and recombinant human bone morphogenetic protein-7 in a rodent model of soft-tissue inflammation. Spine J. 2011;11:568–76.
261. Ratanavaraporn J, Furuya H, Tabata Y. Local suppression of pro-inflammatory cytokines and the effects in BMP-2-induced bone regeneration. Biomaterials. 2012;33:304–16.
262. Tan Y, Montgomery SR, Aghdasi BG, et al. The effect of corticosteroid administration on soft-tissue inflammation associated with rhBMP-2 use in a rodent model of inflammation. Spine (Phila Pa 1976). 2013;38:806–13.

263. Huang RL, Yuan Y, Tu J, Zou GM, Li Q. Opposing TNF-α/IL-1β- and BMP-2-activated MAPK signaling pathways converge on Runx2 to regulate BMP-2-induced osteoblastic differentiation. Cell Death Dis. 2014;5:e1187.
264. Huang R-L, Chen G, Wang W, et al. Synergy between IL-6 and soluble IL-6 receptor enhances bone morphogenetic protein-2/absorbable collagen sponge-induced bone regeneration via regulation of BMPRIA distribution and degradation. Biomaterials. 2015;67:308–22.
265. Ratanavaraporn J, Furuya H, Kohara H, et al. Synergistic effects of the dual release of stromal cell-derived factor-1 and bone morphogenetic protein-2 from hydrogels on bone regeneration. Biomaterials. 2011;32(11):2797–811.
266. Kleinschmidt K, Ploeger F, Nickel J, et al. Enhanced reconstruction of long bone architecture by a growth factor mutant combining positive features of GDF-5 and BMP-2. Biomaterials. 2013;34(24):5926–36.
267. Nakamura Y, Tensho K, Nakaya H, et al. Low dose fibroblast growth factor-2 (FGF-2) enhances bone morphogenetic protein-2 (BMP-2)-induced ectopic bone formation in mice. Bone. 2005;36(3):399–407.
268. Wuertz K, Urban J, Klasen J, et al. Influence of extracellular osmolarity and mechanical stimulation on gene expression of intervertebral disc cells. J Orthop Res. 2007;25:1513–22.
269. Hoppe A, Güldal NS, Boccaccini AR. A review of the biological response to ionic dissolution products from bioactive glasses and glass-ceramics. Biomaterials. 2011;32:2757–74.
270. Jiang C, Liu J, Zhao J, et al. Effects of hypoxia on the immunomodulatory properties of human Gingiva–derived mesenchymal stem cells. J Dent Res. 2015;94:69–77.

Part III
Regeneration of Some Clinic-Targeted Tissues

Chapter 9
Cartilage Regeneration

Yuankun Dai and Changyou Gao

9.1 Introduction

Articular cartilage is a highly developed connective tissue for weight-bearing and friction-reducing. Chondrocyte is the only type of cells in mature articular cartilage, occupying 1–10 % of the tissue volume. Seventy to eighty percent of weight of articular cartilage is water. Collagen, proteoglycans, matrix glycoproteins, and small amount of elastin and phospholipids contribute the other 20–30 % of the weight [1, 2]. Figure 9.1a shows the composition and structure of articular cartilage [3]. Cells and extracellular matrix (ECM) in cartilage distribute laterally in the superficial, randomly in the middle, and vertically in the deep layers of cartilage, respectively.

The avascular structure in the articular cartilage determines that the chondrocytes can only get nutrients from the synovial fluid [4]. After maturation of cartilage, chondrocytes have low ability to migrate and proliferate. Hence, articular cartilage has low possibility of self-healing when lesion occurs. The intrinsic migration of bone marrow mesenchymal stem cells (BMSCs) into cartilage defect always leads to the formation of fibrocartilage [4].

Articular cartilage defects caused by arthritis and trauma severely affect the healthy life of human being. In order to treat cartilage defects, different protocols such as autologous chondrocyte implantation (ACI), mosaicplasty, microfracture, autologous matrix-induced chondrogenesis (AMIC), and cartilage tissue engineering have been developed, as shown in Fig. 9.1b [5].

ACI utilizes autologous chondrocytes grown in culture, which are reimplanted in a second-stage procedure to repair large chondral defects [6]. Mosaicplasty is indicated for the treatment of smaller defects, less than 2–4 cm^2 in size, primarily on the

Y. Dai • C. Gao (✉)
MOE Key Laboratory of Macromolecular Synthesis and Functionalization, Department of Polymer Science and Engineering, Zhejiang University, Hangzhou 310027, China
e-mail: cygao@mail.hz.zj.cn; cygao@zju.edu.cn

© Springer Science+Business Media Singapore 2016

C. Gao (ed.), *Polymeric Biomaterials for Tissue Regeneration*,
DOI 10.1007/978-981-10-2293-7_9

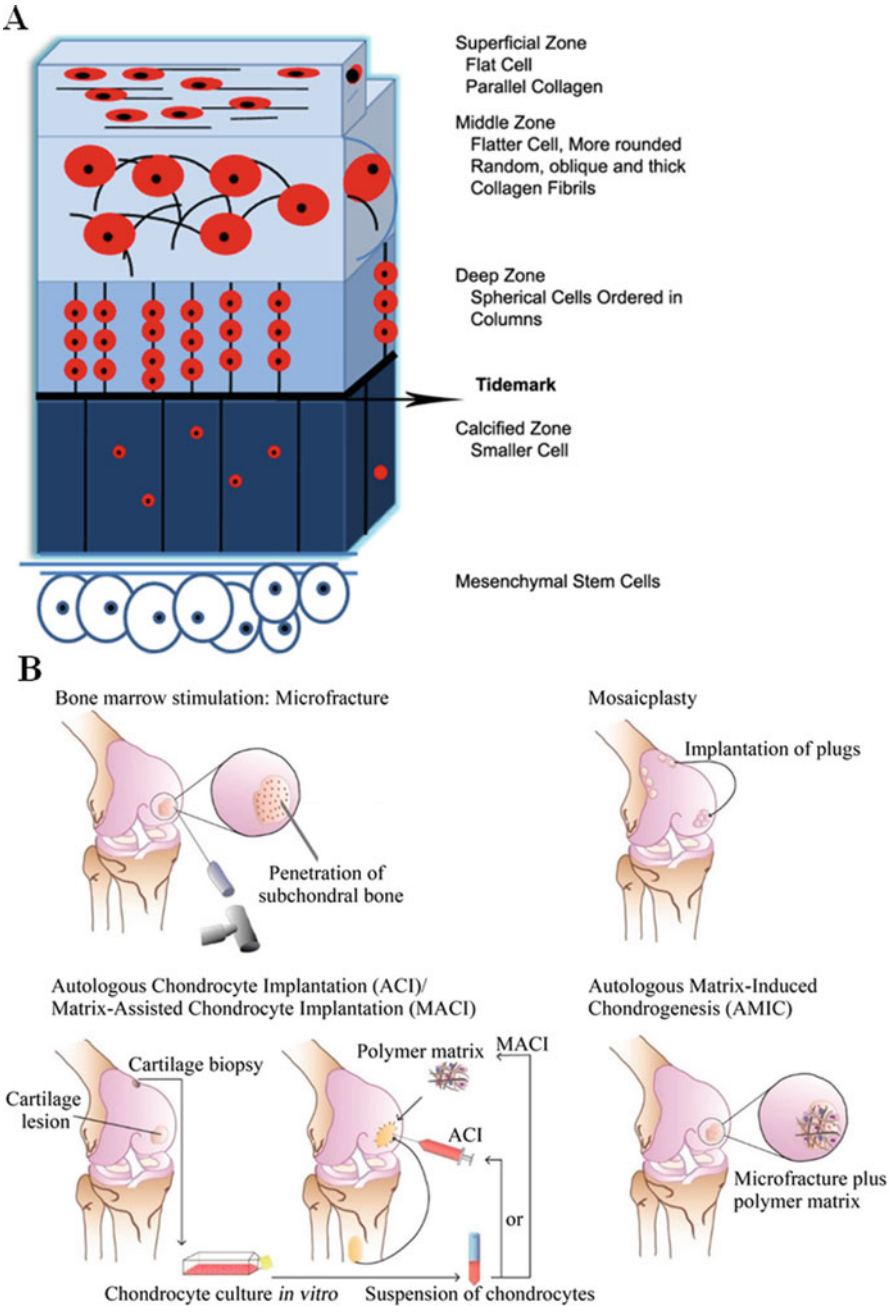

Fig. 9.1 (**a**) Composition and structure of articular cartilage and (**b**) various clinical strategies for regeneration of cartilage [3, 5]

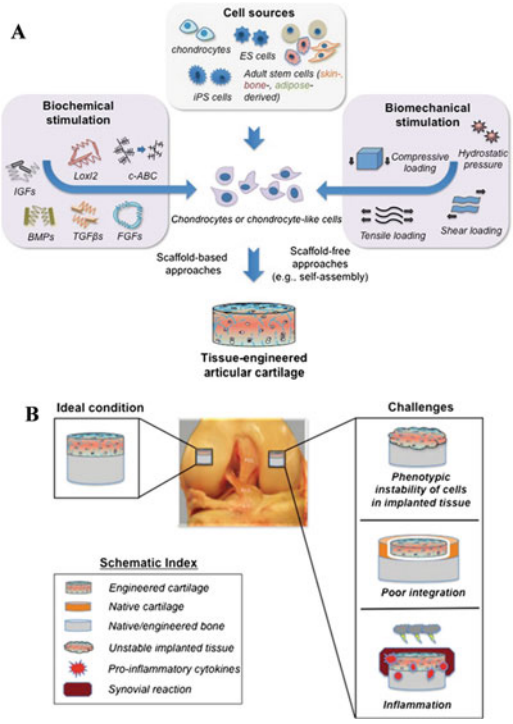

Fig. 9.2 (**a**) Articular cartilage tissue engineering involving the formation of three-dimensional tissues in vitro by seeding cells into scaffolds or through scaffold-free approaches in the presence of biochemical and biomechanical stimuli. (**b**) Challenges in cartilage tissue engineering (Reprinted from Ref. [10] with permission)

femoral condyles. The treatment of larger lesions is limited by donor site morbidity, and the use in the patellofemoral joint is controversial [7]. To overcome these challenges, cartilage tissue engineering has been developed to realize the structural and functional regeneration of damaged cartilage [8]. As shown in Fig. 9.2a, the cells, scaffolds, and bioactive molecules are defined as three essential elements for the traditional cartilage tissue engineering [9, 10]. Various chondrogenetic cell sources are available for the cartilage tissue engineering. The chondrogenesis capability of these cells can be induced or enhanced with many biochemical or biomechanical stimulation in vitro. After culture in vitro, scaffold-based or scaffold-free engineered cartilage could be obtained and implanted for cartilage regeneration in vivo. Hence, cartilage tissue engineering involves direct intra-articular delivery of progenitor cells, progenitor cell delivery on scaffolds, or cell-free scaffolds coated with biological factors to recruit endogenous cells for articular cartilage defect repair [10]. The implantation of biomaterials or cartilage constructs is always accompanied by injury through the surgical procedures.

Inflammatory response takes a pivotal role in tissue repair and regeneration, since injury to the tissue always initiates an inflammatory response to the biomaterials. Moreover, the implantation of engineered cell-material hybrids elicits an adaptive immune reaction toward the cellular component, which in turn influences the host response to the material component [11]. When degradable biomaterials are applied, the immune response is additionally affected by the degradation products

and surface changes of the biomaterials. Chronic inflammation in osteoarthritis develops as inflammatory stimuli persist at the implant site with macrophages, representing the driving force in perpetuating immune responses. Monocytes arriving at the implantation site undergo a phenotypic change to differentiate into macrophages. Their activation leads to further dissemination of chemo-attractants. Macrophages attached to the biomaterials can foster invasion of additional inflammatory cells by secreting chemokines [12]. Taking these concerns into consideration, challenges of articular cartilage tissue engineering are shown in Fig. 9.2b. In summary, difficulty in the regulation and maintenance of cell chondrogenetic phenotype, poor integration between the implanted and the host tissues, and immunoregulation of the implanted biomaterials are the main issues that impede the development of cartilage tissue engineering [10].

9.2 Traditional Cell-Loaded Constructs for Cartilage Regeneration

9.2.1 Biomaterials for Cartilage Regeneration

An ideal cartilage tissue engineering scaffold should preserve the following characteristics: biocompatible, biodegradable, highly porous, suitable for cell attachment, proliferation and differentiation, osteoconductive, noncytotoxic, flexible and elastic, and nonantigenic. Generally, biomaterials used for cartilage tissue engineering can be divided into two categories: natural polymers and synthetic polymers. Each kind of these materials has their own advantages and shortcomings [13]. The natural materials are hydrophilic and bioactive, which enhance the cell-material interactions and facilitate the cells' chondrogenesis to the same extent. Collagen [14–21], fibrin [22–27], silk fibrin [28–32], hyaluronic acid (HA) [33–46], alginate [47–51], gelatin [40, 52–57], chitosan [58–64], etc. have been broadly invested in tissue engineering. The scaffolds based on these natural polymers are usually in a format of hydrogels, either with single or multicomponents. Examples of cartilage tissue engineering scaffolds based on native materials are shown in Fig. 9.3.

9.2.1.1 Natural Materials

Collagen, which constitutes the major part of the extracellular matrix (ECM) and is the essential component and mechanical building block of various physiological systems including cartilage, is highly recommended in cartilage tissue engineering. Collagen has many advantages including favorable biocompatibility and high density of the RGD sequences and other sequences facilitating cell adhesion and cell differentiation [19]. Macroporous scaffolds of collagen can be fabricated conveniently by freeze-drying and chemical cross-linking (Fig. 9.3a) [67]. Vickers et al.

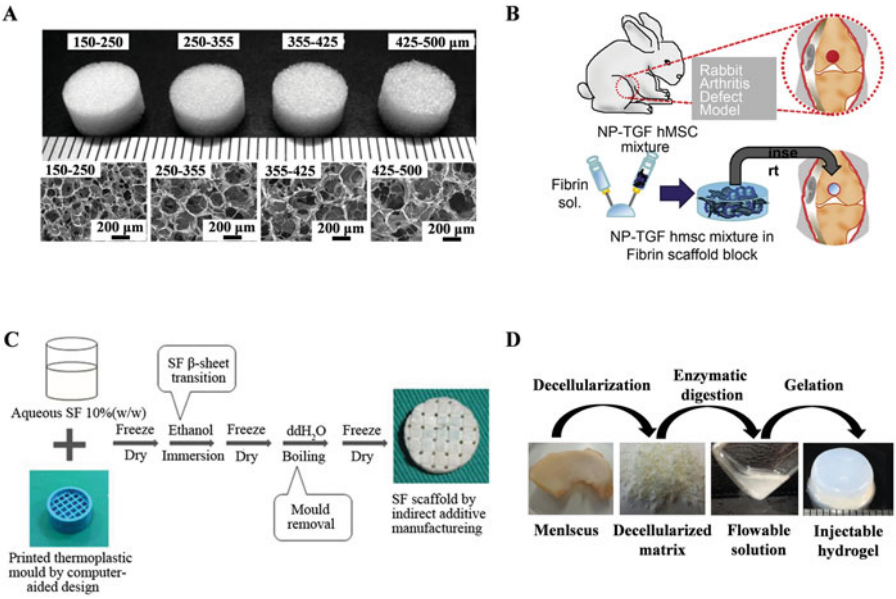

Fig. 9.3 Examples of cartilage tissue engineering scaffolds based on native materials. (**a**) Collagen porous scaffold. (**b**) BMSCs loaded fibrin glue. (**c**) Silk fibroin scaffold. (**d**) Acellular cartilage matrix (Reprinted from Refs. [29, 65–67] with permission)

prepared a chemically cross-linked collagen type II and glycosaminoglycan (GAG) scaffold with a low cross-linking density. Culture of bone marrow stem cells in the scaffold for 4 weeks in vitro found cell-mediated contraction, increased cell number density, and a greater degree of chondrogenesis [68]. Levingstone et al. fabricated a multilayer scaffold consisting of a bone layer composed of collagen type I and hydroxyapatite, an intermediate layer composed of collagen type I and type II and hydroxyapatite, and a superficial layer composed of collagen type I and HA [69]. The scaffolds were implanted into osteochondral defects created in the medial femoral condyle of the knee joint of New Zealand white rabbits, resulting in tissue regeneration with a zonal organization, repair of the subchondral bone, formation of an overlying cartilaginous layer, and evidence of an intermediate tidemark.

Fibrin gel has several features including biocompatibility and biodegradability. The fibronectin-rich fibrin glue is an essential protein in cartilage matrix for chondrocytes-ECM interaction [26]. Fibrin gel could serve as a delivery system for chondrogenetic cells and/or bioactive molecules to facilitate cartilage regeneration (Fig. 9.3b) [65]. Fibrin gel loaded with human bone marrow-derived mesenchymal stem cells (hMSCs) and growth factor could realize full regeneration of cartilage defects in rabbits [65]. Park et al. fabricated a hybrid hydrogel composed of fibrin and HA, into which chondrocytes were implanted for culture in vivo [23]. Cartilage-like tissues were formed in the hybrid hydrogel, showing higher amounts of the ECM components, GAG, and collagen.

Hyaluronic acid (HA) is one of the most extensively studied natural materials for cartilage tissue engineering. HA is a linear polysaccharide found natively in adult articular cartilage that is involved in many cellular processes, including proliferation, morphogenesis, inflammation, and wound repair. Furthermore, HA is also important to cartilage formation and is differentially regulated during limb bud formation and mesenchymal cell condensation. HA hydrogels support chondrocyte matrix deposition and chondrogenic differentiation of mesenchymal stem cells (MSCs) [70]. HA is widely used to functionalize hydrogels or scaffolds for regeneration of cartilage defects. Sheu et al. fabricated a hydrogel based on oxidized HA and resveratrol, into which chondrocytes were implanted for culture in vitro, resulting in upregulated expression of collagen type II, aggrecan, and Sox9 genes and downregulated inflammatory factors [39].

Alginate is a natural anionic and hydrophilic polymer obtained primarily from brown seaweed and bacteria. It is composed of β-D-mannuronate and α-L-guluronate residues [71] and has been widely applied in many biomedical fields due to its excellent biocompatibility, low toxicity, and the mild gelation condition required to form a cross-linked structure [49]. Alginate can be easily modified through chemical and physical reactions to obtain derivatives and can be processed into three-dimensional scaffolds such as hydrogels, microspheres, microcapsules, sponges, foams, and fibers. Studies prove that the alginates would support the chondrogenesis [72, 73]. The cells-alginate constructs are widely used for the regeneration of articular cartilage defects, and some of the researches demonstrate quite positive results. Igarashi et al. delivered BMSCs in an ultra-purified alginate gel into articular cartilage defects in rabbit knees, resulting in complete regeneration of the defects [74].

Gelatin is a denatured collagen, but has relatively low antigenicity compared with collagen. Recently, gelatin-based biomaterials have been widely studied in tissue engineering. However, it is difficult to use pure gelatin scaffold for hard-tissue regeneration such as bone and cartilage due to its weaker mechanical strength. Hence, many studies focus on preparing pure gelatin scaffolds by using proper cross-linking methods [75] or hybrid scaffolds based on gelatin [40, 54, 55, 76]. Some natural materials such as HA, fibrin, chitosan, and synthetic materials have been extensively incorporated to obtain hybrid scaffolds, which not only preserve higher mechanical property but also retain the bioactivity of natural materials.

Chitosan is obtained by deacetylation of chitin which is an abundant natural material. The positive charge in the molecular chain may protect GAGs from hydrolysis [61]. However, the positive charge may also limit the proliferation of chondrocytes. Meanwhile, weaker mechanical property of wet chitosan also limits its application in cartilage tissue engineering [62]. Therefore, the hybrids of one or more materials are always adopted for the application of chitosan in tissue engineering.

Silk fibroin is also a widely used natural material for tissue regeneration. Scaffolds based on silk fibroin for cartilage regeneration can be fabricated through a template/solution-casting method as reported (Fig. 9.3c) [29]. Recently, ECM materials have become more popular because the matrices retain the structure of

native cartilage, which preserve mechanical and chemical signals that can induce cell differentiation and recruitment without additional biologic additives. Cartilage ECM can be obtained from either cell-derived matrices secreted during culture in vitro or from native cartilage (Fig. 9.3d) [66]. Decellularization is an effective way to fully remove all cellular components and nucleic acids or to kill the remnant cells within the matrix [77–80]. The scaffolds based on the decellularized cartilage ECM regenerate hyaline cartilage when combined with rabbit MSCs after transplantation into weight-bearing area of patellar grooves in rabbits for 12 weeks [81].

9.2.1.2 Synthetic Materials

Synthetic polymers are also widely applied in cartilage tissue engineering, but the relatively low cell adhesive ability limits their applications. The widely used synthetic materials include poly(lactide-co-glycolide acid (PLGA) [40, 57, 82–84], polycaprolactone (PCL) [85–89], poly(ethylene glycol) (PEG) [34, 90–98], etc. The scaffolds composted of solely synthetic materials can hardly realize good tissue regeneration. Therefore, the natural materials such as collagen, gelatin, fibrin, HA, and acellular ECMs, as mentioned before, can be compounded or incorporated into the synthetic polymeric scaffolds. Examples of cartilage tissue engineering scaffolds based on synthetic materials are shown in Fig. 9.4.

PCL is a semicrystalline polymer. It belongs to a family of poly α-hydroxyl esters and is one of the most widely used biodegradable polyesters for medical applications because of its biocompatibility, biodegradability, and flexibility [101]. It is widely used to prepare scaffolds for cartilage tissue engineering as well [40, 46, 47, 82, 102–104]. For example, Kim et al. prepared a PCL scaffold constructed with layers of electrospun and salt-leaching PCL membrane, into which chondrocytes were seeded by using an injectable heparin-based hydrogel (Fig. 9.4a). In vivo transplantation of the construct into partial-cartilage defects demonstrates significant cartilage formation with good integration to the surrounding cartilage [85]. Lebourg et al. modified PCL scaffolds with cross-linked HA to grant PCL more hydrophilic and biomimetic microenvironment. Complete regeneration of chondral defects in rabbits in vivo was confirmed by implanting the scaffolds for 24 weeks [38].

PLAG is usually synthesized via ring-opening copolymerization of lactide and glycolide, which has prominent advantages such as adjustable molecular weight and degradation rates, good mechanical properties especially toughness, and excellent processibility [105]. It has been widely used to prepare scaffolds to engineer tissues including cartilage, bone, nerve, etc. [106–111]. Chang et al. seeded endothelial progenitor cells into a highly porous PLGA scaffold and implanted into the osteochondral defect in the medial femoral condyle of rabbits. After 12 weeks, the defects were regenerated with hyaline cartilage, showing a normal columnar chondrocyte arrangement, higher Sox9 expression, and greater contents of GAG and collagen type II [112]. In order to enhance the bioactivity of PLGA scaffolds, bioactive materials such as HA, gelatin, collagen, and fibrinogen can be usually incorporated.

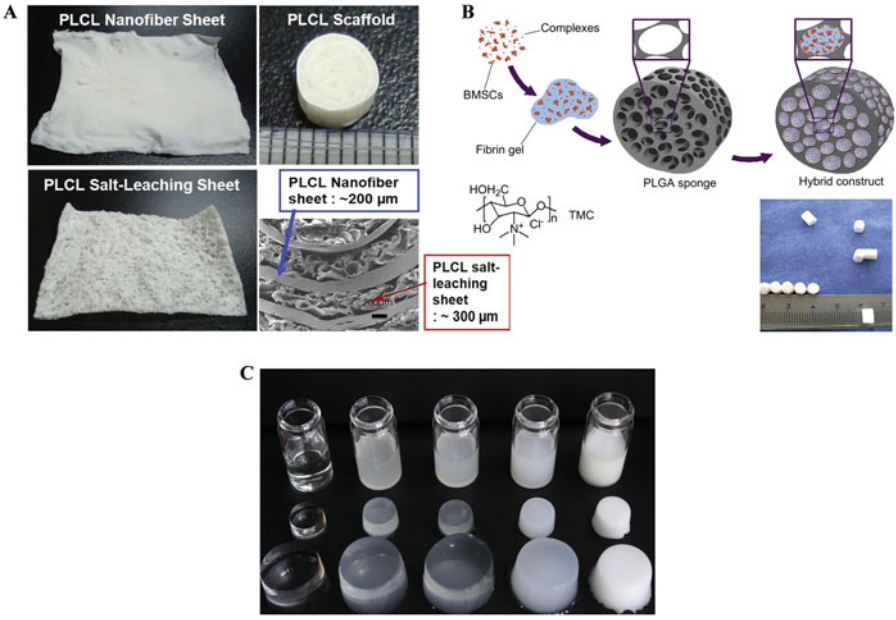

Fig. 9.4 Examples of cartilage tissue engineering scaffolds based on synthetic materials. (**a**) PLCL scaffold. (**b**) PLGA scaffold. (**c**) PEG hydrogel (Reprinted from Refs. [85, 99, 100] with permission)

PLGA/fibrin gel-based constructs combined with MSCs and TGF-β1 chondrogenic genes could facilitate the in vivo regeneration of full-thickness cartilage defects in a rabbit model (Fig. 9.4b) [99, 113, 114]. The PLGA scaffold is fabricated by a gelatin porogen leaching method, into which fibrinogen containing cells and plasmid TGF-β1 gene complexes is infiltrated and then gelated. The chondrocytes cultured in vitro distribute evenly and maintain a round morphology in the hybrid scaffold as that in the normal cartilage [115]. The implantation of PLGA/fibrin gel/N,N,N-trimethyl chitosan chloride (TMC)/pDNA-TGF-β1 construct into osteochondral defects for 12 weeks in vivo results in regenerated cartilage with smooth surface and well integration with its surrounding tissue and subchondral bone [99].

PEG hydrogel has received wide attention due to its injectability, non-cell-adhesive property, cell compatibility, and low immunogenicity. Meanwhile, PEG hydrogel could be prepared for cartilage regeneration (Fig. 9.4c) [100]. The non-degradability of PEG in physiological environment limits its application in tissue engineering, although the PEG molecules of lower molecular weight, like PEG-400, have been proved to metabolize via renal or intestine pathways [116]. Biodegradable segments such as oligo(lactic acid), oligo(ε-caprolactone), oligo(trimethylene carbonate), and phosphate groups have been introduced into the PEG-based macromers. Fan et al. developed a micro-cavitary hydrogel via photo-polymerization of biodegradable oligo(trimethylene carbonate)-poly(ethylene glycol)-

oligo(trimethylene carbonate) diacrylate macromers [96]. The cavitary structure in the hydrogel would accelerate degradation of the hydrogel. Compared with non-cavitary hydrogel, the cell density and total contents of collagen and GAG are significantly higher. The hydrolytically biodegradable PEG hydrogels offer a promising platform for chondrocyte encapsulation and for tuning degradation of cartilage tissue engineering scaffolds. Skaalure et al. prepared a semi-interpenetrating network of bioactive HA and oligo(lactic acid)-PEG hydrogel, into which chondrocytes were encapsulated and cultured for 4 weeks. In this way, the contents of collagen and GAG are significantly increased [34].

9.2.2 Cells for Cartilage Regeneration

Chondrocytes in the cartilage produce cartilage ECMs and therefore have been the first choice for cartilage tissue engineering [117]. They are isolated from various sources such as articular cartilage, nasal septum, ribs, and ear cartilage and are extensively used for the study of cartilage regeneration in vitro and in vivo. However, one of the major limitations of chondrocytes is their instability in the culture in vitro, leading to the loss of expression of cartilage matrices such as collagen type II and aggrecan. Recently, multipotent MSCs have been gained increasing interest in cartilage tissue engineering as an alternative to autologous chondrocytes due to their ease in isolation and high expansion capacity in vitro. MSCs exhibit the potential to differentiate into chondrocytes [118], tenocytes [119], ligament cells [120], neuronal cells [121, 122], cardiomyocyte [123, 124], osteoblasts [125], and other cell types [126]. In particular, bone marrow-derived stem cells (BMSCs), adipose-derived stem cells (ADSCs), and embryonic stem cells (ESCs) are most widely applied in cartilage tissue engineering.

9.2.2.1 Chondrocytes

Chondrocytes are metabolically active cells that synthesize a large spectrum of ECM components such as collagen, glycoproteins, proteoglycans, and HA [117]. Since the chondrocytes are the only type of cells in articular cartilage, they are used for the regeneration of cartilage defects in priority both in vitro and in vivo [117, 127–134]. It is believed that the use of chondrocytes would lead to the formation of neo-tissue with exactly the same ECMs with the native cartilage [135]. The activity of chondrocytes is altered by many factors present within their chemical and mechanical environment. However, the use of chondrocytes for cartilage repair suffers from chondrocyte dedifferentiation. A proper culture and delivery of chondrocytes, including the use of chondrogenetic culture medium, growth factors, and mesenchymal stem cells, need to be well adjusted in order to keep the phenotype of chondrocytes [130]. Three-dimensional scaffolds can better mimic the native microenvironment of chondrocytes in cartilage tissue, promoting cell-cell and cell-matrix

interactions and enforcing round chondrogenetic cell morphology and thereby maintaining their phenotype. Xu et al. encapsulated chondrocytes in alginate gel beads and cultured in spinner flasks in chondrogenic and chondrocyte growth medium and then subcutaneously implanted the cells-loaded beads to evaluate the ectopic chondrogenesis [132]. The results prove high deposition of glycosaminoglycan and expression of cartilage-specific genes. Lohan et al. pre-cultured chondrocytes in polyglycolide (PGA) scaffolds for 3 weeks, which were then implanted into critical-sized osteochondral defect of rabbit knee femoropatellar groove [128, 131]. Twelve weeks after implantation, neo-cartilage was formed in vivo in the PGA constructs seeded with chondrocytes. The results are significantly better than those of the cell-free PGA scaffolds and empty defects.

9.2.2.2 Bone Marrow-Derived Stem Cells (BMSCs)

BMSCs have been extensively used for chondrogenesis in a three-dimensional culture in vitro with addition of chondrogenetic factors and regeneration of cartilage defects in animal models in vivo [33, 136–139]. BMSCs can be isolated via plastic adhesion or negative selection from bone marrow aspirate that includes a highly heterogeneous cell population such as hematopoietic cells, endothelial cells, and adipocytes [140]. However, there are some limitations of BMSCs. The relative number of BMSCs in the marrow blood is rather small, and their differentiation ability decreases significantly with age [141]. Meanwhile, the constructs of cartilage containing BMSCs can raise many problems such as fibrosis, vascularization, the "hollow" phenomenon, and shrinkage likely due to the incomplete differentiation of BMSCs, deterring the clinical translation of tissue-engineered cartilage [139]. Hence chondrogenetic bioactive factors are always applied to promote chondrogenesis differentiation of BMSCs. Li et al. fabricated a bilayered poly(vinyl alcohol)/gelatin/vanillin (PVA/Gel/V) and nano-hydroxyapatite/polyamide-6 (n-HA/PA6) scaffold, into which BMSCs were implanted. The obtained constructs were used for the regeneration of cartilage and subchondral bone defects in rabbits in vivo [142]. With BMSCs loading, the two different layers of the composite biomimetic scaffolds provide a suitable microenvironment for cells to form respective tissues.

9.2.2.3 Adipose-Derived Stem Cells (ADSCs)

ADSCs are becoming more and more attractive because they can be easily isolated from adipose tissues and cultured in vitro for an extended period of time with stable expansion and low levels of senescence [143]. Adipose tissue contains a large proportion of MSCs and is easily accessible in all individuals. Compared with BMSCs, the ADSCs are relatively abundant and can be easily available. In vitro and in vivo studies confirm the chondrogenetic ability of ADSCs and the ability of cartilage regeneration [144–150]. In the presence of platelet-rich plasma (PRP) and cartilage-specific extracellular molecules, the expression of collagen type II and aggrecan can

be significantly upregulated [149, 150]. Wang et al. proved different chondrogenic degrees of ADSCs being cultured in hydrogels composed of chondroitin sulfate, HA, and heparin sulfate, respectively [147]. This chondrogenetic potential of ADSCs makes them a promising candidate for restoration of cartilage defects in vivo. Wang et al. implanted ADSCs into acellular cartilage matrices and used the cell-loading constructs to restore the articular cartilage defects of rabbits [148]. After 12 weeks of implantation, the defects are filled with neo-tissues, showing a smooth surface, highly expressed collagen type II and GAG, and chondrocyte-like cells in the recesses. TEM analysis confirms plenty of secretary matrix particles in the neo-tissue.

9.2.2.4 Embryonic Stem Cells (ESCs)

Recently, several studies have demonstrated the regeneration of cartilage defects in vivo by using ESC progenitor cells [151–154]. ESCs can be obtained from the blastocyst and are able to self-renew for a prolonged period of time without differentiation and, most importantly, can be differentiated into a large variety of tissues derived from all three germ layers. Although the application of ESCs would bring problems such as immunologic incompatibility, possible development of teratomas, and ethical issues in human, the in-depth study of ESCs would promote their applications in healing human diseases. For the cartilage regeneration, ESCs are also a promising choice [151, 153, 155–157]. Pilichi et al. demonstrated a positive result of application of non-differentiated ESCs in vivo for osteochondral regeneration without tumorigenic and teratoma formation [154]. They treated osteochondral defects in a sheep model with ESCs for 24 weeks, proving the regeneration of articular cartilage defects with hyaline cartilage, without signs of immune rejection or teratoma. Toh et al. used TGF-β1 to induce chondrogenic differentiation of ESCs, explored the potential of these ESC-derived chondrogenic cells to produce an ECM-enriched cartilaginous tissue construct when cultured in HA hydrogel, and further investigated the cartilage regenerative ability in an osteochondral defects in a rat model [152]. Twelve weeks after implantation, a hyaline-like neo-cartilage layer is formed, showing good surface regularity and complete integration with the adjacent host cartilage and a regenerated subchondral bone.

9.2.2.5 Other Cells

Besides BMSCs, ADSCs, and ESCs, other types of stem cells from muscle, synovium, and periosteum can also be used for the cartilage regeneration [158–161].

Several works report that synovium-derived MSCs (SMSCs) show a higher colony-forming efficiency than BMSCs. Because the SMSCs display a great potential to differentiate into chondrocytes, they are one of the best candidates for the repair of cartilage defects [162]. SMSCs have the potential for both cartilage tissue

engineering in vitro and cartilage regeneration in vivo. With appropriate stimulation, SMSCs are capable of migrating into articular cartilage defects and differentiating to chondrocytes [162–167]. Fan et al. explored therapeutic chondrogenesis of rabbit SMSCs encapsulated in photopolymerized hydrogels with the treatment of TGF-β1, resulting in positive SMSC chondrogenesis. Meanwhile, SMSCs may be a type of tissue-specific stem cells, because they can respond to signaling in the joint and promote cartilage defect regeneration [168]. Pei et al. isolated SMSCs from synovial tissue of rabbit knee joints and mixed SMSCs with fibrin glue, followed by seeding into a nonwoven PGA mesh. After the constructs were prematured for 1 month in vitro, they were implanted into rabbit knees to repair osteochondral defects. Six months later, the cartilage defects were full of smooth hyaline-like cartilage with high expressions of collagen type II and GAG and were well integrated with the surrounding native cartilage. No detectable collagen type I and macrophages were found [169].

9.2.3 Bioactive Signals for Cartilage Regeneration

The cell growth factors are typical bioactive molecules, which can stimulate or inhibit cellular proliferation, differentiation, migration, and gene expression [171]. There are a number of essential growth factors that have regulatory effects on chondrocytes or stem cells in terms of chondrocyte maturation and cartilage formation. The candidate growth factors include transforming growth factor β (TGF-β), insulin-like growth factor-1 (IGF-1), bone morphogenic proteins (BMPs), fibroblast growth factor (FGF), platelet-derived growth factor (PDGF), etc. [172]. Each growth factor plays a different role in the migration, proliferation, and differentiation of cells as summarized in Fig. 9.5. However, it is difficult to precisely define the function of each growth factor due to the functional overlaps in temporal scale [170].

9.2.3.1 TGF-β

So far four types of TGF-β superfamily, namely, TGF-β1, TGF-β2, TGF-β3, and BMP, have been found in cartilage [171]. Activated TGF-β not only increases the synthesis of proteoglycan but also prevents degradation of cartilage ECM by inhibiting matrix metalloproteinase (MMP). These TGF-β isomers play an important role in the late stage of chondrocyte differentiation and may participate in bone formation as well. TGF-β1 induces early stage of chondrogenesis and increases the production of aggrecan and collagen type II [173]. TGF-β3 plays a role in the maturation of chondrocytes [174]. The TGF-β has been extensively used for the regeneration of cartilage defects in vitro and in vivo [112, 175–184]. For example, Yin et al. fabricated a TGF-β1-immobilized scaffold by incorporating TGF-β1-loaded gelatin microspheres into PLGA framework and evaluated the ADSC differentiation in the scaffold in vitro and regenerative ability of cartilage defect in vivo. The cell

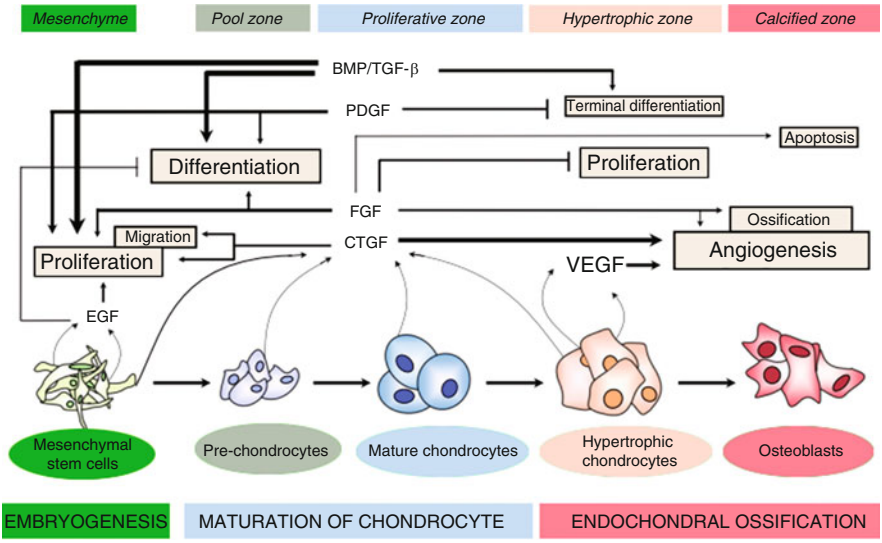

Fig. 9.5 Schematic overview of the role of growth factors at different stages of chondrogenesis (Reprinted from Ref. [170] with permission)

proliferation and GAG deposition in the TGF-β1-immobilized scaffold are significantly increased, and the cartilage regeneration is promoted in the defective articular cartilage in vivo [184]. Lu et al. engineered ADSCs with a baculovirus system that confers prolonged and robust TGF-β3/BMP-6 expression. Culture for 2 weeks in vitro in a porous scaffold leads to the formation of cartilaginous constructs with improved maturity and mechanical properties. After implantation into full-thickness articular cartilage defects in rabbits, these engineered constructs regenerate neo-cartilages that resemble native hyaline cartilage in terms of cell morphology, matrix composition, and mechanical properties. The neo-cartilages also have cartilage-specific zonal structures without signs of hypertrophy and degeneration and integrate well with the native cartilages [180].

9.2.3.2 IGFs

IGFs have a polypeptide sequence similar to proinsulin that allows cells to communicate with their physiologic environment. IGF-1 is well known to promote cell proliferation and inhibit apoptosis. IGF-1 is expressed in developing cartilage, mature cartilage, and synovial fluid of the joint. Both of in vitro and in vivo studies confirm that IGF-1 can induce chondrocyte differentiation and proliferation of MSCs and enhance proteoglycan and collagen type II synthesis [185–192]. Spiller et al. encapsulated IGF-1 in degradable PLGA microparticles and embedded the particles in PVA hydrogel. The PGA fiber scaffolds with chondrocytes were wrapped around the hydrogels and were implanted subcutaneously in athymic mice.

Histology analysis proves enhanced cartilage formation in the layers surrounding the hydrogel with increased content of ECMs, mechanical properties, and integration between the cartilage layers and the hydrogels [191]. The regeneration of cartilage and subchondral bone in vivo was confirmed by injecting IGF-1 suspended HA solution to the temporomandibular in a rabbit model. Twelve and twenty-four weeks after the injection, the defects were well repaired, and nearly normal microarchitectural properties of the subchondral cancellous bone were found in the defects [190].

9.2.3.3 BMPs

BMPs are able to induce the formation of the cartilage and bone, which are required for the formation of pre-chondrogenic condensation and differentiation into chondrocytes. Meanwhile, they can increase the expression of the specific chondrocyte markers such as type X collagen [129, 178, 193–200]. BMP-2, a potent regulator of chondrogenic expression, has received considerable attention in cartilage and osteochondral tissue engineering. Jeong et al. investigated the influence of BMP-2 on the production of cartilage matrix and subsequent bone matrix by using primary chondrocytes seeded on designed three-dimensional PCL scaffolds with chemically conjugated BMP-2. The chemically conjugated BMP-2/PCL scaffolds can significantly promote better cartilage regeneration without particularly accelerating endochondral ossification both in vitro and in vivo compared with those non-BMP-2-treated scaffolds [129].

9.2.3.4 FGF-2

FGF-2 is known as a chondrocyte mitogen found in normal cartilage and has great potential for clinical applications. It can stimulate chondrocytes to synthesize cartilaginous matrix [201–206]. Maehara et al. impregnated a porous hydroxyapatite/collagen scaffold with FGF-2 and used the scaffolds to repair large osteochondral defects in a rabbit model. With the addition of FGF-2, the neo-tissue in the defects displays not only the most abundant bone regeneration but also cartilage regeneration with hyaline-like appearance [205].

9.2.3.5 PDGF

PDGF is a glycolytic protein released by platelets and other cells, which stimulates the growth of cells of mesenchymal origin, for example, the cartilage [207–210]. Meanwhile, the released PDGF-AA from hydrogel being filled in the full-thickness cartilage defects greatly promotes BMSC recruitment into the hydrogel. This confirms the ability of PDGF to recruit BMSCs besides promotion of cell proliferation [210].

9.2.4 Methods for Cartilage Tissue Engineering

9.2.4.1 Pre-culture In Vitro for Cartilage Tissue Engineering

Functional repair of focal cartilage defects requires filling the space with neo-tissue that has compressive properties comparable to native tissue and integration with adjacent host cartilage. One of the main issues in cartilage tissue engineering is represented by the ideal maturation of the construct before implantation in vivo, in order to optimize matrix quality and integration [211]. Considerable progress has been made toward the in vitro tissue engineering of neo-cartilage with compressive properties approaching native levels [212–216]. In 1997, Cao et al. reported a human ear-shaped tissue-engineered construct by using bovine articular chondrocytes and a nonwoven PGA scaffold [217]. Deponti et al. studied the difference of cartilage maturation with or without pre-culture. Articular chondrocytes were embedded in fibrin glue with pre-culture in vitro for 1 week and implanted subcutaneously in rat, proving better tissue maturation compared with the constructs without pre-culture [212]. Pei et al. mixed synovium-derived stem cells with fibrin glue, which were then seeded into nonwoven PGA mesh. After 1-month incubation with growth factors, the premature construct was used to repair osteochondral defects in a rabbit model. Six months later, the defects were full of smooth hyaline-like cartilage with high expression of collagen type II and GAG, which integrated well with the surrounding tissue too [169].

Culture of constructs in a dynamic environment involving fluid flow or agitation is beneficial for cartilage synthesis compared to the static culture conditions [218]. Therefore, various bioreactors have been applied for cartilage tissue engineering, offering advantages such as better control over culture conditions, reduced diffusional limitations for delivery of nutrients and metabolites, enhanced oxygen transfer, and exertion of mechanical and hydrodynamic forces influencing cell and tissue development [219]. Shahin et al. pre-cultured chondrocytes in PGA scaffold for 5 weeks within a bioreactor, confirming improved GAG retention in the scaffolds [220].

9.2.4.2 Regeneration of Cartilage Defects In Situ

With the deep acknowledge of cell behavior regulation and bioactive molecule functions, the in situ regeneration of cartilage defects with direct implantation of cartilage tissue engineering constructs based on biomaterials, cells, and bioactive growth factors has been extensively studied. The scaffolds based on native and/or synthetic materials play a role in supporting the viability of cells and deposition of neo-ECMs, while the bioactive growth factors regulate cell differentiation and physiological activity. Numerous studies give positive regenerative results by using the bioactive constructs in repair of articular cartilage defects. As described early, cells (chondrocytes, BMSCs, ADSCs, ESCs, etc.) and bioactive growth factors (TGF-β, IGF-1,

BMPs, FGF, PDGF, etc.) are loaded into scaffolds (hydrogels, porous scaffolds, etc.), which are then implanted into the cartilage defects without prematuring. Li et al. implanted a PLGA scaffold filled with fibrin gel, mesenchymal stem cells (MSCs), and poly(ethylene oxide)-b-poly(L-lysine) (PEO-b-PLL)/pDNA-TGF-β1 complexes into osteochondral defects, resulting in full in situ regeneration of the defect [113]. However, the application of constructs containing cells and bioactive molecules is still faced with obstacles like source, amount, and phenotype maintenance of MSCs during culture, immune reaction against foreign cells, as well as feasibility of clinical translation considering the ratio of performance to price [221].

9.3 Cell-Free Constructs for Cartilage Regeneration In Situ

Based upon the principles of tissue engineering, the stem cells and chondrocytes are usually used for cartilage regeneration. However the controversy of using cells in tissue engineering still exists because of the uncertainty of dose, time point, as well as side effects [222]. In fact, stem cells are abundant in bone marrow and adult organs such as the brain, peripheral blood, skin, teeth, etc. Once tissues get damaged, endogenous stem/progenitor cells will migrate to the injured site through peripheral blood by responding to the immune cell-secreted biochemical signals [223, 224]. Therefore, homing of endogenous cells for tissue regeneration in situ would be a promising new therapeutic option to bypass the controversial of cell usage. Compared to that of the traditional cartilage tissue engineering, the recruitment of cells into cartilage defect to realize the regeneration in situ still remains rare [225]. Nonetheless, the cell-free scaffolds combined with anti-inflammatory molecules and BMSC-attractive chemokines would have positive influence on the regenerative outcome of cartilage defects. For example, Park et al. studied the in situ recruitment of BMSCs into cartilage defects by transplantation of polylactide/β--tricalcium phosphate (PLA/β-TCP) scaffolds containing IL-8 or MIP-3α [8]. Compared to those scaffolds without chemokines, the scaffolds with IL-8 or MIP-3α can highly facilitate the restoration of cartilage with a smoother surface and higher deposition of collagen. Wang et al. fabricated an anti-inflammatory scaffold composed of resveratrol-grafted polyacrylic acid and atelocollagen [226]. The scaffolds were transplanted into osteochondral defects without the employment of cells. After implantation for 12 weeks, the pro-inflammation genes such as IL-1, MMP13, and COX-2 were downregulated, while the cartilage-related genes were upregulated, leading to efficient regeneration of cartilage defects. For the sake of easier application clinically, a widely accepted biomaterial instead of a brand-new one would be the best choice for fabricating the scaffold. Dai et al. fabricated a macroporous fibrin scaffold with high Fg content and mechanical strength through a porogen leaching method by using PCL microspheres as the porogen. Together with the excellent bioactivity of Fg, the cell-free fibrin scaffold could efficiently regenerate full-thickness cartilage defects in rabbit knees, resulting in neo-cartilage with a smooth surface, well integrity with surrounding tissue, highly deposited GAGs and collagen

type II, and higher expression of cartilage-related genes and proteins, which ensure the great potential for clinical application of Fg scaffold to achieve in situ inductive cartilage regeneration [227]. Meanwhile, the cell-free scaffolds can facilitate cartilage regeneration in clinic too. Roessler et al. implanted a cell-free collagen type I matrix for the treatment of large cartilage defects (mean defect size 3.71 ± 1.93 cm^2, range 1.20–9.00) of the knee and conducted a short-term follow-up after the implantation. Significant pain reduction was achieved after implantation for 6 weeks, while the activity of patients was highly improved and nearly reached to preoperative value after 12 months [228].

9.4 Simultaneous Regeneration of Cartilage and Subchondral Bone

Articular cartilage defects can be divided into two forms, full-thickness cartilage defects without subchondral bone damage and osteochondral defects involving both the cartilage and the underlying subchondral bone [229]. Subchondral bone plays a pivotal role in supporting cartilage and will suffer from deterioration once cartilage is damaged. When damage of subchondral bone occurs, the neo-cartilage has poor integration with the subchondral bone, leading to negative regeneration of the articular cartilage defects [230]. Hence, the regeneration of structure and functions of the articular cartilage defects can be realized only if both cartilage and subchondral bone are simultaneously regenerated with good interface binding [231]. There are several problems that should be overcome for the regeneration of osteochondral defects, including the construction of different layers of scaffolds, well integration of the neo-formed tissues with native tissues, and the effective binding of neo-formed cartilage and subchondral bone [232]. Schematic design of multilayered scaffolds for osteochondral defect regeneration and typical multilayered collagen scaffolds is shown in Fig. 9.6 [69]. Osteochondral tissues encompass cartilage layer, calcified cartilage, and subchondral bone layers in the spatial scale (Fig. 9.6a). The scaffolds with a biphasic structure based on different materials and different chemical or mechanical properties are designed for the regeneration of cartilage and subchondral bone, respectively (Fig. 9.6b) [233–237]. The evaluation of the regenerative ability of the scaffolds in vivo has found some positive results [238–241]. For example, the biphasic PEG/hydroxyapatite scaffold with cartilage- and subchondral bone-like hierarchical nano-roughness, microstructure, and spatiotemporal bioactive cues can be prepared by the 3D printing technology. In vitro culture proves osteochondral differentiation of BMSCs in the scaffold [242]. The bilayered scaffold composed of PLCL, PLGA, and β-tricalcium phosphate (β-TCP) has been prepared by a sintering method and a gel pressing method. The PLGA/β-TCP layer has osteo-conduction activity for bone regeneration, while the elastic PLCL scaffold has mechano-active properties for cartilage regeneration [243]. The biphasic scaffold composed of aragonite-hyaluronic acid (Ar-HA) layers shows full regenerative

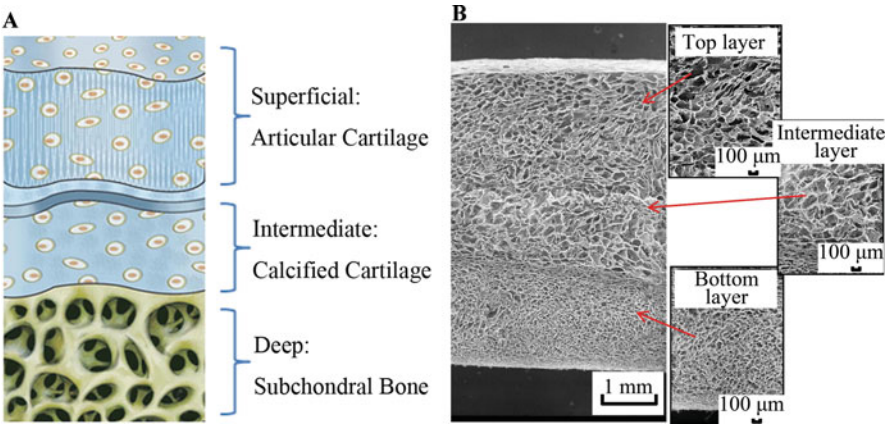

Fig. 9.6 (**a**) Schematic design of multilayered scaffolds for osteochondral defect regeneration. (**b**) Three-layered collagen scaffolds (Reprinted from Ref. [69] with permission)

ability of osteochondral defects with a critical size of 6 mm in diameter and 10 mm in depth in the load-bearing femoral condyle of goats [244].

9.5 Histological Grading of Cartilage

Histological quality of repaired cartilage is one of the most important evaluations of success in cartilage regeneration. Up to present, various histological scoring systems are used to evaluate the quality of cartilage tissues. Basically, a scoring system should be comprehensive but also applicable to researchers with limited knowledge of cartilage histology. In summary, the systems are divided into three categories to describe the osteoarthritic, in vivo repaired, and in vitro engineered cartilage, respectively [245].

Scoring systems for osteoarthritic cartilage focus on the degenerative features of healthy or diseased cartilage. Histological-Histochemical Grading System (HHGS) is the first system for the evaluation of osteoarthritic cartilage [246]. It evaluates the cartilage structure, cell distribution, Safranin-O staining, and tidemark integrity to classify the level of cartilage damage. HHGS is applied in the grading of both human and animal cartilages [247, 248]. Although widely used, HHGS is not efficient to evaluate the specific extent of cartilage deterioration [249]. Osteoarthritis Research Society International (OARSI) developed an Osteoarthritis Cartilage Histopathology Assessment System for better evaluation of the severity and the extent of cartilage surface damage during the arthritic process [250]. The OARSI system is more adequate for the assessment of mild osteoarthritis and could be more conveniently used by less experienced observers [249].

Many scoring systems are developed to evaluate the regeneration of cartilage defect in vivo. O'Driscoll score, Pineda scale, Wakitani score, OsScore, Knutsen

score, and International Cartilage Repair Society (ICRS) score are widely used [245]. O'Driscoll is the first scoring system to assess the repaired cartilage in vivo and is frequently used for cartilage analysis in animal studies [251]. However, many different subitems make it a bit lengthy and complicated to use. Pineda scale is developed to simplify the assessment and is applied to evaluate the self-healing ability of cartilage defect in rabbit at the first beginning [252]. After that, Wakitani introduced a modified scoring system based on Pineda scale, which is extensively applied to evaluate animal cartilage repair in vivo [253]. O'Driscoll, Pineda scale, and Wakitani score are mainly used to evaluate cartilage repair in animal models. In contrast to the animal studies, the study of cartilage repair in human is hard to evaluate due to the infeasible harvest of large biopsy. Considering that, Robert et al. proposed a scoring system for small biopsy of repaired human cartilage, which is named as OsScore [254]. Moreover, ICRS introduced ICRS I and ICRS II scoring systems for more easy and reliable histological evaluation of repaired cartilage [255, 256]. ICRS scoring systems are based on a catalogue of repaired cartilage as a reference for scoring. Distinguished from other systems, ICRS scoring enables discrimination of each subitem, instead of summarizing all the subitems to create a total score. Compared with the ICRS I, the ICRS II contains additional categories, making it more comprehensive. Especially when a scaffold is used in cartilage repair, a category of inflammation can be included to the ICRS II [257].

Scoring system for engineered cartilage should focus on the quality of newly generated cartilage after engineering in vitro. Few histological scoring systems are available for the evaluation of engineered cartilage. O'Driscoll introduced a simple scoring system to evaluate the density of GAGs in the engineered cartilage [258]. This system is not sufficient since many other characteristics, for example, cell morphology, are not included. Another grading system, Bern score, was validated for the evaluation of engineered cartilage [259]. In contrast to O'Driscoll score, Bern score has a broader score range, which gives more information about the characteristics of tissue [260].

9.6 Challenges and Perspectives

Although the cartilage tissue engineering has been investigated for over two decades, rather limited success is achieved to develop clinically relevant outcomes. Nonetheless, significant strides have been made to select optimal cell sources; to identify suitable chemistry, morphology, and compliance of scaffold materials; and to optimize culture conditions and dose and delivery of soluble factors, which are of great importance to develop models of cartilage development in vitro and regeneration of cartilage defects in vivo. Meanwhile, many efforts have been made to overcome the limitations in cell harvesting and to establish culture and implantation techniques in vitro. Novel methods of manufacture such as 3D printing have opened

new horizons for constructing personalized constructs for cartilage regeneration. A thorough understanding of the biological processes at both cellular and molecular levels will ensure the safety and effectiveness of these innovations. With the deep understanding of pathological and healing principles under cartilage defects, cell homing and in situ inductive regeneration of both cartilage and subchondral bone are also full of prospects. All these developments, taken together, may in the future lead to the successful and cost-effective translation from the bench top to the bedside by using novel cell/biomaterial constructs in cartilage regeneration.

References

1. McDevitt CA, Marcelino J. Composition of articular cartilage. Sports Med Arthrosc Rev. 1994;2:1–12.
2. Poole AR, Kojima T, Yasuda T, Mwale F, Kobayashi M, Laverty S. Composition and structure of articular cartilage: a template for tissue repair. Clin Orthop Relat Res. 2001;391:S26–33.
3. Landínez-Parra NS, Garzón-Alvarado DA, Vanegas-Acosta JC. Mechanical behavior of articular cartilage. INTECH Open Access Publisher; 2012.
4. Kay P, Freemont A, Davies D. The aetiology of multiple loose bodies. Snow storm knee. Bone Joint J. 1989;71:501–4.
5. Jeuken RM, Roth AK, Peters RJ, van Donkelaar CC, Thies JC, van Rhijn LW, et al. Polymers in cartilage defect repair of the knee: current status and future prospects. Polymers. 2016;8:219.
6. Gomoll AH, Farr J. Autologous chondrocyte implantation (ACI). Cartilage restoration. New York: Springer; 2014. p. 143–52.
7. Gomoll AH, Farr J. Osteochondral autograft transfer. Cartilage restoration. New York: Springer; 2014. p. 123–9.
8. Park MS, Kim YH, Jung Y, Kim SH, Park JC, Yoon DS, et al. In situ recruitment of human BMSCs using chemokines for articular cartilage regeneration. Cell Transplant. 2014;24(6):1067–83.
9. Bhardwaj N, Devi D, Mandal BB. Tissue-engineered cartilage: the crossroads of biomaterials. Cells and stimulating factors. Macromol Biosci. 2015;15:153–82.
10. Kwon H, Paschos NK, Hu JC, Athanasiou K. Articular cartilage tissue engineering: the role of signaling molecules. Cell Mol Life Sci. 2016;73:1173–94.
11. Babensee JE, Anderson JM, McIntire LV, Mikos AG. Host response to tissue engineered devices. Adv Drug Deliv Rev. 1998;33:111–39.
12. Badylak SF, Gilbert TW. Immune response to biologic scaffold materials. Seminars in immunology. Elsevier; 2008. p. 109–16.
13. Puppi D, Chiellini F, Piras AM, Chiellini E. Polymeric materials for bone and cartilage repair. Prog Polym Sci. 2010;35:403–40.
14. Zheng L, Fan HS, Sun J, Chen XN, Wang G, Zhang L, et al. Chondrogenic differentiation of mesenchymal stem cells induced by collagen-based hydrogel: an in vivo study. J Biomed Mater Res A. 2010;93A:783–92.
15. Cheng H-W, Luk KDK, Cheung KMC, Chan BP. In vitro generation of an osteochondral interface from mesenchymal stem cell-collagen microspheres. Biomaterials. 2011;32:1526–35.
16. Bian W, Li D, Lian Q, Li X, Zhang W, Wang K, et al. Fabrication of a bio-inspired beta-tricalcium phosphate/collagen scaffold based on ceramic stereolithography and gel casting for osteochondral tissue engineering. Rapid Prototyp J. 2012;18:68–80.

17. Park S-H, Song T, Bae TS, Khang G, Choi BH, Park SR, et al. Comparative analysis of collagens extracted from different animal sources for application of cartilage tissue engineering. Int J Precis Eng Manuf. 2012;13:2059–66.
18. Zhang Q, Lu H, Kawazoe N, Chen G. Preparation of collagen scaffolds with controlled pore structures and improved mechanical property for cartilage tissue engineering. J Bioact Compat Polym. 2013;28:426–38.
19. Zheng L, Lu HQ, Fan HS, Zhang XD. Reinforcement and chemical cross-linking in collagen-based scaffolds in cartilage tissue engineering: a comparative study. Iran Polym J. 2013;22:833–42.
20. Yuan T, Zhang L, Li K, Fan H, Fan Y, Liang J, et al. Collagen hydrogel as an immunomodulatory scaffold in cartilage tissue engineering. J Biomed Mater Res B Appl Biomater. 2014;102:337–44.
21. Zheng L, Jiang X, Chen X, Fan H, Zhang X. Biomed Mat. 2014;9.
22. Silverman RP, Passaretti D, Huang W, Randolph MA, Yaremchuk M. Injectable tissue-engineered cartilage using a fibrin glue polymer. Plast Reconstr Surg. 1999;103:1809–18.
23. Park SH, Park SR, Chung SI, Pai KS, Min BH. Tissue-engineered cartilage using fibrin/hyaluronan composite gel and its in vivo implantation. Artif Organs. 2005;29:838–45.
24. Ahmed TAE, Giulivi A, Griffith M, Hincke M. Fibrin glues in combination with mesenchymal stem cells to develop a tissue-engineered cartilage substitute. Tissue Eng Part A. 2011;17:323–35.
25. Singh K, Moyer H, Williams JK, Schwartz Z, Boyan BD. Fibrin glue a scaffold for cellular-based therapy in a critical-sized defect. Ann Plast Surg. 2011;66:301–5.
26. Hong HJ, Lee JS, Choi JW, Min BH, Lee HB, Kim CH. Transplantation of autologous chondrocytes seeded on a fibrin/hyaluronan composite gel into tracheal cartilage defects in rabbits: preliminary results. Artif Organs. 2012;36:998–1006.
27. Cakmak O, Babakurban ST, Akkuzu HG, Bilgi S, Ovali E, Kongur M, et al. Injectable tissue-engineered cartilage using commercially available fibrin glue. Laryngoscope. 2013;123:2986–92.
28. Bhardwaj N, Kundu SC. Chondrogenic differentiation of rat MSCs on porous scaffolds of silk fibroin/chitosan blends. Biomaterials. 2012;33:2848–57.
29. Chen C-H, Liu JM-J, Chua C-K, Chou S-M, Shyu VB-H, Chen J-P. Cartilage tissue engineering with silk fibroin scaffolds fabricated by indirect additive manufacturing technology. Materials. 2014;7:2104–19.
30. Han K-S, Song JE, Tripathy N, Kim H, Moon BM, Park CH, et al. Effect of pore sizes of silk scaffolds for cartilage tissue engineering. Macromol Res. 2015;23:1091–7.
31. Yan L-P, Silva-Correia J, Oliveira MB, Vilela C, Pereira H, Sousa RA, et al. Bilayered silk/silk-nanoCaP scaffolds for osteochondral tissue engineering: in vitro and in vivo assessment of biological performance. Acta Biomater. 2015;12:227–41.
32. Yodmuang S, McNamara SL, Nover AB, Mandal BB, Aganwal M, Kelly T-AN, et al. Silk microfiber-reinforced silk hydrogel composites for functional cartilage tissue repair. Acta Biomater. 2015;11:27–36.
33. Snyder TN, Madhavan K, Intrator M, Dregalla RC, Park D. A fibrin/hyaluronic acid hydrogel for the delivery of mesenchymal stem cells and potential for articular cartilage repair. J Biol Eng. 2014;8:10.
34. Skaalure SC, Dimson SO, Pennington AM, Bryant SJ. Semi-interpenetrating networks of hyaluronic acid in degradable PEG hydrogels for cartilage tissue engineering. Acta Biomater. 2014;10:3409–20.
35. Mintz BR, Cooper JA. Hybrid hyaluronic acid hydrogel/poly(epsilon-caprolactone) scaffold provides mechanically favorable platform for cartilage tissue engineering studies. J Biomed Mater Res A. 2014;102:2918–26.
36. Magalhaes J, Crawford A, Hatton PV, Blanco FJ, Roman JS. Poly(2-ethyl-(2-pyrrolidone) methacrylate) and hyaluronic acid-based hydrogels for the engineering of a cartilage-like tissue using bovine articular chondrocytes. J Bioact Compat Polym. 2014;29:545–59.

37. Levett PA, Hutmacher DW, Malda J, Klein TJ. Hyaluronic acid enhances the mechanical properties of tissue-engineered cartilage constructs. PloS ONE. 2014;9:e113216.
38. Lebourg M, Martinez-Diaz S, Garcia-Giralt N, Torres-Claramunt R, Ribelles JLG, Vila-Canet G, et al. Cell-free cartilage engineering approach using hyaluronic acid-polycaprolactone scaffolds: a study in vivo. J Biomater Appl. 2014;28:1304–15.
39. Sheu SY, Chen WS, Sun JS, Lin FH, Wu T. Biological characterization of oxidized hyaluronic acid/resveratrol hydrogel for cartilage tissue engineering. J Biomed Mater Res A. 2013;101:3457–66.
40. Chang NJ, Jhung YR, Yao CK, Yeh ML. Hydrophilic gelatin and hyaluronic acid-treated PLGA scaffolds for cartilage tissue engineering. J Appl Biomater Funct Mater. 2013;11:45–52.
41. Toh WS, Lim TC, Kurisawa M, Spector M. Modulation of mesenchymal stem cell chondrogenesis in a tunable hyaluronic acid hydrogel microenvironment. Biomaterials. 2012;33:3835–45.
42. Matsiko A, Levingstone TJ, O'Brien FJ, Gleeson JP. Addition of hyaluronic acid improves cellular infiltration and promotes early-stage chondrogenesis in a collagen-based scaffold for cartilage tissue engineering. J Mech Behav Biomed Mater. 2012;11:41–52.
43. Erickson IE, Kestle SR, Zellars KH, Farrell MJ, Kim M, Burdick JA, et al. High mesenchymal stem cell seeding densities in hyaluronic acid hydrogels produce engineered cartilage with native tissue properties. Acta Biomater. 2012;8:3027–34.
44. Tan HP, Chu CR, Payne KA, Marra KG. Injectable in situ forming biodegradable chitosan-hyaluronic acid based hydrogels for cartilage tissue engineering. Biomaterials. 2009;30:2499–506.
45. Park SJ, Yu SM, Chun MH, Chun HJ, Kim CH. Effect of hyaluronic acid on attachment and proliferation of chondrocyte on chitosan/hyaluronic acid bead scaffolds. Tissue Eng Regen Med. 2009;6:438–44.
46. Jung SH, Jang JW, Kim SH, Hong HH, Oh AY, Rhee JM, et al. Articular cartilage regeneration using hyaluronic acid loaded PLGA scaffold by emulsion freeze-drying method. Tissue Eng Regen Med. 2008;5:643–9.
47. Choi SW, Moon SK, Chu JY, Lee HW, Park TJ, Kim JH. Alginate hydrogel embedding poly(D, L-lactide-co-glycolide) porous scaffold disks for cartilage tissue engineering. Macromol Res. 2012;20:447–52.
48. Kim HM, Park JY, Kim EY, Song JE, Kwon SY, Chung JW, et al. Tissue engineered cartilage reconstruction with alginate sponge containing demineralized bone particles. Polym-Korea. 2014;38:278–85.
49. Park H, Lee KY. Cartilage regeneration using biodegradable oxidized alginate/hyaluronate hydrogels. J Biomed Mater Res A. 2014;102:4519–25.
50. Fan CJ, Wang DA. Potential use of alginate beads as a chondrocyte delivery vehicle and stepwise dissolving porogen in a hydrogel scaffold for cartilage tissue engineering. Rsc Adv. 2015;5:80688–97.
51. Reppel L, Schiavi J, Charif N, Leger L, Yu H, Pinzano A, et al. Chondrogenic induction of mesenchymal stromal/stem cells from Wharton's jelly embedded in alginate hydrogel and without added growth factor: an alternative stem cell source for cartilage tissue engineering. Stem Cell Res Ther. 2015;6:260.
52. Xue JX, Feng B, Zheng R, Lu Y, Zhou GD, Liu W, et al. Engineering ear-shaped cartilage using electrospun fibrous membranes of gelatin/polycaprolactone. Biomaterials. 2013;34:2624–31.
53. Levett PA, Melchels FPW, Schrobback K, Hutmacher DW, Malda J, Klein TJ. A biomimetic extracellular matrix for cartilage tissue engineering centered on photocurable gelatin, hyaluronic acid and chondroitin sulfate. Acta Biomater. 2014;10:214–23.
54. Zheng R, Duan HC, Xue JX, Liu Y, Feng B, Zhao SF, et al. The influence of gelatin/PCL ratio and 3-D construct shape of electrospun membranes on cartilage regeneration. Biomaterials. 2014;35:152–64.

55. Kuo CY, Chen CH, Hsiao CY, Chen JP. Incorporation of chitosan in biomimetic gelatin/chondroitin-6-sulfate/hyaluronan cryogel for cartilage tissue engineering. Carbohydr Polym. 2015;117:722–30.
56. Miao T, Miller EJ, McKenzie C, Oldinski RA. Physically crosslinked polyvinyl alcohol and gelatin interpenetrating polymer network theta-gels for cartilage regeneration. J Mater Chem B. 2015;3:9242–9.
57. Yin F, Cai JF, Zen W, Wei YH, Zhou W, Yuan F, et al. Cartilage regeneration of adipose-derived stem cells in the TGF-beta 1-immobilized PLGA-gelatin scaffold. Stem Cell Rev Rep. 2015;11:453–9.
58. Breyner NM, Hell RCR, Carvalho LRP, Machado CB, Peixoto Filho IN, Valerio P, et al. Effect of a three-dimensional chitosan porous scaffold on the differentiation of mesenchymal stem cells into chondrocytes. Cells Tissues Organs. 2010;191:119–28.
59. Ragetly GR, Slavik GJ, Cunningham BT, Schaeffer DJ, Griffon DJ. Cartilage tissue engineering on fibrous chitosan scaffolds produced by a replica molding technique. J Biomed Mater Res A. 2010;93A:46–55.
60. Bi L, Cao Z, Hu Y, Song Y, Yu L, Yang B, et al. Effects of different cross-linking conditions on the properties of genipin-cross-linked chitosan/collagen scaffolds for cartilage tissue engineering. J Mater Sci Mater Med. 2011;22:51–62.
61. Oliveira JT, Crawford A, Mundy JL, Sol PC, Correlo VM, Bhattacharya M, et al. Novel melt-processable chitosan-polybutylene succinate fibre scaffolds for cartilage tissue engineering. J Biomater Sci Polym Ed. 2011;22:773–88.
62. Whu SW, Hung K-C, Hsieh K-H, Chen C-H, Tsai C-L, S-h H. In vitro and in vivo evaluation of chitosan-gelatin scaffolds for cartilage tissue engineering. Mater Sci Eng C Mater Biol Appl. 2013;33:2855–63.
63. Garcia-Lopez J, Garciadiego-Cazares D, Melgarejo-Ramirez Y, Sanchez-Sanchez R, Solis-Arrieta L, Garcia-Carvajal Z, et al. Chondrocyte differentiation for auricular cartilage reconstruction using a chitosan based hydrogel. Histol Histopathol. 2015;30:1477–85.
64. Muzzarelli RAA, El Mehtedi M, Bottegoni C, Aquili A, Gigante A. Genipin-crosslinked chitosan gels and scaffolds for tissue engineering and regeneration of cartilage and bone. Mar Drugs. 2015;13:7314–38.
65. Park JS, Yang HN, Woo DG, Jeon SY, Park K-H. Chondrogenesis of human mesenchymal stem cells in fibrin constructs evaluated in vitro and in nude mouse and rabbit defects models. Biomaterials. 2011;32:1495–507.
66. Wu J, Ding Q, Dutta A, Wang Y, Huang Y-h, Weng H, et al. An injectable extracellular matrix derived hydrogel for meniscus repair and regeneration. Acta Biomater. 2015;16:49–59.
67. Zhang Q, Lu H, Kawazoe N, Chen G. Pore size effect of collagen scaffolds on cartilage regeneration. Acta Biomater. 2014;10:2005–13.
68. Vickers SM, Gotterbarm T, Spector M. Cross-linking affects cellular condensation and chondrogenesis in Type II collagen-GAG scaffolds seeded with bone marrow-derived mesenchymal stem cells. J Orthop Res. 2010;28:1184–92.
69. Levingstone TJ, Thompson E, Matsiko A, Schepens A, Gleeson JP, O'Brien FJ. Multi-layered collagen-based scaffolds for osteochondral defect repair in rabbits. Acta Biomater. 2016;32:149–60.
70. Kim IL, Mauck RL, Burdick JA. Hydrogel design for cartilage tissue engineering: a case study with hyaluronic acid. Biomaterials. 2011;32:8771–82.
71. Sun JC, Tan HP. Alginate-based biomaterials for regenerative medicine applications. Materials. 2013;6:1285–309.
72. Steinert A, Weber M, Dimmler A, Julius C, Schütze N, Nöth U, et al. Chondrogenic differentiation of mesenchymal progenitor cells encapsulated in ultrahigh – viscosity alginate. J Orthop Res. 2003;21:1090–7.
73. Paige KT, Cima LG, Yaremchuk MJ, Schloo BL, Vacanti JP, Vacanti CA. De novo cartilage generation using calcium alginate-chondrocyte constructs. Plast Reconstr Surg. 1996;97:168–78. discussion 79–80.

74. Igarashi T, Iwasaki N, Kasahara Y, Minami A. A cellular implantation system using an injectable ultra-purified alginate gel for repair of osteochondral defects in a rabbit model. J Biomed Mater Res A. 2010;94A:844–55.
75. Lien SM, Li WT, Huang TJ. Genipin-crosslinked gelatin scaffolds for articular cartilage tissue engineering with a novel crosslinking method. Mater Sci Eng C Biomim Supramol Syst. 2008;28:36–43.
76. Kim DH, Heo SJ, Shin JW, Mun CW, Park KM, Park KD, et al. Preparation of thermosensitive gelatin-pluronic copolymer for cartilage tissue engineering. Macromol Res. 2010;18:387–91.
77. Sutherland AJ, Beck EC, Dennis SC, Converse GL, Hopkins RA, Berkland CJ, et al. Decellularized cartilage may be a chondroinductive material for osteochondral tissue engineering. PloS ONE. 2015;10:e0121966.
78. Fermor HL, Russell SL, Williams S, Fisher J, Ingham E. Development and characterisation of a decellularised bovine osteochondral biomaterial for cartilage repair. J Mater Sci Mater Med. 2015;26:186.
79. Chen Y-C, Chen R-N, Jhan H-J, Liu D-Z, Ho H-O, Mao Y, et al. Development and characterization of acellular extracellular matrix scaffolds from porcine menisci for use in cartilage tissue engineering. Tissue Eng Part C Meth. 2015;21:971–86.
80. Benders KEM, van Weeren PR, Badylak SF, Saris DBF, Dhert WJA, Malda J. Extracellular matrix scaffolds for cartilage and bone regeneration. Trends Biotechnol. 2013;31:169–76.
81. Yang Z, Shi Y, Wei X, He J, Yang S, Dickson G, et al. Fabrication and repair of cartilage defects with a novel acellular cartilage matrix scaffold. Tissue Eng Part C Methods. 2009;16:865–76.
82. Fan HB, Hu YY, Zhang CL, Li XS, Lv R, Qin L, et al. Cartilage regeneration using mesenchymal stem cells and a PLGA-gelatin/chondroitin/hyaluronate hybrid scaffold. Biomaterials. 2006;27:4573–80.
83. He X, Lu H, Kawazoe N, Tateishi T, Chen G. A novel cylinder-type poly(L-lactic acid)-collagen hybrid sponge for cartilage tissue engineering. Tissue Eng Part C Meth. 2010;16:329–38.
84. Andreas K, Zehbe R, Kazubek M, Grzeschik K, Sternberg N, Baumler H, et al. Biodegradable insulin-loaded PLGA microspheres fabricated by three different emulsification techniques: investigation for cartilage tissue engineering. Acta Biomater. 2011;7:1485–95.
85. Kim M, Hong B, Lee J, Kim SE, Kang SS, Kim YH, et al. Composite system of PLCL scaffold and heparin-based hydrogel for regeneration of partial-thickness cartilage defects. Biomacromolecules. 2012;13:2287–98.
86. Perez Olmedilla M, Lebourg M, Escobar Ivirico JL, Nebot I, Garcia Giralt N, Gallego Ferrer G, et al. In vitro 3D culture of human chondrocytes using modified epsilon-caprolactone scaffolds with varying hydrophilicity and porosity. J Biomater Appl. 2012;27:299–309.
87. Cai Y, Li J, Poh CK, Tan HC, Thian ES, Fuh JYH, et al. Collagen grafted 3D polycaprolactone scaffolds for enhanced cartilage regeneration. J Mater Chem B. 2013;1:5971–6.
88. Chen C-H, Shyu VB-H, Chen J-P, Lee M-Y. Selective laser sintered poly-epsilon-caprolactone scaffold hybridized with collagen hydrogel for cartilage tissue engineering. Biofabrication. 2014;6:015004.
89. Kundu J, Shim J-H, Jang J, Kim S-W, Cho D-W. An additive manufacturing-based PCL-alginate-chondrocyte bioprinted scaffold for cartilage tissue engineering. J Tissue Eng Regen Med. 2015;9:1286–97.
90. Hwang YS, Sangaj N, Varghese S. Interconnected macroporous poly(ethylene glycol) cryogels as a cell scaffold for cartilage tissue engineering. Tissue Eng Part A. 2010;16:3033–41.
91. Zhang C, Sangaj N, Hwang YS, Phadke A, Chang CW, Varghese S. Oligo(trimethylene carbonate)-poly(ethylene glycol)-oligo(trimethylene carbonate) triblock-based hydrogels for cartilage tissue engineering. Acta Biomater. 2011;7:3362–9.
92. Rennerfeldt DA, Renth AN, Talata Z, Gehrke SH, Detamore MS. Tuning mechanical performance of poly(ethylene glycol) and agarose interpenetrating network hydrogels for cartilage tissue engineering. Biomaterials. 2013;34:8241–57.

93. Roberts JJ, Bryant SJ. Comparison of photopolymerizable thiol-ene PEG and acrylate-based PEG hydrogels for cartilage development. Biomaterials. 2013;34:9969–79.
94. Yu F, Cao XD, Li YL, Zeng L, Yuan B, Chen XF. An injectable hyaluronic acid/PEG hydrogel for cartilage tissue engineering formed by integrating enzymatic crosslinking and Diels-Alder "click chemistry". Polym Chem. 2014;5:1082–90.
95. Yu F, Cao XD, Li YL, Zeng L, Zhu JH, Wang G, et al. Diets-Alder crosslinked HA/PEG hydrogels with high elasticity and fatigue resistance for cell encapsulation and articular cartilage tissue repair. Polym Chem. 2014;5:5116–23.
96. Fan CJ, Wang DA. A biodegradable PEG-based micro-cavitary hydrogel as scaffold for cartilage tissue engineering. Eur Polym J. 2015;72:651–60.
97. Skaalure SC, Chu S, Bryant SJ. An enzyme-sensitive PEG hydrogel based on aggrecan catabolism for cartilage tissue engineering. Adv Healthc Mater. 2015;4:420–31.
98. Sridhar BV, Brock JL, Silver JS, Leight JL, Randolph MA, Anseth KS. Development of a cellularly degradable PEG hydrogel to promote articular cartilage extracellular matrix deposition. Adv Healthc Mater. 2015;4:702–13.
99. Wang W, Li B, Li Y, Jiang Y, Ouyang H, Gao C. In vivo restoration of full-thickness cartilage defects by poly (lactide-co-glycolide) sponges filled with fibrin gel, bone marrow mesenchymal stem cells and DNA complexes. Biomaterials. 2010;31:5953–65.
100. Sharifi S, Blanquer SBG, van Kooten TG, Grijpma DW. Biodegradable nanocomposite hydrogel structures with enhanced mechanical properties prepared by photo-crosslinking solutions of poly(trimethylene carbonate)–poly(ethylene glycol)–poly(trimethylene carbonate) macromonomers and nanoclay particles. Acta Biomater. 2012;8:4233–43.
101. Kim H-J, Lee J-H, Im G-I. Chondrogenesis using mesenchymal stem cells and PCL scaffolds. J Biomed Mater Res A. 2010;92A:659–66.
102. Munirah S, Kim SH, Ruszymah BHI, Khang G. The use of fibrin and poly(lactic-co-glycolic acid) hybrid scaffold for articular cartilage tissue engineering: an in vivo analysis. Eur Cell Mater. 2008;15:41–51.
103. Quinlan E, Lopez-Noriega A, Thompson E, Kelly HM, Cryan SA, O'Brien FJ. Development of collagen-hydroxyapatite scaffolds incorporating PLGA and alginate microparticles for the controlled delivery of rhBMP-2 for bone tissue engineering. J Control Release. 2015;198:71–9.
104. Sato T, Chen GP, Ushida T, Ishii T, Ochiai N, Tateishi T. Tissue-engineered cartilage by in vivo culturing of chondrocytes in PLGA-collagen hybrid sponge. Mater Sci Eng C Biomim Supramol Syst. 2001;17:83–9.
105. Pan Z, Ding J. Poly(lactide-co-glycolide) porous scaffolds for tissue engineering and regenerative medicine. Interface Focus. 2012;2:366–77.
106. Chang N-J, Lin C-C, Shie M-Y, Yeh M-L, Li C-F, Liang P-I, et al. Positive effects of cell-free porous PLGA implants and early loading exercise on hyaline cartilage regeneration in rabbits. Acta Biomater. 2015;28:128–37.
107. Jose MV, Thomas V, Johnson KT, Dean DR, Nyalro E. Aligned PLGA/HA nanofibrous nanocomposite scaffolds for bone tissue engineering. Acta Biomater. 2009;5:305–15.
108. Kim SS, Park MS, Jeon O, Choi CY, Kim BS. Poly(lactide-co-glycolide)/hydroxyapatite composite scaffolds for bone tissue engineering. Biomaterials. 2006;27:1399–409.
109. Lee JY, Bashur CA, Goldstein AS, Schmidt CE. Polypyrrole-coated electrospun PLGA nanofibers for neural tissue applications. Biomaterials. 2009;30:4325–35.
110. Oh SH, Kim JH, Song KS, Jeon BH, Yoon JH, Seo TB, et al. Peripheral nerve regeneration within an asymmetrically porous PLGA/Pluronic F127 nerve guide conduit. Biomaterials. 2008;29:1601–9.
111. Uematsu K, Hattori K, Ishimoto Y, Yamauchi J, Habata T, Takakura Y, et al. Cartilage regeneration using mesenchymal stem cells and a three-dimensional poly-lactic-glycolic acid (PLGA) scaffold. Biomaterials. 2005;26:4273–9.
112. Chang NJ, Lam CF, Lin CC, Chen WL, Li CF, Lin YT, et al. Transplantation of autologous endothelial progenitor cells in porous PLGA scaffolds create a microenvironment for the regeneration of hyaline cartilage in rabbits. Osteoarthritis Cartilage. 2013;21:1613–22.

113. Li B, Yang J, Ma L, Li F, Tu Z, Gao C. Fabrication of poly(lactide-co-glycolide) scaffold filled with fibrin gel, mesenchymal stem cells, and poly(ethylene oxide)-b-poly(L-lysine)/TGF-beta 1 plasmid DNA complexes for cartilage restoration in vivo. J Biomed Mater Res A. 2013;101:3097–108.
114. Wang W, Li B, Yang J, Xin L, Li Y, Yin H, et al. The restoration of full-thickness cartilage defects with BMSCs and TGF-beta 1 loaded PLGA/fibrin gel constructs. Biomaterials. 2010;31:8964–73.
115. Wang W, Li D, Wang M-c, Li Y-l. A hybrid scaffold of poly (lactide-co-glycolide) sponge filled with fibrin gel for cartilage tissue engineering. Chin J Polym Sci. 2011;29:233–40.
116. Robinson GM, Orrego H, Israel Y, Devenyi P, Kapur BM. Low-molecular-weight polyethylene-glycol as a probe of gastrointestinal permeability after alcohol ingestion. Dig Dis Sci. 1981;26:971–7.
117. Akkiraju H, Nohe A. Role of chondrocytes in cartilage formation, progression of osteoarthritis and cartilage regeneration. J Dev Biol. 2015;3:177–92.
118. Mackay AM, Beck SC, Murphy JM, Barry FP, Chichester CO, Pittenger MF. Chondrogenic differentiation of cultured human mesenchymal stem cells from marrow. Tissue Eng. 1998;4:415–28.
119. Wang Q-W, Chen Z-L, Piao Y-J. Mesenchymal stem cells differentiate into tenocytes by bone morphogenetic protein (BMP) 12 gene transfer. J Biosci Bioeng. 2005;100:418–22.
120. Lee IC, Wang J-H, Lee Y-T, Young T-H. The differentiation of mesenchymal stem cells by mechanical stress or/and co-culture system. Biochem Biophys Res Commun. 2007;352:147–52.
121. Dezawa M, Kanno H, Hoshino M, Cho H, Matsumoto N, Itokazu Y, et al. Specific induction of neuronal cells from bone marrow stromal cells and application for autologous transplantation. J Clin Invest. 2004;113:1701–10.
122. Tropel P, Platet N, Platel J-C, Noel D, Albrieux M, Benabid A-L, et al. Functional neuronal differentiation of bone marrow-derived mesenchymal stem cells. Stem Cells. 2006;24:2868–76.
123. Li HW, Yu B, Zhang Y, Pan ZW, Wei XA, Li HL. Jagged1 protein enhances the differentiation of mesenchymal stem cells into cardiomyocytes. Biochem Biophys Res Commun. 2006;341:320–5.
124. Li L, Zhu J, Tian J, Liu X, Feng C. A role for Gcn5 in cardiomyocyte differentiation of rat mesenchymal stem cells. Mol Cell Biochem. 2010;345:309–16.
125. Jaiswal N, Haynesworth SE, Caplan AI, Bruder SP. Osteogenic differentiation of purified, culture-expanded human mesenchymal stem cells in vitro. J Cell Biochem. 1997;64:295–312.
126. Chamberlain G, Fox J, Ashton B, Middleton J. Concise review: mesenchymal stem cells: their phenotype, differentiation capacity, immunological features, and potential for homing. Stem Cells. 2007;25:2739–49.
127. Kim M, Kim SE, Kang SS, Kim YH, Tae G. The use of de-differentiated chondrocytes delivered by a heparin-based hydrogel to regenerate cartilage in partial-thickness defects. Biomaterials. 2011;32:7883–96.
128. Lohan A, Marzahn U, El Sayed K, Haisch A, Kohl B, Mueller RD, et al. In vitro and in vivo neo-cartilage formation by heterotopic chondrocytes seeded on PGA scaffolds. Histochem Cell Biol. 2011;136:57–69.
129. Jeong CG, Zhang H, Hollister SJ. Three-dimensional polycaprolactone scaffold-conjugated bone morphogenetic protein-2 promotes cartilage regeneration from primary chondrocytes in vitro and in vivo without accelerated endochondral ossification. J Biomed Mater Res A. 2012;100A:2088–96.
130. Hubka KM, Dahlin RL, Meretoja VV, Kasper FK, Mikos AG. Enhancing chondrogenic phenotype for cartilage tissue engineering: monoculture and coculture of articular chondrocytes and mesenchymal stem cells. Tissue Eng Part B Rev. 2014;20:641–54.
131. Lohan A, Marzahn U, El Sayed K, Haisch A, Mueller RD, Kohl B, et al. Osteochondral articular defect repair using auricle-derived autologous chondrocytes in a rabbit model. Ann Anat Anat Anz. 2014;196:317–26.

132. Xu F, Xu L, Wang Q, Ye Z, Zhou Y, Tan W-S. 3D dynamic culture of rabbit articular chondrocytes encapsulated in alginate gel beads using spinner flasks for cartilage tissue regeneration. BioMed Res Int. 2014;2014:539789.
133. Li G, Fu N, Xie J, Fu Y, Deng S, Cun X, et al. Poly(3-hydroxybutyrate-co-4-hydroxybutyrate) based electrospun 3D scaffolds for delivery of autogeneic chondrocytes and adipose-derived stem cells: evaluation of cartilage defects in rabbit. J Biomed Nanotechnol. 2015;11:105–16.
134. Omobono MA, Zhao X, Furlong MA, Kwon C-H, Gill TJ, Randolph MA, et al. Enhancing the stiffness of collagen hydrogels for delivery of encapsulated chondrocytes to articular lesions for cartilage regeneration. J Biomed Mater Res A. 2015;103:1332–8.
135. Bryant SJ, Bender RJ, Durand KL, Anseth KS. Encapsulating chondrocytes in degrading PEG hydrogels with high modulus: engineering gel structural changes to facilitate cartilaginous tissue production. Biotechnol Bioeng. 2004;86:747–55.
136. Xue JX, Gong YY, Zhou GD, Liu W, Cao Y, Zhang WJ. Chondrogenic differentiation of bone marrow-derived mesenchymal stem cells induced by acellular cartilage sheets. Biomaterials. 2012;33:5832–40.
137. Deng J, She R, Huang W, Dong Z, Mo G, Liu B. A silk fibroin/chitosan scaffold in combination with bone marrow-derived mesenchymal stem cells to repair cartilage defects in the rabbit knee. J Mater Sci Mater Med. 2013;24:2037–46.
138. Lim CT, Ren X, Afizah MH, Tarigan-Panjaitan S, Yang Z, Wu Y, et al. Repair of osteochondral defects with rehydrated freeze-dried oligo poly(ethylene glycol) fumarate hydrogels seeded with bone marrow mesenchymal stem cells in a porcine model. Tissue Eng Part A. 2013;19:1852–61.
139. Xue K, Qi L, Zhou G, Liu K. A two-step method of constructing mature cartilage using bone marrow-derived mesenchymal stem cells. Cells Tissues Organs. 2013;197:484–95.
140. Wang L, Tran I, Seshareddy K, Weiss ML, Detamore MS. A comparison of human bone marrow-derived mesenchymal stem cells and human umbilical cord-derived mesenchymal stromal cells for cartilage tissue engineering. Tissue Eng Part A. 2009;15:2259–66.
141. Li C, Wei G, Gu Q, Wen G, Qi B, Xu L, et al. Donor Age and cell passage affect osteogenic ability of rat bone marrow mesenchymal stem cells. Cell Biochem Biophys. 2015;72:543–9.
142. Li X, Li Y, Zuo Y, Qu D, Liu Y, Chen T, et al. Osteogenesis and chondrogenesis of biomimetic integrated porous PVA/gel/V-n-HA/pa6 scaffolds and BMSCs construct in repair of articular osteochondral defect. J Biomed Mater Res A. 2015;103:3226–36.
143. Zuk PA, Zhu M, Mizuno H, Huang J, Futrell JW, Katz AJ, et al. Multilineage cells from human adipose tissue: implications for cell-based therapies. Tissue Eng. 2001;7:211–28.
144. Yoon HH, Bhang SH, Shin J-Y, Shin J, Kim B-S. Enhanced cartilage formation via three-dimensional cell engineering of human adipose-derived stem cells. Tissue Eng Part A. 2012;18:1949–56.
145. Jung M-S, Jang HB, Lee S-E, Park J-H, Hwang Y-S. In vitro micro-mineralized tissue formation by the combinatory condition of adipose-derived stem cells, macroporous PLGA microspheres and a bioreactor. Macromol Res. 2014;22:47–57.
146. Veronesi F, Maglio M, Tschon M, Aldini NN, Fini M. Adipose-derived mesenchymal stem cells for cartilage tissue engineering: state-of-the-art in in vivo studies. J Biomed Mater Res A. 2014;102:2448–66.
147. Wang T, Lai JH, Han L-H, Tong X, Yang F. Chondrogenic differentiation of adipose-derived stromal cells in combinatorial hydrogels containing cartilage matrix proteins with decoupled mechanical stiffness. Tissue Eng Part A. 2014;20:2131–9.
148. Wang ZJ, An RZ, Zhao JY, Zhang Q, Yang J, Wang JB, et al. Repair of articular cartilage defects by tissue-engineered cartilage constructed with adipose-derived stem cells and acellular cartilaginous matrix in rabbits. Genet Mol Res. 2014;13:4599–606.
149. Shen J, Gao Q, Zhang Y, He Y. Autologous platelet-rich plasma promotes proliferation and chondrogenic differentiation of adipose-derived stem cells. Mol Med Rep. 2015;11:1298–303.

150. Tang X-B, Dong P-L, Wang J, Zhou H-Y, Zhang H-X, Wang S-Z. Effect of autologous platelet-rich plasma on the chondrogenic differentiation of rabbit adipose-derived stem cells in vitro. Exp Ther Med. 2015;10:477–83.
151. Cheng A, Kapacee Z, Peng J, Lu S, Lucas RJ, Hardingham TE, et al. Cartilage repair using human embryonic stem cell-derived chondroprogenitors. Stem Cells Transl Med. 2014;3:1287–94.
152. Toh WS, Lee EH, Guo X-M, Chan JKY, Yeow CH, Choo AB, et al. Cartilage repair using hyaluronan hydrogel-encapsulated human embryonic stem cell-derived chondrogenic cells. Biomaterials. 2010;31:6968–80.
153. Hwang NS, Varghese S, Elisseeff J. Cartilage tissue engineering – directed differentiation of embryonic stem cells in three-dimensional hydrogel culture. In: Vemuri MC, editor. Methods in molecular biology. New York: Humana Press; 2007. p. 351–73.
154. Pilichi S, Rocca S, Pool RR, Dattena M, Masala G, Mara L, et al. Treatment with embryonic stem-like cells into osteochondral defects in sheep femoral condyles. BMC Vet Res. 2014;10:301.
155. Wakitani S, Aoki H, Harada Y, Sonobe M, Morita Y, Mu Y, et al. Embryonic stem cells form articular cartilage, not teratomas, in osteochondral defects of rat joints. Cell Transplant. 2004;13:331–6.
156. Hwang NS, Varghese S, Elisseeff J. Derivation of chondrogenically-committed cells from human embryonic cells for cartilage tissue regeneration. PloS ONE. 2008;3:e2498.
157. Toh WS, Lee EH, Cao T. Potential of human embryonic stem cells in cartilage tissue engineering and regenerative medicine. Stem Cell Rev Rep. 2011;7:544–59.
158. Chang H, Tate MLK. Concise review: the periosteum: tapping into a reservoir of clinically useful progenitor cells. Stem Cells Transl Med. 2012;1:480–91.
159. De Bari C, Dell'Accio F, Tylzanowski P, Luyten FP. Multipotent mesenchymal stem cells from adult human synovial membrane. Arthritis Rheum. 2001;44:1928–42.
160. Liu Y, Buckley CT, Downey R, Mulhall KJ, Kelly DJ. The role of environmental factors in regulating the development of cartilaginous grafts engineered using osteoarthritic human infrapatellar fat pad–derived stem cells. Tissue Eng Part A. 2012;18:1531–41.
161. Richter W. Mesenchymal stem cells and cartilage in situ regeneration. J Intern Med. 2009;266:390–405.
162. Ogata Y, Mabuchi Y, Yoshida M, Suto EG, Suzuki N, Muneta T, et al. Purified human synovium mesenchymal stem cells as a good resource for cartilage regeneration. PloS ONE. 2015;10:e0129096.
163. Alegre-Aguaron E, Sampat SR, Xiong JC, Colligan RM, Bulinski JC, Cook JL, et al. Growth factor priming differentially modulates components of the extracellular matrix proteome in chondrocytes and synovium-derived stem cells. PloS ONE. 2014;9:e88053.
164. Chang CB, Han SA, Kim EM, Lee S, Seong SC, Lee MC. Chondrogenic potentials of human synovium-derived cells sorted by specific surface markers. Osteoarthritis Cartilage. 2013;21:190–9.
165. Chang C-H, Chen C-C, Liao C-H, Lin F-H, Hsu Y-M, Fang H-W. Human acellular cartilage matrix powders as a biological scaffold for cartilage tissue engineering with synovium-derived mesenchymal stem cells. J Biomed Mater Res A. 2014;102:2248–57.
166. Jones BA, Pei M. Synovium-derived stem cells: a tissue-specific stem cell for cartilage engineering and regeneration. Tissue Eng Part B Rev. 2012;18:301–11.
167. Suzuki S, Muneta T, Tsuji K, Ichinose S, Makino H, Umezawa A, et al. Properties and usefulness of aggregates of synovial mesenchymal stem cells as a source for cartilage regeneration. Arthritis Res Ther. 2012;14:R136.
168. Fan J, Ren L, Liang R, Gong Y, Cai D, Wang D-A. Chondrogenesis of synovium-derived mesenchymal stem cells in photopolymerizing hydrogel scaffolds. J Biomater Sci Polym Ed. 2010;21:1653–67.
169. Pei M, He F, Boyce BM, Kish VL. Repair of full-thickness femoral condyle cartilage defects using allogeneic synovial cell-engineered tissue constructs. Osteoarthritis Cartilage. 2009;17:714–22.

170. Demoor M, Ollitrault D, Gomez-Leduc T, Bouyoucef M, Hervieu M, Fabre H, et al. Cartilage tissue engineering: molecular control of chondrocyte differentiation for proper cartilage matrix reconstruction. Biochim Biophys Acta Gen Subj. 2014;1840:2414–40.
171. Lee S-H, Shin H. Matrices and scaffolds for delivery of bioactive molecules in bone and cartilage tissue engineering. Adv Drug Deliv Rev. 2007;59:339–59.
172. Angel MJ, Sgaglione NA, Grande DA. Clinical applications of bioactive factors in sports medicine – current concepts and future trends. Sports Med Arthrosc Rev. 2006;14:138–45.
173. Kawamura K, Chu CR, Sobajima S, Robbins PD, Fu FH, Izzo NJ, et al. Adenoviral-mediated transfer of TGF-β1 but not IGF-1 induces chondrogenic differentiation of human mesenchymal stem cells in pellet cultures. Exp Hematol. 2005;33:865–72.
174. Bian L, Zhai DY, Tous E, Rai R, Mauck RL, Burdick JA. Enhanced MSC chondrogenesis following delivery of TGF-β3 from alginate microspheres within hyaluronic acid hydrogels in vitro and in vivo. Biomaterials. 2011;32:6425–34.
175. Han Y, Wei Y, Wang S, Song Y. Cartilage regeneration using adipose-derived stem cells and the controlled-released hybrid microspheres. Joint Bone Spine. 2010;77:27–31.
176. Hildner F, Albrecht C, Gabriel C, Redl H, van Griensven M. State of the art and future perspectives of articular cartilage regeneration: a focus on adipose-derived stem cells and platelet-derived products. J Tissue Eng Regen Med. 2011;5:E36–51.
177. Lu C-H, Lin K-J, Chiu H-Y, Chen C-Y, Yen T-C, Hwang S-M, et al. Improved chondrogenesis and engineered cartilage formation from TGF-beta 3-expressing adipose-derived stem cells cultured in the rotating-shaft bioreactor. Tissue Eng Part A. 2012;18:2114–24.
178. Re'em T, Witte F, Willbold E, Ruvinov E, Cohen S. Simultaneous regeneration of articular cartilage and subchondral bone induced by spatially presented TGF-beta and BMP-4 in a bilayer affinity binding system. Acta Biomater. 2012;8:3283–93.
179. Pretzel D, Linss S, Ahrem H, Endres M, Kaps C, Klemm D, et al. A novel in vitro bovine cartilage punch model for assessing the regeneration of focal cartilage defects with biocompatible bacterial nanocellulose. Arthritis Res Ther. 2013;15:R59.
180. Lu C-H, Yeh T-S, Yeh C-L, Fang Y-HD, Sung L-Y, Lin S-Y, et al. Regenerating cartilages by engineered ASCs: prolonged TGF-beta 3/BMP-6 expression improved articular cartilage formation and restored zonal structure. Mol Ther. 2014;22:186–95.
181. Elmallah RK, Cherian JJ, Jauregui JJ, Pierce TP, Beaver WB, Mont MA. Genetically modified chondrocytes expressing TGF-beta 1: a revolutionary treatment for articular cartilage damage? Expert Opin Biol Ther. 2015;15:455–64.
182. Kim SH, Kim SH, Jung Y. TGF-beta(3) encapsulated PLCL scaffold by a supercritical CO2-HFIP co-solvent system for cartilage tissue engineering. J Control Release. 2015;206:101–7.
183. Murphy MK, Huey DJ, Hu JC, Athanasiou KA. TGF-beta 1, GDF-5, and BMP-2 stimulation induces chondrogenesis in expanded human articular chondrocytes and marrow-derived stromal cells. Stem Cells. 2015;33:762–73.
184. Zhang N, Lock J, Sallee A, Liu H. Magnetic nanocomposite hydrogel for potential cartilage tissue engineering: synthesis, characterization, and cytocompatibility with bone marrow derived mesenchymal stem cells. ACS Appl Mater Interfaces. 2015;7:20987–98.
185. Capito RM, Spector M. Collagen scaffolds for nonviral IGF-1 gene delivery in articular cartilage tissue engineering. Gene Ther. 2007;14:721–32.
186. Singh NK, Singh GR, Amarpal, Kinjavdekar P, Sharma AK, Mohanty TR. Articular cartilage repair with autografting under the influence of insulin-like growth factor-1 in rabbits. J Veterinary Med Ser A Physiol Pathol Clin Med. 2007;54:210–8.
187. Davies LC, Blain EJ, Gilbert SJ, Caterson B, Duance VC. The potential of IGF-1 and TGF beta 1 for promoting "Adult" articular cartilage repair: an in vitro study. Tissue Eng Part A. 2008;14:1251–61.
188. Bastiaansen-Jenniskens YM, Koevoet W, Feijt C, Bos PK, Verhaar JAN, Van Osch GJVM, et al. Proteoglycan production is required in initial stages of new cartilage matrix formation but inhibits integrative cartilage repair. J Tissue Eng Regen Med. 2009;3:117–23.

189. An C, Cheng Y, Yuan Q, Li J. IGF-1 and BMP-2 induces differentiation of adipose-derived mesenchymal stem cells into chondrocytes-like cells. Ann Biomed Eng. 2010;38:1647–54.
190. Liu XW, Hu J, Man C, Zhang B, Ma YQ, Zhu SS. Insulin-like growth factor-1 suspended in hyaluronan improves cartilage and subchondral cancellous bone repair in osteoarthritis of temporomandibular joint. Int J Oral Maxillofac Surg. 2011;40:184–90.
191. Spiller KL, Liu Y, Holloway JL, Maher SA, Cao Y, Liu W, et al. A novel method for the direct fabrication of growth factor-loaded microspheres within porous nondegradable hydrogels: controlled release for cartilage tissue engineering. J Control Release. 2012;157:39–45.
192. Joos H, Wildner A, Hogrefe C, Reichel H, Brenner RE. Interleukin-1 beta and tumor necrosis factor alpha inhibit migration activity of chondrogenic progenitor cells from non-fibrillated osteoarthritic cartilage. Arthritis Res Ther. 2013;15:R119.
193. Henson FMD, Vincent T. Chondrocyte outgrowth into a gelatin scaffold in a single impact load model of damage/repair - effect of BMP-2. BMC Musculoskelet Disord. 2007;8:120.
194. Kuo AC, Rodrigo JJ, Reddi AH, Curtiss S, Grotkopp E, Chiu M. Microfracture and bone morphogenetic protein 7 (BMP-7) synergistically stimulate articular cartilage repair. Osteoarthritis Cartilage. 2006;14:1126–35.
195. Matsumoto T, Cooper GM, Gharaibeh B, Meszaros LB, Li G, Usas A, et al. Cartilage repair in a rat model of osteoarthritis through intraarticular transplantation of muscle-derived stem cells expressing bone morphogenetic protein 4 and soluble Flt-1. Arthritis Rheum. 2009;60:1390–405.
196. Menendez MI, Clark DJ, Carlton M, Flanigan DC, Jia G, Sammet S, et al. Direct delayed human adenoviral BMP-2 or BMP-6 gene therapy for bone and cartilage regeneration in a pony osteochondral model. Osteoarthritis Cartilage. 2011;19:1066–75.
197. Nochi H, Sung JH, Lou J, Adkisson HD, Maloney WJ, Hruska KA. Adenovirus mediated BMP-13 gene transfer induces chondrogenic differentiation of murine mesenchymal progenitor cells. J Bone Miner Res. 2004;19:111–22.
198. Shi J, Zhang X, Zhu J, Pi Y, Hu X, Zhou C, et al. Nanoparticle delivery of the bone morphogenetic protein 4 gene to adipose-derived stem cells promotes articular cartilage repair in vitro and in vivo. Arthrosc J Arthrosc Relat Surg. 2013;29:2001–U182.
199. Yang HS, La W-G, Bhang SH, Kim H-J, Im G-I, Lee H, et al. Hyaline cartilage regeneration by combined therapy of microfracture and long-term bone morphogenetic protein-2 delivery. Tissue Eng Part A. 2011;17:1809–18.
200. Zhang Y, Tang CL, Chen WJ, Zhang Q, Wang SL. Dynamic compression combined with exogenous SOX-9 promotes chondrogenesis of adipose-derived mesenchymal stem cells in PLGA scaffold. Eur Rev Med Pharmacol Sci. 2015;19:2671–8.
201. Kaul G, Cucchiarini M, Arntzen D, Zurakowski D, Menger MD, Kohn D, et al. Local stimulation of articular cartilage repair by transplantation of encapsulated chondrocytes overexpressing human fibroblast growth factor 2 (FGF-2) in vivo. J Gene Med. 2006;8:100–11.
202. Takafuji H, Suzuki T, Okubo Y, Fujimura K, Bessho K. Regeneration of articular cartilage defects in the temporomandibular joint of rabbits by fibroblast growth factor-2: a pilot study. Int J Oral Maxillofac Surg. 2007;36:934–7.
203. Ellman MB, An HS, Muddasani P, Im H-J. Biological impact of the fibroblast growth factor family on articular cartilage and intervertebral disc homeostasis. Gene. 2008;420:82–9.
204. Kuroda Y, Akiyama H, Kawanabe K, Tabata Y, Nakamura T. Treatment of experimental osteonecrosis of the hip in adult rabbits with a single local injection of recombinant human FGF-2 microspheres. J Bone Miner Metab. 2010;28:608–16.
205. Maehara H, Sotome S, Yoshii T, Torigoe I, Kawasaki Y, Sugata Y, et al. Repair of large osteochondral defects in rabbits using porous hydroxyapatite/collagen (HAp/Col) and fibroblast growth factor-2 (FGF-2). J Orthop Res. 2010;28:677–86.
206. Kim JH, Lee MC, Seong SC, Park KH, Lee S. Enhanced proliferation and chondrogenic differentiation of human synovium-derived stem cells expanded with basic fibroblast growth factor. Tissue Eng Part A. 2011;17:991–1002.

207. Yuan L-J, Niu C-C, Lin S-S, Chan Y-S, Yang C-Y, Chen W-J, et al. Additive effects of hyperbaric oxygen and platelet-derived growth factor-BB in chondrocyte transplantation via up-regulation expression of platelet-derived growth factor-beta receptor. J Orthop Res. 2009;27:1439–46.
208. Shin SH, Song HY, Kim MY, Do EK, Kim KH, Kim JH. Platelet-activating factor receptor mediates oxidized low density lipoprotein-induced migration of bone marrow-derived mesenchymal stem cells. Cell Physiol Biochem. 2010;26:689–98.
209. Howard D, Shepherd JH, Kew SJ, Hernandez P, Ghose S, Wardale JA, et al. Release of growth factors from a reinforced collagen GAG matrix supplemented with platelet rich plasma: influence on cultured human meniscal cells. J Orthop Res. 2014;32:273–8.
210. Lee JM, Ryu JH, Kim EA, Jo S, Kim B-S, Lee H, et al. Adhesive barrier/directional controlled release for cartilage repair by endogenous progenitor cell recruitment. Biomaterials. 2015;39:173–81.
211. Scotti C, Mangiavini L, Boschetti F, Vitari F, Domeneghini C, Fraschini G, et al. Effect of in vitro culture on a chondrocyte-fibrin glue hydrogel for cartilage repair. Knee Surg Sports Traumatol Arthrosc. 2010;18:1400–6.
212. Deponti D, Di Giancamillo A, Mangiavini L, Pozzi A, Fraschini G, Sosio C, et al. Fibrin-based model for cartilage regeneration: tissue maturation from in vitro to in vivo. Tissue Eng Part A. 2012;18:1109–22.
213. Erickson IE, Kestle SR, Zellars KH, Dodge GR, Burdick JA, Mauck RL. Improved cartilage repair via in vitro pre-maturation of MSC-seeded hyaluronic acid hydrogels. Biomed Mater. 2012;7:024110.
214. Jeon JE, Schrobback K, Meinert C, Sramek V, Hutmacher DW, Klein TJ. Effect of preculture and loading on expression of matrix molecules, matrix metalloproteinases, and cytokines by expanded osteoarthritic chondrocytes. Arthritis Rheum. 2013;65:2356–67.
215. Sabatino MA, Santoro R, Gueven S, Jaquiery C, Wendt DJ, Martin I, et al. Cartilage graft engineering by co-culturing primary human articular chondrocytes with human bone marrow stromal cells. J Tissue Eng Regen Med. 2015;9:1394–403.
216. Zhao X, Bichara DA, Zhou L, Kulig KM, Tseng A, Bowley CM, et al. Conditions for seeding and promoting neo-auricular cartilage formation in a fibrous collagen scaffold. J Cranio-Maxillofac Surg. 2015;43:382–9.
217. Cao Y, Vacanti JP, Paige KT, Upton J, Vacanti CA. Transplantation of chondrocytes utilizing a polymer-cell construct to produce tissue-engineered cartilage in the shape of a human ear. Plast Reconstr Surg. 1997;100:297–302.
218. Freyria A-M, Cortial D, Ronzière M-C, Guerret S, Herbage D. Influence of medium composition, static and stirred conditions on the proliferation of and matrix protein expression of bovine articular chondrocytes cultured in a 3-D collagen scaffold. Biomaterials. 2004;25:687–97.
219. Darling EM, Athanasiou KA. Articular cartilage bioreactors and bioprocesses. Tissue Eng. 2003;9:9–26.
220. Shahin K, Doran PM. Strategies for enhancing the accumulation and retention of extracellular matrix in tissue-engineered cartilage cultured in bioreactors. PloS ONE. 2011;6:e23119.
221. Gaissmaier C, Koh JL, Weise K, Mollenhauer JA. Future perspectives of articular cartilage repair. Injury. 2008;39 Suppl 1:S114–20.
222. Bauge C, Boumediene K. Use of adult stem cells for cartilage tissue engineering: current status and future developments. Stem Cells Int. 2015;2015:438026.
223. Fioretta ES, Fledderus JO, Burakowska-Meise EA, Baaijens F, Verhaar MC, Bouten CV. Polymer–based scaffold designs for in situ vascular tissue engineering: controlling recruitment and differentiation behavior of endothelial colony forming cells. Macromol Biosci. 2012;12:577–90.
224. Vanden Berg-Foels WS. In situ tissue regeneration: chemoattractants for endogenous stem cell recruitment. Tissue Eng. 2013;45:e57.

225. Kon E, Roffi A, Filardo G, Tesei G, Marcacci M. Scaffold-based cartilage treatments: with or without cells? A systematic review of preclinical and clinical evidence. Arthrosc: J Arthrosc Relat Surg. 2015;31:767–75.
226. Wang W, Sun L, Zhang P, Song J, Liu W. An anti-inflammatory cell-free collagen/resveratrol scaffold for repairing osteochondral defects in rabbits. Acta Biomater. 2014;10:4983–95.
227. Dai Y, Liu G, Ma L, Wang D, Gao C. Cell-free macro-porous fibrin scaffolds for in situ inductive regeneration of full-thickness cartilage defects. J Mater Chem B. 2016;4:4410–9.
228. Roessler PP, Pfister B, Gesslein M, Figiel J, Heyse TJ, Colcuc C, et al. Short-term follow up after implantation of a cell-free collagen type I matrix for the treatment of large cartilage defects of the knee. Int Orthop. 2015;39:2473–9. 1–7.
229. Madry H, van Dijk CN, Mueller-Gerbl M. The basic science of the subchondral bone. Knee Surg Sports Traumatol Arthrosc. 2010;18:419–33.
230. Gelse K, Klinger P, Koch M, Surmann-Schmitt C, von der Mark K, Swoboda B, et al. Thrombospondin-1 prevents excessive ossification in cartilage repair tissue induced by osteogenic protein-1. Tissue Eng Part A. 2011;17:2101–12.
231. Ghosh S, Viana J, Reis R, Mano J. Bi-layered constructs based on poly (L-lactic acid) and starch for tissue engineering of osteochondral defects. Mater Sci Eng C. 2008;28:80–6.
232. Nukavarapu SP, Dorcemus DL. Osteochondral tissue engineering: current strategies and challenges. Biotechnol Adv. 2013;31:706–21.
233. Chen GP, Sato T, Tanaka J, Tateishi T. Preparation of a biphasic scaffold for osteochondral tissue engineering. Mater Sci Eng C Biomim Supramol Syst. 2006;26:118–23.
234. Jiang C-C, Chiang H, Liao C-J, Lin Y-J, Kuo T-F, Shieh C-S, et al. Repair of porcine articular cartilage defect with a biphasic osteochondral composite. J Orthop Res. 2007;25:1277–90.
235. Yang Q, Peng J, Lu S-b, Guo Q-y, Zhao B, Zhang L, et al. Evaluation of an extracellular matrix-derived acellular biphasic scaffold/cell construct in the repair of a large articular high-load-bearing osteochondral defect in a canine model. Chin Med J (Engl). 2011;124:3930–8.
236. Duan X, Zhu X, Dong X, Yang J, Huang F, Cen S, et al. Repair of large osteochondral defects in a beagle model with a novel type I collagen/glycosaminoglycan-porous titanium biphasic scaffold. Mater Sci Eng C Mater Biol Appl. 2013;33:3951–7.
237. Liu S, Wu J, Liu X, Chen D, Bowlin GL, Cao L, et al. Osteochondral regeneration using an oriented nanofiber yarn-collagen type I/hyaluronate hybrid/TCP biphasic scaffold. J Biomed Mater Res A. 2015;103:581–92.
238. Jeon JE, Vaquette C, Klein TJ, Hutmacher DW. Perspectives in multiphasic osteochondral tissue engineering. Anat Rec Adv Integr Anat Evol Biol. 2014;297:26–35.
239. Jang K-M, Lee J-H, Park CM, Song H-R, Wang JH. Xenotransplantation of human mesenchymal stem cells for repair of osteochondral defects in rabbits using osteochondral biphasic composite constructs. Knee Surg Sports Traumatol Arthrosc. 2014;22:1434–44.
240. Filardo G, Kon E, Perdisa F, Balboni F, Marcacci M. Autologous osteochondral transplantation for the treatment of knee lesions: results and limitations at two years' follow-up. Int Orthop. 2014;38:1905–12.
241. Zhang S, Chen L, Jiang Y, Cai Y, Xu G, Tong T, et al. Bi-layer collagen/microporous electrospun nanofiber scaffold improves the osteochondral regeneration. Acta Biomater. 2013;9:7236–47.
242. Castro NJ, Patel R, Zhang LG. Design of a novel 3D printed bioactive nanocomposite scaffold for improved osteochondral regeneration. Cel Mol Bioeng. 2015;8:416–32.
243. Kim SH, Kim SH, Jung Y. Bi-layered PLCL/(PLGA/beta-TCP) composite scaffold for osteochondral tissue engineering. J Bioact Compat Polym. 2015;30:178–87.
244. Kon E, Filardo G, Shani J, Altschuler N, Levy A, Zaslav K, et al. Osteochondral regeneration with a novel aragonite-hyaluronate biphasic scaffold: up to 12-month follow-up study in a goat model. J Orthop Surg Res. 2015;10:81.
245. Rutgers M, van Pelt MJP, Dhert WJA, Creemers LB, Saris DBF. Evaluation of histological scoring systems for tissue-engineered, repaired and osteoarthritic cartilage. Osteoarthritis Cartilage. 2010;18:12–23.

246. Mankin HJ, LIPPIELLO L. Biochemical and metabolic abnormalities in articular cartilage from osteo-arthritic human hips. J Bone Joint Surg Am. 1970;52:424–34.
247. Lahm A, Uh M, Erggelet C, Haberstroh J, Mrosek E. Articular cartilage degeneration after acute subchondral bone damage – an experimental study in dogs with histopathological grading. Acta Orthop Scand. 2004;75:762–7.
248. Pearson RG, Kurien T, Shu KSS, Scammell BE. Histopathology grading systems for characterisation of human knee osteoarthritis – reproducibility, variability, reliability, correlation, and validity. Osteoarthritis Cartilage. 2011;19:324–31.
249. Custers RJH, Creemers LB, Verbout AJ, van Rijen MHP, Dhert WJA, Saris DBF. Reliability, reproducibility and variability of the traditional histologic/histochemical grading system vs the new OARSI osteoarthritis cartilage histopathology assessment system. Osteoarthritis Cartilage. 2007;15:1241–8.
250. Pritzker K, Gay S, Jimenez S, Ostergaard K, Pelletier J-P, Revell P, et al. Osteoarthritis cartilage histopathology: grading and staging. Osteoarthritis Cartilage. 2006;14:13–29.
251. O'Driscoll SW, Keeley FW, Salter RB. Durability of regenerated articular cartilage produced by free autogenous periosteal grafts in major full-thickness defects in joint surfaces under the influence of continuous passive motion. A follow-up report at one year. J Bone Joint Surg Am. 1988;70:595–606.
252. Pineda S, Pollack A, Stevenson S, Goldberg V, Caplan A. A semiquantitative scale or histologic grading of articular cartilage repair. Cells Tissues Organs. 1992;143:335–40.
253. Wakitani S, Goto T, Pineda SJ, Young RG, Mansour JM, Caplan AI, et al. Mesenchymal cell-based repair of large, full-thickness defects of articular cartilage. J Bone Joint Surg Am. 1994;76:579–92.
254. Roberts S, McCall IW, Darby AJ, Menage J, Evans H, Harrison PE, et al. Autologous chondrocyte implantation for cartilage repair: monitoring its success by magnetic resonance imaging and histology. Arthritis Res Ther. 2002;5:1.
255. Mainil-Varlet P, Aigner T, Brittberg M, Bullough P, Hollander A, Hunziker E, et al. Histological assessment of cartilage repair. J Bone Joint Surg Am. 2003;85:45–57.
256. Mainil-Varlet P, Van Damme B, Nesic D, Knutsen G, Kandel R, Roberts S. A new histology scoring system for the assessment of the quality of human cartilage repair: ICRS II. Am J Sports Med. 2010;38:880–90.
257. Hoemann CD, Tran-Khanh N, Chevrier A, Chen G, Lascau-Coman V, Mathieu C, et al. Chondroinduction is the main cartilage repair response to microfracture and microfracture with BST-CarGel: results as shown by ICRS-II histological scoring and a novel zonal collagen type scoring method of human clinical biopsy specimens. Am J Sports Med. 2015;43:2469–80.
258. O'Driscoll SW, Marx RG, Beaton DE, Miura Y, Gallay SH, Fitzsimmons JS. Validation of a simple histological-histochemical cartilage scoring system. Tissue Eng. 2001;7:313–20.
259. Grogan SP, Barbero A, Winkelmann V, Rieser F, Fitzsimmons JS, O'driscoll S, et al. Visual histological grading system for the evaluation of in vitro-generated neocartilage. Tissue Eng. 2006;12:2141–9.
260. Bonasia DE, Marmotti A, Mattia S, Cosentino A, Spolaore S, Governale G, et al. The degree of chondral fragmentation affects extracellular matrix production in cartilage autograft implantation: an in vitro study. Arthrosc J Arthrosc Relat Surg. 2015;31:2335–41.

Chapter 10
Skin Regeneration

Xiaowen Zheng, Qian Li, Lie Ma, and Changyou Gao

10.1 Introduction

The skin, the largest organ of the human body, provides a protective barrier against physical, chemical, and biological pathogens to support and maintain human health. In addition, the skin also has the function of temperature regulation, external insult protection, and detoxing. Typically, the skin has hierarchical structures including the upper epidermal layer, interlayer dermis, and subcutaneous tissue. The epidermis whose thickness is 0.1–0.2 mm consists mainly of keratinocytes derived from the capillary network. The dermis layer composes of fibroblasts and extracellular matrix (ECM) including collagen, glycosaminoglycans (GAGs), and elastin. Skin appendages such as hair follicles, sweat glands, and sebaceous glands are from the subcutaneous tissue and play a great role in the sensation, temperature regulation, and detoxing (Fig. 10.1) [1].

Burn, trauma, or chronic diseases frequently cause the loss of the skin, leading to descent of nonspecific immunity and bacterial infection, which is one of the most severe problems affecting human life quality. Thus, skin regeneration has become a major aim in the field of wound healing. In the past several decades, surgical therapies including skin transplantation have been applied to treat the loss of the skin and have achieved great success in skin regeneration. Autologous skin graft is the "gold standard" for clinical treatment of skin defect, and allograft plays a big role in the early period of skin repair as a temporary cover until a permanent skin graft is available. However, skin autograft and allograft are limited by the timely availability and donor sites. In addition, current skin grafts often suffer from a range of problems including incomplete biological functions, scar formation, and bacterial or virus infection during surgical therapies [2]. Thus, it has been becoming more and more

X. Zheng • Q. Li • L. Ma (✉) • C. Gao
MOE Key Laboratory of Macromolecular Synthesis and Functionalization, Department of Polymer Science and Engineering, Zhejiang University, Hangzhou 310027, China
e-mail: liema@zju.edu.cn

© Springer Science+Business Media Singapore 2016

C. Gao (ed.), *Polymeric Biomaterials for Tissue Regeneration*,
DOI 10.1007/978-981-10-2293-7_10

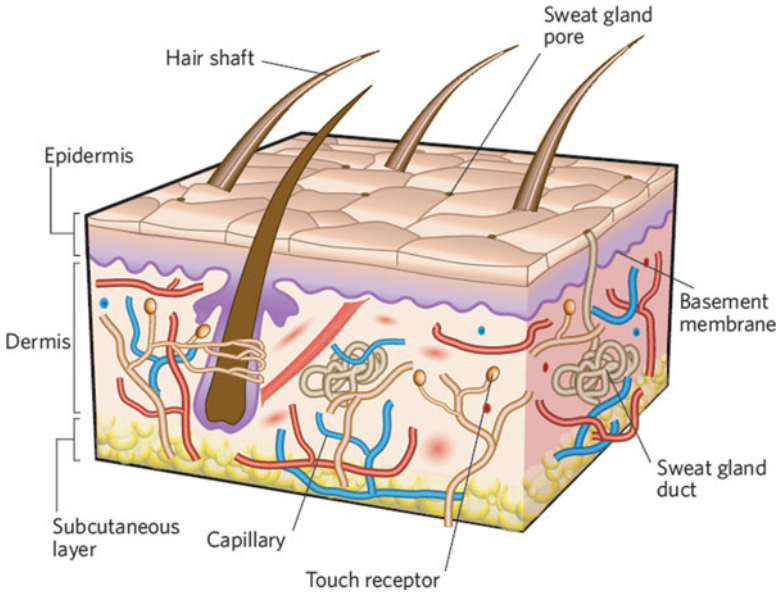

Fig. 10.1 The structure of the human skin (Reprinted from Ref. [1] with permission. Copyright 2007, Rights Managed by Nature Publishing Group)

urgent to find effective therapy strategies for the treatment of skin loss facing with the increasing clinical need and a vast patient resource.

Recently, skin substitute based on tissue engineering is being rapidly developed to bypass the limitations of conventional tissue transplantation and provide new therapeutic strategy to restore skin function [3]. Tissue engineering combines scaffold, cells, and biofactors to remodel the target tissue or organ in vitro, followed by in vivo transplantation according to the principles of materials, medicine, and biology. Skin tissue substitutes based on tissue engineering have been fabricating over the past several decades to provide more suitable therapeutic schemes for skin loss, and some commercial products are available in clinical application. For example, Dermagrafts®, a dermal skin substitute consists of poly(glycolic acid) (PGA), poly(lactic acid) (PLA), and fibroblasts, has been used to treat diabetic ulcers [4]. However, the fully functional skin regeneration is still a big challenge for skin tissue engineering. Better tissue engineering strategy in the aspect of exploitation of new biomaterials and novel design of biomaterial scaffolds should be developed to fulfill the increasing demand of skin regeneration.

This chapter focuses on the application of tissue engineering and regenerative medicine approach for the fabrication of bioengineered constructs for skin regeneration. First of all, the materials and the design of material scaffold for skin regeneration are summarized. Then the bio-functionalization of biomaterial scaffold is reviewed by using proteins, genes, and cytokines. Finally, some important challenges

for skin regeneration including angiogenesis, scarring, appendages regeneration, and in situ tissue regeneration are discussed.

10.2 Materials for Skin Regeneration

10.2.1 Natural Materials

Collagen, one of the most important components of ECM and composed of a triple helix, is widely used in skin regeneration due to its good biocompatibility, biodegradability, flexibility, and structural and functional similarity to ECM [5]. Besides the collagen derived from animal, plant-derived human collagen has been shown to be a promising biomaterial for skin tissue engineering because of its low risk of an allergic response or disease transmission [6]. However, the poor mechanical properties of collagen limit its application in skin substitute. A variety of methods including cross-linking and blending with other substances have been established to improve the mechanical properties of collagen-based scaffold [7]. For example, synthetic human elastin/collagen composite scaffolds were fabricated by electrospinning for tissue engineering dermis [8]. The scaffold supported fibroblast infiltration, de novo collagen deposition, and new capillary formation. Recently, a full-thickness skin equivalent consists of collagen and silk was prepared to study skin biology [9]. In our lab, a collagen/chitosan scaffold cross-linked with glutaraldehyde has been fabricated to promote the growth of fibroblasts and dermis regeneration. The cross-linking of glutaraldehyde and introduction of chitosan can enhance the biostability of the scaffold [10, 11]. Wang et al. used PLGA-knitted mesh to integrate with collagen/chitosan scaffold to improve the mechanical strength of the scaffolds [12]. Some commercial products based on collagen have been applied in clinical practice. For example, Integra® fabricated by cross-linked bovine collagen and chondroitin-6-sulfate was employed for dermal regeneration. Apligraf®, a collagen-based hydrogel seeded with dermal fibroblasts and epidermal cells, has been widely applied to treat burns and several kinds of ulcers in the clinic (Fig. 10.2) [13, 14]. But it remains a challenge to regenerate the skin with complete appendages.

Chitosan, the deacetylated derivative of chitin, is a linear polysaccharide consisting of glucosamine and N-acetyl glucosamine [15]. Chitosan can be tailored with various molecular weights (50–2000 kDa) as well as degrees of deacetylation (30–95 %), allowing wide adjustment of mechanical and biological properties [16]. Cross-linking is usually made to control the degradation rate and enhance the mechanical properties of chitosan matrix for skin tissue engineering as well [17]. Chitosan can be applied to deliver bioactive molecules. For example, the human epidermal growth factor (EGF) and basic fibroblast growth factor (bFGF) were encapsulated in chitosan scaffold to promote wound healing [18, 19]. In addition, membranes based on chitosan are widely used as wound dressings because of the

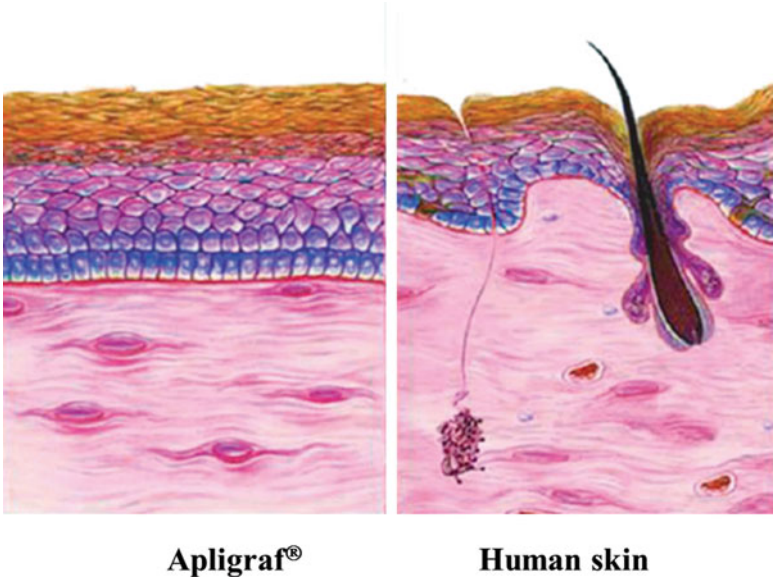

Fig. 10.2 Histology of Apligraf compared with normal human skin (Reprinted from Ref. [13] with permission. Copyright 2010 John Wiley & Sons, Inc)

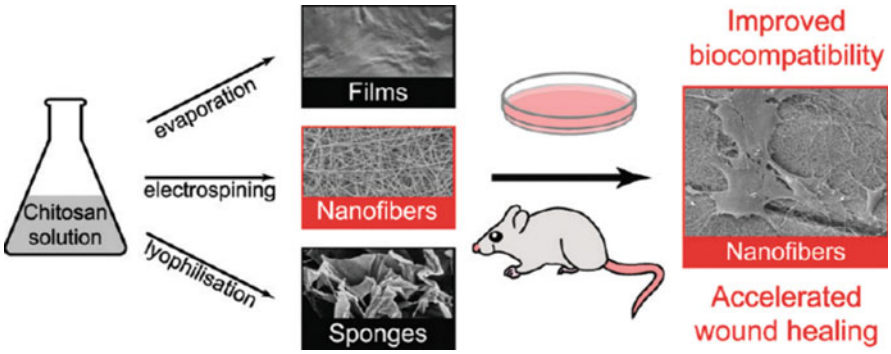

Fig. 10.3 Compared with chitosan films and sponges, the nanofibrillar structure strongly improved cell adhesion and proliferation in vitro. When used as a dressing covering full-thickness skin wounds in mice, chitosan nanofibrils induced a faster regeneration of both the epidermis and dermis compartments (Reprinted from [21] with permission. Copyright 2011 American Chemical Society)

antibacterial capacity of chitosan [20]. However, the most extensive application of chitosan for skin regeneration is serving as a three-dimensional matrix. Tchemtchoua et al. prepared chitosan nanofibrillar scaffold for skin repair. Compared to chitosan sponge, the chitosan nanofibrillar scaffold induced a faster regeneration of both the epidermis and dermis (Fig. 10.3) [21]. Kiyozumi et al. fabricated a photo-cross-linkable chitosan hydrogel containing DMEM/F12 medium (medium-Az-CH-LA)

for skin regeneration [22]. The hydrogel promoted re-epithelialization, vascularization, and wound repair. Moreover, compared to collagen sponge, thicker granulation tissue and earlier neovascularization were found in medium-Az-CH-LA [23].

Other natural biomaterials for skin regeneration including gelatin, hyaluronan, and fibrin are widely used as well. Shevchenko et al. designed a gelatin scaffold with attached silicone pseudo-epidermal layer for wound repair using a cryogelation technique [24]. The mechanical properties of the scaffold were comparable to the clinical product Integra®. In vivo test showed that the gelatin scaffold supports wound healing by allowing host cellular infiltration, bio-integration, and remodeling. Monteiro et al. utilized a spray-assisted layer-by-layer assembly technique to fabricate a multilayer film composed of poly-L-lysine (the epidermal component) and porous hyaluronic acid scaffold (the dermal component) in a rapid and controlled manner for skin tissue engineering [25]. The multilayer film enhances cell adhesion and regeneration of the epidermal barrier functions. Losi et al. prepared a fibrin-based scaffold with incorporated VEGF- and bFGF-loaded nanoparticles to stimulate wound healing [26]. The scaffold induces re-epithelialization and enhances granulation tissue formation/maturity and collagen deposition in genetically diabetic mice. Acellular dermal matrix (ADM) is used to obtain scaffolds with similar components and structure of ECM of the natural skin. For instance, AlloDerm® made of ADM by LifeCell® Corporation is extensively employed for full-thickness skin regeneration.

10.2.2 Synthetic Polymers

The mechanical property is the biggest drawback of natural materials for skin regeneration: thus, natural materials usually need to be cross-linked or combined with other materials. On the contrary, synthetic polymers with predictable and flexible physical and chemical properties including mechanical properties, functional groups, and degradation rate can be obtained under controlled conditions with mature techniques. Besides, synthetic polymers are biodegradable, are less expensive, and have lower immunological response than natural materials [27]. Furthermore, synthetic polymers such as PGA, PLA, poly(lactide-co-glycolide) (PLGA), and polycaprolactone (PCL) have been approved by the Food and Drug Administration (FDA) of the USA.

Synthetic polymers are important materials for skin regeneration. TransCyte® developed by the Advanced Tissue Science Company consisting of PLA scaffold and fibroblasts has been approved by the FDA for the healing of degree III burns [28]. PLGA matrices with fiber diameters varying from 150 to 6000 nm were fabricated via electrospinning [29]. Human skin fibroblasts acquire a well-spreading morphology and show significant growth on fiber matrices in the 350–1100 nm diameter range. Fibrous scaffolds composed of PLA and poly(ethylene glycol) (PEG) were prepared by electrospinning for skin tissue engineering [30]. The scaffold containing 30 % PEG exhibited most beneficial properties including wettability,

and adaptable bulk biodegradation, and promoted the penetration and growth of human dermal fibroblasts. However, synthetic polymers are usually hydrophobic, and their lack of functional groups leads to limited capacity to combine with biomolecules. To enforce the bioactivity of synthetic polymers, natural materials are widely applied with synthetic polymers to design hybrid scaffolds. Chen et al. fabricate a hybrid scaffold composed of knitted PLGA and weblike collagen microsponges to facilitate cell seeding and distribution and rapid formation of the dermal tissue [31]. A porous polycaprolactone (PCL)/collagen membrane was designed by Venugopal et al. via electrospinning. The well-defined nanostructure can well promote the growth and adhesion of cells [32]. The post-modification of synthetic polymers is another important method for the enhancement of bioactivity. Yang et al. used anhydrous ammonia plasma treatment to modify surface properties to improve the cell affinity of a PLA/PLGA scaffold [33]. The modified scaffold facilitated the growth of fibroblasts. Nanofibrous PCL/gelatin scaffolds were modified by collagen type I grafting [34]. The diameter of the fiber and porosity decreased with the increase of grafted collagen, and the collagen-modified nanofibrous PCL/gelatin scaffolds can maintain characteristic shape and promote proliferation of fibroblasts.

10.3 Scaffold Design for Skin Regeneration

The scaffold plays a vital role for skin regeneration by serving as a three-dimensional matrix for maintaining cell activities and promoting extracellular matrix formation, delivering biofactors, preserving tissue volume, and providing temporary mechanical function. As the skin is complicated with a multilayer structure, how to design a scaffold mimicking the hierarchical structure and ultrastructure of ECM of the skin is an issue of great importance. So far different formats of scaffolds have been designed to treat different kinds of damaged skins. For example, chitosan/poly(vinyl alcohol) (PVA) nanofibrous membrane has been prepared by electrospinning as a wound dressing [35]. However, for dermal or even full-thickness skin regeneration, the most common scaffold formats are porous scaffolds and hydrogels.

10.3.1 Porous Scaffolds

The porous scaffold is the most common format for skin regeneration. Typically a porous scaffold possesses unique microstructures similar to native ECM, showing high surface area which facilitates cell attachment and growth. Both natural and synthetic polymers can be fabricated into the porous scaffolds with controlled three-dimensional structures by methods such as gas foaming, freeze-drying, and electrospinning.

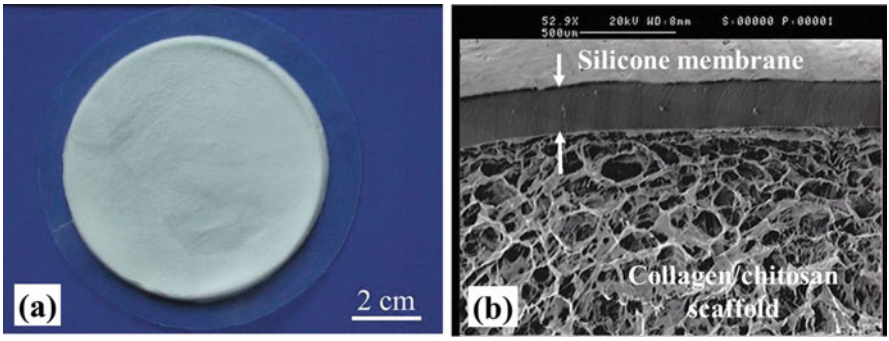

Fig. 10.4 (**a**) A view of the scaffold after being combined with a silicone membrane with a thickness of about 0.14 mm. (**b**) The microstructures of the scaffold observed under a scanning electron microscope (Reprinted from Ref. [38] with permission. Copyright 2006 John Wiley & Sons, Ltd)

A novel porous scaffold composed of collagen, hyaluronic acid, and gelatin was fabricated by freeze-drying for skin repair [36]. The average pore diameter of the scaffold was 132.5 ± 8.4 μm, which is beneficial for cell attachment and infiltration. The in vivo histological results revealed that the scaffold promoted wound healing compared to the group without treatments. Lu et al. fabricated a funnel-like porous PLLA-collagen and PLLA-gelatin hybrid scaffolds by forming collagen or gelatin sponge on a woven PLLA mesh for skin tissue engineering [37]. PLLA-collagen and PLLA-gelatin porous scaffolds promoted the regeneration of the dermal tissue and reduced contraction during the formation of new tissues. In our lab, Ma et al. have developed a collagen/chitosan hybrid porous scaffold which was cross-linked by glutaraldehyde (GA) to improve their biostability for skin regeneration [11]. Collagen and chitosan are evenly distributed in the scaffolds with high porosity and good interconnectivity. In vitro culture suggested that the porous scaffold could maintain the original good cytocompatibility of collagen and effectively accelerate infiltration and proliferation of human dermal fibroblasts. In vivo test revealed that the scaffold could induce the fibroblast infiltration from the surrounding tissues. Besides, collagen/chitosan-silicone membrane bilayer dermal equivalent (BDE) was designed, in which the silicone membrane covers the hybrid scaffold to prevent water evaporation and infection (Fig. 10.4) [38]. The porous BDE can be functionalized by plasmid DNA to form a gene-activated scaffold for more complicated reconstruction of the damaged skin. For example, the porous BED combined with *N*,*N*,*N*-trimethyl chitosan chloride (TMC)/pDNA-VEGF complexes can significantly enhance the expression of VEGF, which in turn facilitates the regeneration of full-thickness incisional wounds [39]. To inhibit the scar formation during wound healing, TMC/siRNA-TGF-β1complexes were incorporated into the BDE to interfere in transforming growth factor-β1 (TGF-β1) signal pathway and suppress the expression of TGF-β1 [40]. The functionalized porous BDE can inhibit scar formation compared to the normal BDE. These results indicate that the porous BDE holds great promise for skin regeneration in clinical application.

10.3.2 Hydrogel

Hydrogels are three-dimensional cross-linked polymer networks that are capable of absorbing large amount of water, which is important for the absorption of the excess of wound exudates [41]. In addition, hydrogels can protect the wound site from infection and promote the healing process by providing a moisturized environment. Moreover, hydrogels can preserve the bioactivity of growth factors, antibiotics, cytokines, and cells, making them ideal carriers for the delivery of biomolecules to realize complete skin regeneration. Many studies have been focused on the applications of hydrogel for skin regeneration [42–45].

Chitosan hydrogel is well known as a wound dressing, showing good biocompatibility, anti-infective activity, and the ability to accelerate wound healing. Thermoresponsive hydrogel was developed by using chitosan and agarose for skin regeneration [46]. The hydrogel prevented water loss and wound dehydration and was in favor of cell internalization and proliferation. A bilayer physical hydrogel of chitosan without any external cross-linking agent was used to induce inflammatory cell migration and angiogenesis [47]. A hydrogel sheet composed of alginate, chitin/chitosan, and fucoidan (ACF-HS) has been developed for wound dressing (Fig. 10.5) [48]. The hydrogel can provide a moist environment for rapid wound healing. Significantly advanced granulation tissue was observed in the healing-impaired wounds being treated with the hydrogel. Wong et al. fabricated a pullulan-collagen composite hydrogel by using a salt-induced phase inversion technique, which can recapitulate the reticular structure of human dermal ECM [49]. The hydrogel promoted wound closure due to the increased recruitment of stromal cells as well as the formation of the granulation tissue. A versatile, nontoxic, in situ cross-linkable biodegradable dextran hydrogel loaded with chitosan microparticles containing VEGF and EGF was designed for skin regeneration. In vivo results showed that the hydrogel improved the physical, chemical, and biological protection of the damaged skin [50]. Besides, the spatiotemporally controlled release of VEGF- and EGF-enhanced angiogenesis and re-epithelialization are crucial for the reconstruction of the native skin. More excitingly, a recent study shows that dextran-based hydrogels supported the infiltration of inflammatory cells, resulting in its rapid degradation and promoted infiltration of angiogenic cells and endothelial cells into the healing wounds [51]. In addition, the remarkable neovascularization and regeneration with hair follicles and sebaceous glands were observed after 21 days, and new hair was observed 5 weeks later. These results indicate that dextran-based hydrogel alone without bioactive factors can promote complete skin regeneration with appendages.

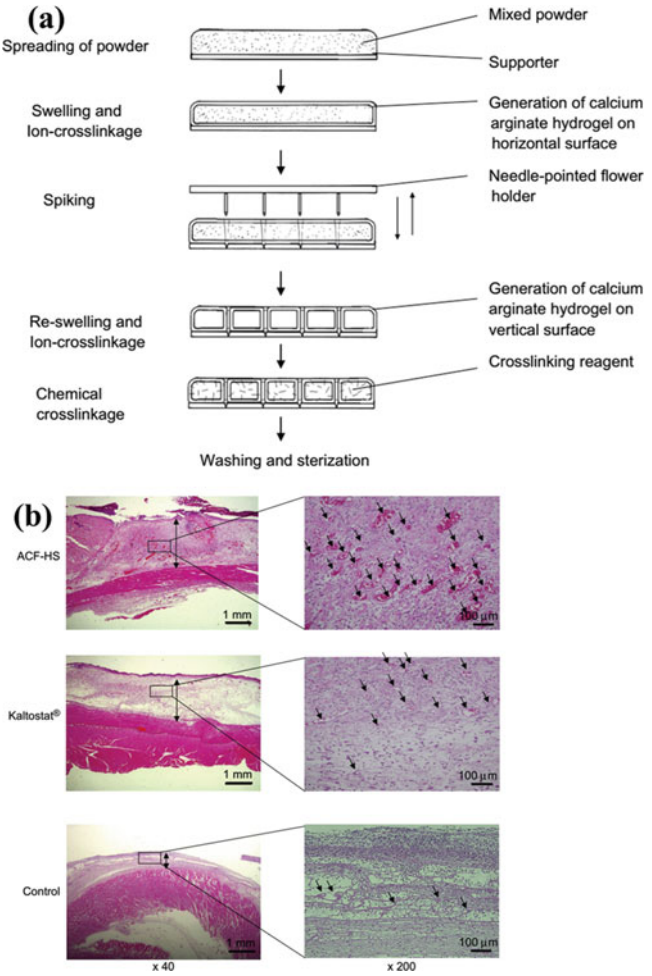

Fig. 10.5 (**a**) Preparative procedures for ACF-HS. (**b**) Histological examination of wounds covered with ACF-HS or Kaltostat® and controls (uncovered). In the *left panel*, *black arrows* show formed granulation tissues. In the *right panel*, *squares* show the sites for microphotographs, and *black arrows* show blood vessels containing erythrocytes (Reprinted from Ref. [48] with permission. Copyright 2009 Published by Elsevier Ltd)

10.4 Bio-functionalization of Skin Regeneration Scaffolds

Skin repair is the result of synergistic effect of different kinds of cells whose proliferation, migration, differentiation, and ECM secretion are well regulated by bioactive factors such as growth factors, genes, and cytokines. Combining bioactive factors with scaffolds is a promising way to promote the efficiency and quality of the regenerated skin.

10.4.1 Growth Factors

Growth factors are capable of stimulating cellular growth, cellular proliferation, and cellular differentiation. Usually they are proteins or steroid hormones regulating a variety of cellular processes. Growth factors typically act as signaling molecules between cells to promote cell differentiation or maturation and have been widely used in tissue engineering skin constructs. Some growth factors are promising mediators of wound healing, such as the epidermal growth factor (EGF), fibroblast growth factor (FGF), vascular endothelial growth factors (VEGF), platelet-derived growth factor (PDGF), insulin-like growth factor-1 (IGF-1), transforming growth factors α and β (TGF-α and TGF-β), and hepatocyte growth factor (HGF). Site-specific delivery of growth factors in micro-devices could provide an efficient means of stimulating localized recruitment to the cell transplants and would ensure cell survival and functions. By combining growth factors with micro-vehicles, bioactive skin scaffolds can be constructed. Richardson et al. incorporated VEGF and PDGF into a porous PLGA scaffold to realize a controlled dose and rate of delivery, pioneering the research of a vehicle delivering multiple angiogenic factors with distinct kinetics [52]. Perets et al. incorporated bFGF-loaded microspheres with three-dimensional porous alginate scaffolds, achieving enhanced vascularization in vivo [53]. Tabata et al. combined FGF, HGF, and VEGF with collagen gels to promote the regeneration of hair follicles after implantation [54]. Mao et al. combined FGF on a substrate via a layer-by-layer technique to fabricate bioactive films, on which fibroblasts proliferated better and secreted more ECM [55]. Regarding to hair follicle regeneration, HGF, a mitogen, motogen, and morphogen for lots of different organs, is expressed by the cells in human hair follicles and involved in the cycle of hair growth. Uijtdewilligen et al. incorporated insulin-like growth factor-2 (IGF-2) and sonic hedgehog (SHH) into a collagen type I heparin scaffold to form an embryonic-like scaffold which could help to repair the skin without contraction or scar formation [56].

10.4.2 Genes

As summarized above, with the ability to modulate and direct cells efficiently, the growth factors have been extensively used as bioactive factors to combine with tissue engineering scaffolds. However the most challenging limitation is their short half-lives. The emerging gene technique provides an optional method to make cells produce growth factors constantly. Hence, functional genes can be incorporated into scaffolds as bioactive factors and are locally expressed to encode specific growth factors at wound site. Specific examples of application of gene therapy in skin tissue engineering will be introduced below.

Shea et al. incorporated plasmid DNA encoding platelet-derived growth factor (PDGFB) into a three-dimensional PLGA sponge, implantation of which in a rat

dermis showed enhancement of granulation tissue and vascularization [57]. Other types of matrices such as collagen and PVA sponges loaded with genes are also developed and used to treat cutaneous wounds, resulting in improvement of flap survival, granulation tissue formation, angiogenesis, and re-epithelialization [39, 58].

Alternatively, the nucleic acids (e.g., plasmid, siRNA) are complexed with cationic polymers or lipids, with the design of these transfection reagents depending upon the nucleic acid properties, such as size [59]. Complexation with polymers or lipids protects against degradation, creates a less negative particle relative to naked plasmid, and facilitates internalization and intracellular trafficking [60].

10.4.3 Cytokines

Cytokines, a family of small molecules of approximately 8–10 kDa in size, are key regulators of cell migration, immune responses, and wound healing [61]. Pro-inflammatory cytokines, particularly IL-1 and IL-6 and TNF-α, are upregulated during the inflammatory phase of wound healing.

IL-1 is produced by monocytes, neutrophils, macrophages, and keratinocytes and is immediately released by keratinocytes during wound healing. IL-1 activates fibroblasts and promotes the secretion of FGF [62]. IL-6 is secreted by neutrophils and monocytes and has been shown to be involved in healing response. Evidence shows that IL-6 is closely related with wound healing by regulating leukocyte infiltration, angiogenesis, and collagen accumulation [63]. TNF-α can promote the expression of FGF-7, indicating that it can favor the process of re-epithelialization [64].

Stromal cell-derived factor-1α (SDF-1α, CXCL12) chemokine is a member of the CXC family and works via the CXCR4 receptor. It plays a role in the inflammatory response by recruiting lymphocytes to the wound and promoting angiogenesis. Endothelial cells, myofibroblasts, and keratinocytes express SDF-1. A number of researches have proved that SDF-1α plays a pivotal role in the recruitment of stem cells. For example, PLGA scaffolds incorporated with SDF-1α can recruit more stem cells, which favors angiogenesis and decreases fibrotic and inflammatory responses. More interestingly, mechanical stretch can upregulate SDF-1α in the skin tissue and promote migration of circulating bone marrow-derived mesenchymal stem cells (BMSCs) [65]. The application of SDF-1α provides an avenue for the recruitment of stem cells, which is crucial for the in situ skin regeneration. For example, Nakamura et al. used mesenchymal stem cells (MSCs) genetically engineered with (SDF-1α) to heal skin wounds [66]. SDF-1α-engineered MSCs (SDF-MSCs) expressed more SDF-1α and enhanced the migration of MSCs and dermal fibroblasts and promoted skin wound closure.

10.5 Important Challenges and Strategies

Although many significant milestones of bioengineered skin have been reached for clinical therapies of full-thickness defects, challenges still remain to fulfill the criteria of "regenerated skin" with complete structural, esthetic, and functional properties as the nature of the skin. How to achieve rapid angiogenesis, inhibited scarring, and regeneration of appendages is a key issue related to the quality of the regenerated skin. In addition, in situ regeneration, which should be particularly concerned, would be less costly and complex than those approaches that require ex vivo cell manipulation.

10.5.1 Angiogenesis

One of the most critical issues for most bioengineered tissues is the rapid and appropriate angiogenesis of the constructs, since a tissue beyond a certain size generally cannot survive without the supply of nutrients and oxygen, and removal of waste products of cells [67]. For materials with a thickness larger than 0.4 mm, new blood vessels are not able to penetrate rapidly [68]. The delayed or poor angiogenesis of the reconstructed skin will hinder the nourishment of the overlaying epidermal layer and result in the failure of the graft. Moreover, if the transplantation of split-thickness skin grafts is delayed, the timely healing of the damaged skin will be hampered and the risk of death will increase [69]. It is clear that the blood supply is essential to realize the long-term integration of the reconstructed skin with the host tissue. Therefore, acceleration of the angiogenesis rate to achieve rapid formation of new blood capillaries is urgently required, whereas still remains a research focus for improvement of existing skin substitutes.

Suitable pore size of tissue-engineered scaffold plays an important role in improving permeability, facilitating cell migration, and enhancing angiogenesis. Yannas et al. found that a pore size ranging from 90 to 150 μm and porosity larger than 90 % promote vessel formation [70]. Pruitt et al. reported that only when pore size of scaffold is larger than 80 μm it can be conducive to the ingrowth of connective tissue and neovascularization [71]. Another possible approach to enhance the angiogenesis of the tissue-engineered skin is to combine the prefabricated vessels with some special kinds of cells to achieve better initial onset of revascularization for early anastomoses between graft and bed vessels. As one example, human dermal microvascular endothelial cells were incorporated into collagen or fibrin hydrogels. Three-dimensional capillaries were formed after transplantation of the pre-vascularized substitutes [72]. The engineered capillaries were further stabilized by pericytes and smooth muscle cells and ultimately connected to the microvessels of the wound ground. It is also found some glycosaminoglycans have angiogenetic effect. Pieper et al. reported that the incorporation of glycosaminoglycans could

increase angiogenesis degree in vivo [73]. However, a sufficient vasculature still takes more than 4 weeks to develop.

The most powerful approach to induce angiogenesis in the engineered tissues is to use angiogenetic growth factors such as bFGF, VEGF, and PDGF. So far many efforts have been made to enhance angiogenesis by incorporation of angiogenic growth factors into tissue engineering scaffolds. With the loading of bFGF, the fibrin and collagen scaffolds show enhanced angiogenesis when applied to the rabbit ear ulcers, therefore greatly improving the healing of full-thickness skin defects [74]. Wissink et al. used heparin to realize a controlled release of bFGF through specific binding, which is effective in promoting the growth of endothelial cells within the collagen scaffold in vitro [75]. Perets et al. encapsulated bFGF into PLGA microspheres and then loaded the microspheres into a porous sodium alginate scaffold [53]. The formation of large mature vessels was greatly promoted by the bFGF-loaded scaffold in a rat peritoneal model.

However, delivery of the growth factors faces some challenges due to their sensitivity and instability, and their half-lives are only on the order of minutes in serum. In addition, the high cost of growth factors also limits their trial in practice. The gene technique has been considered as an alternative way in order to overcome the drawbacks of growth factors. By loading of more stable and functional genes into the scaffolds, the gene-activated matrix (GAMs) can be generated to locally transfect cells and constantly produce targeted growth factors at wound site. Endowed with the advantages of localized treatment, maintenance of effective amount of bioactive DNAs, and protection of DNAs against immune responses and nuclease degradation, the GAMs have shown great promise for the enhanced angiogenesis of the engineered skin. Mao et al. used TMC as a cationic gene delivery vector to carry plasmid DNA encoding VEGF (pDNA-VEGF) and constructed a gene-activated collagen scaffold for skin repair [76]. The in vivo application to Sprague-Dawley mice demonstrated that the TMC/pDNA-VEGF complexes remarkably promoted the in vivo expression of VEGF and thus enhanced the angiogenesis of the scaffolds. Recently, a gene-activated collagen-chitosan/silicone membrane bilayer dermal equivalent (BDE) has been prepared and evaluated for treatment of the full-thickness incisional wounds in terms of histology, immunohistochemistry, immunofluorescence, real-time quantitative PCR, and Western blotting analysis in a porcine model [39]. The TMC/pDNA-VEGF group shows highest level of VEGF expression at both mRNA and protein levels, resulting in the highest densities of newly formed and mature vessels. After 112 days of ultrathin skin graft transplantation, the healing skin has a similar structure and ~80 % tensile strength of the normal skin. Exploitation of the gene-activated BDE for the healing of full-thickness burns was also performed, showing very positive angiogenesis and repair results similar to those for incisional wounds (Fig. 10.6) [77].

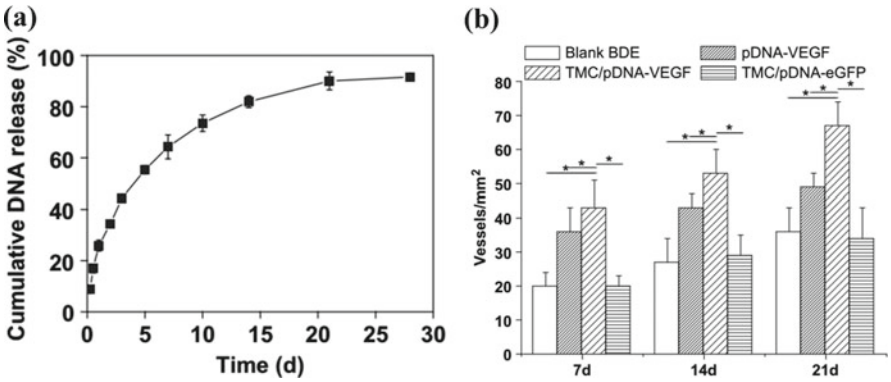

Fig. 10.6 (**a**) Cumulative release of DNA from the scaffolds as a function of time. (**b**) TMC/pDNA-VEGF group had a significantly higher number of newly formed and mature blood vessels (Reprinted from Ref. [77] with permission. Copyright 2010 Elsevier Ltd)

10.5.2 Scarring

Although skin substitutes based on principle of regeneration have achieved important progresses, scarring still remains a problem which results in issues such as disfiguration, itching, and local ulceration [78]. Prevention of scarring is therefore a major challenge to be addressed for the repair and regeneration of skin defects, and anti-scarring technologies should be incorporated for the new generation of the skin constructs.

Scars are the outcome of postnatal healing process of normal acute mammalian tissue repair including integration of bioengineered skins [79]. Scarring is a rapid tissue repairing process driven by an evolutionarily devised mechanism, allowing rapid recover of tissue integrity to fill tissue voids. Scarring involves a series of cellular events related to tissue repair including inflammation, migration/proliferation and ECM deposition, and also the inputs of numerous cell types, matrix components, and signaling molecules. Essentially, the excessive and disordered accumulation of ECM such as collagen, as well as the imbalance of new deposition and destruction of collagen, directly leads to the scar formation. By contrast, the scar-free regeneration should have features including complete restoration of skin structure, normal collagen deposition, and regular distribution of hair follicles, capillaries, and glands, which reflects a focus of interest for the emerging fields of regenerative medicine. Central to a material-based approach for skin regeneration is to build a suitable environment where cells are exposed to a complex pattern of bioactive molecules, which direct desired cell behaviors and right tissue regeneration.

Fetal wound repair is essentially a scar-free regenerative process. It has been extensively studied and confirmed that embryonic scarless wound repair exhibits

reduced fibrin clots and platelet degranulation, and suppressed inflammatory response, which has provided therapeutic strategies for scar-free repair. Most importantly, the growth factor profile is also quite different for embryonic wound and adult wound. The large family of TGF-β protein, which can be secreted by multiple cell types such as platelets, macrophages, and fibroblasts, is one of the most important biosignal molecules during the wound healing process. It acts as a chemokine for fibroblasts, induces differentiation of myofibroblasts, regulates the collagen synthesis, and modulates the matrix turnover. Recent investigations have confirmed that the level of TGF-β1 and TGF-β2 in fetal skin injuries is lower than that in adult skin, while the level of TGF-β3 is elevated [80]. Inspired by these findings, successful reduction of scarring of adult skin wounds has been reported by interrupting TGF-β1 and TGF-β2 signaling pathway through neutralization with antibodies, inactivation by proteoglycan-like decorin, and blockage of function by exogenous receptors, as well as exogenous addition of the TGF-β3 isoforms. Samuels et al. [81] found that hypertrophic scar was induced in a rabbit embryos subcutaneous model by injecting the TGF-β1 and TGF-β2, while the addition of their polyclonal neutralizing antibody could inhibit scarring and generate a normal tensile strength and more physical dermal architecture. A recent research proves that after infected by adenovirus encoding a truncated TGF-β receptor II, normal dermal fibroblasts could result in wounds with an average of 49 % reduction of the scar area and less inflammatory reaction in the full-thickness incisional wounds in rats [82].

The recently emerging biomolecular cues of RNA interference (RNAi) offer a fascinating and prospective alternative to specifically silence targeted genes and downregulate targeted protein levels [83]. Delivery of exogenous small interfering RNA (siRNA) mediated by three-dimensional scaffolding materials is right now at the frontier of current research. Compared with other strategies, the RNAi not only shows higher efficiency and specificity during a long duration time but also avoids risks of immunogenicity and inactivation in the antibody method. In a recent research in our lab, TMC/siRNA complexes targeting TGF-β1 were incorporated into the collagen-chitosan/silicone membrane bilayer dermal equivalent (BDE) to fabricate an RNAi functionalized bioengineered skin (RNAi-BDE), aiming to interfere TGF-β1 signal pathway, directing cell behaviors, and ultimately inhibiting scarring (Fig. 10.7). The RNAi-BDE functioned as a reservoir for the incorporated TMC/siRNA complexes, enabling a prolonged siRNA release. Application of the RNAi-BDE on the full-thickness skin defects of pig backs confirmed the in vivo inhibition of TGF-β1 expression by immunohistochemistry, real-time quantitative PCR, and Western blotting during 30 days post-surgery. The levels of other scar-related factors such as collagen type I, collagen type III, and α-smooth muscle actin (α-SMA) were also downregulated. In combination with the ultrathin skin graft transplantation for 73 days, the regenerated skin by RNAi-BDE had an extremely similar structure to that of the normal one with significant scar inhibition.

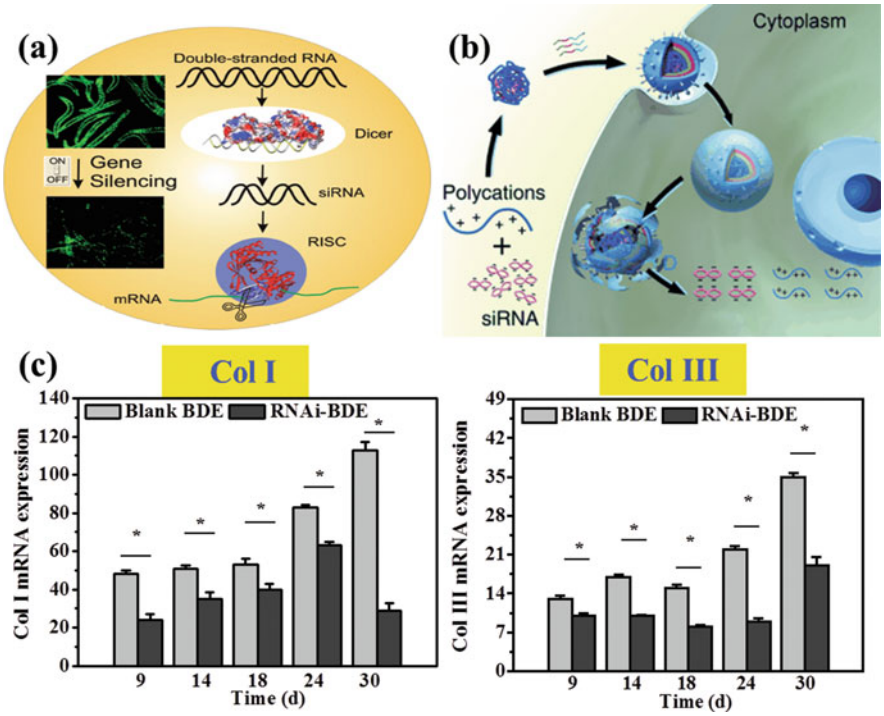

Fig. 10.7 (**a**) The siRNA could silence special gene expression. (**b**) Combination of polycations TMC with siRNA to form complexes which could be transfected into cells. Wound formation is mainly caused by massive and disordered deposition of Col I and Col III. (**c**) TMC/siRNA can suppress the expression of both Col I and Col III significantly (Reprinted from Ref. [40] with permission. Copyright 2012 Elsevier Ltd)

10.5.3 Appendages

Skin appendages such as hair follicle, sweat gland, sebaceous gland make skin functions well in touch, temperature sensation, excretion, perspiration, and thermoregulation. Regeneration of skin appendages is an important symbol of skin recovery and functionalization. Although some commercial artificial skin substitutions can achieve a structural repair in the epidermis and the dermis, it remains a challenge to regenerate the skin with complete appendages [84]. Hence, regenerated skin cannot fully replace normal skin in function.

Hair follicle is a mini-organ which produces hair. It is composed of hair papilla, matrix, root sheath, hair fiber, bulge, and so on. There are three stages in hair growth: the growth phase (anagen), the regressing phase (catagen), and the quiescent phase (telogen). Growth cycles are controlled by chemical signals like epidermal growth factor. Efforts of reconstructing hair follicles have been made decades ago. Lin et al. combined epidermal stem cells in collagen/gelatin scaffold with fibroblasts; hair

follicle-like structure was formed after implantation. It is also reported that the interaction between epidermal cells and mesenchymal cells contributes to the formation of hair follicles. More recently, MSCs are induced into hair papilla-like cells [85]. Moreover, polysaccharide, as one main component of dermal ECM, is reported to induce the regeneration of hair follicles on a mice model [51]. Recently, it was reported that hair growth was promoted by adipose-derived stem cell (ASC) transplantation in animal experiments, and a conditioned medium of ASCs (ASC-CM) induced the proliferation of hair-compositing cells in vitro. Jin et al. introduced some ASC stimulators in preconditioning to enhance hair regeneration [86]. They also highlighted the functional role of ASCs in hair cycle progression and concluded the advantages and disadvantages of their application in hair regeneration.

Sweat glands are small tubular structures of the skin that can produce sweat. There are two kinds of sweat glands. Eccrine sweat glands are distributed all over the body (except for the lips, tip of the penis, and the clitoris), although their density varies a lot from region to region, while apocrine sweat glands are larger, having different mechanisms of secretion, and are limited to axilla (armpits) and perianal areas. Sweat glands play a key role in thermoregulation and inner balance. Therefore, it is vital to reconstruct sweat glands especially for large-area burns. Fu et al. cultured sweat gland cells (SGCs) on gelatin microspheres containing EGF and delivered the SGCs-microspheres complex into an engineered skin construct mainly composed of a fibroblast-embedded collagen-based matrix [87]. This engineered skin construct was then transplanted onto full-thickness cutaneous wound in an athymic murine model. Remarkably, sweat gland-like structure can be achieved in vitro within the hybrid matrix. Huang Sha et al. designed a functional in vitro cell-laden three-dimensional extracellular matrix mimics (3D-ECM) with composite hydrogels based on gelatin and sodium alginate. It provides the spatial inductive cues for enhancing specific differentiation of epidermal lineages to regenerate sweat glands [88].

Sebaceous glands are kind of microscopic glands in the skin that secrete an oily/waxy matter, called sebum, to lubricate and waterproof the skin and hair of mammals. In human beings, they are found in greatest abundance on the face and scalp, though distributed throughout all skin sites except the palms and soles. Compared with hair follicles and sweat glands, sebaceous glands are later to be studied. But exciting progress has been made related to reconstruction of sebaceous glands. Hair bulge cells have been reported to possess the potential of differentiating into sebaceous glands. Horsley et al. firstly found a kind of progenitor cells that can secret factor Blimp1, which can stimulate the regeneration of sebaceous glands when they get hurt [89].

Appendages do have a firm interaction rather than separate growth, although most researches are still confined to one certain appendage. With further study of biology of appendages, and clarifying the interaction of materials and related cells (specifically stem cells) and appendages themselves, it is quite possible to functionalize skin constructs by reconstructing different appendages together in the future.

10.5.4 In Situ Skin Regeneration

Along with the advancement of science and technology in biology, medicine, and material science, the insight mechanism of wound healing is better understood. Diverse methods for skin repair and regeneration have also been developed. Stem cell-based therapy, which is a promising cure for a multitude of diseases and disorders, has been one of the best documented approaches in regenerative medicine. However, the ex vivo expansion of stem cells and their in vivo delivery are restricted by the low survival rate and the limited availability of stem cell sources.

It has been demonstrated that endogenous stem cells can be actively attracted to sites of injury [3]. Thus, recruiting sufficient endogenous stem cells to the wound area and inducing them to repair the structure and functions of skin become a key challenge. This technique, known as in situ regeneration, has the potential to provide new therapeutic options for all kinds of tissues and organs. The in situ tissue regeneration method relies on endogenous stem cell homing, proliferation, differentiation, and rebuilding functional skins. Such options would be less costly and complex than the traditional approaches which require substantial ex vivo cell manipulation.

Microenvironment, which could be changed by cytokines, surface topology, and so on, could influence stem cell recruiting. Some cytokines can enhance tissue regeneration by facilitating cell homing. Chen et al. fabricated a radially oriented scaffold which could effectively promote BMSCs migration, whose effect was further enhanced by addition of stromal cell-derived factor-1 (SDF-1) (Fig. 10.8) [90]. It is reported that the migration abilities of PDMSCs exposed to hypoxic conditions are significantly increased. Interestingly, decreased integrin alpha4 in PDMSCs under hypoxia increases PDMSC migration ability [91]. In addition, bone morphogenetic protein-7 (BMP-7) is another cell homing factor [3]. Shao et al. found that a peptide sequence (E7, EPLQLKM) with seven amino acids has a high specific affinity to bone marrow-derived MSCs [92]. In the subsequent work, E7 peptide was immobilized to a collagen scaffold via a collagen-binding domain (CBD) to construct a functional collagen scaffold, which could enhance the speed of healing process [93]. It is reported that E7-modified scaffolds incorporated with rhTGF-β1 could maintain a sustained release and bioactivity. A series of analyses indicate that the E7 peptide promotes BMSC initial adhesion and that the scaffolds containing both E7 and rhTGF-β1 are the most favorable for BMSC survival (Fig. 10.9) [94].

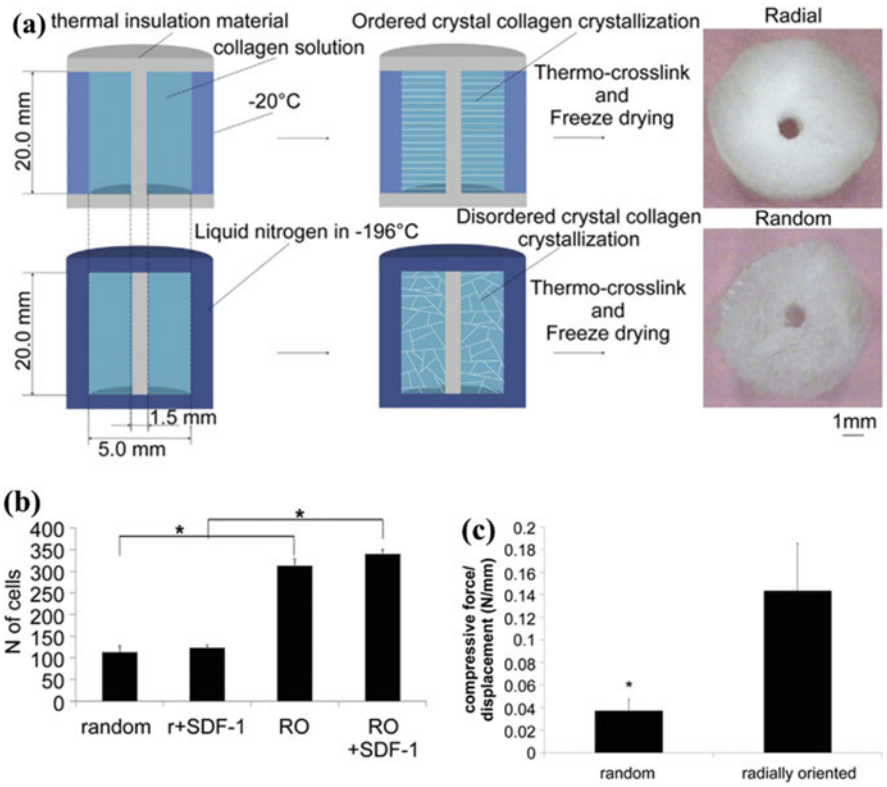

Fig. 10.8 (**a**) Fabrication of the radially oriented (RO) and random collagen scaffolds. (**b**) The radially oriented scaffolds had significantly better mechanical property compared with the random scaffolds. (**c**) The cell number was quantified at low magnification and the radially oriented scaffolds accelerated cell infiltration (Reprinted from Ref. [90] with permission. Copyright 2014 Elsevier Ltd)

10.6 Conclusions and Future Perspectives

Skin regeneration is one of the most serious problems in clinical medicine. The use of skin grafts is still an important therapy for damaged skin. So far decades of efforts have focused on the development of the tissue-engineered skin based on material technologies, chemistry, biology, and medicine. Bioengineered skins for epidermal, dermal, and full-thickness defects have been fabricated, and some of them are currently commercially available. However, most of them are not sufficient to regenerate new skin similar with native skin.

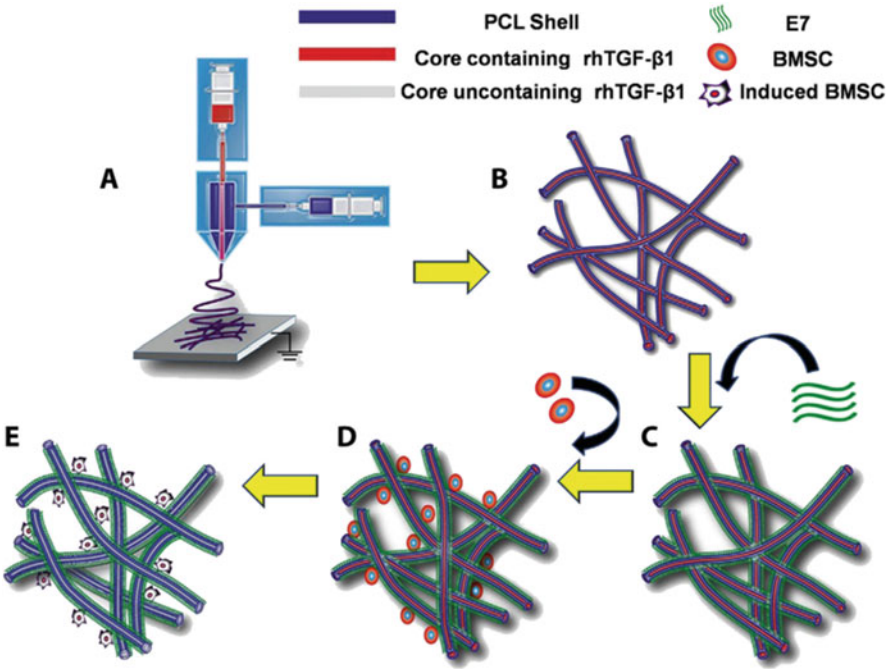

Fig. 10.9 The preparation process for coaxial electrospun fiber scaffolds. (**a**) The process of coaxial electrospinning: the spinneret is composed of two concentric needles; the outer needle is used to deliver the shell solution (*blue*, PCL), while the inner needle is used to eject the core solution (*red*, rhTGF-β 1). (**b**) Scaffold composed of electrospun coaxial fibers, with core (*red*) and shell (*blue*) structure. (**c**) Scaffold conjugated with the BMSC-specific affinity peptide (E7) (*green*). (**d**) E7-modified scaffold facilitates adhesion of BMSCs onto the surface. (**e**) The E7-modified surface and sustained release of rhTGF-β 1 in the core of the coaxial fibers promote adhesion and differentiation of BMSCs [94] (Reprinted from Ref. [94] with permission. Copyright 2014 Elsevier Ltd)

To realize the regeneration of the skin with a complicated structure and complete functions, it is becoming increasingly popular to design "smart biomaterial system" to provide instructive signals to stimulate target cell responses in the processes of skin regeneration. "Smart biomaterials" can be obtained by adjusting the properties of biomaterials including physical properties, chemical compositions, and biofunctions. Meanwhile, the application of electronic devices into skin tissue engineering is able to regulate and control the environment such as temperature and wettability of the wound and thereby to provide more suitable conditions for skin regeneration. Moreover, by the combination of stem cells and in situ skin regeneration, the induced differentiation of endogenous stem cells for the in situ skin regeneration with appendages has attracted more and more interest. We believe that with the development of biomaterial science and regenerative medicine, the skin with a complicated structure and multifunction similar to those of the native skin can be regenerated sooner or later.

Acknowledgement We acknowledge financial support by the Key Science Technology Innovation Team of Zhejiang Province (2013TD02), the Natural Science Foundation of China (51322302, 20934003) and the National Key Research Program of China (2016YFC1101001).

References

1. MacNeil S. Progress and opportunities for tissue-engineered skin. Nature. 2007;445:874–80.
2. Tabata Y. Biomaterial technology for tissue engineering applications. J R Soc Interface. 2009;6(35, Suppl 3):S311–24.
3. Chen FM, Wu LA, Zhang M, et al. Homing of endogenous stem/progenitor cells for in situ, tissue regeneration: promises, strategies, and translational perspectives. Biomaterials. 2011;32(12):3189–209.
4. Marston WA. Dermagraft, a bioengineered human dermal equivalent for the treatment of chronic nonhealing diabetic foot ulcer. Expert Rev Med Devices. 2004;1(1):21–31.
5. Parenteau-Bareil R, Gauvin R, Berthod F. Collagen-based biomaterials for tissue engineering applications. Materials. 2010;3:1863–87.
6. Willard JJ, Drexler JW, Das A, et al. Plant-derived human collagen scaffolds for skin tissue engineering. Tissue Eng Part A. 2013;19(13–14):1507–18.
7. Cao H, Chen MM, Liu Y, et al. Fish collagen-based scaffold containing PLGA microspheres for controlled growth factor delivery in skin tissue engineering. Colloids Surf B Biointerfaces. 2015;136:1098–106.
8. Rnjak-Kovacina J, Wise SG, Zhe L, et al. Electrospun synthetic human elastin: collagen composite scaffolds for dermal tissue engineering. Acta Biomater. 2012;8(10):3714–22.
9. Bellas E, Seiberg M, Garlick J, et al. In vitro 3D full-thickness skin-equivalent tissue model using silk and collagen biomaterials. Macromol Biosci. 2012;12(12):1627–36.
10. Ma L, Gao C, Mao Z, et al. Thermal dehydration treatment and glutaraldehyde cross-linking to increase the biostability of collagen-chitosan porous scaffolds used as dermal equivalent. J Biomater Sci Polym Ed. 2003;14(8):861–74.
11. Ma L, Gao C, Mao Z, et al. Collagen/chitosan porous scaffolds with improved biostability for skin tissue engineering. Biomaterials. 2003;24(26):4833–41.
12. Wang X, You C, Hu X, et al. The roles of knitted mesh-reinforced collagen-chitosan hybrid scaffold in the one-step repair of full-thickness skin defects in rats. Acta Biomater. 2013;9(8):7822–32.
13. Zhong SP, Zhang YZ, Lim CT. Tissue scaffolds for skin wound healing and dermal reconstruction. Wiley Interdiscip Rev Nanomed Nanobiotechnol. 2010;2:510–25.
14. Edmonds M. Apligraf in the treatment of neuropathic diabetic foot ulcers. Int J Lower Extrem Wounds. 2009;8(1):11–8.
15. Montembault A, Viton C, Domard A. Physico-chemical studies of the gelation of chitosan in a hydroalcoholic medium. Biomaterials. 2005;26(8):933–43.
16. Ribeiro MP, Ana E, Daniela S, et al. Development of a new chitosan hydrogel for wound dressing. Wound Repair Regen. 2009;17(6):817–24.
17. Adekogbe I, Ghanem A. Fabrication and characterization of DTBP-crosslinked chitosan scaffolds for skin tissue engineering. Biomaterials. 2005;26(35):7241–50.
18. Hong JP, Kim YW, Lee SK, et al. The effect of continuous release of recombinant human epidermal growth factor (rh-EGF) in chitosan film on full thickness excisional porcine wounds. Ann Plast Surg. 2008;61(4):457–62.
19. Mizuno K, Yamamura K, Yano K, et al. Effect of chitosan film containing basic fibroblast growth factor on wound healing in genetically diabetic mice. J Biomed Mater Res A. 2003;64(1):177–81.

20. Abdelgawad AM, Hudson SM, Rojas OJ. Antimicrobial wound dressing nanofiber mats from multicomponent (chitosan/silver-NPs/polyvinyl alcohol) systems. Carbohydr Polym. 2014;100(100):166–78.
21. Tchemtchoua VT, Atanasova G, Aqil A, et al. Development of a chitosan nanofibrillar scaffold for skin repair and regeneration. Biomacromolecules. 2011;12(9):3194–204.
22. Kiyozumi T, Kanatani Y, Ishihara M, Saitoh D, Shimizu J, Yura H, et al. Medium (DMEM/F12)-containing chitosan hydrogel as adhesive and dressing in autologous skin grafts and accelerator in the healing process. J Biomed Mater Res B Appl Biomater. 2006;79:129–36.
23. Kiyozumi T, Kanatani Y, Ishihara M, et al. The effect of chitosan hydrogel containing DMEM/F12 medium on full-thickness skin defects after deep dermal burn. Burns. 2007;33(5):642–8.
24. Shevchenko RV, Eeman M, Rowshanravan B, et al. The in vitro characterization of a gelatin scaffold, prepared by cryogelation and assessed in vivo as a dermal replacement in wound repair. Acta Biomater. 2014;10(7):3156–66.
25. Monteiro IP, Shukla A, Marques AP, et al. Spray-assisted layer-by-layer assembly on hyaluronic acid scaffolds for skin tissue engineering. J Biomed Mater Res A. 2015;103(1):330–40.
26. Losi P, Briganti E, Errico C, et al. Fibrin-based scaffold incorporating VEGF- and bFGF-loaded nanoparticles stimulates wound healing in diabetic mice. Acta Biomater. 2013;9(8):7814–21.
27. Rezwan K, Chen QZ, Blaker JJ, et al. Biodegradable and bioactive porous polymer/inorganic composite scaffolds for bone tissue engineering. Biomaterials. 2006;27(18):3413–31.
28. Amani H, Dougherty WR, Blome S. Use of Transcyte® and dermabrasion to treat burns reduces length of stay in burns of all size and etiology. Burns J Int Soc Burn Injuries. 2006;32(7):828–32.
29. Kumbar SG, Nukavarapu SP, James R, et al. Electrospun poly(lactic acid-co-glycolic acid) scaffolds for skin tissue engineering. Biomaterials. 2008;29(30):4100–7.
30. Cui W, Zhu X, Yang Y, et al. Evaluation of electrospun fibrous scaffolds of poly(dl -lactide) and poly(ethylene glycol) for skin tissue engineering. Mater Sci Eng C. 2009;29(6):1869–76.
31. Chen G, Sato T, Ohgushi H, et al. Culturing of skin fibroblasts in a thin PLGA-collagen hybrid mesh. Biomaterials. 2005;26(15):2559–66.
32. Venugopal JR, Zhang Y, Ramakrishna S. In vitro culture of human dermal fibroblasts on electrospun polycaprolactone collagen nanofibrous membrane. Artif Organs. 2006;30(6):440–6.
33. Yang J, Shi G, Bei J, Wang S, Cao Y, Shang Q, et al. Fabrication and surface modification of macroporous poly (L-lactic acid) and poly (L-lactic-co-glycolic acid)(70/30) cell scaffolds for human skin fibroblast cell culture. J Biomed Mater Res. 2002;62:438–46.
34. Gautam S, Chou CF, et al. Surface modification of nanofibrous polycaprolactone/gelatin composite scaffold by collagen type I grafting for skin tissue engineering. Mater Sci Eng C Mater Biol Appl. 2014;34C(1):402–9.
35. Zhou Y, Yang D, Chen X, et al. Electrospun water-soluble carboxyethyl chitosan/poly(vinyl alcohol) nanofibrous membrane as potential wound dressing for skin regeneration. Biomacromolecules. 2008;9(1):349–54.
36. Wang HM, Chou YT, Wen ZH, et al. Novel biodegradable porous scaffold applied to skin regeneration. Plos One. 2013;8(6):e56330.
37. Lu H, Oh HH, Kawazoe N, et al. PLLA-collagen and PLLA-gelatin hybrid scaffolds with funnel-like porous structure for skin tissue engineering. Sci Technol Adv Mater. 2012;13(6):64210–8.
38. Shi Y, Ma L, Zhou J, et al. Collagen/chitosan-silicone membrane bilayer scaffold as a dermal equivalent. Polym Adv Technol. 2005;16(11–12):789–94.
39. Rui G, Xu S, Ma L, et al. Enhanced angiogenesis of gene-activated dermal equivalent for treatment of full thickness incisional wounds in a porcine model. Biomaterials. 2010;31(28):7308–20.
40. Liu X, Liang J, Zhang B, et al. RNAi functionalized collagen-chitosan/silicone membrane bilayer dermal equivalent for full-thickness skin regeneration with inhibited scarring. Biomaterials. 2013;34(8):2038–48.

41. Vlierberghe SV, Dubruel P, Schacht E. Biopolymer-based hydrogels as scaffolds for tissue engineering applications: a review. Biomacromolecules. 2011;12(5):1387–408.
42. Yanchun Liu MD, Cai S, Xiao ZS, et al. Release of basic fibroblast growth factor from a cross-linked glycosaminoglycan hydrogel promotes wound healing. Wound Repair Regen. 2007;15(2):245–51.
43. Shepherd J, Sarker P, Rimmer S, et al. Hyperbranched poly(NIPAM) polymers modified with antibiotics for the reduction of bacterial burden in infected human tissue engineered skin. Biomaterials. 2011;32(32):258–67.
44. Peattie RA, Nayate AP, Firpo MA, et al. Stimulation of in vivo angiogenesis by cytokine-loaded hyaluronic acid hydrogel implants. Biomaterials. 2004;25(14):2789–98.
45. Lee PY, Cobain E, Huard J, et al. Thermosensitive hydrogel PEG-PLGA-PEG enhances engraftment of muscle-derived stem cells and promotes healing in diabetic wound. Mol Ther J Am Soc Gene Ther. 2007;15(6):1189–94.
46. Miguel SP, Ribeiro MP, Brancal H, et al. Thermoresponsive chitosan-agarose hydrogel for skin regeneration. Carbohydr Polym. 2014;111(20):366–73.
47. Boucard N, Viton C, Agay D, et al. The use of physical hydrogels of chitosan for skin regeneration following third-degree burns. Biomaterials. 2007;28(24):3478–88.
48. Murakami K, Aoki H, Nakamura S, et al. Hydrogel blends of chitin/chitosan, fucoidan and alginate as healing-impaired wound dressings. Biomaterials. 2010;31(1):83–90.
49. Wong VW, Rustad KC, Galvez MG, et al. Engineered pullulan-collagen composite dermal hydrogels improve early cutaneous wound healing. Tissue Eng Part A. 2011;17(5–6):631–44.
50. Ribeiro MP, Morgado PI, Miguel SP, et al. Dextran-based hydrogel containing chitosan microparticles loaded with growth factors to be used in wound healing. Mater Sci Eng C. 2013;33(5):2958–66.
51. Sun G, Zhang X, Shen YI, et al. Dextran hydrogel scaffolds enhance angiogenic responses and promote complete skin regeneration during burn wound healing. Proc Natl Acad Sci U S A. 2011;108(52):20976–81.
52. Richardson TP, Peters MC, Ennett AB, et al. Polymeric system for dual growth factor delivery. Nat Biotechnol. 2001;19(11):1029–34.
53. Perets A, Baruch Y, Weisbuch F, et al. Enhancing the vascularization of three-dimensional porous alginate scaffolds by incorporating controlled release basic fibroblast growth factor microspheres. J Biomed Mater Res A. 2003;65a(65):489–97.
54. Ozeki M, Tabata Y. In vivo promoted growth of mice hair follicles by the controlled release of growth factors. Biomaterials. 2003;24(13):2387–94.
55. Mao Z, Ma L, Zhou J, et al. Bioactive thin film of acidic fibroblast growth factor fabricated by layer-by-layer assembly. Bioconjug Chem. 2005;16(5):1316–22.
56. Uijtdewilligen PJE, Versteeg EMM, Gilissen C, et al. Towards embryonic-like scaffolds for skin tissue engineering: identification of effector molecules and construction of scaffolds. J Tissue Eng Regen Med. 2013;10(1):E34–44.
57. Shea LD, Smiley E, Bonadio J, et al. DNA delivery from polymer matrices for tissue engineering. Nat Biotechnol. 1999;17(6):551–4.
58. Hijjawi J, Mogford JE, Chandler LA, et al. Platelet-derived growth factor B, but not fibroblast growth factor 2, plasmid DNA improves survival of ischemic myocutaneous flaps. Arch Surg. 2004;139(2):142–7.
59. Putnam D, Doody A. RNA-interference effectors and their delivery. Crit Rev Ther Drug Carrier Syst. 2006;23(2):137–64.
60. Laporte LD, Rea JC, Shea LD. Design of modular non-viral gene therapy vectors. Biomaterials. 2006;27(7):947–54.
61. Vanden BergFoels WS. In situ tissue regeneration: chemoattractants for endogenous stem cell recruitment. Tissue Eng Part B Rev. 2014;20(1):28–39.
62. Tang A, Gilchrest BA. Regulation of keratinocyte growth factor gene expression in human skin fibroblasts. J Dermatol Sci. 1996;11(1):41–50.

63. Lin ZQ, Kondo T, Ishida Y, et al. Essential involvement of IL-6 in the skin wound-healing process as evidenced by delayed wound healing in IL-6-deficient mice. J Leukoc Biol. 2003;73(6):713–21.
64. Barrientos S, Stojadinovic O, Golinko MS, et al. Growth factors and cytokines in wound healing. Wound Repair Regen. 2008;16(5):333.
65. Zhou SB, Wang J, Chiang CA, et al. Mechanical stretch upregulates SDF-1α in skin tissue and induces migration of circulating bone marrow-derived stem cells into the expanded skin. Stem Cells. 2013;31(12):2703–13.
66. Nakamura Y, Ishikawa H, Kawai K, et al. Enhanced wound healing by topical administration of mesenchymal stem cells transfected with stromal cell-derived factor-1. Biomaterials. 2013;34(37):9393–400.
67. Zhang B, Liu X, Wang C, et al. Chapter 52 – bioengineering skin constructs. In: Stem cell biology and tissue engineering in dental sciences. London: Academic; 2015. p. 703–19.
68. Black AF, Berthod F, L'Heureux N, et al. In vitro reconstruction of a human capillary-like network in a tissue-engineered skin equivalent. Faseb J. 1998;12(13):1331–40.
69. O'Ceallaigh S, Herrick SE, Bluff JE, et al. Quantification of total and perfused blood vessels in murine skin autografts using a fluorescent double-labeling technique. Plast Reconstruct Surg. 2006;117(1):140–51.
70. O'Brien FJ, Harley BA, Yannas IV, et al. The effect of pore size on cell adhesion in collagen-GAG scaffolds. Biomaterials. 2005;26(4):433–41.
71. Pruitt Jr B, Levine NS. Characteristics and uses of biologic dressings and skin substitutes. Arch Surg. 1984;119(3):312–22.
72. Böttcher-Haberzeth S, Biedermann T, Klar AS, et al. Tissue engineering of skin: human tonsil-derived mesenchymal cells can function as dermal fibroblasts. Pediatr Surg Int. 2014;30(2):213–22.
73. Pieper JS, Wachem PBV, Luyn MJAV, et al. Attachment of glycosaminoglycans to collagenous matrices modulates the tissue response in rats. Biomaterials. 2000;21(16):1689–99.
74. Pandit AS, Feldman DS, Caulfield J. In vivo wound healing response to a modified degradable fibrin scaffold. J Biomater Appl. 1998;12(3):222–36.
75. Wissink MJB, Beernink R, Poot AA, et al. Improved endothelialization of vascular grafts by local release of growth factor from heparinized collagen matrices. J Control Release. 2000;64(1–3):103–14.
76. Mao Z, Shi H, Rui G, et al. Enhanced angiogenesis of porous collagen scaffolds by incorporation of TMC/DNA complexes encoding vascular endothelial growth factor. Acta Biomater. 2009;5(8):2983–94.
77. Guo R, Xu S, Ma L, et al. The healing of full-thickness burns treated by using plasmid DNA encoding VEGF-165 activated collagen-chitosan dermal equivalents. Biomaterials. 2011;32(4):1019–31.
78. Costa AMA, Desmoulire A. Mechanisms and factors involved in development of hypertrophic scars. Eur J Plast Surg. 1998;21(1):19–23.
79. Lappert PW. Scarless fetal skin repair: "unborn patients" and "fetal material". Plast Reconstr Surg. 1996;98(6):1125.
80. Chalmers RL. The evidence for the role of transforming growth factor-beta in the formation of abnormal scarring. Int Wound J. 2011;8(3):218–23.
81. Samuels P, Tan AK. Fetal scarless wound healing. J Otolaryngol. 1999;28(5):296–302.
82. Liu W, Chua C, Wu X, et al. Inhibiting scar formation in rat wounds by adenovirus-mediated overexpression of truncated TGF-beta receptor II. Plast Reconstr Surg. 2005;115(3):860–70.
83. Monaghan M, Pandit A. RNA interference therapy via functionalized scaffolds. Adv Drug Deliv Rev. 2011;63:197–208.
84. Zhong SP, Zhang YZ, Lim CT. Tissue scaffolds for skin wound healing and dermal reconstruction. Wiley Interdiscip Rev Nanomed Nanobiotechnol. 2010;2(5):510–25.
85. Yoo BY. Application of mesenchymal stem cells derived from bone marrow and umbilical cord in human hair multiplication. J Dermatol Sci. 2010;60(2):74–83.

86. Jin SE, Sung JH. Hair regeneration using adipose-derived stem cells. Histol Histopathol. 2015;31:249–56.
87. Huang S, Xu Y, Wu C, et al. In vitro, constitution and in vivo, implantation of engineered skin constructs with sweat glands. Biomaterials. 2010;31(21):5520–5.
88. Huang S, Yao B, Xie J, et al. 3D bioprinted extracellular matrix mimics facilitate directed differentiation of epithelial progenitors for sweat gland regeneration. Acta Biomater. 2015;32:170–7.
89. Horsley V, O'Carroll D, Tooze R, et al. Blimp1 defines a progenitor population that governs cellular input to the sebaceous gland. Cell. 2006;126(3):597–609.
90. Chen P, Tao J, Zhu S, et al. Radially oriented collagen scaffold with SDF-1 promotes osteochondral repair by facilitating cell homing. Biomaterials. 2015;39:114–23.
91. Ho CJ, Mook LS, In YY, et al. Microenvironmental interaction between hypoxia and endothelial cells controls the migration ability of placenta-derived mesenchymal stem cells via alpha4 integrin and rho signaling. J Cell Biochem. 2015;117(5):1145–57.
92. Shao Z, Zhang X, Pi Y, et al. Polycaprolactone electrospun mesh conjugated with an MSC affinity peptide for MSC homing in vivo. Biomaterials. 2012;33(12):3375–87.
93. Wang H, Yan X, Shen L, et al. Acceleration of wound healing in acute full-thickness skin wounds using a collagen-binding peptide with an affinity for MSCs. Burns Trauma. 2014;2(4):181–6.
94. Man Z, Yin L, Shao Z, et al. The effects of co-delivery of BMSC-affinity peptide and rhTGF-β1 from coaxial electrospun scaffolds on chondrogenic differentiation. Biomaterials. 2014;35:5250–60.

Chapter 11
Regeneration of Blood Vessels

Kai Wang, Weilong Cui, Yongzhen Wei, Meifeng Zhu, Qiang Zhao, and Deling Kong

11.1 Introduction

Blood vessels transport blood to deliver oxygen and nutrients. Vascular diseases such as atherosclerosis may result in obstruction of blood vessels and tissue ischemia [1]. Vascular graft has proven to be an effective strategy for the treatment of these vascular diseases [2]. In the United States, there are over 500,000 vascular grafts being used for bypass surgery each year, most of which are autologous venous and arterial grafts. However, autologous grafts are limited by availability, need for additional surgeries, donor site morbidity, and 30 % 10-year failure rate [1]. Artificial blood vessels become indispensable and have received increasing attention. Up to now, some products have gained success and have been commercialized, such as expanded polytetrafluoroethylene (ePTFE) and poly(ethylene terephthalate) (Dacron). Dacron and Teflon work well for large-diameter (>6 mm internal diameter) vascular grafts, where the rate of blood flow is high, but these materials yield disappointing clinical results in small-diameter (<6 mm internal diameter) coronary artery grafts [3]. In addition, nondegradation of the polymer graft often leads to the calcification during long-term implantations [4]. In this regard, development of vascular grafts with relatively slow degradation and controlled regenerative process has become a new concept and direction. These grafts provide a favorable environment for the recruitment of autogenous vascular cells. After a full degradation of the polymer scaffold, "neoartery" could be generated [5]. With the recent advancement of knowledge and technologies in the small-diameter vascular grafts, there are still many scientific questions to be addressed. Among these questions, vascular regeneration and their long-term patency and function should be mentioned.

K. Wang • W. Cui • Y. Wei • M. Zhu • Q. Zhao • D. Kong (✉)
College of Life Sciences, Nankai University, Tianjin, China
e-mail: kongdeling@nankai.edu.cn

© Springer Science+Business Media Singapore 2016

C. Gao (ed.), *Polymeric Biomaterials for Tissue Regeneration*,
DOI 10.1007/978-981-10-2293-7_11

11.1.1 Endothelialization of Vascular Grafts

The endothelium is not a smooth inert surface that facilitates laminar blood flow through the blood vessel but a dynamic organ with an active role in coagulation homeostasis, the sensing and transduction of the hemodynamic forces of circulation, and the cellular metabolism of the vascular wall [2]. It is understandable that the main focus of vascular graft studies is endothelialization. Within many general functions, the endothelium is equipped with a number of mechanisms that prevents thrombus formation in the circulatory system. It harbors factors that interrupt the coagulation cascade, such as antithrombin III, the protein C receptor thrombomodulin, and tissue factor pathway inhibitor. It prevents platelet activation by the production of nitric oxide and prostacyclin, exonucleotidases, and surface heparan sulfates [6]. All of these functions make the endothelium an important physiological barrier to maintain the patency and homeostasis of blood vessels. However, a vascular graft that can resist thrombosis by forming a confluent luminal endothelium in vivo is still a dream in the field of vascular tissue engineering.

11.1.2 Restenosis of Vascular Grafts

Transplantation of small-diameter vascular grafts is often accompanied by restenosis, including short- and midterm restenosis. The reasons for short-term restenosis include platelet adhesion and aggregation and the resulting thrombus formation. While those for midterm restenosis include over-proliferation of vascular smooth muscle cells (VSMCs) and neointimal hyperplasia. Generally speaking, the main problem could be ascribed to the poor blood compatibility of artificial vascular grafts, which leads to the adhesion of platelets and plasma protein, and subsequent aggregation and thrombus formation [7]. In addition to biomaterial incompatibility, physical forces have been associated with vascular graft intimal hyperplasia [8]. Prominent among these suggestions have been compliance mismatch between the graft and host artery, which result in adverse local hemodynamic effects at the anastomosis with consequent greater intimal thickening and eventual graft failure [9]. There has been a great deal of work recently on developing more compliant sutures, suturing techniques, mechanical clips, biological glue, and laser-based solder techniques [10]. The aim of this has been to improve pulsatile laminar blood flow in arteries propagation across the anastomosis and to reduce damage to the surrounding endothelium [9]. But beyond that, there is evidence that a confluent endothelium is crucial in prevention of the initiation and progression of the process. One aspect of endothelial protection is the physical barrier, which forms to prevent contact with subendothelial components of the arterial wall and activation of the coagulation cascade. In addition, early events in the cascade, such as platelet degranulation following contact with type-I collagen, have been shown to induce mitogenic factors such as transforming growth factor β (TGF-β) [2]. Animal models in which

endothelial injury was induced show that loss of an intact endothelium results in a change of VSMCs phenotype to a proliferative state. It is widely accepted that increased proliferation of terminally differentiated vascular SMCs contribute significantly to lesional neointima formation [11]. Conversely, such a change was inhibited by the presence of endothelial cells [2]. Therefore, how to construct a hemocompatible surface or interface with antithrombogenic properties is the key issue in research on vascular grafts.

11.1.3 Anticoagulation of Vascular Grafts

Small-diameter prosthetic grafts undergo early thrombotic occlusion limiting their clinical utility for coronary or peripheral revascularization procedures. Several different antithrombotic agents have been evaluated experimentally [12]. One pharmacologic agent that has received wide research focus as a means to reduce neointimal hyperplasia is heparin, which is a mucopolysaccharide found in most tissues. Heparin inhibits thrombin and activated factors IX, X, XI, and XII, which is involved in the conversion of prothrombin to thrombin, thereby reducing thrombin formation. In addition, heparin has a potent antiproliferative effect on vascular VSMCs, and this effect is independent of its anticoagulant activity. Its inhibitory effect on VSMCs is mediated in part through interactions with cell receptors, growth factors, adhesion molecules, and protease inhibitors [13]. Unfortunately, systemic administration of effective levels of antithrombotic drugs is expensive and may be associated with serious hemorrhagic complications. An alternative approach is to immobilize an antithrombotic agent at the graft site. This strategy offers the advantage of inhibiting the thrombotic process at a specific site while avoiding systemic side effects [14]. Beyond that, some groups take the advantage of enzyme prodrug therapy (EPT) technique in the fabrication of anticoagulant vascular grafts [15]. EPT is a versatile technique that allows synthesis of drugs at the site of action when prodrugs are systemically administrated. In addition to targeted and localized drug delivery, the advantage of EPT also includes the fine tune of drug dosage, duration, and administration [16].

11.1.4 Calcification of Vascular Grafts

In the field cardiovascular implants, calcification of heart valves and conduits used in congenital cardiac surgery has been extensively described, and their prevention has been a challenge for researchers and industry for decades [17]. The presence of cardiovascular calcification significantly predicts patients' morbidity and mortality. Calcific mineral deposition within the soft cardiovascular tissues disrupts the normal biomechanical function of these tissues, leading to complications such as heart failure, myocardial infarction and stroke. The realization that calcification results

from active cellular processes offers hope that therapeutic intervention may prevent or reverse the disease. To this point, however, no clinically viable therapies have emerged. This may be due to the lack of certainty that remains in the mechanisms by which mineral is deposited in cardiovascular tissues [18].

11.1.5 Animal Models for the Assessment of Vascular Grafts

In order to assess the capacity of the new conduits to maintain physiologic function in the circulatory system and to determine the response of both the host and the conduits to implantation, evaluation of the grafts in preclinical animal studies is required [19]. Preclinical assessment of vascular grafts using appropriate animal models is essential to determine the clinical potential of engineered tissues. With the advancement of knowledge and technologies in the vascular grafts, there are many criteria that are utilized in the assessment of clinical potential. Each of these criteria may be best analyzed in different experimental settings. At first, the selection of an appropriate animal model needs to include criteria relevant to the vascular graft such as implantation site, vascular diameter and length, and time frame of implantation. Equally important are criteria relevant to the animal species selected such as cost, availability, ease of handling, animal response to surgical procedure, target vessel diameter and length, and target physiology. Optimally, an animal model needs to be selected that meets most of these criteria. It is best to match site and diameter to test the hemodynamics and implantability; use longer grafts (>4 cm) to test patency; select the type of anastomosis (end to end, end to side) to test shear stress; or select species that exhibit similar immunogenicity and thrombogenicity mechanisms as those at work in humans. The type of analysis, for example, serial imaging or monitoring versus a single measurement at the end of the experiment – is also important in determining the choice of animal model. Secondly, similarity to human physiology is one major factor that is considered when assessing criteria specifically related to translational studies. For example, ovine and nonhuman primate models show greater similarity to humans in terms of thrombogenicity mechanisms as compared to dogs or pigs. On the other hand, dogs exhibit lack of spontaneous endothelialization of vascular grafts, and they tend to be hyperthrombogenic, similar to humans. These two features make the dog model more stringent for vascular grafts testing. By contrast, lack of similarity in vascular dimensions and hemodynamics makes small animals like mice and rats poor models for long-term grafts evaluation. However, the plethora of transgenic mice presents a very useful resource to dissect molecular mechanisms related to immune response, remodeling, vascular reactivity, and other aspects of graft physiology. Sometimes the age and gender of recipient animals also should be mentioned. The age of recipient animals may affect the microenvironmental factors that are critical for successful grafting and long-term tissue regeneration. As the concerns of animal rights and limitations on the use of nonhuman primate increase, the pig and sheep models have become more widely used in recent years. In addition to the ethical considerations, cost is

also a factor, making the pig and sheep the models of choice. There are no absolute ideal animal models or international consensus on standards associated with the development and testing of vascular grafts. The lack of standardized models makes it difficult to compare results among investigators. In order to best evaluate the implantation of vascular grafts in such a variety of animal models, it requires optimal model selection and use of proper internal controls [20].

In the next section, we will discuss other factors that influence vascular regeneration and their long-term patency and function. Among these factors, we focus on the selection of suitable polymers, their degradation and elasticity, the scaffolds' structure, and necessary functional modification to the scaffolds.

11.2 Selection of Polymers for Vascular Grafts

11.2.1 Synthetic Polymers

ePTFE Initial vascular prostheses used nondegradable polymers like ePTFE or Teflon. Polytetrafluoroethylene (PTFE) was patented by DuPont as Teflon in 1937, and ePTFE was patented by Gore as Gore-Tex in 1969. ePTFE is an expanded polymer which is manufactured by a heating, stretching, and extruding process resulting in a non-textile porous tube [21]. The ePTFE tubes have an electronegative luminal surface that is antithrombotic. A 5-year patency of 91–95 % is achieved when used as arterial substitute with neither transanastomotic nor transmural endothelialization of this graft. Although these substitutes dominat the clinical market of vascular substitutes for large-diameter vessels, vascular regeneration is nil, and lack of patency limits the use of these as small vessel substitutes and further regeneration. Decreased patency (45 %) is observed when it is used in femoropopliteal bypass surgery [22]. Several attempts have been adopted to improve the patency of ePTFE. Studies showed that seeding ePTFE graft with autologous endothelial cells (ECs) can give adequate ECs coverage. Patency was improved considerably in dogs when compared to unseeded ePTFE grafts [23]. Compared with degradable materials, long immune response can be induced due to its nondegradable properties. Last but not the least, ePTFE is much stiffer than arteries or veins. Those problems limit their use in current practice.

PCL Poly (ε-caprolactone) (PCL) is a promising polymer for the construction of small-diameter vascular grafts due to its good biocompatibility, suitable mechanical strength, and slow biodegradation rate. Pektok et al. [24] compared the electrospun PCL grafts and the ePTFE grafts (2 mm diameter) by implanting them in rat abdominal aorta for 24 weeks. They found that PCL grafts showed better healing characteristics than ePTFE grafts. Fast endothelialization and extracellular matrix (ECM) formation, accompanied by degradation of graft fiber, seem to be the major advantages of PCL vascular graft. Walpoth's group [4] implanted electrospun PCL

vascular grafts into rat abdominal aorta. Results showed no aneurysmal dilation, perfect patency, excellent structural integrity, and limited intimal hyperplasia throughout the study. Endothelialization, cell invasion, and neovascularization of the graft wall rapidly increased until 6 months. However, from 6 to 18 months, regression of cell number and capillary density and severe calcification were observed within the graft wall. The calcification may be linked to the hypoxic conditions and oxidative stress due to the graft dense fibrous structure or the local low compliance. Kong's group [5] fabricated a macroporous electrospun PCL grafts with thicker fibers (5–6 μm) and larger pores (~30 μm). They demonstrated that thicker-fiber electrospun PCL vascular grafts could enhance vascular regeneration and remodeling process by mediating macrophage polarization into M2 phenotype.

PLCL Poly(l-lactide-co-ε-caprolactone) (PLCL) copolymers have been applied as a biomaterial for the construction of vascular grafts due to the high elastic properties. In previous reports, PLCL vascular grafts were fabricated by an extrusion-particulate leaching technique, but there were a few problems for extruded PLCL grafts in cell seeding efficiency, cell ingrowth, and mechanical strength. Sang-Heon et al. [25] fabricated and characterized a new tubular, macroporous, fibrous PLCL (5:5) graft using gel spinning. Compared to extruded PLCL scaffolds, the fibrous PLCL scaffold showed improved biological activities, such as cell seeding efficiency and proliferation, and improved mechanical properties, such as tensile strength and viscoelastic properties. Shafiq et al. [26] fabricated scaffolds by mixing appropriate proportions of linear PLCL and substance P (SP)-immobilized PLCL, using electrospinning to develop vascular grafts. PLCL-SP showed significantly higher host cell infiltration, blood vessel formation, and mesenchymal stem cells (MSCs) recruitment in vivo. Mun et al. [27] seeded VCMSs onto electrospun PLCL scaffolds to construct a three-dimensional network. The vascular grafts constructed using cell-matrix engineering were similar to the native vessels in their mechanical properties, such as tensile strength, tensile strain, and e-modulus.

PGA Poly(glycolic acid) (PGA) is a polyester obtained by the ring-opening polymerization of glycolide. Cho et al. [28] fabricated a hybrid biodegradable polymer scaffold from PLCL copolymer reinforced with PGA fibers. The PGA/PLCL vascular patches were seeded with ECs and VSMCs differentiated from bone marrow stromal cells (BMSCs) and implanted in the inferior vena cava (IVC) of bone marrow donor dogs. Compared with PLCL scaffolds, PGA/PLCL scaffolds exhibited tensile mechanical properties more similar to those of dog inferior vena cava. Eight weeks after implantation, the vascular patches remained patent with no sign of thrombosis, stenosis, or dilatation. Kobayashi et al. [29] produced the composite nanofiber composed of PGA and collagen to accomplish the recruitment of host cells and peripheral blood vessels without the bio-derived matter-like growth factors. Structural analysis revealed that the fiber has the sheath-core-like structure in which the surface region is abundant in PGA and the core region is abundant in collagen. The results of the animal experiment demonstrated that the PGA-collagen nanofiber sponge was entirely populated and vascularized within 5 days after the implantation. Rapoport

et al. [30] utilized electrospinning technique to form tubular scaffold composites with structural features reminiscent of the corrugated laminae seen in blood vessels. This tubular scaffold was fabricated with complex "J"-shaped behavior through the use of elastic polyurethane and reinforcing polyglycolic acid (PGA) woven mesh. The mechanical behavior of this tubular scaffold achieved from a low-stiffness highly elastic zone giving rise to a high-stiffness zone, and the value of burst pressures and toughness was 3095 ± 1016 mmHg and 6.3 ± 1.9 MJ/m^3, respectively.

PLA Poly(lactic acid) (PLA) is a biodegradable thermoplastic polyester that can be produced through ring-opening polymerization of lactic acid. Since lactic acid is a chiral molecule, it exists in two forms, D-PLA and L-PLA. Poly(l-lactic acid) (PLLA) is the result of L-PLA polymerization. Zhu et al. [31] reported novel scaffolds which were fabricated by co-electrospinning collagen/chitosan and PLA. The scaffolds had a more biomimetic structure than PLA, as the fiber diameters approached the size of the ECM. Axially aligned nanofibrous matrices were evaluated as small-diameter cardiovascular grafts. Sankaran et al. [32] fabricated a graft using the PLA and PCL physical blends in the ratios of 75:25 and 25:75 by electrospinning. Hydrophobicity and tensile stress were significantly higher in PLA-PCL (75:25), whereas tensile strain and fiber density were significantly higher in PLA-PCL (25:75). Human umbilical vein endothelial cells (HUVECs) adhesion experiment showed cell viability and proliferation were rationally influenced by the aligned nanofibers, and gene expression revealed the grafts' thromboresistivity, elasticity, and aided neovascularization. A graft comprised of a polyetherurethane scaffold and sealed with polyethylene glycol (PEG)/PLA copolymer exhibited good compliance, and the compliance increased with the degradation of the PEG/PLA components in vitro. Yet, when implanted in vivo, the compliance reduced 20 % after 12 weeks [33].

PGS Polycondensation of glycerol and sebacic acid forms the elastomeric poly(glycerol sebacate) (PGS). PGS shows appreciable mechanical properties and biocompatibility and degrades within 2 months in vivo [34]. In vitro hemocompatibility evaluation of PGS-based biphasic scaffolds were shown to be nonthrombogenic compared to other synthetic grafts [35]. Single-layered three-dimensional microfluidic PGS scaffolds also achieved biomimetic fluid properties [36]. Wang's group investigated the effect of pore size in PGS porous scaffold on VSMCs organization. They found that pores of 25–32 μm increased VSMCs alignment, elastin, and collagen production [37]. Subsequently, Wang's group fabricated a PGS porous tube with an average pore size of 21.2 ± 0.79 μm enveloped by a thin PCL fiber sheath [38]. After implanting the cell-free biodegradable elastomeric grafts into rat abdominal aorta, they found that the grafts degraded rapidly to yield neoarteries nearly free of foreign materials at 3 months. Based on this success, Khosravi et al. [39] developed a novel method for electrospinning smaller grafts composed of a PGS microfibrous core enveloped by a thin PCL outer sheath. Electrospun PGS-PCL composites were implanted as infrarenal aortic interposition grafts in mice and remained patent up to the 12-month endpoint without thrombosis or stenosis.

PU Polyurethane (PU) exhibits good biocompatible, optimum tensile strength and high elasticity, which make it an appealing choice for construction of small-diameter vascular conduits [40]. Recently, results of a study indicated intravascular implant patency of 95 % when an electrospun PU scaffold was implanted into the abdominal aorta of rats. Luminal surface was covered with intact endothelial cell lining, and there was no evidence of neointima formation [41]. He et al. [42] investigated the performance of small-caliber PU vascular prosthesis generated using the electrospinning technique. The results showed that cell proliferation was not inhibited as the small-caliber PU synthetic vascular grafts showed little cytotoxicity. The endothelial cells had faster adherence to the PU scaffolds than to the PTFE surface during the initial contact. Punnakitikashem et al. [43] prepared a biodegradable fibrous scaffold that contained biodegradable elastic polyurethane urea (BPU) and the drug dipyridamole (DPA) by electrospinning. The resulting scaffolds had tensile strengths and strains comparable with human coronary artery. It confirmed that the DPA-loaded BPU scaffolds could extend human blood clotting time and reduce human platelet deposition and hemolysis. Furthermore, the DPA-loaded BPU scaffolds had no adverse effect on human aortic endothelial cell growth, yet it improved their proliferation. Thermoplastic polyurethane (TPU) as a class of PU has linear segmented molecular chains, good processability, high elongation, and excellent biocompatibility. Bergmeister et al. [44] investigated the biocompatibility of TPU grafts in vitro and in vivo. TPU grafts showed significantly increased endothelial cell proliferation in vitro. Population by host cells increased significantly in the TPU conduits within 1 month of implantation. After long-term implantation, TPU implants showed 100 % patency (ePTFE: 93 %) with no signs of aneurysmal dilatation. Enayati et al. [45] also evaluated biodegradable TPU vascular graft by implanting into the infrarenal aorta of rats. After 1 month the results showed that the porous structure of the TPU graft allowed cell migration and proliferation, resulting in a highly cellular graft.

PHA Polyhydroxyalkanoate (PHA) is a polyester produced by microbes like bacteria under nutrient-limited conditions with excess carbon supply [46]. PHA shows good biocompatibility and a wide range of mechanical properties and biodegradation rates. These make it attractive for vascular conduit construction. A 7-mm-long PHA-PGA tubular scaffold seeded with ovine carotid artery cells, implanted into a lamb aorta, showed patency for 5 months and stress-strain behavior similar to a native vessel [47].

11.2.2 Natural Polymers

Collagen is the major component of the ECM in the body. It is a structural protein whose main function is to provide mechanical integrity to different tissues and organs such as tendon, bone, etc. Collagen gels as scaffolds for engineering vascular substitutes were first reported by Weinberg CB in 1986 in the first attempt to

produce a tubular construct in vitro that mimicked the structure of an artery [48]. Building on his early work, Achilli et al. [49] investigated UV-C-treated collagen gels to improve the integrity of collagen-based scaffold by adding cross-links. Schutte et al. [50] used a bioreactor to apply mechanical conditioning through cyclic strain. Mechanical stimulation improved tissue strength through increasing collagen content as well as some radial tissue compaction. Wu et al. [51] cocultured the endothelial and smooth muscle cells on a collagen membrane. This tissue-engineered vascular substitute had not only enough tensile strength and good biocompatibility but also advanced vascular regeneration.

Elastin is a protein normally found in the wall of arteries and in several mammalian tissues. Its main function is to provide elasticity, allowing high strain and efficient elastic energy storage in arteries, to ensure blood flow and perfusion to the rest of the body's tissues. Leach et al. [52] recently detailed a protocol to process elastin with ethylene glycol diglycidyl ether (EGDE), a diepoxy cross-linker, to develop an elastin-based scaffold. In order to imitate the native three-layered architecture, Koens et al. [53] prepared a triple-layered construct consisting of elastin and collagen. The highly purified type-I collagen fibrils and elastin fibers used did not evoke platelet aggregation in vitro. Some researchers also discovered that elastin addition to a porous collagen scaffold played a major role in altering its biological and mechanical response [54]. Smith et al. [55] fabricated cross-linked suture-reinforced polydioxanone (PDO)-elastin tubes. These tubes exhibited a range of compliance values, including those matching native artery. These tubes display many characteristics of the ideal small-diameter grafts.

Fibrin is an insoluble body protein largely involved in blood clotting. It is formed through fibrillogenesis of a monomer (called fibrinogen) that flows in the blood. In 2000, Ye et al. [56] prepared a three-dimensional matrix of fibrin gel for cardiovascular tissue engineering and reported uniform cell growth and collagen deposition into the gel. Syedain et al. [57] fabricated a tissue-engineered arteries based on entrapment of human dermal fibroblasts in fibrin gel. The completely biological vascular grafts that possessed circumferential alignment characteristic of native arteries, which was essential to their mechanical properties. Recently, this group confirmed that hypoxia coupled with insulin supplementation was also shown to improve the strength of fibrin-based tissue-engineered vascular grafts (TEVGs) by enhancing collagen deposition in the entrapped cells [58]. Additionally, Swartz et al. [59] have examined a fibrin-based TEVGs in an ovine model. In this study, fibrin tubes with entrapped vascular VSMCs were implanted as vein interposition grafts in lambs. At 15 weeks of postimplantation, TEVGs exhibited remarkable matrix remodeling with production of collagen and elastin fibers and orientation of VSMCs perpendicular to the direction of blood flow. Implanted vessels gained significant mechanical strength and reactivity that were comparable to those of native veins.

Chitin is, after cellulose, the most common polysaccharide found in nature. Chupa et al. [60] introduced a method to produce a porous scaffold by freezing and lyophilizing chitosan. Ling et al. [61] used a mesh of knitted chitosan fibers, coated in a chitosan and gelatin solution and then freeze-dehydrated. The scaffold possessed proper swelling property, burst strength of almost 4000 mmHg, and high

suture retention strength. An alternative, constructed from cross-linked and freeze-dried chitosan and collagen, had also been shown to support vascular cell adhesion and proliferation, and additionally, exhibited suitable biocompatibility in vivo when implanted in rabbit livers [62]. Chitosan could also be fabricated with PCL by sequential quantity grading co-electrospinning. To prevent thrombosis, researchers used heparinization and immobilization of vascular endothelial growth factor (VEGF) in the gradient CS/PCL [63].

Hyaluronic acid (HA) (or sodium hyaluronate) is a non-sulfated glycosaminoglycan (GAG). It is comprised of linear, unbranching, polyanionic disaccharide units consisting of glucuronic acid and N-acetyl glucosamine. Milella et al. [64] characterized the physicochemical properties of nonwoven hyaluronan benzylic esters (Hyaff 11) as a tissue engineering scaffold. Zhu et al. [65] developed a suitable intimal layer scaffold for endothelialization using novel humanlike collagen/HA. The result showed the scaffold with an interconnected porous network, better mechanical properties, and excellent biocompatibility. Joo et al. [66] reported that bioactive HA could be chemically modified into hyaluronic acid-catechol by a single-step method. This method could enhance endothelialization in vitro.

ECM serves as a biologically active scaffold on which cells can migrate or adhere. Li et al. [67] demonstrated that elastin haploinsufficiency led to compensatory increase in VSMCs number which resulted in profound arterial thickening. It may regulate the phenotype of the cells. It has been demonstrated that VSMCs rapidly lose their contractile apparatus and adopt a synthetic phenotype in culture [68]. The ECM serves as an anchor for many proteins including growth factors and enzymes such as proteases and their inhibitors.

Rothuizen et al. [69] presented a novel approach to generate autologous tissue-engineered blood vessels (TEBVs) in vivo. Polymer rods were engineered and implanted, evoking an inflammatory response that culminates in encapsulation by a fibrocellular capsule. After 4 weeks, rods with tissue capsules grown around it were harvested. Tissue capsules were grafted bilaterally as carotid artery interposition. Patency was 100 % after 1 week and 87.5 % after 4 weeks. Wall thickness and α-smooth muscle actin (α-SMA)-positive area significantly increased. The lumen was largely covered with ECs.

By combining ultrahigh hydrostatic pressure (UHP)-decellularized ostrich carotid arteries with the peptide modifier, Mahara et al. [70] created a tissue-engineered small-caliber long-bypass grafts measuring 20–30 cm in length and having a 2-mm inner diameter. A novel peptide modifier containing a collagen-binding peptide sequence and an endothelial cell-binding sequence improved the affinity of the luminal surface for endothelial cells. The decellularized carotid artery modified with the peptide demonstrated good patency and stable pulsatile blood flow in pig femoral-femoral bypass model.

Small intestinal submucosa (SIS) is a natural biodegradable material derived from the small intestine of vertebrates, usually from swine. Vascular grafts were engineered using SIS-fibrin hybrid scaffold and implanted interpositionally into the arterial circulation of an ovine model. No occlusions or anastomotic complications were observed in 18 animals that received these grafts. Notably, the grafts exhibited unprecedented levels of host cell infiltration [71].

11.2.3 Hybrid Materials: Synthetic and Natural Polymers

Autologous saphenous vein is used as a conduit to bypass atherosclerotic lesions in both the coronary artery (coronary artery bypass graft surgery [CABG]) and in femoral arteries (infrainguinal bypass graft surgery [IIBS]). Despite the undoubted success and benefits of the procedures, graft failure occurs in 50 % of cases within 10 years after surgery. A principal cause of late vein graft failure is intimal and medial hyperplasia caused by medial vascular VSMCs migration, proliferation, and ECM deposition, followed later by superimposed atherosclerosis. These changes directly compromise graft blood flow and provoke thrombosis.

Jeremy et al. [72] studied the effect of external synthetic stents and sheaths in pig models of vein into artery interposition grafting and showed a profound effect on vein graft remodeling and thickening. It has been clearly demonstrated that external synthetic stents or sheaths elicit a complete inhibition of neointima formation, an axiomatic lesion in vein graft disease, and an overall reduction of graft thickening. These effects appear to be mediated by the promotion of angiogenesis which is mediated by the accumulation of a proangiogenic exudate in the space between the graft and the sheath or stent. Macroporosity is also a crucial factor since it allows for a fully integrated and functional microvascular system to develop. Ultimately, they suggest that the profound local accumulation of inflammatory cells, in particular, macrophages and giant cells, play a key role in that they initiate accumulation of ECs and VSMCs in and around the material and promote angiogenesis. Another facet of the external stents or sheaths is that they impose symmetry on the graft.

Decellularized xenografts are commonly used as a tissue engineering substitute for vascular reconstructive procedures. Although acellular allogeneic vascular grafts have good histocompatibility and antithrombotic properties, the decellularization process may damage the biomechanics and accelerate the elastin deformation and degradation, finally resulting in vascular graft expansion and even aneurysm formation. Here, to address these problems, Gong et al. [73] combined synthetic polymers with natural decellularized small-diameter vessels to fabricate hybrid tissue-engineered vascular grafts (HTEV). The donor aortic vessels were decellularized with a combination of different detergents and dehydrated under a vacuum freeze-drying process. PCL nanofibers were electrospun outside the acellular aortic vascular grafts to strengthen the decellularized matrix. The intimal surfaces of the hybrid small-diameter vascular grafts were coated with heparin before the allograft transplantation. Mechanical testing of scaffolds showed that electrospun PCL fibers significantly enhanced the biomechanics of decellularized vessels. Vascular ultrasound and micro-CT angiography showed that all grafts after implantation in a rat model were satisfactorily patent for up to 6 weeks. Electrospun PCL fibers successfully prevented the occurrence of vasodilation and aneurysm formation after transplantation and reduced the cell inflammatory infiltration.

Hemodynamic factors play a major role in the development of intimal hyperplasia and subsequent bypass failure. To evaluate the potential protective effect of

external reinforcement on such a failure, Longchamp et al. [74] developed an ex vivo model for the perfusion of segments of human saphenous veins under arterial shear stress. The data showed that, in an experimental ex vivo setting, an external scaffold decreased intimal hyperplasia and maintained the integrity of veins exposed to arterial pressure, via increase in shear stress and decrease wall tension, that likely contributed to trigger selective molecular and cellular changes. Ex vivo, such reinforcement prevented the dilatation of the vessel, decreased the development of intimal hyperplasia, and preserved the architecture of the media layer by reducing the apoptosis of VSMCs and subsequent fibrosis. At the molecular level, the mesh prevented the upregulation of matrix metalloproteinases (MMP-2, MMP-9) and plasminogen activator type I, which are involved in the remodeling of the ECM.

11.3 Fabrication of Vascular Grafts

To date, numerous techniques such as electrospinning, particle leaching, melt spinning, and 3D printing have been used to fabricate vascular grafts with synthetic and natural materials. Each of these methods has its own unique advantages and disadvantages. Microstructure of vascular grafts formed by those methods has a great effect on their regeneration and remolding. An important factor in vascular grafts is pore size. Too small pores will hinder cell infiltration, but too large pores can cause problems such as blood leakage. Current studies tend to fabricate vascular grafts using combination of two or more approaches. The following are some typical technique usually applied in fabrication of polymer-based vascular grafts.

Electrospinning is the most commonly used method to fabricate vascular graft. It is a simple and effective way to produce fibers ranging from 50 nm to 10 μm. It consists of a syringe pump, a high-voltage power supply, a grounded iron rod, and a spinneret. Using this technique, fibers are collected on the target and can be modified by regulating parameters such as rod rotating speed, voltage, flow velocity, and solution concentration. As discussed in greater detail above, a number of synthetic and natural polymers have been explored for the fabrication of nanofibers [75]. Walpoth's group fabricated PCL vascular grafts by electrospinning and evaluated the long-term performance of grafts in the rat abdominal aorta replacement model. Results showed excellent structural integrity during 18 months, with no aneurysmal dilation, and perfect patency with no thrombosis and limited intimal hyperplasia. However, calcification took place on the medium term, and a cellular regression was observed at 12 and 18 months [4]. In order to prevent blood leakage and facilitate cell infiltration and applicability of vascular grafts in the clinic, bilayered grafts were prepared by electrospinning a high-porosity layer with a low-porosity layer on external or internal side. In vitro blood leakage through these bilayered grafts was significantly reduced compared with a high-porosity graft. The study showed that most of the cellular infiltration came from the graft surrounding tissues and not from the blood flow [76]. This phenomenon owns important directive significance for fabrication of biodegradable vascular grafts.

Limited cell infiltration into the grafts will hamper the regeneration and remodeling of the grafts into neoarteries. To overcome this problem, macroporous electrospun PCL grafts with thicker fibers (5–6 μm) and larger pores (30 μm) were fabricated in Kong's lab. In vivo implantation by replacing rat abdominal aorta demonstrated that the macroporous grafts markedly improved cell infiltration and ECM secretion. The regenerated arteries demonstrated contractile response to adrenaline and acetylcholine-induced relaxation. Analysis of the cellularization process revealed that the thicker-fiber scaffolds induced a large number of M2 macrophages to infiltrate into the graft wall, which further promoted cellular infiltration and vascularization [5] (Fig. 11.1). Regeneration of VSMCs with circumferential orientation within the grafts is crucial for functional vascular reconstruction in vivo. Thus, Kong's lab designed a bilayered vascular graft, of which the internal layer was composed of circumferentially aligned microfibers prepared by wet spinning and an external layer was composed of random nanofibers prepared by electrospinning. The internal circumferentially aligned microfibers provided topographic guidance for in vivo regeneration of circumferentially aligned VSMCs, and the external random nanofibers could offer enhanced mechanical property and prevent bleeding during and after graft implantation (Fig. 11.2). The results demonstrated that the circumferentially oriented VSMCs and longitudinally aligned ECs were successfully regener-

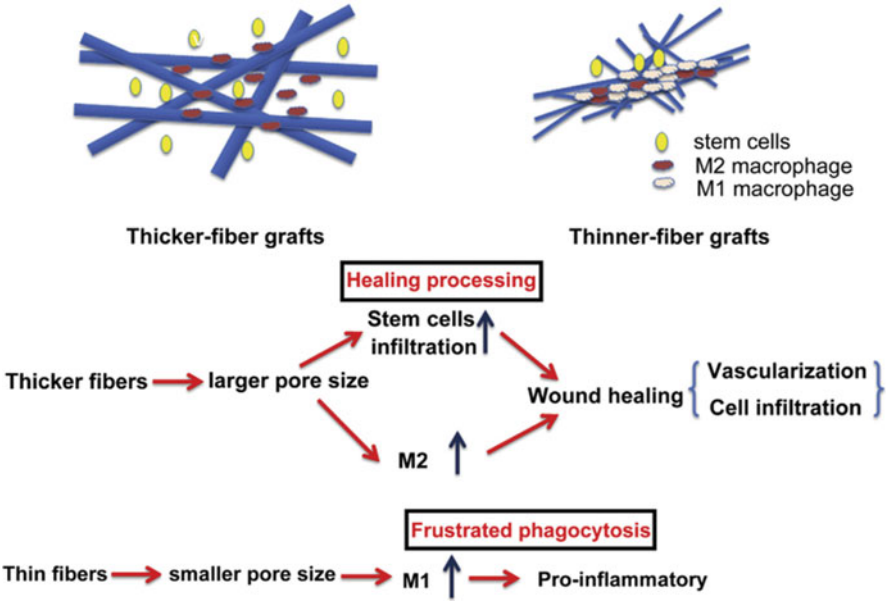

Fig. 11.1 Schematic illustrates that the pore size of electrospun PCL grafts may modulate the polarization of macrophages phenotype (Reprinted from Ref. [5] with permission, Copyright 2014 Elsevier Ltd.)

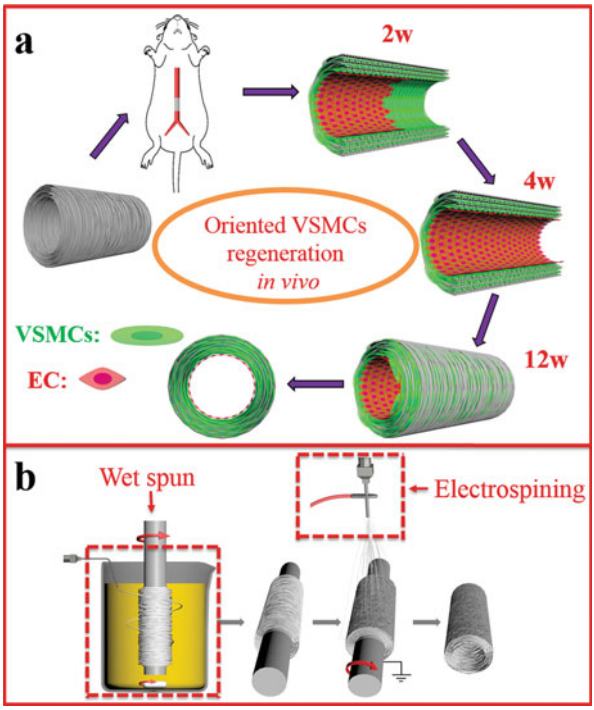

Fig. 11.2 (**a** Schematic illustration shows the circumferentially aligned microfibers of the grafts which guide VSMCs' regeneration in circumferential orientation. (**b**) The bilayered grafts are prepared by wet spinning and electrospinning method (Reprinted from Ref. [77] with permission. Copyright 2015 Elsevier Ltd.)

ated in vivo after the bilayered vascular grafts were implanted in rat abdominal aorta, and the regenerated neoartery exhibited contraction and relaxation property in response to vasoactive agents [77].

Despite great progress has been made over recent decades and various techniques have been developed to fabricate a TEVGs, only one kind of polymer-based graft has been successfully executed in clinical application, which was described by Hibino et al. in 2001 in a high-flow, low-pressure pulmonary venous system. A hybrid biodegradable polymer vascular graft degrade within a certain period of time was fabricated by pouring a solution of the copolymer of PCL-PLA (50:50) onto the PGA woven fabric sheet, followed by freeze-drying [78]. Twenty five grafts were implanted (median patient age, 5.5 years) and underwent a Fontan procedure under informed consent and institutional review board approval. Six of these 25 patients died, although no graft-related mortality occurred. There was no evidence of aneurysm formation, graft infection, graft rupture, or ectopic calcification [79, 80].

Particle leaching method also has been developed for fabrication of vascular grafts. Wang's lab developed bilayered vascular grafts composed of PGS layer fabricated by salt leaching method and PCL sheath generated by electrospinning which increased graft strength and prevented bleeding. Three months' postimplantation in rat abdominal aorta, the neoarteries resembled native arteries in several aspects: a

confluent endothelium and contractile smooth muscle layers and regular, strong, and synchronous pulsation [38]. The long-term study showed that the neoarteries contained nerves and had the same amount of mature elastin as native arteries and responded to vasomotor agents, although with smaller magnitude than native aortas [81]. Also, Wu's study confirmed that the thickness and density of PCL sheath in bilayered grafts could affect the vascular remodeling and regeneration [82].

Sugar spheres can also be used as porogen to produce highly interconnected vascular graft by several steps. Polymer solution was firstly cast into an assembled sugar template under a mild vacuum. The polymer-sugar composite was phase separated at low temperature overnight and then immersed into cyclohexane to exchange Tetrahydrofuran (THF). The consequential composites were freeze-dried, and the sugar spheres were leached out in distilled water and freeze-dried again. In vivo subcutaneous implantation studies indicated VSMCs differentiation and host tissue infiltration in the scaffolds [83]. A thin dense layer needed to prevent leakage of blood after this kind of macroporous vascular graft was implanted in vivo.

The technique of phase separation can generate macroporous scaffolds which can increase cell migration and cell seeding efficiency. Polymer dissolution is processed by liquid-liquid phase separation and polymer gelation to generate a nanofibrous sponge. Then the solvent is extracted and the foam is freeze-dried. Many parameters such as gelation temperature, polymer concentration, solvent characteristics, and thermal treatment can affect scaffolds morphology, Young's modulus, and tensile strength. Ma's lab developed a porous vascular grafts with biodegradable PLLA through thermally induced phase-separation (TIPS) techniques. The grafts with oriented gradient microtubular structures in the axial or radial direction can be produced by utilizing different thermal conductivities of the mold materials and using benzene as the solvent. The porosity, tubular size, and the orientational direction of the microtubules can be regulated by the TIPS temperature, the polymer concentration, and by utilizing materials of different thermal conductivities [84].

Bilayered vascular grafts of poly(ester urethane) urea (PEUU) were fabricated by electrospinning and TIPS and implanted in vivo after seeded with pericytes. Cell-seeded TEVGs showed extremely higher patency rate than the unseeded control. The remodeled vascular grafts consisted of multiple layers of α-SMA- and calponin-positive cells and a von Willebrand factor-positive monolayer in the lumen [85, 86].

Sugiura et al. developed a novel bioresorbable vascular graft with a porous PLCL sponge-type scaffold reinforced by PLA nanofibers which is fabricated by phase-separation method and electrospinning. The animal experiments show that it has potential to be applied as small-diameter arterial grafts [87].

Despite these promising results from the preclinical studies, it is too early to evaluate the full potential of these grafts in clinical applications. Future studies should include long-term implantation of grafts in large animals as well as more rigorous functional evaluations.

11.4 Functional Modification of Vascular Grafts

11.4.1 Nitric Oxide-Releasing Materials

Commercialized Dacron, ePTFE, and microporous PU vascular prostheses have been widely used in clinical practice as large-diameter (>6 mm) vascular grafts. However, these polymers have been proven inadequate when used as small-diameter (<6 mm) grafts due to occlusion and restenosis. To solve this problem, researchers used different nitric oxide (NO)-based strategies to modify these polymer materials. NO-releasing materials were firstly reported by Smith et al. in 1996 [88]. Covalent attachment of NO donors directly to the polymer backbone has been recognized as a further route for fabrication of ePTFE bypass grafts (W.L. Gore & Associates, Inc.). NONOate formed by using gaseous NO demonstrates potent antiplatelet activity to predict the inhibition of thrombosis. Many researchers incorporated NO donors into PU to prepare novel NO-releasing materials for promoting graft endothelialization while preventing thrombus formation and intimal hyperplasia. Among those studies, Fleser et al. [89] implanted small-diameter (5 mm) PU vascular grafts coated with a polymer containing the NO donors (dialkyl hexanediamine diazeniumdiolate) in a sheep arteriovenous bridge-graft model for 21 days. Approximately 80 % of the NO-eluting grafts were found to remain patent in vivo compared with only a 50 % patency rate with control grafts. Although the improvement in patency between NO-releasing grafts and control grafts was not statistically significant, control grafts contained significant adherent thrombus and fibrin matrix with inflammatory and red blood cells, an observation not found in NO-releasing grafts.

There has been substantial effort directed to fabricating materials that mimic endothelial properties. Kushwaha et al. [90] developed a nanofibrous matrix, which is formed by self-assembly of peptide amphiphiles (PAs), containing NO donating residues and Tyr-Ile-Gly-Ser-Arg (YIGSR) peptide sequence, a laminin-derived cell-adhesive peptide sequence. The NO-releasing nanofibrous matrix demonstrated a significantly enhanced proliferation of ECs but reduced VSMCs proliferation and platelet attachment. Andukuri et al. [91] reported a similar design in which electrospun PCL nanofibers were coated with NO-releasing PAs containing cell-adhesive ligands (YIGSR and KKKKK) by a solvent evaporation technique. The presence of YIGSR ligands and release of NO promoted the adhesion and proliferation of ECs while simultaneously limiting the adhesion and proliferation of VSMCs and the adhesion and activation of platelets.

Besides immobilization of NO donors on polymer matrix, there are many studies on modification of polymers by catalysts for promoting the transfer of NO from NO donors in blood. Wang et al. [15] constructed a functional vascular graft by immobilization of β-galactosidase on vascular graft surface for catalyzing prodrug to release NO locally and sustainably (Fig. 11.3). The functional vascular grafts were implanted into the rat abdominal aorta with a 1-month monitoring period. Results in vivo showed effective inhibition of thrombus formation and enhancement of vascular tissue regeneration and remodeling on the grafts. Lewis and coworkers

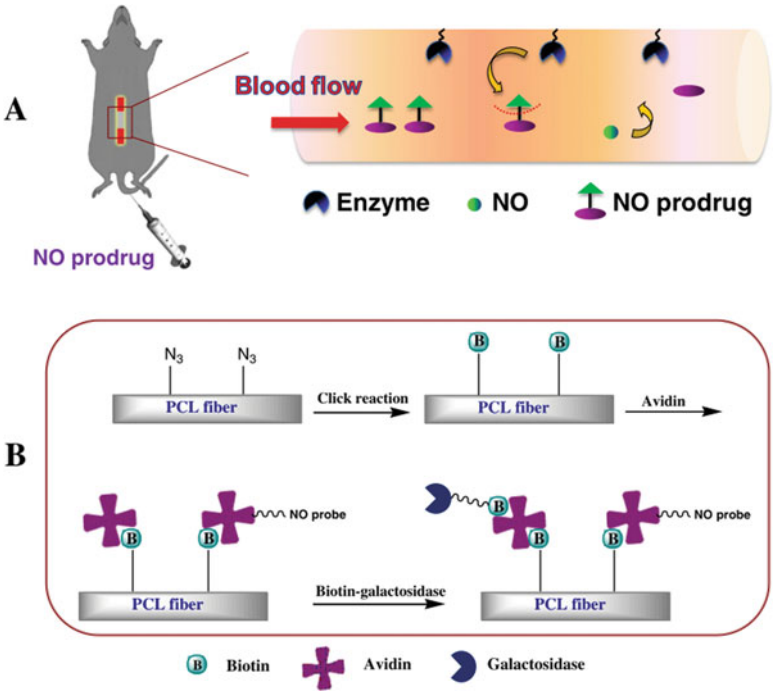

Fig. 11.3 Illustration for the enzyme immobilized on the vascular grafts to catalyze the decomposition of exogenously administrated NO prodrug to release NO. (**a**) Pathway for the surface enzyme functionalization of PCL vascular grafts (**b**) (Reprinted from Ref. [15] with permission. Copyright 2015 Elsevier B.V.)

modified polyethylene terephthalate (PET) and PU with thiol groups that could promote the release of NO from S-nitrosothiol compounds (RSNO) naturally found in plasma and whole blood solutions and thus inhibited platelet adhesion [92, 93]. Chen et al. prepared a novel vascular graft in situ with catalytic generation of NO [94]. PGA and poly α-lysine were deposited alternately onto the surface of electrospun PCL matrices, and selenocystamine (SeCA) was loaded as a catalyst. Cellular compatibility of the new material was shown to be good in the fibroblast proliferation experiment. In biological function evaluations, the catalyst-loaded material could inhibit the spread of VSMCs in the presence of NO donors and prevent acute thrombosis when in contact with blood. An et al. developed an electrospun PCL matrix loaded with organoselenium-immobilized polyethyleneimine (SePEI) as NO donor catalyst via electrostatic layer-by-layer self-assembly [95]. This material revealed significant NO generation when contacting NO donor S-nitrosoglutathione (GSNO). Modified material could inhibit adhesion and spreading of VSMCs and promote proliferation of ECs. In addition, antithrombotic properties of these NO-generating materials were proven by reduced platelet adhesion and prevention of acute thrombosis.

Other studies demonstrated the immobilization of NO-releasing catalysts on the surface of stents for localized delivery of NO. Huang's group coated metallic stents with titanium dioxide (TiO_2) films, followed by immobilization of cystamine and selenocystamine (Se) on TiO_2 film surface for catalytic generation of NO by decomposing endogenous S-nitrosothiols (RSNO) [96, 97]. Results in vitro showed that both modifications reduced collagen-induced platelet activation. In addition, the Se-modified stents inhibited neointimal hyperplasia in dog femoral artery model. Recently, the group developed a NO-catalytic bioactive coating that obtained by covalent conjugation of 3,3-diselenodipropionic acid (SeDPA) with glutathione peroxidase (GPx)-like catalytic activity to generate NO from RSNO via specific catalytic reaction [98]. Results in vivo showed SeDPA-PPAam-coated stents remarkably reduced neointimal stenosis compared with bare stent by promoting re-endothelialization and reducing proliferation and migration of VSMCs.

11.4.2 Polypeptide Modification

In general, biological recognition between cell-surface receptors and their ligands is the key switch to mediate cell migration and adhesion in physiological environments. Verhaar's group reported that stromal cell-derived factor 1α (SDF1α)-derived peptides can be chemically modified with a supramolecular fourfold hydrogen bonding ureido-pyrimidinone (UPy) moiety that allowed for the convenient incorporation of the UPy-SDF1α-derived peptides into a UPy-modified polymer scaffold [99]. The chain-extended UPy-poly(l-lactic acid caprolactone) (CE-UPy-PLLCL) polymer was obtained by replacing the poly(2-methyle1, 3-propylene adipate) diol of chain-extended UPy-poly(2-methyle1, 3-propylene adipate) with poly(l-lactic acid caprolactone) diol. The CE-UPy-PLLCL and either the UPy-SDF1a(R) peptide or the UPy-SDF1a(NR) peptide were dissolved in a mixture of chloroform and hexafluoroisopropanol and then produced fibrous tubular graft by electrospinning. This kind of graft can retain and stimulate leukocyte populations in an anti-inflammatory, pro-tissue formation signaling environment.

Mahara et al. demonstrated the excellent patency of tissue-engineered small-caliber long-bypass grafts [70]. The inner surface of an acellular ostrich carotid artery was modified with a novel heterobifunctional peptide composed of a collagen-binding region $(Pro\text{-}Hyp\text{-}Gly)_n$, $(POG)_n$, and the integrin α4β1 ligand, Arg-Glu-Asp-Val (REDV), which was expressed on ECs and circulating endothelial progenitor cells (EPCs). The $(Pro\text{-}Hyp\text{-}Gly)_7$ (POG_7) peptide was conjugated to Arg-GluAsp-Val (REDV) through Gly-Gly-Gly (G_3) spacer domain, which was termed $(Pro\text{-}Hyp\text{-}Gly)_7$-Gly-Gly-Gly-Arg-Glu-Asp-Val (POG_7G_3REDV). Decellularized carotid arteries were immersed in this peptide solution and incubated at 60 °C for 1 h and then cooled down to room temperature to accomplish peptide modification. The modified graft was transplanted into Gottingen minipig femoral arteries and observed for 20 days and received no anticoagulant medica-

tion. Five cases were patent and no thrombogenesis was observed on the luminal surface. In contrast, all unmodified grafts became occluded, and severe thrombosis was observed. This vascular graft is the first successful demonstration of short-term patency at clinically applicable sizes.

The tripeptide sequence of Arg-Gly-Asp (RGD) was identified by Pierschbacher and Ruoslahti in 1984 as a minimal essential cell adhesion peptide sequence in fibronectin. Kong's lab modified electrospun PCL scaffold with RGD containing molecule (Nap-FFRGD) using a surface coating method. The Nap-FFRGD molecule contains both the RGD peptide and hydrophobic naphthalene group, which can self-assemble onto hydrophobic PCL surfaces to form an RGD coating layer. The modified surface was shown to improve hydrophilicity and enhance cell adhesion and spread in vitro [100]. And then, the electrospun PCL grafts were functionally modified by Nap-FFGRGD molecule through self-resembling. The potential of the grafts as small-diameter vascular grafts was investigated in a rabbit carotid arterial implantation model. The modified grafts exhibited an improved inhibition of platelet adhesion, enhanced cell infiltration, endothelium formation, smooth muscle regeneration, and patency, which suggested that the as-prepared PCL-RGD graft may be a promising candidate for the small-diameter vascular grafts [101].

The tetrapeptide, REDV, is a fibronectin-derived peptide that can specifically bind to the α4β1 integrin, which is abundant on ECs, whereas scarce on VSMCs. Wang et al. constructed an NO and REDV dual modificated vascular graft and examined its effect on enhancing rapid in situ endothelialization. [102]. A macroporous electrospun PCL graft was prepared and modified via layer-by-layer self-assembly. Assembly of PCL grafts was performed with constant-flow pumps driving the solutions through the grafts at a very slow rate. To prepare catalyst-loaded material, deposition was continued until ten SePEI/hyaluronic acid (SePEI/HA) bilayers were obtained. To get REDV peptide functionalized material, a SePEI/HA-REDV bilayer was deposited after nine bilayers of SePEI/HA, and the sample was marked as PCL-$(S/H)_9$-S/H-R. The cooperation of NO and REDV promoted ECs adhesion with an increased ECs/SMCs ratio in a coculture system. Grafts built by this method exhibited rapid endothelialization and a well-organized ECs pattern. The dual modification proposed in this study may be a promising approach to improve the endothelialization and long-term performance of small-diameter vascular grafts.

Larsen et al. reported a peptide fluorosurfactant polymer (FSP) biomimetic construct that promoted ECs selective attachment, growth, shear stability, and function on ePTFE [103]. The peptide FSP consisted of a flexible poly(vinyl amine) backbone with ECs-selective peptide ligands (primary sequence: Cys-Arg-Arg-Glu-Thr-Ala-Trp-Ala-Cys, CRRETAWAC) and pendant fluorocarbon branches for stable anchorage to underlying ePTFE. This peptide has demonstrated high binding affinity for the α5β1 integrin found on ECs, which was attributed to Arg-Arg-Glu (RRE) motif interaction with the β1 subunit and Trp interaction with a Trp residue in the α5 integrin subunit. They demonstrated low affinity of CRRETAWAC for platelets and platelet integrins, thus providing it with EC selectivity. This EC

selectivity could potentially facilitate rapid in vivo endothelialization and healing without thrombosis for small-diameter ePTFE vascular grafts.

Zhou et al. reported that a short peptide REDV was linked to trimethyl chitosan (TMC) via a bifunctional (Polyethylene Glycol) PEG linker for the targeted delivery of microRNA-126 to vascular endothelial cells [104]. TMC was reacted with a bifunctional PEG, ω-2-pyridyldithio polyethylene glycol α-succinimidylester (OPSS-PEG-SCM), in distilled water for 6 h, allowing the primary amino groups on TMC to react specifically with the SCM group of the heterobifunctional PEG. After lyophilized, the obtained TMC-g-PEG-OPSS reacted with REDV-Cys to link the REDV peptide by means of a specific reaction between the OPSS group in TMC-g-PEG-OPSS and the thiol group in the REDV-Cys peptide. By REDV modification, the TMC-g-PEG-REDV/miRNA complex showed negligible cytotoxicity, increased expression of miRNA-126, and enhanced ECs proliferation compared with the TMC/miRNA and TMC-g-PEG/miRNA complexes. It was suggested that the REDV peptide-modified TMC-g-PEG polyplex could be potentially used as a miRNA carrier in artificial blood vessels for rapid endothelialization.

Ji et al. developed a method for the dual functionalization of a PCL surface through the supramolecular assembly technology [105]. Functionalization of PCL-cyclodextrin (PCL-CD) through host-guest inclusion complexation was performed in aqueous medium. PEG can decrease protein adsorption, and TPSLEQRTVYAK (TPS) peptide can specifically bind EPCs. The two kinds of functional molecular were immobilized on the PCL surface through host-guest inclusion complexation (Fig. 11.4). Aqueous solution of adamantine (AD) conjugated guest compounds (PEG-AD and TPS-AD) alone or in combination was prepared. Typically, the total concentration of guest compounds was kept at 1 mg/mL irrespective of the composition. Then PCL-CD films were put into the solutions, incubated and dried. The relative composition of the PEG and TPS could be further fine-tuned by adjusting the feeding ratio. The PEG functionation significantly inhibited the adsorption of fibrinogens and the adhesion of platelets, thus reducing the possibility of thrombus formation. Moreover, the TPS-functionalized surface showed enhanced attachment toward EPCs compared with the one without TPS functionalization. The dual functions provided by the corresponding functional molecules were well preserved, which indicated that the host-guest supramolecular assembly technology is particularly useful for covalent immobilization of bioactive molecules onto polymeric scaffolds.

Hydrophobin HGFI is a member of amphiphilic proteins, which can form a self-assembly layer on the surface of hydrophobic polymer scaffolds and convert their wettability. A fusion protein, TPS-linker-HGFI (TLH), which was composed of HGFI that originated from *Grifola frondosa* and functional peptide TPS, was expressed by *Pichia pastoris* expression system. PCL scaffolds were incubated overnight in a sterilized aqueous TLH solution, followed by blowing off the excess protein solution and drying in a super clean bench. Cell adhesion test showed that the TLH-modified PCL could specially enhance the adhesion of ECs and EPCs [106, 107]. This work presented a new perspective to apply hydrophobin in tissue

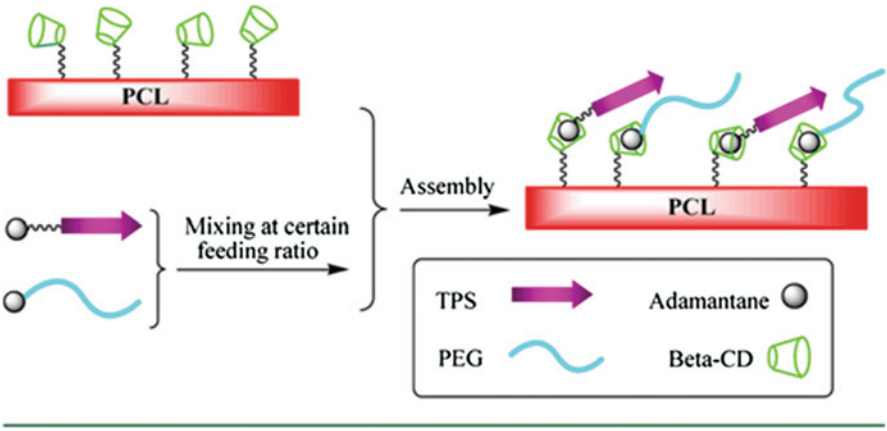

Fig. 11.4 Schematic illustration for the supramolecular assembly of functional molecules on the surface of PCL-CD film (Reprinted from Ref. [105] with permission. Copyright 2013 American Chemical Society)

engineering and regenerative medicine and provided an alternative approach in surface modification.

11.4.3 Incorporation of Growth Factors

Endothelialization is a complex process that mainly relate to ECs adhesion, migration, proliferation and differentiation. Numerous growth factors are involved in the regulation of ECs activities and new blood vessel formation. So there are many researchers committed to investigate how to modify the artificial vascular graft with growth factors and other bioactive molecules.

Fibroblast growth factors (FGFs) can promote fibroblast mitosis, ECs migration, and VSMCs proliferation. Brewster et al. [108] engineered a thrombin-resistant mutant of FGF-1 through a lysine (K) for arginine (R) base substitution at residue 136 (termed R136K), the primary thrombin-induced cleavage site Then R136K was bound to a collagen-binding domain (CBD) to generate R136K-CBD. Comparing with control group, the R136K-CBD has significantly better angiogenic activity, ECs sprout lengthening, and mitogenic activity.

Researchers found that the regeneration potential of endogenous cells could be contributed to blood vessel regeneration. Since adult vascular cells lack expansion capability, it will be highly desirable to develop vascular grafts that can recruit endogenous stem cells or progenitor cells of both ECs and VSMCs. Stromal cell-derived factor-1a (SDF-1α) is considered to be a potent factor for EPCs homing and neovascularization. Yu et al. [109] use di-NH-PEG as a linker molecule and Sulfo-n-hydroxysuccinimide (NHS) and 1-ethyl-3-(3-dimethylaminopropyl)carbodiimide (EDC) as cross-linking agents, to make heparin connect to PLLA scaffold surface.

Following heparin conjugation, SDF-1α in PBS was incubated with the scaffolds over night at 4 °C to allow it to bind to heparin immobilized on the scaffolds. They implanted the heparin-SDF-1α-treated PLLA scaffold into the left common carotid artery of rats. The result demonstrated that heparin could stabilize the immobilized SDF-1α on microfibers, which enhanced the self-regeneration capability of the grafts by recruiting EPCs and smooth muscle progenitor cells, contributing to endothelialization and the remodeling of the vascular wall.

In small animals, transanastomotic cell ingrowth can trigger vascular regeneration. That is very rare in humans. To prove that functional blood vessels can be formed in situ through the host inflammatory response solely by circulating cells, Talacua et al. [110] utilize Gore-Tex sheet and masterly constructed a novel rat model. In addition, this group modified PCL conduit with MCP-1 through impregnating PCL conduit into fibrin gel added monocyte chemoattractant protein–1 (MCP-1). Then the conduit was implanted into the abdominal aorta of rats, and an end-to-end anastomosis was made to a 4 × 10 mm^2 impenetrable Gore-Tex strip using 10-0 interrupted sutures distally and proximally of the electrospun tube. Then Gore-Tex was wrapped around the PCL in samples, creating an impenetrable outer layer. The results demonstrated that Gore-Tex shielding led to a significant reduction of cell ingrowth from neighboring tissues and MCP-1 was beneficial to endothelialization and tissue formation.

VEGFs can induce enhancement of the endothelial functions that mediate the inhibition of VSMCs proliferation, suppression of thrombosis, and anti-inflammatory effects. Thus, there are many approaches to immobilize VEGF on scaffold surface. Koobatian et al. [111] used NHS and EDC as cross-linking agents to make heparin bind to SIS surface, and the heparin-bound SIS was immersed in PBS with recombinant human VEGF-165 to make VEGF immobilize on the heparin surface by utilizing the heparin-binding domain. This acellular tissue-engineered vessel was implanted into the carotid artery of an ovine model. The result showed that the grafts possessed of high patency rates, fast endothelialization, high elastin and collagen content, as well as impressive mechanical properties and vascular contractility comparable to native arteries. Wang's group also used heparin to immobilize VEGF to obtain the same effect [112]. PCL scaffolds were prepared by electrospinning, followed by treatment with ammoniating ethylenediamine (EDA). Heparin was covalently cross-linked through EDC and NHS. Finally, heparin-loaded PCL was incubated with VEGF solution. Shin et al. [113] dissolved PLCL in chloroform and poured it onto a glass plate walled with aluminum tape and covered with aluminum foil. The polydopamine formed by oxidizing and cross-linking dopamine was coated on the PLCL film. Subsequently, the polydopamine-deposited films were immersed and shaken in solutions containing growth factors for immobilization of VEGF. And they found that VEGF-immobilized substrate could effect on adhesion of HUVECs, significantly enhance proliferation of HUVECs, and improve their migration. This modification method could act as a versatile tool to modify surface characteristics of vascular grafts potentially for accelerated endothelialization.

An ideal vascular graft should be noncytotoxic, nonthrombogenic, and infection resistant; have appropriate mechanical properties; minimize intimal hyperplasia; and support the regeneration of vascular tissue. In order to achieve these purposes, Han et al. [114] prepared a multilayered small-diameter vascular scaffold dual loaded with VEGF and platelet-derived growth factor-bb (PDGF). The multilayered grafts including inner, middle and outer layer were prepared by dual-source and dual-power electrospinning. The inner layer consisited of poly(ethylene glycol)-b-poly(Llactide-co-ε-caprolactone) (PELCL) and gelatin fibers. The PELCL fibers containing chitosan hydrogel loaded with VEGF were fabricated by suspension electrospinning. The middle layer consisted of PLGA and gelatin fibers. The PLGA fibers loading PDGF were prepared through emulsion electrospinning. The outer layer consisited of PCL and gelatin fibers. The PCL fibers were obtained via electrospinning of PCL solution in chloroform with N,N-Dimethylformamide. All gelatin fibers were fabricated by dissolving gelatin in tetrafluoroethylene and electrospinning. The results suggested that the small-diameter vascular scaffold dual-loading VEGF and PDGF could enhance vascular regeneration maintain patency in rabbit left common carotid artery for 8 weeks.

Besides growth factors, researchers also adopted other bioactive molecules to modify the scaffolds to accelerate endothelialization. Lu et al. [115] used anti-CD133 antibody to coat the ePTFE grafts. After adsorption of PEI, dipped alternately in heparin solution and collagen solution, synthetic ePTFE grafts coated with five bilayers of heparin/collagen were prepared. Then the multilayers were immersed in glutaraldehyde to promote cross-linking and to immobilize the anti-CD133 antibody. Finally, they implanted the graft into the carotid artery of pig. The results demonstrated that these synthetic ePTFE grafts coated with anti-CD133 antibody-functionalized heparin/collagen multilayer may achieve rapid endothelialization.

11.4.4 Gene Modification

Dannowski et al. [116] developed a nonviral gene carrier based on liposomes and transfected plasmids coding for the acidic fibroblast growth factor (aFGF) and enhanced green fluorescent protein (eGFP) into human corneal ECs. The transfection efficiency, toxicity of the gene carriers, and the proliferation of ECs were investigated. The liposome gene carrier showed high transfection efficiency.

Vein graft failure caused by narrowing and occlusion after coronary artery bypass grafting with saphenous veins is a major clinical problem and is an important target for gene therapy. Akowuah et al. [117] engineered vascular grafts with genetically modified BMSCs on poly(propylene carbonate) graft, which delivered the tissue inhibitor of metalloproteinase 3 (TIMP-3) plasmid to the saphenous vein graft in vitro by ultrasound exposure (USE) in the presence of echo contrast microbubbles (ECM). Then the transgened vein graft was tested by the model of Yorkshire White pigs' carotid model. At 28 days post-grafting, lumen and total vessel area were significantly greater in the TIMP-3 group compared to the untransfected or con-

trol group. Meng et al. [118] developed a receptor-targeted nanocomplex (RTN) vector system. The RTN vector was composed of cationic liposome lipofectin, a peptide (Peptide-Y: K16GACYGLPHKFCG), and plasmid DNA. Vein grafts were transgened by RTN with a plasmid-encoding inducible nitric oxide synthase (iNOS) and then engrafted into the rabbit's carotid artery to inhibit the neointimal hyperplasia. Fluorescent immunohistochemistry analysis of samples from rabbits killed at 7 days after surgery showed that mostly ECs and macrophages were transfected. Morphometric analysis of vein graft samples from the 28-day groups showed approximately a 50 % reduction of neointimal thickness and 64 % reduction of neointimal area in the iNOS-treated group compared with the surgery control group. Zhong et al. [119] developed a novel recombinant lentivirus for the delivery of hepatocyte growth factor (HGF) and Bax in a rabbit vein graft model of bypass grafting. Rabbit vein segments were dissected and transgened by the lentivirus vector harboring HGF and Bax cDNAs (Lenti-HGF-Bax) and then were interposed into the rabbit's carotid arteries. HGF and Bax expression in vein grafts was detected by immunohistochemical and western blot analysis. The result showed that vein graft thickening was remarkably reduced in Lenti-HGF-Bax-treated rabbits compared to controls.

Zhang et al. [120] created small-diameter vessels by seeding and culture of genetically modified MSCs onto a synthetic polymer scaffold produced by an electrospinning technique. Rat MSCs were modified with nitric oxide synthase (eNOS). The results showed that the seeded cells integrated with the microfibers of the scaffold to form a three-dimensional cellular network, indicating a favorable interaction between this synthetic scaffold with MSCs. High transduction efficiency was obtained with the use of concentrated retrovirus in the gene transfection of MSCs. The use of MSCs and therapeutic genes in tissue engineering of blood vessels could be helpful in improving vessel regeneration and patency.

11.5 The Mechanical Properties of Vascular Grafts

11.5.1 Synthetic Polymers

Human mammary arteries and saphenous veins have burst pressures between 2031 and 4225 mmHg [121] and 1250 ± 500 mmHg [85], respectively. Mechanical characteristics of vascular grafts, such as compliance and Young's modulus, have significant potential to influence their long-term patency [122].

Surgeons have used nondegradable synthetic PTFE or Dacron medium-to-large-diameter grafts which provide 10 years of symptom-free lifestyle. However, they have extremely poor performance in replacement of small-diameter (<6 mm) blood vessels due to neointimal hyperplasia and thrombosis [123]. The commercial grafts such as woven and knitted Dacron and ePTFE usually show a low radial compliance [8]. A high-porosity ePTFE graft demonstrated no significant deterioration in suture

retention strength, radial tensile strength, or longitudinal tensile strength for periods ranging from 2 to 80 weeks compared to preimplantation grafts [124].

PCL has excellent mechanical characteristics, and it does not undergo plastic deformation and failure when exposed to long cyclic strain. Therefore, it can be a critical component in vascular graft application [125]. Sang et al. [126] indicated that the PCL/collagen composite graftss, with fiber diameters of approximately 520 nm, possessed appropriate tensile strength (4.0 ± 0.4 MPa) and adequate elasticity (2.7 ± 1.2 MPa). The burst pressure of the composite grafts was 4912 ± 155 mmHg, which was much greater than that of the pure PCL grafts (914 ± 130 mmHg) and native vessels. Ángel et al. [127] synthesized biocompatible and biodegradable PCL urethane macromers to fabricate hollow fiber membranes of different sizes as small-diameter vascular graft candidates. Their tensile stiffness ranged from 0.09 to 0.11 N/mm and their maximum tensile force from 0.86 to 1.03 N, with minimum failure strains of approximately 130 % and burst pressures from 1158 to 1468 mmHg.

The polyethylene terephthalate (PET)/PGA graft was woven to be partially degradable with a double-layered fiber (core; PET and sheath; PGA). The PGA component had degraded and been replaced by host tissue that contained a mixture of α-SMA positive cells and other host cells. The graft was a unified structure with the aorta. The adhesion strength between the graft and aortic wall was significantly enhanced in the PET/PGA group. The vascular graft demonstrated histologic and mechanical integration with the native aorta [128].

Porous elastomeric grafts made of PGS enforced with PCL nanofibers degraded rapidly and yielded neoarteries nearly free of foreign materials in rat abdominal aorta. 3 to 12 months after implantation in rat abdominal aortas, the PGS grafts with rationally strengthened sheath were remodeled into neoarteries that resembled native arteries in the following aspects: high patency rate and even vessel wall thickness; a confluent endothelium and contractile smooth muscle layers; expression of elastin, collagen, and GAG; and tough and compliant mechanical properties. This study confirmed that adequate density of PCL sheath in PGS grafts could initiate stable and high-quality muscular remodeling, which contributed to long-term success in arterial circulation before clinical translation [82]. Similarly, Ramak et al. [39] developed a novel method for electrospinning smaller grafts composed of a PGS microfibrous core enveloped by a thin PCL outer sheath. Electrospun PGS-PCL composites were implanted as infrarenal aortic interposition grafts in mice and remained patent up to the 12-month endpoint without thrombosis or stenosis. Lack of rupture over 12 months confirmed sufficient long-term strength, due primarily to the persistent PCL sheath.

PU can potentially provide a greater degree of graft-artery compliance match than ePTFE prostheses [129]. Finer tensile strength and elastic property facilitates the usage of PU as a vascular scaffold, but it is shown to have less compliance and a biologically unstable nature. The compliance values of poly(carbonate)polyurethane (CPU) and artery (mean over the pressure range) were 8.1(0.4) and 8.0(5.9)

percent per mmHg × 10^{-2}, respectively, although the elastic behavior of artery was anisotropic unlike CPU, which was isotropic [130]. Uttayarat et al. [131] combined electrospinning with the spin casting method to pattern microfibers and microgrooves on the electrospun PU tubular scaffold. The elastic modulus of the grafts in the axial direction was also in a range similar to those of native vascular grafts.

Poliglecaprone (PGC) in the form of monocryl monofilament sutures displayed excellent tensile properties and 20–30 % reduction in strength after 2 weeks in vivo [132]. In another study, blends of PGC and PCL of varying compositions were electrospun into tubular conduits and their mechanical, morphological, thermal, and in vitro degradation properties were evaluated under simulated physiological conditions. Generally, mechanical strength, modulus, and hydrophilic nature were enhanced by the addition of PGC to PCL. A 3:1 PCL/PGC blend was concluded to be a judicious blend composition for tubular grafts based on overall results on the mechanical properties and performance after a 1-month in vitro degradation study [133].

Electrospun PLLA scaffolds with NaCl-made pores had a lower elastic modulus (8.05 MPa) and yield stress (349 kPa) and a higher yield strain (0.04) compared to their traditional counterparts (40.36 MPa, 676 kPa, and 0.0188) [134]. Grafts were prepared using the PLA and PCL physical blends in the ratios of 75:25 and 25:75 with the dimension of (40 × 0.2 × 4) millimeter by electrospinning. Hydrophobicity and tensile stress were significantly higher in PLA-PCL (75:25), whereas tensile strain and fiber density were significantly higher in PLA-PCL (25:75). Cell viability and proliferation were rationally influenced by the aligned nanofibers. Gene expression revealed the grafts' thromboresistivity, elasticity, and aided neovascularization. Thus, these scaffolds could be an ideal candidate for small-diameter blood vessel engineering [32].

11.5.2 Natural Polymers

Collagen-based scaffolds have been the platform for a number of exploratory clinical trials that shows the true potential of tissue engineering for repairing significant tissue damage. Hirai et al. [135] specifically worked on the original development of a collagen-based construct for a low-pressure-loaded venous system. By pouring a solution of bovine aortic VSMCs and type-I collagen into a tubular glass mold and using a Dacron mesh support, a vascular construct that could tolerate luminal pressures as great as 100 mmHg was obtained in 24 weeks of culture [136]. Vivek et al. [137] proposed a design strategy for the fabrication of tubular conduits comprising collagen fiber networks and elastin-like protein polymers to mimic native tissue structure and function. Comparing favorably to an ultimate tensile strength (UTS) and a Young's modulus for native blood vessels of 1.4–11.1 MPa and 1.5 ± 0.3 MPa, dense fibrillar collagen networks exhibited an UTS of 0.71 ± 0.06 MPa, strain to failure of 37.1 ± 2.2 %, and Young's modulus of 2.09 ± 0.42 MPa, respectively.

Elastin is found to be very brittle and shows mechanical properties lower than those of native elastin. As such, the material was suggested as a provisional matrix for in vivo remodeling. Buijtenhuijs et al. [138] used a freeze-drying method with insoluble type-I collagen and insoluble elastin to produce a porous scaffold with fibers of collagen and elastin interspersed together. Elastin exhibited less stress relaxation than intact or decellularized aorta. The rate of stress relaxation of intact and decellularized aorta was linearly dependent on the initial stress levels. The rate of stress relaxation for elastin increased linearly at stress levels below about 60 kPa [139]. McKenna et al. [140] fabricated a tubular construct using electrospun recombinant human tropoelastin (rTE). The electrospun scaffolds were formed by using 1,1,1,3,3,3-hexafluro-2-propanol (HFP) as the solvent and disuccinimidyl suberate (DSS) as the cross-linking agent to stabilize the fibers in aqueous solution. The fabricated scaffold had an elastic modulus in the range of 0.15–0.91 MPa and an ultimate tensile strength of 0.36 MPa. The results of in vitro studies demonstrated that the fabricated electrospun rTE scaffolds supported ECs growth with typical ECs cobblestone morphology following 48 h in culture, which confirmed the suitability of this biomaterial for application in vascular grafts. Vaibhav et al. [141] used biaxial force-controlled experiments to quantify regional variations in the anisotropy and nonlinearity of elastin isolated from bovine aortic tissues proximal and distal to the heart. Results from this study showed that tissue nonlinearity significantly increased distal to the heart as compared to proximally located regions. Their studies suggested that it was important to consider elastin fiber orientations in investigations that used microstructure-based models to describe the contributions of elastin and collagen to arterial mechanics.

Esterified hyaluronic acid (HYAFF) is routinely used for clinical tissue engineering applications. The problems that are generally associated with hyaluronic acid (HA)-based biopolymers are their poor mechanical properties and their rapid degradation rate. In order to increase their mechanical properties, Arrigoni et al. [142] added sodium ascorbate (SA) to a culture of VSMCs seeded in HYAFF nonwoven sheets, and SA improved mechanical properties of the vascular construct lowering material stiffness and increasing tensile strength. Amaliris et al. [143] demonstrated the ability of PU containing HA in its backbone structure to reduce protein adsorption, platelet and bacterial adhesion, and fibroblast and macrophage proliferation while allowing the retention of both ECs and vascular-appropriate mechanics. The molecular weight of the HA oligosaccharides influenced the mechanical properties of the PU-HA copolymers. In another study, PU materials modified with HA were more effective than either PEG- or heparin-grafted materials with respect to limiting protein adsorption and platelet adhesion. These modifications in PU chemistry were performed while retaining material mechanics in the range of native vascular tissue. Thus, this study described the generation of materials that possessed the unique ability to display excellent hemocompatibility while simultaneously supporting extensive endothelialization and retaining vascular-appropriate mechanics [144].

It is increasingly recognized that biomimetic, natural polymers mimicking the ECM have low thrombogenicity and functional motifs that regulate cell-matrix interactions, with these factors being critical for TEVGs, especially small diameter grafts. Elsayed et al. [145] devised the fabrication of novel, electrospun, multilayer, gelatin fiber scaffolds, with controlled fiber layer orientation and optimized gelatin cross-linking to achieve not only compliance equivalent to that of coronary artery but also for the first time strength of the wet tubular acellular scaffold (swollen with absorbed water) same as that of the tunica media of coronary artery in both circumferential and axial directions. Most importantly, the suture retention strength of gelatin scaffolds firstly achieved in the range of 1.8–1.94 N for wet acellular scaffolds, and was same or better than that for fresh saphenous vein.

11.5.3 Hybrid Materials: Synthetic and Natural Polymers

A synthetic polymer will provide mechanical integrity, and natural proteins provide biocompatibility and ECM-mimicking environment for better cell attachment and proliferation. Ju et al. [146] used a co-electrospinning technique to fabricate PCL/collagen bilayer scaffolds with an outer layer containing large pores that enhanced VSMCs infiltration and an inner layer with smaller pore sizes that facilitated ECs attachment. Thus, the microstructure and mechanical properties of the resultant scaffolds could be controlled by the fiber diameter. Increasing the fiber diameter from 0.27 to 4.45 μm enhanced the scaffold's porosity and reduced its Young's modulus from 2.03 to 0.26 MPa. Stitzel et al. [147] discovered that controlling the ratio of collagen, elastin, and PLGA could improve electrospinning characteristics and physical strength of the scaffolds, which resisted bursting at nearly 12 times normal systolic pressure.

As for chitosan, its poor mechanical properties represent a major limit to its development. PCL can increase the mechanical properties. A mixture of 1:1 chitosan and PCL demonstrated an ultimate strength twice than that of chitosan alone [148]. In another study, Chen et al. [149] fabricated electrospun collagen/chitosan/TPU nanofibrous scaffolds with functional and structural properties resembling the native ECM. The tensile strength of scaffolds with random and aligned fibers was 4.6 MPa and 10.3 MPa, respectively. In addition, the mechanical properties of resultant scaffolds were significantly improved by cross-linking the fibers. The tensile strength of glutaraldehyde cross-linked scaffold with random fibers was twofold higher than uncross-linked samples. The fabricated scaffolds could support the growth and alignment of ECs and were used to form a vascular graft in vitro.

11.6 The Degradation of Vascular Grafts

The degradation rate of these polymers is determined by initial molecular weight, exposed surface area, crystallinity, and ratio of monomers. ePTFE is very stable in vivo with no reported failures due to degradation of the graft. PGA is a biodegradable macromolecular material that degrades through hydrolysis of its ester bonds in vivo, loses 100 % of its strength within 4 weeks and is completely absorbed within 6 months [150].

Both PCL and PLLA are slowly degrading polymers. PLA is less crystalline than PGA but more hydrophobic, making it less susceptible to hydrolysis. Surgical sutures made of PLA require more than a year to lose their tensile strength. Walpoth's group [4] reported that electrospun PCL grafts were degraded to 20 % of original molecular weight at 18 months of postimplantation. But the grafts neither dilated nor had a significant increase in compliance. Tara et al. [151] have shown that the PLCL coating completely degrades 4 months after implantation in a mouse model.

Random copolymerization of PLA (both L- and D,L-lactide forms) and PGA, known as PLGA, is the most investigated degradable polymer for biomedical applications and has been used in sutures, drug delivery devices, and tissue engineering scaffolds. With a number of commercial manufacturers and easy polymer processability, researchers do not have to be polymer synthesis experts to utilize PLGA in their work. Because PLA and PGA have significantly different properties, careful choice of copolymer composition allows for the optimization of PLGA for intended applications. Property modulation is even more significant for PLGA copolymers because with 25–75 % lactide composition, PLGA forms amorphous polymers, which are very hydrolytically unstable compared with the more stable homopolymers. This is evident in the degradation times of 50:50 PLGA, 75:25 PLGA, and 85:15 PLGA being 1–2 months, 4–5 months, and 5–6 months, respectively [152].

Ye et al. [153] described that PGS elastomer was used to construct the microvessel framework. In vivo studies of scaffolds implanted subcutaneously and intraperitoneally, without or with exogenous cells, into nude rats demonstrated biodegradation of the membrane interface and host blood cell infiltration of the microvessels. This modular, implantable scaffold could serve as a basis for building tissue constructs of increasing scale and clinical relevance.

References

1. Song L, Sengupta D, Shu C. Vascular tissue engineering: from in vitro to in situ. Wiley Interdiscip Rev Syst Biol Med. 2014;6:61–76.
2. You KH, Ingram J, Korossis SA, Ingham E, Homer-Vanniasinkam S. Tissue engineering of vascular conduits. Br J Surg. 2006;93:652–61.
3. Baguneid MS, Seifalian AM, Salacinski HJ, Murray D, Hamilton G, Walker MG. Tissue engineering of blood vessels. J Cell Mol Med. 2006;11:945–57.

4. Valence SD, Tille JC, Mugnai D, Mrowczynski W, Gurny R, Möller M, et al. Long term performance of polycaprolactone vascular grafts in a rat abdominal aorta replacement model. Biomaterials. 2012;33:38–47.
5. Wang Z, Cui Y, Wang J, Yang X, Wu Y, Wang K, et al. The effect of thick fibers and large pores of electrospun poly(ε-caprolactone) vascular grafts on macrophage polarization and arterial regeneration. Biomaterials. 2014;35:5700–10.
6. Hinsbergh VWMV. The endothelium: vascular control of haemostasis. Eur J Obstet Gynecol Reprod Biol. 2001;95:198–201.
7. Yao Y, Wang J, Cui Y, Xu R, Wang Z, Zhang J, et al. Effect of sustained heparin release from PCL/chitosan hybrid small-diameter vascular grafts on anti-thrombogenic property and endothelialization. Acta Biomater. 2014;10:2739–49.
8. Sarkar S, Salacinski HJ, Hamilton G, Seifalian AM. The mechanical properties of infrainguinal vascular bypass grafts: their role in influencing patency. Eur J Vasc Endovasc Surg. 2006;31:627–36.
9. Tiwari A, Cheng KS, Salacinski H, Hamilton G, Seifalian AM. Improving the patency of vascular bypass grafts: the role of suture materials and surgical techniques on reducing anastomotic compliance mismatch * ☆☆. Eur J Vasc Endovasc Surg Off J Eur Soc Vasc Surg. 2003;25:287–95.
10. Salacinski HJ, Goldner S, Giudiceandrea A, Hamilton G, Seifalian AM, Edwards A, et al. The mechanical behavior of vascular grafts: a review. J Biomater Appl. 2001;15:241–78.
11. Tang Z, Wang A, Yuan F, Yan Z, Liu B, Chu JS, et al. Differentiation of multipotent vascular stem cells contributes to vascular diseases. Nat Commun. 2012;3:177–80.
12. Oltrona L, Eisenberg PR, Abendschein DR, Rubin BG. Efficacy of local inhibition of procoagulant activity associated with small-diameter prosthetic vascular grafts. J Vasc Surg. 1996;24:624–31.
13. Lin PH, Chen C, Bush RL, Yao Q, Lumsden AB, Hanson SR. Small-caliber heparin-coated ePTFE grafts reduce platelet deposition and neointimal hyperplasia in a baboon model ☆. J Vasc Surg. 2004;39:1322–8.
14. Letourneur D, Caleb BL, Castellot JJ. Heparin binding, internalization, and metabolism in vascular smooth muscle cells: I. Upregulation of heparin binding correlates with antiproliferative activity. J Cell Physiol. 1995;165:676–86.
15. Wang Z, Lu Y, Qin K, Wu Y, Tian Y, Wang J, et al. Enzyme-functionalized vascular grafts catalyze in-situ release of nitric oxide from exogenous NO prodrug. J Control Release. 2015;210:179–88.
16. Mendes AC, Zelikin AN. Enzyme prodrug therapy engineered into biomaterials. Adv Funct Mater. 2014;24:5202–10.
17. Levy RJ, Schoen FJ, Anderson HC, Harasaki H, Koch TH, Brown W, et al. Cardiovascular implant calcification: a survey and update ☆. Biomaterials. 1991;12:707–14.
18. Hutcheson JD, Goettsch C, Rogers MA, Aikawa E. Revisiting cardiovascular calcification: a multifaceted disease requiring a multidisciplinary approach. Semin Cell Dev Biol. 2015;46:68–77.
19. Byrom MJ, Bannon PG, White GH, Ng MKC. Animal models for the assessment of novel vascular conduits. J Vasc Surg. 2010;52:176–95.
20. Swartz DD, Andreadis ST. Animal models for vascular tissue-engineering. Curr Opin Biotechnol. 2013;24:916–25.
21. Chlupác J, Filová E, Bacáková L. Blood vessel replacement: 50 years of development and tissue engineering paradigms in vascular surgery. Physiol Res. 2009;58 Suppl 2:119–39.
22. Deutsch M, Meinhart J, Zilla P, Howanietz N, Gorlitzer M, Froeschl A, et al. Long-term experience in autologous in vitro endothelialization of infrainguinal ePTFE grafts. J Vasc Surg. 2009;49:352–62.
23. Budd JS, Allen KE, Hartley G, Bell PRF. The effect of preformed confluent endothelial cell monolayers on the patency and thrombogenicity of small calibre vascular grafts *. Eur J Vasc Surg. 1991;5:397–405.

24. Pektok E, Nottelet B, Tille JC, Gurny R, Kalangos A, Moeller M, et al. Degradation and healing characteristics of small-diameter poly(epsilon-caprolactone) vascular grafts in the rat systemic arterial circulation. Circulation. 2008;118:2563–70.
25. Sang-Heon K, Jae Hyun K, Sub CM, Eunna C, Youngmee J, Soo Hyun K, et al. Fabrication of a new tubular fibrous PLCL scaffold for vascular tissue engineering. J Biomater Sci Polym Ed. 2006;17:1359–74.
26. Shafiq M, Jung Y, Kim SH. In situ vascular regeneration using substance P-immobilised poly(L-lactide-co-ε-caprolactone) scaffolds: stem cell recruitment, angiogenesis, and tissue regeneration. Eur Cell Mater. 2015;30:282–302.
27. Mun CH, Jung Y, Kim SH, Lee SH, Kim HC, Kwon IK, et al. Three-dimensional electrospun poly(lactide-co-ε-caprolactone) for small-diameter vascular grafts. Tissue Eng Part A. 2012;18:1608–16.
28. Cho SW, Jeon O, Lim JE, Gwak SJ, Kim SS, Choi CY, et al. Preliminary experience with tissue engineering of a venous vascular patch by using bone marrow–derived cells and a hybrid biodegradable polymer scaffold. J Vasc Surg. 2006;44:1329–40.
29. Kobayashi H, Terada D, Yokoyama Y, Moon DW, Yasuda Y, Koyama H, et al. Vascular-inducing poly(glycolic acid)-collagen nanocomposite-fiber scaffold. J Biomed Nanotechnol. 2013;9:1318–26.
30. Rapoport HS, Fish J, Basu J, Campbell J, Genheimer C, Payne R, et al. Construction of a tubular scaffold that mimics J-shaped stress/strain mechanics using an innovative electrospinning technique. Tissue Eng Part C Methods. 2012;18:567–74.
31. Zhu C, Ma X, Xian L, Zhou Y, Fan D. Characterization of a co-electrospun scaffold of HLC/CS/PLA for vascular tissue engineering. Biomed Mater Eng. 2014;24:1999–2005.
32. Sankaran KK, Krishnan UM, Sethuraman S. Axially aligned 3D nanofibrous grafts of PLA-PCL for small diameter cardiovascular applications. J Biomater Sci Polym Ed. 2014;25:1791–812.
33. Izhar U, Schwalb H, Borman JB, Hellener G, Hotoveli-Salomon A, Marom G, Stern T, et al. Novel synthetic selectively degradable vascular prostheses: a preliminary implantation study. J Surg Res. 2001;95:152–60.
34. Hashi CK, Derugin N, Janairo RRR, Lee R, Schultz D, Lotz J, et al. Antithrombogenic modification of small-diameter microfibrous vascular grafts. Arterioscler Thromb Vasc Biol. 2010;30:1621–7.
35. Motlagh D, Yang J, Lui KY, Webb AR, Ameer GA. Hemocompatibility evaluation of poly(glycerol-sebacate) in vitro for vascular tissue engineering. Biomaterials. 2006;27:4315–24.
36. Mcclure MJ, Sell SA, Bowlin GL, Bowlin GL. Electrospun polydioxanone, elastin, and collagen vascular scaffolds: uniaxial cyclic distension. J Eng Fibers Fabr. 2009;4:18–25.
37. Lee K-W, Stolz DB, Wang Y. Substantial expression of mature elastin in arterial constructs. Proc Natl Acad Sci. 2011;108:2705–10.
38. Wu W, Allen RA, Wang Y. Fast-degrading elastomer enables rapid remodeling of a cell-free synthetic graft into a neoartery. Nat Med. 2012;18:1148–53.
39. Khosravi R, Best CA, Allen RA, Stowell CET, Onwuka E, Zhuang JJ, et al. Long-term functional efficacy of a novel electrospun poly(glycerol sebacate)-based arterial graft in mice. Ann Biomed Eng. 2016;44:2402–16. 1–15.
40. Grasl C, Bergmeister H, Stoiber M, Schima H, Weigel G. Electrospun polyurethane vascular grafts: in vitro mechanical behavior and endothelial adhesion molecule expression. J Biomed Mater Res A. 2010;93:716–23.
41. Bergmeister H, Grasl C, Walter I, Plasenzotti R, Stoiber M, Schreiber C, et al. Electrospun small-diameter polyurethane vascular grafts: ingrowth and differentiation of vascular-specific host cells. Artif Organs. 2012;36:54–61.
42. He W, Hu Z, Xu A, Liu R, Yin H, Wang J, et al. The preparation and performance of a new polyurethane vascular prosthesis. Cell Biochem Biophys. 2013;66:855–66.

43. Punnakitikashem P, Truong D, Menon JU, Nguyen KT, Yi H. Electrospun biodegradable elastic polyurethane scaffolds with dipyridamole release for small diameter vascular grafts. Acta Biomater. 2014;10:4618–28.
44. Bergmeister H, Seyidova N, Schreiber C, Strobl M, Grasl C, Walter I, et al. Biodegradable, thermoplastic polyurethane grafts for small diameter vascular replacements. Acta Biomater. 2015;11:104–13.
45. Enayati M, Eilenberg M, Grasl C, Riedl P, Kaun C, Messner B, et al. Biocompatibility assessment of a new biodegradable vascular graft via in vitro co-culture approaches and in vivo model. Ann Biomed Eng. 2016. doi:10.1007/s10439-016-1601-y.
46. Zinn M, Witholt B, Egli T. Occurrence, synthesis and medical application of bacterial polyhydroxyalkanoate. Adv Drug Deliv Rev. 2001;53:5–21.
47. Shum-Tim D, Stock U, Hrkach J, Shinoka T, Lien J, Moses MA, et al. Tissue engineering of autologous aorta using a new biodegradable polymer. Ann Thorac Surg. 1999;68:2298–304.
48. Weinberg CB, Bell E. A blood vessel model constructed from collagen and cultured vascular cells. Science. 1986;231:397–400.
49. Achilli M, Lagueux J, Mantovani D. On the effects of UV-C and pH on the mechanical behavior, molecular conformation and cell viability of collagen-based scaffold for vascular tissue engineering. Macromol Biosci. 2010;10:307–16.
50. Schutte SC, Chen Z, Brockbank KG, Nerem RM. Cyclic strain improves strength and function of a collagen-based tissue-engineered vascular media. Tissue Eng Part A. 2010;16:3149–57.
51. Wu HC, Wang TW, Kang PL, Tsuang YH, Sun JS, Lin FH. Coculture of endothelial and smooth muscle cells on a collagen membrane in the development of a small-diameter vascular graft. Biomaterials. 2007;28:1385–92.
52. Leach JB, Wolinsky JB, Stone PJ, Wong JY. Crosslinked α-elastin biomaterials: towards a processable elastin mimetic scaffold. Acta Biomater. 2005;1:155–64.
53. Koens MJW, Faraj KA, Wismans RG, Vliet JAVD, Krasznai AG, Cuijpers VMJI, et al. Controlled fabrication of triple layered and molecularly defined collagen/elastin vascular grafts resembling the native blood vessel. Acta Biomater. 2010;6:4666–74.
54. Ryan AJ, O'Brien FJ. Insoluble elastin reduces collagen scaffold stiffness, improves viscoelastic properties, and induces a contractile phenotype in smooth muscle cells. Biomaterials. 2015;73:296–307.
55. Smith MJ, Mcclure MJ, Sell SA, Barnes CP, Walpoth BH, Simpson DG, et al. Suture-reinforced electrospun polydioxanone–elastin small-diameter tubes for use in vascular tissue engineering: a feasibility study. Acta Biomater. 2008;4:58–66.
56. Ye Q, Zund G, Benedikt P, Sockenhoevel J, Hoerstrup SP, Sakyama S, et al. Fibrin gel as a three dimensional matrix in cardiovascular tissue engineering. Eur J Cardiothorac Surg. 2000;17:587–91.
57. Syedain ZH, Meier LA, Bjork JW, Ann L, Tranquillo RT. Implantable arterial grafts from human fibroblasts and fibrin using a multi-graft pulsed flow-stretch bioreactor with noninvasive strength monitoring. Biomaterials. 2010;32:714–22.
58. Bjork JW, Meier LA, Johnson SL, Syedain ZH, Tranquillo RT. Hypoxic culture and insulin yield improvements to fibrin-based engineered tissue. Tissue Eng Part A. 2012;18:785–95.
59. Swartz DD, Russell JA, Andreadis ST. Engineering of fibrin-based functional and implantable small-diameter blood vessels. Am J Physiol Heart Circ Physiol. 2005;288:867.
60. Chupa JM, Foster AM, Sumner SR, Madihally SV, Matthew HWT. Vascular cell responses to polysaccharide materials: in vitro and in vivo evaluations. Biomaterials. 2000;21:2315–22.
61. Ling Z, Qiang A, Wang A, Lu G, Kong L, Gong Y, et al. A sandwich tubular scaffold derived from chitosan for blood vessel tissue engineering. J Biomed Mater Res A. 2006;77A:277–84.
62. Zhu C, Fan D, Duan Z, Xue W, Shang L, Chen F, et al. Initial investigation of novel human-like collagen/chitosan scaffold for vascular tissue engineering. J Biomed Mater Res A. 2009;89:829–40.

63. Du F, Wang H, Zhao W, Li D, Kong D, Yang J, et al. Gradient nanofibrous chitosan/poly ε-caprolactone scaffolds as extracellular microenvironments for vascular tissue engineering. Biomaterials. 2011;33:762–70.
64. Milella E, Brescia E, Massaro C, Ramires PA, Miglietta MR, Fiori V, et al. Physico-chemical properties and degradability of non-woven hyaluronan benzylic esters as tissue engineering scaffolds. Biomaterials. 2002;23:1053–63.
65. Zhu C, Fan D, Wang Y. Human-like collagen/hyaluronic acid 3D scaffolds for vascular tissue engineering. Mater Sci Eng C Mater Biol Appl. 2014;34C:393–401.
66. Joo H, Byun E, Lee M, Hong Y, Lee H, Kim P. Biofunctionalization via flow shear stress resistant adhesive polysaccharide, hyaluronic acid-catechol, for enhanced in vitro endothelialization. J Ind Eng Che. 2016;34:14.
67. Li DY, Brooke B, Davis EC, Mecham RP, Sorensen LK, Boak BB, et al. Elastin is an essential determinant of arterial morphogenesis. Nature. 1998;393:276–80.
68. Chamley-Campbell J, Campbell GR, Ross R. The smooth muscle in culture. Physiol Rev. 1979;59:1–61.
69. Rothuizen TC, Damanik FF, Lavrijsen T, Visser MJ, Hamming JF, Lalai RA, et al. Development and evaluation of in vivo tissue engineered blood vessels in a porcine model. Biomaterials. 2016;75:82–90.
70. Mahara A, Somekawa S, Kobayashi N, Hirano Y, Kimura Y, Fujisato T, et al. Tissue-engineered acellular small diameter long-bypass grafts with neointima-inducing activity. Biomaterials. 2015;58:54–62.
71. Row S, Peng H, Schlaich EM, Koenigsknecht C, Andreadis ST, Swartz DD. Arterial grafts exhibiting unprecedented cellular infiltration and remodeling invivo: the role of cells in the vascular wall. Biomaterials. 2015;50:115–26.
72. Jeremy J, Gadsdon P, Vijayan V, Wyatt M, Newby A, Angelini G. On the biology of saphenous vein grafts fitted with external synthetic sheaths and stents ☆. Biomaterials. 2007;28:895–908.
73. Gong W, Lei D, Li S, Huang P, Qi Q, Sun Y, et al. Hybrid small-diameter vascular grafts: anti-expansion effect of electrospun poly ε-caprolactone on heparin-coated decellularized matrices. Biomaterials. 2016;76:359–70.
74. Longchamp A, Alonso F, Dubuis C, Allagnat F, Berard X, Meda P, et al. The use of external mesh reinforcement to reduce intimal hyperplasia and preserve the structure of human saphenous veins. Biomaterials. 2014;35:2588–99.
75. Hasan A, Memic A, Annabi N, Hossain M, Paul A, Dokmeci MR, et al. Electrospun scaffolds for tissue engineering of vascular grafts. Acta Biomater. 2014;10:11–25.
76. Valence SD, Tille JC, Giliberto JP, Mrowczynski W, Gurny R, Walpoth BH, et al. Advantages of bilayered vascular grafts for surgical applicability and tissue regeneration. Acta Biomater. 2012;8:3914–20.
77. Zhu M, Wang Z, Zhang J, Wang L, Yang X, Chen J, et al. Circumferentially aligned fibers guided functional neoartery regeneration invivo. Biomaterials. 2015;61:85–94.
78. Hibino N, Imai Y, Shinoka T, Aoki M, Watanabe M, Kosaka Y, et al. First successful clinical application of tissue engineered blood vessel. Kyobu Geka Jpn J Thorac Surg. 2002;55:368–73.
79. Shin'Oka T, Matsumura G, Hibino N, Naito Y, Watanabe M, Konuma T, et al. Midterm clinical result of tissue-engineered vascular autografts seeded with autologous bone marrow cells. J Thorac Cardiovasc Surg. 2005;129:1330–8.
80. Hibino N, McGillicuddy E, Matsumura G, Ichichara Y, Naito Y, Breuer C, et al. Late-term results of tissue-engineered vascular grafts in humans. J Thorac Cardiovasc Surg. 2010;139:431–6.
81. Allen RA, Wu W, Yao M, Dutta D, Duan X, Bachman TN, et al. Nerve regeneration and elastin formation within poly(glycerol sebacate)-based synthetic arterial grafts one-year post-implantation in a rat model. Biomaterials. 2014;35:165–73.

82. Yang X, Wei J, Lei D, Liu Y, Wu W. Appropriate density of PCL nano-fiber sheath promoted muscular remodeling of PGS/PCL grafts in arterial circulation. Biomaterials. 2016;88:34–47.
83. Hu J, Sun X, Ma H, Xie C, Chen YE, Ma PX. Porous nanofibrous PLLA scaffolds for vascular tissue engineering. Biomaterials. 2010;31:7971–7.
84. Ma H, Hu J, Ma PX. Polymer scaffolds for small-diameter vascular tissue engineering. Adv Funct Mater. 2010;20:2833–41.
85. Soletti L, Yi H, Guan J, Stankus JJ, El-Kurdi MS, Wagner WR, et al. A bilayered elastomeric scaffold for tissue engineering of small diameter vascular grafts. Acta Biomater. 2010;6:110–22.
86. Wei H, Alejandro N, Lorenzo S, Yi H, Burhan G, Mihaela C, et al. Pericyte-based human tissue engineered vascular grafts. Biomaterials. 2010;31:8235–44.
87. Sugiura T, Tara S, Nakayama H, Kurobe H, Yi T, Lee YU, et al. Novel bioresorbable vascular graft with sponge-type scaffold as a small-diameter arterial graft. Ann Thorac Surg. 2016;102:720–7.
88. Smith DJ, Chakravarthy D, Pulfer S, Simmons ML, Hrabie JA, Citro ML, et al. Nitric oxide-releasing polymers containing the [N (O) NO]-group. J Med Chem. 1996;39:1148–56.
89. Fleser PS, Nuthakki VK, Malinzak LE, Callahan RE, Seymour ML, Reynolds MM, et al. Nitric oxide–releasing biopolymers inhibit thrombus formation in a sheep model of arteriovenous bridge grafts. J Vasc Surg. 2004;40:803–11.
90. Kushwaha M, Anderson JM, Bosworth CA, Andukuri A, Minor WP, Lancaster JR, et al. A nitric oxide releasing, self assembled peptide amphiphile matrix that mimics native endothelium for coating implantable cardiovascular devices. Biomaterials. 2010;31:1502–8.
91. Andukuri A, Kushwaha M, Tambralli A, Anderson JM, Dean DR, Berry JL, et al. A hybrid biomimetic nanomatrix composed of electrospun polycaprolactone and bioactive peptide amphiphiles for cardiovascular implants. Acta Biomater. 2011;7:225–33.
92. Duan X, Lewis RS. Improved haemocompatibility of cysteine-modified polymers via endogenous nitric oxide. Biomaterials. 2002;23:1197–203.
93. Gappa-Fahlenkamp H, Lewis RS. Improved hemocompatibility of poly (ethylene terephthalate) modified with various thiol-containing groups. Biomaterials. 2005;26:3479–85.
94. Chen S, An J, Weng L, Li Y, Xu H, Wang Y, et al. Construction and biofunctional evaluation of electrospun vascular graft loaded with selenocystamine for in situ catalytic generation of nitric oxide. Mater Sci Eng C. 2014;45:491–6.
95. An J, Chen S, Gao J, Zhang X, Wang Y, Li Y, et al. Construction and evaluation of nitric oxide generating vascular graft material loaded with organoselenium catalyst via layer-by-layer self-assembly. Sci China Life Sci. 2015;58:765–72.
96. Weng Y, Song Q, Zhou Y, Zhang L, Wang J, Chen J, et al. Immobilization of selenocystamine on TiO 2 surfaces for in situ catalytic generation of nitric oxide and potential application in intravascular stents. Biomaterials. 2011;32:1253–63.
97. Zhou Y, Weng Y, Zhang L, Jing F, Huang N, Chen J. Cystamine immobilization on TiO_2 film surfaces and the influence on inhibition of collagen-induced platelet activation. Appl Surf Sci. 2011;258:1776–83.
98. Yang Z, Yang Y, Xiong K, Li X, Qi P, Tu Q, et al. Nitric oxide producing coating mimicking endothelium function for multifunctional vascular stents. Biomaterials. 2015;63:80–92.
99. Muylaert DE, van Almen GC, Talacua H, Fledderus JO, Kluin J, Hendrikse SI, et al. Early in-situ cellularization of a supramolecular vascular graft is modified by synthetic stromal cell-derived factor-1α derived peptides. Biomaterials. 2016;76:187–95.
100. Wang Z, Wang H, Zheng W, Zhang J, Zhao Q, Wang S, et al. Highly stable surface modifications of poly (3-caprolactone)(PCL) films by molecular self-assembly to promote cells adhesion and proliferation. Chem Commun. 2011;47:8901–3.
101. Zheng W, Wang Z, Song L, Zhao Q, Zhang J, Li D, et al. Endothelialization and patency of RGD-functionalized vascular grafts in a rabbit carotid artery model. Biomaterials. 2012;33:2880–91.

102. Wang Y, Chen S, Pan Y, Gao J, Tang D, Kong D, et al. Rapid in situ endothelialization of a small diameter vascular graft with catalytic nitric oxide generation and promoted endothelial cell adhesion. J Mater Chem B. 2015;3:9212–22.
103. Larsen CC, Kligman F, Tang C, Kottke-Marchant K, Marchant RE. A biomimetic peptide fluorosurfactant polymer for endothelialization of ePTFE with limited platelet adhesion. Biomaterials. 2007;28:3537–48.
104. Zhou F, Jia X, Yang Q, Yang Y, Zhao Y, Fan Y, et al. Targeted delivery of microRNA-126 to vascular endothelial cells via REDV peptide modified PEG-trimethyl chitosan. Biomater Sci. 2016;4:849–56.
105. Ji Q, Zhang S, Zhang J, Wang Z, Wang J, Cui Y, et al. Dual functionalization of poly (ε-caprolactone) film surface through supramolecular assembly with the aim of promoting in situ endothelial progenitor cell attachment on vascular grafts. Biomacromolecules. 2013;14:4099–107.
106. Niu B, Huang Y, Zhang S, Wang D, Xu H, Kong D, et al. Expression and characterization of hydrophobin HGFI fused with the cell-specific peptide TPS in Pichia pastoris. Protein Expr Purif. 2012;83:92–7.
107. Huang Y, Zhang S, Niu B, Wang D, Wang Z, Feng S, et al. Poly(ε-caprolactone) modified with fusion protein containing self-assembled hydrophobin and functional peptide for selective capture of human blood outgrowth endothelial cells. Colloids Surf B Biointerfaces. 2013;101:361–9.
108. Brewster LP, Washington C, Brey EM, Gassman A, Subramanian A, Calceterra J, et al. Construction and characterization of a thrombin-resistant designer FGF-based collagen binding domain angiogen. Biomaterials. 2008;29:327–36.
109. Yu J, Wang A, Tang Z, Henry J, Lee LP, Zhu Y, et al. The effect of stromal cell-derived factor-1α/heparin coating of biodegradable vascular grafts on the recruitment of both endothelial and smooth muscle progenitor cells for accelerated regeneration. Biomaterials. 2012;33:8062–74.
110. Talacua H, Smits AI, Muylaert DE, van Rijswijk JW, Vink A, Verhaar MC, et al. In situ tissue engineering of functional small-diameter blood vessels by host circulating cells only. Tissue Eng Part A. 2015;21:2583–94.
111. Koobatian MT, Row S, Jr RJS, Koenigsknecht C, Andreadis ST, Swartz DD. Successful endothelialization and remodeling of a cell-free small-diameter arterial graft in a large animal model. Biomaterials. 2016;76:344–58.
112. Wang Z, Sun B, Zhang M, Ou L, Che Y, Zhang J, et al. Functionalization of electrospun poly(-caprolactone) scaffold with heparin and vascular endothelial growth factors for potential application as vascular grafts. J Bioact Compat Polym. 2013;28:154–66.
113. Shin YM, Lee YB, Kim SJ, Kang JK, Park JC, Jang W, et al. Mussel-inspired immobilization of vascular endothelial growth factor (VEGF) for enhanced endothelialization of vascular grafts. Biomacromolecules. 2012;13:2020–8.
114. Han F, Jia X, Dai D, Yang X, Zhao J, Zhao Y, et al. Performance of a multilayered small-diameter vascular scaffold dual-loaded with VEGF and PDGF. Biomaterials. 2013;34:7302–13.
115. Lu S, Peng Z, Sun X, Gong F, Yang S, Li S, et al. Synthetic ePTFE grafts coated with an anti-CD133 antibody-functionalized heparin/collagen multilayer with rapid in vivo endothelialization properties. ACS Appl Mater Interfaces. 2013;5:7360–9.
116. Dannowski H, Bednarz J, Reszka R, Engelmann K, Pleyer U. Lipid-mediated gene transfer of acidic fibroblast growth factor into human corneal endothelial cells. Exp Eye Res. 2005;80:93–101.
117. Akowuah EF, Gray C, Lawrie A, Sheridan PJ, Su CH, et al. Ultrasound-mediated delivery of TIMP-3 plasmid DNA into saphenous vein leads to increased lumen size in a porcine interposition graft model. Gene Ther. 2005;12:1154–7.
118. Meng QH, Irvine S, Tagalakis AD, Mcanulty RJ, Mcewan JR, Hart SL. Inhibition of neointimal hyperplasia in a rabbit vein graft model following non-viral transfection with human iNOS cDNA. Gene Ther. 2013;20:979–86.

119. Jing-Tao Z, Qing C, Yan S, Hong-Bo G, Ping X. Lentiviral vector mediated expression of Bax and hepatocyte growth factor inhibits vein graft thickening in a rabbit vein graft model. Pharmazie. 2014;69:809–13.
120. Zhang J, Qi H, Wang H, Hu P, Ou L, Guo S, et al. Engineering of vascular grafts with genetically modified bone marrow mesenchymal stem cells on poly (propylene carbonate) graft. Artif Organs. 2006;30:898–905.
121. Yin A, Zhang K, Mcclure MJ, Huang C, Wu J, Fang J, et al. Electrospinning collagen/chitosan/poly(L -lactic acid- co -ϵ-caprolactone) to form a vascular graft: mechanical and biological characterization †. J Biomed Mater Res A. 2013;101:1292–301.
122. Qiu Y, Tarbell JM. Computational simulation of flow in the end-to-end anastomosis of a rigid graft and a compliant artery. ASAIO J. 1996;42:M702–9.
123. Song Y, Feijen J, Grijpma DW, Poot AA. Tissue engineering of small-diameter vascular grafts: a literature review. Clin Hemorheol Microcirc. 2011;49:357–74.
124. Isaka M, Nishibe T, Okuda Y, Saito M, Seno T, Yamashita K, et al. Experimental study on stability of a high-porosity expanded polytetrafluoroethylene graft in dogs. Ann Thorac Cardiovasc Surg Off J Assoc Thorac Cardiovasc Surg Asia. 2006;12:37–41.
125. Lu XL, Sun ZJ, Cai W, Gao ZY. Study on the shape memory effects of poly(l -lactide-co-ϵ-caprolactone) biodegradable polymers. J Mater Sci Mater Med. 2008;19:395–9.
126. Sang JL, Jie L, Oh SH, Soker S, Atala A, Yoo JJ. Development of a composite vascular scaffolding system that withstands physiological vascular conditions. Biomaterials. 2008;29:2891–8.
127. Mercado-Pagán ÁE, Stahl AM, Ramseier ML, Behn AW, Yang Y. Synthesis and characterization of polycaprolactone urethane hollow fiber membranes as small diameter vascular grafts. Mater Sci Eng C Mater Biol Appl. 2016;64:61–73.
128. Takeuchi M, Kuratani T, Miyagawa S, Shirakawa Y, Shimamura K, Kin K, et al. Tissue-engineered stent-graft integrates with aortic wall by recruiting host tissue into graft scaffold. J Thorac Cardiovasc Surg. 2014;148:1719–25.
129. Giudiceandrea A, Seifalian AM, Krijgsman B, Hamilton G. Effect of prolonged pulsatile shear stress in vitro on endothelial cell seeded PTFE and compliant polyurethane vascular grafts. Eur J Vasc Endovasc Surg Off J Eur Soc Vasc Surg. 1998;15:147–54.
130. Tai NR, Salacinski HJ, Edwards A, Hamilton G, Seifalian AM. Compliance properties of conduits used in vascular reconstruction. Br J Surg. 2000;87:1516–24.
131. Uttayarat P, Perets A, Li M, Pimton P, Stachelek SJ, Alferiev I, et al. Micropatterning of three-dimensional electrospun polyurethane vascular grafts. Acta Biomater. 2010;6:4229–37.
132. Odermatt EK, Funk L, Bargon R, Martin DP, Rizk S, Williams SF. MonoMax suture: a new long-term absorbable monofilament suture made from poly-4-hydroxybutyrate. Int J Polym Sci. 2012;2012:216137.
133. Patel HN, Garcia R, Schindler C, Dean D, Pogwizd SM, Singh R, et al. Fibro-porous poliglecaprone/polycaprolactone conduits: synergistic effect of composition and in vitro degradation on mechanical properties. Polym Int. 2015;64:547–55.
134. Wright LD, Andric T, Freeman JW. Utilizing NaCl to increase the porosity of electrospun materials. Mater Sci Eng C. 2011;31:30–6.
135. Hirai J, Matsuda T. Venous reconstruction using hybrid vascular tissue composed of vascular cells and collagen: tissue regeneration process. Cell Transplant. 1996;5:93–105.
136. Offeddu GS, Ashworth JC, Cameron RE, Oyen ML. Structural determinants of hydration, mechanics and fluid flow in freeze-dried collagen scaffolds. Acta Biomater. 2016;41:193–203.
137. Kumar VA, Caves JM, Haller CA, Dai E, Liu L, Grainger S, et al. Acellular vascular grafts generated from collagen and elastin analogs. Acta Biomater. 2013;9:8067–74.
138. Buijtenhuijs P, Buttafoco L, Poot AA, Daamen WF, Kuppevelt THV, Dijkstra PJ, et al. Tissue engineering of blood vessels: characterization of smooth-muscle cells for culturing on collagen-and-elastin-based scaffolds. Biotechnol Appl Biochem. 2004;39:141–9.

139. Yu Z, Zhang Y. The orthotropic viscoelastic behavior of aortic elastin. Biomech Model Mechanobiol. 2010;10:613–25.
140. Mckenna KA, Hinds MT, Sarao RC, Wu PC, Maslen CL, Glanville RW, et al. Mechanical property characterization of electrospun recombinant human tropoelastin for vascular graft biomaterials. Acta Biomater. 2011;8:225–33.
141. Agrawal V, Kollimada SA, Byju AG, Gundiah N. Regional variations in the nonlinearity and anisotropy of bovine aortic elastin. Biomech Model Mechanobiol. 2013;12:1181–94.
142. Arrigoni C, Camozzi D, Imberti B, Mantero S, Remuzzi A. The effect of sodium ascorbate on the mechanical properties of hyaluronan-based vascular constructs. Biomaterials. 2006;27:623–30.
143. Ruiz A, Flanagan CE, Masters KS. Differential support of cell adhesion and growth by copolymers of polyurethane with hyaluronic acid. J Biomed Mater Res A. 2013;101:2870–82.
144. Chuang TW, Masters KS. Regulation of polyurethane hemocompatibility and endothelialization by tethered hyaluronic acid oligosaccharides. Biomaterials. 2009;30:5341–51.
145. Elsayed Y, Lekakou C, Labeed F, Tomlins P. Fabrication and characterisation of biomimetic, electrospun gelatin fibre scaffolds for tunica media-equivalent, tissue engineered vascular grafts. Mater Sci Eng C. 2015;61:473–83.
146. Ju YM, Jin SC, Atala A, Yoo JJ, Sang JL. Bilayered scaffold for engineering cellularized blood vessels. Biomaterials. 2010;31:4313–21.
147. Stitzel J, Jie L, Sang JL, Komura M, Berry J, Soker S, et al. Controlled fabrication of a biological vascular substitute. Biomaterials. 2006;27:1088–94.
148. Sarasam A, Madihally SV. Characterization of chitosan–polycaprolactone blends for tissue engineering applications. Biomaterials. 2005;26:5500–8.
149. Chen F, Su Y, Mo X, He C, Wang H, Ikada Y. Biocompatibility, alignment degree and mechanical properties of an electrospun chitosan–P(LLA-CL) fibrous scaffold. J Biomater Sci Polym Ed. 2009;20:2117–28.
150. Reed AM, Gilding DK. Biodegradable polymers for use in surgery – poly(ethylene oxide)/poly(ethylene terephthalate) (PEO/PET) copolymers: 2. In vitro degradation. Polymer. 1979;20:1454–8.
151. Tara S, Kurobe H, Maxfield MW, Rocco KA, Bagi P, Yi T, et al. Comparison of the biological equivalence of two methods for isolating bone marrow mononuclear cells for fabricating tissue-engineered vascular grafts. Tissue Eng C Methods. 2015;21(6):597–604.
152. Ulery BD, Nair LS, Laurencin CT. Biomedical applications of biodegradable polymers. J Polym Sci B. 2011;49:832–64.
153. Ye X, Lu L, Kolewe ME, Park H, Larson BL, Kim ES, et al. A biodegradable microvessel scaffold as a framework to enable vascular support of engineered tissues. Biomaterials. 2013;34:10007–15.

Chapter 12
Myocardial Regenerative Medicine

Zhaobo Fan*, Xiaofei Li*, Hong Niu*, and Jianjun Guan

12.1 Introduction

Cardiovascular disease is a high morbidity and mortality disease in western countries. Myocardial infarction (MI) or heart attack is a major cardiovascular disease that affects millions of people. In the USA alone, MI affects eight million people [1]. The most common cause of MI is thrombosis formed inside the coronary artery or its branches. It blocks the blood flow to a part of the myocardium leading to massive cell death in the affected area. These cells include cardiomyocytes, cardiac fibroblasts, smooth muscle cells, and endothelial cells. Thirty minutes after MI, the damaged tissue starts an irreversible necrosis process. Polymorphonuclear leukocytes are then accumulated in the infarcted tissue and the neutrophils infiltrate inside to begin the phagocytosis of dead cells. Meanwhile, the upregulated matrix metalloproteinases (MMPs) degrade extracellular matrix in the infarcted area leading to wall thinning and left ventricle dilation. After 4 days, collagen deposition begins to initiate cardiac fibrosis for the purpose of protecting the thin wall from rupture. After 3 weeks, a dense scar tissue is formed [2, 3]. Cardiac fibrosis does not stop but propagates over time. Meanwhile, the cardiac wall dilation continues and cardiac function gradually decreases, which eventually progress the infarcted hearts toward heart failure stage.

Current clinical intervention for MI is mainly focused on coronary reperfusion, which aims to reintroduce nutrient and oxygen in the infarcted heart. However, reperfusion therapy does not regenerate new cardiac muscle. Unlike many other tissues in the body, the damaged heart tissue cannot self-regenerate to restore normal

*Author contributed equally with all other contributors.

Z. Fan • X. Li • H. Niu • J. Guan (✉)
Department of Materials Science and Engineering, The Ohio State University,
2041 College Road, Columbus, OH 43210, USA
e-mail: guan.21@osu.edu

© Springer Science+Business Media Singapore 2016

C. Gao (ed.), *Polymeric Biomaterials for Tissue Regeneration*,
DOI 10.1007/978-981-10-2293-7_12

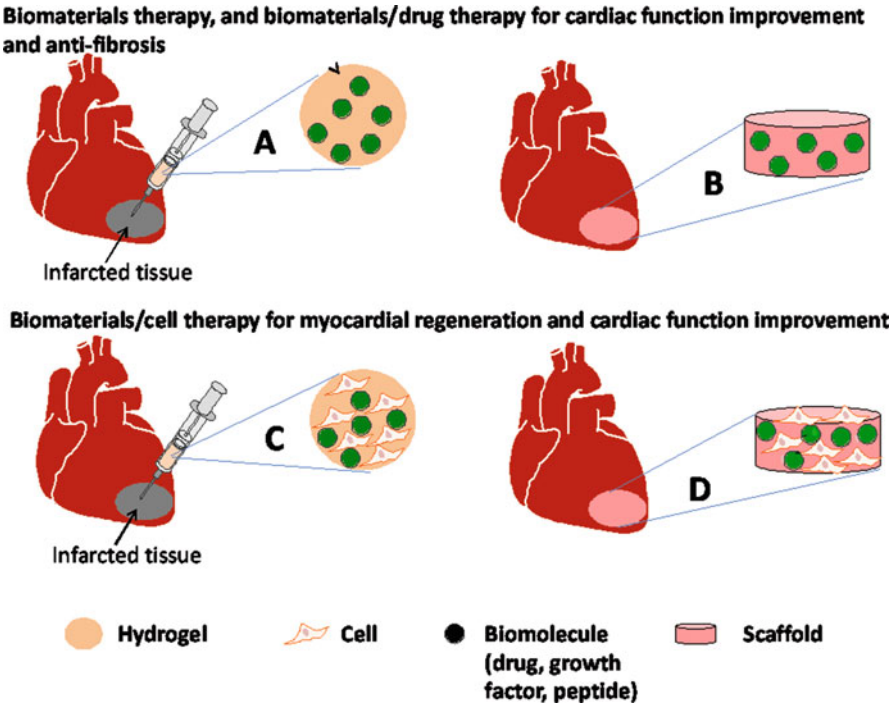

Fig. 12.1 Current biomaterials-based therapies after MI in order to improve cardiac function

tissue features and function. This is because adult cardiomyocytes are unable to grow, and endogenous cardiac stem/progenitor cells cannot spontaneously generate enough cardiomyocytes to assemble new myocardium [4]. Consequently, it is necessary to transplant cells to the infarcted region to compensate the lost cardiac cells. This is cardiac cell therapy. It has been considered as a promising approach for MI. Therapies that improve the function of damaged heart tissue other than fully regeneration have also been explored. These include using acellular biomaterials and control of cardiac fibrosis (Fig. 12.1). This chapter summarizes current approaches for cardiac regeneration and cardiac function improvement.

12.2 Biomaterial-Based Myocardial Repair

12.2.1 Injectable Hydrogels

It has been established that injection of hydrogels into infarcted hearts improves cardiac function and reduces infarct size. The injected hydrogels may also decrease cardiac cell apoptosis and promote angiogenesis. After MI, the MMPs are upregulated, which degrade cardiac ECM causing tissue thickness decrease [5]. The hydrogels provide structural and mechanical support to the infarcted tissue. Hydrogels are

hydrophilic and exhibit many similarities as the extracellular matrices (ECMs) in cardiac tissue [6]. The hydrogels can be injected into the cardiac tissue in a liquid form, which then solidifies in response to physical or chemical stimuli, based on the characteristics of the specific hydrogels. Current hydrogels used for myocardial injection are either natural or synthetic. The natural hydrogels are derived from tissues and other natural sources, thus possessing excellent biocompatibility. However, natural hydrogels usually have low mechanical properties, batch-to-batch variation, and vulnerable to chemical modification. Synthetic hydrogels overcome these disadvantages through tailoring of chemical structure and composition. A potential concern for synthetic hydrogels is toxicity before and after degradation. An alternative approach to avoid potential toxicity is to use natural/synthetic hydrogel composites.

12.2.1.1 Natural Hydrogels for Cardiac Repair

The commonly used natural hydrogels for cardiac repair include decellularized extracellular matrix, chitosan, hyaluronic acid, alginate, and Matrigel. These injectable hydrogels have been tested in infarcted hearts for functional improvement and/or regeneration. The hydrogels can also be modified or combined with drugs and growth factors to further enhance the therapeutic efficacy.

Decellularized Extracellular Matrix

Decellularized ECM is a naturally derived matrix that has shown promise for treating infarcted hearts after MI [7]. It provides cardiac cells with biochemical cues important for cell migration and differentiation and tissue regeneration [7]. Decellularized ECM can be obtained after removal of cells from the tissues. Optimized decellularization processes allow the decellularized tissue to have similar chemical compositions as the native tissues. In most cases, the decellularized ECMs show excellent biocompatibility as evidenced by the lack of cytotoxic effect and minor foreign body response [7].

The decellularized ECMs can be fabricated into thermal-sensitive hydrogels. At a lower temperature, the matrices can dissolve or suspend in the acidic aqueous solution. When the temperature is elevated to 37 °C, the solution forms solid hydrogel. The decellularized ECM solution may be delivered into infarcted hearts by a minimally invasive cardiac surgery. Various studies have demonstrated that the injected matrices improve cardiac function. Okada et al. injected decellularized small intestinal submucosa into infarcted mouse hearts using an acute MI model [8]. When examined at 2 weeks of postimplantation, the end-systolic area and fractional area change were significantly increased. The injected matrix also increased capillary density in the infarcted area. Compared to decellularized small intestinal submucosa, decellularized cardiac tissue better resembles the ECM composition in the native heart tissue. It may thus be more suitable for cardiac repair [9]. Singelyn et al. generated injectable porcine myocardium hydrogel and tested in rat MI model [10].

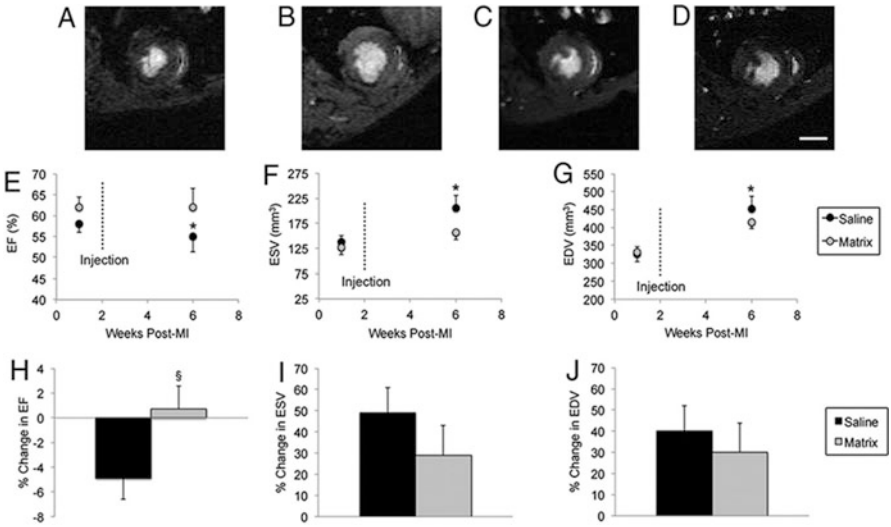

Fig. 12.2 MRI analysis in rat MI model after injection of myocardial matrix [10]. (**A**) Baseline (1 week post-myocardial infarction [MI], 1 week pre-injection) and (**B**) 4 weeks post-injection images of saline-injected heart. (**C**) Baseline and (**D**) 4 weeks post-injection images of myocardial matrix–injected heart. Scale bar = 0.5 cm. (**E**) Ejection fraction (EF) of saline controls significantly declined ($p = 0.04$), whereas the (**F**) end-systolic volume (ESV) ($p = 0.01$) and (**G**) end-diastolic volume (EDV) ($p = 0.01$) significantly expanded between 1 week and 6 weeks post-MI. By contrast, there was no statistical significance for EF ($p = 0.8$), ESV ($p = 0.054$), and EDV ($p = 0.06$) between time points in the myocardial matrix group. Myocardial matrix–injected animals had an overall increase in the percent change in EF ($p = 0.054$) (**H**), and overall decrease in the percent change in volume (**I** and **J**) between time points compared to saline, although these were not statistically significant. Data are presented as the mean ± SEM; $^*p < 0.05$. MRI = magnetic resonance imaging

When evaluated after 4 weeks of injection, the preservation of ejection fraction, end-diastolic volume, and end-systolic volume was observed. In a subsequent porcine MI model, the animals injected with decellularized cardiac tissue exhibited significantly higher ejection fraction, lower end-diastolic volume, and end-systolic volume than the controls (Fig. 12.2) [9]. Histological analysis demonstrated that the injected hydrogel promoted cardiac muscle regeneration and neovascularization. Overall, decellularized ECMs are promising for cardiac repair. However, there are disadvantages associated with them: (1) the remaining immunogenic proteins may initiate immune rejection (posttreatment is necessary to guarantee that the decellularized extracellular matrix is free of immunogenic proteins); and (2) the hydrogels have long gelation time. They may enter into vasculature and block it after gelation.

Chitosan

Chitosan is a polysaccharide derived from chitin. Chitosan is attractive for cardiac repair because of its good biocompatibility, biodegradability, bioactivity, and low toxicity. The chitosan hydrogels can be achieved by neutralizing acidic chitosan

solution or cross-linking the polymer chains [11]. Adding glycerophosphate (GP) in the chitosan solution can make the hydrogel thermosensitive. The gelation time is around 10 min. To decrease gelation time, chitosan chloride can be used. It reduces the gelation time to approximately 1 min [12]. Chitosan-based hydrogels are capable of providing mechanical support and promoting angiogenesis in infarcted heart tissue. When injecting chitosan into the damaged rat hearts after MI, heart function and vessel density were significantly increased [13]. Chitosan hydrogel may also promote cardiac cell survival by scavenging reactive oxygen species (ROS) [14].

Hyaluronic Acid

Hyaluronic acid (HA) is a polysaccharide found in almost all adult connective tissues, including the joint, ligament, tendon, and skin. HA hydrogels have high biocompatibility and are typically degraded by enzymes in the tissues. HA hydrogels can be injected into infarcted hearts with and without prior modification. The modification imparts the hydrogels with improved mechanical properties, cell adhesive property, and biodegradation. Ifkovits et al. injected methacrylated hyaluronic acid into the hearts after MI and cross-linked with tetramethylethylenediamine and ammonium persulfate [15]. The injected HA significantly increased the wall thickness in the apex and basilar infarct regions. The degree of cardiac function improvement was dependent on modulus of the HA hydrogel. When comparing the cardiac function of the hearts injected with 8- and 43-kPa hydrogels, those injected with 43-kPa hydrogel showed a statistically smaller infarct area and better functional outcomes (cardiac output and ejection fraction).

Alginate

Alginate is attractive in cardiac tissue engineering due to its good biocompatibility and gentle gelation conditions [16]. When injecting alginate solution into infarcted hearts, it can be solidified by Ca^{2+} in the heart. Landa et al. demonstrated the feasibility of using alginate in the infarcted hearts for functional improvement [17]. When the alginate hydrogel was delivered into subacute (1 week) MI hearts and late infarcts (8 weeks), the wall thickness was significantly increased even after 2 months of injection. This resulted in an increase in systolic and diastolic cardiac function. Similar functional improvement results were seen when using large animal MI models [18]. Modification of alginate hydrogels by blending with other natural polymers such as fibrin and collagen or conjugating with cell adhesive peptide may improve cell adhesive property of alginate and augment the therapeutic efficacy [19, 20]. Mukherjee et al. mixed alginate and fibrin hydrogels followed by injection into porcine myocardium 7 days after MI [21]. A remarkable reduction of infarct size was observed 3 weeks after injection compared with saline injection group. So far, alginate hydrogel is the first injectable hydrogel tested in clinical trial.

Matrigel

Matrigel is a mixture of basement membrane components derived from sarcoma, a tumor rich in laminin, collagen IV, heparin, and a number of growth factors. It resembles the extracellular environment found in many tissues. Matrigel has been served as a substrate for tissue culture [22]. It has also been widely used as a native-mimicking environment to test cell response to different drugs and growth factors in vitro [23]. Matrigel is in liquid form at 4 °C and turns into solid hydrogel at 37 °C. Injection of Matrigel into infarcted hearts after MI led to an increase in wall thickness and capillary density [24]. When compared with saline injection group, Matrigel injection significantly improved ejection fraction after 4 weeks of implantation. Interestingly, it also induced the recruitment of CD34+ and c-Kit+ stem cells to the infarcted area. Despite the advantages the Matrigel has, its clinical application may be impractical in the near future due to its tumor origin.

Hydrogel Composites

Different types of hydrogel composites have emerged for cardiac repair. Typical examples are alginate-HA hydrogel [25], alginate-chitosan hydrogel [19], and decellularized ECM-fibrin hydrogels [26]. Nanoparticles including carbon nanotubes (CNTs), dendrimers, and graphene were also incorporated into natural hydrogels to form nanocomposites [27]. Nanocomposites reinforced by CNTs have been used to engineer cardiac tissues because of their excellent electrical property. However, many challenges such as toxicity and biodegradability remain to be solved before the wide application of these nanocomposites in cardiac repair.

12.2.1.2 Synthetic Polymer-Based Hydrogels

Synthetic hydrogels, including degradable poly(N-isopropylacrylamide) (PNIPAAm)-based hydrogels [28], PEG and copolymers [29, 30], poly(D-lysine) (PDL) [31], and self-assembly peptide [32], have been injected into infarcted hearts for cardiac repair. Compared with natural polymer-based hydrogels, the properties of synthetic hydrogels such as gelation time, modulus, and degradation rate can be readily tuned by synthesis method, composition, and chemistry [33].

Poly(N-Isopropylacrylamide)-Based Hydrogels

Among the different injectable hydrogels used for heart repair, poly(N-isopropylacrylamide) (PNIPAAm)-based hydrogels have the advantage of fast gelation, which can increase gel retention in the heart tissue. The fast gelation also allows higher cell and drug retention when the hydrogels are used for cell and drug delivery. PNIPAAm is not degradable. The degradable PNIPAAm can be

synthesized by copolymerization with degradable components [2, 25, 34–44]. These hydrogels have lower critical solution temperatures (LCSTs) below 32 °C before degradation, which are increased above 37 °C after degradation. Therefore, the degraded hydrogels can dissolve in the body fluid and be removed from the body. When adding pH-sensitive component to the PNIPAAm-based hydrogels, LCSTs become pH dependent. Li et al. synthesized a family of pH- and thermal-sensitive hydrogels based on NIPAAm, propylacrylic acid, hydroxyethyl methacrylate-co-oligo(trimethylene carbonate), and methacrylate poly(ethylene oxide) methoxy ester [36]. The hydrogels had LCSTs above 37 °C at pH 8.0 and below 37 °C at pH 6.8 before degradation. These hydrogels are clinically attractive because they can be delivered into hearts by catheter using minimally invasive approach.

Injection of PNIPAAm-based hydrogels into infarcted hearts has been shown to increase cardiac function [28, 45–48]. Fujimoto et al. injected a PNIPAAm-based hydrogel into rat chronic infarction model with PBS as a control. In the PBS group, the left ventricle cavity area was increased and contractility was decreased after 6 weeks of injection, while in the hydrogel group, both parameters were preserved [28]. In addition, a thicker left ventricle wall and higher capillary density were found for the hydrogel group. When using PNIPAAm-based hydrogels to improve cardiac function, the time of the injection affects therapeutic efficacy [46, 49]. This is because the wall stress of the infarcted tissue varies when the MI evolves from early to late stages. In general, the wall stress gradually increases from the necrotic phase to the fibrotic phase [50]. Therefore, the same hydrogel may have different efficacy in reducing wall stress [46]. Yoshizumi et al. injected a PNIPAAm-based hydrogel into rat hearts at three different time points: immediately after MI, 3 days after MI, and 2 weeks after MI [46]. These three time points correspond to the beginnings of the necrotic, fibrotic, and chronic remodeling phases. While all injection time points increased the left ventricle function and wall thickness, the injection after 3 days of MI group exhibited better cardiac function than the other injection time points (Fig. 12.3). The above results suggest that timing of hydrogel injection should be considered in order to achieve optimal therapeutic effect.

PNIPAAm-based hydrogels can be used as growth factor and drug carriers for enhanced cardiac repair [2, 51, 52]. Guan et al. functionalized the PNIPAAm hydrogels with growth factors [2] and antioxidants [25]. The results showed that functionalization enhanced mesenchymal stem cell (MSC) growth within the hydrogels, offering a suitable environment for cells delivered into the heart.

Polyethylene Glycol (PEG) and Copolymers

PEG has been approved by FDA for some medical uses because of its low toxicity and nonimmune response [53]. Injection of PEG hydrogel has been shown to increase cardiac function in different studies. For example, Kraehenbuehl et al. developed an injectable MMP-responsive PEG hydrogel and injected it into infarcted hearts 1 h following MI. After 6 weeks, the hearts injected with PEG

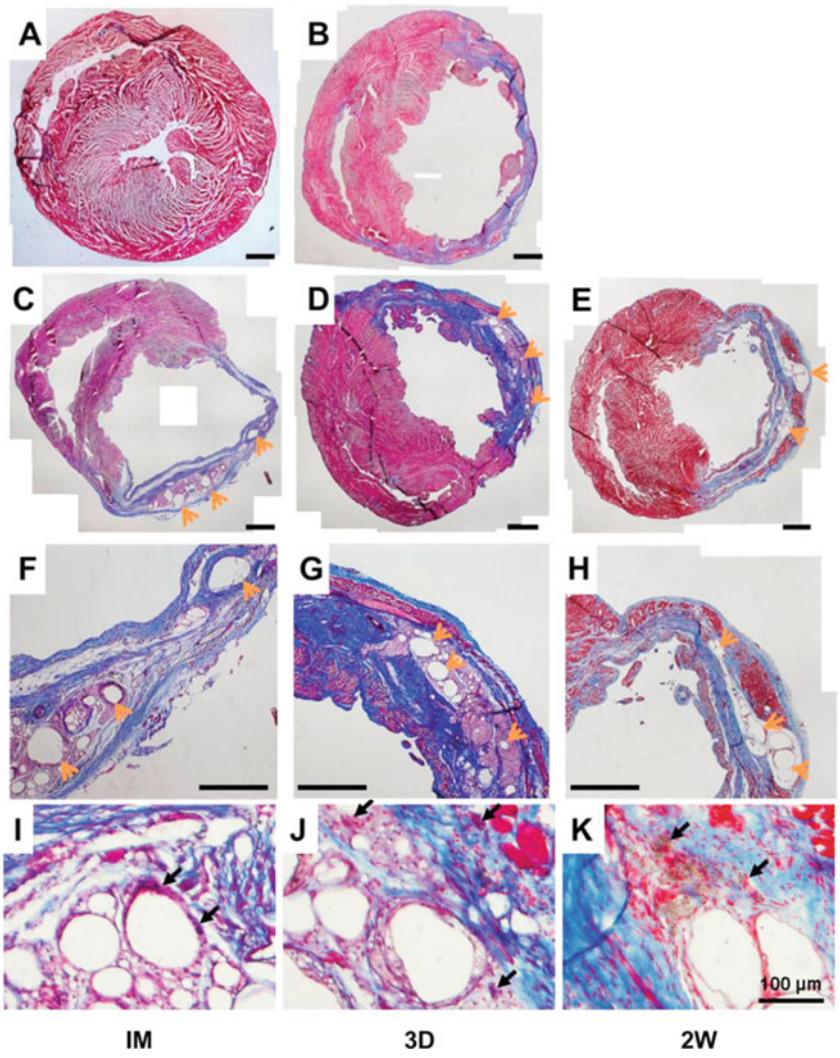

Fig. 12.3 Ventricular wall histology for rat hearts 10 w after MI [46]. Representative Masson's trichrome-stained cross sections: (**A**) healthy control, (**B**) MI control, (**C**, **F**, **I**) immediately after MI (IM) group, (**D**, **G**, **J**) injection after 3 days (3D) group, (**E**, **H**, **K**) injection after 2 weeks (2W) group. (**A**–**H**) Scale bars 1 mm. *Orange arrows* point to the hydrogel residues; *black arrows* point to foreign body giant cells. Wall thickness (L) and infarction size (M) were measured from the complete set of these images. * indicates significant differences between groups. Echocardiographic assessment of long-term cardiac functions: (**N**) end-systolic area (ESA), (**O**) end-diastolic area (EDA), (**P**) fractional area change (% FAC), (**Q**) ejection fraction (EF). # indicates significant differences between 3D group and other injection groups and MI control group. * indicates significant differences between MI control and all injection groups. & indicates significant differences between MI control and the 3D and 2W groups

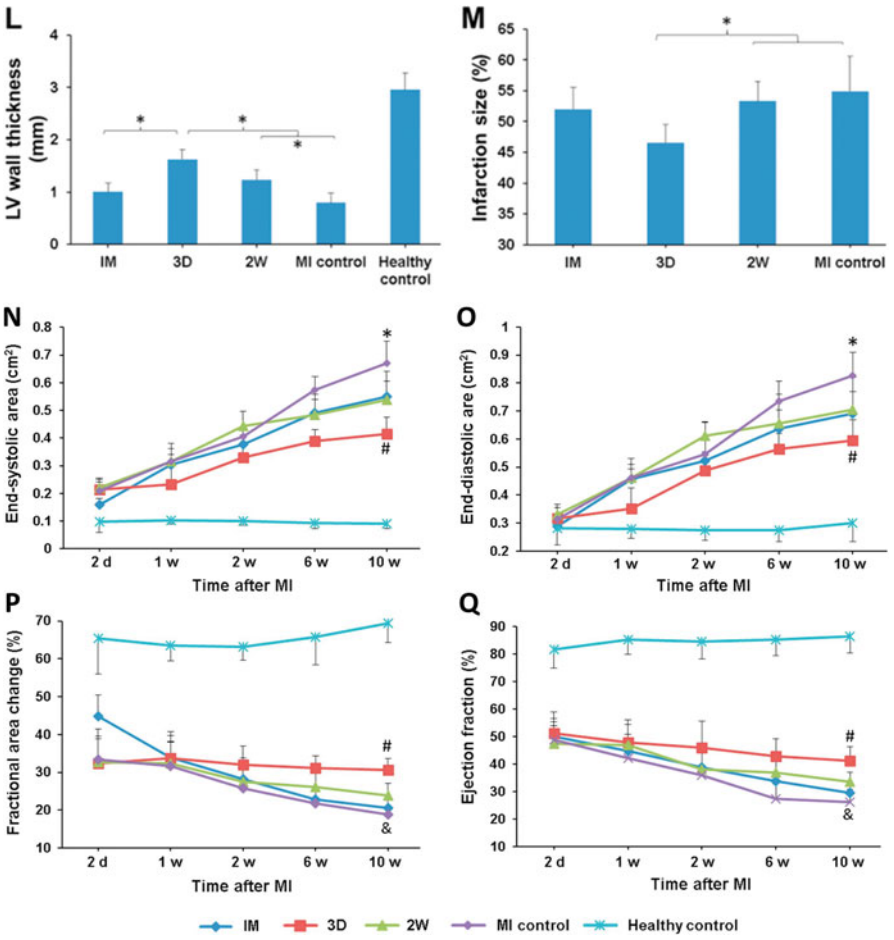

Fig. 12.3 (continued)

hydrogel demonstrated significantly lower infarct size, end-diastolic volume, and end-systolic volume compared with those hearts injected with PBS. Meanwhile, the PEG hydrogel-injected hearts had significantly higher ejection fraction [54].

The hydrogels based on PEG copolymers have also been developed for cardiac repair. Xu et al. fabricated hydrogels based on thiolated collagen (Col-SH) and oligo(acryloyl carbonate)-b-poly(ethylene glycol)-b-oligo(acryloyl carbonate) (OAC-PEG-OAC) [26]. Echocardiographic results showed that the injected hydrogels increased ejection fraction at 28 days compared to the PBS group. In addition, the injected hydrogels significantly reduced the infarct size and increased the wall thickness. Similar results were seen with the injection of hydrogel composed of α-cyclodextrin and mPEG-PCL-mPEG [55].

Polypeptides

Polypeptide hydrogels have emerged as promising matrices for cardiac repair because their compositions mimic the natural extracellular matrix. Self-assembling peptides are a class of polypeptides that spontaneously assemble into nanostructures. Rational design of self-assembling peptides can avoid immune response. In vivo, they degrade by enzymes into nontoxic amino acids and short peptides. The mechanical and bioactive properties of self-assembling peptides can be readily tuned by modulating amino acid building blocks to mimic natural microenvironments. Self-assembling peptides are injectable. They have the potential for minimally invasive delivery to the myocardium [56]. Davis et al. injected a self-assembling peptide hydrogel into the heart tissue and found that the hydrogel was rapidly cellularized within days by endothelial cells, smooth muscle cells, and cardiac cells [57]. Self-assembling peptide hydrogels can also be used for the delivery of growth factors and cells into infarct hearts. A variety of growth factors and different cell types have been incorporated into the hydrogels for enhanced cell survival, vascularization, myocardial regeneration, and heart function.

12.2.2 Acellular Scaffolds

Acellular scaffolds can serve as cardiac patches to augment cardiac function. These scaffolds are typically sutured or glued on the surface of infarcted heart tissue. The cells from the surrounding healthy heart tissue then migrate and populate inside to vascularize and/or regenerate cardiac tissue. The acellular scaffolds improve cardiac function by providing mechanical support, vascularization the tissue and/or regeneration of new heart tissue. Different types of biomaterials have been fabricated into acellular scaffolds for cardiac repair, including collagen [58], fibrin [59], decellularized extracellular matrix [60], degradable polyurethane [61, 62], poly(glycolide-co-caprolactone) [63], and poly(lactide-co-caprolactone) [64]. The scaffolds are either in gel, foam, or fibrous form. The gel-type scaffolds are more easily shaped to a complex geometry than foams and fibrous scaffolds. The foams and fibrous scaffolds have controlled structure, pore size, and orientation. Fibrous scaffolds can also mimic the morphology of the collagen fibers in tissues and thus are considered more suitable for tissue regeneration.

Fibrin gel possesses excellent biocompatibility. It has been used for engineering different tissues. Zhang et al. employed fibrin gel as cardiac patches for murine heart regeneration [59]. The fibrin gel was first conjugated with PEG and then placed on the infarct surface. To increase stem cell recruitment in the fibrin gel, SDF-1α was bound to the gel. The growth factor was able to release from the gel for up to 10 days. Two weeks after implantation, the number of recruited c-kit+ cells was significantly higher in the gel with SDF-1α. In addition, the left ventricle function was significantly better than in the control group. Callegari et al. placed porous collagen foam on infarcted rat hearts [58]. After 15 and 60 days of implantation, the

scaffolds were populated with endothelial and smooth muscle cells, resulting in an increase of vessel density for arterioles and capillaries. These results demonstrated that porous collagen scaffold is a powerful angiogenetic and arteriogenetic promoter. The use of decellularized ECM as cardiac patches can also promote heart tissue regeneration and improve cardiac function. For example, decellularized small intestinal submucosa was used as a cardiac patch in rabbit MI model [60]. Four weeks after transplantation, the left ventricle end-systolic volume and end-diastolic volume were significantly decreased while ejection fraction was increased.

Besides naturally derived cardiac patches, synthetic polymer-based cardiac patches have been explored. These scaffolds are typically elastic with mechanical properties similar to those of the heart tissue. On the other hand, stiff scaffolds may further damage infarcted heart tissue. Fujimoto et al. fabricated microporous elastic poly(ester urethane)urea scaffolds and tested in rat hearts 2 weeks after MI [61]. The scaffolds significantly increased wall thickness after 4 and 8 weeks of implantation. Interestingly, the scaffolds were populated with mature smooth muscle cells (Fig. 12.4). In addition, the capillary density was significantly increased. Poly(ester urethane)urea scaffold implantation did not change end-diastolic cavity area (EDA) and increased the fractional area change (FAC), while EDA increased and FAC decreased in the infarction control group. Similar results were found when tested in porcine acute MI model [62].

12.3 Cell Therapy for Myocardial Regeneration

12.3.1 Cell Types and Current Limitations

The delivery of exogenous cell capable of directly and indirectly promoting cardiac regeneration is considered as a promising approach for regenerating new myocardium. Various cell types have been explored in clinical and preclinical models for cardiac therapy. Cardiomyocytes and stem cells capable of differentiating into cardiomyocytes can be used to regenerate cardiac tissue. These stem cells include cardiac stem/progenitor cells [65–69], pluripotent stem cell [embryonic stem cells (ESCs) and induced pluripotent stem cells (iPSCs)]-derived cardiovascular progenitor cells [70–72], and cardiosphere-derived cells [73–83]. Some stem cell types do not differentiate into cardiomyocytes to directly regenerate cardiac tissue, but can indirectly promote the regeneration. These cell types typically provide paracrine effects to augment the survival of resident cardiac cells, recruit endogenous stem cells, and vascularize the damaged heart tissue [84–90]. Some cell types also directly participate in tissue vascularization. Examples include bone marrow mesenchymal stem cells (BMMSCs) [91–105] and adipose-derived stem cells (ADSCs) [106–109].

To deliver cells into infarcted hearts, a commonly used approach is to suspend the cells in buffer and then inject into the infarct area. This direct injection approach

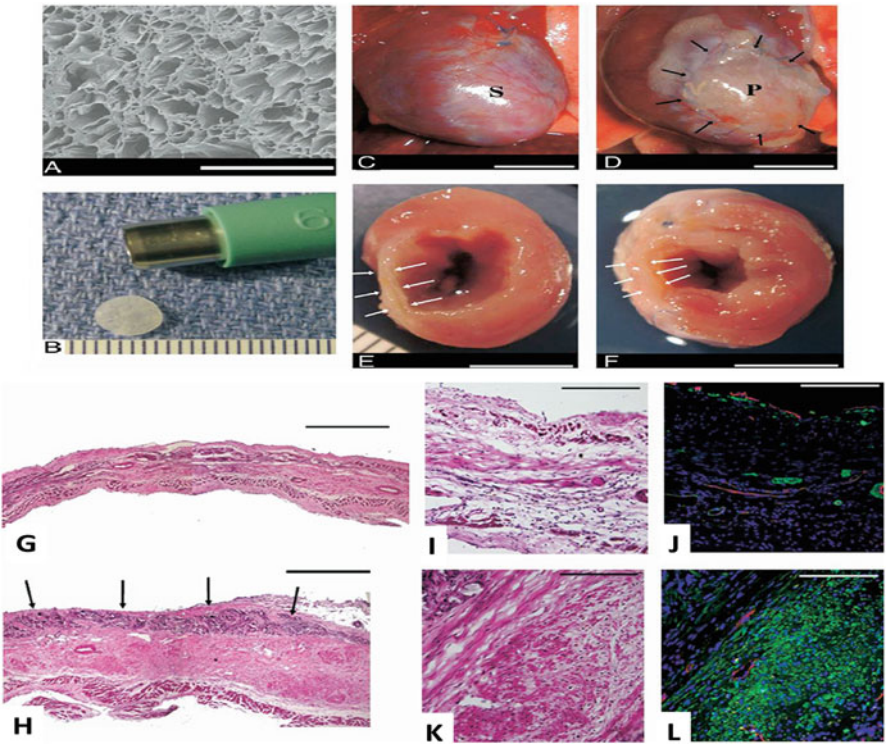

Fig. 12.4 Features of PEUU and representative images at 8 weeks after implantation [61]. Electron micrograph of the polyester urethane urea (PEUU) material (**A**). Polyester urethane urea patch in final format (6-mm diameter, 300-μm thick) (**B**). Representative images, 8 weeks after implantation, of the anterior view of infarction control (**C**) and PEUU-patched (**D**) hearts. The cross-sectional view of both groups is shown in (**E**, **F**), respectively. *Black arrows* point to the implanted PEUU patch, and *white arrows* indicate the infarcted anterior wall. Scale bars, 500 μm in A, 1 mm in B, and 55 mm in C to F. P, the patch implanted area; S, the infarcted scar. Representative histological sections of the infarction control (**G**) and PEUU-patched (**H**) myocardial wall 8 weeks after implantation stained with hematoxylin and eosin. *Black arrows* indicate the top of the PEUU implanted area, which appears *dark violet*. Higher magnification of hematoxylin and eosin staining and immunohistochemical staining appears in (**I**–**L**) where (**I**, **J**) are infarcted control and (**K**, **L**) are PEUU patched. α-SMA staining appears *green*, CD31 staining appears *red*, and nuclear staining appears *blue*. Increased smooth muscle actin is apparent in the PEUU-patched group. *Scale bars* in (**G**, **H**) are 500 μm. For (**I**–**L**), *scale bars* are 200 μm

has low efficacy because of inferior cell retention in the tissue. During the injection, greater than 90 % of injected cells were squeezed out of the heart tissue as a result of heart tissue contraction and low viscosity of the buffer. For those retained cells, a large portion dies within couple of weeks. The cell death can be a result of anoikis, apoptosis, and necrosis. In normal conditions, the cells adhere to ECM, which is a proper environment for cell growth and differentiation. Anoikis is induced from apoptosis under conditions of weak or improper adhesion between the cell and

ECM or even cell detachment from the ECM. Frisch and Francis first reported in 1994 that cell death following anoikis mechanism is because of lack of cell adhesion [110]. Necrosis can cause significant cell death within the first day after transplantation. Apoptosis is the process of programmed killing of the damaged cells during acute MI [111, 112]. In the infarcted hearts, the harsh low oxygen and nutrient environment leads to ischemic pathway-initiated cell death. Meanwhile, phagocytosis releases apoptotic cytokines and cytotoxic reactive oxygen species (ROS), resulting in cell death. In addition, the transplanted cells may be attacked by proinflammatory cytokines like TNF-α and IL-1-β [2, 113].

12.3.2 Approaches to Augment Cell Retention, Survival, and Engraftment for Enhanced Cardiac Repair

To increase cell retention, cells can be encapsulated into injectable biomaterials such as hydrogels. The viscous hydrogels have been shown to efficiently hold cells in heart tissue upon solidification. The cells can also be loaded into porous scaffolds or hydrogels and then patch on the infarcted tissue surface. In order to improve cell survival and promote cell differentiation (for stem cells), cells may be encapsulated into hydrogels and scaffolds with appropriate properties [114]. These biomaterials may provide an ideal environment for cells to survive and differentiate in the harsh environment of MI hearts. In addition, preexposure of cells to ischemia, genetic modification of cells, and delivery of growth factors and oxygen to cells have been used to augment survival of transplanted cells [39, 115, 116]. To prevent cell death caused by immune proteins and proinflammatory cytokines, hydrogels and scaffolds can be modified to prevent them from penetrating inside to attack the encapsulated cells [117]. An additional benefit for using hydrogels and scaffolds is that they act as a mechanical support, which decreases elevated wall stress to improve cardiac function.

12.3.2.1 Injectable Hydrogel-Based Cell Delivery System

Hydrogels have been widely used as supporting matrices to deliver cells into infarcted heart tissue. Bioactive and biocompatible hydrogels mimicking biochemical and biomechanical microenvironments in native tissue are ideal for successful cardiac repair and regeneration. Many hydrogel types, including natural polymer hydrogels, synthetic polymer hydrogels, and natural/synthetic hybrid hydrogels (introduced in Sect. 2), can be used to deliver cells. In general, hydrogel-based cell delivery system has several key advantages in cardiac repair after MI:

1. The hydrogels provide mechanical support to the ischemic left ventricle wall [118]. After MI, the infarct heart tissue led to the left ventricle wall remodeling

which includes the formation of scar tissue, thinning of myocardial wall, and dilation of ventricle. The injected hydrogels with proper mechanical properties provide structural support for the weakened cardiac wall.
2. The hydrogels not only retain cells in the infarcted area but also offer a biocompatible microenvironment for cells to attach, proliferate, differentiate, and function.
3. The injectable hydrogels allow to readily load drugs and biomolecules inside. The drugs and biomolecules can sustain release for a period of time. The released drugs or biomolecules can directly or indirectly enhance the cell survival and promote differentiation or even tissue angiogenesis.

A well-studied drug delivery system to augment cell survival in ischemic environment is to introduce growth factors to the system. By using prosurvival growth factor-loaded hydrogel systems, a short-term cell survival rate can be increased. To enhance long-term cell survival, angiogenic growth factors can be used to stimulate vessel formation to provide adequate oxygen and nutrient for cells [119–121]. However, a concern for directly applying growth factors in cell transplantation is that most of the growth factors have a relatively short half-life and the stimulative effect cannot last long [122, 123]. Encapsulation of growth factors in hydrogels not only protects the growth factors but also allows them to gradually release out [124–126]. IGF-1 and HGF are two well-known prosurvival growth factors. Fibroblast growth factor (FGF) [127], platelet-derived growth factor (PDGF) [128], and vascular endothelial growth factor (VEGF) [129] are the commonly used angiogenic growth factors. bFGF also has prosurvival function as it enhanced MSC survival under ischemic conditions [130]. To accelerate the regeneration of cardiac tissue, specific growth factors can be applied together with prosurvival and angiogenic growth factors to promote stem cell differentiation into functional cardiomyocytes and/or augment maturation of cardiomyocytes [131–133].

Li et al. fabricated a bFGF-releasing system based on a thermosensitive and degradable hydrogel [130]. The bFGF was able to sustainably release from the hydrogel in a 2-week period (Fig. 12.5). The released bFGF significantly enhanced MSC survival under ischemic conditions typical of the infarcted heart tissue. Koudstaal et al. developed an IGF-1- and HGF-releasing system that activated and increased the proliferation of endogenous cardiac stem/progenitor cells (eCSCs) after MI [134]. When the system is applied into porcine MI model, a new cardiomyocyte formation and capillary density increase were observed. In addition, cardiac function was improved.

Besides the ischemic effect, immune rejection also compromises the survival of transplanted cells. Small cytotoxic molecules secreted by neutrophils and macrophages, such as reactive oxygen species (ROS), TNF-α, and IL-1-β, are able to infiltrate into the hydrogel, triggering cell apoptotic pathways and leading to cell death and additional cytokine secretion [135–142]. Anti-inflammatory molecules either bind to proinflammatory cytokines or reduce their bioactivity. Therefore, combining hydrogels with anti-inflammatory molecules may provide immune protection for the transplanted cells. Hume et al. modified PEG hydrogel with superox-

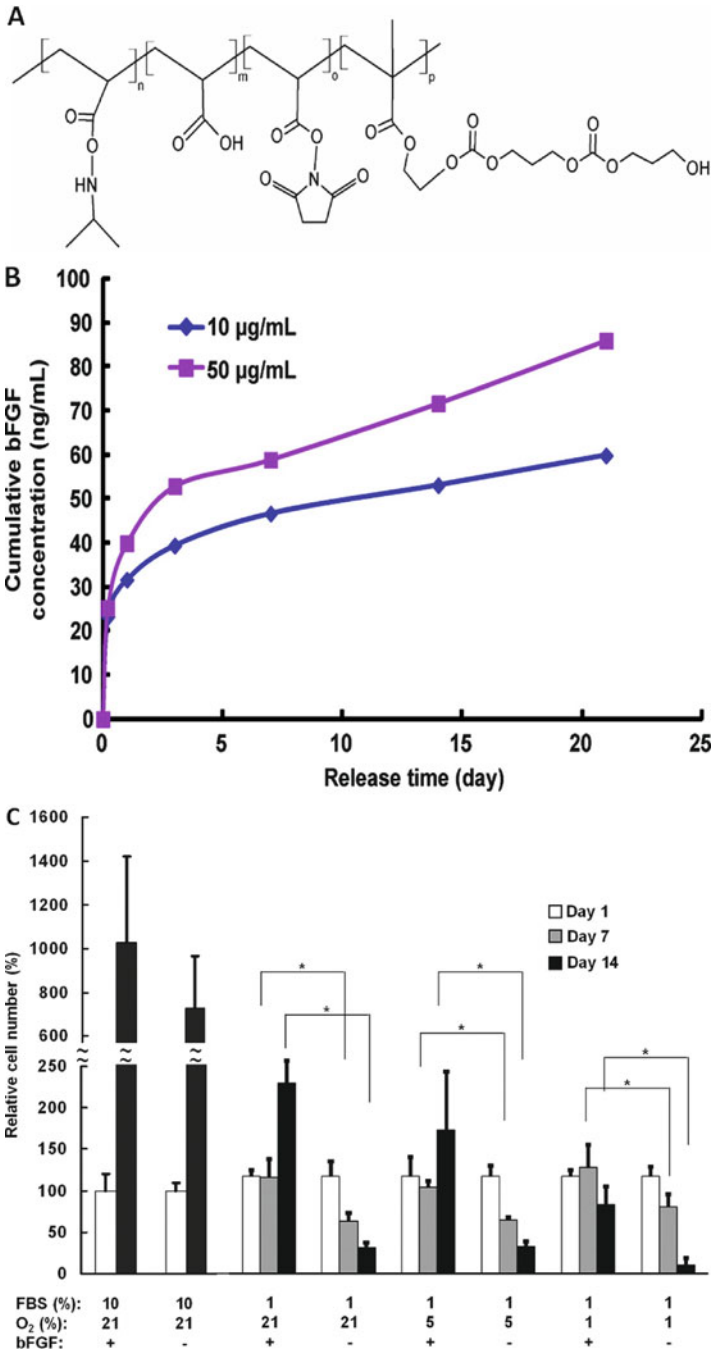

Fig. 12.5 Release of bFGF to augment MSC survival under low nutrient and oxygen conditions [132]. (**A**) Hydrogel structure; (**B**) release kinetics of bFGF loaded in the hydrogel. bFGF loading was 10–50 μg/mL, respectively. The error bars are small; (**C**) MSC survival in hydrogels cultured under different conditions. Culture conditions, 10 % FBS and 21 % oxygen, 1 % FBS and 21 % oxygen, 1 % FBS and 5 % oxygen, and 1 % FBS and 1 % oxygen. dsDNA content was used to quantify cell number in the hydrogels. The dsDNA content at day 1 was used for normalization

ide dismutase mimetic (SODm). After encapsulation of cells in the functionalized hydrogel system, the cells showed improved metabolic activity [143], indicating that the transplanted cells were protected from ROS damage. Lin et al. conjugated peptide WP9QY (YCWSQYLCY) on to PEG hydrogel to prevent attack of TNF-α cytokine to the encapsulated cells [144]. Su et al. modified PEG hydrogel with anti-inflammatory peptides and RGD peptide to provide early protection of encapsulated cells in the presence of TNF-α and IL-1-β [117]. In both studies, cell survival and engraftment improvement were observed and cell function was prolonged. Guo et al. found that IGF-1 offered MSCs the ability to play antiapoptotic and anti-inflammation roles in post-myocardial infarction [145]. Therefore, encapsulation of IGF-1 in the hydrogel may be a good approach to increase survival of the engrafted cells in the ischemic hearts, decrease cell apoptosis, and inhibit secretion of inflammation cytokines like TNF-α, IL-1-β, and IL-6.

12.3.2.2 Cardiac Patch-Based Cell Delivery System

Three forms of cardiac patches have been used for cardiac cell delivery, i.e., hydrogel, microporous foam, and fibrous scaffold. The hydrogels have small pores usually in nanometer scale. The microporous foams and fibrous scaffolds have larger pore size which may allow encapsulated cells to proliferate inside.

A widely used hydrogel-based cardiac patch is collagen. Collagen has excellent biocompatibility and bioactivity. Eschenhagen et al. developed a cardiac patch based on collagen gel and rat cardiomyocytes [146]. The cardiomyocytes were first mixed with collagen solution followed by collagen gelation to form 3D tissue constructs. The tissue constructs were able to contract. The contraction force can be significantly improved by incorporation of Matrigel into collagen. After 12 days of culture, the 3D tissue constructs were implanted into infarcted rat hearts. By 4 weeks, cardiac function was significantly improved as the myocardial dilation was attenuated and the wall thickness was increased. One of the advantages of using collagen gel is that cells can elongate inside which may improve cell functioning and cell-cell communication [2]. A major disadvantage of collagen-based patch is weak mechanical properties. To increase mechanical properties, collagen gel was combined with methylated hyaluronic acid. The mechanical properties can be readily modulated by the concentration of the methylated hyaluronic acid [25].

Microporous foams have larger pores than intact hydrogels, thus facilitating the transport of nutrients, oxygen, and metabolic molecules and removal of waste. Microporous foams also possess large surface area and high porosity, which make them suitable for cell attachment, cell migration, and cell-cell communication. In addition, the interconnected pores allow for vascularization. Microporous foams can be prepared by techniques like thermally induced phase separation [147], salt leaching [148], and microfabrication (for creating complex geometries) [149]. The microporous foams can be designed with ordered channels or accordion-like honeycombs to induce cell alignment [149]. For example, poly(glycerol sebacate) scaf-

fold with accordion-like structure induced cardiomyocytes to form anisotropic morphology and possess mechanical properties closely matching those of the native heart tissues [150]. Microporous collagen scaffold can be tailored to have an elasticity modulus matching that of native heart tissue (10–15 kPa) [151]. Induced pluripotent stem cell-derived cardiomyocytes (iPSC-CMs) were seeded in the collagen scaffold and implanted into infarcted hearts following 3 days of in vitro culture. After 2 weeks of implantation, the constructs and iPSC-CMs integrated with host myocardium resulting in augmented cardiac function [152]. One of the limitations in using microporous foams is the difficulty to homogeneously seed high density of cells within the 3-D structure, and cells are unable to migrate into the inner parts of the foam due to the limited diffusion length of the nutrients and oxygen. In addition, a risk of residual chemicals exists if harsh chemical conditions are required to fabricate the porous structure [153].

Fibrous scaffolds have also been utilized for cardiac tissue regeneration because of their capacity of closely mimicking the nanoscale of collagen fibers within the myocardium. The fibers can also be fabricated to follow an aligned morphology of collagen fibers. The aligned fibers have two advantages: (1) facilitating the seeded cardiomyocytes to align and assume the morphology exhibited in the native myocardium [154] (the aligned cells have been shown to generate higher contraction force) [154] and (2) allowing to mimic anisotropic mechanical properties of the myocardium. The fibrous scaffolds are usually fabricated by electrospinning. In a typical electrospinning setup, an electric field is created between a positively charged needle and a negatively charged collector. The polymer solution is ejected from the needle, and the fibers are formed after solvent evaporation. The properties of the fibrous scaffolds, like fiber morphology, alignment, diameter, and density, are tunable by adjusting the polymer type, solvent type, polymer solution concentration, ejection rate, electric voltage, and rotation speed of the collector [155]. Guan et al. developed a nanofibrous poly(ester carbonate urethane)urea (PECUU) scaffold seeded with MSCs [156]. The electrospun scaffolds had a similar anisotropic structure and stiffness along a cross fiber-aligned orientation to native myocardium. The cells were electrosprayed and homogeneously distributed within the scaffolds. After 7 days of culture, the seeded cells were aligned within the scaffolds. Interestingly, the alignment induced the MSCs to differentiate toward cardiac lineage (Fig. 12.6).

Besides fiber alignment, fiber modulus and density have potential effect on cardiac differentiation. Xu et al. fabricated fibrous scaffolds seeded with cardiosphere-derived cells (CDCs) using a simultaneous electrospinning/electrospraying technique [157]. Tissue constructs with similar cell adhesion property but different global modulus, single fiber modulus, fiber density, and fiber alignment were developed. The CDC cardiac differentiation was found to be dependent on the scaffold modulus, fiber volume fraction, and fiber alignment. The constructs with modulus of ~50–60 kPa most significantly directed the cardiac differentiation. Comparing constructs with similar modulus, the extent of differentiation was greater for lower fiber alignment and higher fiber volume fraction.

12.4 Antifibrotic Therapy

After MI, cardiac fibrosis (scar tissue) naturally forms. It is characterized by excessive accumulation of collagen and other ECM components at the infarcted area. Myofibroblasts have been found to be responsible for the cardiac fibrosis. After MI, myofibroblasts secrete excessive stiff collagen type I, leading to the increase in ratio of collagen type I/III and tissue stiffness. Cardiac fibrosis expands during the MI and develops from acute to later stages. This negatively affects systole and diastole function of the myocardium and ultimately leads to congestive heart failure if no effective treatment is made.

The goal of myocardial antifibrotic therapy is to prevent cardiac fibrosis from expanding in the infarcted area. Since it is widely accepted that activated myofibroblasts are responsible for cardiac fibrosis, preventing myofibroblast formation represents a strategy to control cardiac fibrosis. Myofibroblasts are mainly differentiated from cardiac fibroblasts. As a major cell type in the myocardium, cardiac fibroblasts have a larger quantity than cardiomyocytes [158]. Cardiac fibroblasts play the role of maintaining ECM during homeostasis while keeping their quiescent form in a healthy heart [159]. After MI, cardiac fibroblasts interact with upregulated transforming growth factor-β1 (TGF-β1) to differentiate into myofibroblasts [160, 161]. It has been confirmed that the activated TGF-β binds to type II and type I serine/threonine kinase receptors to activate the TGF-β/SMAD signaling pathway, which then drives the differentiation [162–164]. The hypersecretory myofibroblasts produce

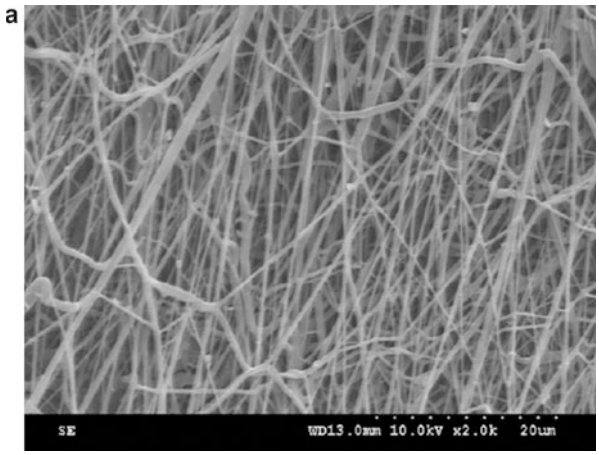

Fig. 12.6 Aligned fibers and uniaxial strain induced cell alignment and promoted cardiac differentiation [158]. (**a**) SEM image of aligned fibers; (**b**) representative Z-stack confocal images and cell anisotropic index (CAI) of MSCs in the tissue constructs stretched at different strains (0, 25, 50, and 75 %) on day 7. F-actins of the cells were stained with rhodamine phalloidin. All images were taken at a depth of 45 μm; (**c**) real-time RT-PCR analysis of cardiac-specific genes, GATA4, Nkx2.5, and MEF2C, and calcium channel CACNA1c. MSCs cultured on tissue culture plate were used as control (ctrl). The expression of these genes in control group was used for normalization

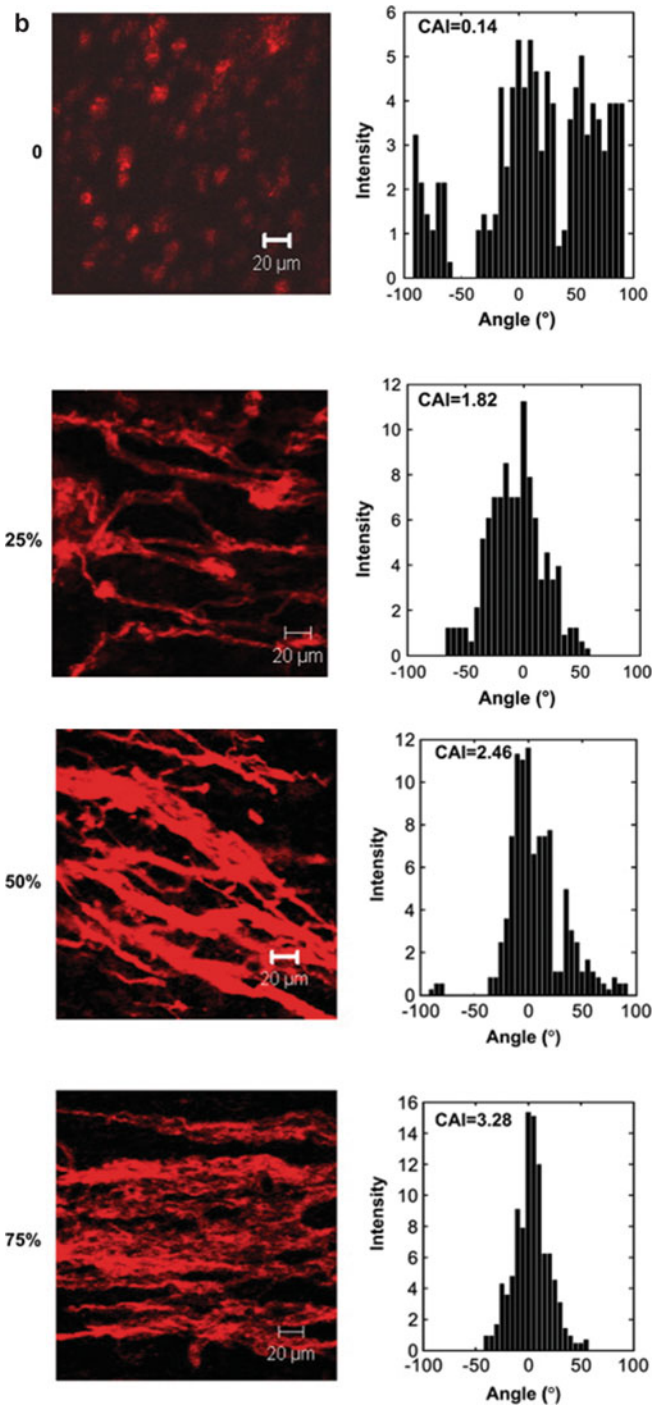

Fig. 12.6 (continued)

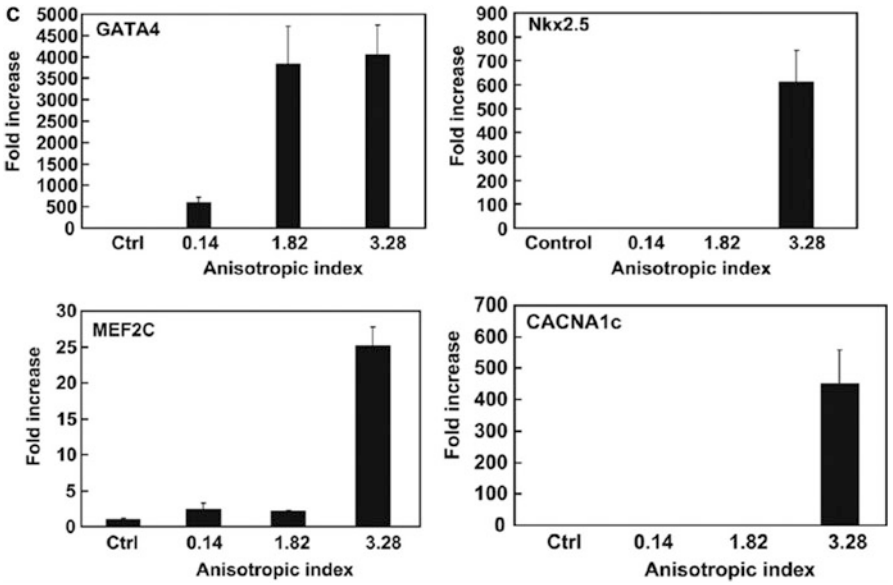

Fig. 12.6 (continued)

cytokines TGF-β to continuously promote the cardiac fibroblast differentiation into myofibroblasts. Unlike the myofibroblast in other organs, cardiac myofibroblast remains alive for years to keep contributing to the scar tissue formation [165].

Fibrocyte differentiation is another source of myofibroblasts. After MI, fibrocyte, a type of fibroblast-like peripheral cell, migrates to the infarcted site induced by chemokines such as CCL21 and CXCL12 [166, 167]. Besides morphological similarities, fibrocytes express the fibroblast-specific proteins, CD45 (leukocyte common antigen) and CD34 (hematopoietic and vascular cell marker). The expression of these two proteins concurrently decreases when the fibrocytes differentiate into myofibroblasts [168]. Besides CCL21 and CXCL12, IL-14, IL-13, and PDGF are also capable of regulating the fibrocyte differentiation [167, 169]. Epithelial-to-mesenchymal transition (EMT) is also a source of myofibroblasts, which is involved in transdifferentiation of epithelial cells into myofibroblast-like cells. During the transition, epithelial marker expression is downregulated while the mesenchymal marker expression is upregulated simultaneously [170, 171]. TGF-β contributes to the EMT process. Besides TGF-β, whether some other cytokines regulate this transition is still on debate [172, 173]. Endothelial-to-mesenchymal transition (EnMT) has emerged as a potential myofibroblast source in wound healing and progression of fibrosis. During the EnMT, the expression of endothelial cell markers, such as vascular endothelial cadherin (VE cadherin), is repressed. Meanwhile, endothelial cells are induced to express the mesenchymal cell products including α-SMA, collagen type I, and vimentin [174]. Besides the phenotypic change, the involved cells become motile and are able to migrate to the surrounding tissues. Similar to EMT, EnMT can also be driven by TGF-β [174].

12.4.1 Approaches Toward Antifibrotic Therapy

Once MI occurs, the differentiation of cardiac fibroblasts to myofibroblasts is the key step for the fibrosis cascade. Consequently, inhibiting the formation of myofibroblast is of great importance in the antifibrotic therapy. Since the upregulated cytokines and growth factors, such as TGF-β, Ang-II, and PDGF, drive the cellular transition to myofibroblasts, the current antifibrotic therapy mainly focused on reducing the amount of these cytokines and growth factors and attenuating their bioactivity. The antifibrotic drugs are typically administrated systemically by IV injection or oral intake. They can also be locally delivered using biomaterials as drug carriers. Besides antifibrotic drug therapy, biomaterial and biomaterial/cell therapies can also attenuate cardiac fibrosis (discussed in Sects. 2 and 3).

12.4.1.1 Systemic Delivery of Antifibrotic Reagent

The antifibrotic drugs capable of reducing the amount and activity of the growth factors and cytokines can directly/indirectly inhibit the formation of myofibroblasts. It has been widely accepted that TGF-β is the major mediator that induces the fibroblast-to-myofibroblast transition. Preventing the TGF-β from interacting with fibroblasts may thus inhibit myofibroblast formation. TGF-β receptor I (ALK5)-specific inhibitors have been developed for this purpose. Various reports demonstrated that these inhibitors can largely reduce cardiac fibrosis leading to an improvement of heart function [175, 176]. In cardiac fibroblasts, angiotensin II induces the expression of TGF-β1 through angiotensin type I receptor [177]. Therefore, angiotensin receptor inhibitors may be used to reduce cardiac fibrosis [178, 179]. In addition, inflammation plays a role in the formation of myofibroblasts since the cytokines released in this process, such as IL-1β and TNF-α, can promote the proliferation of cardiac fibroblasts [180]. Drugs capable of suppressing inflammation in the infarcted area may thus decrease the proliferation and reduce cardiac fibrosis [181].

The antifibrotic drugs introduced above are mainly administrated through either IV injection or oral intake. These systemic drug delivery approaches are convenient to operate. However the disadvantage is that extremely low dosage can be allocated to the infarcted area. Increasing the initial drug dosage may lead to toxic effect. Localized delivery of these drugs is a potential approach to address these concerns.

12.4.1.2 Localized Delivery of Antifibrotic Agents with Biomaterials

Localized delivery of antifibrotic agents with biomaterials has two advantages: (1) increases the drug retention in infarcted area and (2) allows drugs to be continuously released from biomaterials. Repeated injection of drugs is thus unnecessary. Studies have demonstrated that delivery of antifibrotic growth factors with

injectable hydrogels is an effective way to reduce cardiac fibrosis. HGF is known as an antifibrotic growth factor, due to its function of binding c-met and promoting apoptosis of myofibroblasts via PI3K/Akt/p70 signaling pathway [182–184]. Besides antifibrotic property, HGF possesses proangiogenic, antiapoptotic, and cardioprotective effects [185–188]. Nakano et al. developed a novel porous gelatin patch for HGF delivery. The advantage of using gelatin is that it can be entirely proteolyzed in the body, therefore minimizing the inflammatory and pharmacological responses in vivo [189]. The HGF was able to continuously release from the patch for 2 weeks in vitro [190]. After 2 and 4 weeks of implantation, the scar size was significantly decreased. This led to the increase of cardiac function.

Co-delivery of growth factors may better attenuate cardiac fibrosis than delivery of single growth factor. IGF-1 has strong antiapoptotic effect [191–193]. The delivery of IGF-1 together with HGF can largely decrease tissue apoptosis, resulting in reduced scar size. The delivery of two growth factors can also induce resident cardiac stem cell migration and activation to promote new myocardium formation [194]. Ruvinov et al. developed an alginate-based IGF-1/HGF co-delivery system and tested in rat acute MI model [195]. In vitro, the IGF-1 and HGF are completely released from the alginate for 3 and 7 days, respectively. The faster release of IGF-1 was due to its lower molecular weight. The burst release of IGF-1 provided a pro-survival signal to the cardiac cells to reduce apoptosis [196], while a relatively slower HGF release was able to play anti-inflammation, pro-angiogenesis, and anti-fibrosis roles in the later phases (Fig. 12.7). VEGF is a potent proangiogenic factor that improves regional blood flow following MI [171, 197]. HGF and VEGF were encapsulated into a degradable PEG hydrogel and delivered into infarcted hearts [198]. Twenty-one days after the implantation, the fibrosis was remarkably reduced. The delivered VEGF also exerted its proangiogenic effect as the vessel density was remarkably increased [199, 200].

Besides approaches discussed above, delivery of pure biomaterials and biomaterials/cells in the infarcted hearts has been found to decrease cardiac fibrosis. The underlying mechanisms include decreasing tissue inflammation, promoting cardiac tissue regeneration, augmenting native cell survival, and increasing tissue vascularization [201].

12.5 Conclusions and Prospectives

Biomaterials and cell therapies are promising approaches to treat MI. Biomaterial-only therapy improves cardiac function by providing mechanical support and an environment for host cell survival and proliferation. Addition of biomolecules such as drug, growth factor, and peptide may facilitate cardiac function improvement by further promoting host cell survival and proliferation, stimulating cell recruitment, controlling inflammation, and inducing angiogenesis. However, myocardial regeneration may not be readily achieved by biomaterials or biomaterial/biomolecule therapy. Cell therapy is necessary. Cardiomyocytes and stem cells that differentiate

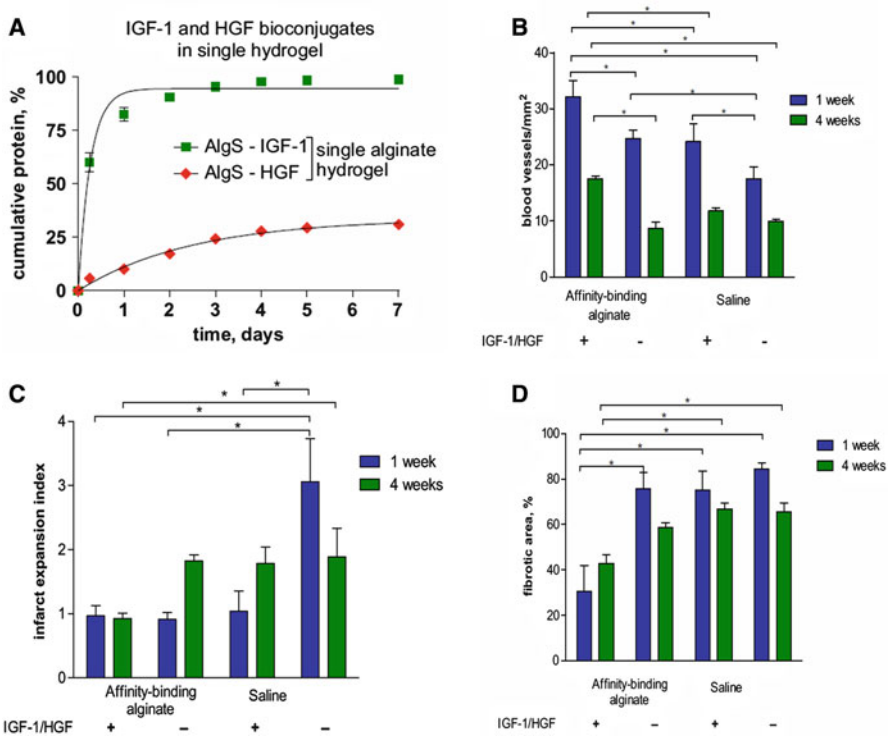

Fig. 12.7 The promotion of myocardial repair by the sequential delivery of IGF-1 and HGF from an injectable alginate biomaterial in a model of acute myocardial infarction [197]. (**A**) IGF-1 and HGF release from affinity-binding alginate microbeads was analyzed by ELISA using antibodies specific to human IGF-1 and HGF. The sequential IGF-1/HGF delivery promotes angiogenesis (**B**), attenuates infarct expansion, (**C**) and reduces fibrosis (**D**)

into cardiomyocytes can directly regenerate myocardium, while those stem cells that do not differentiate into cardiomyocytes but provide paracrine effects can indirectly regenerate myocardium. However, the efficacy of current cell therapy is low because of low cell engraftment. Low cell retention and inferior cell survival are two major causes. Using biomaterials like injectable hydrogels and scaffolds may improve cell retention. Yet current hydrogels have long gelation time. This makes it impossible to largely increase cell retention. The development of hydrogels with a fast gelation rate may address this issue. Different approaches have been explored to augment survival of transplanted cells in the ischemic conditions of infarcted hearts. While they can improve cell survival to some extent, further studies on the long-term effect of these approaches on cell survival, functioning, and differentiation are needed.

Control of cardiac fibrosis after MI is necessary because it will prevent the damaged hearts from progressing into heart failure. Systemic delivery of antifibrotic drugs is a convenient approach and widely used in clinics. However, the low drug

dosage allocated to the heart and side effects limits the therapeutic efficacy. Localized delivery of antifibrotic drugs together with biomaterials can improve the efficacy. Since the delivered biomaterials may prevent the heart tissue from rupture, this approach may control cardiac fibrosis immediately after MI so that the processes that initiate the cardiac fibrosis can be inactivated. The biomaterials may also decrease the elevated wall stress-induced inflammation. The gradual release of antifibrotic drug from the biomaterials can extend the therapeutic effect for long-term control of cardiac fibrosis. Overall, the current antifibrotic therapy has low efficacy. The development of new and translational delivery approaches to improve the efficacy will push the antifibrotic therapy toward clinical application.

Acknowledgments This work was supported by the US National Institutes of Health (R01EB022018, R01HL124122, and R21EB021896), US National Science Foundation (1006734 and 1160122), and American Heart Association (15GRNT25830058 and 13GRNT17150041).

References

1. Mozaffarian D, Benjamin EJ, Go AS, Arnett DK, Blaha MJ, Cushman M, et al. Heart disease and stroke statistics – 2015 update: a report from the American Heart Association. Circulation. 2015;131:e29–322.
2. Wang F, Li Z, Khan M, Tamama K, Kuppusamy P, Wagner WR, et al. Injectable, rapid gelling and highly flexible hydrogel composites as growth factor and cell carriers. Acta Biomater. 2010;6:1978–91.
3. Li Z, Guan J. Hydrogels for cardiac tissue engineering. Polymers. 2011;3:740–61.
4. Etzion S, Kedes LH, Kloner RA, Leor J. Myocardial regeneration: present and future trends. Am J Cardiovasc Drugs: Drugs, Devices, Other Interv. 2001;1:233–44.
5. Mann DL. Mechanisms and models in heart failure: a combinatorial approach. Circulation. 1999;100:999–1008.
6. Kim D-H, Kim P, Song I, Cha JM, Lee SH, Kim B, et al. Guided three-dimensional growth of functional cardiomyocytes on polyethylene glycol nanostructures. Langmuir. 2006;22:5419–26.
7. Wang RM, Christman KL. Decellularized myocardial matrix hydrogels: in basic research and preclinical studies. Adv Drug Deliv Rev. 2016;96:77–82.
8. Okada M, Payne TR, Oshima H, Momoi N, Tobita K, Huard J. Differential efficacy of gels derived from small intestinal submucosa as an injectable biomaterial for myocardial infarct repair. Biomaterials. 2010;31:7678–83.
9. Seif-Naraghi SB, Singelyn JM, Salvatore MA, Osborn KG, Wang JJ, Sampat U, et al. Safety and efficacy of an injectable extracellular matrix hydrogel for treating myocardial infarction. Sci Transl Med. 2013;5:173ra25.
10. Singelyn JM, Sundaramurthy P, Johnson TD, Schup-Magoffin PJ, Hu DP, Faulk DM, et al. Catheter-deliverable hydrogel derived from decellularized ventricular extracellular matrix increases endogenous cardiomyocytes and preserves cardiac function post-myocardial infarction. J Am Coll Cardiol. 2012;59:751–63.
11. Chenite A, Chaput C, Wang D, Combes C, Buschmann M, Hoemann C, et al. Novel injectable neutral solutions of chitosan form biodegradable gels in situ. Biomaterials. 2000;21:2155–61.
12. Léobon B, Garcin I, Menasché P, Vilquin J-T, Audinat E, Charpak S. Myoblasts transplanted into rat infarcted myocardium are functionally isolated from their host. Proc Natl Acad Sci. 2003;100:7808–11.

13. Lu W-N, Lü S-H, Wang H-B, Li D-X, Duan C-M, Liu Z-Q, et al. Functional improvement of infarcted heart by co-injection of embryonic stem cells with temperature-responsive chitosan hydrogel. Tissue Eng Part A. 2008;15:1437–47.
14. Liu Z, Wang H, Wang Y, Lin Q, Yao A, Cao F, et al. The influence of chitosan hydrogel on stem cell engraftment, survival and homing in the ischemic myocardial microenvironment. Biomaterials. 2012;33:3093–106.
15. Ifkovits JL, Tous E, Minakawa M, Morita M, Robb JD, Koomalsingh KJ, et al. Injectable hydrogel properties influence infarct expansion and extent of postinfarction left ventricular remodeling in an ovine model. Proc Natl Acad Sci. 2010;107:11507–12.
16. Draget KI, Østgaard K, Smidsrød O. Homogeneous alginate gels: a technical approach. Carbohydr Polym. 1990;14:159–78.
17. Landa N, Miller L, Feinberg MS, Holbova R, Shachar M, Freeman I, et al. Effect of injectable alginate implant on cardiac remodeling and function after recent and old infarcts in rat. Circulation. 2008;117:1388–96.
18. Leor J, Tuvia S, Guetta V, Manczur F, Castel D, Willenz U, et al. Intracoronary injection of in situ forming alginate hydrogel reverses left ventricular remodeling after myocardial infarction in Swine. J Am Coll Cardiol. 2009;54:1014–23.
19. Dahlmann J, Krause A, Möller L, Kensah G, Möwes M, Diekmann A, et al. Fully defined in situ cross-linkable alginate and hyaluronic acid hydrogels for myocardial tissue engineering. Biomaterials. 2013;34:940–51.
20. Tsur-Gang O, Ruvinov E, Landa N, Holbova R, Feinberg MS, Leor J, et al. The effects of peptide-based modification of alginate on left ventricular remodeling and function after myocardial infarction. Biomaterials. 2009;30:189–95.
21. Mukherjee R, Zavadzkas JA, Saunders SM, McLean JE, Jeffords LB, Beck C, et al. Targeted myocardial microinjections of a biocomposite material reduces infarct expansion in pigs. Ann Thorac Surg. 2008;86:1268–76.
22. Kleinman HK, Martin GR. Matrigel: basement membrane matrix with biological activity. Semin Cancer Biol. 2005;15:378–86.
23. Tai KF, Chen PJ, Chen DS, Hwang LH. Concurrent delivery of GM-CSF and endostatin genes by a single adenoviral vector provides a synergistic effect on the treatment of orthotopic liver tumors. J Gene Med. 2003;5:386–98.
24. Ou L, Li W, Zhang Y, Wang W, Liu J, Sorg H, et al. Intracardiac injection of matrigel induces stem cell recruitment and improves cardiac functions in a rat myocardial infarction model. J Cell Mol Med. 2011;15:1310–8.
25. Li Z, Wang F, Roy S, Sen CK, Guan J. Injectable, highly flexible, and thermosensitive hydrogels capable of delivering superoxide dismutase. Biomacromolecules. 2009;10:3306–16.
26. Xu G, Wang X, Deng C, Teng X, Suuronen EJ, Shen Z, et al. Injectable biodegradable hybrid hydrogels based on thiolated collagen and oligo (acryloyl carbonate)–poly (ethylene glycol)–oligo (acryloyl carbonate) copolymer for functional cardiac regeneration. Acta Biomater. 2015;15:55–64.
27. Williams C, Budina E, Stoppel WL, Sullivan KE, Emani S, Emani SM, et al. Cardiac extracellular matrix–fibrin hybrid scaffolds with tunable properties for cardiovascular tissue engineering. Acta Biomater. 2015;14:84–95.
28. Fujimoto KL, Ma Z, Nelson DM, Hashizume R, Guan J, Tobita K, et al. Synthesis, characterization and therapeutic efficacy of a biodegradable, thermoresponsive hydrogel designed for application in chronic infarcted myocardium. Biomaterials. 2009;30:4357–68.
29. Jiang XJ, Wang T, Li XY, Wu DQ, Zheng ZB, Zhang JF, et al. Injection of a novel synthetic hydrogel preserves left ventricle function after myocardial infarction. J Biomed Mater Res A. 2009;90:472–7.
30. Bawa P, Pillay V, Choonara YE, du Toit LC. Stimuli-responsive polymers and their applications in drug delivery. Biomed Mater (Bristol, England). 2009;4:022001.
31. Crompton KE, Goud JD, Bellamkonda RV, Gengenbach TR, Finkelstein DI, Horne MK, et al. Polylysine-functionalised thermoresponsive chitosan hydrogel for neural tissue engineering. Biomaterials. 2007;28:441–9.

32. Davis ME, Hsieh PC, Takahashi T, Song Q, Zhang S, Kamm RD, et al. Local myocardial insulin-like growth factor 1 (IGF-1) delivery with biotinylated peptide nanofibers improves cell therapy for myocardial infarction. Proc Natl Acad Sci U S A. 2006;103:8155–60.
33. Li Y, Rodrigues J, Tomás H. Injectable and biodegradable hydrogels: gelation, biodegradation and biomedical applications. Chem Soc Rev. 2012;41:2193–221.
34. Guan J, Hong Y, Ma Z, Wagner WR. Protein-reactive, thermoresponsive copolymers with high flexibility and biodegradability. Biomacromolecules. 2008;9:1283–92.
35. Li H, Duann P, Lin PH, Zhao L, Fan Z, Tan T, et al. Modulation of wound healing and scar formation by MG53 protein-mediated cell membrane repair. J Biol Chem. 2015;290:24592–603.
36. Li Z, Fan Z, Xu Y, Lo W, Wang X, Niu H, et al. pH-sensitive and thermosensitive hydrogels as stem-cell carriers for cardiac therapy. ACS Appl Mater Interfaces. 2016;8:10752–60.
37. Li Z, Fan Z, Xu Y, Niu H, Xie X, Liu Z, et al. Thermosensitive and highly flexible hydrogels capable of stimulating cardiac differentiation of cardiosphere-derived cells under static and dynamic mechanical training conditions. ACS Appl Mater Interfaces. 2016;8:15948–57.
38. Li Z, Guo X, Guan J. A thermosensitive hydrogel capable of releasing bFGF for enhanced differentiation of mesenchymal stem cell into cardiomyocyte-like cells under ischemic conditions. Biomacromolecules. 2012;13:1956–64.
39. Li Z, Guo X, Guan J. An oxygen release system to augment cardiac progenitor cell survival and differentiation under hypoxic condition. Biomaterials. 2012;33:5914–23.
40. Li Z, Guo X, Matsushita S, Guan J. Differentiation of cardiosphere-derived cells into a mature cardiac lineage using biodegradable poly(N-isopropylacrylamide) hydrogels. Biomaterials. 2011;32:3220–32.
41. Li Z, Guo X, Palmer AF, Das H, Guan J. High-efficiency matrix modulus-induced cardiac differentiation of human mesenchymal stem cells inside a thermosensitive hydrogel. Acta Biomater. 2012;8:3586–95.
42. Wang F, Li Z, Lannutti JL, Wagner WR, Guan J. Synthesis, characterization and surface modification of low moduli poly(ether carbonate urethane)ureas for soft tissue engineering. Acta Biomater. 2009;5:2901–12.
43. Xu Y, Fu M, Li Z, Fan Z, Li X, Liu Y, et al. A prosurvival and proangiogenic stem cell delivery system to promote ischemic limb regeneration. Acta Biomater. 2016;31:99–113.
44. Xu Y, Li Z, Li X, Fan Z, Liu Z, Xie X, et al. Regulating myogenic differentiation of mesenchymal stem cells using thermosensitive hydrogels. Acta Biomater. 2015;26:23–33.
45. Nelson DM, Hashizume R, Yoshizumi T, Blakney AK, Ma Z, Wagner WR. Intramyocardial injection of a synthetic hydrogel with delivery of bFGF and IGF1 in a rat model of ischemic cardiomyopathy. Biomacromolecules. 2014;15:1–11.
46. Yoshizumi T, Zhu Y, Jiang H, D'Amore A, Sakaguchi H, Tchao J, et al. Timing effect of intramyocardial hydrogel injection for positively impacting left ventricular remodeling after myocardial infarction. Biomaterials. 2016;83:182–93.
47. Wall ST, Yeh CC, Tu RY, Mann MJ, Healy KE. Biomimetic matrices for myocardial stabilization and stem cell transplantation. J Biomed Mater Res A. 2010;95:1055–66.
48. Garbern JC, Minami E, Stayton PS, Murry CE. Delivery of basic fibroblast growth factor with a pH-responsive, injectable hydrogel to improve angiogenesis in infarcted myocardium. Biomaterials. 2011;32:2407–16.
49. Blackburn NJ, Sofrenovic T, Kuraitis D, Ahmadi A, McNeill B, Deng C, et al. Timing underpins the benefits associated with injectable collagen biomaterial therapy for the treatment of myocardial infarction. Biomaterials. 2015;39:182–92.
50. Holmes JW, Borg TK, Covell JW. Structure and mechanics of healing myocardial infarcts. Annu Rev Biomed Eng. 2005;7:223–53.
51. Li X, Zhou J, Liu Z, Chen J, Lü S, Sun H, et al. A PNIPAAm-based thermosensitive hydrogel containing SWCNTs for stem cell transplantation in myocardial repair. Biomaterials. 2014;35:5679–88.

52. Chen Y-S, Tsou P-C, Lo J-M, Tsai H-C, Wang Y-Z, Hsiue G-H. Poly (N-isopropylacrylamide) hydrogels with interpenetrating multiwalled carbon nanotubes for cell sheet engineering. Biomaterials. 2013;34:7328–34.
53. Odian G. Principles of polymerization. Hoboken: Wiley; 2004.
54. Kraehenbuehl TP, Ferreira LS, Hayward AM, Nahrendorf M, van der Vlies AJ, Vasile E, et al. Human embryonic stem cell-derived microvascular grafts for cardiac tissue preservation after myocardial infarction. Biomaterials. 2011;32:1102–9.
55. Wang T, Jiang XJ, Tang QZ, Li XY, Lin T, Wu DQ, et al. Bone marrow stem cells implantation with alpha-cyclodextrin/MPEG-PCL-MPEG hydrogel improves cardiac function after myocardial infarction. Acta Biomater. 2009;5:2939–44.
56. French KM, Somasuntharam I, Davis ME. Self-assembling peptide-based delivery of therapeutics for myocardial infarction. Adv Drug Deliv Rev. 2016;96:40–53.
57. Davis ME, Motion JP, Narmoneva DA, Takahashi T, Hakuno D, Kamm RD, et al. Injectable self-assembling peptide nanofibers create intramyocardial microenvironments for endothelial cells. Circulation. 2005;111:442–50.
58. Callegari A, Bollini S, Iop L, Chiavegato A, Torregrossa G, Pozzobon M, et al. Neovascularization induced by porous collagen scaffold implanted on intact and cryoinjured rat hearts. Biomaterials. 2007;28:5449–61.
59. Zhang G, Nakamura Y, Wang X, Hu Q, Suggs LJ, Zhang J. Controlled release of stromal cell-derived factor-1 alpha in situ increases c-kit+ cell homing to the infarcted heart. Tissue Eng. 2007;13:2063–71.
60. Tan MY, Zhi W, Wei RQ, Huang YC, Zhou KP, Tan B, et al. Repair of infarcted myocardium using mesenchymal stem cell seeded small intestinal submucosa in rabbits. Biomaterials. 2009;30:3234–40.
61. Fujimoto KL, Tobita K, Merryman WD, Guan J, Momoi N, Stolz DB, et al. An elastic, biodegradable cardiac patch induces contractile smooth muscle and improves cardiac remodeling and function in subacute myocardial infarction. J Am Coll Cardiol. 2007;49:2292–300.
62. Fujimoto KL, Tobita K, Guan J, Hashizume R, Takanari K, Alfieri CM, et al. Placement of an elastic biodegradable cardiac patch on a subacute infarcted heart leads to cellularization with early developmental cardiomyocyte characteristics. J Card Fail. 2012;18:585–95.
63. Piao H, Kwon JS, Piao S, Sohn JH, Lee YS, Bae JW, et al. Effects of cardiac patches engineered with bone marrow-derived mononuclear cells and PGCL scaffolds in a rat myocardial infarction model. Biomaterials. 2007;28:641–9.
64. Jin J, Jeong SI, Shin YM, Lim KS, Shin H, Lee YM, et al. Transplantation of mesenchymal stem cells within a poly(lactide-co-epsilon-caprolactone) scaffold improves cardiac function in a rat myocardial infarction model. Eur J Heart Fail. 2009;11:147–53.
65. Hosoda T, Zheng H, Cabral-da-Silva M, Sanada F, Ide-Iwata N, Ogorek B, et al. Human cardiac stem cell differentiation is regulated by a mircrine mechanism. Circulation. 2011;123:1287–96.
66. Chugh AR, Beache GM, Loughran JH, Mewton N, Elmore JB, Kajstura J, et al. Administration of cardiac stem cells in patients with ischemic cardiomyopathy: the SCIPIO trial: surgical aspects and interim analysis of myocardial function and viability by magnetic resonance. Circulation. 2012;126:S54–64.
67. Bolli R, Tang XL, Sanganalmath SK, Rimoldi O, Mosna F, Abdel-Latif A, et al. Intracoronary delivery of autologous cardiac stem cells improves cardiac function in a porcine model of chronic ischemic cardiomyopathy. Circulation. 2013;128:122–31.
68. Latham N, Ye B, Jackson R, Lam BK, Kuraitis D, Ruel M, et al. Human blood and cardiac stem cells synergize to enhance cardiac repair when cotransplanted into ischemic myocardium. Circulation. 2013;128:S105–12.
69. Williams AR, Hatzistergos KE, Addicott B, McCall F, Carvalho D, Suncion V, et al. Enhanced effect of combining human cardiac stem cells and bone marrow mesenchymal stem cells to reduce infarct size and to restore cardiac function after myocardial infarction. Circulation. 2013;127:213–23.

70. Spater D, Abramczuk MK, Buac K, Zangi L, Stachel MW, Clarke J, et al. A HCN4+ cardiomyogenic progenitor derived from the first heart field and human pluripotent stem cells. Nat Cell Biol. 2013;15:1098–106.
71. Nsair A, Schenke-Layland K, Van Handel B, Evseenko D, Kahn M, Zhao P, et al. Characterization and therapeutic potential of induced pluripotent stem cell-derived cardiovascular progenitor cells. PLoS One. 2012;7:e45603.
72. Hudson J, Titmarsh D, Hidalgo A, Wolvetang E, Cooper-White J. Primitive cardiac cells from human embryonic stem cells. Stem Cells Dev. 2012;21:1513–23.
73. Smith RR, Barile L, Cho HC, Leppo MK, Hare JM, Messina E, et al. Regenerative potential of cardiosphere-derived cells expanded from percutaneous endomyocardial biopsy specimens. Circulation. 2007;115:896–908.
74. Davis DR, Zhang Y, Smith RR, Cheng K, Terrovitis J, Malliaras K, et al. Validation of the cardiosphere method to culture cardiac progenitor cells from myocardial tissue. PLoS One. 2009;4:e7195.
75. Johnston PV, Sasano T, Mills K, Evers R, Lee ST, Smith RR, et al. Engraftment, differentiation, and functional benefits of autologous cardiosphere-derived cells in porcine ischemic cardiomyopathy. Circulation. 2009;120:1075–83.
76. Chimenti I, Smith RR, Li TS, Gerstenblith G, Messina E, Giacomello A, et al. Relative roles of direct regeneration versus paracrine effects of human cardiosphere-derived cells transplanted into infarcted mice. Circ Res. 2010;106:971–80.
77. Mishra R, Vijayan K, Colletti EJ, Harrington DA, Matthiesen TS, Simpson D, et al. Characterization and functionality of cardiac progenitor cells in congenital heart patients. Circulation. 2011;123:364–73.
78. Li TS, Cheng K, Malliaras K, Smith RR, Zhang Y, Sun B, et al. Direct comparison of different stem cell types and subpopulations reveals superior paracrine potency and myocardial repair efficacy with cardiosphere-derived cells. J Am Coll Cardiol. 2012;59:942–53.
79. Maxeiner H, Mufti S, Krehbiehl N, Dulfer F, Helmig S, Schneider J, et al. Interleukin-6 contributes to the paracrine effects of cardiospheres cultured from human, murine and rat hearts. J Cell Physiol. 2014;229:1681–9.
80. Xie Y, Ibrahim A, Cheng K, Wu Z, Liang W, Malliaras K, et al. Importance of cell-cell contact in the therapeutic benefits of cardiosphere-derived cells. Stem Cells (Dayton, Ohio). 2014;32:2397–406.
81. Davis DR, Kizana E, Terrovitis J, Barth AS, Zhang YQ, Smith RR, et al. Isolation and expansion of functionally-competent cardiac progenitor cells directly from heart biopsies. J Mol Cell Cardiol. 2010;49:312–21.
82. Davis DR, Zhang YQ, Smith RR, Cheng K, Terrovitis J, Malliaras K, et al. Validation of the cardiosphere method to culture cardiac progenitor cells from myocardial tissue. Plos One. 2009;4:e7195.
83. Lee ST, White AJ, Matsushita S, Malliaras K, Steenbergen C, Zhang Y, et al. Intramyocardial injection of autologous cardiospheres or cardiosphere-derived cells preserves function and minimizes adverse ventricular remodeling in pigs with heart failure post-myocardial infarction. J Am Coll Cardiol. 2011;57:455–65.
84. Forrester JS, Makkar RR, Marban E. Long-term outcome of stem cell therapy for acute myocardial infarction: right results, wrong reasons. J Am Coll Cardiol. 2009;53:2270–2.
85. Wang F, Guan J. Cellular cardiomyoplasty and cardiac tissue engineering for myocardial therapy. Adv Drug Deliv Rev. 2010;62:784–97.
86. Don CW, Murry CE. Improving survival and efficacy of pluripotent stem cell-derived cardiac grafts. J Cell Mol Med. 2013;17:1355–62.
87. Tang YL, Wang YJ, Chen LJ, Pan YH, Zhang L, Weintraub NL. Cardiac-derived stem cell-based therapy for heart failure: progress and clinical applications. Expl Biol Med (Maywood, NJ). 2013;238:294–300.
88. Garbern JC, Lee RT. Cardiac stem cell therapy and the promise of heart regeneration. Cell Stem Cell. 2013;12:689–98.

89. Rosen MR, Myerburg RJ, Francis DP, Cole GD, Marban E. Translating stem cell research to cardiac disease therapies: pitfalls and prospects for improvement. J Am Coll Cardiol. 2014;64:922–37.
90. van Berlo JH, Molkentin JD. An emerging consensus on cardiac regeneration. Nat Med. 2014;20:1386–93.
91. Nagaya N, Kangawa K, Itoh T, Iwase T, Murakami S, Miyahara Y, et al. Transplantation of mesenchymal stem cells improves cardiac function in a rat model of dilated cardiomyopathy. Circulation. 2005;112:1128–35.
92. Gnecchi M, He H, Noiseux N, Liang OD, Zhang L, Morello F, et al. Evidence supporting paracrine hypothesis for Akt-modified mesenchymal stem cell-mediated cardiac protection and functional improvement. FASEB J: Off Publ Fed Am Soc Exp Biol. 2006;20:661–9.
93. Ripa RS, Haack-Sorensen M, Wang Y, Jorgensen E, Mortensen S, Bindslev L, et al. Bone marrow derived mesenchymal cell mobilization by granulocyte-colony stimulating factor after acute myocardial infarction: results from the Stem Cells in Myocardial Infarction (STEMMI) trial. Circulation. 2007;116:I24–30.
94. Hare JM, Traverse JH, Henry TD, Dib N, Strumpf RK, Schulman SP, et al. A randomized, double-blind, placebo-controlled, dose-escalation study of intravenous adult human mesenchymal stem cells (prochymal) after acute myocardial infarction. J Am Coll Cardiol. 2009;54:2277–86.
95. Traverse JH, McKenna DH, Harvey K, Jorgenso BC, Olson RE, Bostrom N, et al. Results of a phase 1, randomized, double-blind, placebo-controlled trial of bone marrow mononuclear stem cell administration in patients following ST-elevation myocardial infarction. Am Heart J. 2010;160:428–34.
96. Duran JM, Makarewich CA, Sharp TE, Starosta T, Zhu F, Hoffman NE, et al. Bone-derived stem cells repair the heart after myocardial infarction through transdifferentiation and paracrine signaling mechanisms. Circ Res. 2013;113:539–52.
97. Toma C, Pittenger MF, Cahill KS, Byrne BJ, Kessler PD. Human mesenchymal stem cells differentiate to a cardiomyocyte phenotype in the adult murine heart. Circulation. 2002;105:93–8.
98. Balana B, Nicoletti C, Zahanich I, Graf EM, Christ T, Boxberger S, et al. 5-Azacytidine induces changes in electrophysiological properties of human mesenchymal stem cells. Cell Res. 2006;16:949–60.
99. Qian Q, Qian H, Zhang X, Zhu W, Yan YM, Ye SQ, et al. 5-azacytidine induces cardiac differentiation of human umbilical cord-derived mesenchymal stem cells by activating extracellular regulated kinase. Stem Cells Dev. 2012;21:67–75.
100. Wang CC, Chen CH, Lin WW, Hwang SM, Hsieh PCH, Lai PH, et al. Direct intramyocardial injection of mesenchymal stem cell sheet fragments improves cardiac functions after infarction. Cardiovasc Res. 2008;77:515–24.
101. Martinez EC, Kofidis T. Adult stem cells for cardiac tissue engineering. J Mol Cell Cardiol. 2011;50:312–9.
102. Perin EC, Tian M, Marini FC, Silva GV, Zheng Y, Baimbridge F, et al. Imaging long-term fate of intramyocardially implanted mesenchymal stem cells in a porcine myocardial infarction model. Plos One. 2011;6:e22949.
103. Pittenger MF, Martin BJ. Mesenchymal stem cells and their potential as cardiac therapeutics. Circ Res. 2004;95:9–20.
104. Mias C, Lairez O, Trouche E, Roncalli J, Calise D, Seguelas MH, et al. Mesenchymal stem cells promote matrix metalloproteinase secretion by cardiac fibroblasts and reduce cardiac ventricular fibrosis after myocardial infarction. Stem Cells (Dayton, Ohio). 2009;27:2734–43.
105. Zuo S, Jones WK, Li HX, He ZS, Pasha ZS, Yang YT, et al. Paracrine effect of Wnt11-overexpressing mesenchymal stem cells on ischemic injury. Stem Cells Dev. 2012; 21:598–608.

106. Mazo M, Planat-Benard V, Abizanda G, Pelacho B, Leobon B, Gavira JJ, et al. Transplantation of adipose derived stromal cells is associated with functional improvement in a rat model of chronic myocardial infarction. Eur J Heart Fail. 2008;10:454–62.
107. Mazo M, Hernandez S, Gavira JJ, Abizanda G, Arana M, Lopez-Martinez T, et al. Treatment of reperfused ischemia with adipose-derived stem cells in a preclinical Swine model of myocardial infarction. Cell Transplant. 2012;21:2723–33.
108. Shevchenko EK, Makarevich PI, Tsokolaeva ZI, Boldyreva MA, Sysoeva VY, Tkachuk VA, et al. Transplantation of modified human adipose derived stromal cells expressing VEGF165 results in more efficient angiogenic response in ischemic skeletal muscle. J Transl Med. 2013;11:138.
109. Rigol M, Solanes N, Roura S, Roque M, Novensa L, Dantas AP, et al. Allogeneic adipose stem cell therapy in acute myocardial infarction. Eur J Clin Invest. 2014;44:83–92.
110. Frisch SM, Francis H. Disruption of epithelial cell-matrix interactions induces apoptosis. J Cell Biol. 1994;124:619–26.
111. Baldi A, Abbate A, Bussani R, Patti G, Melfi R, Angelini A, et al. Apoptosis and post-infarction left ventricular remodeling. J Mol Cell Cardiol. 2002;34:165–74.
112. Khoynezhad A, Jalali Z, Tortolani AJ. Apoptosis: pathophysiology and therapeutic implications for the cardiac surgeon. Ann Thorac Surg. 2004;78:1109–18.
113. Reinecke H, Murry CE. Taking the death toll after cardiomyocyte grafting: a reminder of the importance of quantitative biology. J Mol Cell Cardiol. 2002;34:251–3.
114. Li X, Tamama K, Xie X, Guan J. Improving cell engraftment in cardiac stem cell therapy. Stem Cells Int. 2016;2016:7168797.
115. Jiang S, Haider H, Idris NM, Salim A, Ashraf M. Supportive interaction between cell survival signaling and angiocompetent factors enhances donor cell survival and promotes angiomyogenesis for cardiac repair. Circ Res. 2006;99:776–84.
116. Maulik N, Yoshida T, Engelman RM, Deaton D, Flack 3rd JE, Rousou JA, et al. Ischemic preconditioning attenuates apoptotic cell death associated with ischemia/reperfusion. Mol Cell Biochem. 1998;186:139–45.
117. Su J, Hu BH, Lowe Jr WL, Kaufman DB, Messersmith PB. Anti-inflammatory peptide-functionalized hydrogels for insulin-secreting cell encapsulation. Biomaterials. 2010;31:308–14.
118. Kadner K, Dobner S, Franz T, Bezuidenhout D, Sirry MS, Zilla P, et al. The beneficial effects of deferred delivery on the efficiency of hydrogel therapy post myocardial infarction. Biomaterials. 2012;33:2060–6.
119. Deuse T, Peter C, Fedak PWM, Doyle T, Reichenspurner H, Zimmermann WH, et al. Hepatocyte growth factor or vascular endothelial growth factor gene transfer maximizes mesenchymal stem cell-based myocardial salvage after acute myocardial infarction. Circulation. 2009;120:S247–54.
120. Lee TJ, Bhang SH, Yang HS, La WG, Yoon HH, Shin JY, et al. Enhancement of long-term angiogenic efficacy of adipose stem cells by delivery of FGF2. Microvasc Res. 2012;84:1–8.
121. Nor JE, Christensen J, Mooney DJ, Polverini PJ. Vascular endothelial growth factor (VEGF)-mediated angiogenesis is associated with enhanced endothelial cell survival and induction of Bcl-2 expression. Am J Pathol. 1999;154:375–84.
122. Lynch SE, Decastilla GR, Williams RC, Kiritsy CP, Howell TH, Reddy MS, et al. The effects of short-term application of a combination of platelet-derived and insulin-like growth-factors on periodontal wound-healing. J Periodontol. 1991;62:458–67.
123. Nixon AJ, Brower-Toland BD, Bent SJ, Saxer RA, Wilke MJ, Robbins PD, et al. Insulinlike growth factor-I gene therapy applications for cartilage repair. Clin Orthop Rel Res. 2000;379:S201–13.
124. Martens TP, Godier AFG, Parks JJ, Wan LQ, Koeckert MS, Eng GM, et al. Percutaneous cell delivery into the heart using hydrogels polymerizing in situ. Cell Transplant. 2009;18:297–304.

125. Li Z, Guan J. Thermosensitive hydrogels for drug delivery. Expert Opin Drug Deliv. 2011;8:991–1007.
126. Babensee JE, McIntire LV, Mikos AG. Growth factor delivery for tissue engineering. Pharm Res. 2000;17:497–504.
127. Ma F, Xiao Z, Chen B, Hou X, Han J, Zhao Y, et al. Accelerating proliferation of neural stem/progenitor cells in collagen sponges immobilized with engineered basic fibroblast growth factor for nervous system tissue engineering. Biomacromolecules. 2014;15:1062–8.
128. Chen Y, Xu H, Liu J, Zhang C, Leutz A, Mo X. The c-Myb functions as a downstream target of PDGF-mediated survival signal in vascular smooth muscle cells. Biochem Biophys Res Commun. 2007;360:433–6.
129. Haider H, Ye L, Jiang S, Ge R, Law PK, Chua T, et al. Angiomyogenesis for cardiac repair using human myoblasts as carriers of human vascular endothelial growth factor. J Mol Med (Berlin, Germany). 2004;82:539–49.
130. Xu P, Liu J, Derynck R. Post-translational regulation of TGF-beta receptor and Smad signaling. FEBS Lett. 2012;586:1871–84.
131. Xue YY, Yan Y, Gong H, Fang B, Zhou Y, Ding ZW, et al. Insulin-like growth factor binding protein 4 enhances cardiomyocytes induction in murine-induced pluripotent stem cells. J Cell Biochem. 2014;115:1495–504.
132. Minato A, Ise H, Goto M, Akaike T. Cardiac differentiation of embryonic stem cells by substrate immobilization of insulin-like growth factor binding protein 4 with elastin-like polypeptides. Biomaterials. 2012;33:515–23.
133. Choi KC, Yoo DS, Cho KS, Huh PW, Kim DS, Park CK. Effect of single growth factor and growth factor combinations on differentiation of neural stem cells. J Korean Neurosurg Soc. 2008;44:375–81.
134. Koudstaal S, Bastings MM, Feyen DA, Waring CD, van Slochteren FJ, Dankers PY, et al. Sustained delivery of insulin-like growth factor-1/hepatocyte growth factor stimulates endogenous cardiac repair in the chronic infarcted pig heart. J Cardiovasc Transl Res. 2014;7:232–41.
135. Li RH. Materials for immunoisolated cell transplantation. Adv Drug Deliv Rev. 1998;33:87–109.
136. Wilson JT, Chaikof EL. Challenges and emerging technologies in the immunoisolation of cells and tissues. Adv Drug Deliv Rev. 2008;60:124–45.
137. Weber LM, Hayda KN, Anseth KS. Cell-matrix interactions improve beta-cell survival and insulin secretion in three-dimensional culture. Tissue Eng Part A. 2008;14:1959–68.
138. Weber LM, Anseth KS. Hydrogel encapsulation environments functionalized with extracellular matrix interactions increase islet insulin secretion. Matrix Biol: J Int Soc Matrix Biol. 2008;27:667–73.
139. Lin CC, Anseth KS. Glucagon-like peptide-1 functionalized PEG hydrogels promote survival and function of encapsulated pancreatic beta-cells. Biomacromolecules. 2009;10:2460–7.
140. Shuh M, Bohorquez H, Loss Jr GE, Cohen AJ. Tumor necrosis factor-alpha: life and death of hepatocytes during liver ischemia/reperfusion injury. Ochsner J. 2013;13:119–30.
141. de Vos P, Marchetti P. Encapsulation of pancreatic islets for transplantation in diabetes: the untouchable islets. Trends Mol Med. 2002;8:363–6.
142. Jang JY, Lee DY, Park SJ, Byun Y. Immune reactions of lymphocytes and macrophages against PEG-grafted pancreatic islets. Biomaterials. 2004;25:3663–9.
143. Hume PS, Anseth KS. Polymerizable superoxide dismutase mimetic protects cells encapsulated in poly(ethylene glycol) hydrogels from reactive oxygen species-mediated damage. J Biomed Mater Res A. 2011;99:29–37.
144. Lin CC, Metters AT, Anseth KS. Functional PEG-peptide hydrogels to modulate local inflammation induced by the pro-inflammatory cytokine TNFalpha. Biomaterials. 2009;30:4907–14.
145. Guo J, Zheng D, Li WF, Li HR, Zhang AD, Li ZC. Insulin-like growth factor 1 treatment of MSCs attenuates inflammation and cardiac dysfunction following MI. Inflammation. 2014;37:2156–63.

146. Eschenhagen T, Fink C, Remmers U, Scholz H, Wattchow J, Weil J, et al. Three-dimensional reconstitution of embryonic cardiomyocytes in a collagen matrix: a new heart muscle model system. FASEB J. 1997;11:683–94.
147. Shapiro L, Cohen S. Novel alginate sponges for cell culture and transplantation. Biomaterials. 1997;18:583–90.
148. Caspi O, Lesman A, Basevitch Y, Gepstein A, Arbel G, Huber I, et al. Tissue engineering of vascularized cardiac muscle from human embryonic stem cells. Circ Res. 2007;100:263–72.
149. Engelmayr Jr GC, Cheng M, Bettinger CJ, Borenstein JT, Langer R, Freed LE. Accordion-like honeycombs for tissue engineering of cardiac anisotropy. Nat Mater. 2008;7:1003–10.
150. Masoumi N, Johnson KL, Howell MC, Engelmayr Jr GC. Valvular interstitial cell seeded poly(glycerol sebacate) scaffolds: toward a biomimetic in vitro model for heart valve tissue engineering. Acta Biomater. 2013;9:5974–88.
151. Berry MF, Engler AJ, Woo YJ, Pirolli TJ, Bish LT, Jayasankar V, et al. Mesenchymal stem cell injection after myocardial infarction improves myocardial compliance. Am J Physiol Heart Circ Physiol. 2006;290:10.
152. Joanne P, Kitsara M, Boitard SE, Naemetalla H, Vanneaux V, Pernot M, et al. Nanofibrous clinical-grade collagen scaffolds seeded with human cardiomyocytes induces cardiac remodeling in dilated cardiomyopathy. Biomaterials. 2016;80:157–68.
153. Janik H, Marzec M. A review: fabrication of porous polyurethane scaffolds. Mater Sci Eng C Mater Biol Appl. 2015;48:586–91.
154. Khan M, Xu Y, Hua S, Johnson J, Belevych A, Janssen PM, et al. Evaluation of changes in morphology and function of Human Induced Pluripotent Stem Cell Derived Cardiomyocytes (HiPSC-CMs) cultured on an aligned-nanofiber cardiac patch. PLoS One. 2015;10:e0126338.
155. Sill TJ, von Recum HA. Electrospinning: applications in drug delivery and tissue engineering. Biomaterials. 2008;29:1989–2006.
156. Guan J, Wang F, Li Z, Chen J, Guo X, Liao J, et al. The stimulation of the cardiac differentiation of mesenchymal stem cells in tissue constructs that mimic myocardium structure and biomechanics. Biomaterials. 2011;32:5568–80.
157. Xu Y, Patnaik S, Guo X, Li Z, Lo W, Butler R, et al. Cardiac differentiation of cardiosphere-derived cells in scaffolds mimicking morphology of the cardiac extracellular matrix. Acta Biomater. 2014;10:3449–62.
158. Nag AC. Study of non-muscle cells of the adult mammalian heart: a fine structural analysis and distribution. Cytobios. 1980;28:41–61.
159. Border WA, Noble NA. Transforming growth factor beta in tissue fibrosis. N Engl J Med. 1994;331:1286–92.
160. Desmouliere A, Geinoz A, Gabbiani F, Gabbiani G. Transforming growth factor-beta 1 induces alpha-smooth muscle actin expression in granulation tissue myofibroblasts and in quiescent and growing cultured fibroblasts. J Cell Biol. 1993;122:103–11.
161. Sime PJ, Xing Z, Graham FL, Csaky KG, Gauldie J. Adenovector-mediated gene transfer of active transforming growth factor-beta1 induces prolonged severe fibrosis in rat lung. J Clin Invest. 1997;100:768–76.
162. Roberts AB, Russo A, Felici A, Flanders KC. Smad3: a key player in pathogenetic mechanisms dependent on TGF-β. Ann N Y Acad Sci. 2003;995:1–10.
163. Derynck R, Zhang YE. Smad-dependent and Smad-independent pathways in TGF-beta family signalling. Nature. 2003;425:577–84.
164. Leask A. Getting to the heart of the matter: new insights into cardiac fibrosis. Circ Res. 2015;116:1269–76.
165. Willems IE, Havenith MG, De Mey JG, Daemen MJ. The alpha-smooth muscle actin-positive cells in healing human myocardial scars. Am J Pathol. 1994;145:868–75.
166. Bucala R, Spiegel LA, Chesney J, Hogan M, Cerami A. Circulating fibrocytes define a new leukocyte subpopulation that mediates tissue repair. Mol Med. 1994;1:71–81.
167. Chesney J, Bucala R. Peripheral blood fibrocytes: novel fibroblast-like cells that present antigen and mediate tissue repair. Biochem Soc Trans. 1997;25:520–4.

168. Mori L, Bellini A, Stacey MA, Schmidt M, Mattoli S. Fibrocytes contribute to the myofibroblast population in wounded skin and originate from the bone marrow. Exp Cell Res. 2005;304:81–90.
169. Aiba S, Tagami H. Inverse correlation between CD34 expression and proline-4-hydroxylase immunoreactivity on spindle cells noted in hypertrophic scars and keloids. J Cutan Pathol. 1997;24:65–9.
170. Kalluri R, Neilson EG. Epithelial-mesenchymal transition and its implications for fibrosis. J Clin Invest. 2003;112:1776–84.
171. Jain R, Shaul PW, Borok Z, Willis BC. Endothelin-1 induces alveolar epithelial-mesenchymal transition through endothelin type A receptor-mediated production of TGF-beta1. Am J Respir Cell Mol Biol. 2007;37:38–47.
172. Doerner AM, Zuraw BL. TGF-beta1 induced epithelial to mesenchymal transition (EMT) in human bronchial epithelial cells is enhanced by IL-1beta but not abrogated by corticosteroids. Respir Res. 2009;10:1465–9921.
173. Yamauchi Y, Kohyama T, Takizawa H, Kamitani S, Desaki M, Takami K, et al. Tumor necrosis factor-alpha enhances both epithelial-mesenchymal transition and cell contraction induced in A549 human alveolar epithelial cells by transforming growth factor-beta1. Exp Lung Res. 2010;36:12–24.
174. Zeisberg EM, Tarnavski O, Zeisberg M, Dorfman AL, McMullen JR, Gustafsson E, et al. Endothelial-to-mesenchymal transition contributes to cardiac fibrosis. Nat Med. 2007;13:952–61.
175. Engebretsen KVT, Skårdal K, Bjørnstad S, Marstein HS, Skrbic B, Sjaastad I, et al. Attenuated development of cardiac fibrosis in left ventricular pressure overload by SM16, an orally active inhibitor of ALK5. J Mol Cell Cardiol. 2014;76:148–57.
176. Tan SM, Zhang Y, Connelly KA, Gilbert RE, Kelly DJ. Targeted inhibition of activin receptor-like kinase 5 signaling attenuates cardiac dysfunction following myocardial infarction. Am J Physiol Heart Circ Physiol. 2010;298:H1415–25.
177. Campbell SE, Katwa LC. Angiotensin II stimulated expression of transforming growth factor-beta1 in cardiac fibroblasts and myofibroblasts. J Mol Cell Cardiol. 1997;29:1947–58.
178. De Mello WC, Specht P. Chronic blockade of angiotensin II AT1-receptors increased cell-to-cell communication, reduced fibrosis and improved impulse propagation in the failing heart. J Renin Angiotensin Aldosterone Syst. 2006;7:201–5.
179. Shibasaki Y, Nishiue T, Masaki H, Tamura K, Matsumoto N, Mori Y, et al. Impact of the angiotensin II receptor antagonist, losartan, on myocardial fibrosis in patients with end-stage renal disease: assessment by ultrasonic integrated backscatter and biochemical markers. Hypertens Res. 2005;28:787–95.
180. Ortiz LA, Lasky J, Gozal E, Ruiz V, Lungarella G, Cavarra E, et al. Tumor necrosis factor receptor deficiency alters matrix metalloproteinase 13/tissue inhibitor of metalloproteinase 1 expression in murine silicosis. Am J Respir Crit Care Med. 2001;163:244–52.
181. Westermann D, Rutschow S, Van Linthout S, Linderer A, Bucker-Gartner C, Sobirey M, et al. Inhibition of p38 mitogen-activated protein kinase attenuates left ventricular dysfunction by mediating pro-inflammatory cardiac cytokine levels in a mouse model of diabetes mellitus. Diabetologia. 2006;49:2507–13.
182. Shukla MN, Rose JL, Ray R, Lathrop KL, Ray A, Ray P. Hepatocyte growth factor inhibits epithelial to myofibroblast transition in lung cells via Smad7. Am J Respir Cell Mol Biol. 2009;40:643–53.
183. Mizuno S, Matsumoto K, Li MY, Nakamura T. HGF reduces advancing lung fibrosis in mice: a potential role for MMP-dependent myofibroblast apoptosis. Faseb J. 2005;19:580–2.
184. Singh S, Saraiva L, Elkington PT, Friedland JS. Regulation of matrix metalloproteinase-1, -3, and -9 in Mycobacterium tuberculosis-dependent respiratory networks by the rapamycin-sensitive PI3K/p70(S6K) cascade. Faseb J. 2014;28:85–93.

185. Nakamura T, Matsumoto K, Mizuno S, Sawa Y, Matsuda H. Hepatocyte growth factor prevents tissue fibrosis, remodeling, and dysfunction in cardiomyopathic hamster hearts. Am J Physiol Heart Circ Physiol. 2005;288:H2131–9.
186. Taniyama Y, Morishita R, Aoki M, Hiraoka K, Yamasaki K, Hashiya N, et al. Angiogenesis and antifibrotic action by hepatocyte growth factor in cardiomyopathy. Hypertension. 2002;40:47–53.
187. Nakamura T, Sakai K, Matsumoto K. Hepatocyte growth factor twenty years on: much more than a growth factor. J Gastroenterol Hepatol. 2011;1:188–202.
188. Ueda H, Nakamura T, Matsumoto K, Sawa Y, Matsuda H. A potential cardioprotective role of hepatocyte growth factor in myocardial infarction in rats. Cardiovasc Res. 2001;51:41–50.
189. Sakaguchi G, Tambara K, Sakakibara Y, Ozeki M, Yamamoto M, Premaratne G, et al. Control-released hepatocyte growth factor prevents the progression of heart failure in stroke-prone spontaneously hypertensive rats. Ann Thorac Surg. 2005;79:1627–34.
190. Nakano J, Marui A, Muranaka H, Masumoto H, Noma H, Tabata Y, et al. Effects of hepatocyte growth factor in myocarditis rats induced by immunization with porcine cardiac myosin. Interact Cardiovasc Thorac Surg. 2014;18:300–7.
191. Ren J, Samson WK, Sowers JR. Insulin-like growth factor I as a cardiac hormone: physiological and pathophysiological implications in heart disease. J Mol Cell Cardiol. 1999;31:2049–61.
192. Li Q, Li B, Wang X, Leri A, Jana KP, Liu Y, et al. Overexpression of insulin-like growth factor-1 in mice protects from myocyte death after infarction, attenuating ventricular dilation, wall stress, and cardiac hypertrophy. J Clin Invest. 1997;100:1991–9.
193. Conti E, Carrozza C, Capoluongo E, Volpe M, Crea F, Zuppi C, et al. Insulin-like growth factor-1 as a vascular protective factor. Circulation. 2004;110:2260–5.
194. Urbanek K, Rota M, Cascapera S, Bearzi C, Nascimbene A, De Angelis A, et al. Cardiac stem cells possess growth factor-receptor systems that after activation regenerate the infarcted myocardium, improving ventricular function and long-term survival. Circ Res. 2005;97:663–73.
195. Ruvinov E, Leor J, Cohen S. The promotion of myocardial repair by the sequential delivery of IGF-1 and HGF from an injectable alginate biomaterial in a model of acute myocardial infarction. Biomaterials. 2011;32:565–78.
196. Suleiman MS, Singh RJR, Stewart CEH. Apoptosis and the cardiac action of insulin-like growth factor I. Pharmacol Ther. 2007;114:278–94.
197. Ozawa CR, Banfi A, Glazer NL, Thurston G, Springer ML, Kraft PE, et al. Microenvironmental VEGF concentration, not total dose, determines a threshold between normal and aberrant angiogenesis. J Clin Invest. 2004;113:516–27.
198. Salimath AS, Phelps EA, Boopathy AV, Che P-l, Brown M, García AJ, et al. Dual delivery of hepatocyte and vascular endothelial growth factors via a protease-degradable hydrogel improves cardiac function in rats. PLoS One. 2012;7:e50980.
199. Schwarz ER, Speakman MT, Patterson M, Hale SS, Isner JM, Kedes LH, et al. Evaluation of the effects of intramyocardial injection of DNA expressing vascular endothelial growth factor (VEGF) in a myocardial infarction model in the rat – angiogenesis and angioma formation. J Am Coll Cardiol. 2000;35:1323–30.
200. Kloner RA, Dow J, Chung G, Kedes LH. Intramyocardial injection of DNA encoding vascular endothelial growth factor in a myocardial infarction model. J Thromb Thrombolysis. 2000;10:285–9.
201. Fan Z, Guan J. Antifibrotic therapies to control cardiac fibrosis. Biomater Res. 2016;20:13.